DOE/ET/53088-182 IFSR #182

PROCEEDINGS OF
US-JAPAN WORKSHOP
MAGNETIC RECONNECTION

DECEMBER 10-13, 1984

AUSTIN, TEXAS

FORWARD

The Magnetic Reconnection Workshop held at the University of Texas at Austin, December 10–13, 1984 was organized by the Institute for Fusion Studies, in connection with the Joint Institute for Fusion Theory, to exchange information in theoretical plasma physics. There were approximately thirty-five scientists participating which included six visitors from Japan. There were eight sessions with formal presentations on key issues related to magnetic reconnection.

The main goal of the workshop was to exchange recent results and ideas between theorists, computer simulationists, and experimentalists. Leading scientists representing these three categories made presentations in their respective areas. Each session included stimulated interaction between the speaker and his audience.

TABLE OF CONTENTS

MAGNETIC RECONNECTION

December 10–13, 1984
Institute for Fusion Studies
Austin, Texas

Sponsored By
US–Japan Joint Institute for Fusion Theory

Agenda

Monday, December 10, 1984

8:20 AM	Registration
8:50 AM	Opening Remarks: P. Diamond
Morning Session	Chairman: A. Bhattacharjee
9:00–9:45 AM	T. Sato, "3D Simulations of Energy Relaxation Processes"
9:55 AM	Break
10:15–11:00 AM	R. Nebel, "Flux Regeneration in ZT-40M at High θ and the MHD Model"
11:10–11:55 AM	D. Spicer, "Reconnection and Its Role in Solar Flares"
12:05 PM	Lunch
Afternoon Session	Chairman: T. Sato
2:00–2:40 PM	J. Holmes, "Nonlinear Coupling of Tearing Modes in the Reversed Field Pinch and the Tokamak Disruption"
2:50–3:30 PM	H. Strauss, "RFP: Mean Field MHD Model"
3:40 PM	Break
4:00–4:40 PM	T. Amano, "Nonlinear Evolution of Tearing Modes In Reversed Field Pinches"

Tuesday, December 11, 1984

Morning Session	Chairman: P. Diamond
9:00-9:45 AM	W. Park, "Magnetic Reconnection in Tokamaks"
9:55 AM	Break
10:15-11:00 AM	R. Pellat, "Half Coalescense of Non-linear m=1 Mode"
11:10-11:50 AM	T. Jensen, "A Sawtooth Oscillation Model"
12:00 noon	Lunch
Afternoon Session	Chairman: R. Kulsrud
2:00-2:30 PM	S. Kim, "Soft X-ray Imaging of Transient and Double Sawteeth on TEXT"
2:40-3:10 PM	A. Aydemir, "Half Coalescence of the m=1 Island in Tokamaks"
3:20 PM	Break
3:30-4:10 PM	R. Kleva, "Are Vacuum Bubbles a Cause of Major Disruptions?"
4:20-5:00 PM	Y. Kondoh, "Energy Principle for Toroidal Plasma With Boundary"

Wednesday 12, 1984

Morning Session	Chairman: W. Park
9:00-9:45 AM	T. Hayashi, "Spheromak and Magnetic Reconnection"
9:55 AM	Break
10:15-11:00 AM	R. Moses, "Kinetic Theory of Driven Reconnection At An X-Point"
11:10-11:50 AM	G. Kurita, "Bubble Formation Due to Surface Tearing Modes"
12:00 noon	Lunch
Afternoon Session	Chairman: T. Amano
2:00-2:40 PM	R. Steinolfson, "Reverse Flow Vortices and Current Sheets in Nonlinear Tearing"
2:50-3:20 PM	B. McNamara, "Lie Transform Approach To Drift-Resonant Interactions in Fluid and Plasma Turbulence"
3:30 PM	Break
3:50-4:20 PM	M. Kotschenreuther, "Resistive Dynamics of Magnetic Islands With Curvature and Pressure"
4:30-5:00 PM	A. Bhattacharjee, "Relaxation of Toroidal Plasmas"
7:00 PM	BANQUET DINNER The Old Pecan Street Cafe (Transportation provided)

Thursday, December 13, 1984

Morning Session	Chairman:
9:00-9:45 AM	J. Mizushima, "Statistical Properties of MHD Turbulence"
9:55 AM	Break
10:15-11:00 AM	D. Schnack, "Relaxation, Turbulence, and Dynamo Action In Driven Systems"
11:10-11:50 PM	S. Cowley, "The Dynamics of Tearing Modes"
12:00 noon	Lunch
Afternoon Session	Chairman: R. Moses
1:30-2:00 PM	J.N. Leboeuf, "Computer Modeling of Fast Collisionless Reconnection"
2:10-2:40 PM	T. Tajima, "Explosive Coalescence"
2:50 PM	M.N. Rosenbluth, Concluding Remarks

US–Japan Workshop Participants

December 10–13, 1984

Prof. T. Amano
Nagoya University
Nagoya, JAPAN
052–781–5111

Dr. A. Aydemir
IFS
512–471–6157 (FTS 770–5619)

Dr. Dan Barnes
Science Applications, Inc.
1406 Camp Craft Road, Suite 202A
Austin, TX 78746

Dr. Amitava Bhattacharjee
Columbia University
Department of Applied Physics
S.W. Mudd 210
New York, NY 10027
212–280–8417

Mr. Steve Cowley
Princeton Plasma Physics Lab
P.O. Box 451
Princeton, NJ 08544
609–683–2613

Mr. Gary Craddock
IFS
512–471–4378 (FTS 770–5270)

Dr. Pat H. Diamond
IFS
512–471–1485 (FTS 770–5271)

Dr. Taiksoo Hahm
IFS
512–471–7770 (FTS 770–5340)

Dr. Takaya Hayashi
Hiroshima University
Institute for Fusion Theory
JAPAN

Dr. Jeffrey A. Holmes
Oak Ridge National Lab
P.O. Box Y   Bldg. 9104-2
Oak Ridge, TN 37830
615-574-0622 (FTS 624-0622)

Dr. Wendell Horton
IFS
512-471-1594 (FTS 770-5269)

Dr. Torkil Jensen
GA Technologies Inc.
P.O. Box 85608
San Diego, CA 92138
619-455-4233

Mr. Sung B. Kim
FRC
512-471-4380

Dr. Robert Kleva
University of Maryland
Lab for Plasma Fusion Energy Studies
College Park, MD 20742
301-454-7107

Dr. Y. Kondoh
Gunma University
JAPAN

Mike Kotschenreuther
IFS
512-471-4367 (FTS 770-5619)

Dr. Russell Kulsrud
Princeton Plasma Physics Lab
P.O. Box 451
Princeton, NJ 08544
609-683-2613

Dr. G. Kurita
J.A.E.R.I.
Naka-Gun, Ibaraki-Ken
JAPAN

Jean-Noel Leboeuf
IFS
512-471-6123 (FTS 770-5270)

Dr. Brendan McNamara
Lawrence Livermore National Lab
P.O. Box 5511   L-630
Livermore, CA 94550
415-422-9821

Dr. Ron Moses
Los Alamos National Lab
P.O. Box 1663
Los Alamos, NM 87545
FTS 843-5622

Dr. J. Mizushima
Department of Information Science
Sagami Institute of Technology
1-15-5 Tsujido Nishikaigan
Fujisawa 251
JAPAN

Dr. Rick Nebel
Los Alamos National Laboratory
P.O. Box 1663 F642
Los Alamos, NM 87545
505-667-4394

Dr. Wonchull Park
Princeton Plasma Physics Lab
P.O. Box 451
Princeton, NJ 08544
609-683-2637

Dr. Rene Pellat
Centre de Physique Theorique
Ecole Polytechnique
91128 Palaiseau
FRANCE

Dr. M.N. Rosenbluth
IFS
512-471-1322 (FTS 770-5269)

Prof. Tetsuya Sato
Institute for Fusion Theory
Hiroshima University
Higashisnda-Machi,Hiroshima
JAPAN

Dr. Dalton D. Schnack
Science Applications, Inc.
P.O. Box 2351
La Jolla, CA 92038
619-456-6021

Dr. Daniel Spicer
Naval Research Laboratory
Plasma Physics Division
Washington, DC 20375
703-620-0492

Dr. R.S. Steinolfson
Univ. of Calif. at Irvine
Department of Physics
Irvine, CA 92717
714-856-6280

Dr. Hank Strauss
Courant Institute, New York Univ.
251 Mercer Street
New York, NY 10012
212-460-7127

Dr. Toshi Tajima
IFS
512-471-4574 (FTS 770-5270)

Dr. Jiro Todoroki
IFS
512-471-5427 (FTS 770-5269)

3D SIMULATIONS OF ENERGY RELAXATION PROCESSES

T. SATO

HIROSHIMA UNIVERSITY

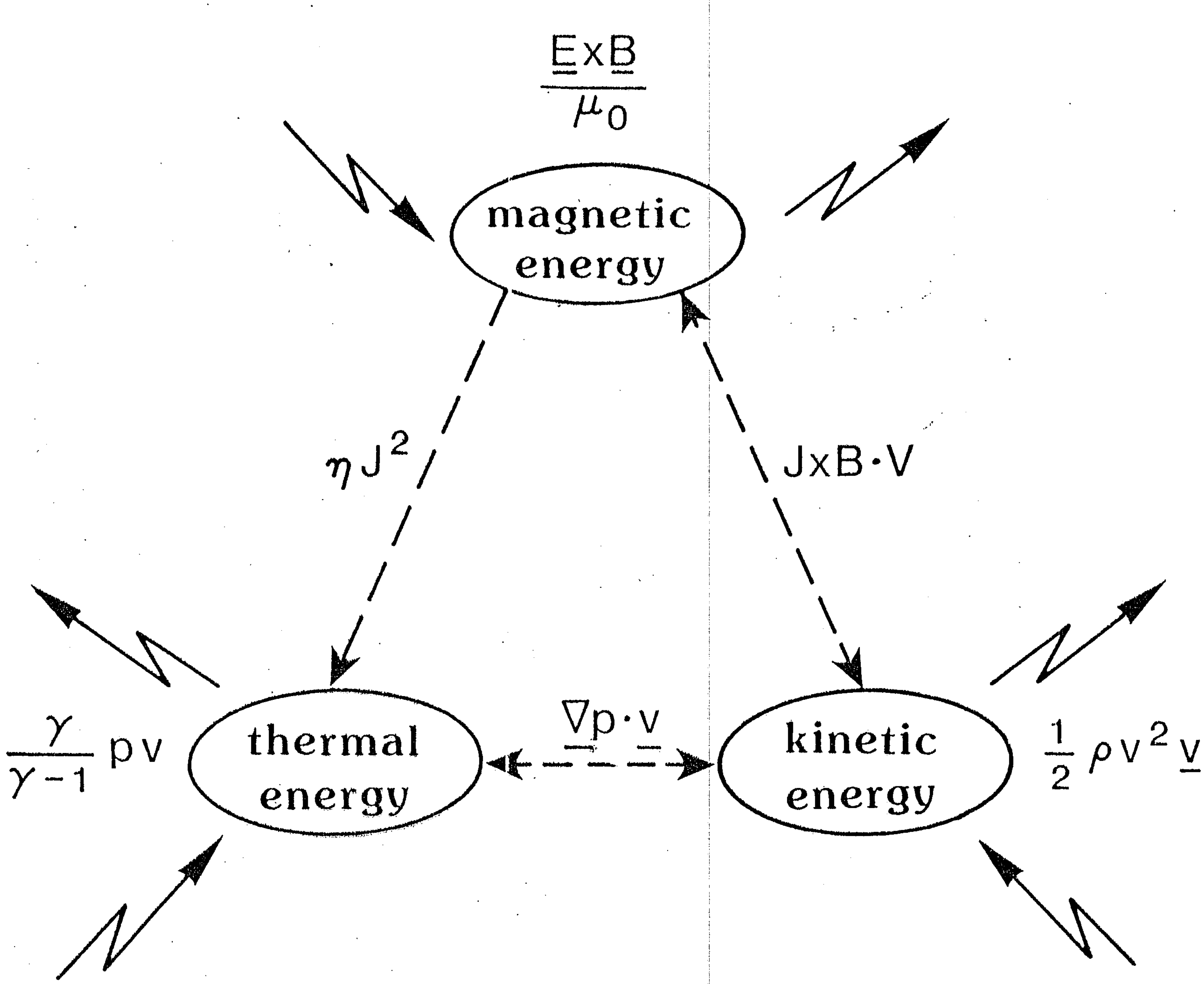

ExB / μ0
magnetic energy
ηJ2
JxB·V
thermal energy
kinetic energy
∇p·v
γ/(γ-1) pv
1/2 ρv2v

Energy Relaxation

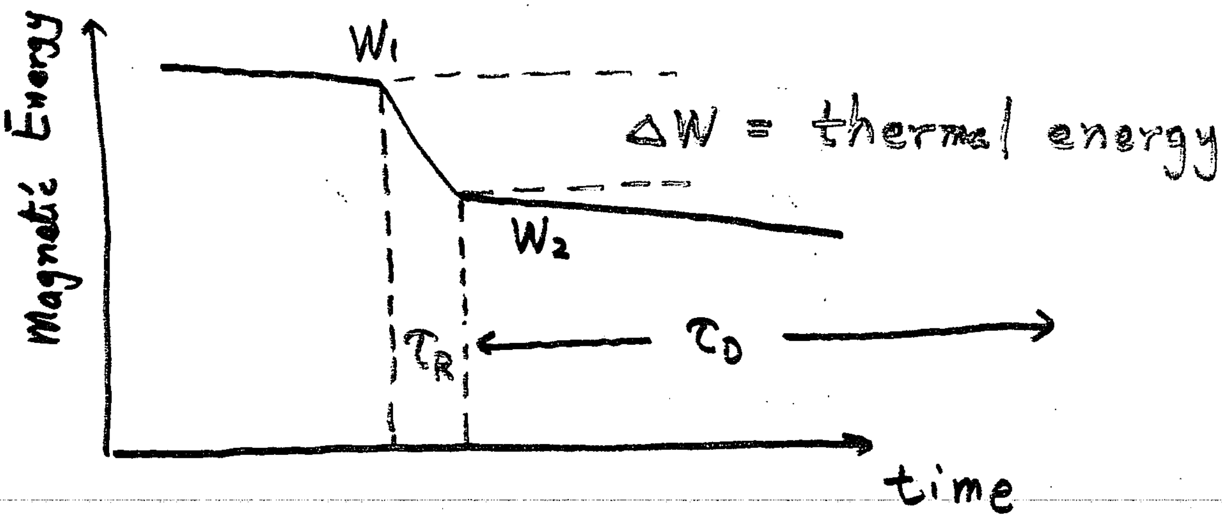

$$\tau_R \ll \tau_D$$

What can cause rapid energ dissipation ?

1. Turbulence $\rightarrow$ $\tau_R = k^2 D$
   (large k)
2. Driven Reconnection $\rightarrow$ $\tau_R = \eta j^2$
   (large j)

Driven Reconnection

- Initially no anti-parallel configuration is required.
- Plasma convection creates anti-parallel configuration.

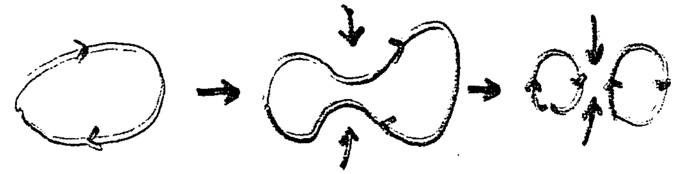

Cause : Converging plasma flows $\underline{V_D}$

or convection electric field $\underline{E_D}$

$$(E_D = - V_D \times B)$$

Effect : Generation of neutral sheet current J_{NS}

$$\left(\underline{J_{NS}} = \frac{E_D}{\eta} \right)$$

Enhancement of local dissipation

$$\eta \underline{J_{NS}}^2 = \frac{E_D^2}{\eta}$$

(inversely proportional to η)

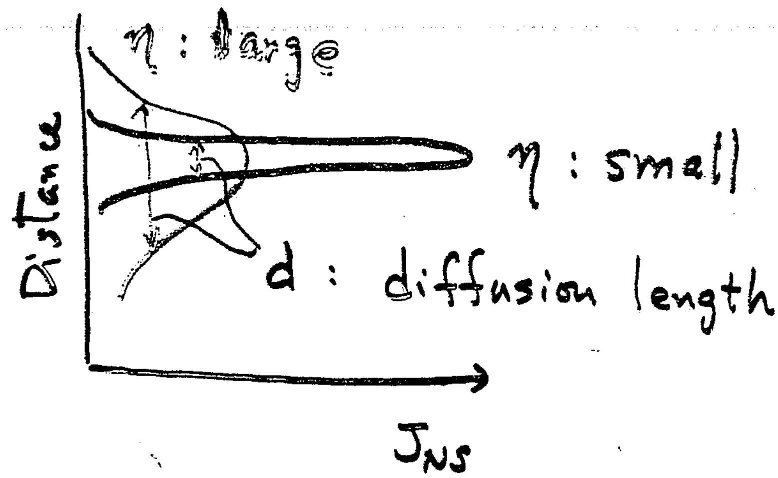

Dissipation Rate

$$\tau_R^{-1} \approx \int \eta J_{NS}^2 \, dV \propto \eta J_{NS}^2 d$$

$$\eta J_{NS} = E_D$$

$$\mu_0 J_{NS} = \frac{B}{d}$$

$$\therefore \quad \tau_R^{-1} \propto \frac{E_D B}{\mu_0} = \underline{\text{indep. of } \eta} \quad !!$$

Single helicity kink instability

$$\psi(r, \theta, z) = \psi_0(r) + \psi_1(r) \sin\left(\theta - \frac{2\pi}{L} z\right)$$

$$B_{1\theta} \propto \frac{\partial \psi_1(r)}{\partial r} \sin\left(\theta - \frac{2\pi}{L} z\right)$$

$$B_{1r} \propto \psi_1(r) \cos\left(\theta - \frac{2\pi}{L} z\right)$$

Toroidal flux converted from B_{1r} through driven reconnection

$$\Delta \chi^- = 2\pi \int_0^{\frac{L}{2}} a\, B_{1r}\, dz = -\frac{\psi_1(a)}{\pi}$$

$$\Delta \chi^+ = 2\pi \int_{-\frac{L}{2}}^{0} a\, B_{1r}\, dz = \frac{\psi_1(a)}{\pi}$$

$$(\Delta \chi^- + \Delta \chi^+ = 0)$$

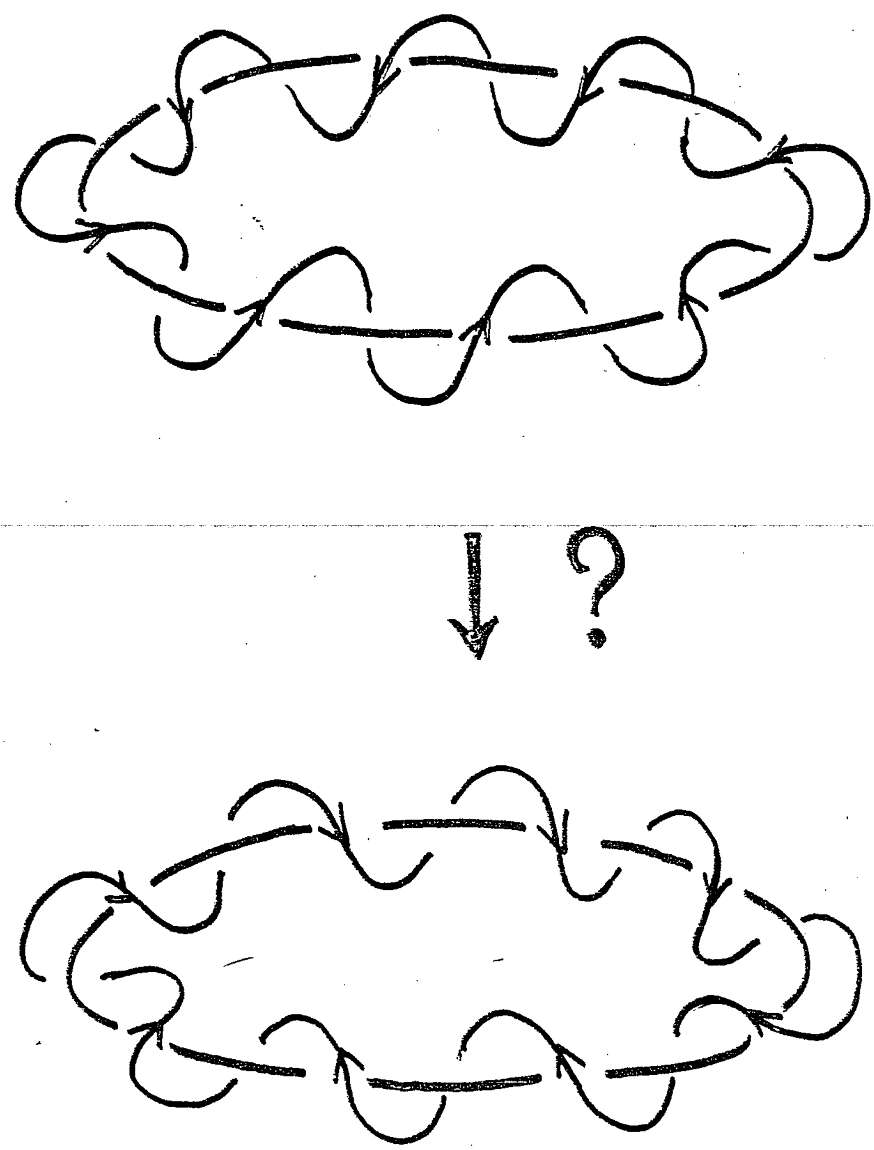

Proposed Model

m = 1 helical kink instability

⇨ { axial plasma flows
  nonlinear distortion
  ⇨ generation of B_r

⇨ non-linear driven reconnection

⇩

self-reversal

Basic flow pattern induced by a helical kink instability on a toroidal plane

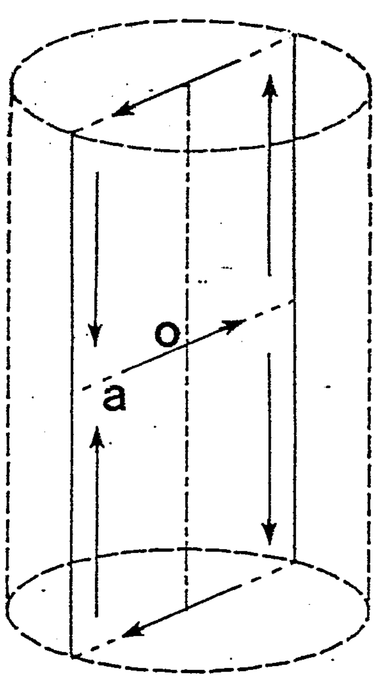

Helically distorted magnetic field configuration

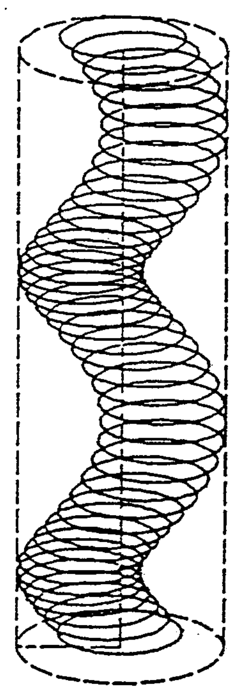

Radial fields induced by nonlinear development of a helical kink mode

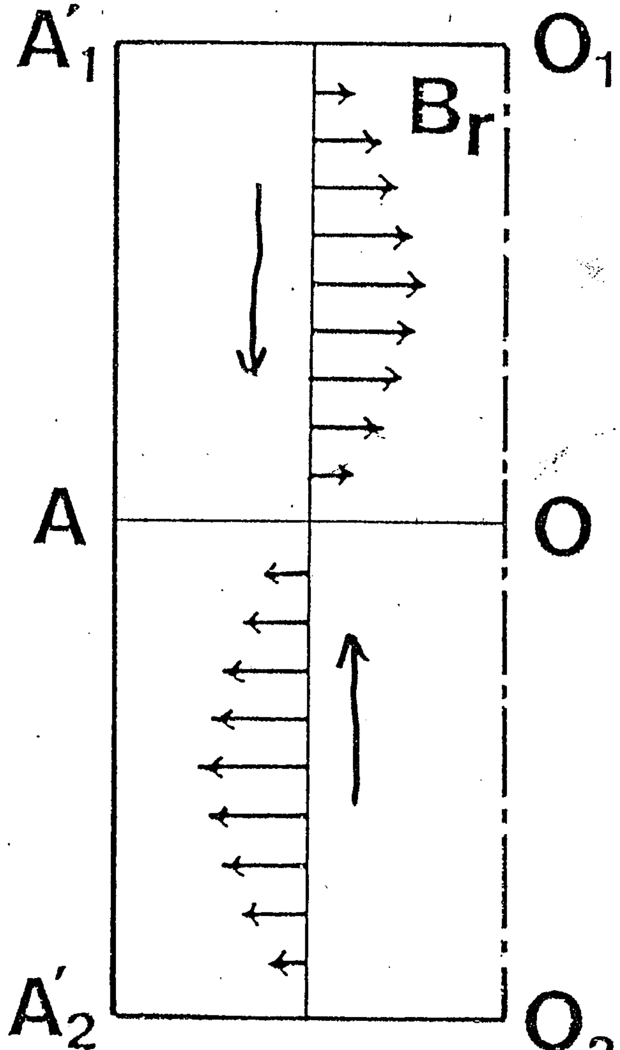

Top view of nonlinearly deformed poloidal fields

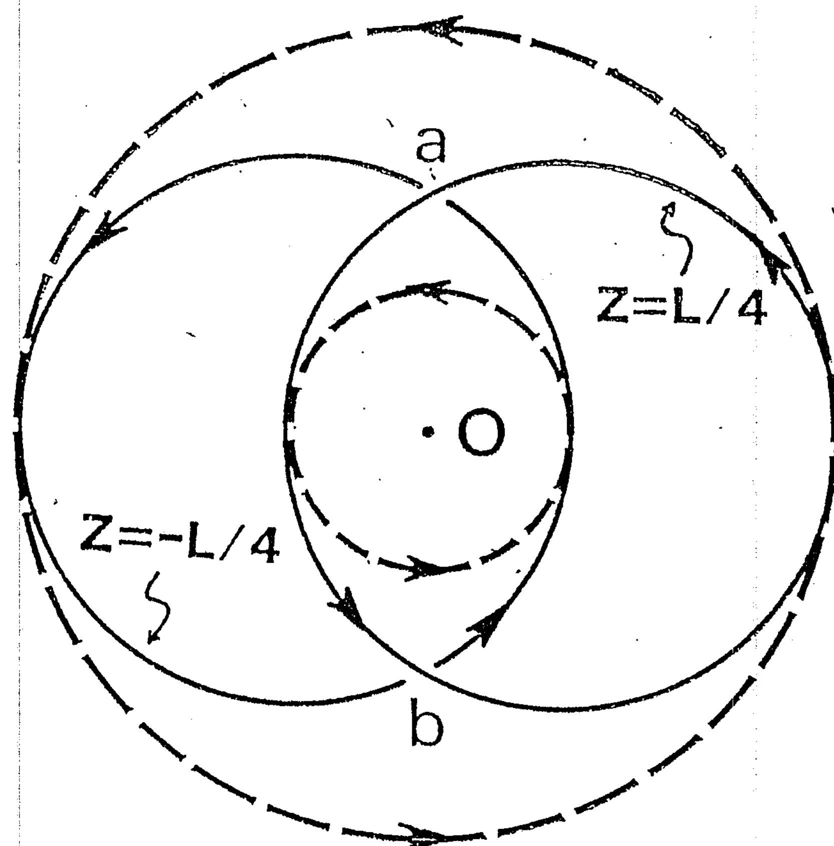

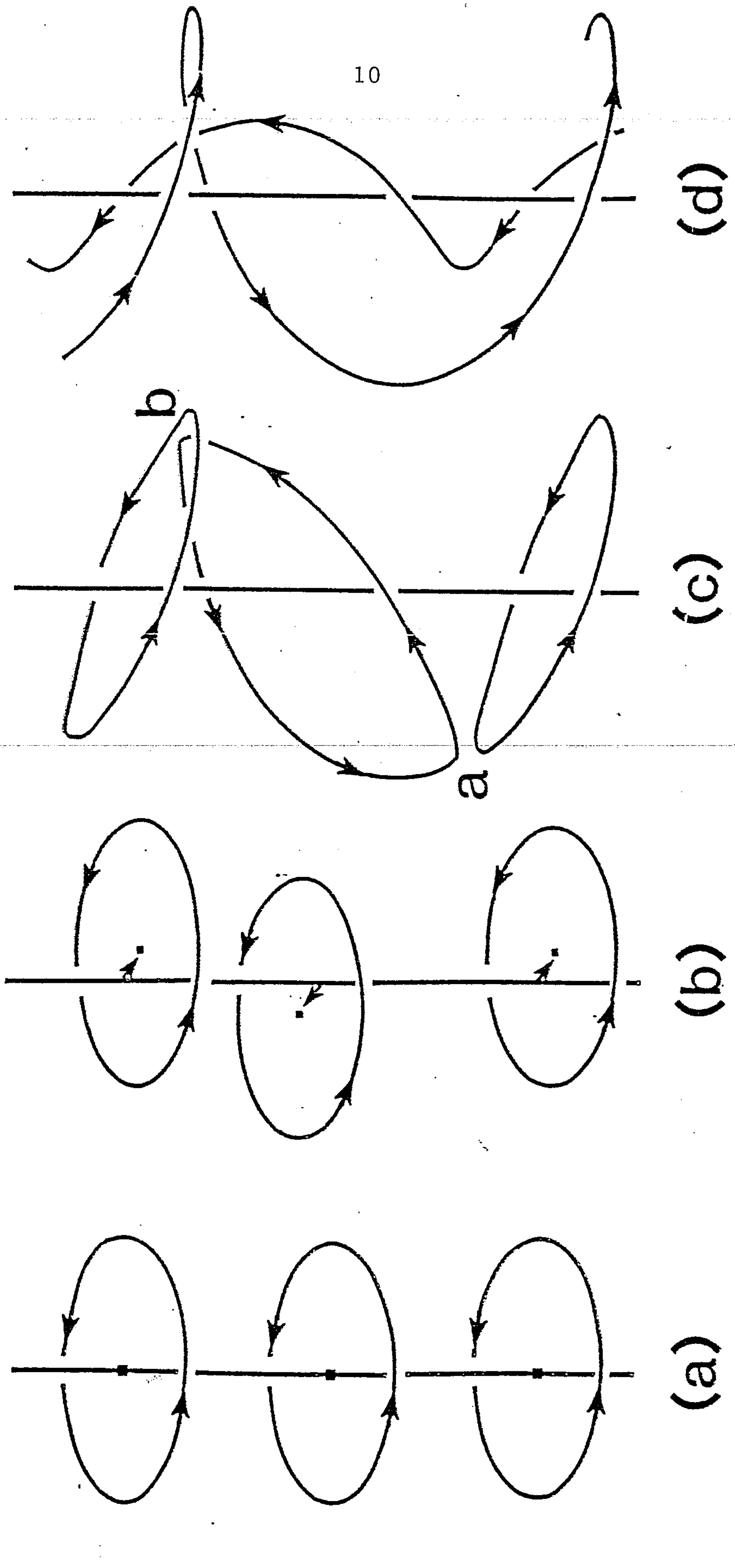
(a)
(b)
(c)
(d)
a
b

SIMULATION STUDY OF REVERSED FIELD GENERATION AND MEINTENANCE IN THE RFP

Kanya Kusano and Tetsuya Sato

Institute for Fusion Theory
Hiroshima University
Hiroshima, Japan

Initial Conditions

Force-free equilibrium

$$\mu B = \mathrm{rot}\, B, \quad B_r = 0,$$

where

$$\mu = \begin{cases} \lambda \ (\text{const.}) & 0<r<\xi \\ \dfrac{\lambda}{2}\left\{\cos\left(\pi \dfrac{r-\xi}{a-\xi}\right) + 1\right\} & \xi<r<a \end{cases}$$

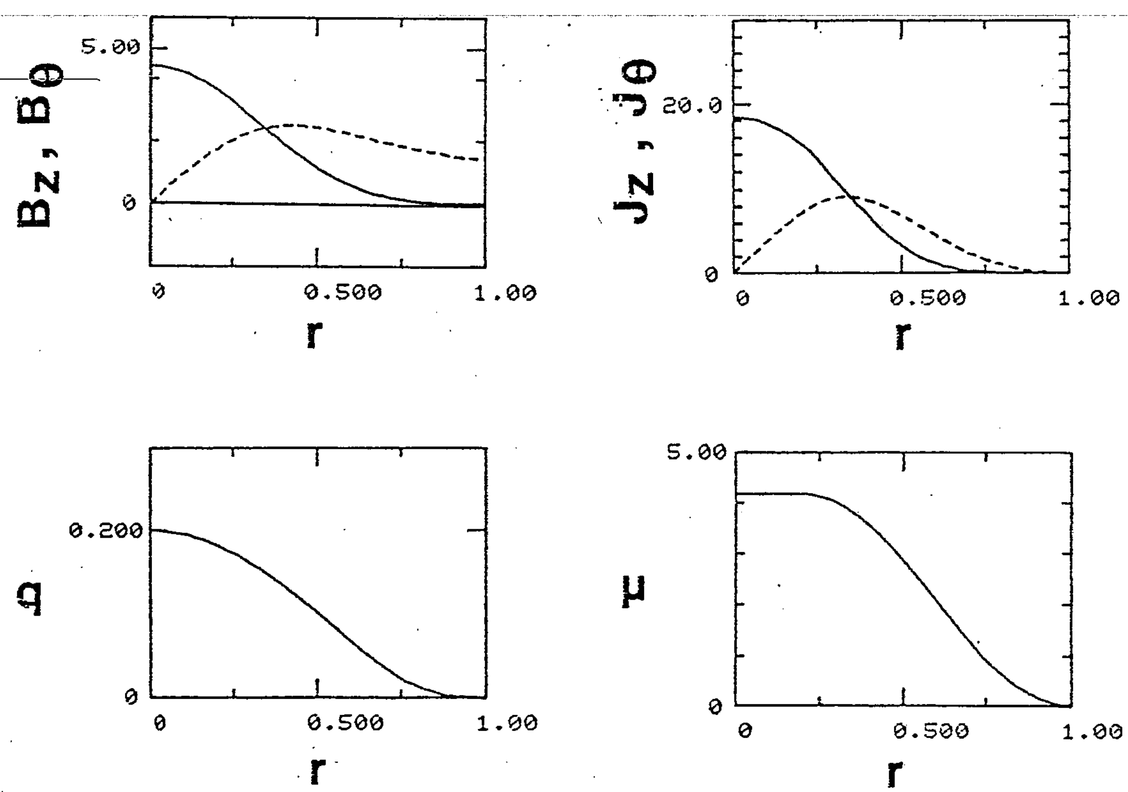

$F = 0$

$\Theta = 1.73$

Imposed Perturbations at t=0

$$\partial v_{m,n} = \partial v_0 \exp i\,(\, m\theta - 2\pi nz/L\,)$$

	m	n
case 1	1	5
case 2	1	6
case 3	1	4~7

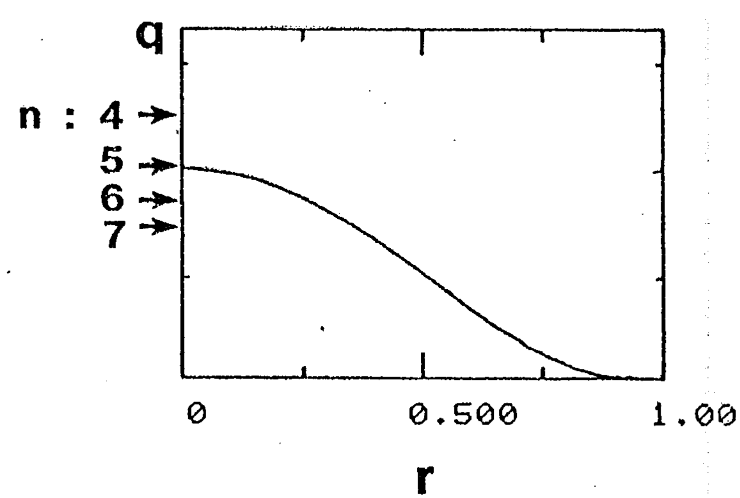

Simulation Model

3-D Cylindrical MHD Code

Dimensions

$a = 0.1$ m

$L = 1.5$ m

Grid points

r	44
θ	16
z	160

Boundary conditions

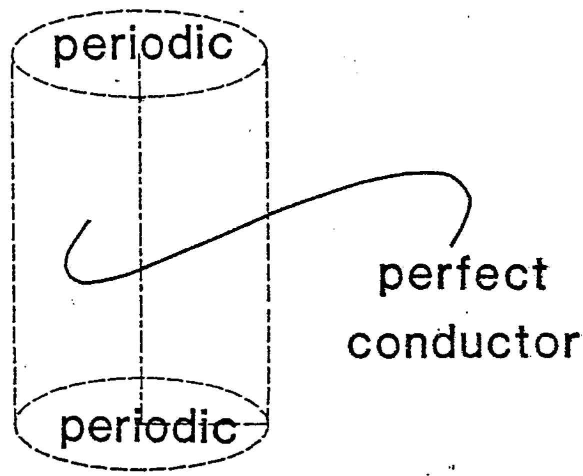

Equations (zero-β model)

$$\frac{\partial \rho}{\partial t} = -\nabla \cdot (\rho v)$$

$$\frac{\partial \rho v}{\partial t} = -\nabla \cdot [\rho v v - \frac{1}{\mu_0}(BB - \frac{B^2}{2}\mathbf{I})]$$

$$\frac{\partial B}{\partial t} = \nabla \times (v \times B) - \nabla \times (\eta J)$$

$$\mu_0 J = \nabla \times B$$

η : resistivity (constant and uniform)

Radial q-profile, Axial profiles of the radial field and the axial plasma flow

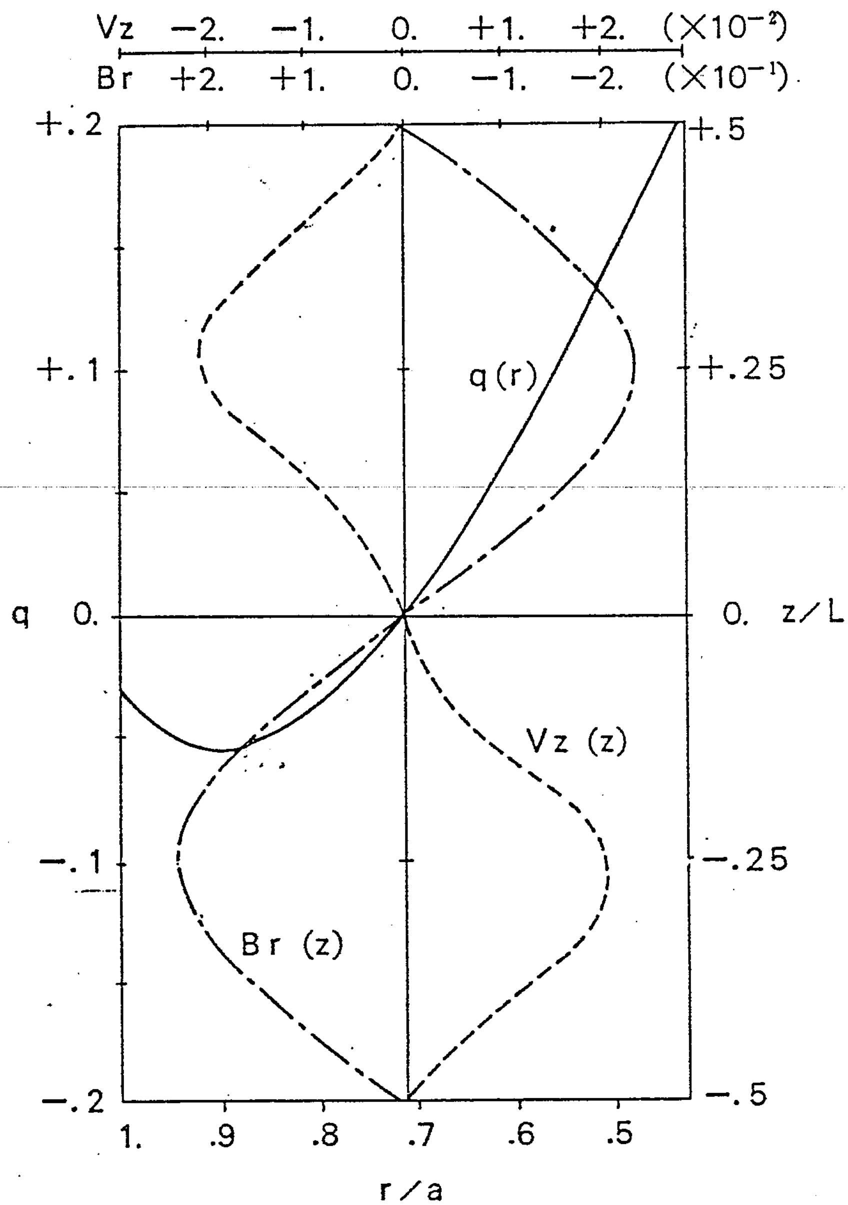

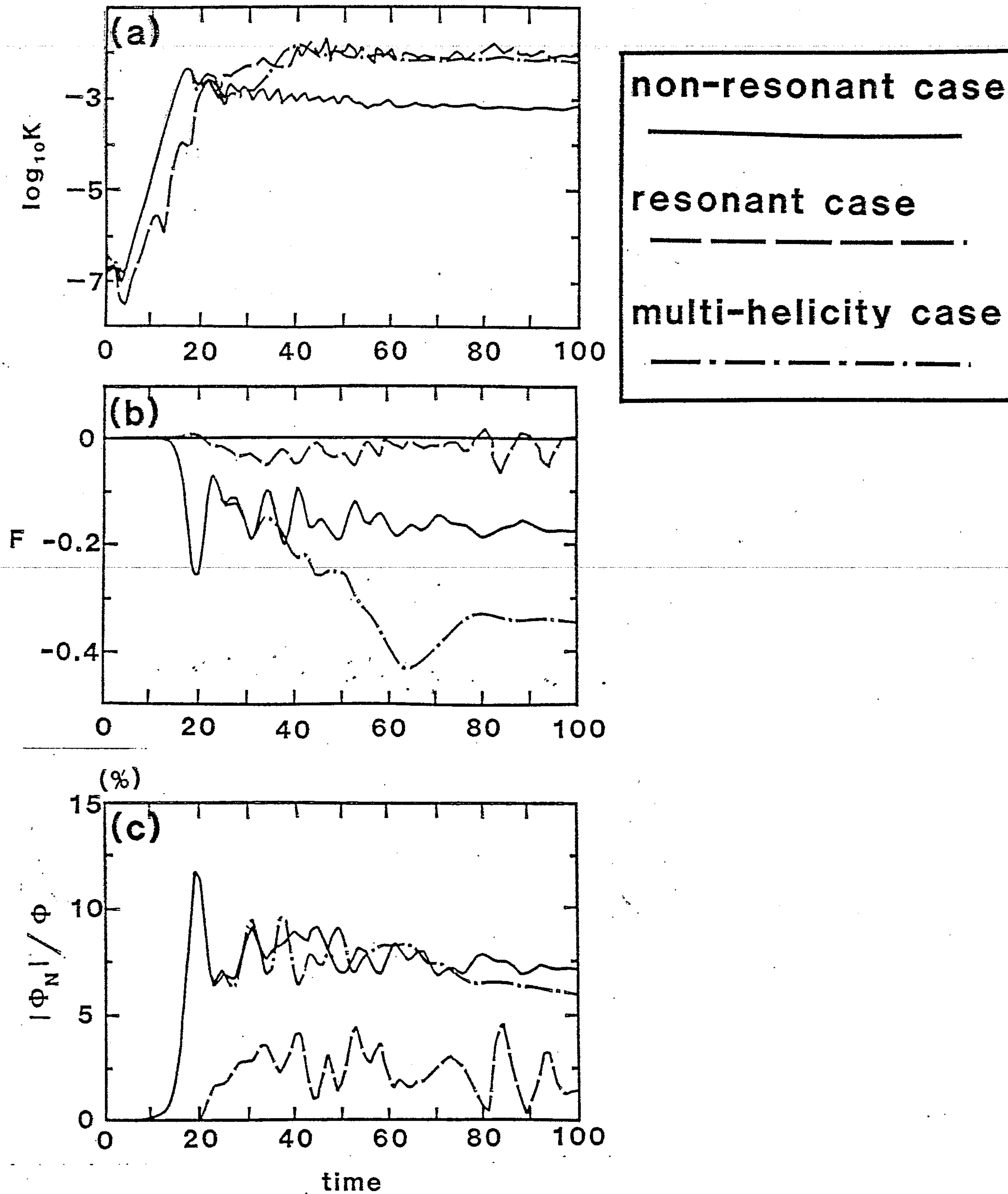
(a)
$\log_{10}K$
-3
-5
-7
0
20
40
60
80
100
non-resonant case
resonant case
multi-helicity case
(b)
F
0
-0.2
-0.4
0
20
40
60
80
100
(c)
(%)
15
10
5
0
$|\Phi_N|/\Phi$
0
20
40
60
80
100
time

temporal evolutions of Fourier amplitudes

of kinetic energy

non-resonant case

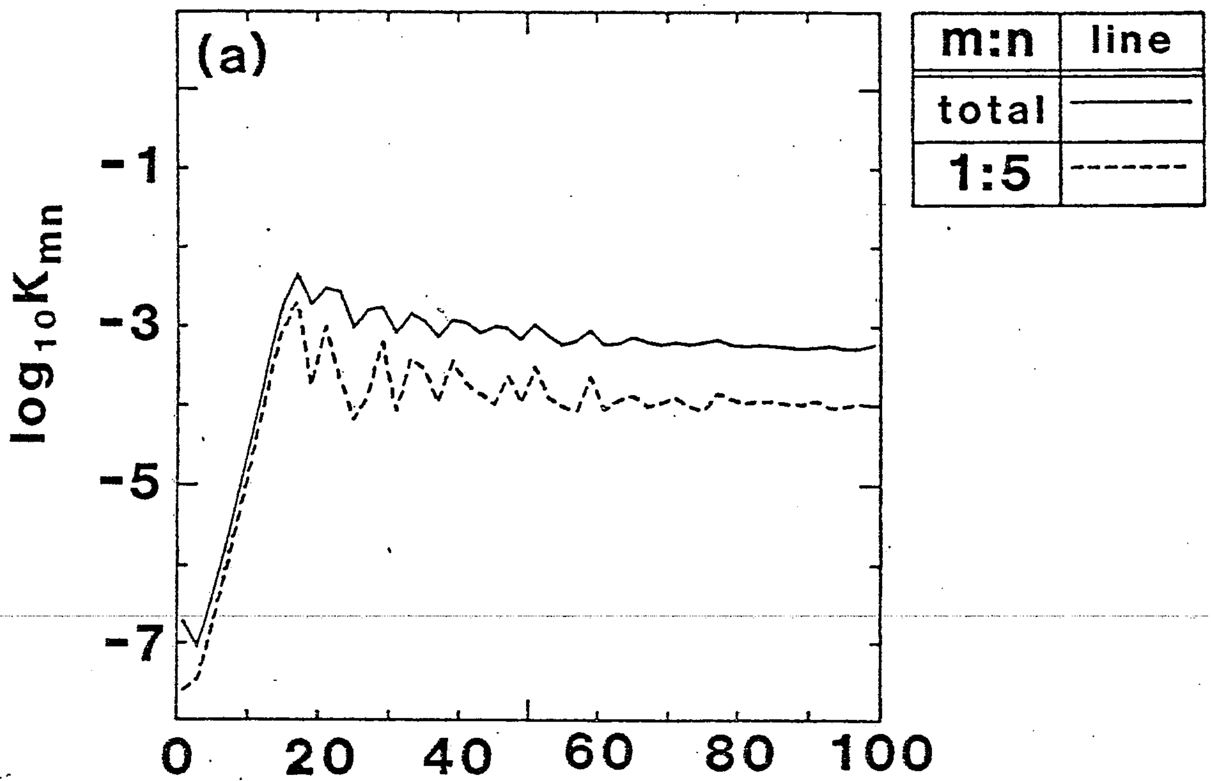

multi-helicity case

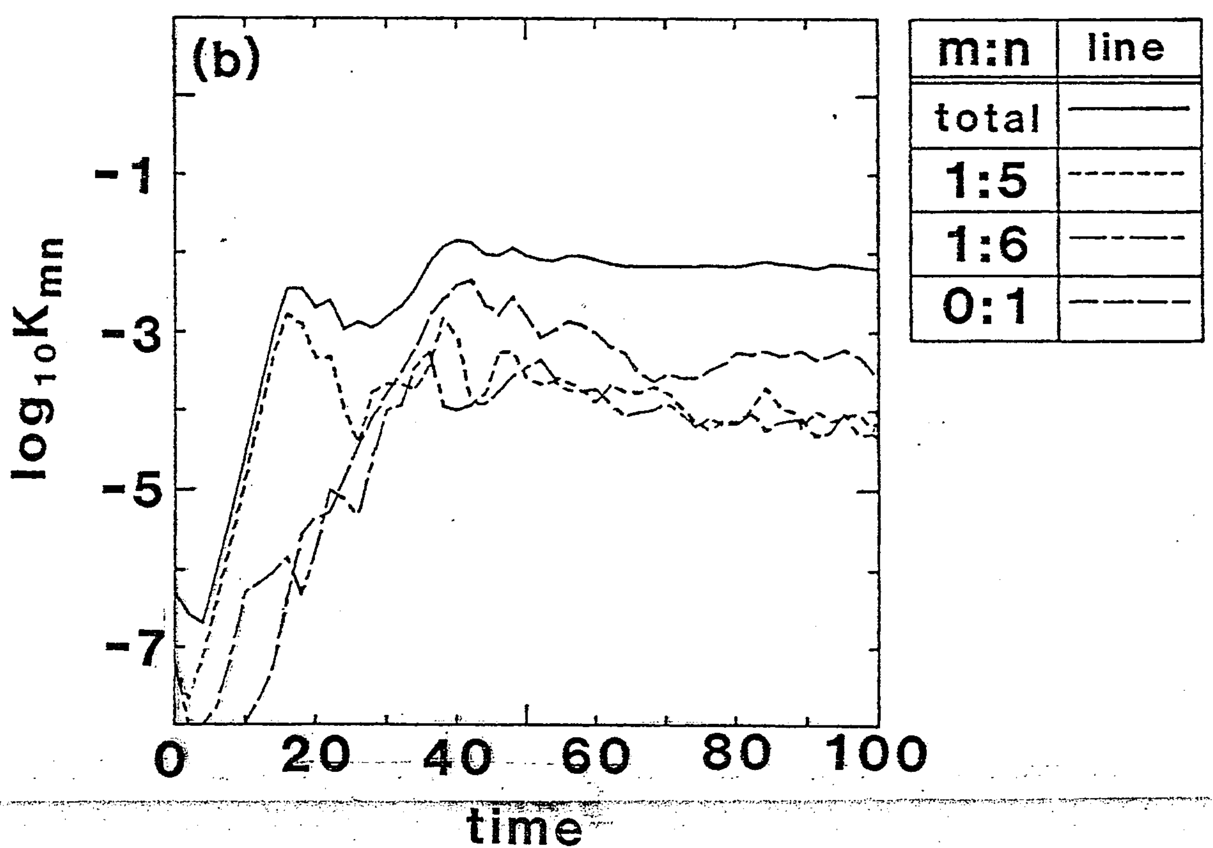

contours of negative toroidal field

in poloidal section for non-resonant case

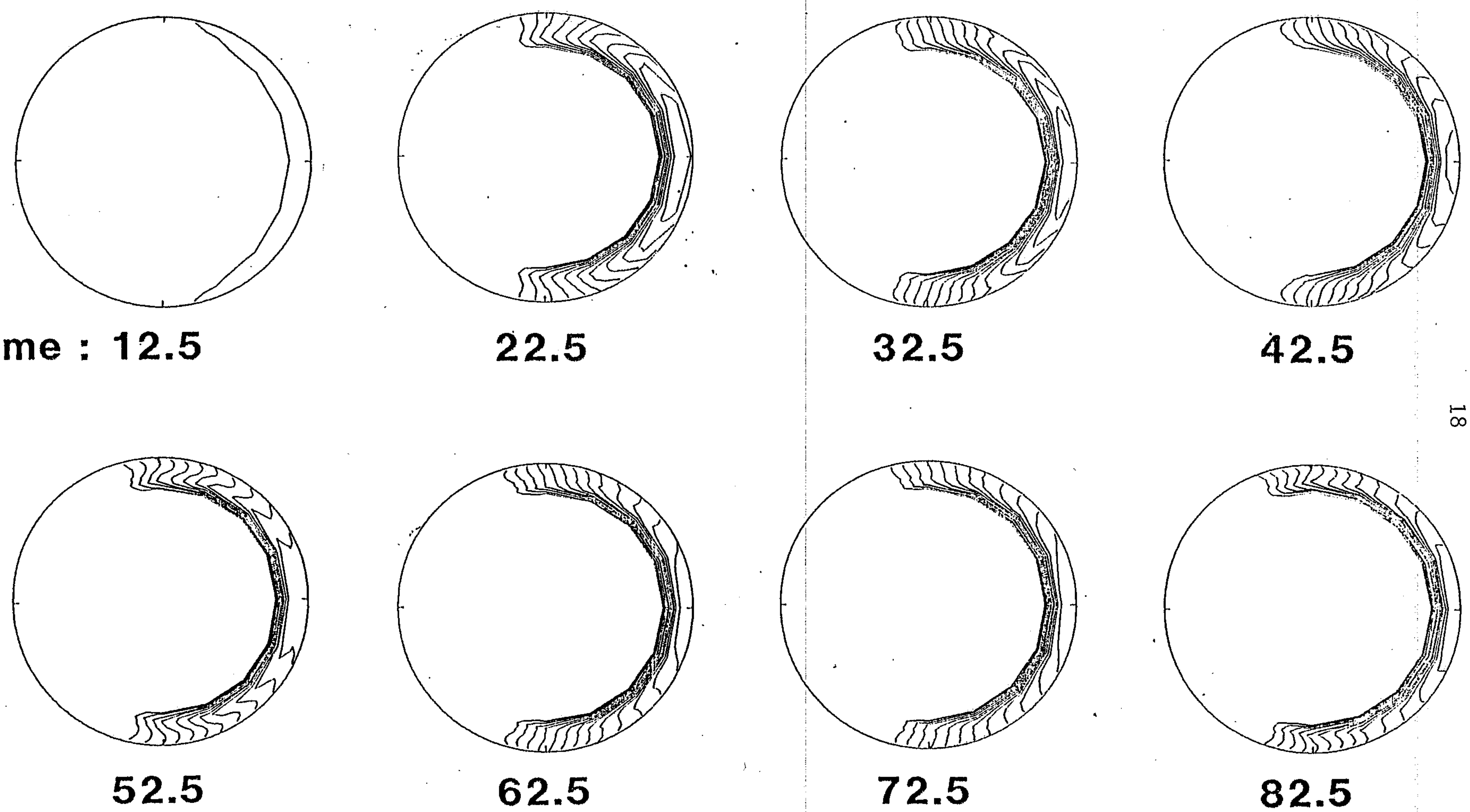

contours of negative toroidal field

in poloidal section for multi-helicity case

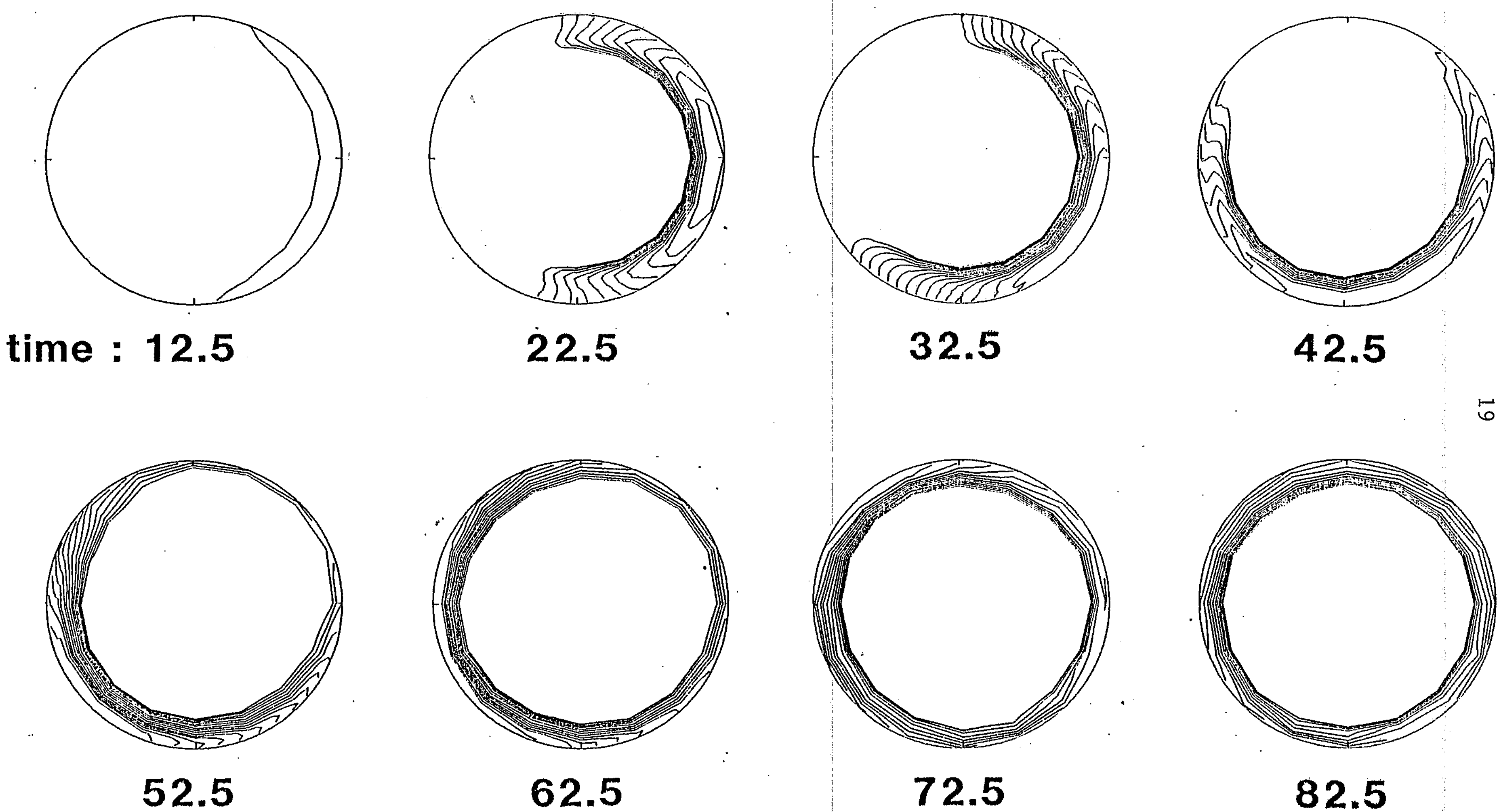

temporal evolutions of generated reversed flux for several single helicity cases

Current is not sustained.

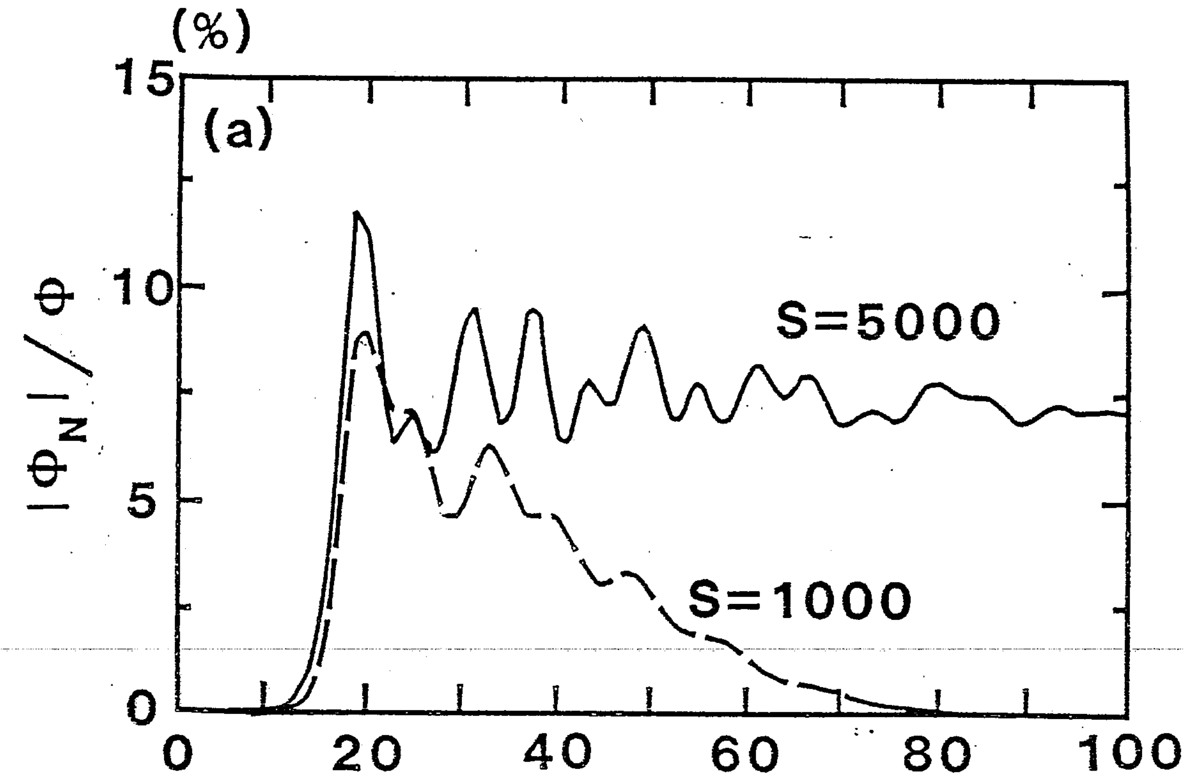

Current is sustained.

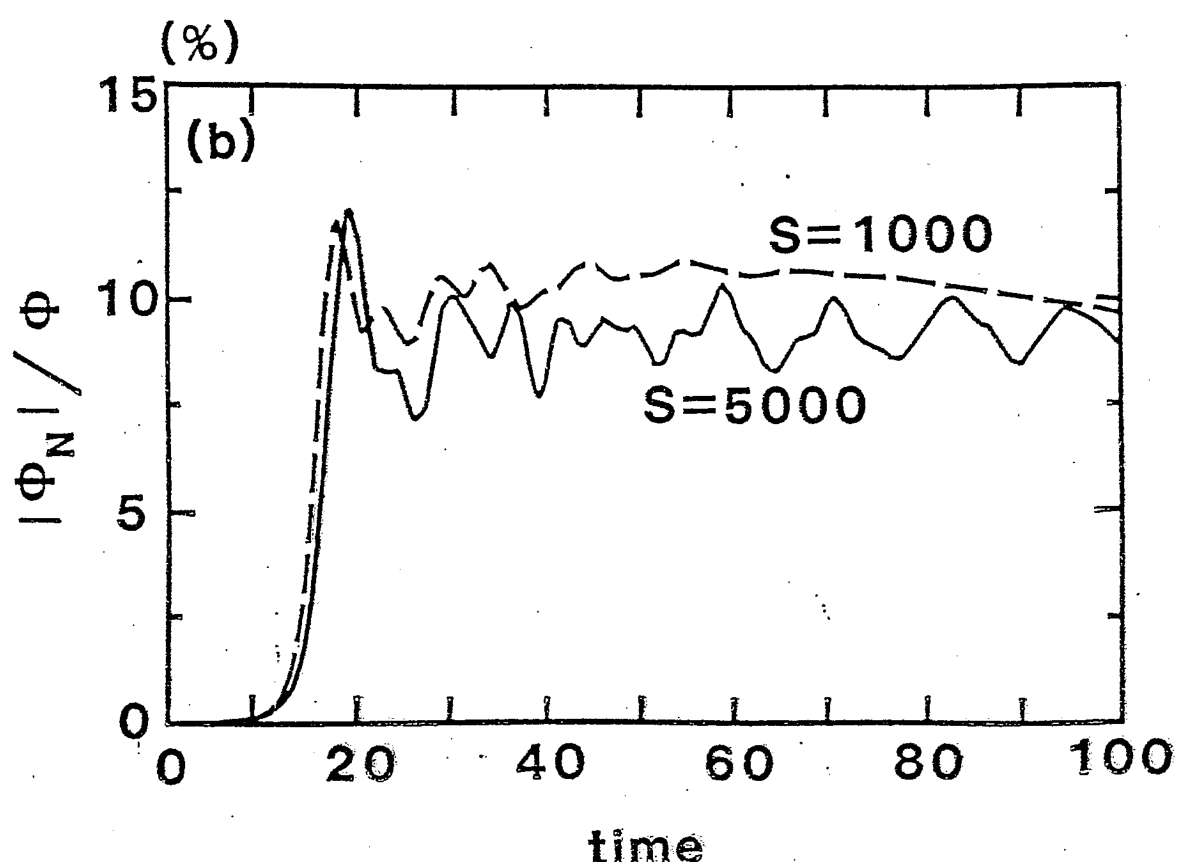

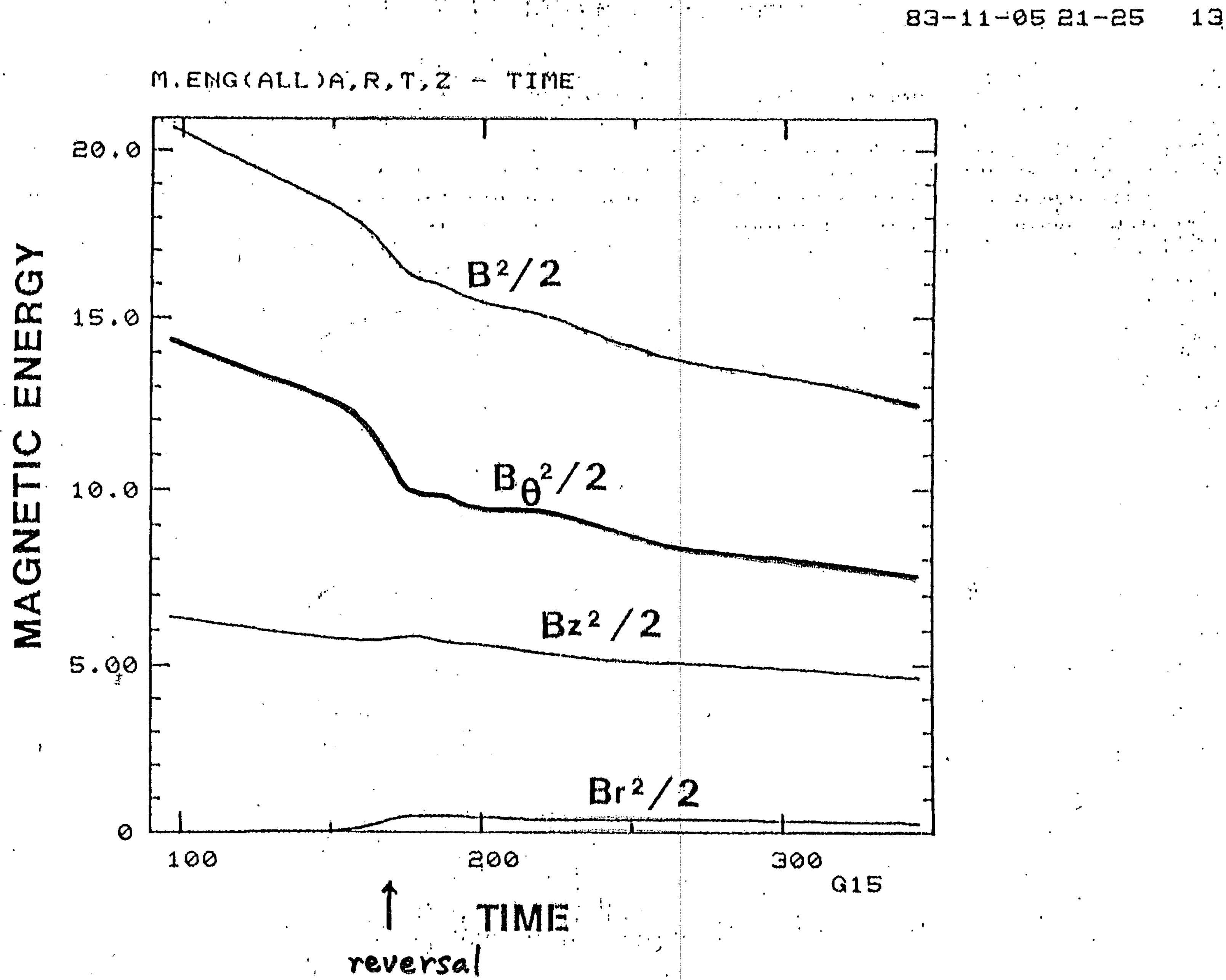
83-11-05 21-25 13
M.ENG(ALL)A,R,T,Z - TIME
MAGNETIC ENERGY
20.0
15.0
10.0
5.00
0
100
200
300
G15
TIME
reversal
$B^2/2$
$B_\theta^2/2$
$Bz^2/2$
$Br^2/2$

Simulation of Self-Reversal in RFP

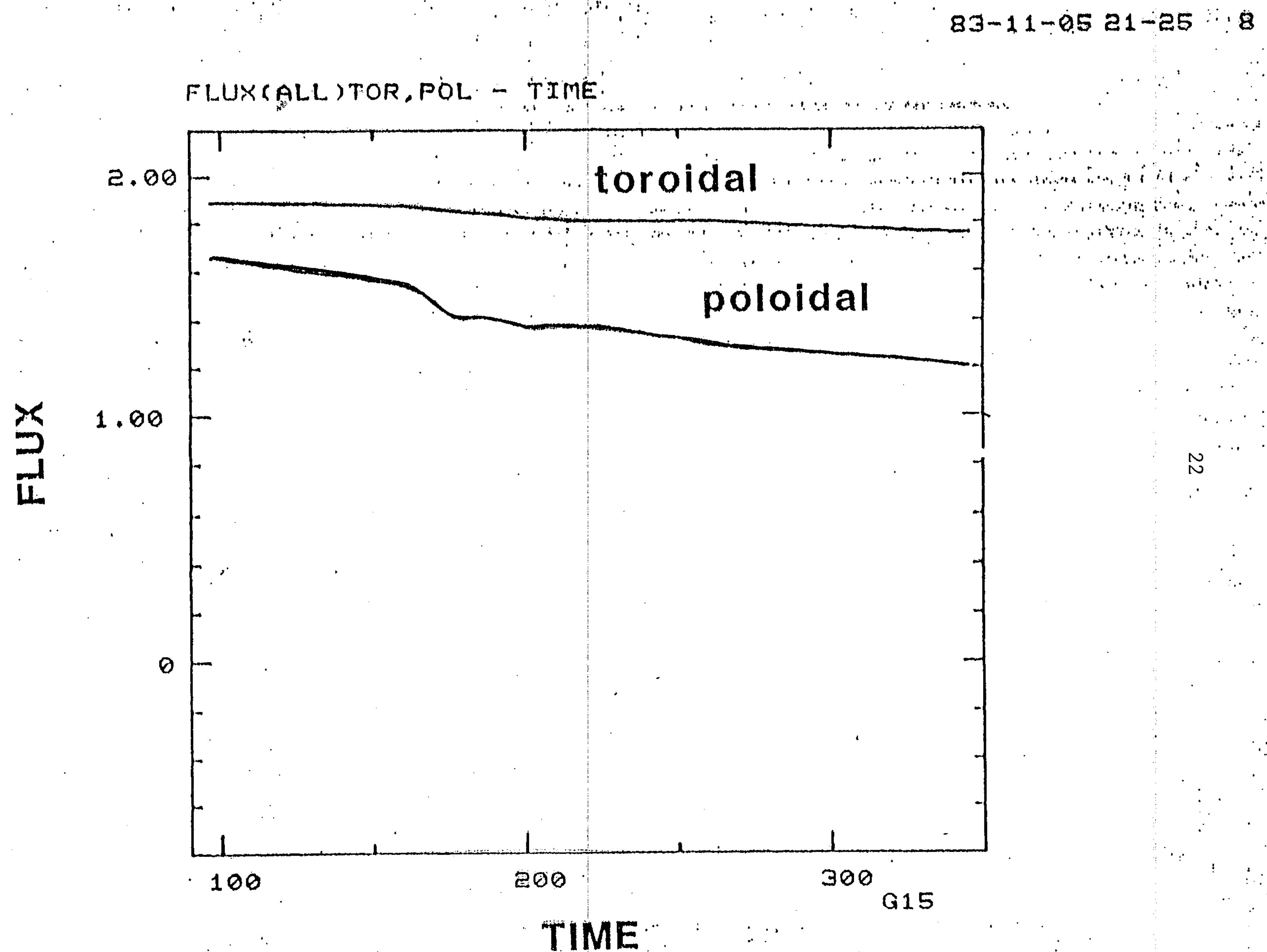

Simulation of Spheromak Merging

different

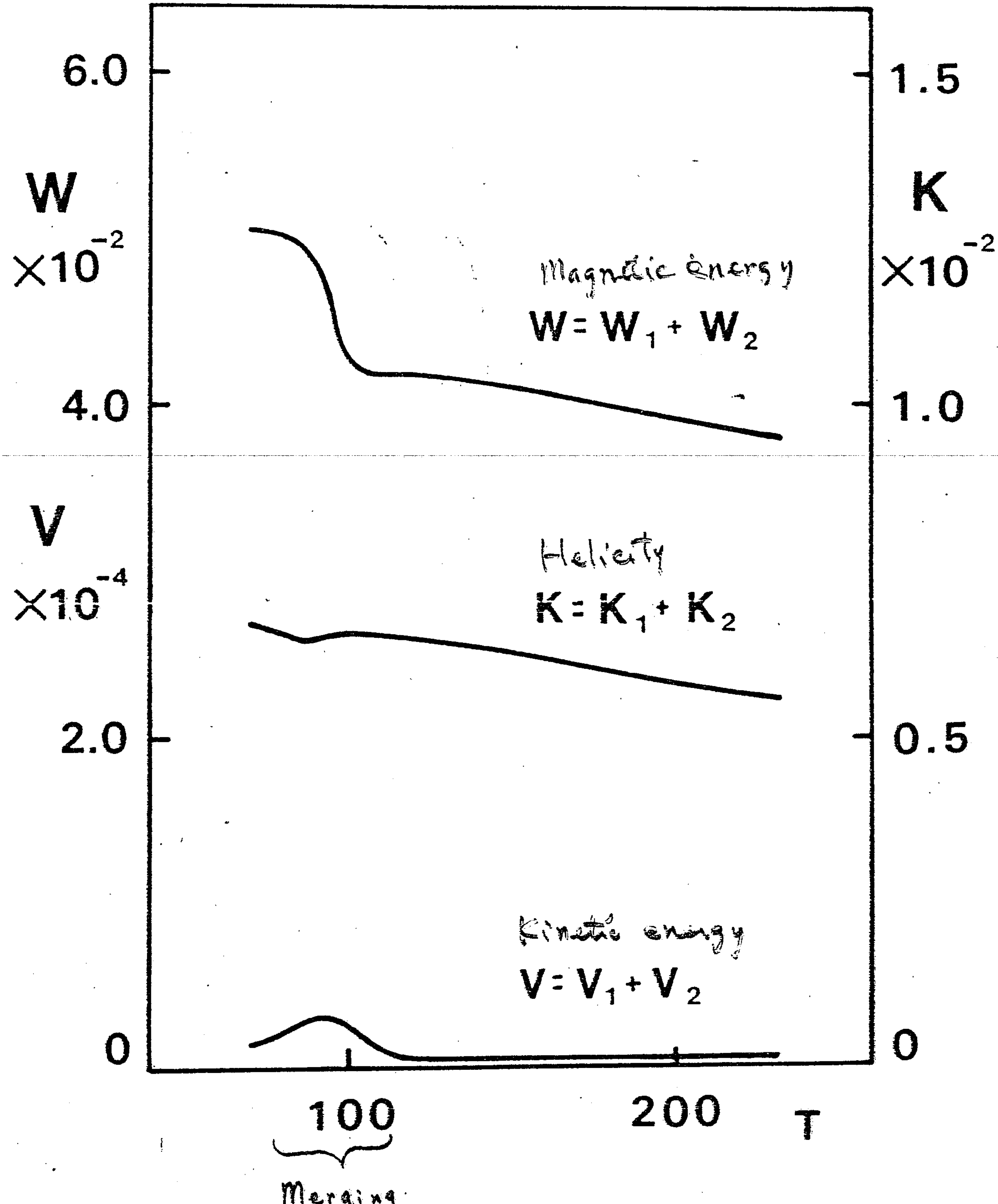

scenario of setting-up process in the RFP

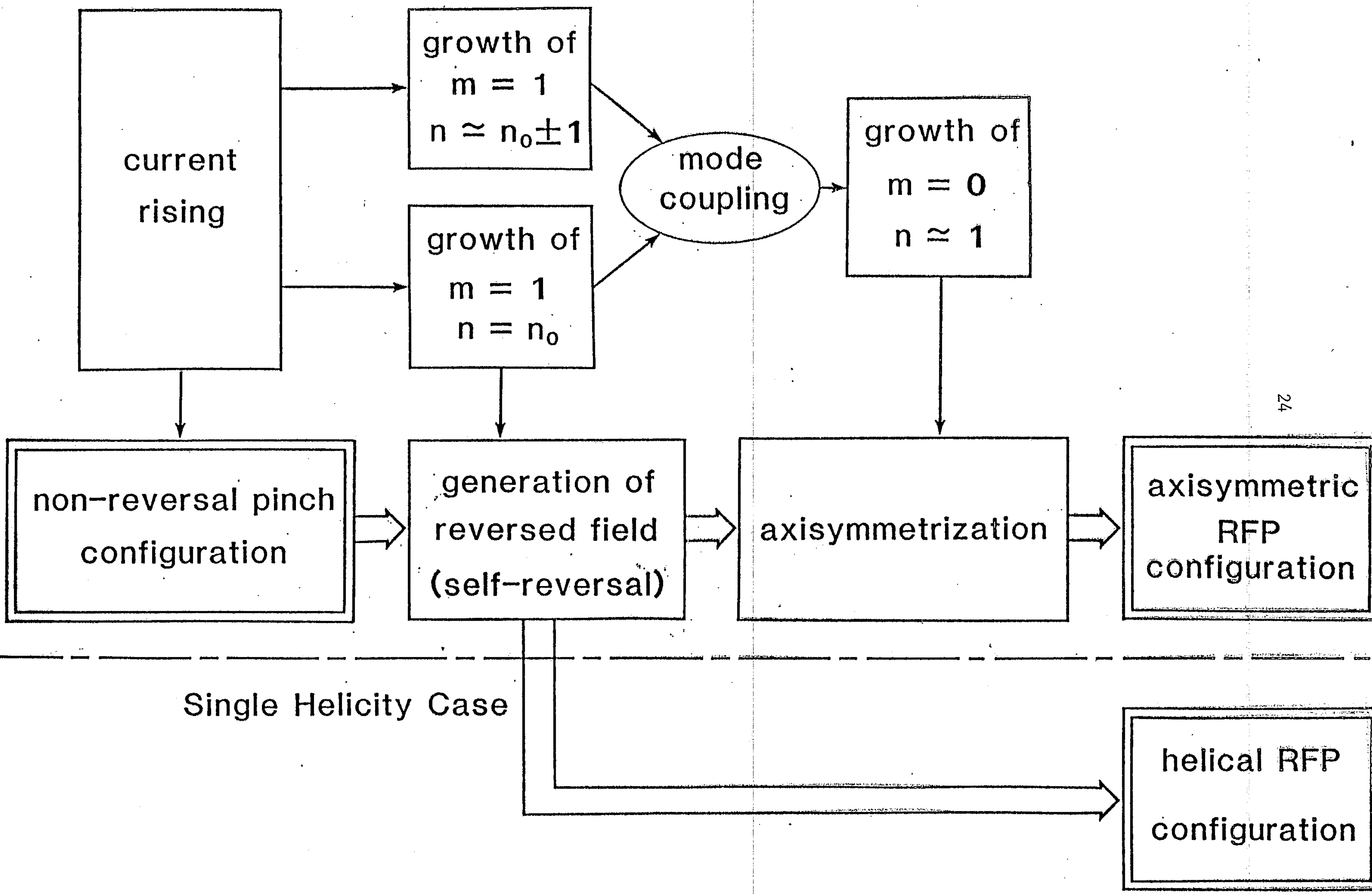

MAGNETOHYDRODYNAMIC SELF-ORGANIZATION IN THREE DIMENSIONS

RITOKU HORIUCHI AND TETSUYA SATO

INSTITUTE FOR FUSION THEORY,
HIROSHIMA UNIVERSITY
HIRORHIMA 730, JAPAN

Initial Field Pattern in 3D

NO.H08

T = 0

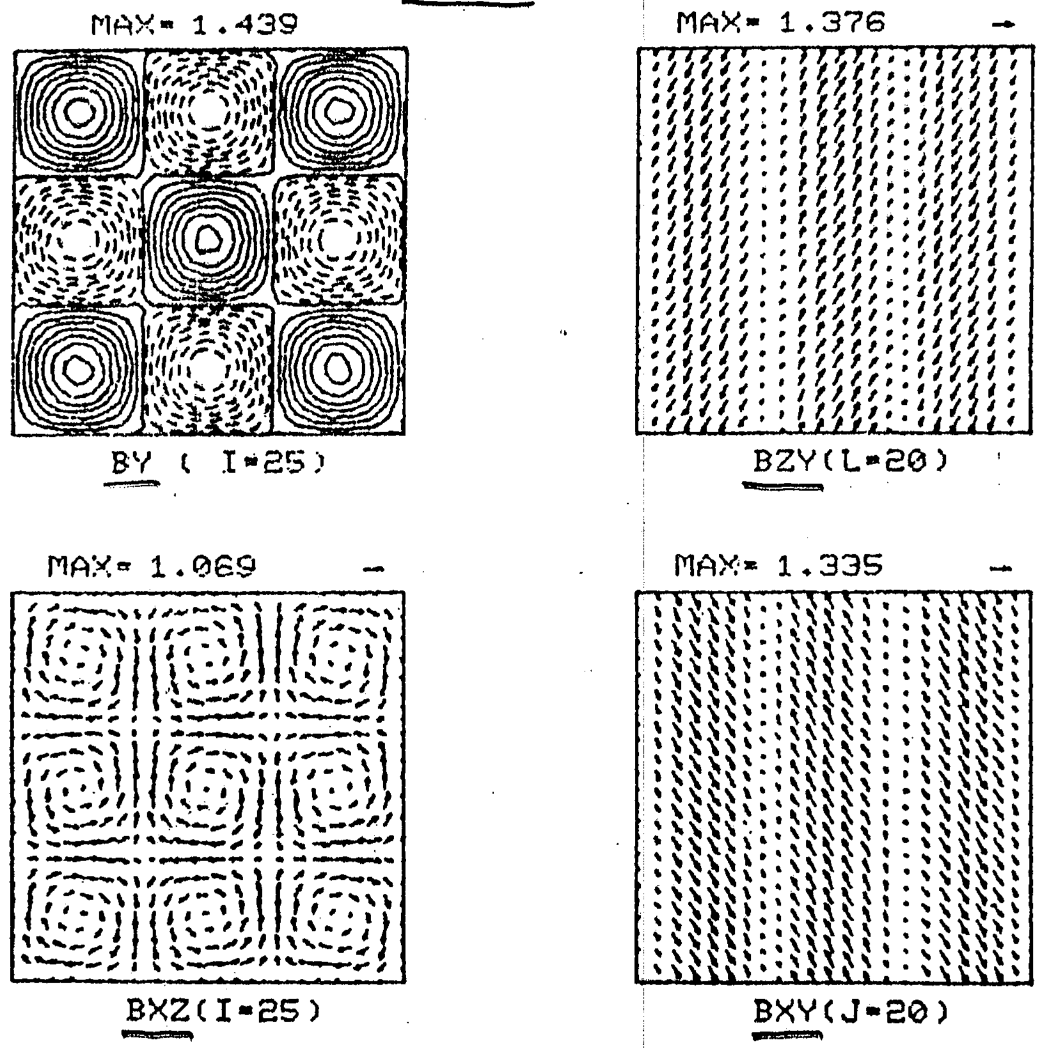

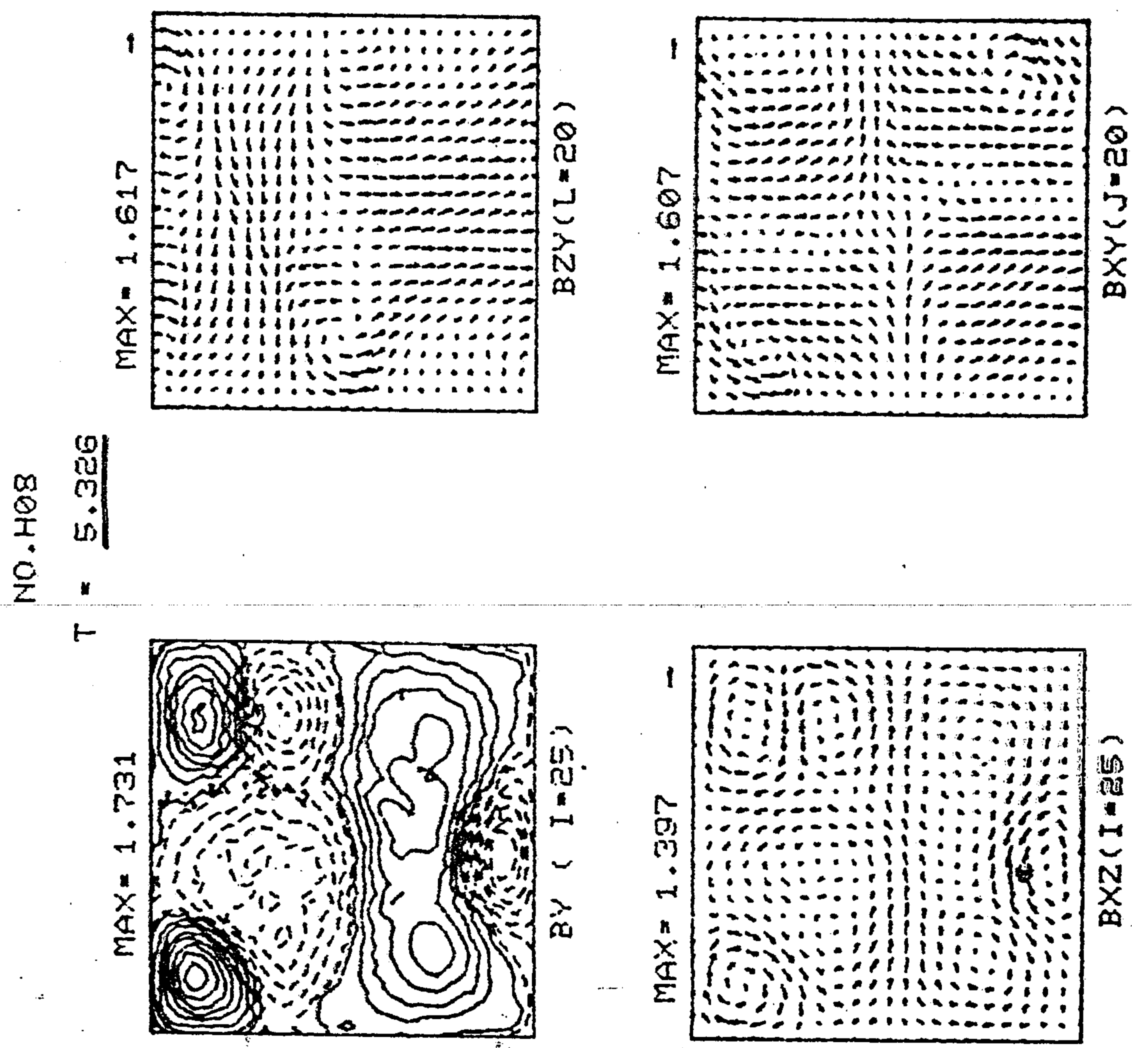
NO.H08
T = 5.326
MAX= 1.617
BZY(L=20)
MAX= 1.607
BXY(J=20)
MAX= 1.731
BY (I=25)
MAX= 1.397
BXZ(I=25)

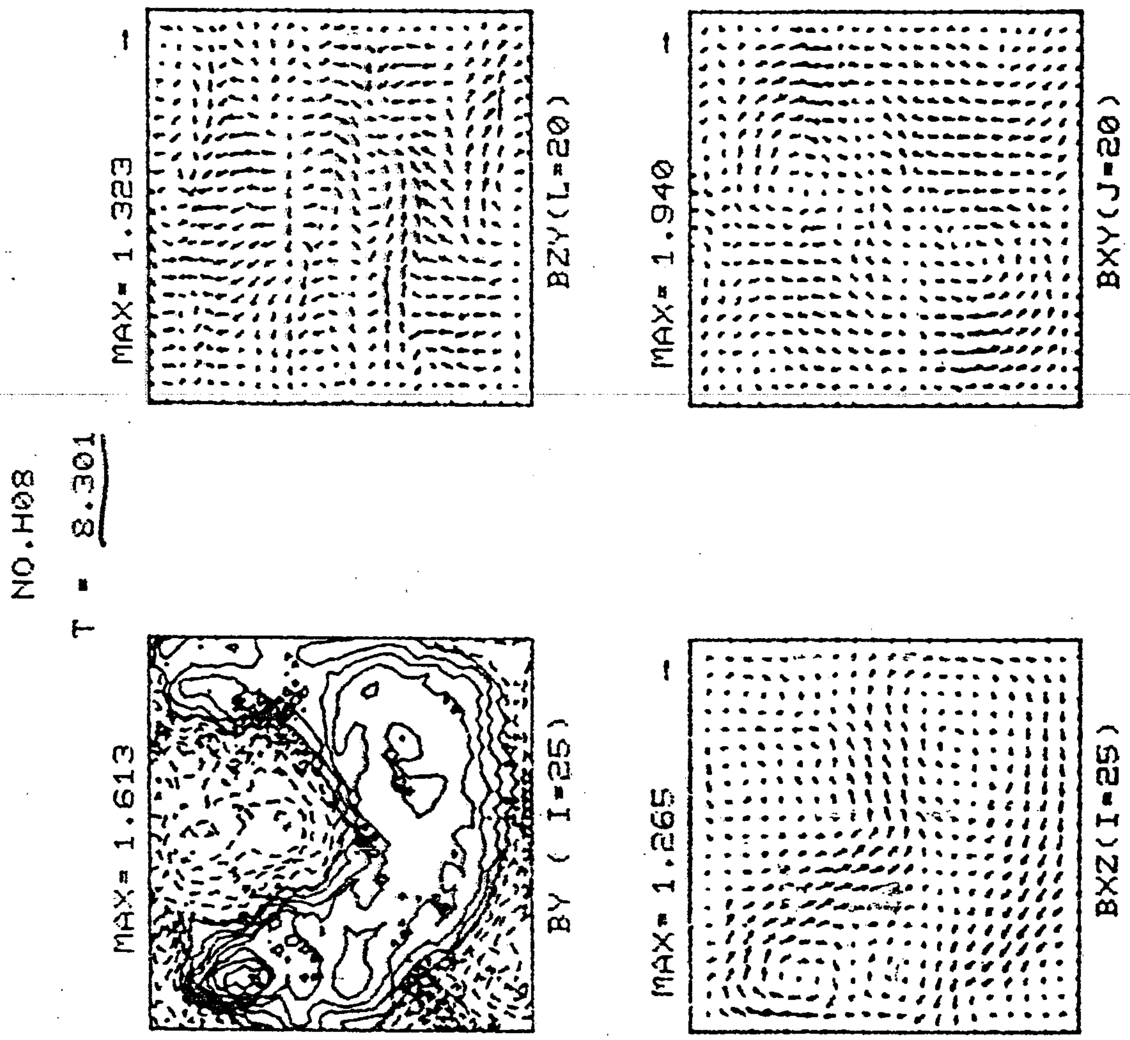
NO.H08
T = 8.301
MAX= 1.323
BZY(L=20)
MAX= 1.940
BXY(J=20)
MAX= 1.613
BY (I=25)
MAX= 1.265
BXZ(I=25)

SPECTRUM OF MAGNETIC FIELD (1)

NO.H08

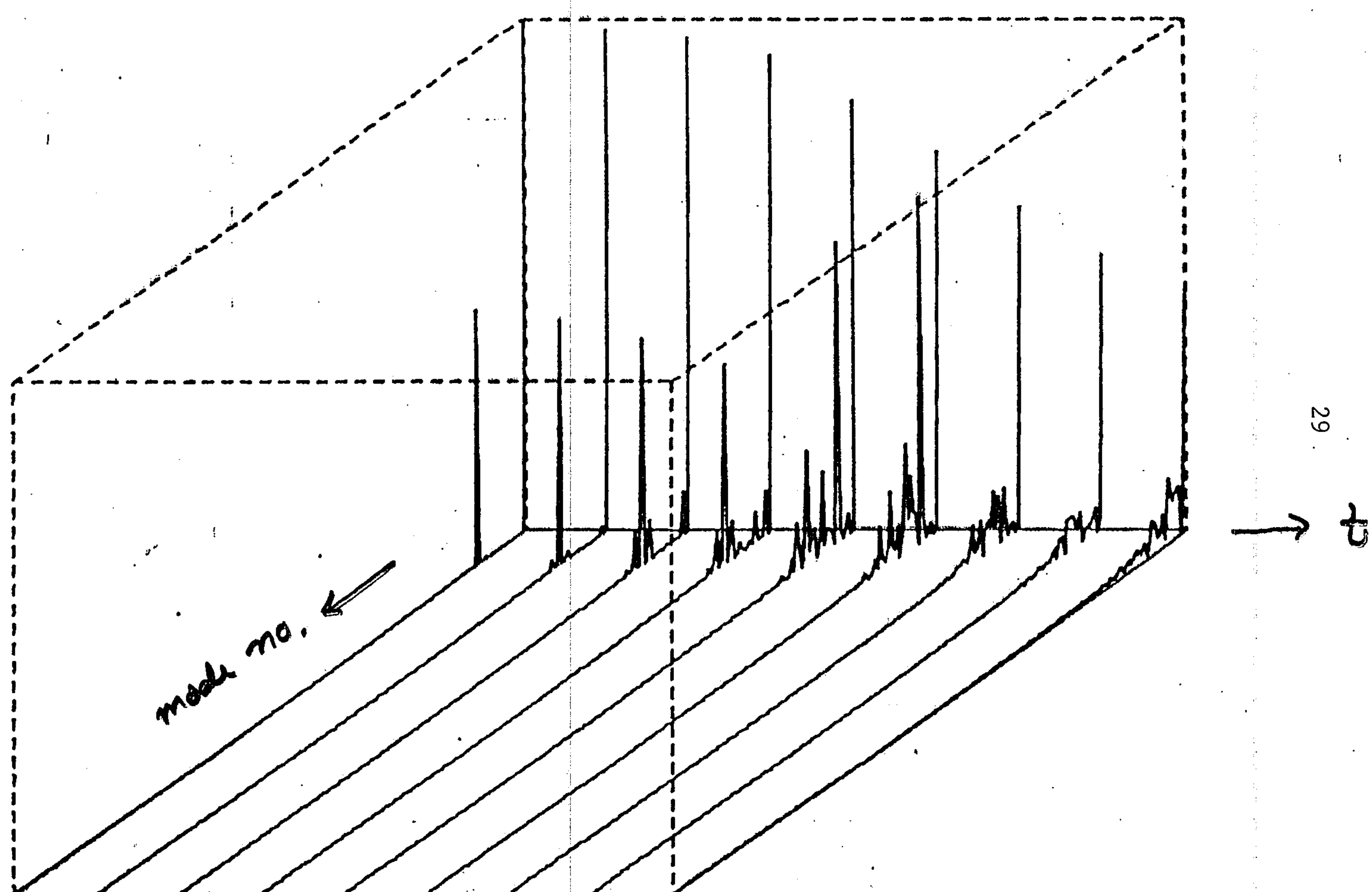

FLUX REGENERATION IN ZT-40M AT HIGH θ AND THE MHD MODEL

R. NEBEL

LOS ALAMOS NATIONAL LABORATORY

Flux Regeneration in ZT-40M at High θ and the MHD Model

R. Nebel

K. Werley

Conclusions

1. Any toroidally asymmetric flux regeneration mechanism must arise from the $m = 0$ component of the dynamics.

   - torus → periodic cylinder
   - quadratically non linear Ohm's law

2. The flux regeneration mechanism in ZT-40M at high Θ is toroidally asymmetric.

3. $m = 0$ single mode MHD instabilities always oppose flux regeneration. (anti-dynamo)

Conclusions cont.

4. $m=0$ magnetic perturbations driven nonlinearly by multi-helicity $m=1$ tearing modes can qualitatively produce toroidally asymmetric flux regeneration, but it usually is smaller than the symmetric component.
   - Algebraically: lowest order interactions
   - Numerically: 3 D simulations.

5. Hall effects may couple the spectrum in such a way as to enhance the asymmetric component of the toroidal flux regeneration mechanism.
   - Speculative, only phasings have been computed. signs and magnitude are unknown.
   - Island distortions and toroidal phasings of $m=1$ and $m=0$ peaks arise from these terms

Conceptual Picture

1. Multiple helicity $m=1$ modes driven unstable by diffusion.

2. Non linear beatings of the $m=1$ modes cause the $m=0, n=1$ mode's "O" point to become a flux source.

3. Magnetic pressure from the "O" point causes V_z to carry flux from the "O" point to the "X" point where it reconnects to form equal and opposite amounts of positive and negative flux.

4. Hall terms may enhance this process as well as distort the $m=0$ island.

Toroidal Behavior of Flux Regeneration

Assume (for convenience) a resistive MHD ohm's Law:

$$\vec{E} + \vec{V} \times \vec{B} = \eta \vec{J} \qquad (1)$$

Expand in Fourier series (periodic cylinder):

$$\vec{E}(r,\theta,z) = \sum_{m=0}^{\infty} \sum_{n=-\infty}^{\infty} \left[\vec{E}_s^{m,n}(r) \sin(m\theta + k_n z) + \vec{E}_c^{m,n}(r) \cos(m\theta + k_n z) \right] \qquad (2)$$

$$\vec{V}(r,\theta,z) = \sum_{m_1=0}^{\infty} \sum_{n_1=-\infty}^{\infty} \left[\vec{V}_s^{m_1,n_1}(r) \sin(m_1\theta + k_{n_1} z) + \vec{V}_c^{m_1,n_1}(r) \cos(m_1\theta + k_{n_1} z) \right] \qquad (3)$$

$$\vec{B}(r,\theta,z) = \sum_{m_2=0}^{\infty} \sum_{n_2=-\infty}^{\infty} \left[\vec{B}_s^{m_2,n_2}(r) \sin(m_2\theta + k_{n_2} z) + \vec{B}_c^{m_2,n_2}(r) \cos(m_2\theta + k_{n_2} z) \right] \qquad (4)$$

$$\vec{J}(r,\theta,z) = \sum_{m_3=0}^{\infty} \sum_{n_3=-\infty}^{\infty} \left[\vec{J}_s^{m_3,n_3}(r) \sin(m_3\theta + k_{n_3} z) + \vec{J}_c^{m_3,n_3}(r) \cos(m_3\theta + k_{n_3} z) \right] \qquad (5)$$

where $K_n \equiv n/R$ and R is major radius.

$$\left\langle \dot{\Phi}_z(r_v) \right\rangle \equiv \frac{-r_v}{2\pi R} \int_0^{2\pi R} \int_0^{2\pi} E_\theta(r_v, \theta, z)\, d\theta\, dz$$

$$\equiv \left\langle \dot{\Phi}_z(r_v) \right\rangle^{\eta \vec{J}} + \left\langle \dot{\Phi}_z(r_v) \right\rangle^{\vec{v} \times \vec{B}} \qquad (6)$$

where
$$\left\langle \dot{\Phi}_z(r_v) \right\rangle^{\eta \vec{J}} \equiv -2\pi r_v\, \eta\, J_\theta^{0,0}(r_v) \qquad (7)$$

$$\left\langle \dot{\Phi}_z(r_v) \right\rangle^{\vec{v} \times \vec{B}} \equiv \frac{r_v \int_0^{2\pi R} \int_0^{2\pi} (\vec{v} \times B)_\theta\, d\theta\, dz}{2\pi R} \qquad (8)$$

Cowling's theorum:

$$\left\langle \dot{\Phi}_z(r_v) \right\rangle^{\vec{v} \times \vec{B}} = 0 \Rightarrow \left\langle \dot{\Phi}_z(r_v) \right\rangle < 0 \qquad (9)$$

Necessary condition for flux regeneration:

$$\boxed{\left\langle \dot{\Phi}_z(r_v) \right\rangle^{\vec{v} \times \vec{B}} \neq 0} \qquad (10)$$

Note that numerator of eq. (8) is the norm for Fourier series. Consequently only terms that contribute have:

$$\boxed{\begin{matrix} m_1 = m_2 \\ n_1 = n_2 \end{matrix}} \qquad (11)$$

Consider toroidal dependence of $\dot{\Phi}^{\vec{V}\times\vec{B}}(r_v,z)$ keeping only terms which contribute to $\langle\dot{\Phi}_z(r_v)\rangle^{\vec{V}\times\vec{B}}$ (i.e. $m_1 = m_2$, $n_1 = n_2$)

$$\dot{\Phi}_z(r_v, z) = r_v \int_0^{2\pi} (\vec{V}\times\vec{B})_\theta \, d\theta \tag{12}$$

$$= \pi r_v \sum_{m=1}^{\infty} \sum_{n=-\infty}^{\infty} \Big[V_{z,s}^{m,n}(r_v)\, B_{r,s}^{m,n}(r_v) + V_{z,c}^{m,n}(r_v)\, B_{r,c}^{m,n}(r_v) - V_{r,s}^{m,n}(r_v)\, B_{z,s}^{m,n}(r_v) - V_{r,c}^{m,n}(r_v)\, B_{z,c}^{m,n}(r_v) \Big]$$

$$+ 2\pi r_v \sum_{n=-\infty}^{\infty} \Big[\big(V_{z,s}^{0,n}(r_v)\, B_{r,s}^{0,n}(r_v) - V_{r,s}^{0,n}(r_v)\, B_{z,s}^{0,n}(r_v) \big) \sin^2 K_n z + \big(V_{z,c}^{0,n}(r_v)\, B_{r,s}^{0,n}(r_v) +$$

$$V_{z,s}^{0,n}(r_v)\, B_{r,c}^{0,n}(r_v) - V_{r,c}^{0,n}(r_v)\, B_{z,s}^{0,n}(r_v) - V_{r,s}^{0,n}(r_v)\, B_{z,c}^{0,n}(r_v) \big) \sin K_n z \cos K_n z +$$

$$\big(V_{z,c}^{0,n}(r_v)\, B_{r,c}^{0,n}(r_v) - V_{r,c}^{0,n}(r_v)\, B_{z,c}^{0,n}(r_v) \big) \cos^2 K_n z \Big]$$

- Only terms with z dependence are $m=0$ terms

- Procedure works for any quadratically nonlinear term in Ohm's law, not just $\vec{V}\times\vec{B}$.

Figure 1

ZT-40M DIAGNOSTIC PORTS USAGE

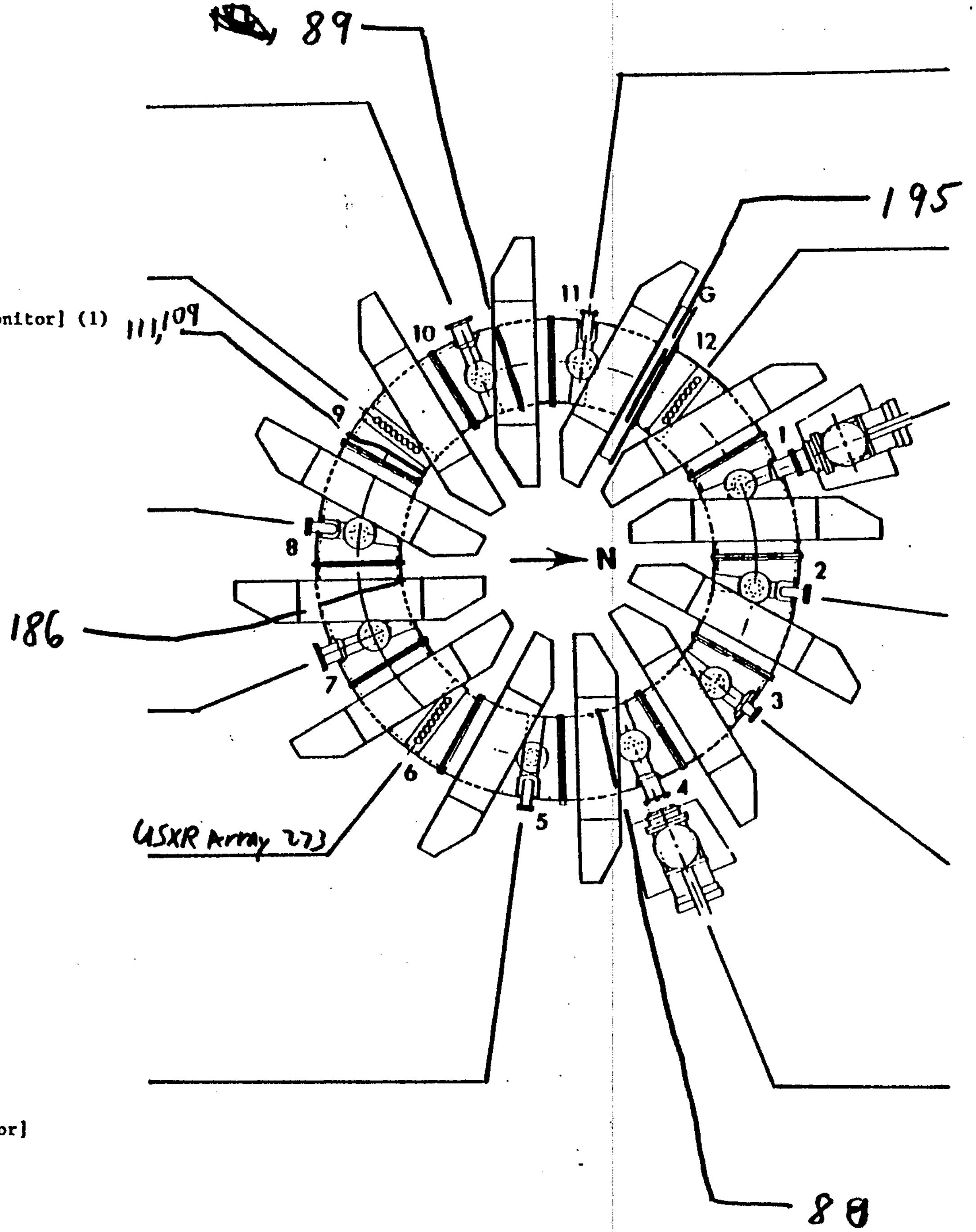

<u>Section 10</u>

TOP: USXR

SIDE: Grazing Incidence

BOTTOM: PI Loop + PGF

<u>Section 9</u>

TOP: FIR Interf. (1) + SB (1)

BOTTOM: FIR Interf. (1) + [D_α Monitor] (1)

<u>Section 8</u>

TOP: SB Diodes (2)

SIDE: B.O.
Unused
PGF (GA)

BOTTOM: B.O.

<u>Section 7</u>

TOP: 2-color Interf. + PGF

SIDE: Flash Lamp

BOTTOM: 2-color Interferometer

<u>Section 6</u>

TOP: Multichord Spectrom. (6)

BOTTOM: SBD (8)

<u>Section 5</u>

TOP: Window

SIDE: Spectrometer (Mc Pherson)
Window
Window + PGF (GA)

BOTTOM: Spectr. cal., [D_α Monitor]

<u>Section 11</u>

TOP: IR Interferometer

SIDE: [D_α Monitor]
UV Spectrometer
PGF (GA)

BOTTOM: IR Interferometer

<u>Section 12</u>

TOP: IR Interferometer (8 ports)

BOTTOM: IR Interferometer (8 ports)

<u>Section 1</u>

TOP: PGF + PI Electrode

SIDE: Pump + [D_α Monitor]

BOTTOM: Fast IG + Flash Lamp

<u>Section 2</u>

TOP: SP Thomson scattering

SIDE: SP Thomson scattering
SP Thomson scattering
Window + PGF (GA)

BOTTOM: SP Thomson scattering

<u>Section 3</u>

TOP: Bolometer

SIDE: J.H. VUV Spectrometer

BOTTOM: B.O.

<u>Section 4</u>

TOP: PGF + Spectrometer (Hilger)
+ Gas Supply

SIDE: Pump

BOTTOM: Si(Li) Detector

<u>Status</u>: March 2, 1984

[ ] means temporary diagnostic

Figure 4

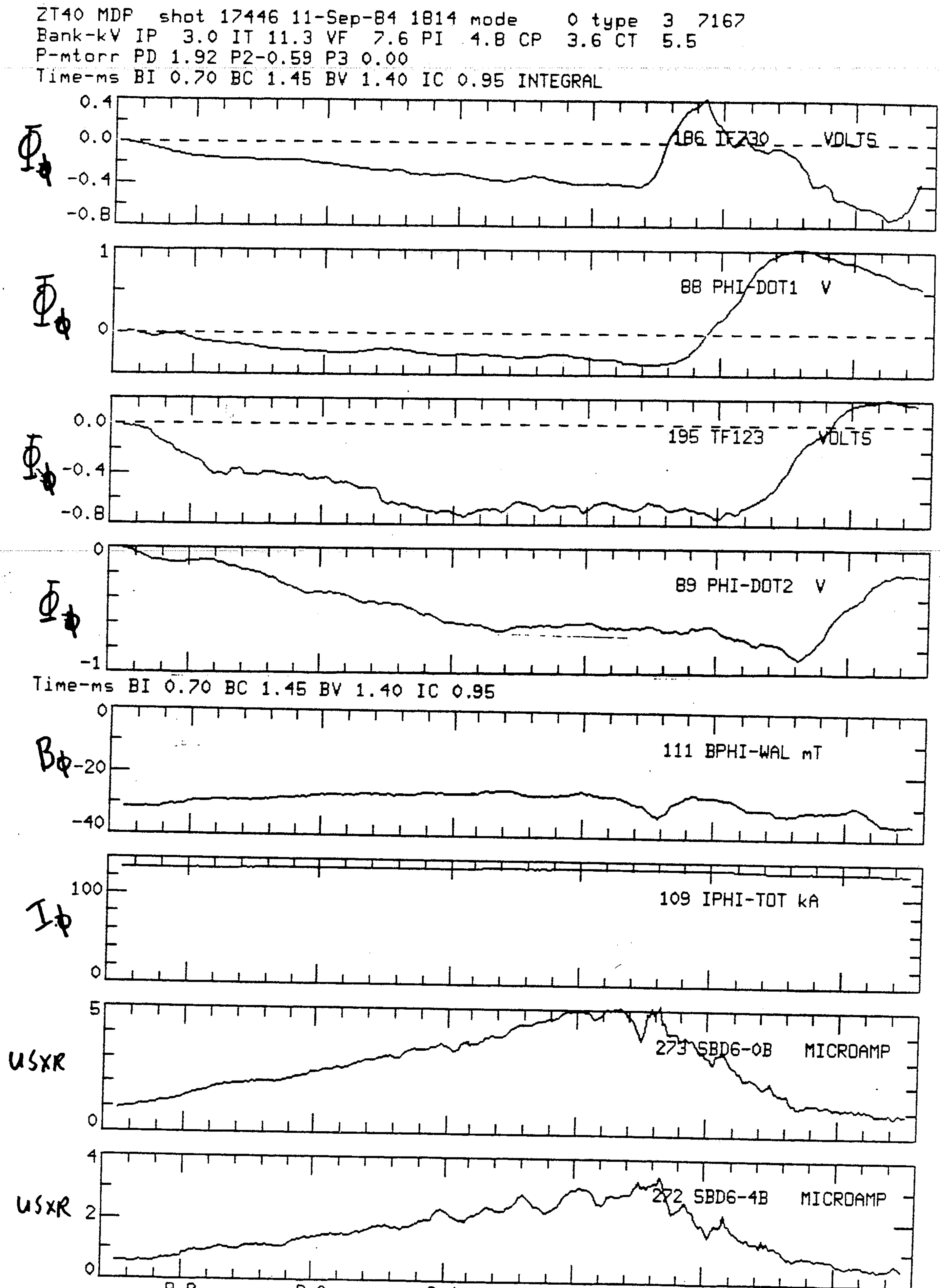
ZT40 MDP shot 17446 11-Sep-84 1814 mode 0 type 3 7167
Bank-kV IP 3.0 IT 11.3 VF 7.6 PI 4.8 CP 3.6 CT 5.5
P-mtorr PD 1.92 P2-0.59 P3 0.00
Time-ms BI 0.70 BC 1.45 BV 1.40 IC 0.95 INTEGRAL
0.4
0.0
-0.4
-0.8
186 TF230 VOLTS
1
0
88 PHI-DOT1 V
0.0
-0.4
-0.8
195 TF123 VOLTS
0
-1
89 PHI-DOT2 V
Time-ms BI 0.70 BC 1.45 BV 1.40 IC 0.95
0
-20
-40
111 BPHI-WAL mT
100
0
109 IPHI-TOT kA
5
0
273 SBD6-0B MICROAMP
4
2
0
272 SBD6-4B MICROAMP
USXR
USXR

Figure 5
F-Θ diagram

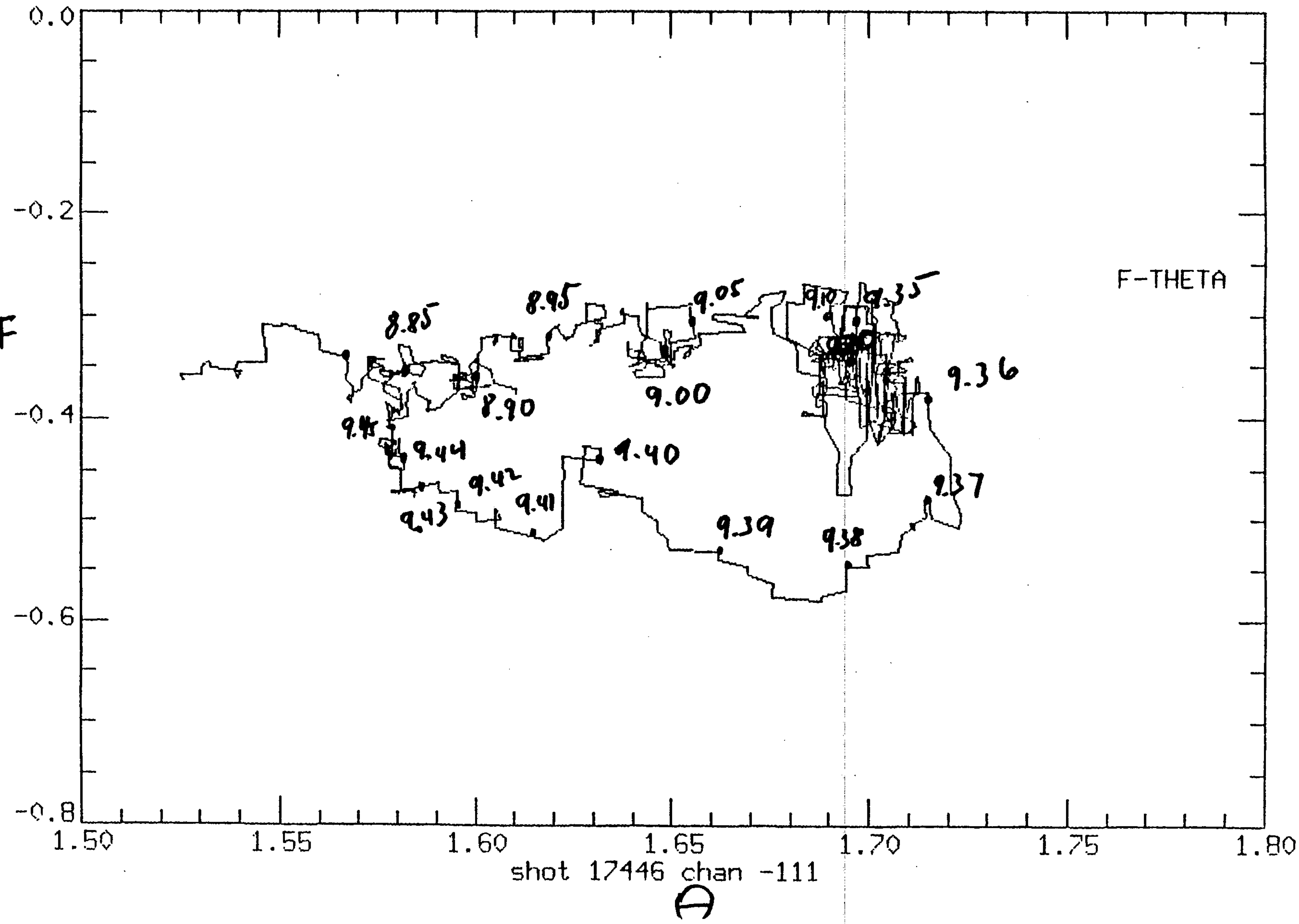

Experimental Results

- Relaxation occurs when traveling magnetic disturbance reaches toroidal observation point.

- Positive flux (inside reversal surface) increases ~20% during passage of disturbance.

Conclusion :

- Traveling disturbance is the source of the flux regeneration, and it is toroidally asymmetric.

$m=0$ Instabilities (Resistive MHD)

Standard $m=0, n=1$ reconnection

$$B_r^{0,1}(r,z) = B_r^{0,1}(r) \sin z/R \tag{13}$$

$$V_r^{0,1}(r,z) = V_r^{0,1}(r) \cos z/R \tag{14}$$

$$V_z^{0,1}(r,z) = V_z^{0,1}(r) \sin z/R \tag{15}$$

$$B_z^{0,1}(r,z) = B_z^{0,1}(r) \cos z/R \tag{16}$$

$$E_\theta^{0,1}(r,z) = E_\theta^{0,1}(r) \cos z/R \tag{17}$$

$$J_\theta^{0,1}(r,z) = J_\theta^{0,1}(r) \cos z/R \tag{18}$$

and
$$V_r^{0,1}(r_r) = 0, \quad V_z^{0,1}(r_r) < 0, \quad B_r^{0,1}(r_r) > 0, \quad B_z^{0,1}(r_r) = 0, \quad E_\theta^{0,1}(r_r) > 0, \quad J_\theta^{0,1}(r_r) > 0 \tag{19}$$

Figure 6

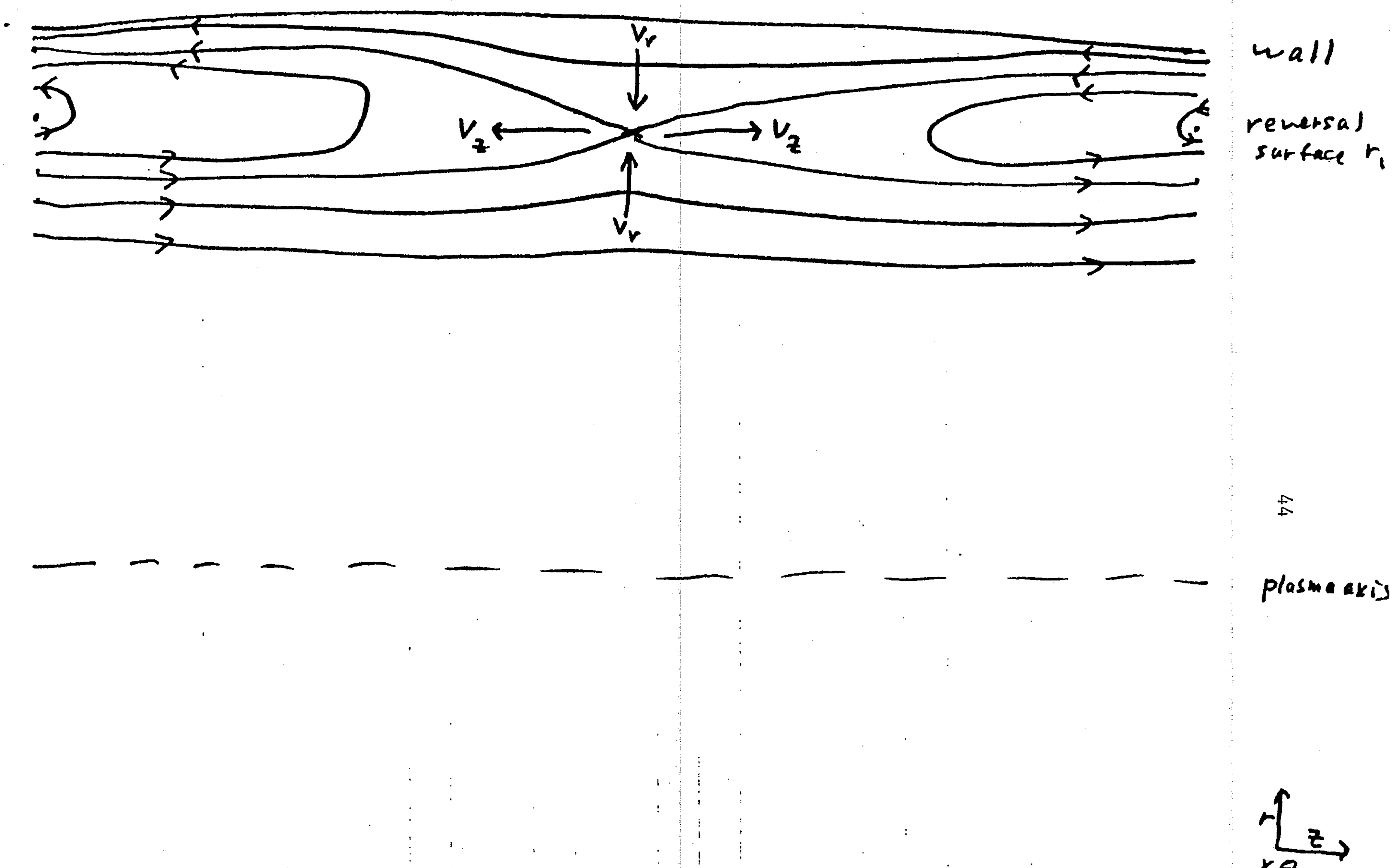
wall
reversal surface r_1
V_r
V_z
V_z
V_r
plasma axis
r
z
$\times\theta$

Now

$$\langle \dot{\Phi}_z(r_v) \rangle = -2\pi r_v \left[\eta J_\theta^{0,0}(r_v) - \tfrac{1}{2} V_z^{0,1}(r_v) B_r^{0,1}(r_v) \right]$$

$$< 0 \tag{20}$$

since $J_\theta^{0,0}(r_v) > 0$, $V_z^{0,1}(r_v) < 0$, $B_r^{0,1}(r_v) > 0$.

$\therefore$ $m = 0$ instabilities oppose flux regeneration.

"Kerstian" Interepretation

Flux reconnects through "X" point and then flows to the "O" point where it is annihilated (i.e. "O" point is a flux sink)

Consider flux enclosed by "O" point

$$\dot{\Phi}_z(r_v, 0) = -\int_0^{2\pi} E_\theta(r_v, 0)\, r_v\, d\theta \tag{21}$$

$$= -2\pi r_v \eta \left(J_\theta^{0,0}(r_v, 0) + J_\theta^{0,1}(r_v, 0) \right)$$

$$< 0$$

$\therefore$ Flux always decreases inside the "O" point for a single mode, hence "O" point is a flux sink.

Multihelicity Instabilities

- Can multihelicity $m=1$ tearing mode interactions turn $m=0$ "o" point from a flux sink into a flux source?

- Consider only lowest order interactions.

Principal modes: $m=1, n=-10$
$m=1, n=-11$

Lowest order nonlinearly driven modes
$m=0, n=1$
$m=2, n=-21$ ← ignore

$$V_r^{1,-11}(r,\theta,z) = V_r^{1,-11}(r)\left[\cos\left(\theta-\tfrac{11}{R}z\right)+\sin\left(\theta-\tfrac{11}{R}z\right)\right] \qquad (22)$$

$$V_z^{1,-11}(r,\theta,z) = V_z^{1,-11}(r)\left[\cos\left(\theta-\tfrac{11}{R}z\right)-\sin\left(\theta-\tfrac{11}{R}z\right)\right] \qquad (23)$$

$$B_r^{1,-11}(r,\theta,z) = B_r^{1,-11}(r)\left[\cos\left(\theta-\tfrac{11}{R}z\right)-\sin\left(\theta-\tfrac{11}{R}z\right)\right] \qquad (24)$$

$$B_z^{1,-11}(r,\theta,z) = B_z^{1,-11}(r)\left[\cos\left(\theta-\tfrac{11}{R}z\right)+\sin\left(\theta-\tfrac{11}{R}z\right)\right] \qquad (25)$$

$$V_r^{1,-10}(r,\theta,z) = V_r^{1,-10}(r)\left[\cos\left(\theta-\tfrac{10}{R}z\right)+\sin\left(\theta-\tfrac{10}{R}z\right)\right] \qquad (26)$$

$$V_z^{1,-10}(r,\theta,z) = V_z^{1,-10}(r)\left[\cos\left(\theta-\tfrac{10}{R}z\right)-\sin\left(\theta-\tfrac{10}{R}z\right)\right] \qquad (27)$$

$$B_r^{1,-10}(r,\theta,z) = B_r^{1,-10}(r)\left[\cos\left(\theta-\tfrac{10}{R}z\right)-\sin\left(\theta-\tfrac{10}{R}z\right)\right] \qquad (28)$$

$$B_z^{1,-10}(r,\theta,z) = B_z^{1,-10}(r)\left[\cos\left(\theta-\tfrac{10}{R}z\right)+\sin\left(\theta-\tfrac{10}{R}z\right)\right] \qquad (29)$$

Considering these modes along with the (0,1) mode described in eqs (13)-(18) one finds:

$$\langle \dot{\Phi}_z(r_v) \rangle = -2\pi r_v \Big[\eta J_\theta^{0,0}(r_v) - .5 V_z^{0,1}(r_v) B_r^{0,1}(r_v) + V_r^{1,-10}(r_v) B_z^{1,-10}(r_v)$$
$$+ V_r^{1,-11}(r_v) B_z^{1,-11}(r_v) - V_z^{1,-10}(r_v) B_r^{1,-10}(r_v) - V_z^{1,-11}(r_v) B_r^{1,-11}(r_v) \Big] \qquad (30)$$

and

$$\dot{\Phi}_z(r_v, z) = -2\pi r_v \Big[\eta \left(J_\theta^{0,0}(r_v) + J_\theta^{0,1}(r_v) \cos z/R \right) + V_r^{1,-10}(r_v) B_z^{1,-10}(r_v)$$
$$+ V_r^{1,-11}(r_v) B_z^{1,-11}(r_v) + V_r^{0,1}(r_v) B_z^{0,1}(r_v) \cos^2 z/R - V_z^{1,-10}(r_v) B_r^{1,-10}(r_v) - V_z^{1,-11}(r_v) B_r^{1,-11}(r_v)$$
$$- V_z^{0,1}(r_v) B_r^{0,1}(r_v) \sin^2 z/R + \Big(V_r^{1,-10}(r_v) B_z^{1,-11}(r_v) + V_r^{1,-11}(r_v) B_z^{1,-10}(r_v) - V_z^{1,-10}(r_v) B_r^{1,-11}(r_v)$$
$$- V_z^{1,-11}(r_v) B_r^{1,-10}(r_v) \Big) \cos z/R \Big] \qquad (31)$$

Assume that the toroidally symmetric components of eq. (31) are small (in rough agreement with ZT-40)

$$V_r^{1,-10}(r_v) B_z^{1,-10}(r_v) + V_r^{1,-11}(r_v) B_z^{1,-11}(r_v) - V_z^{1,-10}(r_v) B_r^{1,-10}(r_v) - V_z^{1,-11}(r_v) B_r^{1,-11}(r_v) = 0 \qquad (32)$$

Then $\dot{\Phi}_z(r_v, 0)$ (i.e. Φ_z at the "O" point) becomes:

$$\dot{\Phi}(r_v, 0) = -2\pi r_v \Big\{ \eta \left(J_\theta^{0,0}(r_v) + J_\theta^{0,1}(r_v) \right) + V_r^{1,-11}(r_v) B_z^{1,-10}(r_v) + V_r^{1,-10}(r_v) B_z^{1,-11}(r_v)$$
$$- V_z^{1,-10}(r_v) B_r^{1,-11}(r_v) - V_z^{1,-11}(r_v) B_r^{1,-10}(r_v) \Big\} \qquad (33)$$

In this case the "O" point becomes a flux source if:

$$\begin{bmatrix} V_r^{1,-11}(r_0)\, B_z^{1,-10}(r_0) + V_r^{1,-10}(r_0)\, B_z^{1,-11}(r_0) \\ -V_z^{1,-10}(r_0)\, B_r^{1,-11}(r_0) - V_z^{1,-11}(r_0)\, B_r^{1,-10}(r_0) \end{bmatrix} \leftarrow \eta\left(J_\theta^{0,0}(r_0) + J_\theta^{0,1}(r_0)\right) \tag{34}$$

$\boxed{\text{∴ Nonlinear beatings of } m=1 \text{ tearing modes may cause the } m=0, n=1 \text{ "O" point to become a flux source.}}$

Question: Do the nonlinear beatings of $m=1$ tearing modes provide the correct flows? Recall that $V_z^{0,1}(r_0) \sim \sin Z/R$ from eq. (15). Check to see that proper phasing is obtained from momentum equation's z component:

$$\rho \frac{\partial V_z(r,\theta,z)}{\partial t} + \rho \frac{V_\theta(r,\theta,z)}{r} \frac{\partial V_z(r,\theta,z)}{\partial \theta} + \rho V_r(r,\theta,z) \frac{\partial V_z(r,\theta,z)}{\partial r} \tag{35}$$

$$+ \rho V_z(r,\theta,z) \frac{\partial V_z(r,\theta,z)}{\partial z} = J_r(r,\theta,z) B_\theta(r,\theta,z) - J_\theta(r,\theta,z) B_r(r,\theta,z)$$

Equations (22)-(29) also have:

$$V_\theta^{1,-11}(r,\theta,z) = V_\theta^{1,-11}(r)\left[\cos\left(\theta - \frac{11z}{R}\right) - \sin\left(\theta - \frac{11z}{R}\right)\right] \quad (36)$$

$$V_\theta^{1,-10}(r,\theta,z) = V_\theta^{1,-10}(r)\left[\cos\left(\theta - \frac{10}{R}z\right) - \sin\left(\theta - \frac{10}{R}z\right)\right] \quad (37)$$

$$B_\theta^{1,-11}(r,\theta,z) = B_\theta^{1,-11}(r)\left[\cos\left(\theta - \frac{11}{R}z\right) + \sin\left(\theta - \frac{11}{R}z\right)\right] \quad (38)$$

$$B_\theta^{1,-10}(r,\theta,z) = B_\theta^{1,-10}(r)\left[\cos\left(\theta - \frac{10}{R}z\right) + \sin\left(\theta - {}^{10}/_{R}z\right)\right] \quad (39)$$

$$J_r^{1,-11}(r,\theta,z) = J_r^{1,-11}(r)\left[\cos\left(\theta - {}^{11}/_{R}z\right) - \sin\left(\theta - {}^{11}/_{R}z\right)\right] \quad (40)$$

$$J_r^{1,-10}(r,\theta,z) = J_r^{1,-10}(r)\left[\cos\left(\theta - \frac{10}{R}z\right) - \sin\left(\theta - {}^{11}/_{R}z\right)\right] \quad (41)$$

$$J_\theta^{1,-11}(r,\theta,z) = J_\theta^{1,-11}(r)\left[\cos\left(\theta - \frac{11z}{R}\right) + \sin\left(\theta - {}^{11}/_{R}z\right)\right] \quad (42)$$

$$J_\theta^{1,-10}(r,\theta,z) = J_\theta^{1,-10}(r)\left[\cos\left(\theta - \frac{10z}{R}\right) + \sin\left(\theta - \frac{10}{R}z\right)\right] \quad (43)$$

$$J_z^{1,-11}(r,\theta,z) = J_z^{1,-11}(r)\left[\cos\left(\theta - \frac{11}{R}z\right) + \sin\left(\theta - \frac{11}{R}z\right)\right] \quad (44)$$

$$J_z^{1,-10}(r,\theta,z) = J_z^{1,-10}(r)\left[\cos\left(\theta - \frac{10}{R}z\right) + \sin\left(\theta - \frac{10}{R}z\right)\right] \quad (45)$$

Substituting eqs. (22-29) and (36)-(45) into the

(0,1) component of equation (35) yields:

$$\rho \frac{\partial V_{z,c}^{0,1}(r)}{\partial t} \cos z/R + \rho \frac{\partial V_{z,s}^{0,1}(r)}{\partial t} \sin z/R = \Big[\rho \frac{V_\theta^{1,-11}(r)\, V_z^{1,-10}(r)}{r} - \rho \frac{V_\theta^{1,-10}(r)\, V_z^{1,-11}(r)}{r}$$

$$+ \rho V_r^{1,-11}(r) \frac{\partial V_z^{1,-10}(r)}{\partial r} - \rho V_r^{1,-10}(r) \frac{\partial V_z^{1,-11}(r)}{\partial r}$$

$$- \frac{\rho}{R} V_z^{1,-10}(r)\, V_z^{1,-11}(r) + J_r^{0,1}(r)\, B_\theta^{0,0}(r) \qquad (46)$$

$$- J_\theta^{0,0}(r)\, B_r^{0,1}(r) + J_r^{1,-11}(r)\, B_\theta^{1,-10}(r) - J_r^{1,-10}(r)\, B_\theta^{1,-11}(r)$$

$$+ J_\theta^{1,-11}(r)\, B_r^{1,-10}(r) - J_\theta^{1,-10}(r)\, B_r^{1,-11}(r) \Big] \sin z/R .$$

Note that all of the nonlinear convolutions beat into the $\sin z/R$ velocity component, consistent with the reconnection picture. A net flux regeneration will occur when:

$$V_z^{0,1}(r_0)\; B_r^{0,1}(r_0) > 2\, \eta J_\theta^{0,0}(r_0) \qquad (47)$$

Question: Does this scenario work out with the correct signs and magnitudes numerically?

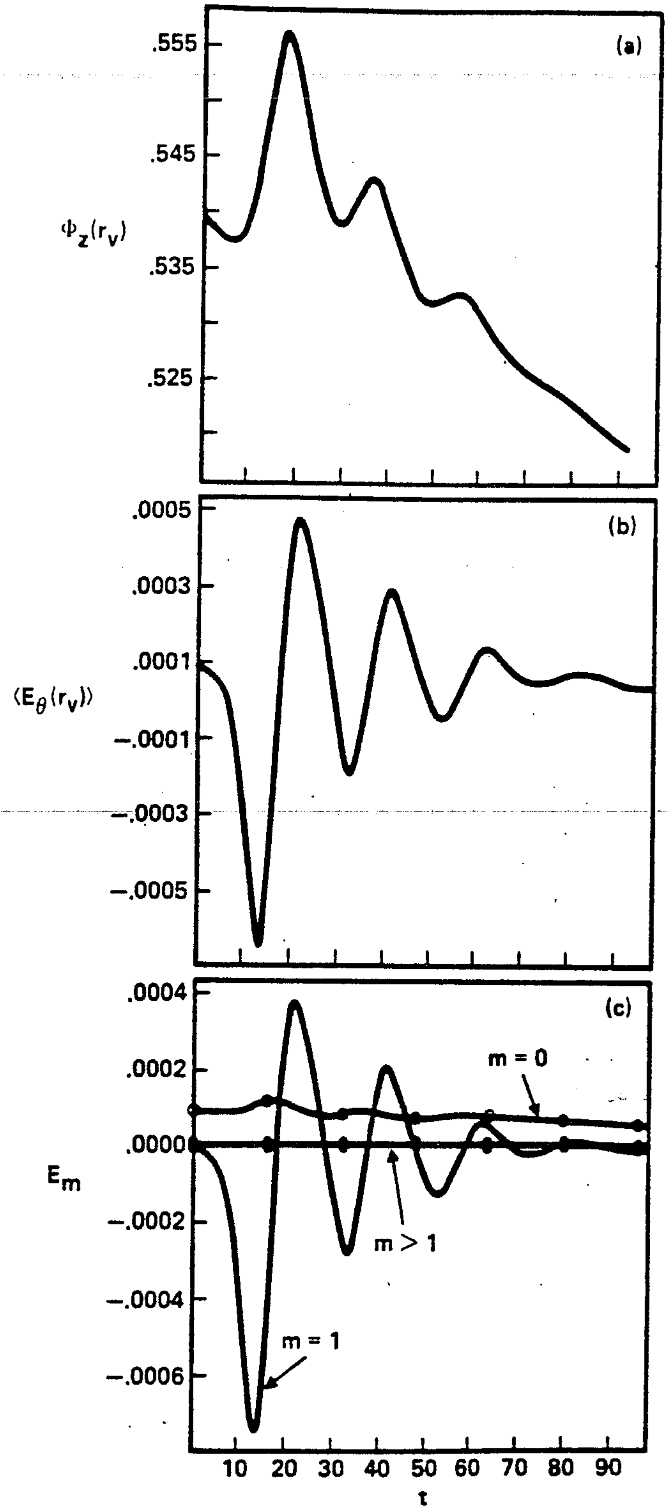

Fig. 19. (a) axial magnetic flux contained within the field reversal surface r_v; (b) m = 0, n = 0 component of the poloidal electric field at the field reversal surface; and (c) poloidal mode contributions to the mean poloidal electric field at the field reversal surface, as functions of time for the three-dimensional high-θ case.

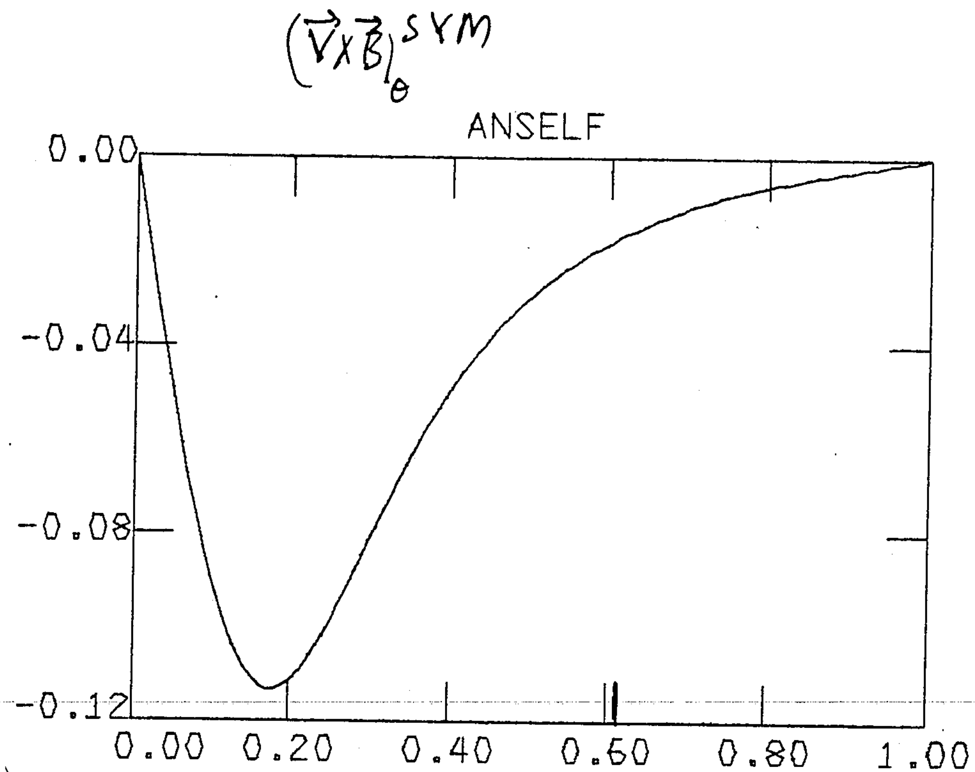

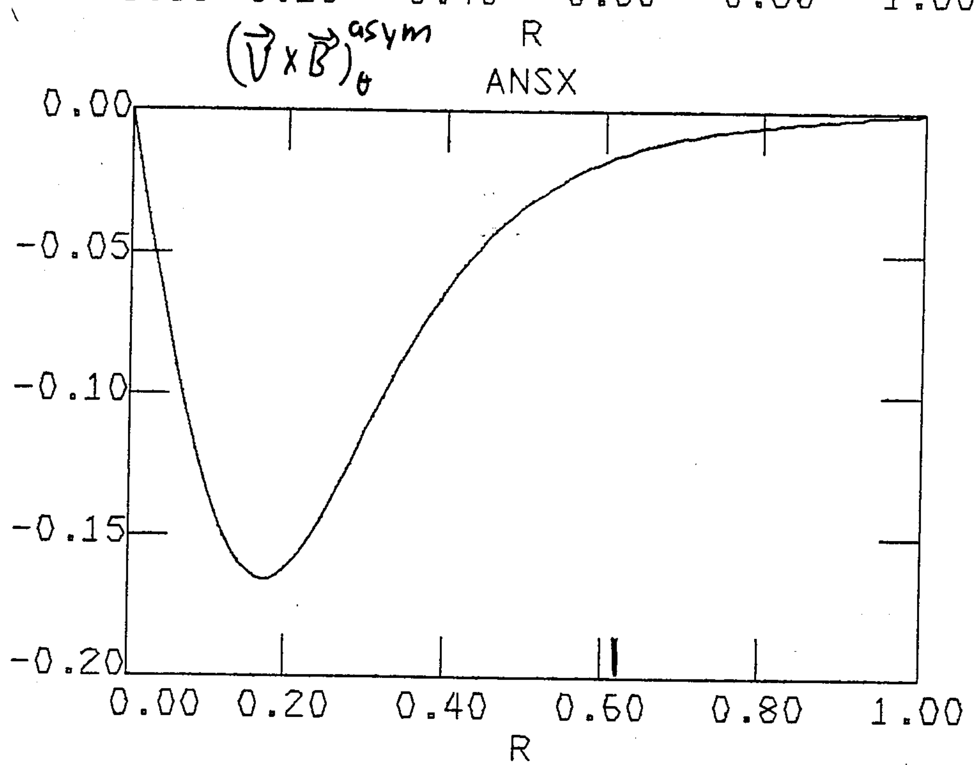

12:38:53
11/28/84

Result: $\vec{V} \times \vec{B} \gg \vec{V} \cdot \vec{B}$ for instabitres implies that nonlinear beating induced electric fields are always smaller than the self-beating induced electric fields. Hence, symmetric regeneration > asymmetric regeneration.

MHD Conclusions:

1. $m=0$ instabilities do not produce flux regeneration.

2. $m=1$ nonlinear couplings can produce asymmetric flux regeneration but it is usually smaller than the symmetric component.

3. MHD may lead to an asymmetric dynamo if:
   a. There are several $m=1$ modes of comparable magnitude present
   b. They are phase locked to beat into the same $m=0, n=1$ mode.

4. An essential part of this picture is the $m=0, n=1$ "O" point becoming a toroidal flux source.

Hall Effect

Ohm's law now becomes:

$$\vec{E} + \vec{V}\times\vec{B} + \frac{\vec{J}\times\vec{B}}{n} = \eta\vec{J} \qquad (48)$$

Combining eqs (48), (6), (13), (16), (24), (25), (28), (29), (40), (41), (44) and (45) one finds (assuming $n = n^{0,0}(r)$):

$$\langle \dot{\Phi}_z^{Hall}(r_v) \rangle \equiv \frac{-r_v}{2\pi R} \int_0^{2\pi R}\int_0^{2\pi} \frac{(\vec{J}\times\vec{B})_\theta}{n}\, d\theta\, dz$$

$$= \frac{-r_v}{2\pi R n} \int_0^{2\pi R}\int_0^{2\pi} \Big\{ J_z^{1,-11}(r_v)\, B_r^{1,-11}(r_v) \left[\cos^2(\theta - \tfrac{11z}{R}) - \sin^2(\theta - \tfrac{11z}{R})\right]$$

$$+ J_z^{1,-10}(r_v)\, B_r^{1,-10}(r_v) \left[\cos^2(\theta - \tfrac{10}{R}z) - \sin^2(\theta - \tfrac{10}{R}z)\right] + J_z^{0,1}(r_v)\, B_r^{0,1}(r_v) \qquad (49)$$

$$\cdot \sin\tfrac{z}{R} \cos\tfrac{z}{R} - J_r^{1,-11}(r_v)\, B_z^{1,-11}(r_v) \left[\cos^2(\theta - \tfrac{11z}{R}) - \sin^2(\theta - \tfrac{11z}{R})\right]$$

$$- J_r^{1,-10}(r_v)\, B_z^{1,-10}(r_v) \left[\cos^2(\theta - \tfrac{10}{R}z) - \sin^2(\theta - \tfrac{10}{R}z)\right] - J_r^{0,1}(r_v)\, B_z^{0,1}(r_v) \sin\tfrac{z}{R}\cos\tfrac{z}{R} \Big\}$$

$$= 0$$

∴ Hall effect produces <u>no</u> <u>net</u> <u>flux</u> <u>regeneration</u> but it does couple the spectrum.

We now have

$$
\begin{aligned}
\dot{\Phi}_z(r_v, z) = -2\pi r_v \Big\{ & \eta \left[J_\theta^{0,0}(r_v) + J_{\theta,c}^{0,1}(r_v) \cos z/R + J_{\theta,s}^{0,1}(r_v) \sin z/R \right] \\
& + V_r^{1,-10}(r_v)\, B_z^{1,-10}(r_v) + V_r^{1,-11}(r_v)\, B_z^{1,-11}(r_v) + V_{r,c}^{0,1}(r_v)\, B_{z,c}^{0,1}(r_v) \cos^2 z/R \\
& + V_{r,s}^{0,1}(r_v)\, B_{z,s}^{0,1}(r_v) \sin^2 z/R - V_z^{1,-10}(r_v)\, B_r^{1,-10}(r_v) - V_z^{1,-11}(r_v)\, B_r^{1,-11}(r_v) \\
& - V_{z,s}^{0,1}(r_v)\, B_{r,s}^{0,1}(r_v) \sin^2 z/R - V_{z,c}^{0,1}(r_v)\, B_{r,c}^{0,1}(r_v) \cos^2 z/R + V_r^{1,-10}(r_v)\, B_z^{1,-11}(r_v) \cos z/R \\
& + V_r^{1,-11}(r_v)\, B_z^{1,-10}(r_v) \cos z/R - V_z^{1,-10}(r_v)\, B_r^{1,-11}(r_v) \cos z/R - V_z^{1,-11}(r_v)\, B_r^{1,-10}(r_v) \\
& \cdot \cos z/R - \frac{J_z^{1,-11}(r_v)\, B_r^{1,-10}(r_v)}{n} \sin z/R + \frac{J_z^{1,-10}(r_v)\, B_r^{1,-11}(r_v)}{n} \sin z/R \\
& - \frac{J_r^{1,-11}(r_v)\, B_z^{1,-10}(r_v)}{n} \sin z/R + \frac{J_r^{1,-10}(r_v)\, B_z^{1,-11}(r_v)}{n} \sin z/R \Big\}.
\end{aligned}
\tag{50}
$$

Note that the $m=0, n=1$ configuration described in eqs (13)-(19) is no longer valid, but instead there are both sine and cosine terms in the equations (i.e. the "o" point is no longer at $z=0$).

The "X" and "O" points are located at

$$z = R \operatorname{Arctan}\left[\frac{-B_{r,c}^{0,1}(r_0)}{B_{r,s}^{0,1}(r_0)} \right] \qquad (51)$$

From eqs. (50) and (51) it is obvious that both the $\vec{\nabla}\times\vec{B}$ terms and the Hall terms contribute at the "o" point unless

$$B_{r,c}^{0,1}(r_0) = 0 \qquad (52)$$

which is unlikely since

$$\frac{\partial B_{r,c}^{0,1}(r_0,t)}{\partial t} = \frac{J_z^{1,-11}(r_0)\, B_r^{1,-10}(r_0)}{n} - \frac{J_z^{1,-10}(r_0) B_r^{1,-11}(r_0)}{n} + \frac{J_r^{1,-11}(r_0)\, B_z^{1,-10}(r_0)}{n} - \frac{J_r^{1,-10}(r_0)\, B_z^{1,-11}(r_0)}{n} \qquad (53)$$

Note that the Hall terms do not enter directly into the momentum equation, but rather indirectly:

$$\rho \frac{\partial V_{z,c}^{0,1}(r_0)}{\partial t} = J_{r,c}^{0,1}(r_0)\, B_\theta^{0,0}(r_0) - J_\theta^{0,0}(r_0)\, B_{r,c}^{0,1}(r_0) \qquad (54)$$

whereas the cosine component was zero in the MHD model.

Experimental Implications

- Narrowing in Θ space of high current operation
  - $m=0, n=1$ reconnection is not proceeding fast enough.
  - Cure : Keep resistivity at reversal surface high by keeping plasma cold.

    i.e. gas refuel

- Quiescence
  - Proper balance of different nonlinearities to minimize $\delta B/B$.

RECONNECTION AND ITS ROLE IN SOLAR FLARES

D. SPICER

NAVAL RESEARCH LABORATORY

SOME MAJOR QUESTIONS CONCERNING SOLAR ACTIVITY

- THE SOURCE(S) OF SOLAR MAGNETIC FIELDS.
- THE EMERGENCE AND DISAPPEARANCE OF MAGNETIC FLUX.
- THE FORMATION OF ACTIVE REGIONS.
- THE CAUSE(S) OF SOLAR FLARES.
- THE CAUSE(S) OF CORONAL TRANSIENTS.
- THE CAUSE(S) OF CORONAL HEATING.

SOURCES OF SOLAR FLARES: MAJOR ISSUES

- SOURCE OF FREE ENERGY.
- MECHANISM(S) THAT DISSIPATE THE AVAILABLE FREE ENERGY.

SOURCE OF FREE ENERGY: MAGNETIC

- HOW IS THIS FREE MAGNETIC ENERGY STORED?

  (A) REMOTELY (SUBPHOTOSPHERICALLY).

  (B) INSITU CORONAL STORAGE (ORTHODOX VIEW).

- THERE ARE SERIOUS QUESTIONS WITH BOTH POSSIBILITIES.

INSITU CORONAL MAGNETIC ENERGY STORAGE

- CONSTRAINTS IMPOSED BY ALL KNOWN MAGNETIC DISSIPATION MECHANISMS THAT THE AVAILABLE INSITU CORONAL FREE MAGNETIC ENERGY AND ITS CORRESPONDING ENERGY DENSITY BE HIGH CAUSE SERIOUS DIFFICULTIES FOR INSITU STORAGE (E.G., INSITU STORAGE REQUIRES FREE MAGNETIC ENERGY WITH ENERGY DENSITIES OF ORDER 10^4 ERGS/CM^3 WHICH IS APPROXIMATELY 10^4 GREATER THAN THE AMBIENT GAS PRESSURES).

- SOLAR MAGNETIC FIELDS ARE NOT FORCE-FREE SINCE THERE EXIST FINITE FORCES (GLOBAL CURVATURE, GRAVITY AND PRESSURE GRADIENTS, BOTH GAS AND MAGNETIC) WHICH MUST BALANCE ONE ANOTHER.

- THE USUAL ASSUMPTION OF CONSTANT ALPHA FOR FORCE-FREE FIELDS IS DUBIOUS SINCE SUCH AN ASSUMPTION IMPLICITLY NEGLECTS CORONAL POTENTIAL FIELDS DUE TO SUB-PHOTOSPHERIC CURRENTS.

- INDUCTIVE INSITU CORONAL STORAGE OF MAGNETIC ENERGY IMPOSES THE CONSTRAINT THAT AT MOST APPROXIMATELY 10^{32} ELECTRONS/S CAN BE DIRECTLY ACCELERATED BY ANY FLARE MECHANISM THAT DISSIPATES THE INDUCTIVELY STORED ENERGY.

FLARE MECHANISMS

- PRINCIPAL MECHANISMS:

  (A) RECONNECTION

  (B) DOUBLE LAYERS

  (C) ANOMALOUS RESISTIVITY

- MECHANISM MUST DISSIPATE APPROXIMATELY 10^{32} OF MAGNETIC ENERGY IN APPROXIMATELY 10-100 SECS.

- MECHANISM MUST RESULT IN TEMPORAL STRUCTURE WITH AN HIERHARCHY OF TIME 10^{-3} TO 10^{2} SEC.

- THE RELEASED ENERGY MUST SPREAD THROUGHOUT A VOLUME OF APPROXIMATELY 10^{30} CM^{3} IN APPROXIMATELY 10-100 SECS.

- THE MECHANISMS(S) MUST BE CAPABLE OF PRODUCING 10^{35}-10^{38} 20 KEV ELECTRONS/S IN SIMILAR TIMES.

MAGNETIC STRUCTURE AT THE SOLAR SURFACE

- FLUX EMERGES IN CONCENTRATED "ACTIVE" REGIONS WHICH OCCUPY ONLY A SMALL FRACTION OF THE SOLAR SURFACE.
- THESE REGIONS ARE MADE UP OF NUMEROUS FLUX "BUNDLES" (ALSO SOMETIMES CALLED "ROPES" OR "TUBES"). THESE BUNDLES ARE A FEW HUNDRED KILOMETERS IN SIZE WITH FIELD STRENGTHS APPROACING 1500 GAUSS.
- BUNDLES APPEAR WITH A BROAD SPECTRUM OF SIZES.
- THE LARGEST ACTIVE REGIONS CONTAIN UP TO 10^{23} Mx (Mx = 1 GAUSS CM^2).
- SMALLEST EPHERMERAL REGIONS HAVE ONLY 10^{18}-10^{19} Mx, BUT APPEAR IN GREAT NUMBERS.
- UNIPOLAR FLUX IS OBSERVED. THE EXPLANATION FOR THIS APPARENT CONTRADICTION WITH PHYSICAL LAW APPEARS TO BE DUE TO OUR INABILITY TO RESOLVE FINER STRUCTURE BUNDLES OF THE OPPOSITE POLARITY AT THE PERIPHERY OF THE OBSERVABLE ACTIVE REGION.
- EMERGING FLUX CARRIES DENSE PLASMA FROM THE CONVECTION ZONE INTO THE PHOTOSPHERE.

- AS A LOOP OF MAGNETIC FLUX EMERGES, THE FOOTPRINTS OF THE LOOP MOVE STEADILY APART.

- THE USUAL VIEW OF EMERGENCE IS OF A TWISTED SUBSURFACE ROPE OF MAGNETIC FLUX WHICH DEVELOPS A RISING LOOP OR KINK THAT BREAKS THROUGH THE SURFACE.

- TURBULENCE AND FLOWS EXCLUDE MAGNETIC FLUX FROM THE CENTER OF THE CELLS AND VORTICES WHICH FILL THE CONVECTION ZONE AND CONCENTRATE IT IN ROPES AT THE PERIPHERY OF CELLS.

- OBSERVATIONS SHOW THAT FLUX, PARTICULARLY IN THE FORM OF SUNSPOTS, ROTATES ACROSS THE VISIBLE SURFACE AT A FASTER RATE THAN THE SURFACE PLASMA. THIS SUGGESTS THAT THIS FLUX IS CONNECTED MAGNETICALLY TO THE MORE RAPIDLY ROTATING, DEEPER LAYERS. DRAG AND THUS HEATING SHOULD RESULT.

- LITTLE IS KNOWN ABOUT THE RATE OF EMERGENCE OF FLUX.

NONLINEAR COUPLING OF TEARING MODES IN THE REVERSED FIELD PINCH AND THE TOKAMAK DISRUPTION

J. HOLMES

OAK RIDGE NATIONAL LAB

NONLINEAR COUPLING OF TEARING MODES IN THE REVERSED FIELD PINCH AND THE TOKAMAK DISRUPTION

BY J. A. Holmes

Collaborators:

B. A. Carreras
T. C. Hender
H. R. Hicks
V. E. Lynch
} ORNL

Z. G. An
P. H. Diamond
} IFS

For presentation at the US-Japan Joint Institute for Fusion Theory Workshop on Magnetic Reconnection, Austin, Tx, Dec. 1984.

TOKAMAK

Two tearing modes unstable (2/1 and 3/2)

↓

Island overlap

↓

Stochastization of field lines
+
Explosive growth

↓

loss of confinement

⇣

Disruption (bad!)

RFP

Many m=1 tearing modes unstable with singular surfaces close together

↓

Island overlap

↓

Stochastization of field lines

⇣

Dynamo (good!)

MOTIVATION: TO STUDY HOW THE NONLINEAR COUPLING OF RESISTIVE TEARING MODES CAN LEAD TO SUCH DIFFERENT PHENOMENA AS

DISRUPIONS IN TOKAMAKS AND

SUSTAINMENT OF PROFILES AGAINST RESISTIVE DIFFUSION (DYNAMO) IN RFP'S.

OUTLINE OF TALK

- Computational Models
- Tokamak Disruptions
  - Description
  - Nonlinear Coupling Mechanism
- RFP Tearing Modes
  - Description
  - Nonlinear Coupling Behavior
  - Consistency with Tokamak Disruption Mechanism
- Conclusions and Future Direction

COMPUTATIONAL MODEL

- Resistive MHD
- Cylindrical Geometry Adequate for Tearing Modes
- Full Set of Equations with Constant Mass Density Valid for RFP and Tokamak
  - Compressible or Incompressible
  - With or Without Equilibrium Resistive Diffusion
  - Options on Equation for Pressure Evolution
- Reduced Set of (Strauss) Equations Valid for Tokamak Only.
- Solution by Initial Value Approach
  - Cylindrical Coordinates (r, θ, z)
  - Finite Difference in r and time t.
  - Fourier Expansion in θ and z using Periodic Boundary Conditions.

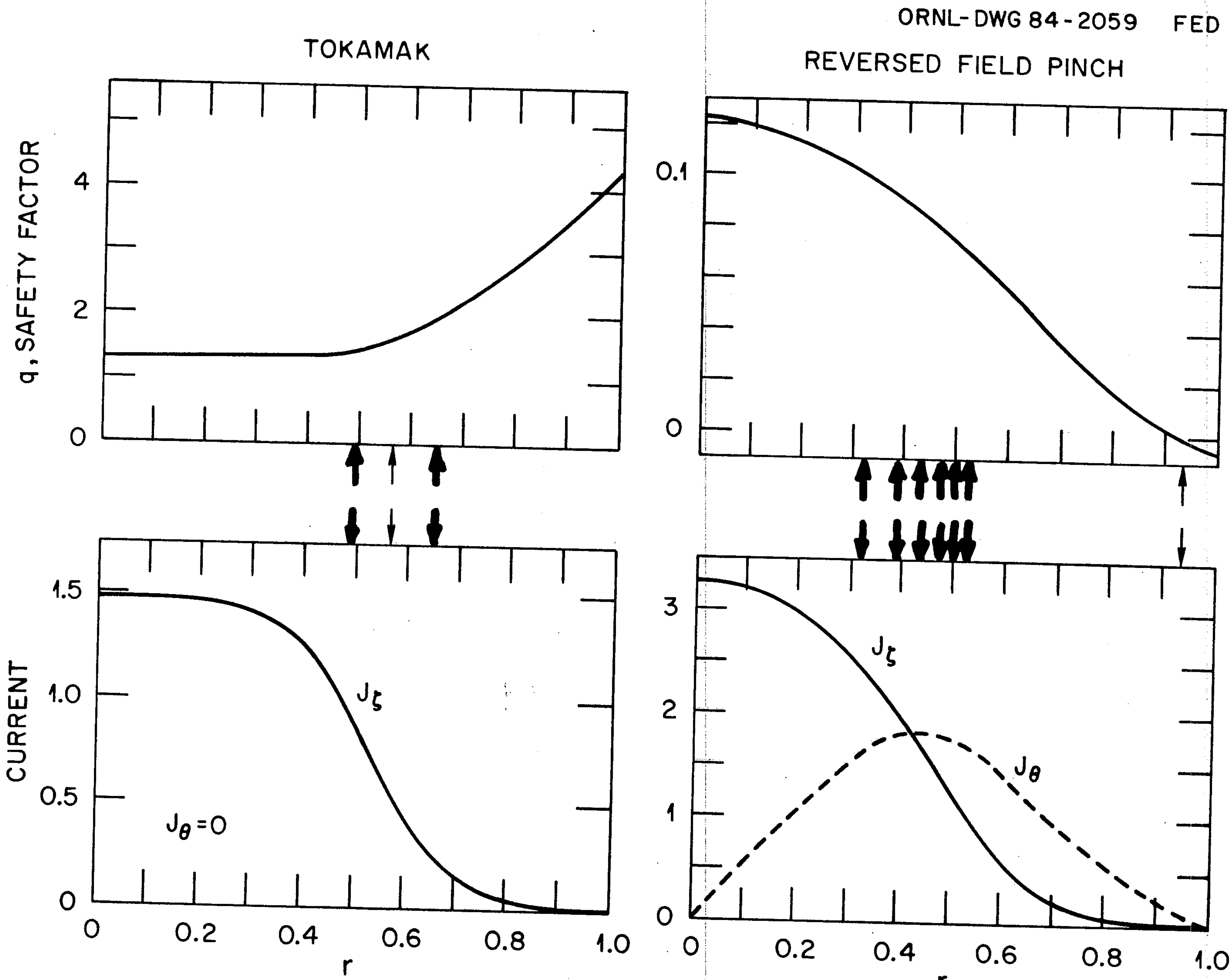

Caramana, Nebel, Schnack

MULTIPLE HELICITY TEARING MODE EVOLUTION

TOKAMAK DISRUPTION

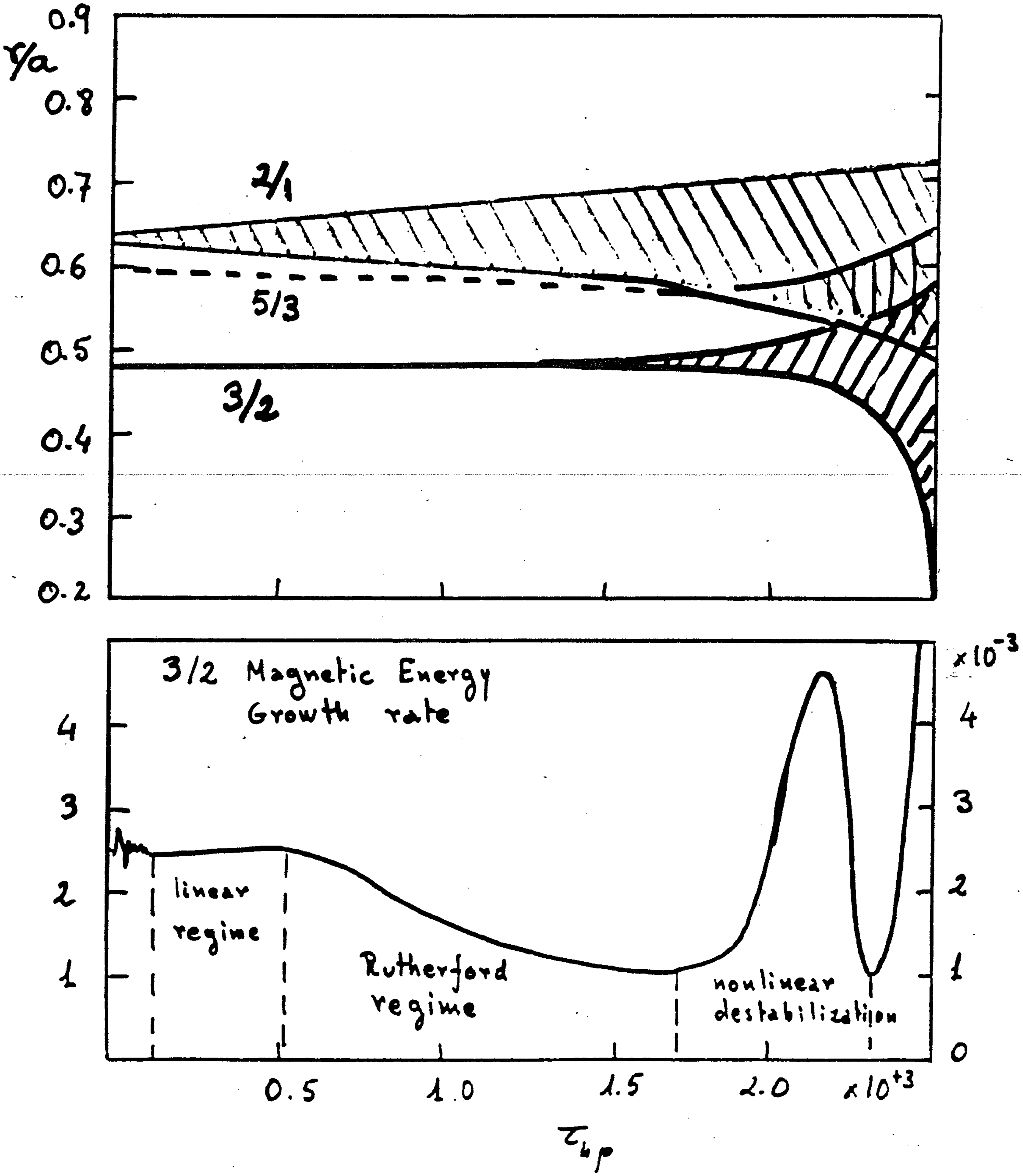

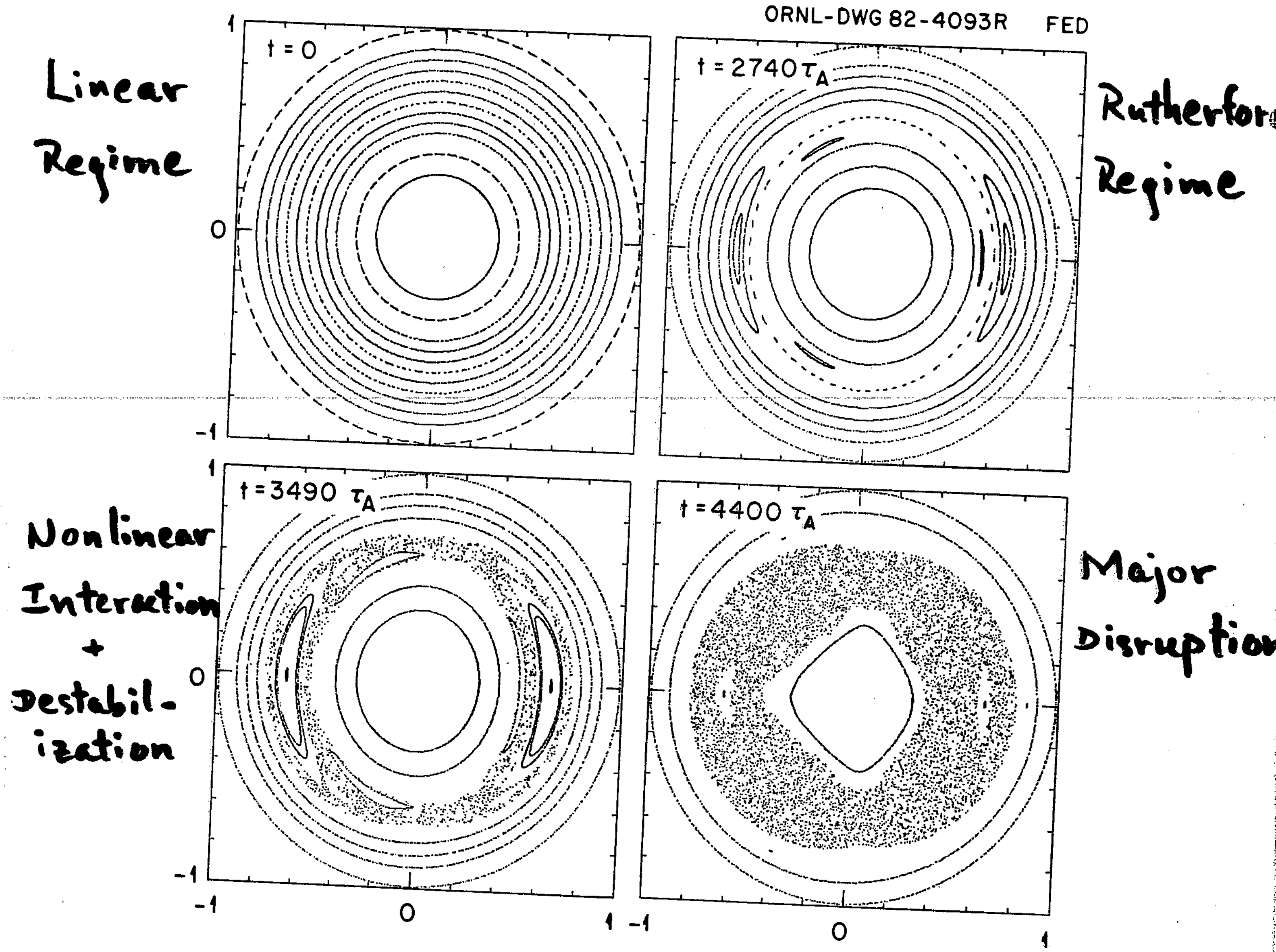
ORNL-DWG 82-4093R FED
Linear Regime
t = 0
t = 2740 τ_A
Rutherford Regime
Nonlinear Interaction + Destabil-ization
t = 3490 τ_A
t = 4400 τ_A
Major Disruption
1
0
-1
-1
0
1
-1
0
1

NONLINEAR MODE INTERACTION MODEL

(Carreras, Rosenbluth, Hicks), (An, Diamond)

- Assume:
  - Sheared Slab Model ($q = q(x)$).
  - Low β Reduced Resistive MHD Equations.
  - Modes: $\vec{k}$ a test mode (unstable)

    $\vec{k}'$ a passive background

    $\vec{k}+\vec{k}'$ a nonlinearly driven mode.

- Results:
  - Driven field associated with localized current $\tilde{J}_{\vec{k}+\vec{k}'}$.
  - Nonlinear beating of $\tilde{\vec{J}}_{k+\vec{k}'}$ and $\tilde{\vec{B}}_{k'}$ generates vorticity change for the k mode.
  - If driven mode unstable ($\Delta'_{k+k'} > 0$), test mode k further destabilized by nonlinear coupling to new free energy source.
  - If driven mode stable ($\Delta'_{k+k'} < 0$), nonlinear coupling opens new energy sink for the mode k, which is stabilized.

NONLINEAR COUPLING TOKAMAK DISRUPTION MECHANISM

(Carreras, Rosenbluth, Hicks)

- Modes Involved: (0;0) Equilibrium.
  (2;1) and (3;2) Linearly Unstable.
  (5;3) and (1;1) Lowest Order Couplings.
  Can neglect nonresonant (1;1).

- (2;1) and (3;2) Magnetic Islands Alter Current Profile Quasi-Linearly, Destabilizing (5;3)

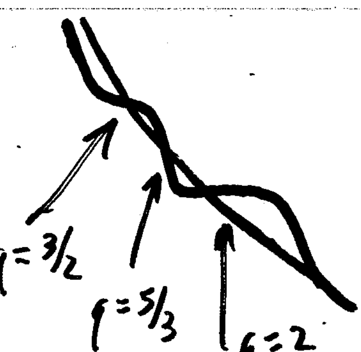

- Nonlinear Coupling of Destabilized (5;3) and (2;1) through $\vec{J}\times\vec{B}$ force drives rapid increase in kinetic energy of (3;2)

- $\gamma^{k_2}_{(3;2)} \approx \frac{1}{\sqrt{\pi}} \left|\tilde{B}_r^{(2;1)}\right| \underline{\Delta'_{(5;3)}} \frac{a^2}{B_0 W_{(2;1)} \tau_{Hp}^2}$ for $\underline{\Delta'_{(5;3)} > 0}$

$\underline{\Delta'_{(5;3)} < 0 \quad \text{Tends to stabilize}}$ the (3;2)

Linear Destabilization of (5;3) Nonlinearly Destabilizes the (3;2).

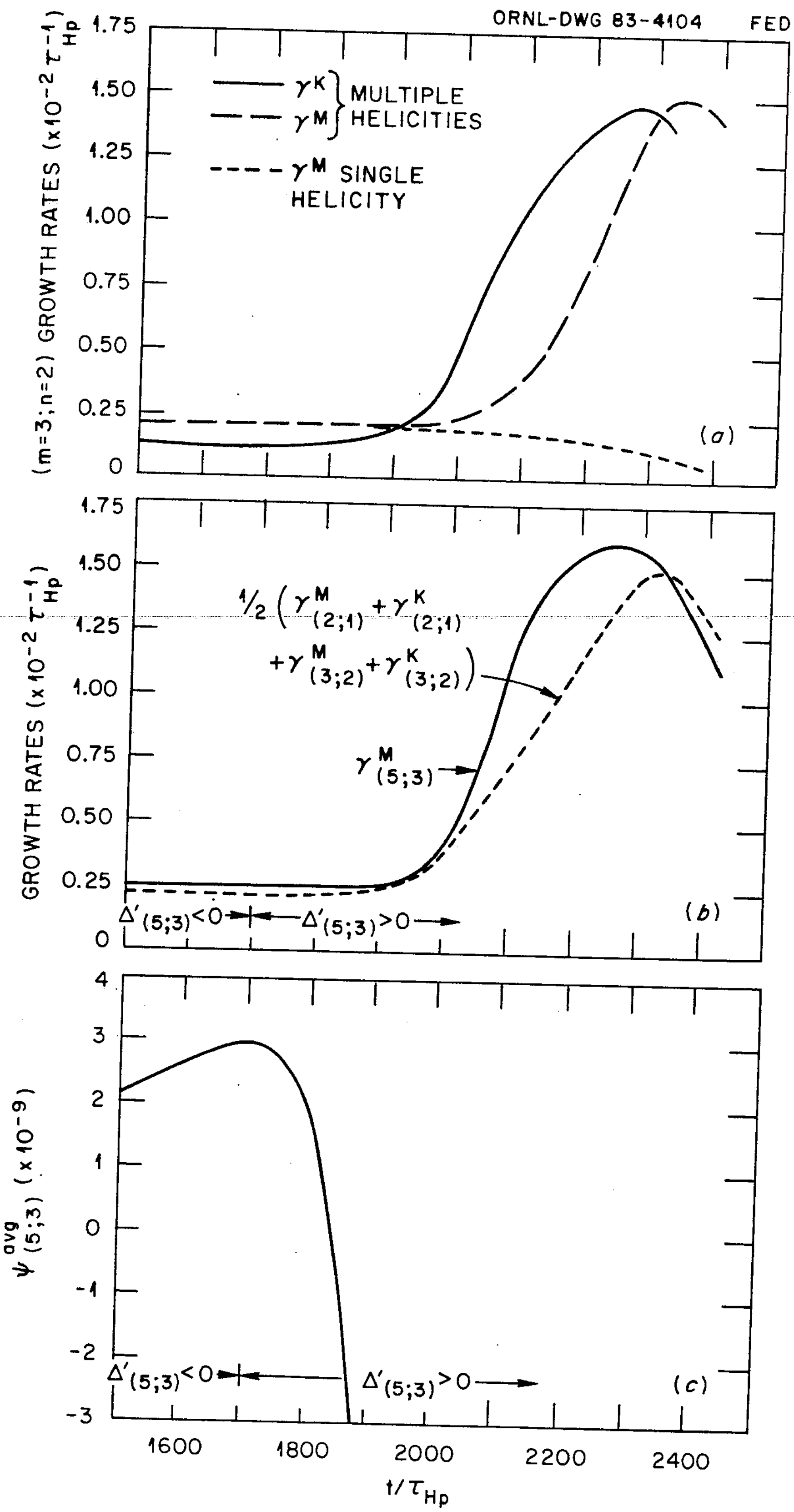

NONLINEAR COUPLING IN THE RFP

- Modes Involved: (0;0) Equilibrium.
  (1;n), (1;n+1), etc. Linearly Unstable ($n \sim 10$).
  (2;2n+1) and (0;1) Lowest Order Couplings.
  (0;1) Not resonant between (1;n) and (1;n+1).

- Contrast with Tokamak: Close spacing of (1;n) and (1;n+1) ⇒ Strong Interaction and Island Overlap "Earlier" than in Tokamak. **Quasilinear current profile modification will be small.**

- To compare with Tokamak, let us regard (1;n) as (2;1), (1;n+1) as (3;2), and (2;2n+1) as (5;3).

The (1;12) Mode is Nonlinearly Stabilized.
The (2;23) is always stable.

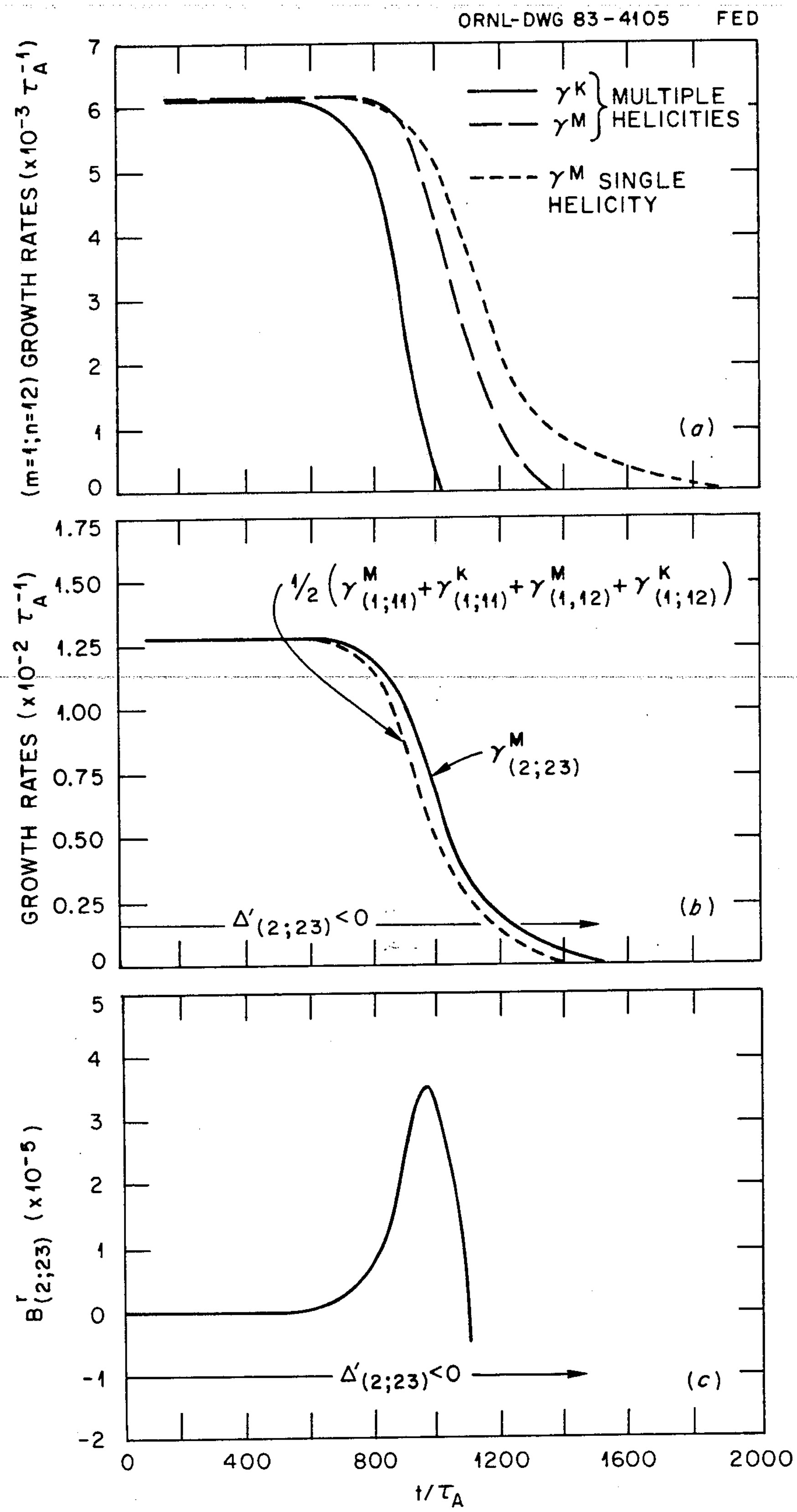

Saturated Island Width is Smaller in the Presence of Nonlinear Couplings.

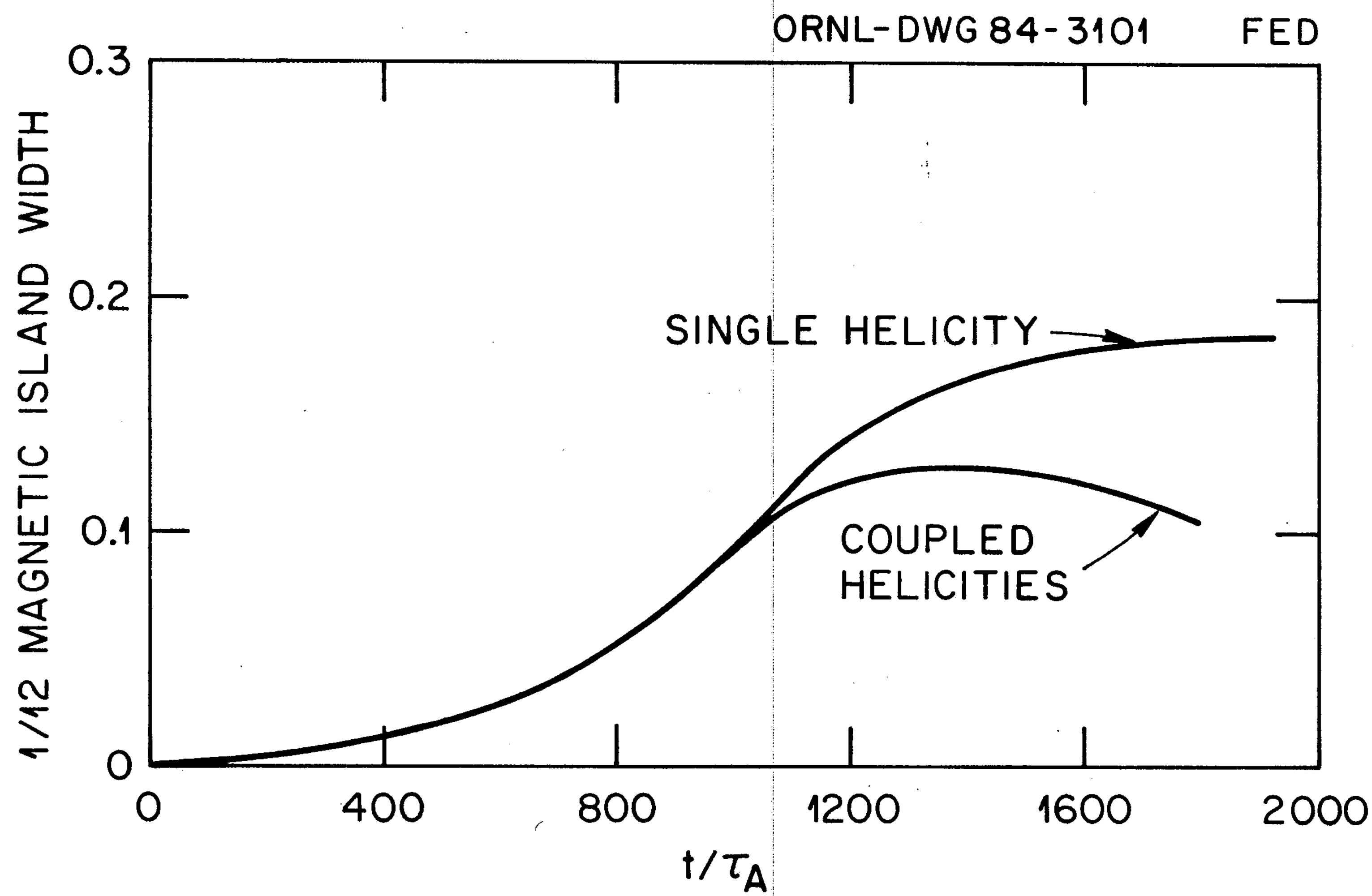

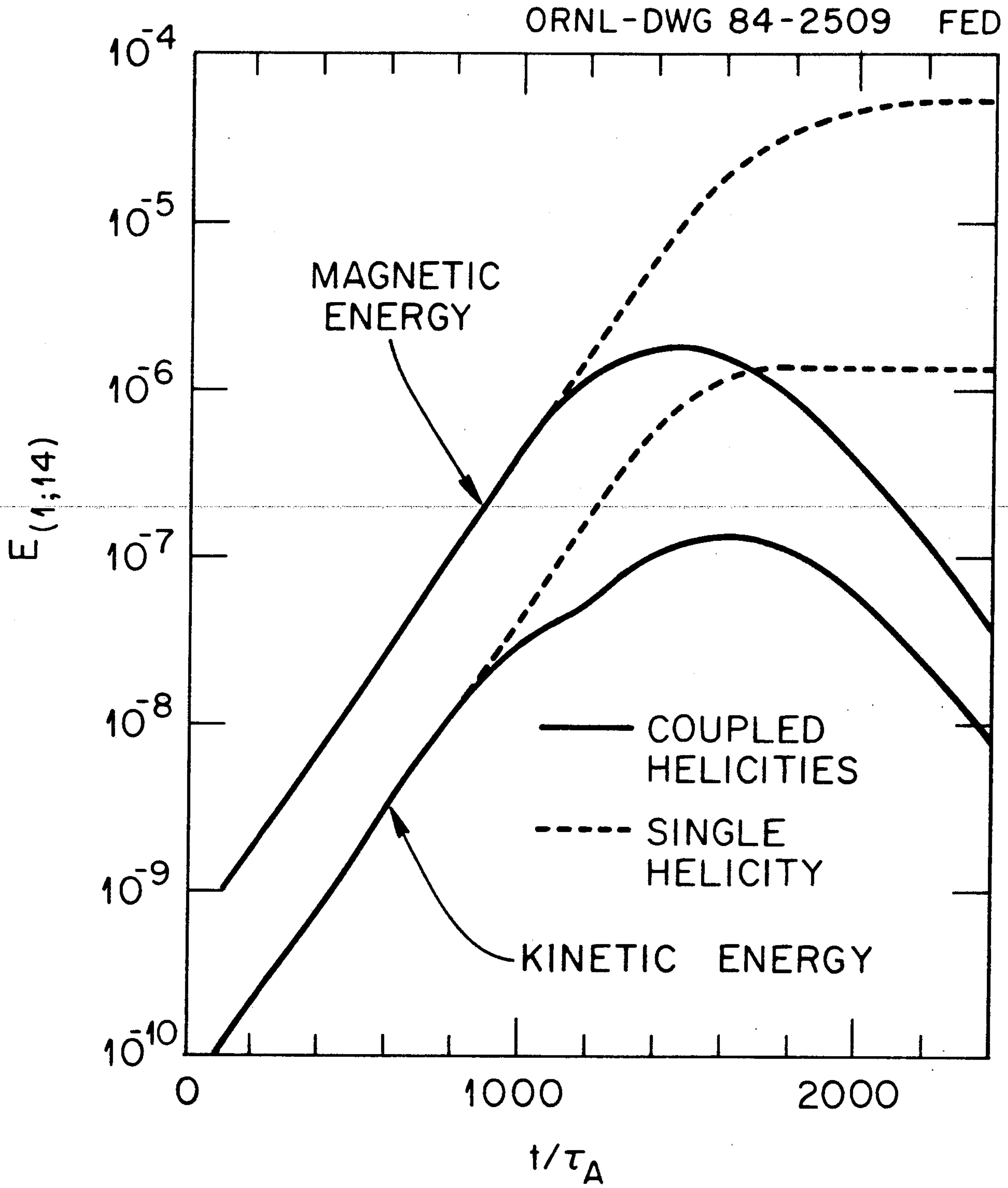
ORNL-DWG 84-2509 FED
10^{-4}
10^{-5}
10^{-6}
10^{-7}
10^{-8}
10^{-9}
10^{-10}
$E_{(1;14)}$
MAGNETIC ENERGY
COUPLED HELICITIES
SINGLE HELICITY
KINETIC ENERGY
0
1000
2000
t/τ_A

The stabilization carries over to many mode cases.

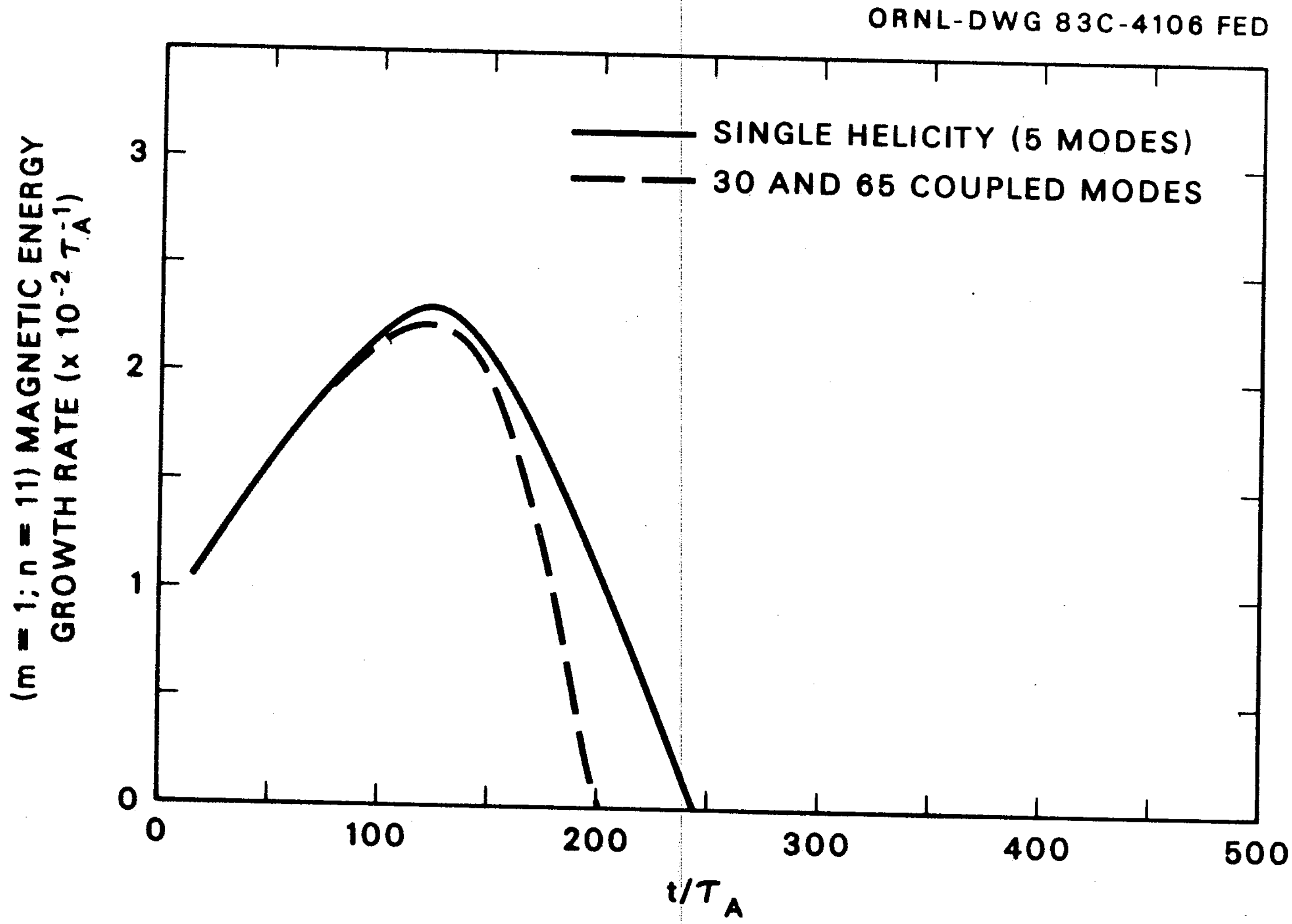

Removing the m=2 modes reduces the nonlinear stabilizing effect.

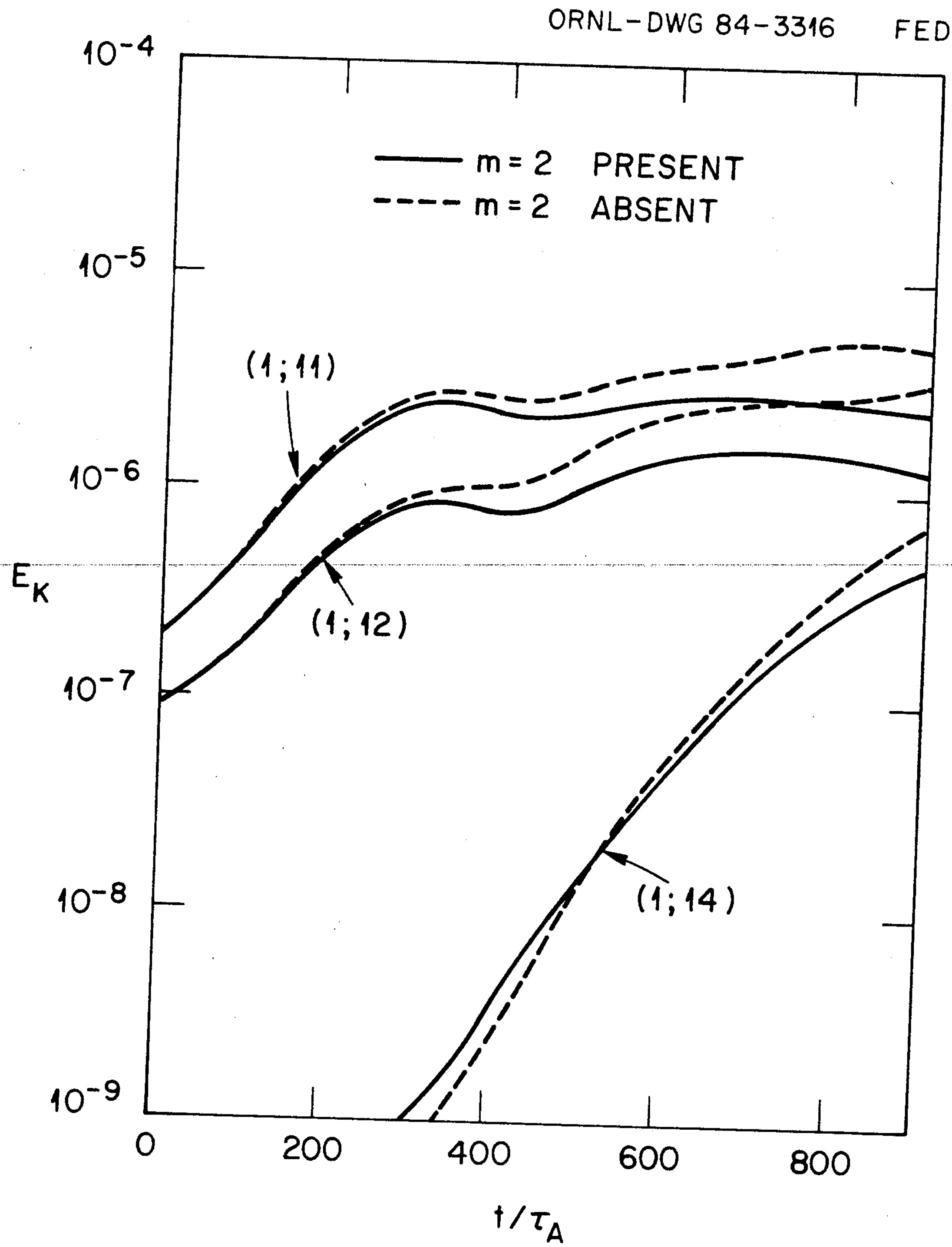

Though the driven modes play a crucial role, they are not easy to detect.

ORNL-DWG 84-2978 FED

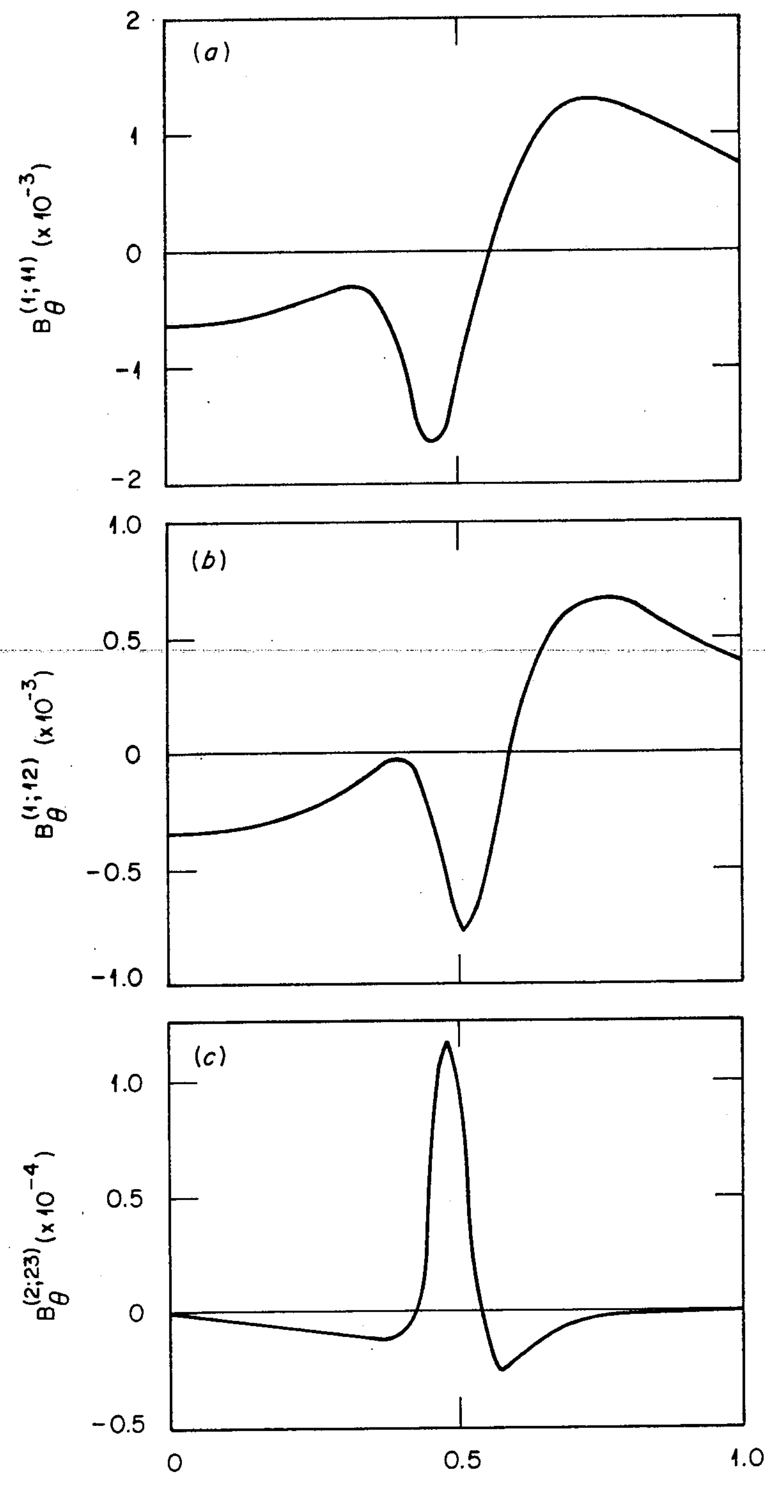

In spite of the stabilization effects, large regions of stochastic field lines are generated.

ORNL-DWG 83-4112 FED

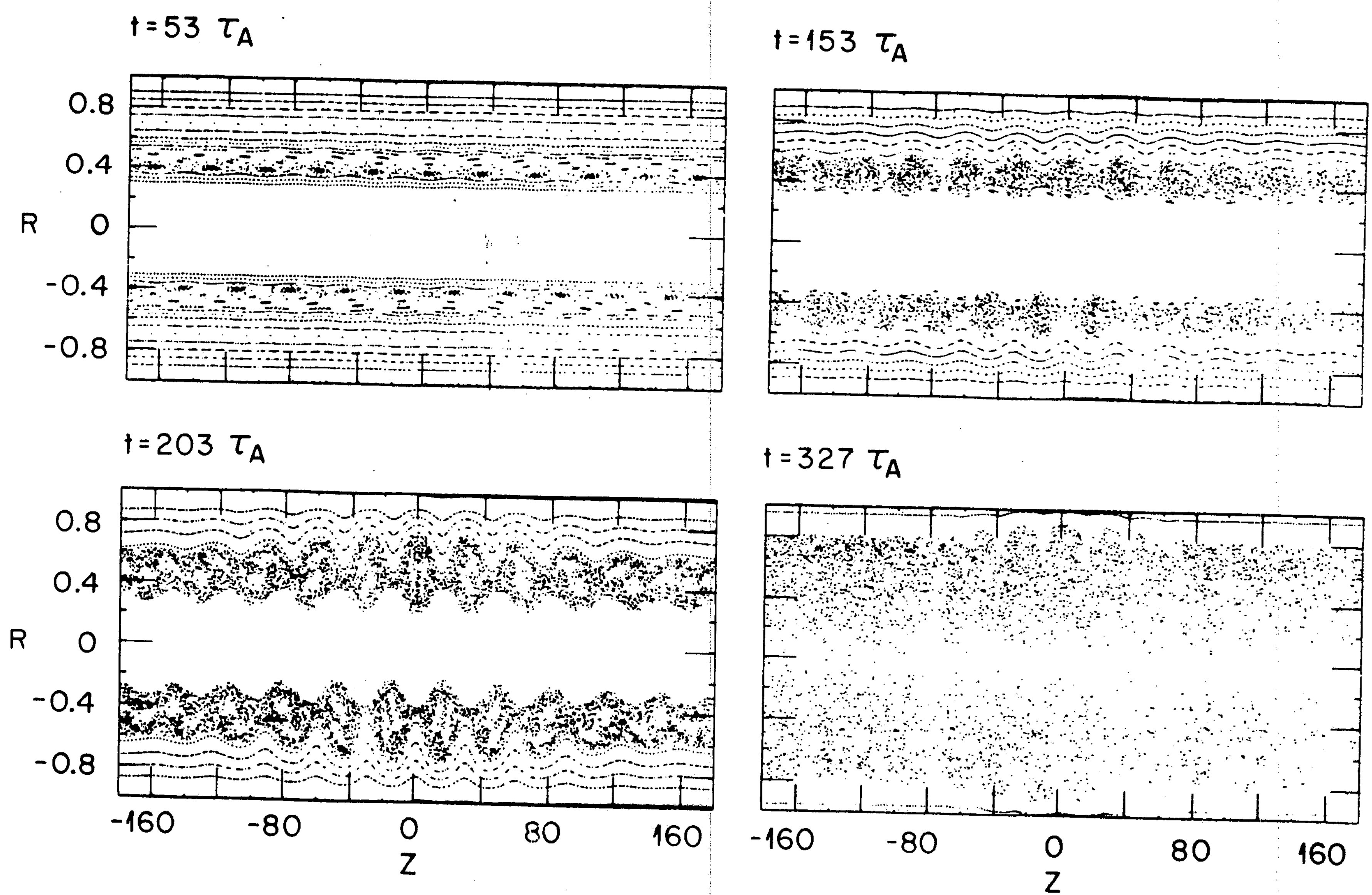

Conclusions + Future Direction

- Nonlinear couplings of two unstable tearing modes are
  - Destabilizing in tokamak disruptions.
  - Stabilizing in the RFP.
  - Understandable in terms of an analytic model.

- The nonlinear stabilization observed in the RFP carries over to cases for which many modes are included.

- Future work should attempt to couple analytic and numerical efforts to understand steady state turbulence in RFP's.

RFP: MEAN FIELD MHD MODEL

H. STRAUSS

COURANT INSTITUTE

RFP : Mean Field MHD Model

H Strauss

I

(1) MHD "explains" RFP

a) α effect

b) transport : $\beta \sim 20\%$

Tokamak : $q \sim 1$, $q' > 0$ RFP $q \sim a/R$, $q' < 0$

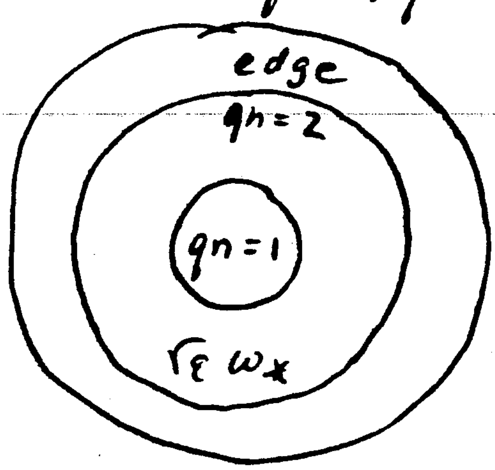

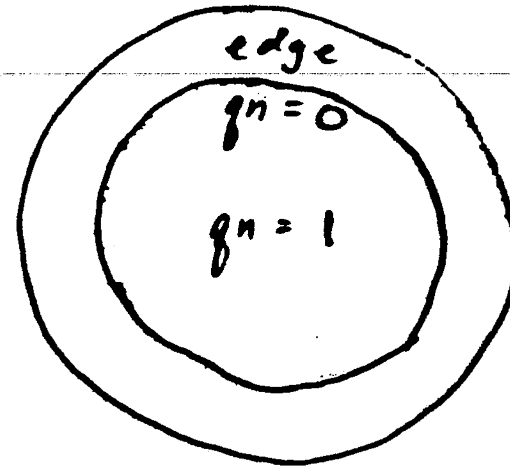

(2) Transport-like MHD model

a) simpler

b) good agreement (better than incomp MHD)

c) generalized quasilinear

II $\beta = 0$ derivation

III α effect

IV $\beta \neq 0$

V numerical

$$\underset{\sim}{B} = \overline{\underset{\sim}{B}} + \hat{\underset{\sim}{B}}$$

$$\overline{\underset{\sim}{B}} = \oint \frac{d\theta\, dz}{2\pi R} \underset{\sim}{B}$$

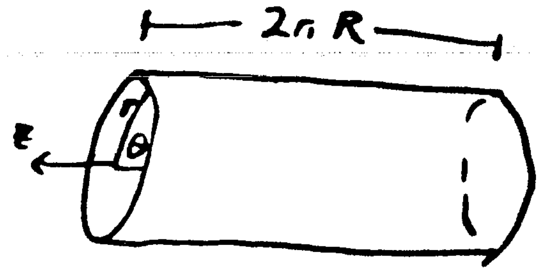

$$|\hat{\underset{\sim}{B}}| \ll |\overline{\underset{\sim}{B}}|$$

Mean Field $\overline{\underset{\sim}{B}} = \nabla \times \underset{\sim}{\bar{A}}$

$$\dot{\bar{A}} = \dot{\bar{\psi}}\, \underset{\sim}{\bar{B}} + \dot{\bar{\chi}}\, \nabla r \times \underset{\sim}{\bar{B}} = \overline{V \times B} + E_z \hat{z} - \eta \bar{J}$$

$$\frac{\partial}{\partial z}\left(\underset{\sim}{\bar{J}} \times \underset{\sim}{\bar{B}} \cdot \nabla r\right) = 0$$

$$\dot{\bar{\psi}} = \alpha + \left(E_z^0 \bar{B}_z - \eta \bar{J} \cdot \bar{B}\right) / \bar{B}^2$$

$$\left(\frac{1}{r}\frac{\partial}{\partial r} r \bar{B}^2 \frac{\partial}{\partial r} - \frac{\bar{B}^2}{r^2} - \frac{1}{r}\frac{\partial \bar{B}_\theta^2}{\partial r}\right)\dot{\bar{\chi}} = \frac{\partial}{\partial r}\left(\underset{\sim}{\bar{J}} \cdot \underset{\sim}{\bar{B}}\, \dot{\bar{\psi}}\right) - \frac{2\bar{B}_\theta}{r}\frac{\partial}{\partial r}\left(\bar{B}_z \dot{\bar{\psi}}\right)$$

$$\alpha = \overline{\hat{\underset{\sim}{V}} \times \hat{\underset{\sim}{B}}} \cdot \overline{\underset{\sim}{B}} \,/\, \bar{B}^2$$

Steady State
$$\begin{cases} \bar{J}_\theta \bar{B}_z = \bar{J}_z \bar{B}_\theta \\ \eta\, \underset{\sim}{\bar{J}} \cdot \underset{\sim}{\bar{B}} = \alpha\, \underset{\sim}{\bar{B}}^2 + \bar{E}_z \bar{B}_z \end{cases}$$

Fluctuations

1. Small amplitude

   $|\hat{B}| / |\bar{B}| \sim \lambda \ll 1$

   exp, overlap

2. all linear terms

3. $\bar{B} \cdot \nabla \sim \hat{B} \cdot \nabla \sim \lambda$ at B kinks

4. $\frac{\partial}{\partial r} \sim \frac{1}{\lambda}$ boundary layer

5. $\frac{\partial}{\partial t} |\hat{B}| \sim \lambda |\hat{B}|$ small inertia

6. $\eta \sim \lambda^3$ nonlinear tearing

$$\frac{\partial}{\partial t}\hat{A} = \frac{\partial\hat{\psi}}{\partial t}\bar{B} + \frac{\partial\hat{\phi}}{\partial t}\nabla r$$

$$= v \times B + \nabla\hat{u} - \eta\hat{J}$$

$$\bar{B}\cdot \Rightarrow \dot{\hat{\psi}}$$

$$J \times B \cdot \nabla r \times \bar{B} = 0 \Rightarrow \hat{\phi}$$

$$(\bar{B}_{\sim} \cdot \hat{B}_{\sim} \approx 0)$$

$$\hat{v} \approx (\nabla\hat{u} - \dot{\hat{\phi}}\nabla r) \times \bar{B} / \bar{B}^2$$

$$\nabla \cdot \left(\rho \frac{dv}{dt} \times \bar{B} / \bar{B}^2\right) = B \cdot \nabla \frac{J \cdot B}{B^2} \Rightarrow \dot{\hat{u}}$$

$$\left[\begin{array}{l} \frac{\partial}{\partial t}\bar{B} \sim \eta\bar{J} \ll \frac{\partial}{\partial t}\hat{B} \\ \hat{B} = \nabla \times (\hat{\psi}\bar{B} + \hat{\varphi}\nabla r) \end{array}\right]$$

RFP eqs. $(\beta = 0)$

$$\frac{\partial}{\partial t}\hat{\psi} = \frac{B \cdot \nabla u}{\bar{B}^2} + \eta \hat{\sigma}$$

$$\frac{d}{dt}\nabla \cdot \frac{\rho}{\bar{B}^2}\nabla \hat{u} = B \cdot \nabla(\hat{\sigma} + \bar{\sigma})$$

$$\left(\frac{1}{r^2}\frac{\partial^2}{\partial \theta^2} + \frac{\partial^2}{\partial z^2}\right)\hat{\varphi} = \bar{B} \cdot \nabla \frac{\partial \hat{\psi}}{\partial r}$$

$$\sigma = \bar{J} \cdot \bar{B} / \bar{B}^2$$

$$\hat{\sigma} = \frac{1}{\bar{B}^2}\nabla \cdot (\hat{B} \times \bar{B})$$

$$\frac{\partial}{\partial t}\bar{\psi} = \alpha + (E_z^{\circ} B_z - \eta \underset{\sim}{\bar{J}} \cdot \underset{\sim}{\bar{B}}) / \bar{B}^2$$

$$\mathcal{L}(\dot{\bar{\chi}}) = \mathcal{F}(\dot{\bar{\psi}})$$

$$\dot{\underset{\sim}{B}} = \nabla \times (\dot{\psi}\bar{B} + \dot{\bar{\chi}}\nabla r \times \bar{B} + \dot{\hat{\phi}}\nabla r)$$

$$\alpha = \overline{B \cdot \nabla u} - \overline{B_r \frac{\partial \phi}{\partial t}}$$

$$F = \frac{B_z(a)}{\langle B_z \rangle}$$

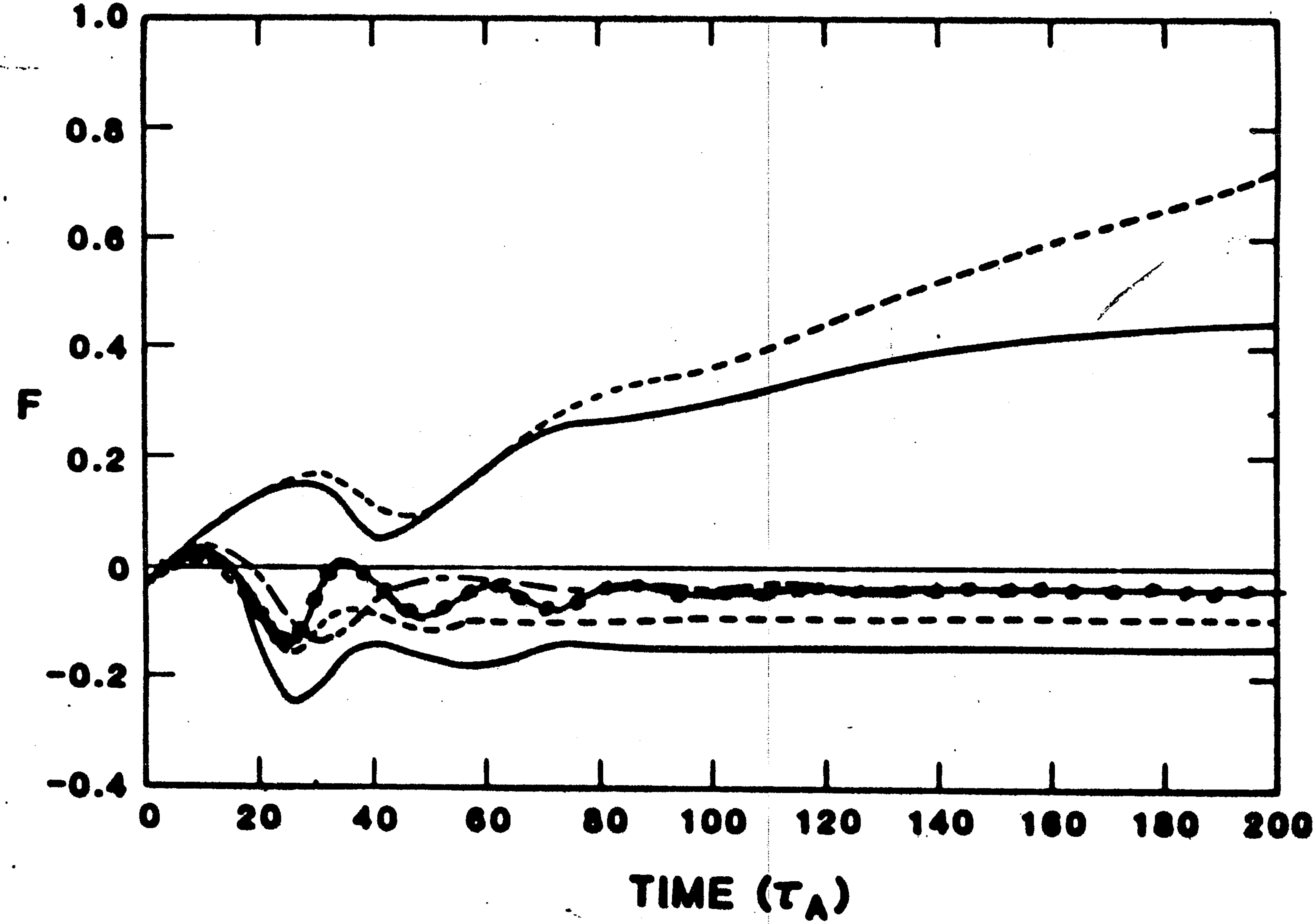

Fig. 3

8/84e1r5510

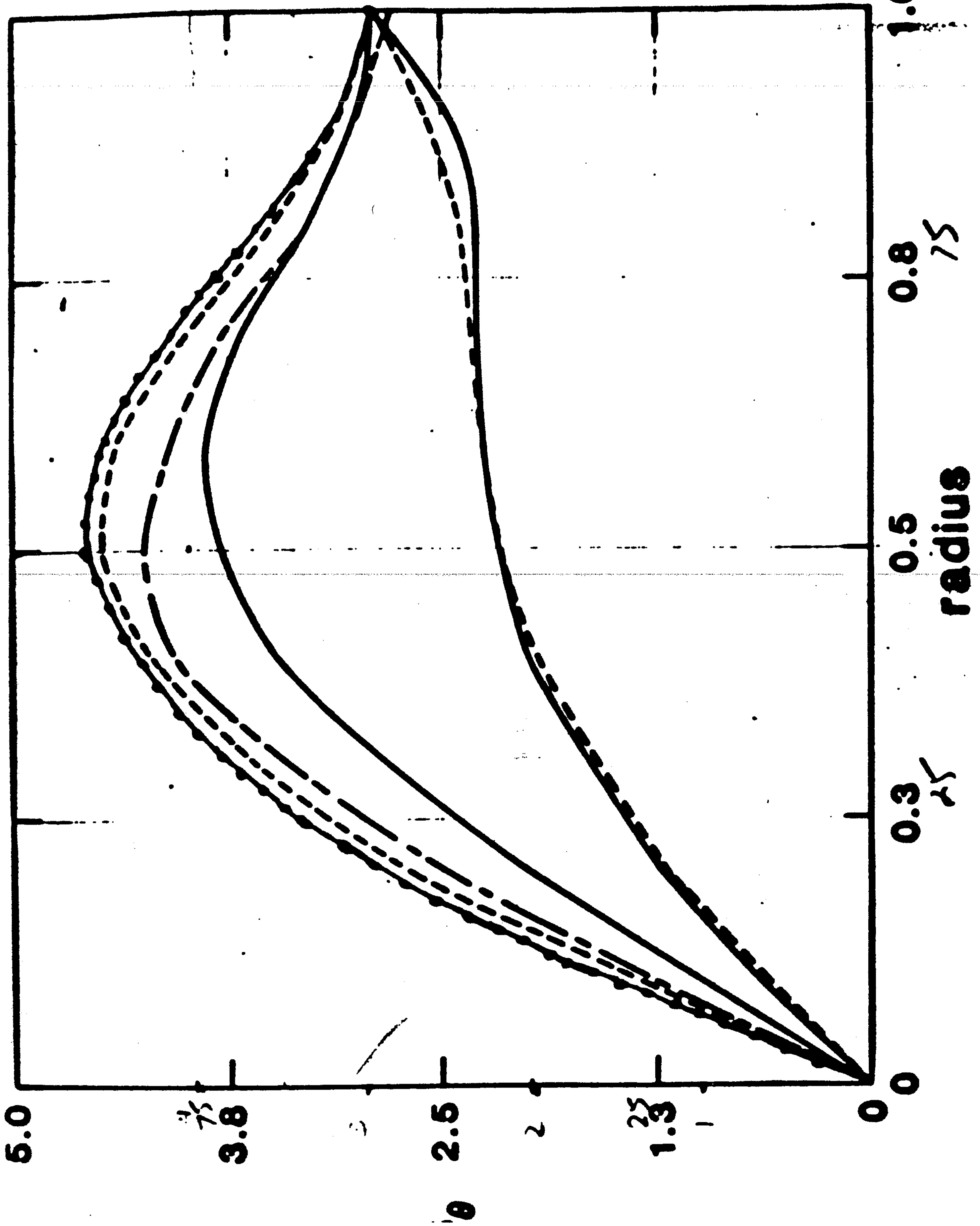

Fig. 1

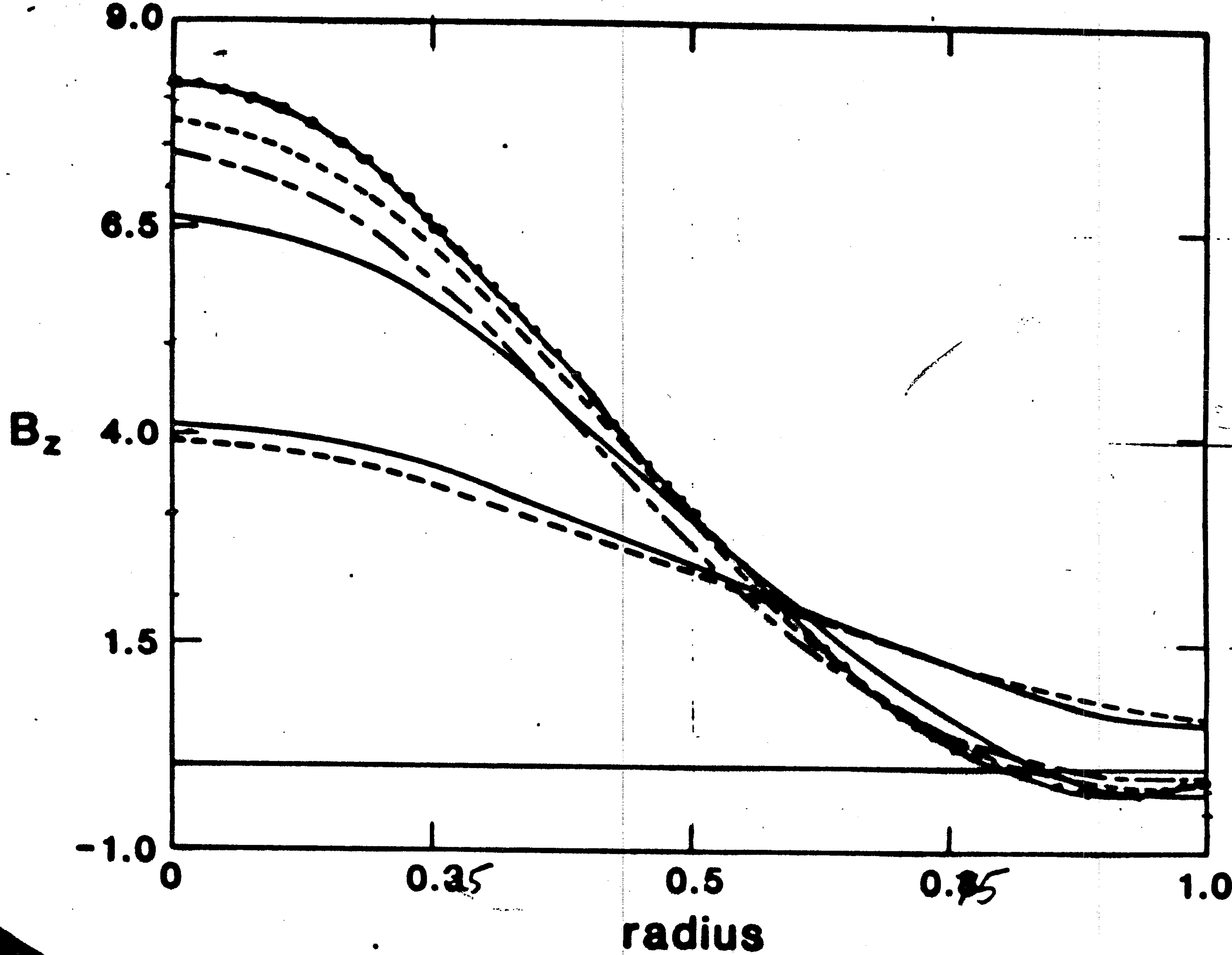

Fig. 2

8/84ctr5620

Energy :

$$\mathcal{E} = \frac{1}{2} \left\langle \bar{\rho} (\nabla U / \bar{B})^2 + \bar{\underline{B}}^2 + \hat{\underline{B}}^2 \right\rangle$$

$$\frac{\partial}{\partial t} \mathcal{E} = \left\langle (E_z^\circ \hat{z} - \eta \underline{J}) \cdot \underline{J} \right\rangle + O\left(\hat{B}^2 \frac{\partial \bar{B}}{\partial \tau}, \hat{V}^2 \frac{\partial \bar{B}}{\partial \tau} \right)$$

α effect

① No current drive in steady state

$$\alpha \bar{B}^2 = \overline{B \cdot \nabla U} - \cancel{B_r \frac{\partial \hat{\phi}}{\partial \tau}} \to 0$$

$$\langle \alpha \bar{B}^2 \rangle = 0$$

$$\langle \bar{B}^2 \dot{\psi} \rangle = 0 = \langle \eta J \cdot B \rangle = E_z^\circ \langle B_z \rangle$$

(2) Quasilinear α $\qquad U \sim U_{\underset{\sim}{k}}(r,t)\exp(im\theta - inz/R)$

$$\alpha \bar{B}^2 \approx \frac{1}{r}\frac{\partial}{\partial r}\left(r\,\overline{U B_r}\right)$$

a) steady state $\partial/\partial t = 0$

$$0 = \bar{B}\cdot\nabla U + \eta\hat{\sigma}$$

$$0 = \bar{B}\cdot\nabla\hat{\sigma} + B_r\bar{\sigma}'$$

$$\alpha\bar{B}^2 = \frac{1}{r}\frac{\partial}{\partial r}\left[r\,\eta\bar{B}^2\sum_k \frac{|B_{r\underset{\sim}{k}}|^2}{|\underset{\sim}{k}\cdot\bar{B}|^2}\frac{\partial}{\partial r}\left(\frac{\bar{J}\cdot\bar{B}}{\bar{B}^2}\right)\right]$$

(Taylor: $J\cdot B/B^2 = \sigma = \text{const}$)

b) Growing modes – at wall

$$\alpha\bar{B}^2 = -\frac{1}{2}\sum_k\left(\frac{k\times B\cdot\hat{r}}{k\cdot B}\right)\frac{\partial}{\partial t}\frac{\partial}{\partial r}|\psi_k|^2$$

$$\frac{k\cdot B}{k\times B\cdot\hat{r}} = \left(\frac{m-nq}{mq+nr^2/R^2}\right)\frac{r}{R} \qquad \begin{array}{ll} \text{RFP} & \alpha > 0 \\ \text{Tok} & \alpha < 0 \end{array}$$

c) Growing modes – at center

$$U = \frac{\partial\xi}{\partial t} \sim r$$

$$\frac{\partial}{\partial t}q = \frac{q}{r}\frac{dq}{dr}\frac{\partial}{\partial t}\left|\frac{\partial\xi}{\partial r}\right|^2 \qquad \begin{array}{ll} \text{RFP} & \dot{q} < 0 \\ \text{Tok} & \dot{q} > 0 \end{array}$$

("1st reconnection")

$\beta \neq 0$

model: p = const, [redacted]

$$\frac{\partial}{\partial t} p = -v \cdot \nabla p - \Gamma p \nabla \cdot v + (\Gamma - 1)\eta J^2 + \nabla \cdot \chi \cdot \nabla p$$

$$v = \left(\nabla U - \frac{\partial A}{\partial t}\right) \times B / \bar{B}^2 + V_{\parallel} \underset{\sim}{B} / \bar{B}$$

Mean field

$$\bar{J} \times \bar{B} \cdot \nabla r = \frac{d\bar{p}}{dr}$$

$$\dot{\bar{\psi}} = \alpha + (E_z B_z - \eta \bar{J} \cdot \bar{B}) / \bar{B}^2$$

$$\frac{\partial \bar{p}}{\partial t} = -\nu \bar{B}^2 + (\Gamma - 1)\eta \bar{J}^2 + \frac{1}{r}\frac{\partial}{\partial r} r \chi_{\perp} \frac{d\bar{p}}{dr}$$

$$\mathcal{L}(\dot{\bar{x}}) = \mathcal{G}(\dot{\bar{\psi}}, \dot{\bar{p}})$$

$$\nu = +\overline{\bar{v} \cdot \nabla \bar{p}} + \Gamma \bar{p}\, \nabla \cdot \bar{v}$$
$$+ \hat{v} \cdot \nabla \hat{p} + \Gamma \overline{\hat{p}\, \nabla \cdot \hat{v}} - \frac{1}{r}\frac{\partial}{\partial r} r \frac{\chi_{\parallel} \overline{B \cdot \nabla p\, \bar{B}_r}}{B^2}$$

Fluctuations

$$\frac{\partial}{\partial t}\hat{\psi} = \frac{B \cdot \nabla u}{\bar{B}^2} + \eta\hat{\sigma}$$

$$\left(\frac{1}{r^2}\frac{\partial^2}{\partial\theta^2} + \frac{\partial^2}{\partial z^2}\right)\hat{\varphi} = \underset{\sim}{\bar{B}} \cdot \nabla\left(\frac{\partial\hat{\psi}}{\partial r} - \frac{\bar{p}'}{\bar{B}^2}\hat{\psi}\right) + \underset{\sim}{\bar{B}} \times \nabla r \cdot \nabla\hat{p}$$

$$\frac{d}{dt}\nabla \cdot \frac{\bar{\rho}}{\bar{B}^2}\nabla\hat{u} = \underset{\sim}{B} \cdot \nabla\hat{\sigma} + \hat{B}_r\left(\bar{\sigma}' - \frac{2\bar{\sigma}}{\bar{B}^2}\bar{p}'\right)$$
$$+ \frac{2\bar{B}_\theta^2}{r\bar{B}^4}\nabla r \times \bar{B} \cdot \nabla\hat{p}$$

$$\frac{\partial}{\partial t}\hat{p} = -\frac{\nabla p \times \nabla u \cdot \bar{B}}{\bar{B}^2} - \Gamma\bar{p}\,\nabla \cdot \hat{v}_\perp - \frac{\Gamma\bar{p}}{\bar{B}}\underset{\sim}{B} \cdot \underset{\sim}{\nabla}\hat{v}_\parallel$$
$$+ \chi\nabla_\perp^2\hat{p} + B \cdot \nabla\left(\frac{\chi_\parallel}{\bar{B}^2}B \cdot \nabla p\right)$$

$$\bar{\rho}\frac{d}{dt}v_\parallel = -B \cdot \nabla p / \bar{B}$$

$\beta \neq 0$ Numerical example

shows effect of ν

$\chi_{\parallel} = 0 \quad \chi_{\perp} = 4\eta = \text{const}$

Initially $\alpha = \nu = 0$, $\beta = 0.8$, $B_z(0) = 1$

$t = 100 \qquad \beta = 0.3$, $B_z(0) = 1.3$

dynamo

INITIAL EQUILIBRIUM

$T=0 \quad \beta_0 = 80\%$

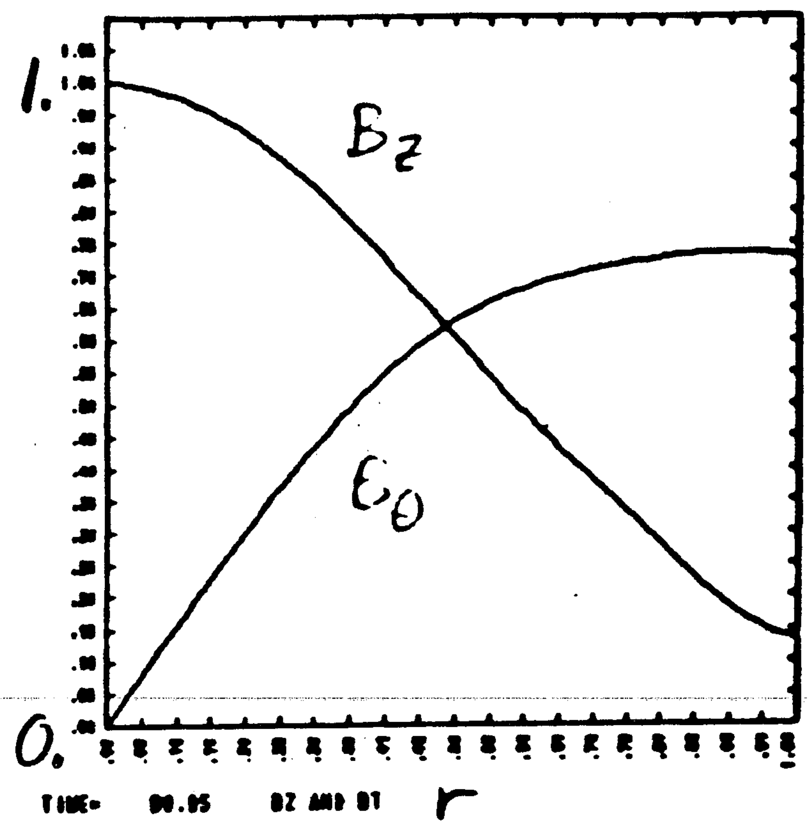

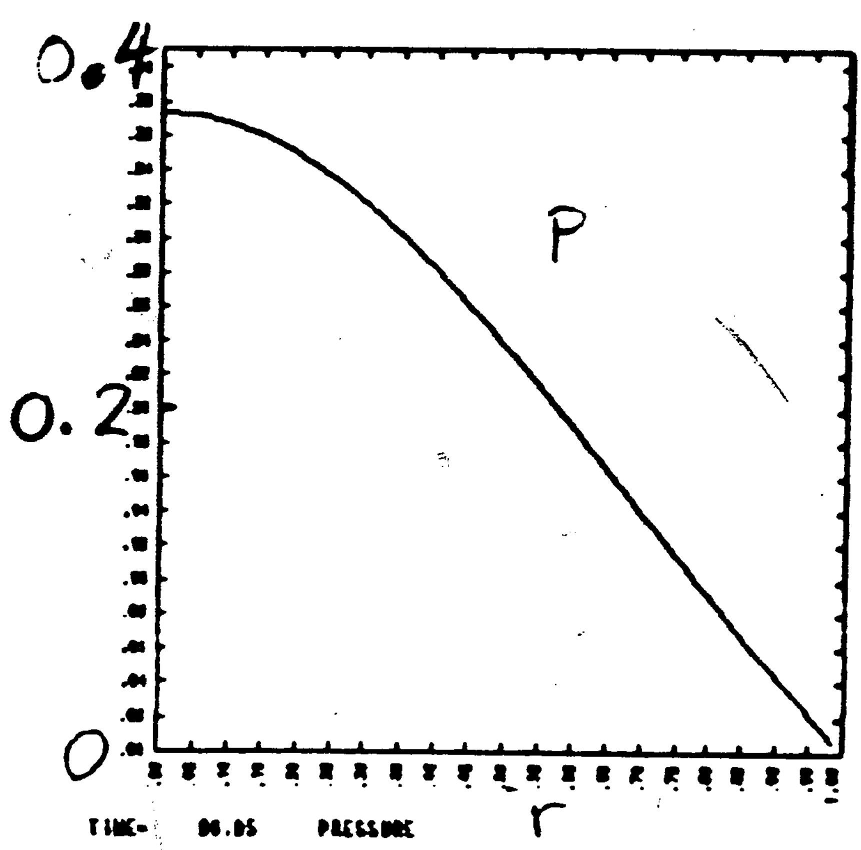

T = 100 ($\eta = 10^{-3}$) $\beta_0 = 30\%$

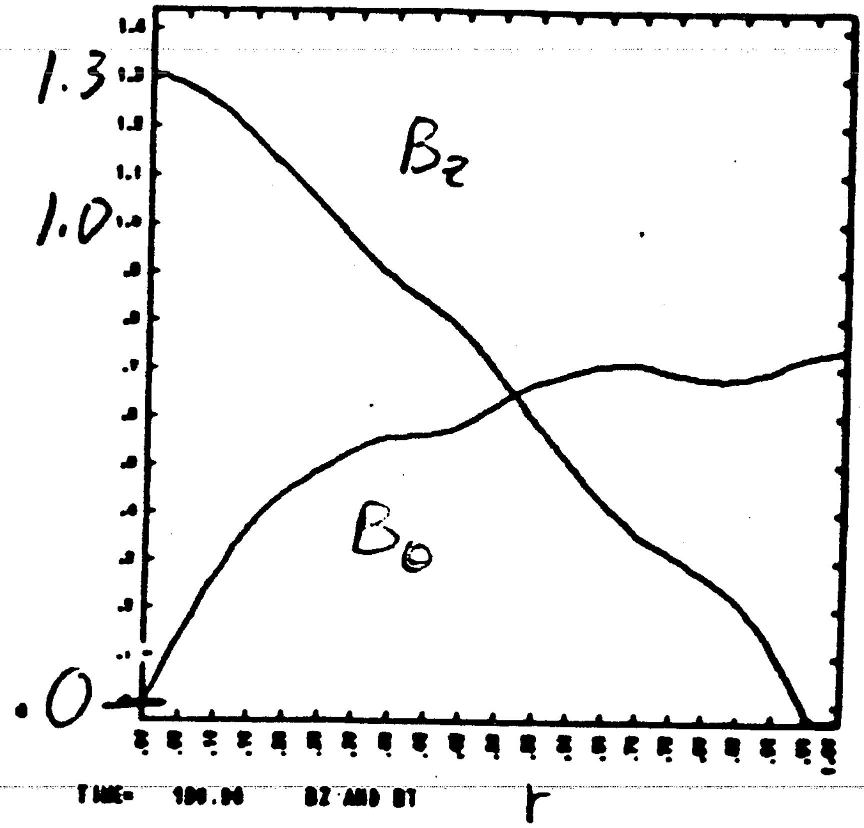

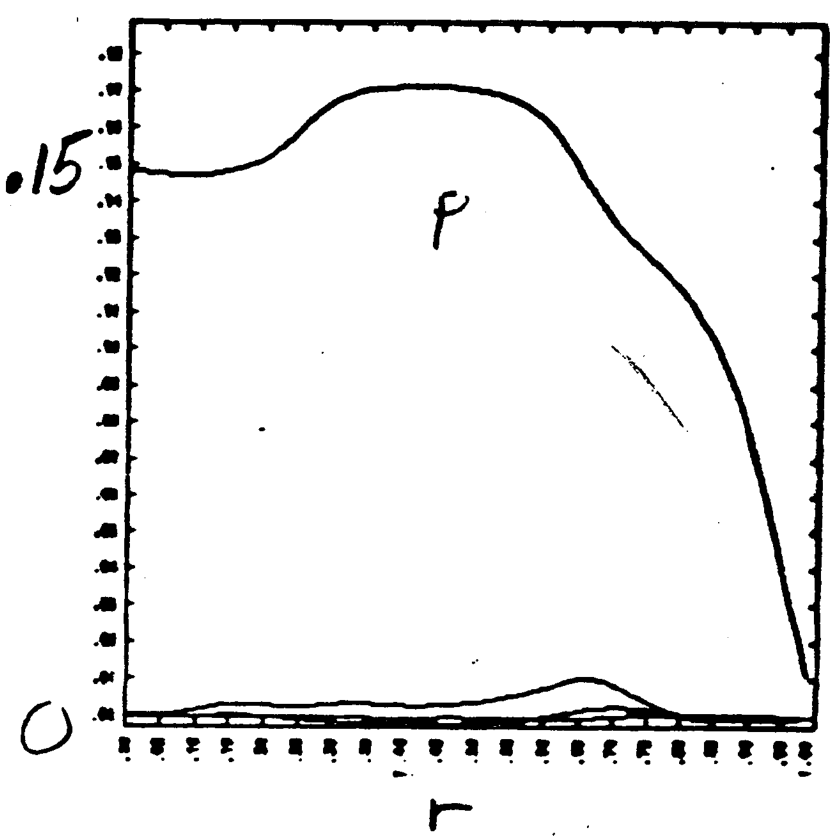

current

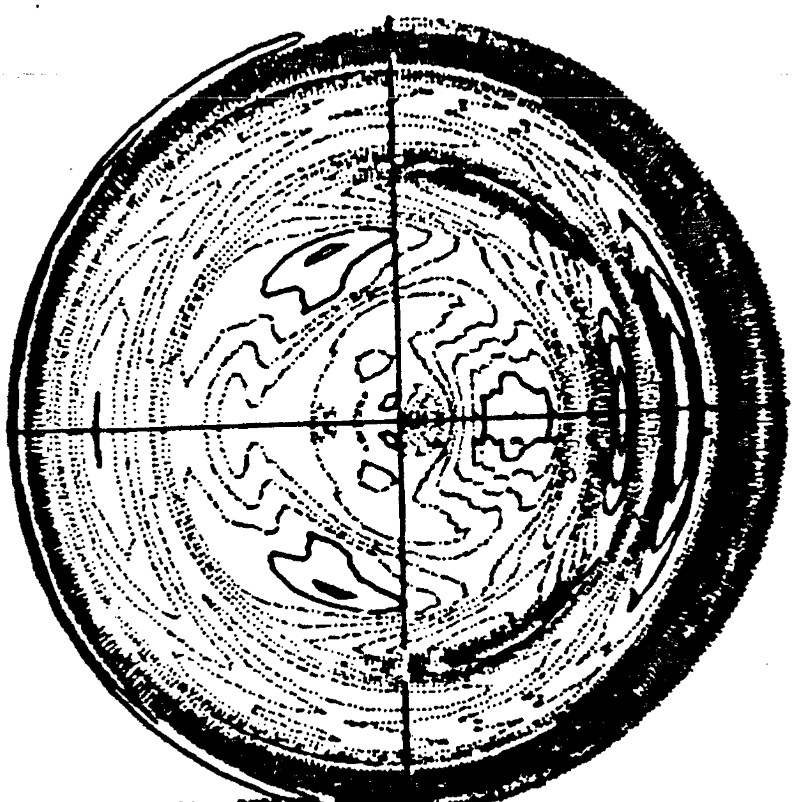

pressure

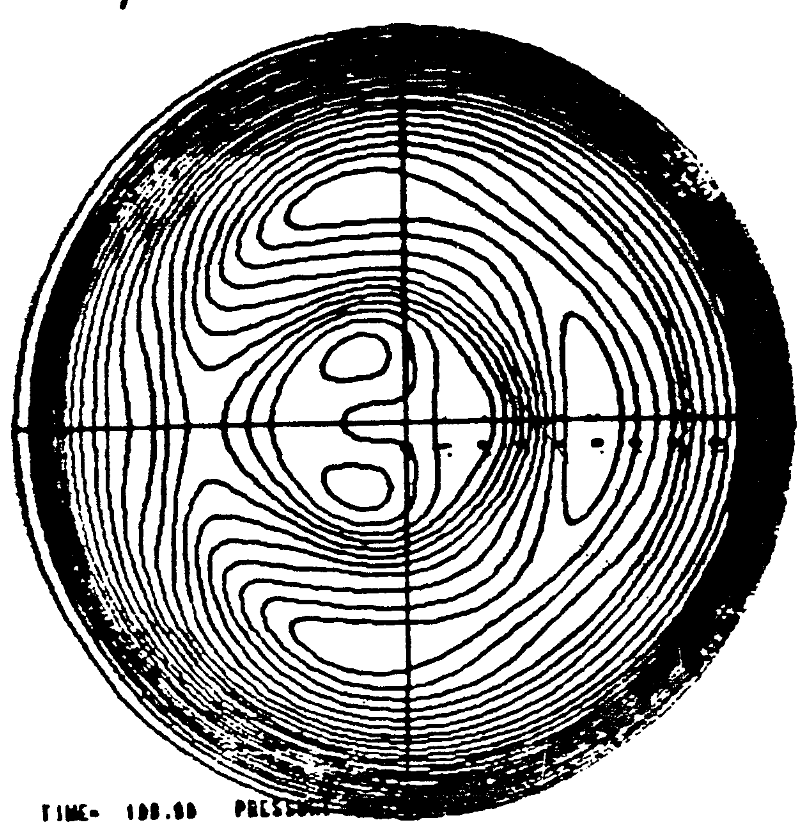

Energy vs time

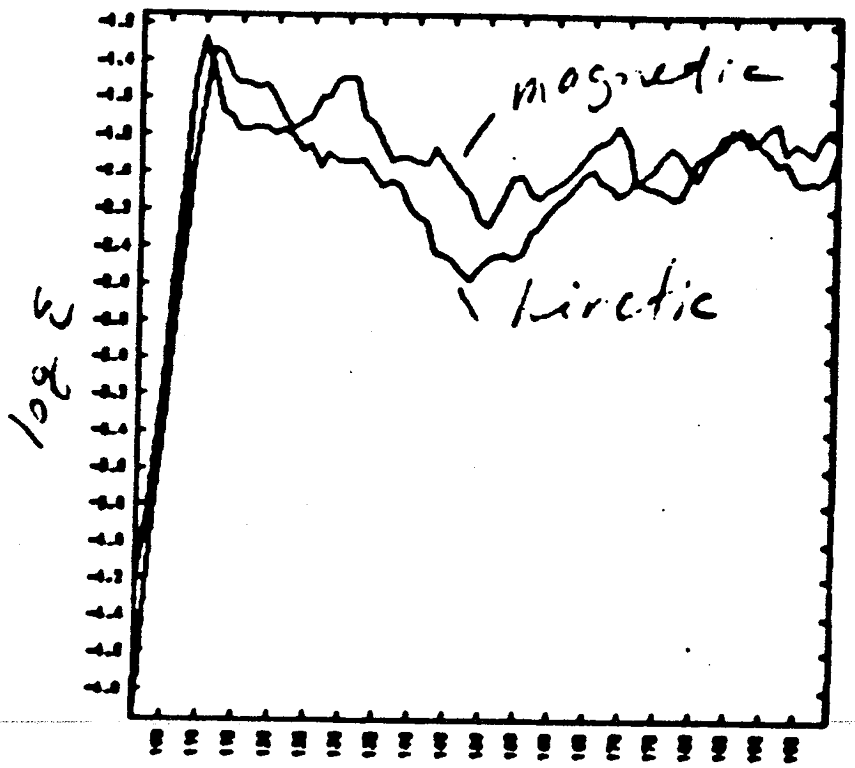

P.E. AND K.E. VS. TIME

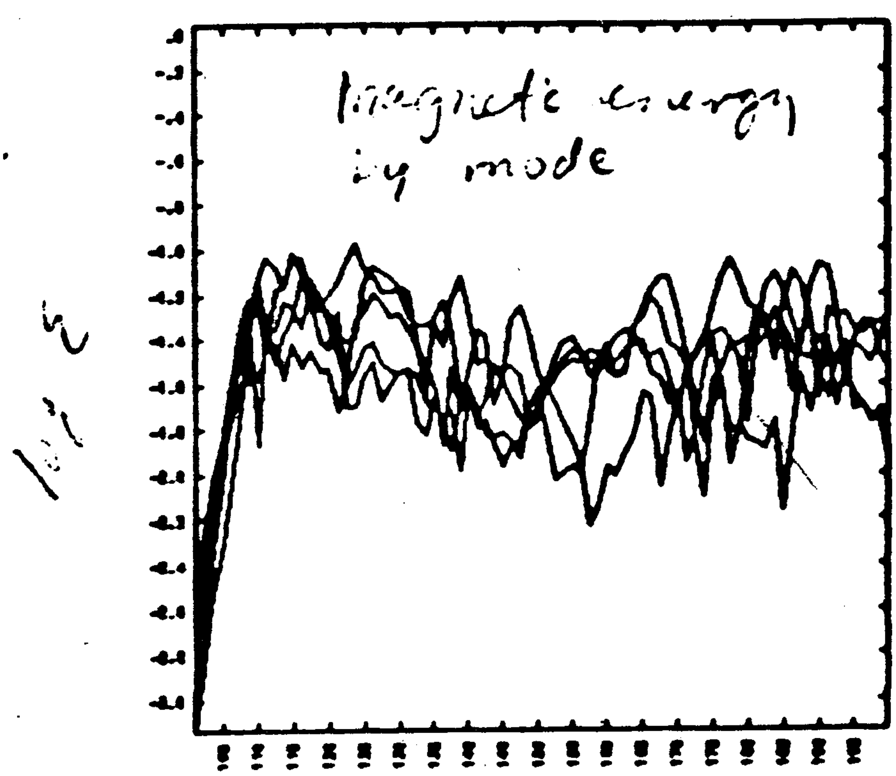

LOG(P.E.) VS. TIME

p(0) vs time

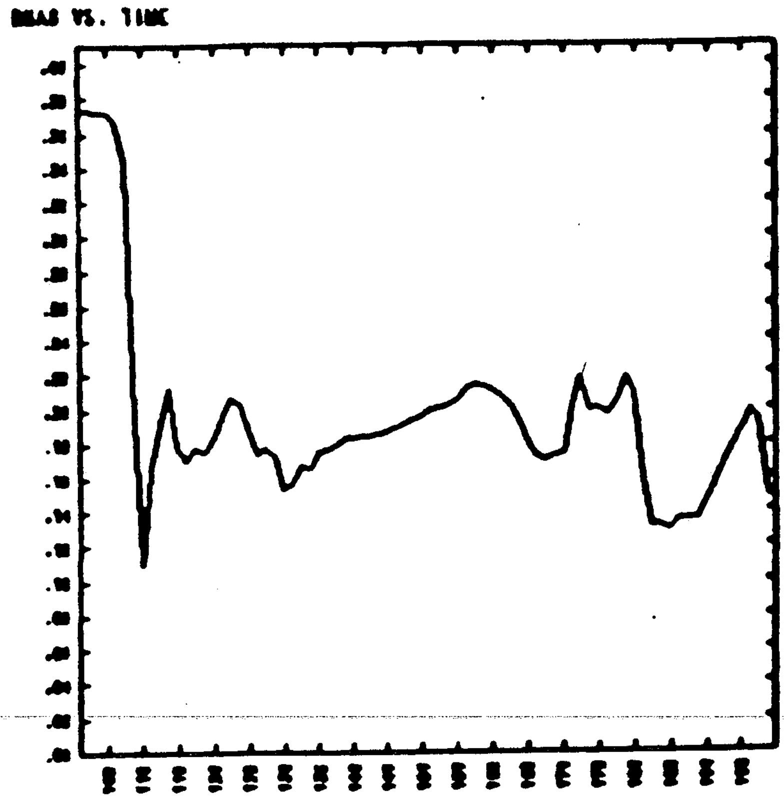

P(0) VS. TIME

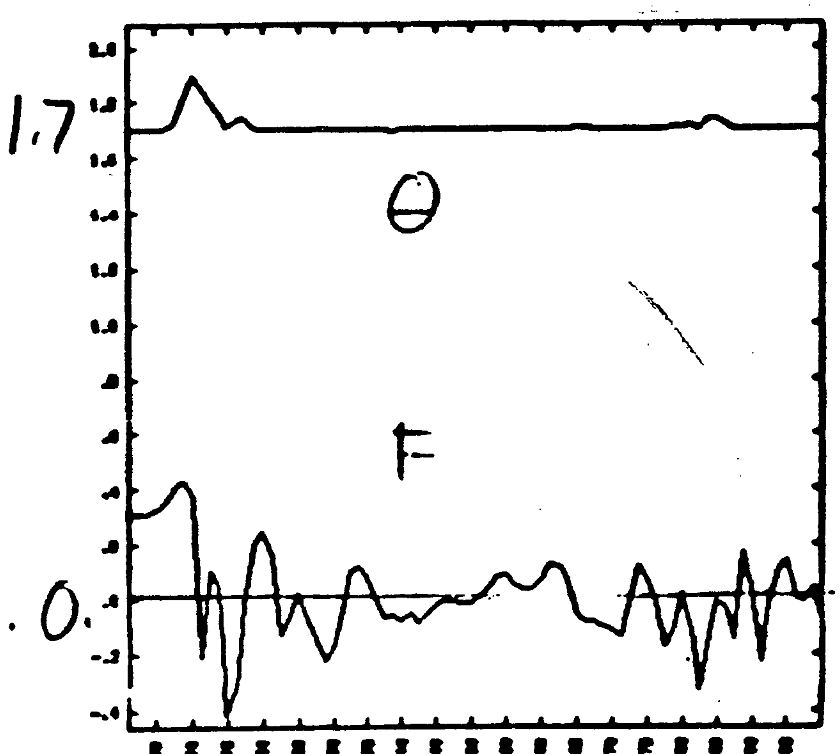

THETA AND F VS. TIME

NONLINEAR EVOLUTION OF TEARING MODES IN REVERSED FIELD PINCHES

T. AMANO

NAGOYA UNIVERSITY

Nonlinear Evolution of Tearing Mode in Reversed Field Pinches

H. Ashida*, Y. Maejima*, A. Nagata**, T. Amano

*Electrotechnical Laboratory

**Fac. of Eng., Hiroshima Univ.

Institute of Plasma Physics, Nagoya Univ.

~~1). What is RFP~~ ?

~~present status of experiment and theory~~

1). Code description, test,

comparison with other simulations

2). Ergodic Field Lines, K-S entropy,

Diffusion.

3). Dynamo Effect

4). Discussion.

Basic Equations

$$\frac{\partial}{\partial t}\underset{\sim}{v} = -\underset{\sim}{v}\cdot\nabla\underset{\sim}{v} - \nabla p + S^2 \underset{\sim}{j}\times\underset{\sim}{B}$$

$$\frac{\partial}{\partial t}\underset{\sim}{\omega} = \underset{\sim}{\omega}\cdot\nabla\underset{\sim}{v} - \underset{\sim}{v}\cdot\nabla\underset{\sim}{\omega} + S^2(\underset{\sim}{B}\cdot\nabla\underset{\sim}{j} - \underset{\sim}{j}\cdot\nabla\underset{\sim}{B})$$

$$\underset{\sim}{\omega} = \mathrm{rot}\,\underset{\sim}{v}$$

$$\mathrm{div}\,\underset{\sim}{v} = 0$$

$$\frac{\partial}{\partial t}\underset{\sim}{B} = \underset{\sim}{B}\cdot\nabla\underset{\sim}{v} - \underset{\sim}{v}\cdot\nabla\underset{\sim}{B} - \mathrm{rot}\,\eta\,\underset{\sim}{j}$$

$$\underset{\sim}{j} = \mathrm{rot}\,\underset{\sim}{B}$$

$S = \tau_r/\tau_A$ at Plasma Center

$\tau_r = 4\pi a_w^2/C^2\eta$: Resistive Diffusion Time

$\tau_A = a_w\sqrt{4\pi\rho}/B_0$: Alfvén Transit Time

$$\nabla^2 p = -\nabla\cdot(\underset{\sim}{v}\cdot\nabla\underset{\sim}{v}) + \nabla\cdot[S^2(j\times B)]$$

cylindrical approx.

Mode Expansion

We use the cylindrical coordinates ;

$$(r, \theta, \zeta), \quad \zeta = z/R$$

(i) $f_{m,n}(r)\cos(m\theta + n\zeta)$

$$v_r, \ \omega_\theta, \ \omega_\zeta$$

$$B_\theta, \ B_\zeta, \ j_\theta, \ j_\zeta$$

(ii) $f_{m,n}(r)\sin(m\theta + n\zeta)$

$$v_\theta, \ v_\zeta, \ \omega_r$$

$$B_r, \ j_r$$

(iii) $m > 0 \quad (-\infty < n < +\infty)$

$m = 0 \quad n < 0$

$$\underset{\sim}{v}_{m=n=0} = 0 \quad (\mathrm{div}\, \underset{\sim}{v} = 0)$$

Boundary Conditions

$r = a$

$$v_r = 0\,,$$
$$\underset{\sim}{n} \times \underset{\sim}{w} = 0$$
$$B_r = 0$$
$$\underset{\sim}{n} \times \underset{\sim}{j} = 0$$

$$B_{\theta 0}(a) = \text{const.}$$
$$B_{\varphi 0}(a) = \text{const.}$$

VII Resistivity

$$\eta_{\alpha\beta} = \eta_\perp - \eta_\parallel \frac{B_\alpha B_\beta}{B^2}$$

$$\eta_\perp = 2\eta_\parallel$$

$$\underline{E_\zeta = \eta_\parallel(0)\, j_\zeta(0) = \eta_{\zeta\zeta}\, j_\zeta + \eta_{\zeta\theta}\, j_\theta}$$

($\eta_\parallel, \eta_\perp$ are independent of time.)

or $\quad \eta_\perp = 2\eta_\parallel = \text{const (in } r)$

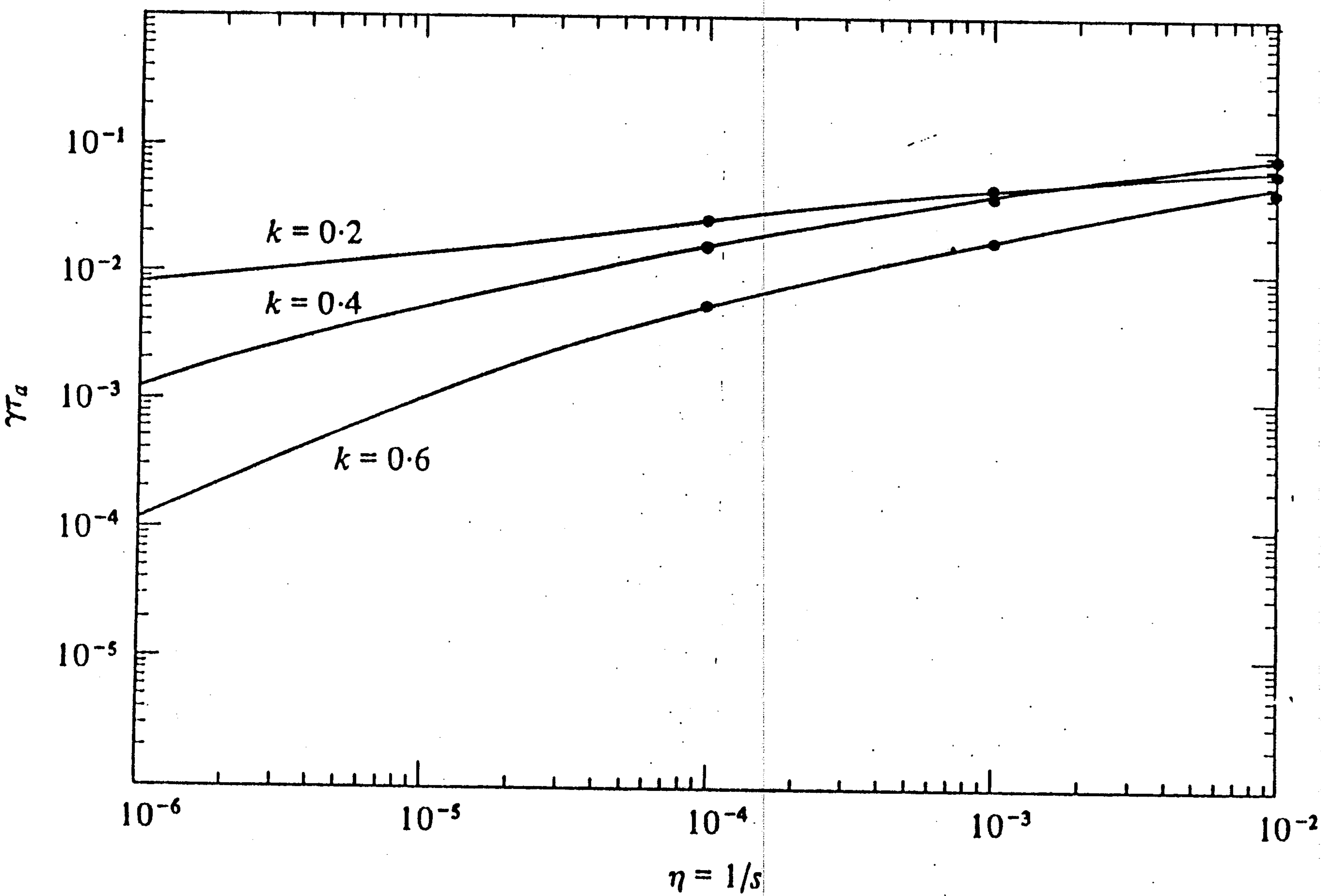

Growth rate γ *versus* S for $m = 1$ and $\beta = 0$.

J. P. Freidberg & D.W. Hewett, J. Plasma Physics (1981) 26, 1 pp. 177-192.

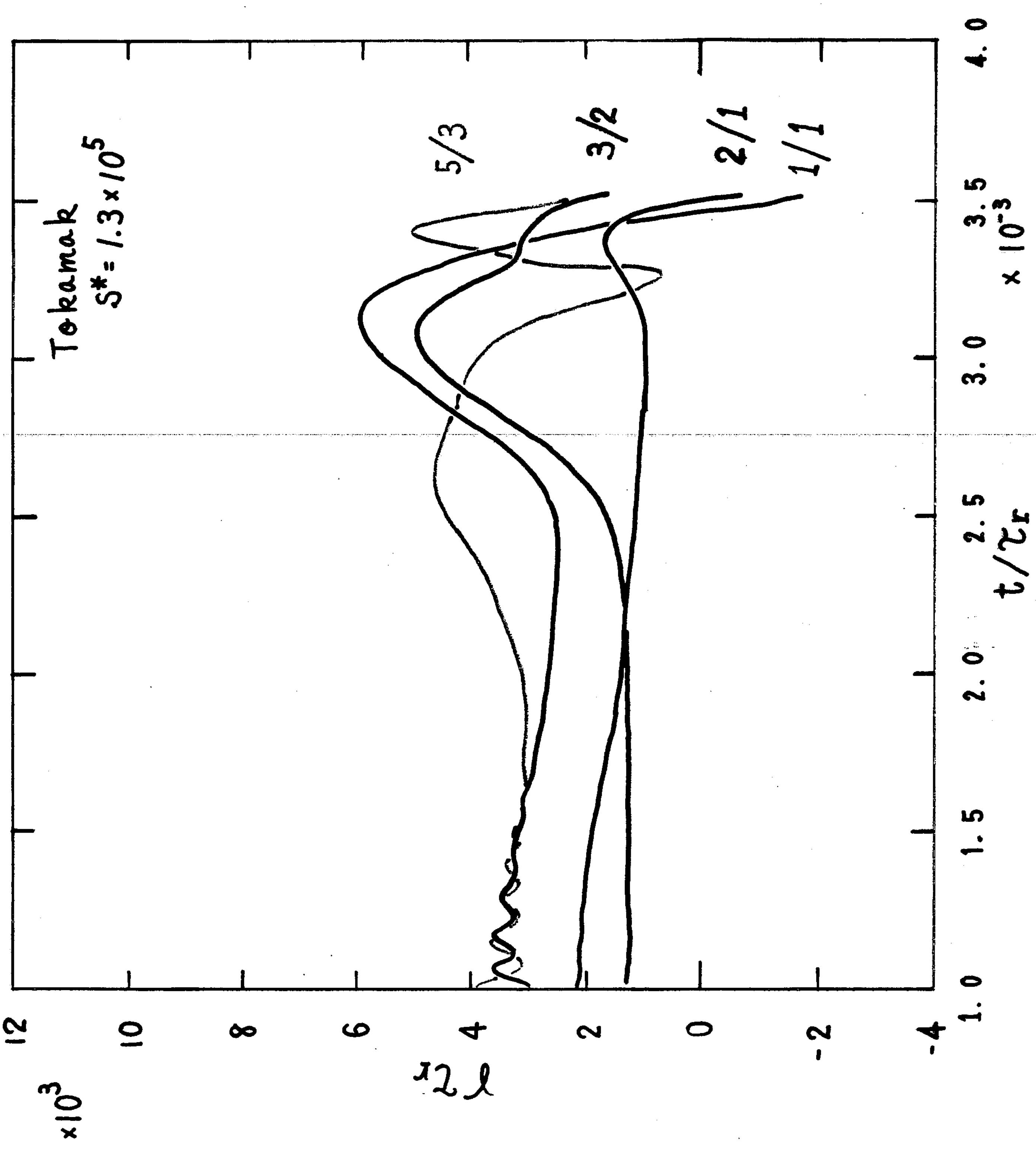
Tokamak
S* = 1.3 × 10^5
5/3
3/2
2/1
1/1
12
10
8
6
4
2
0
-2
-4
×10^3
γτ_r
1.0
1.5
2.0
2.5
3.0
3.5
4.0
t/τ_r
× 10^-3

Caramana, Nebel, Shanak, Phys. Fluids 26 1305(1983).

Holmes, Carreras et al. ORNL/TM-9148(1984).

$q(r) = 0.1225(1-1.87r^2 + 0.8323r^4)$.

$\beta = 0$.

$q(0) = 0.1225 > q(r) > q(1) = -0.005145$.

field reversal surface $r = 0.93$.

 decaying mag. field.

Results. (imcompressible case).

1) m/n = 1/10 single helicity

complete reconnection of the magnetic island and expulsion of the magnetic axis followed by a slow, second reconnection and the re-emergence of the original magnetic axis.

2) m/n = 1/11 single helicity

the magnetic islands saturates without expulsion of the magnetic axis.

Electron Heat Transport in a Tokamak with Destroyed Magnetic Surfaces ;

Rechster, Rosenbluth, P.R.L 40 38 (1978).

White, Handbook of Plasma Physics, vol. I (1983), North-Holland Publishing Co.

$$\vec{B} = B_z \vec{z} + B_\theta(r)\vec{\theta} + \delta\vec{B}$$

$$\delta\vec{B} = \sum \vec{b}_{mn}(r) \exp\left[i\left(m\theta - n\frac{z}{R}\right)\right] + \text{C.C.}$$

island width

$$\Delta_{mn} = 4\left[2\frac{R}{m} \Big/ \frac{|b_{mn}(r)|}{B_z}\left(\frac{dL}{dr}\right)\Big|_{r=r_{mn}}\right]^{\frac{1}{2}}$$

stochasticity parameter

$$S = \frac{1}{2}\left(\Delta_{mn} + \Delta_{m'n'}\right) \Big/ |r_{mn} - r_{m'n'}|$$

$\underline{S > 1}$

$$\boxed{l(z) = l_0 \exp(z/L_c)}$$

diffusion of field lines

$$\langle (\Delta r)^2 \rangle = 2L D_{st}$$

$$D_{st}(r) = \pi R \sum_{m,n} \frac{b_{mn}(r)}{B_z^2} \delta\left(\frac{m}{q(r)} - n\right)$$

Rechster, Rosenbluth, White, *Phys. Rev. Lett.*

$$h = \frac{1}{L_c} = \lim_{z\to\infty} \lim_{d_0\to 0} \left[\frac{1}{z} \ln\left(\frac{d(z)}{d_0}\right)\right]$$

$$\boxed{h = \frac{1}{4}\frac{\left(\frac{2}{3}\right)!}{\left(\frac{1}{3}\right)!}(3D_{st})^{\frac{1}{3}} = 0.3645\, D_{st}^{\frac{1}{3}}}$$

direct measurement of D_{st}

$$\boxed{D_{st} = \lim_{\substack{z\to\infty \\ L\to\infty}} \frac{1}{Lz}\sum_{n=1}^{L} x_n^2}$$

$$x_n = r - r_0$$

$$\boxed{\chi_r = \langle(\Delta r)^2\rangle/2\tau = D_{st}\, v_{the}}$$

for $\lambda \gg L_c$ Collision-less case

K-S Entropy

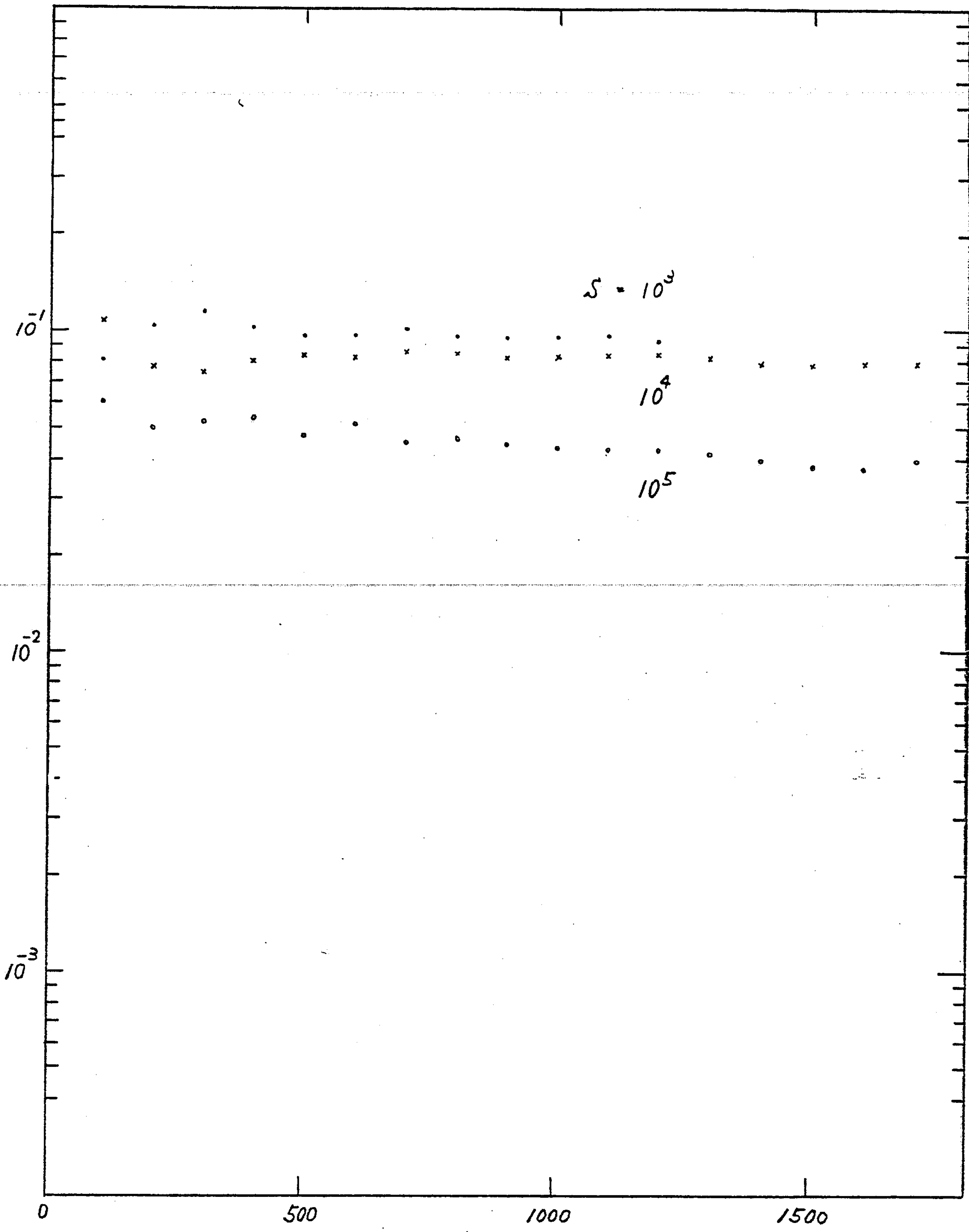

HBTX-1A :

$a = 26$ cm

$T_e = 100 - 200$ eV

$n_e = 10^{13} - 10^{14}$ cm^{-3}

$B = 10^3$

$S = 10^5$

$\tau_E = a^2/4\chi_r = 26^2/\ 4 \times 20 \times (4 \times 10^{-2})^3 v_{the}$

$= 1.3 \times 10^{-4}$ sec

$B_z(\text{bias}) = 500$ Gauss

$B_z(\text{reverse}) = -120$ Gauss

$B_\theta(a) = 1.54$ kG at $I_p = 200$ kA

Robinsons Model

Initial Equilibrium

safety factor q

Suydam parameter $C1$

(Suydam condition $C1 < 1/8$)

$$q(r) = \frac{S_0}{R}\left(1 + \frac{r^2}{\alpha} + \frac{r^4}{\beta} + \frac{r^6}{\gamma} + \frac{r^8}{\delta}\right)$$

$$C1(r) = -\frac{4\pi p'}{r B_\rho^2}\left(\frac{q}{q'}\right)^2 = c_0\left(1 + c_1 r^2 + \cdots\right)$$

$$B_\rho(r) = \frac{q(r)}{q(0)} \exp\left\{\int_0^r \frac{R^2}{q^2R^2 + r^2}\left(C1\, r q'^2 - q q' - \frac{2r}{R^2}\right)\right\}$$

$S_0 = 2,\ \alpha = -8,\ \beta = -400,\ \gamma = 2450,\ \delta = -110000$

$C_0 = 0.19;\quad C_1 = -0.85$

$$\boxed{\begin{array}{ll} \text{Plasma radius} & = 4.2 \\ \text{Aspect ratio} & = 4 \end{array}}$$

$S = 10^5,\ \beta = 8.2\%,\ F = -0.83,\ \theta = 2.87$

$\eta_\perp = 2\eta_\parallel,\quad \eta_\parallel = 1$

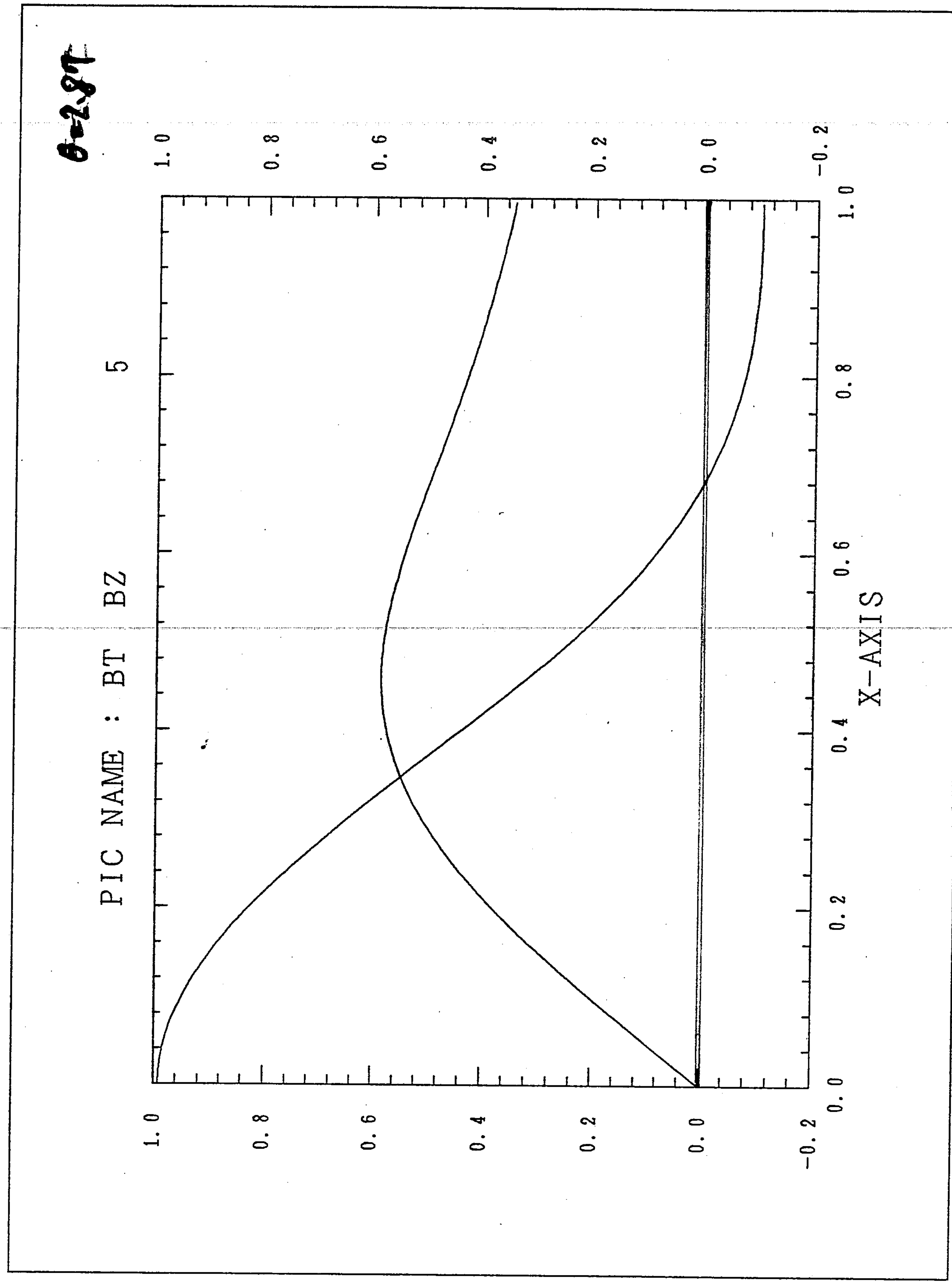

700

MODE NO.	M	N
	0	0
	1	-9
	2	-18
	3	-27
	1	-10
	2	-20
	3	-30
	1	-11
	2	-22
	3	-33
	1	-12
	2	-24
	3	-36
	1	-13
	2	-26
	3	-39
	2	-19
	2	-21
	2	-23
	2	-25
	3	-21
	3	-22
	3	-23
	0	-1
	0	-2
	0	-3
	0	-4

700

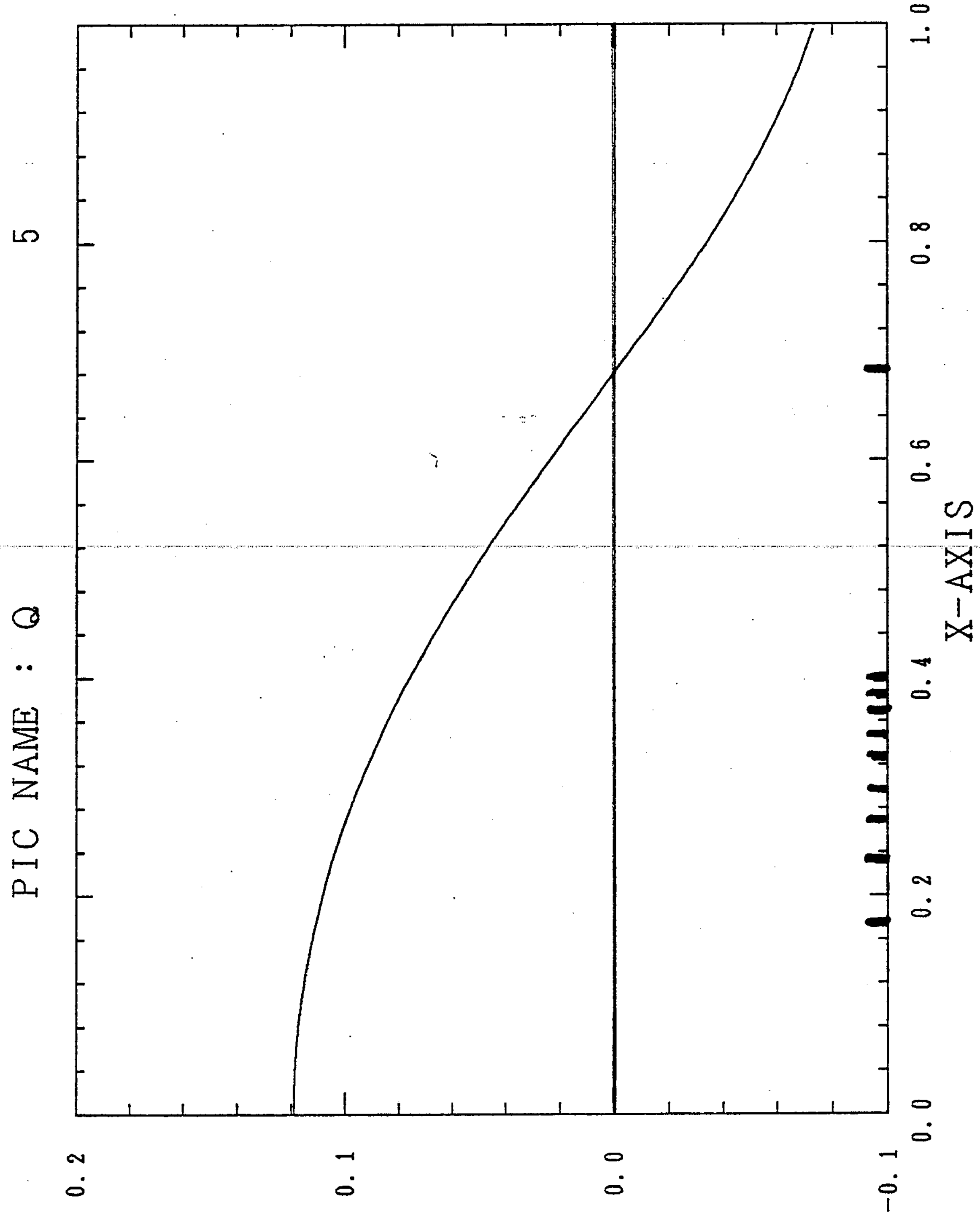

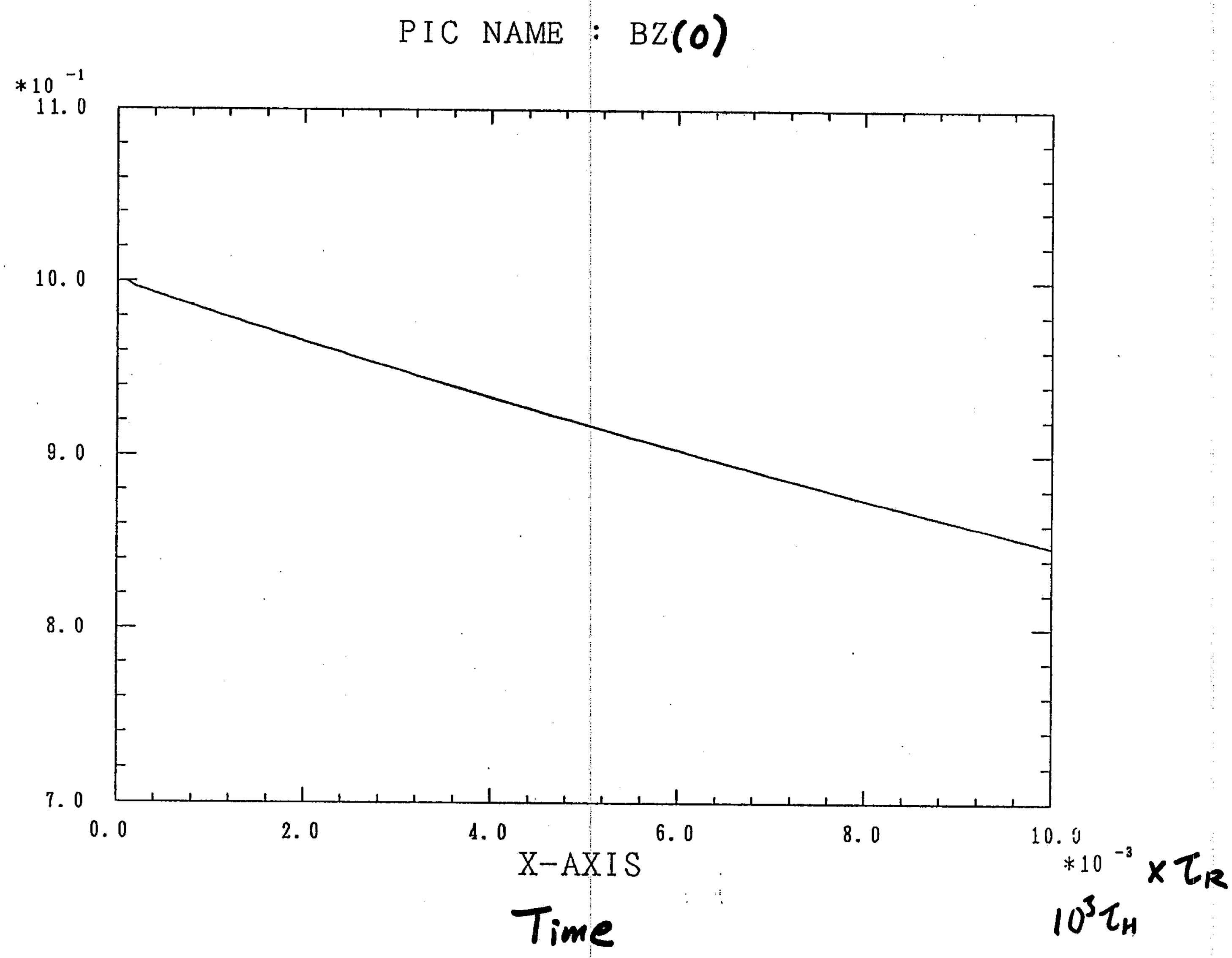

PIC NAME : BZ(0)
*10 -1
11.0
10.0
9.0
8.0
7.0
0.0
2.0
4.0
6.0
8.0
10.0
X-AXIS
*10 -3
Time
× τR
10³ τH

500

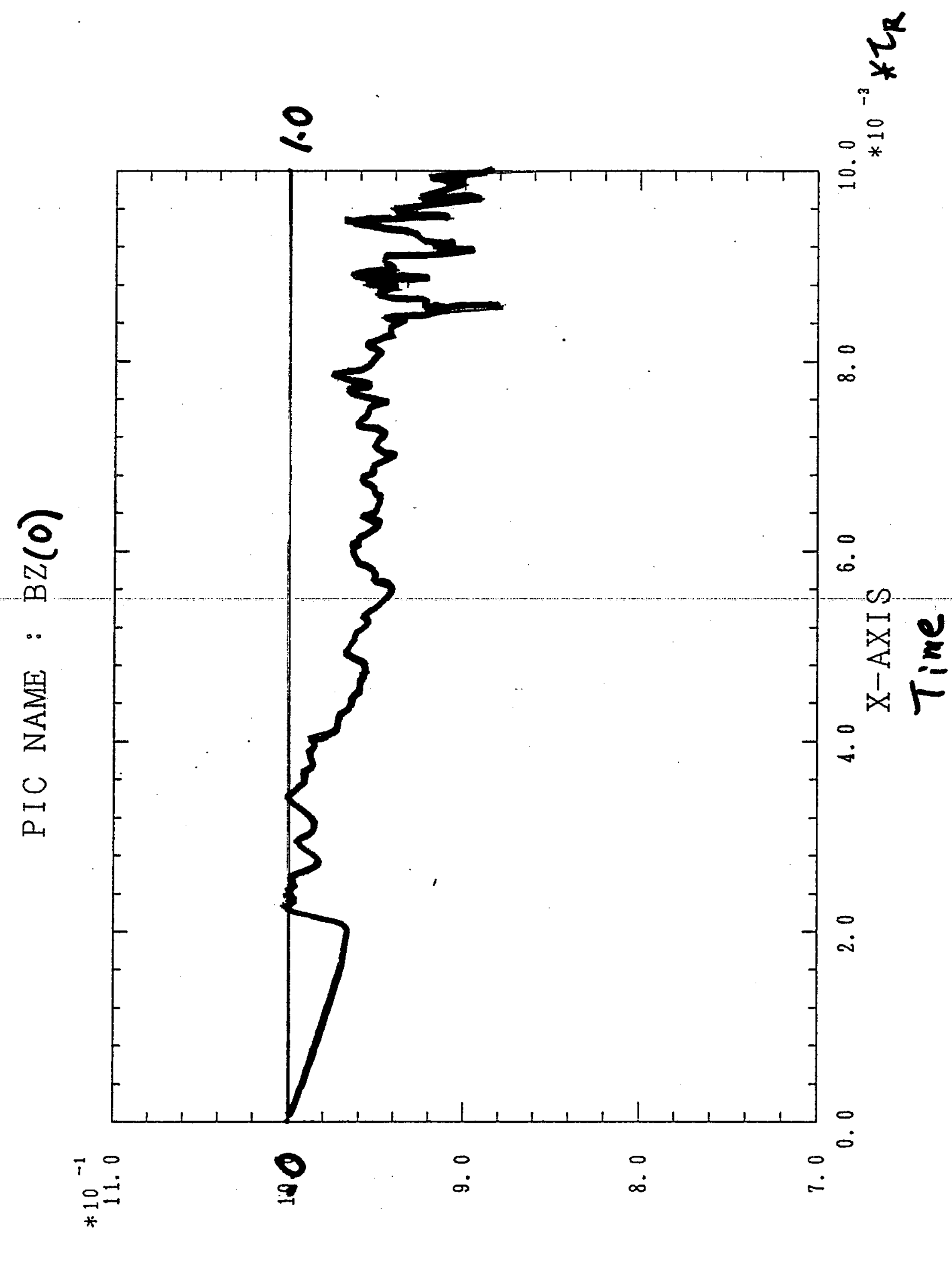
PIC NAME : BZ(0)
X-AXIS
Time
*10 -3 *τR
0.0
2.0
4.0
6.0
8.0
10.0
1.0
*10 -1
11.0
10.0
9.0
8.0
7.0

$\Phi = \frac{2}{a^2}\int_0^a r B_s \, dr$

PIC NAME : RTFL(t) = $\Phi(t)/\Phi(0)$

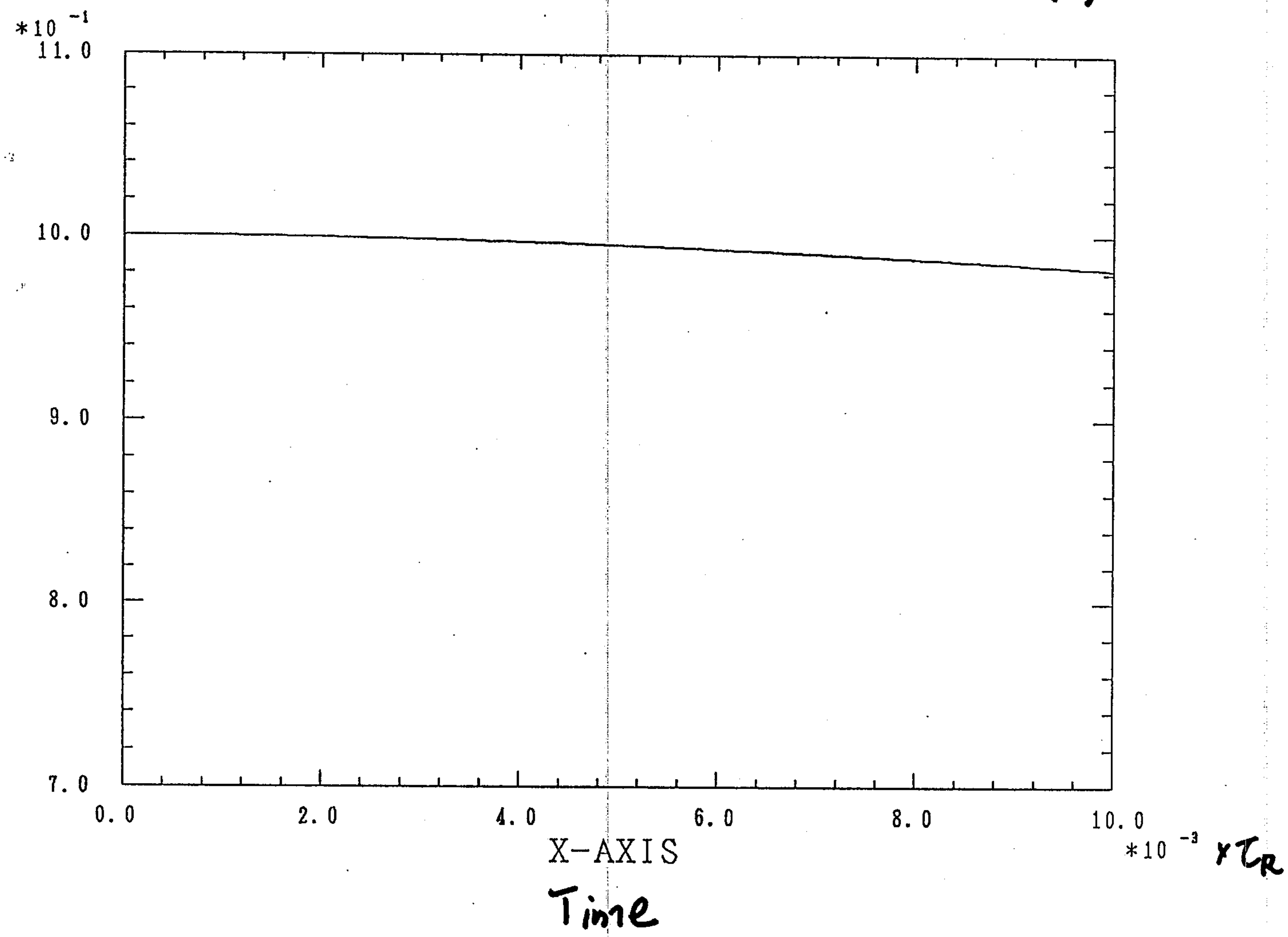

500

PIC NAME : RTFL

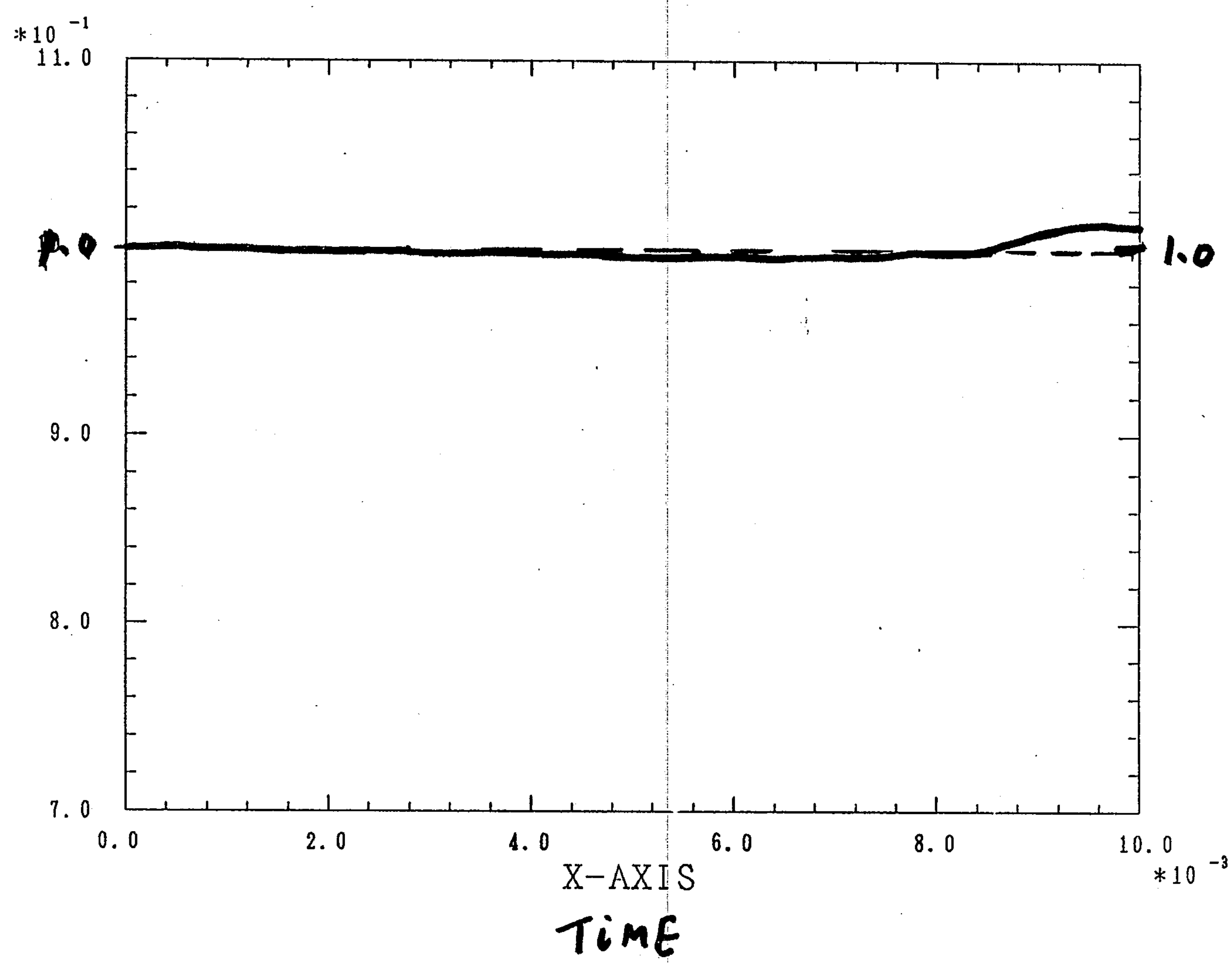

70

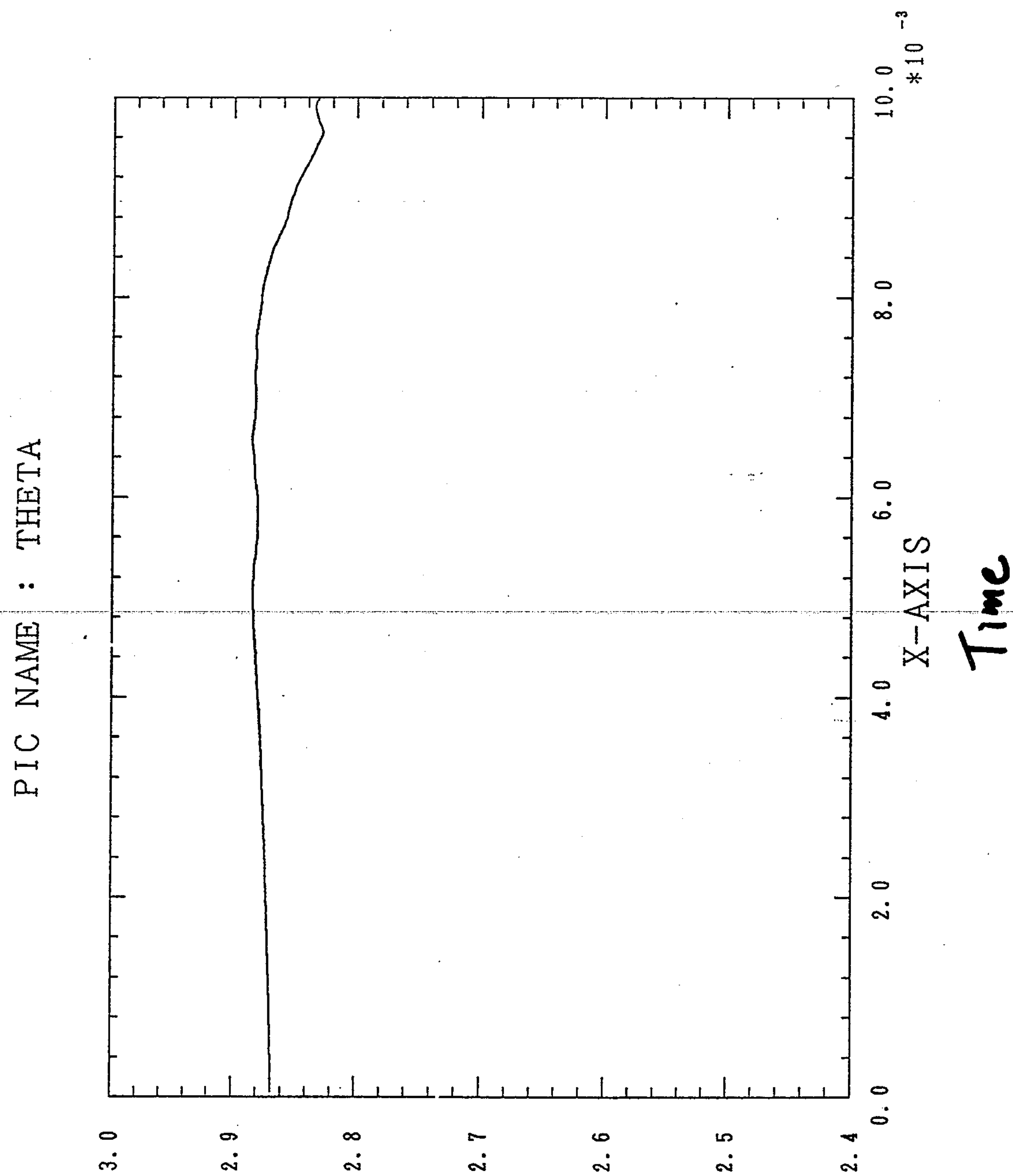
PIC NAME : THETA
X-AXIS
Time
*10 -3
0.0
2.0
4.0
6.0
8.0
10.0
3.0
2.9
2.8
2.7
2.6
2.5
2.4

q(0)

PIC NAME : Q0

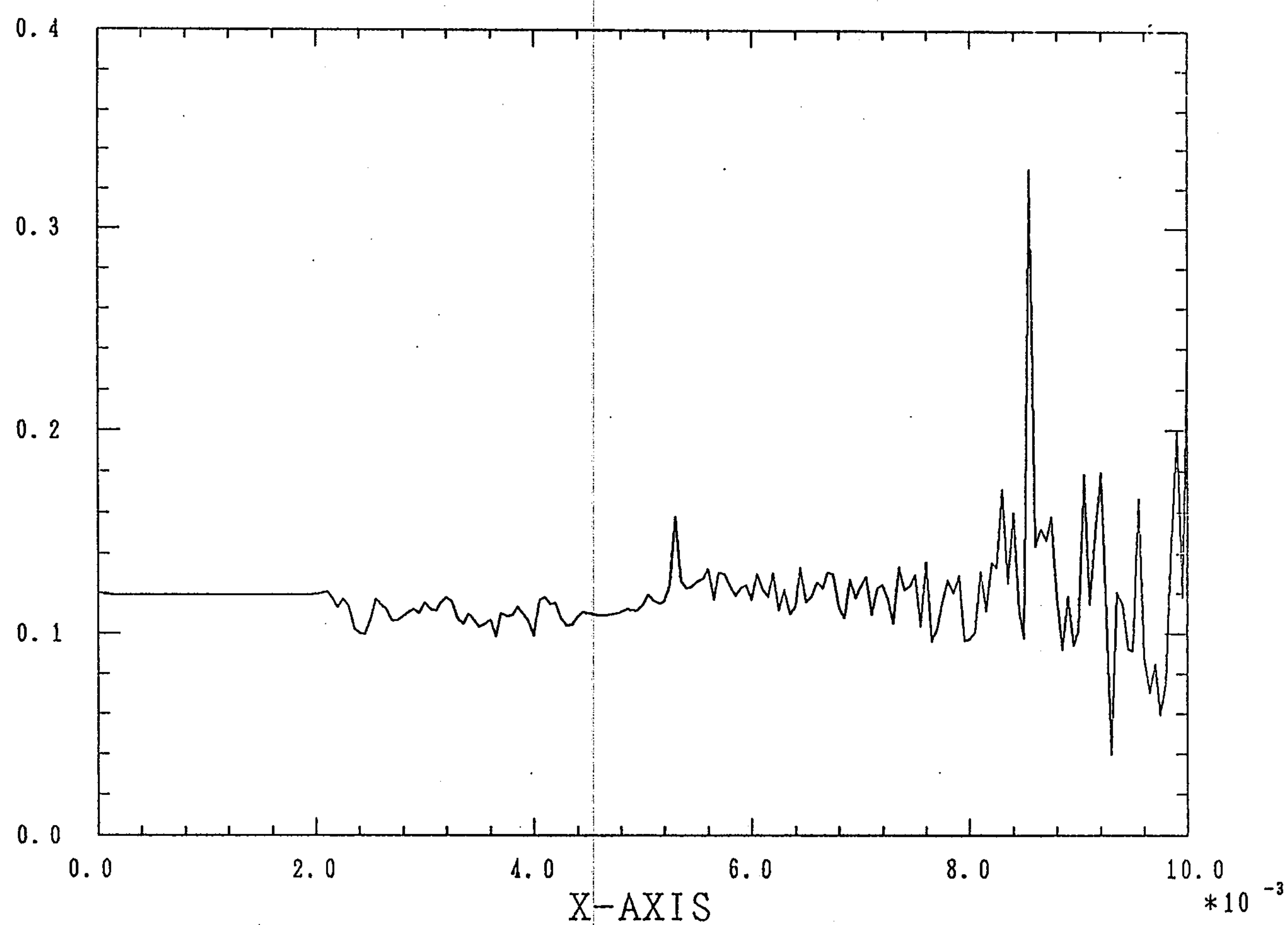

Time

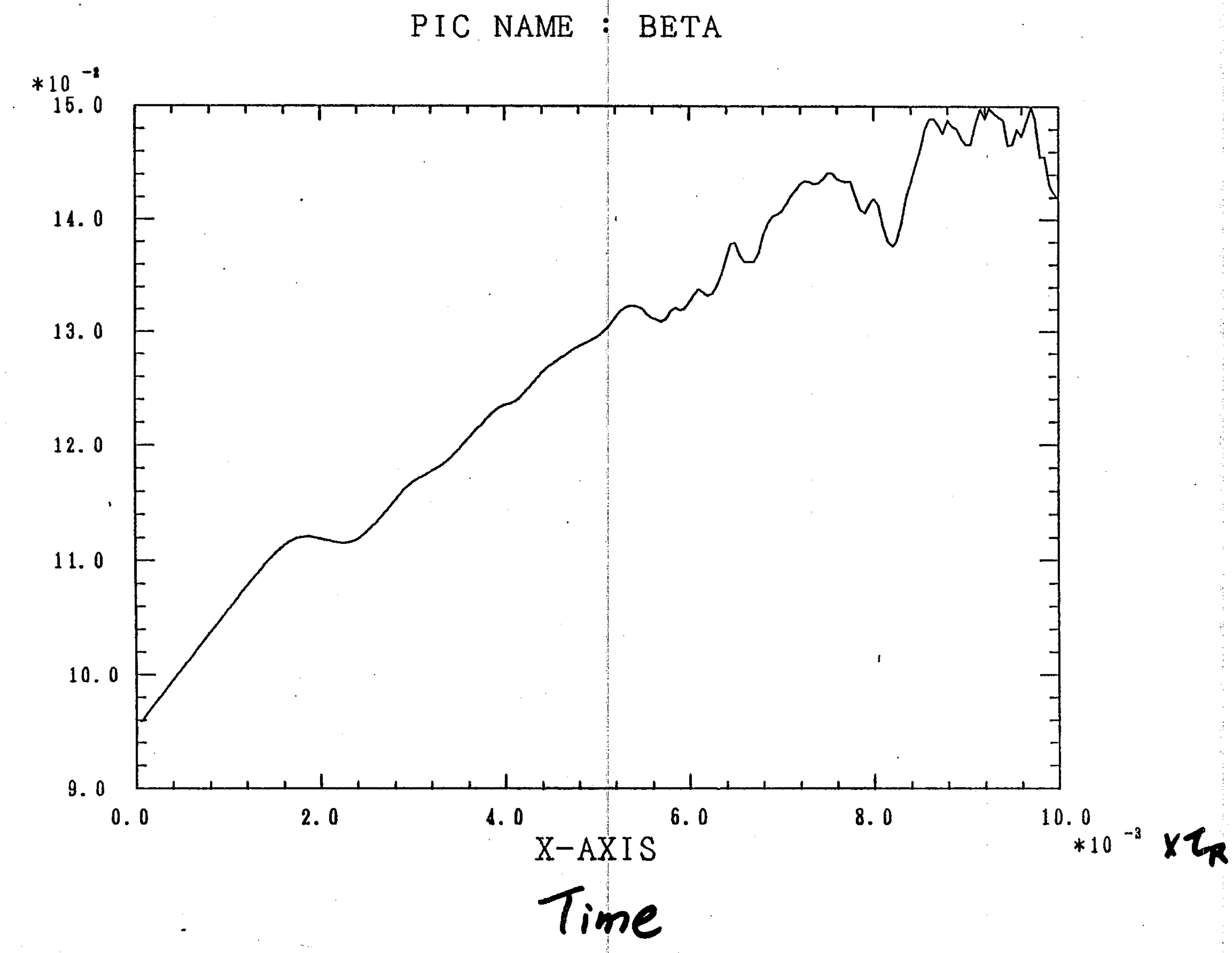
PIC NAME : BETA
*10 ⁻²
15.0
14.0
13.0
12.0
11.0
10.0
9.0
0.0
2.0
4.0
6.0
8.0
10.0
*10 ⁻³
X-AXIS
Time

706

Discussion

1) K-S entropy Diffusion

D measurement.

2) more modes. -------- pseudo-spectral code.

3) dynamo effect. lower Θ model.

4) div v $\neq$ 0.

energy equation.

Joule heating, anomalous loss.

MAGNETIC RECONNECTION IN TOKAMAKS

W. PARK

PRINCETON PLASMA PHYSICS LAB

Magnetic Reconnection in Tokamaks

W. Park
D. Monticello
R. White

Outline

- Ways of Reconnection.
  Reconnection rate $\dot{\psi}_s(\eta, \mu)$.
- Comparison with numerical simulation results.
  - external coil driven reconnection
  - $m=1$ nonlinear internal kink.
  - $m=2$ nonlinear tearing mode.
- Application and comparison with tokamak experiment.
- Simulation of enhanced (double) sawtooth oscillation.

(Park, Monticello, White, Phys. of Fluids (27) 137 (1984))

Ways of Reconnection

— Magnetic topology change

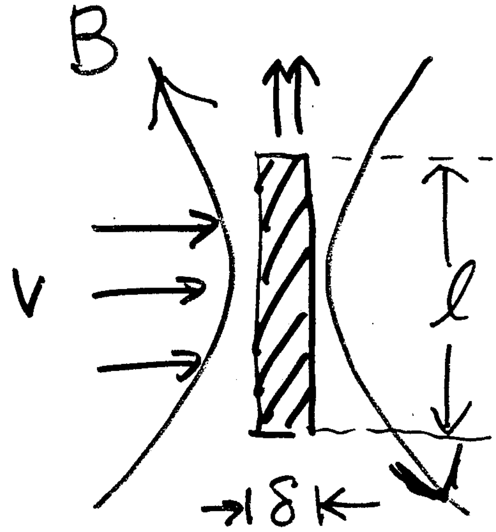

$$J_s \simeq \frac{\Delta B}{\delta}, \quad \dot{\psi}_s = \eta J_s$$

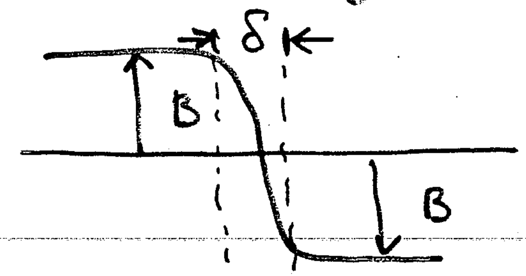

A) $J_s \to \infty$ as $\eta \to 0$.

$$\dot{\psi}_s = \eta J_s = \eta^{\alpha} \quad (0 \leq \alpha < 1)$$

- $\ell \sim \delta$: Petschek type layer

$$\dot{\psi}_s \sim (1 + \mu/\eta)^{-1/2}$$

- $\ell \sim 1$: Sweet – Parker type layer

$$\dot{\psi}_s \sim \eta^{1/2} (1 + \mu/\eta)^{-1/4}$$

B) $J_s \to$ finite as $\eta \to 0$ (i.e., no current singularity)

$$\dot{\psi}_s = \eta J_s \sim \eta$$

Equations

2-D Reduced tokamak eqs.

$$\begin{cases} \dfrac{d\psi}{dt} = -\eta J & \left(J = -\nabla^2\psi - 2\alpha\dfrac{B_0}{R_0}\right) \\[2ex] \dfrac{d\nabla^2 u}{dt} = -\vec{B}\cdot\nabla J + \mu\nabla^2\nabla^2 u & \end{cases}$$

$$\vec{B} = \nabla\psi \times \hat{e} + B_0\hat{e}$$

$$\vec{V} = \nabla u \times \hat{e}$$

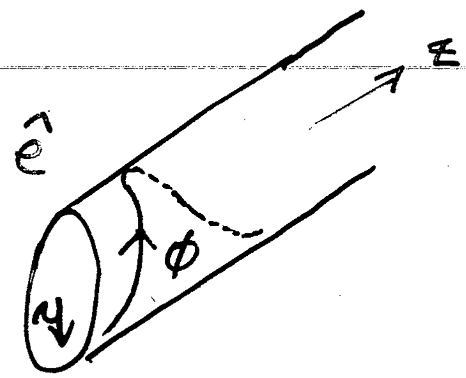

$\psi(r, \phi)$ $\qquad$ $\phi = \theta + \alpha z$

$\hat{e} = \hat{r} \times \hat{\phi}$

- r – finite difference.
  Packed grid inside a layer.

  ϕ – fourier space

- quantitative study.

Helical coil driven Reconnection

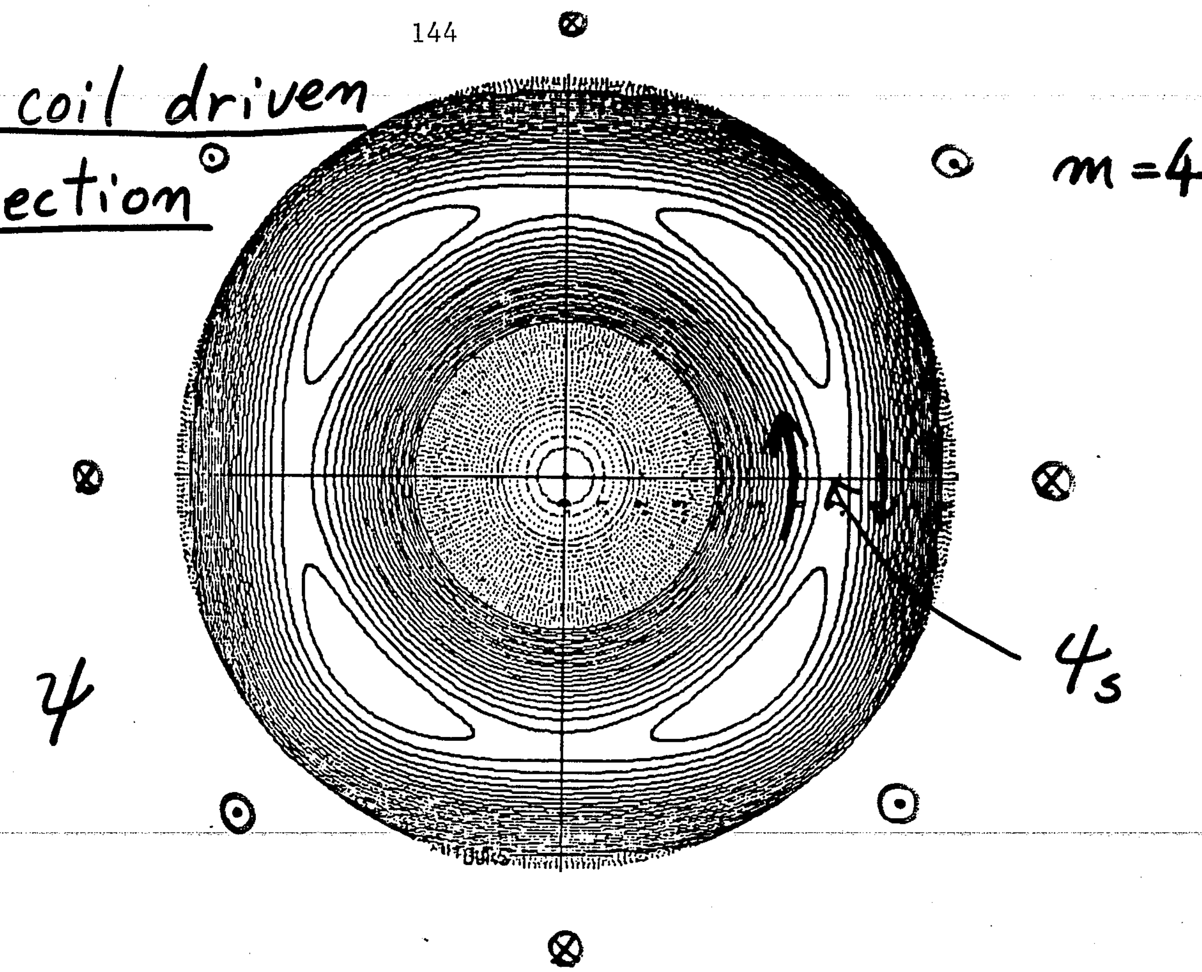

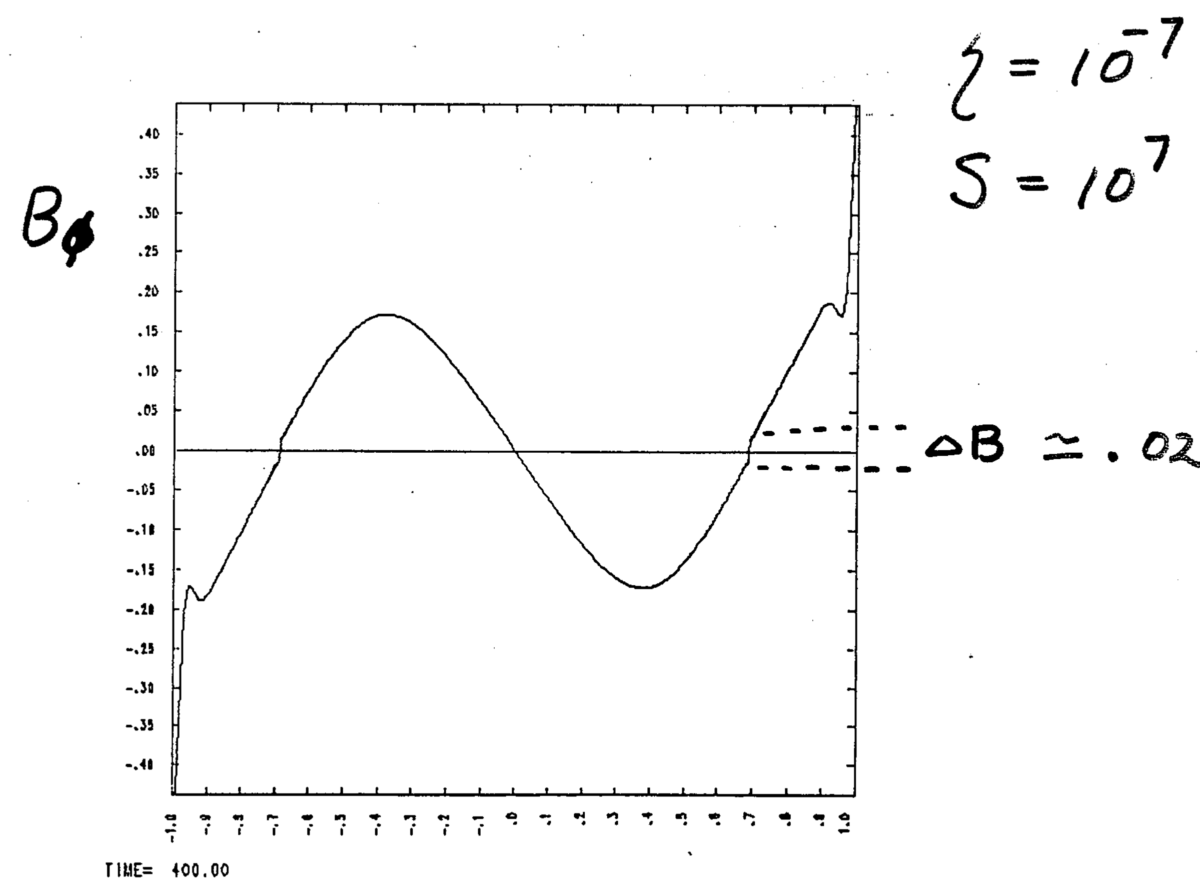

J

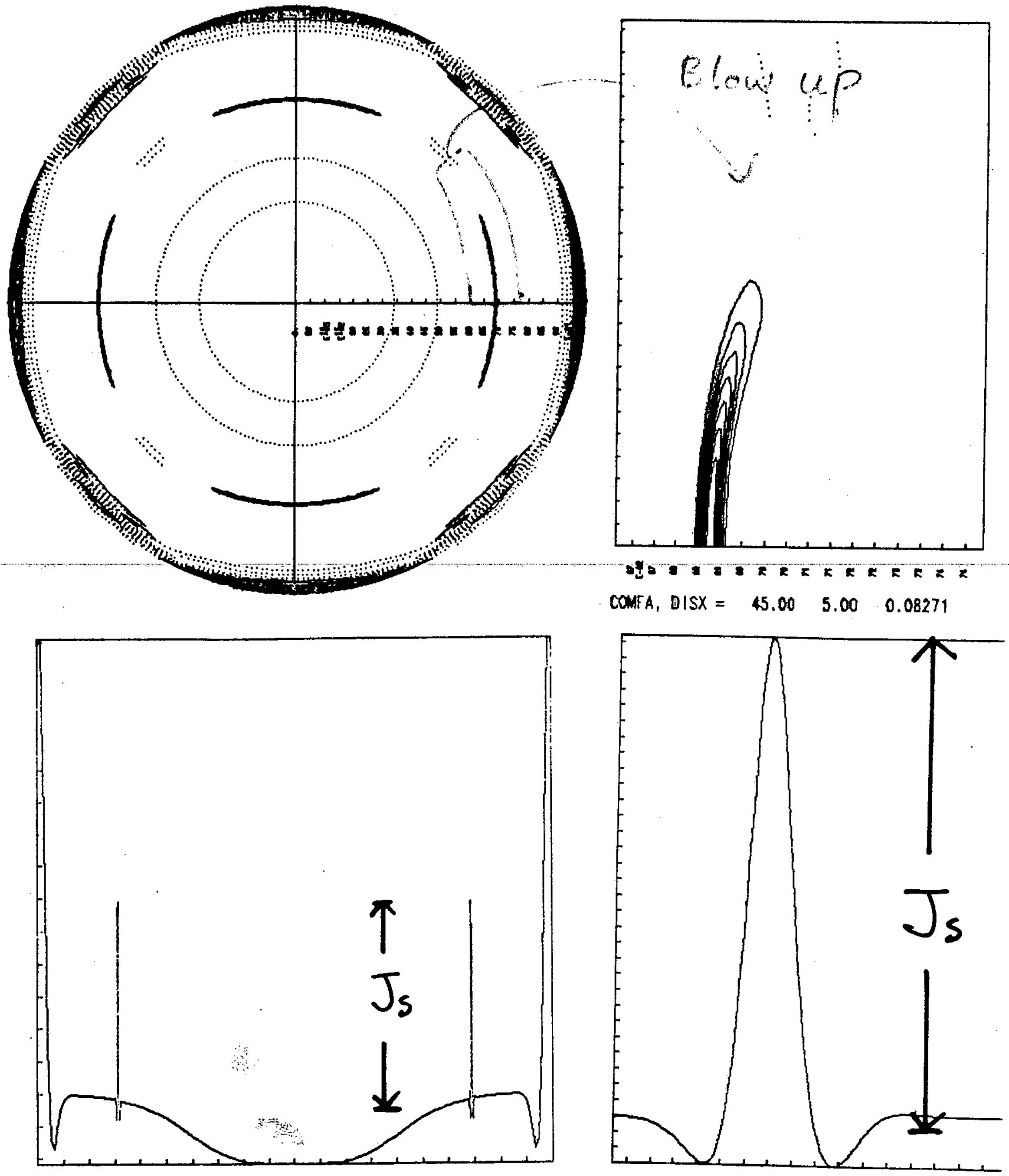

$\dot{\psi}_s = \eta\, J_s$

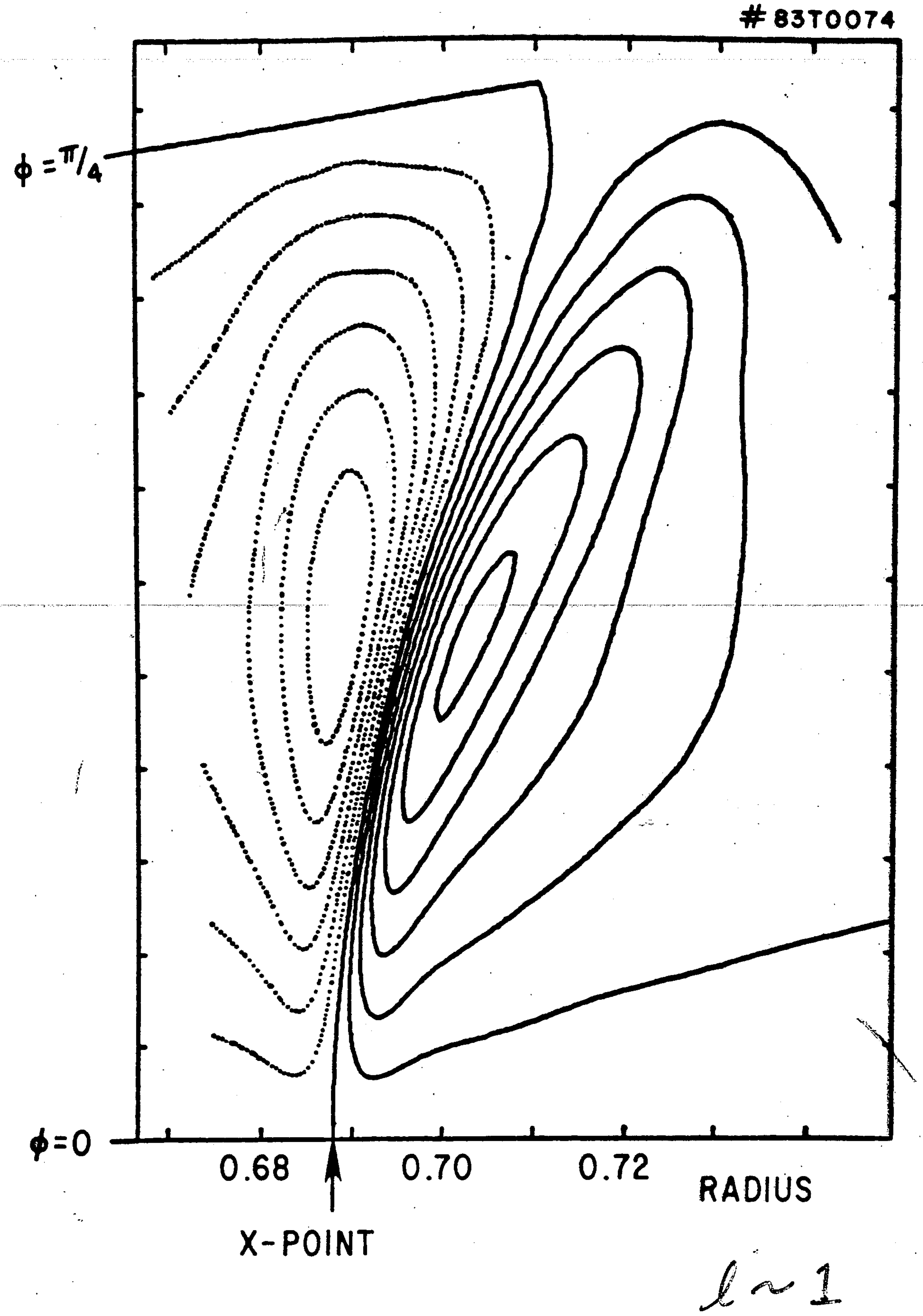

83T0074
φ = π/4
φ=0
0.68
0.70
0.72
RADIUS
X-POINT
ℓ ~ 1

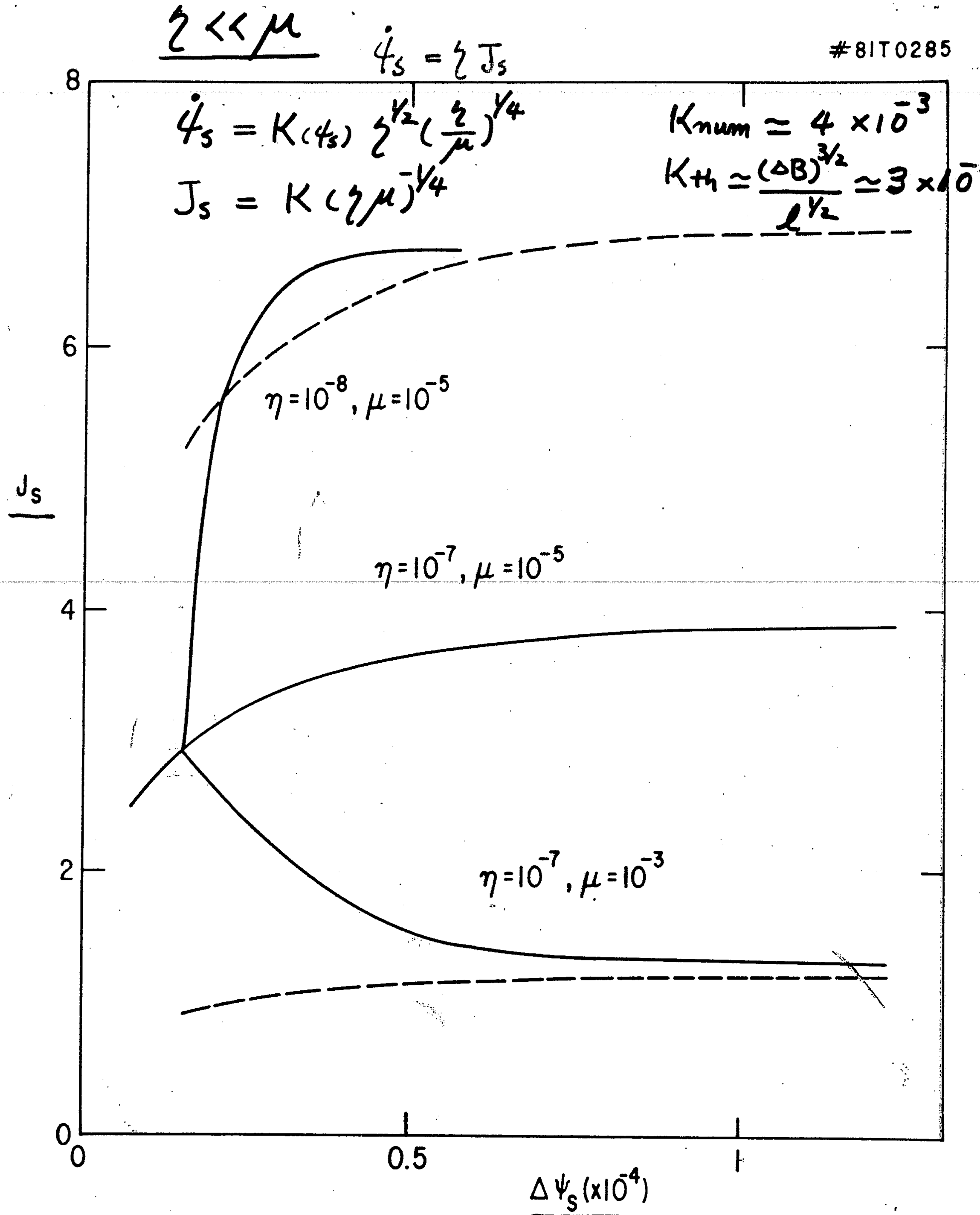

$\eta \ll \mu$
$\dot{\psi}_s = \eta J_s$
#81T0285
$\dot{\psi}_s = K(\psi_s)\, \eta^{1/2} (\frac{\eta}{\mu})^{1/4}$
$J_s = K(\eta\mu)^{-1/4}$
$K_{num} \simeq 4 \times 10^{-3}$
$K_{th} \simeq \frac{(\Delta B)^{3/2}}{\ell^{1/2}} \simeq 3 \times 10^{-3}$
$\eta = 10^{-8}, \mu = 10^{-5}$
$\eta = 10^{-7}, \mu = 10^{-5}$
$\eta = 10^{-7}, \mu = 10^{-3}$
J_s
$\Delta\psi_s (\times 10^{-4})$
0
2
4
6
8
0.5
1

m=1 Internal Kink

– Kadomtzev–Monticello flip

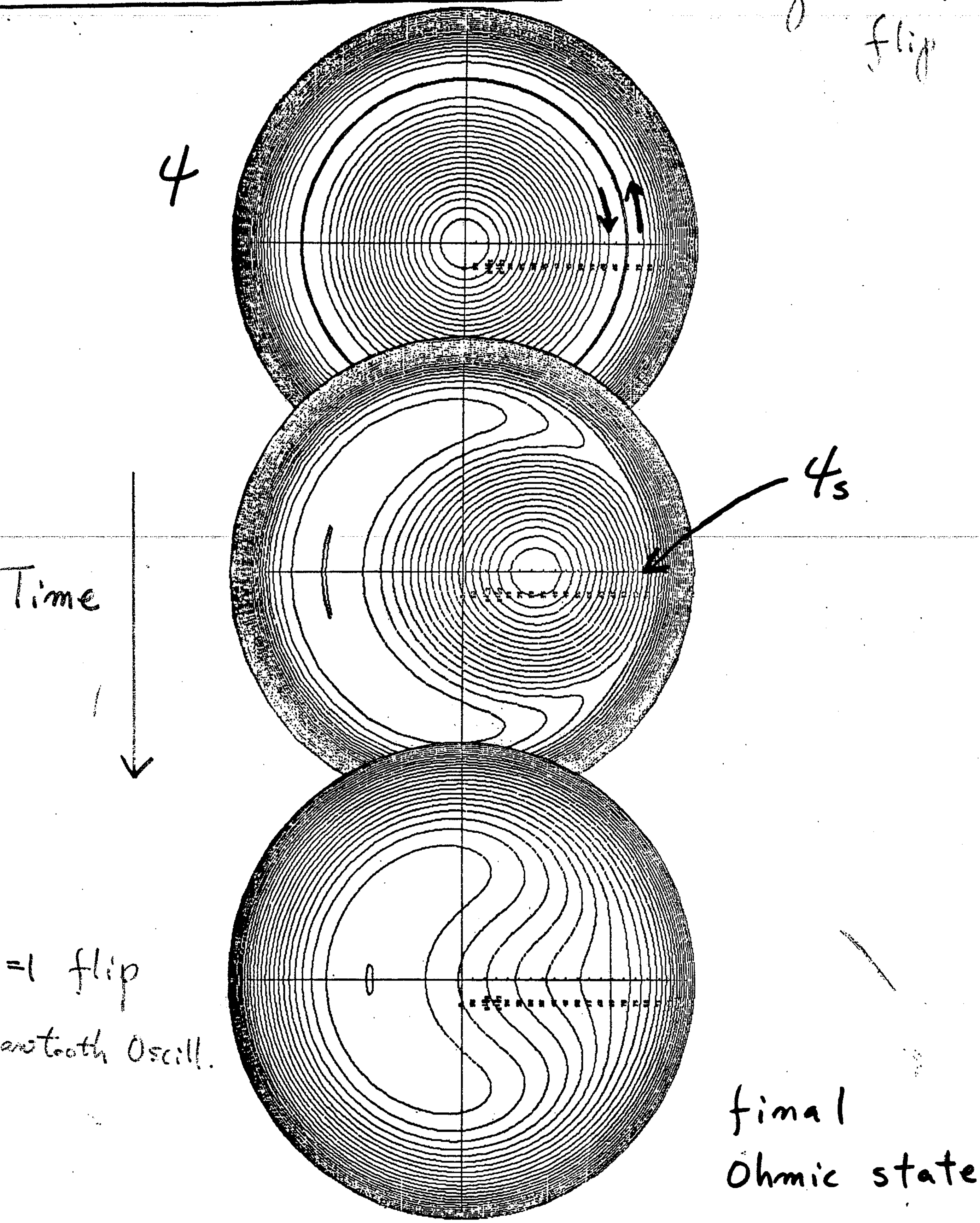

- m=1 flip
- Sawtooth Oscill.

$\xi \lesssim \mu$ $S \sim 10^8$

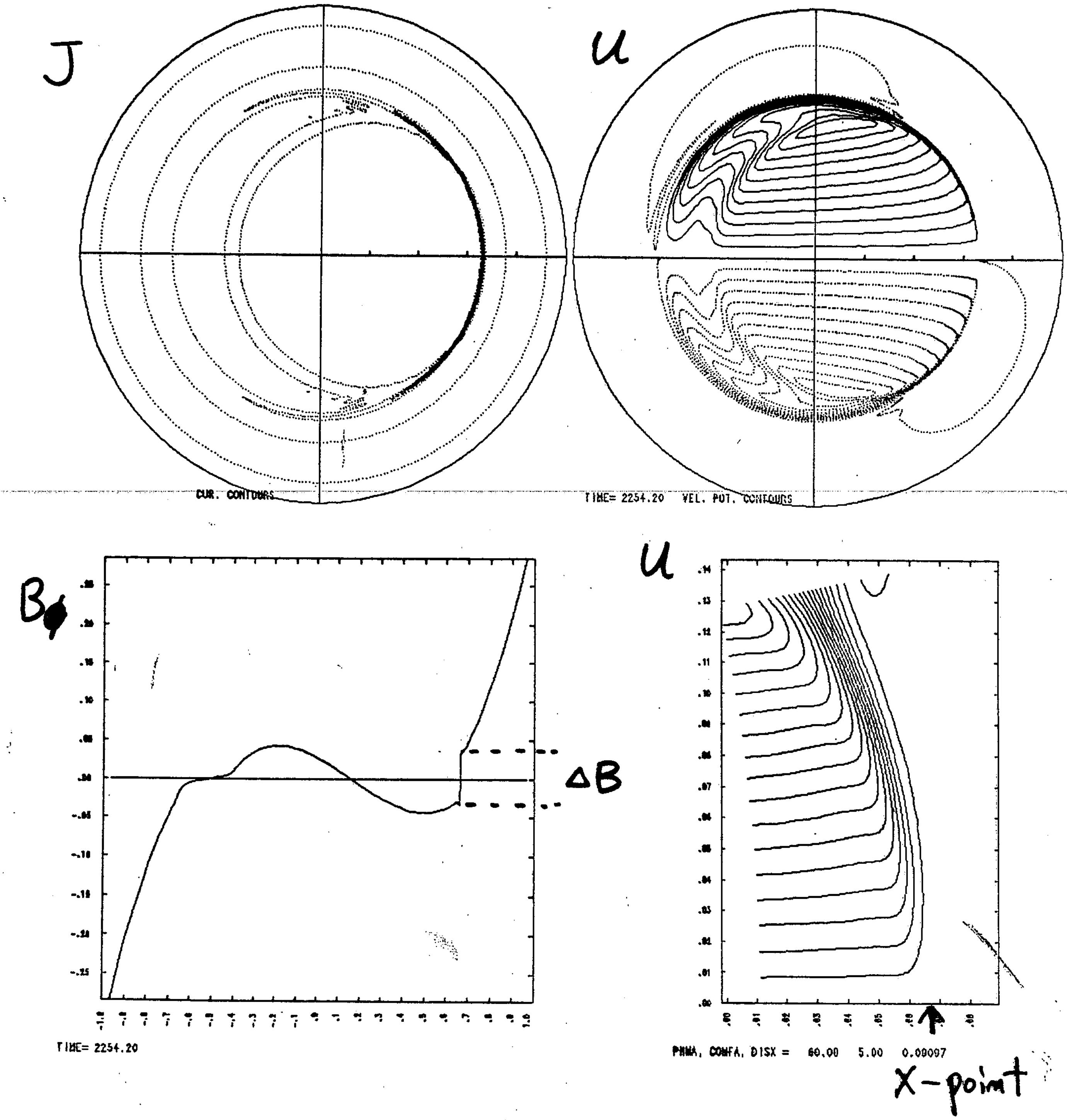

$\xi \gg \mu$ → higher m tearing

$\eta >> \mu$

#81T0281

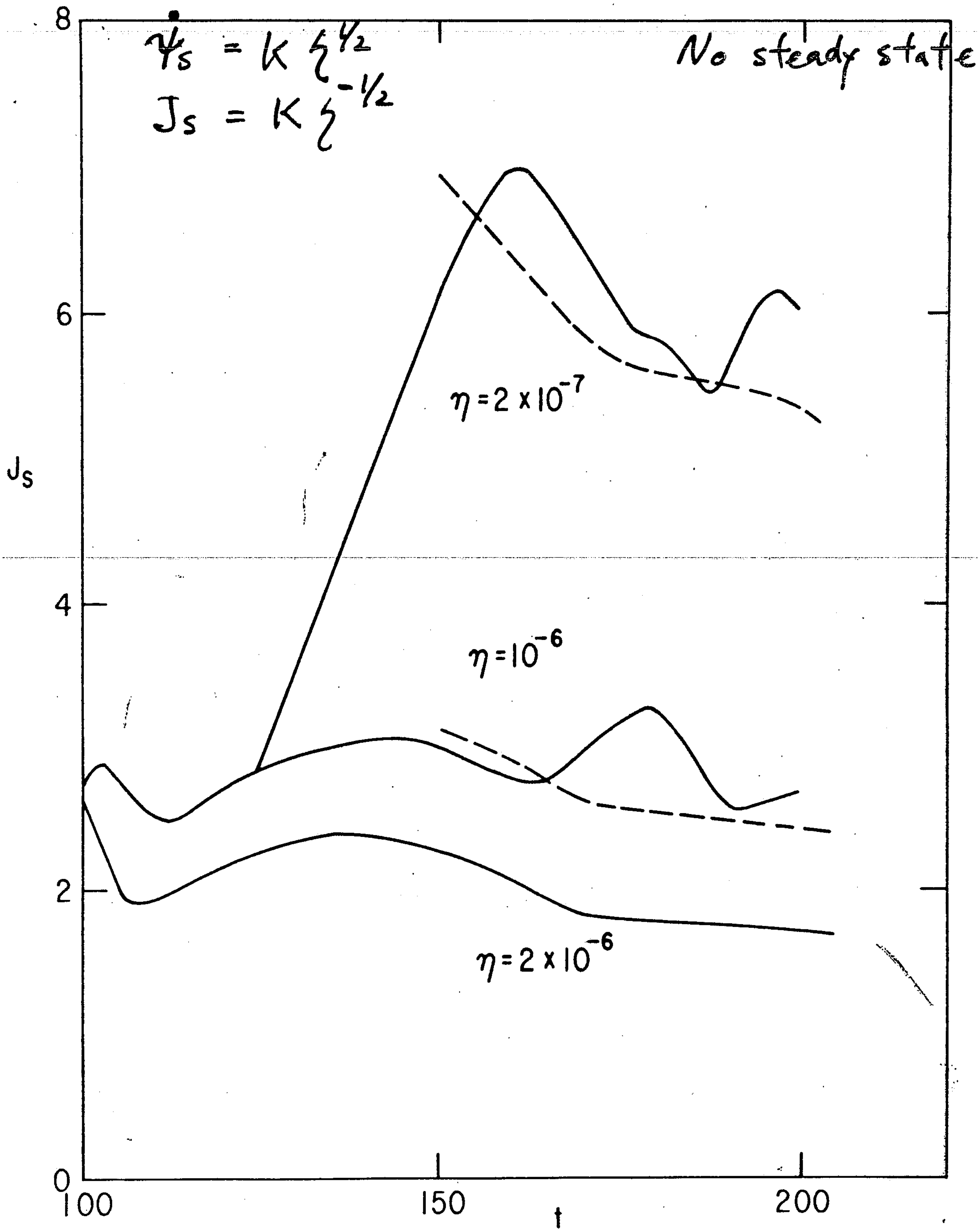

#81T0286

$\eta \ll \mu$

$\dot{\psi}_s \sim \eta^{1/2} \left(\frac{\eta}{\mu}\right)^{1/4}$

$J_s \sim (\eta\mu)^{-1/4}$

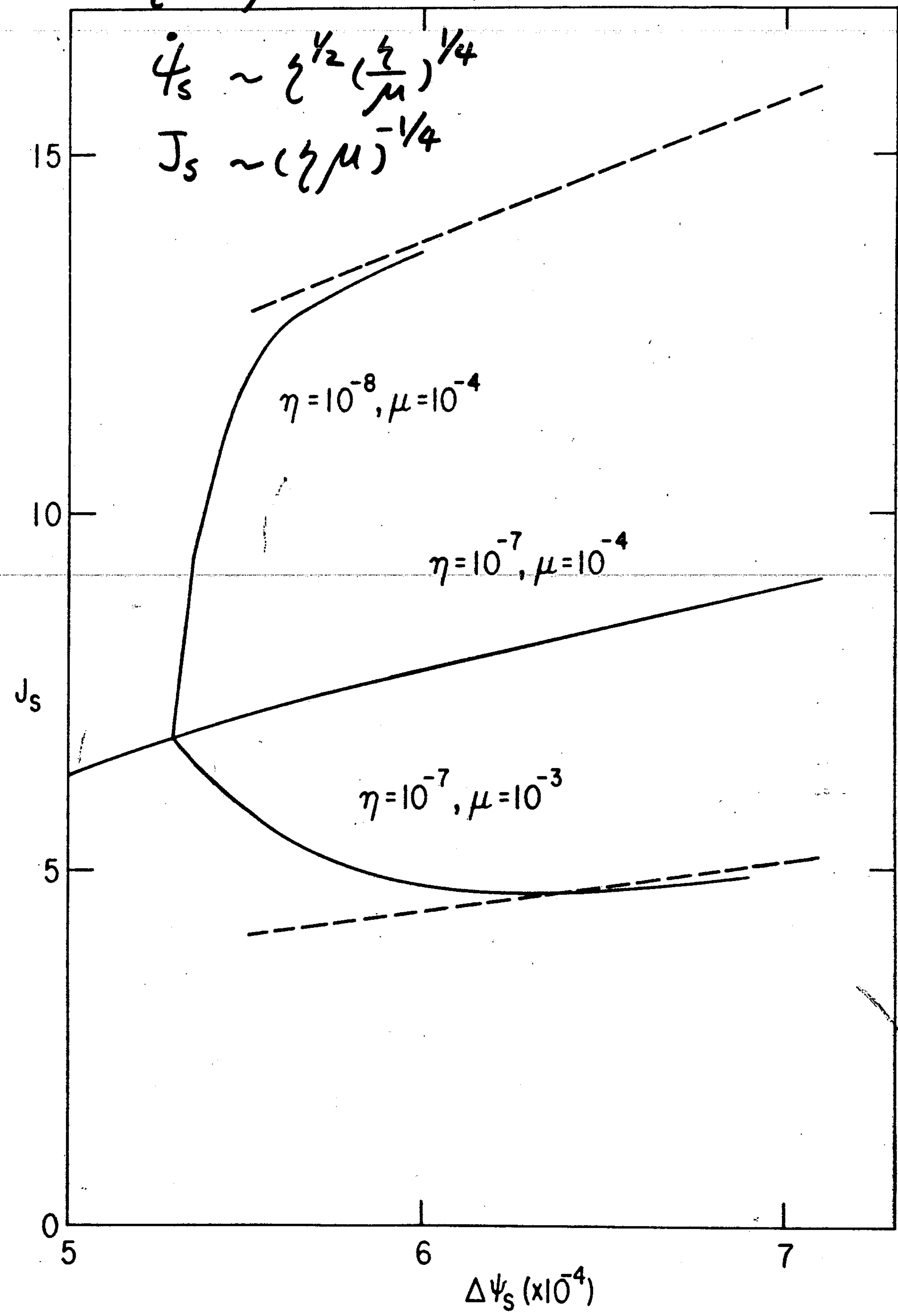

PDX Tokamak

Elec. g.r. $\simeq .005$ cm, Ion g.r. $\simeq .5$ cm, Collisionless s.d. $\simeq .0$ cm

Resistive layer thickness $= .05$ cm, $\mu \le \eta \simeq .5 \times 10^{-7}$

$\dot{\psi} \simeq K \eta^{1/2} \left(\frac{\mu}{\eta}+1\right)^{-1/4}$, $K \simeq \frac{\Delta B^{3/2}}{l^{1/2}} \simeq .04$

$\tau = 3000\, \tau_A \simeq .4$ msec

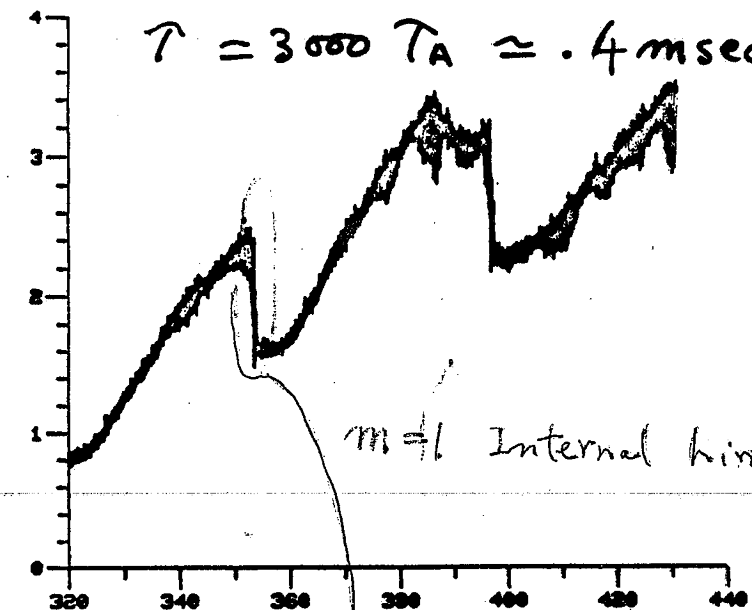

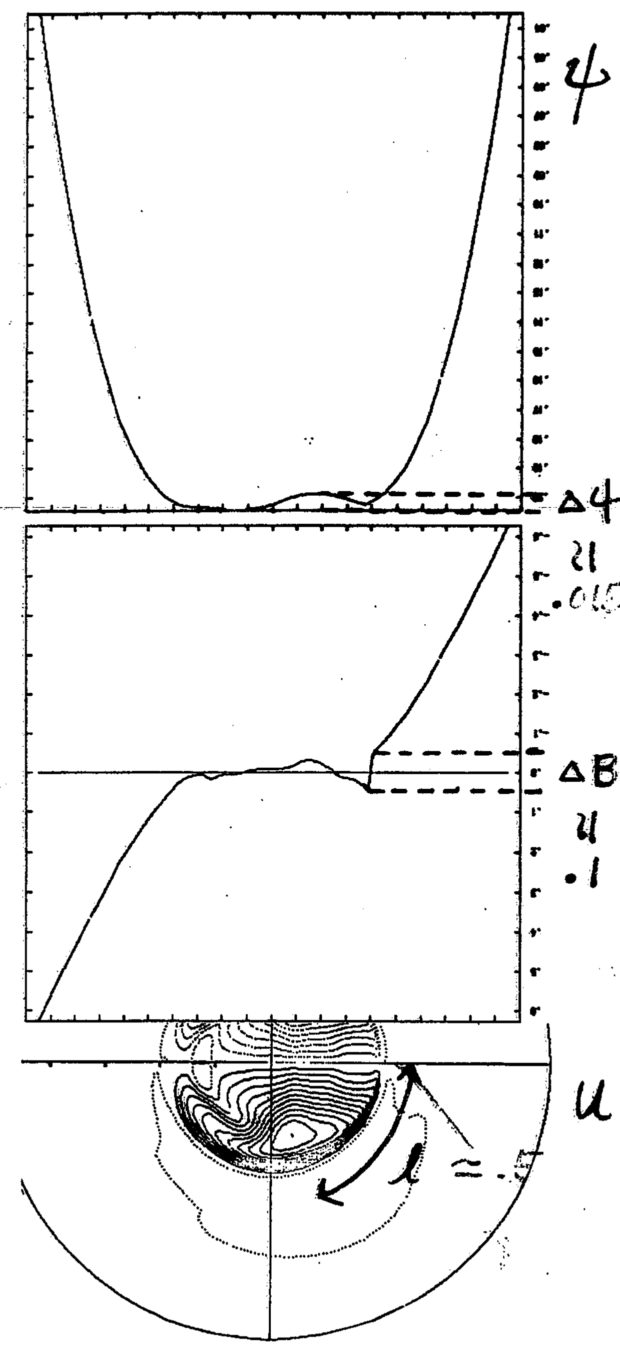

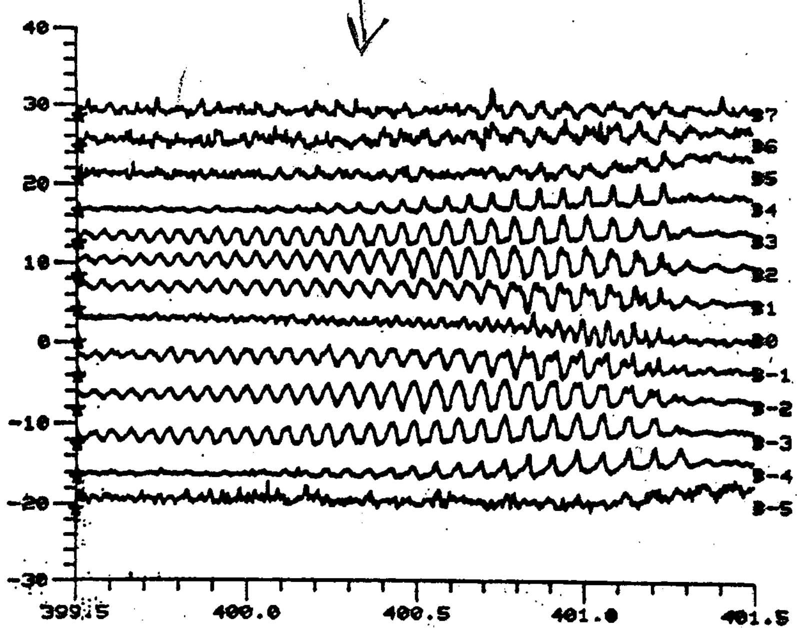

1 msec

o ST tokamak : 100 μs : 70 μs

$J_s \sim O(1) \rightarrow$ No singularity

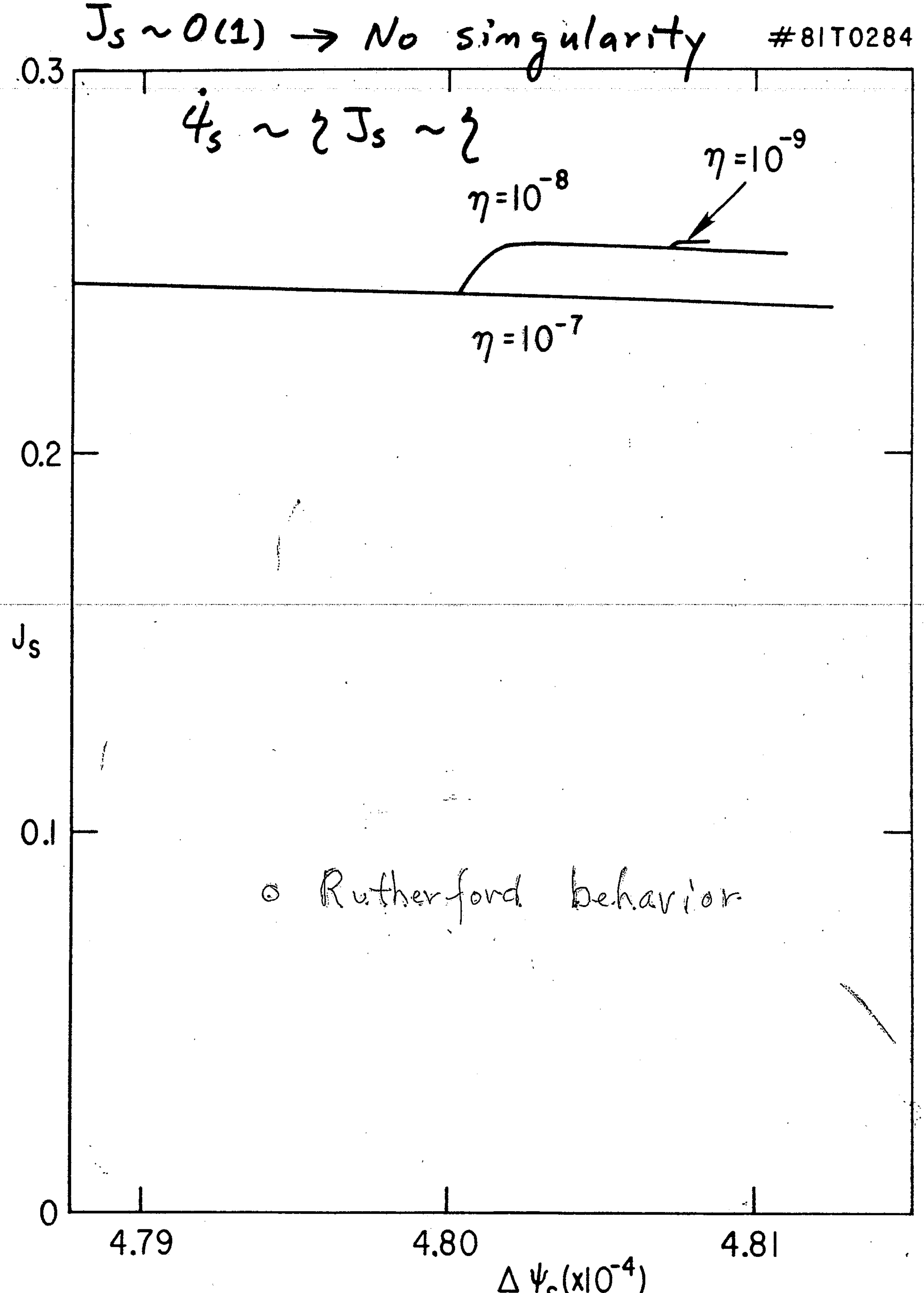

m=2 Tearing

stable if $\eta=0$

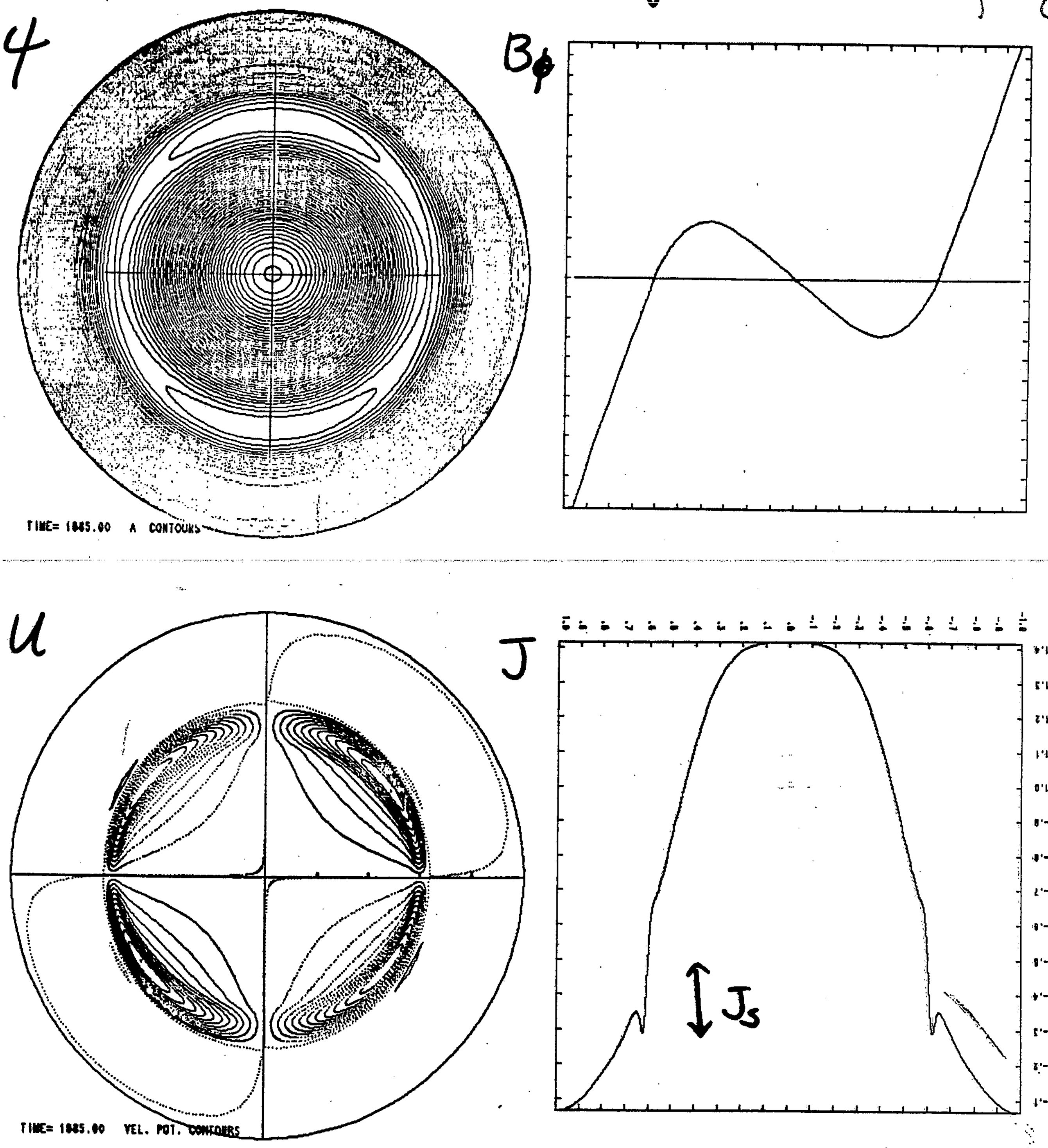

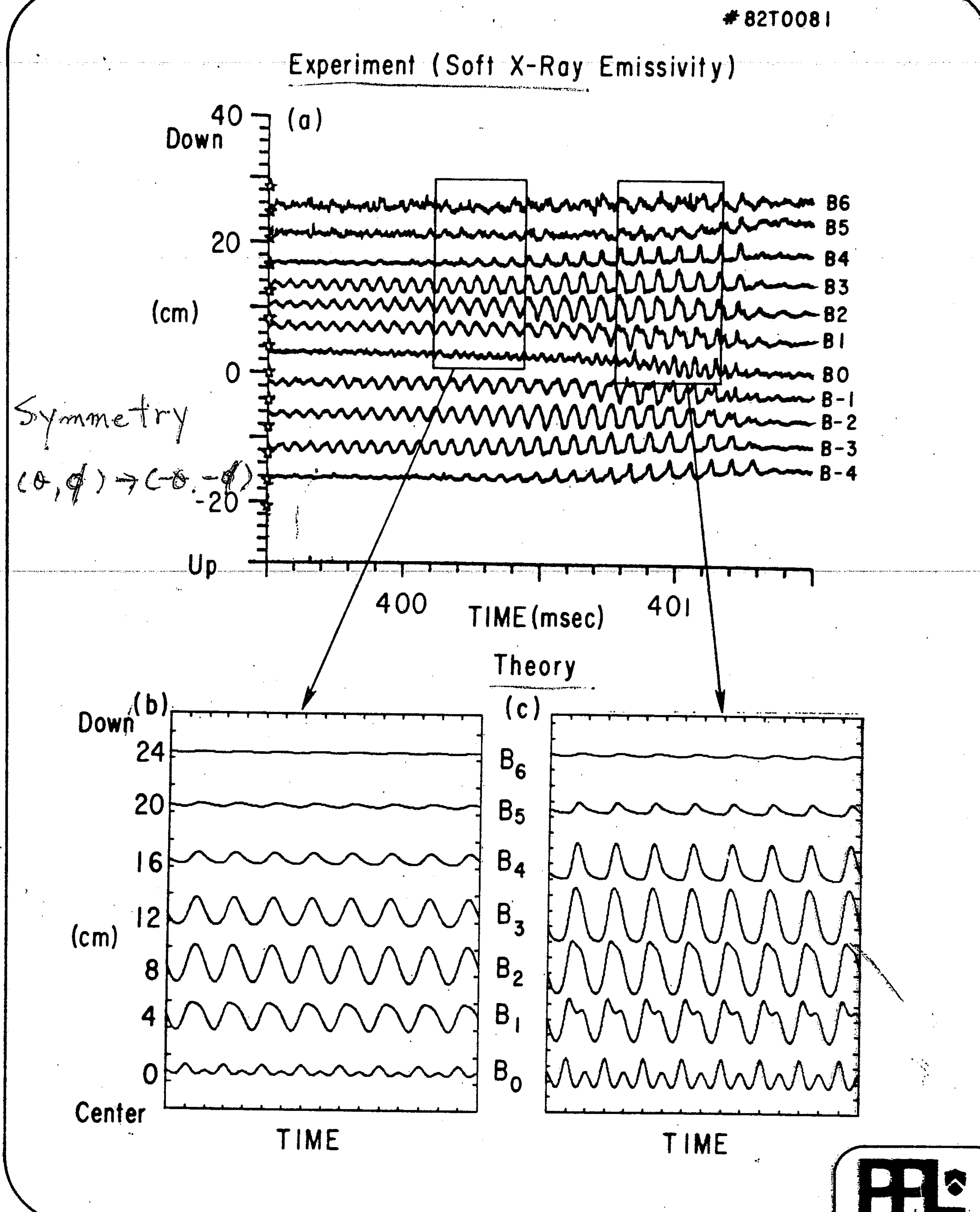

#82T0081
Experiment (Soft X-Ray Emissivity)
(a)
40
Down
20
(cm)
0
-20
Up
B6
B5
B4
B3
B2
B1
B0
B-1
B-2
B-3
B-4
400
TIME (msec)
401
Symmetry
$(\theta, \phi) \to (-\theta, -\phi)$
Theory
(b)
Down
24
20
16
12
(cm)
8
4
0
Center
TIME
(c)
B_6
B_5
B_4
B_3
B_2
B_1
B_0
TIME

Nonlinear Evolution of highly conducting confined plasmas

- Topology change
  - $J \to \infty$ as $\eta \to 0$ at the x-point:

    $$\dot{\psi}_s \sim \eta^{1/2}(1+\mu/\eta)^{-1/4}$$

  - no singularity : $\dot{\psi}_s \sim \eta$
- Doublet or Spheromak formation :

  $$\dot{\psi}_s \sim \eta^{1/2}(1+\mu/\eta)^{-1/4}$$

- 3-dimensionally current singularities can occur any place – (X-line → x-point) – determined globally.
- Magnetic helicity is conserved in the fast reconnection time scale

$$\frac{d}{dt}\left(\int \vec{A}\cdot\vec{B}\, d\Omega\right) \sim \int \eta\, \vec{J}\cdot\vec{B}\, d\Omega \sim \eta \int_{\delta} J\, d\Omega$$

$$\sim \eta$$

Time scales

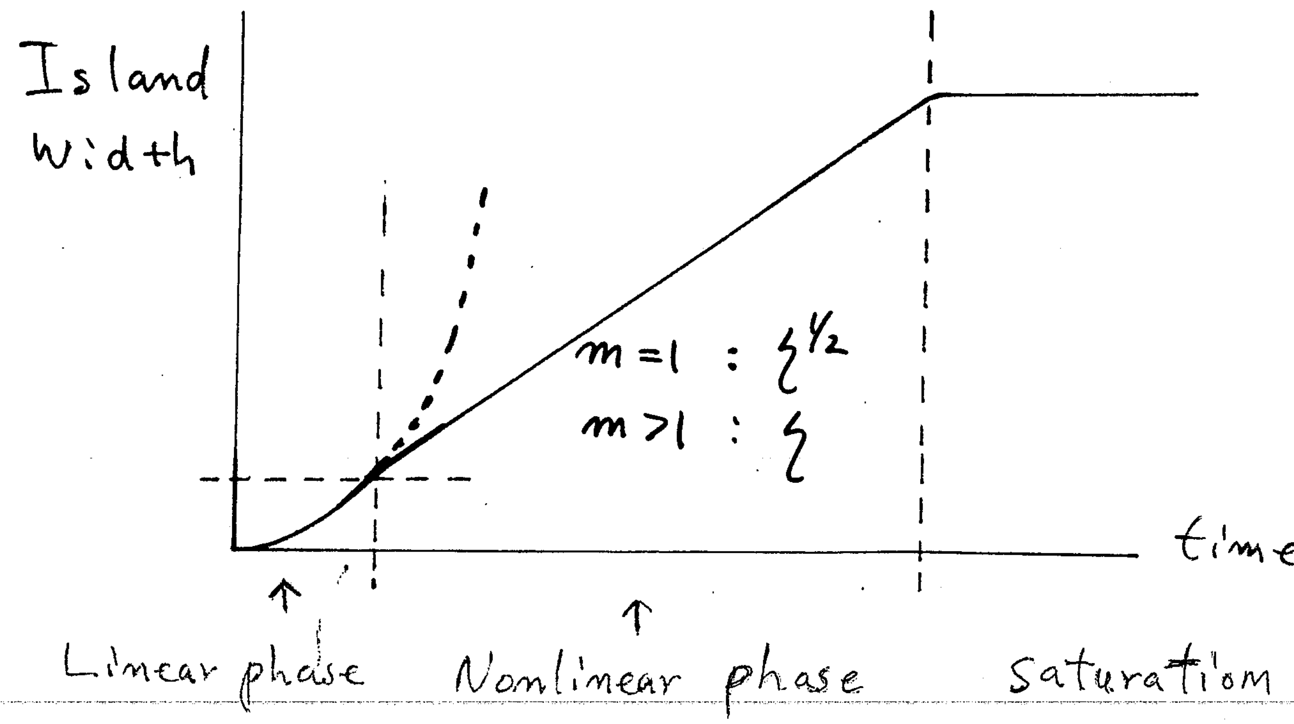

$$\begin{cases} \tau_A \sim .1\ \mu sec \\ \tau_s \sim a^2/\eta \sim 1\ sec \\ \zeta \sim 10^{-7} \end{cases}$$

Time scales of magnetic island growth

M = 1 : <u>1 msec</u> fast

M > 1 : <u>1 sec</u> slow

Enhanced (double) Sawtooth

Soft X-ray

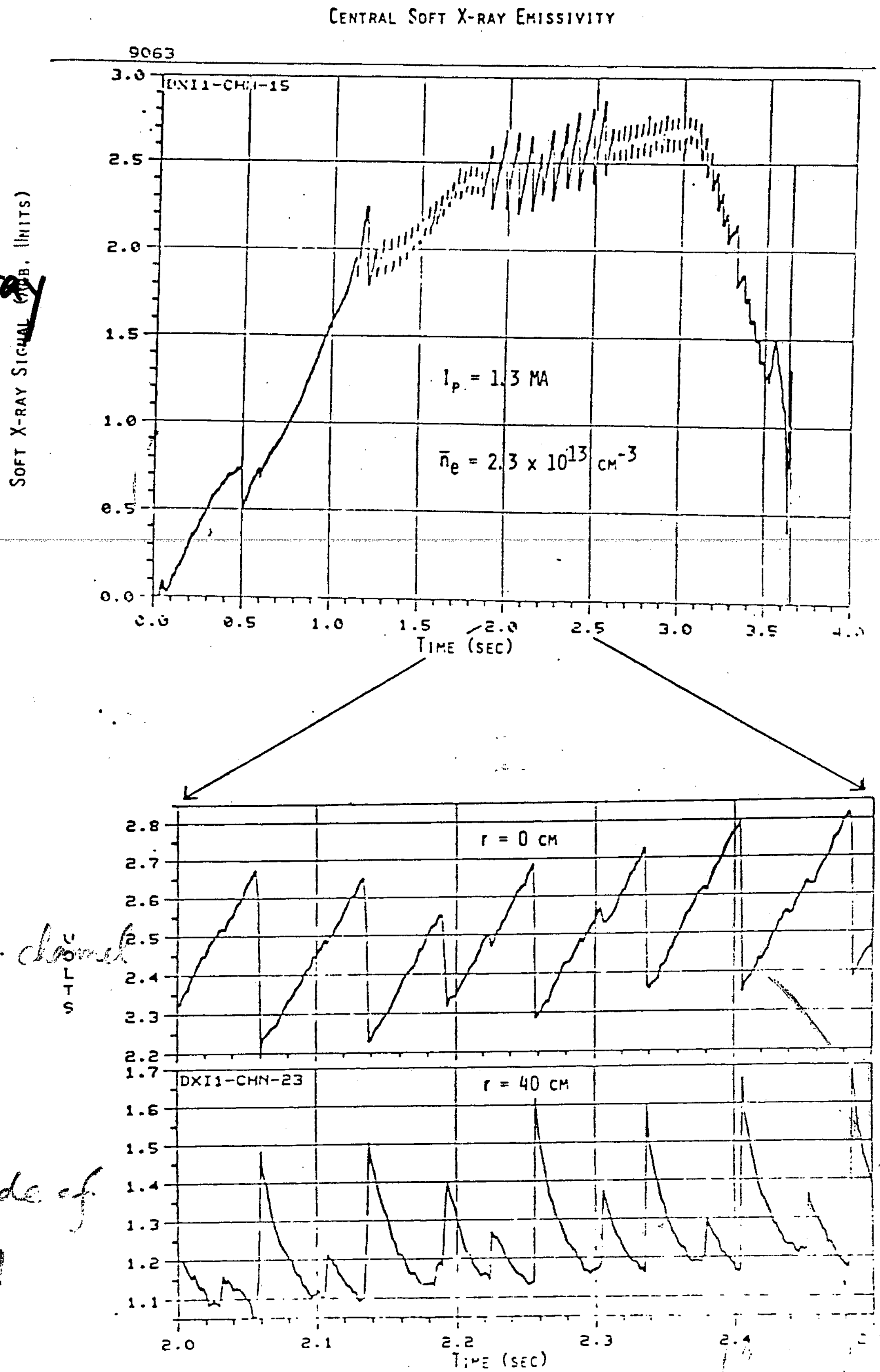

Center channel

Outside of $q = 1$

Kadomtzev - Monticello flip

83T0073

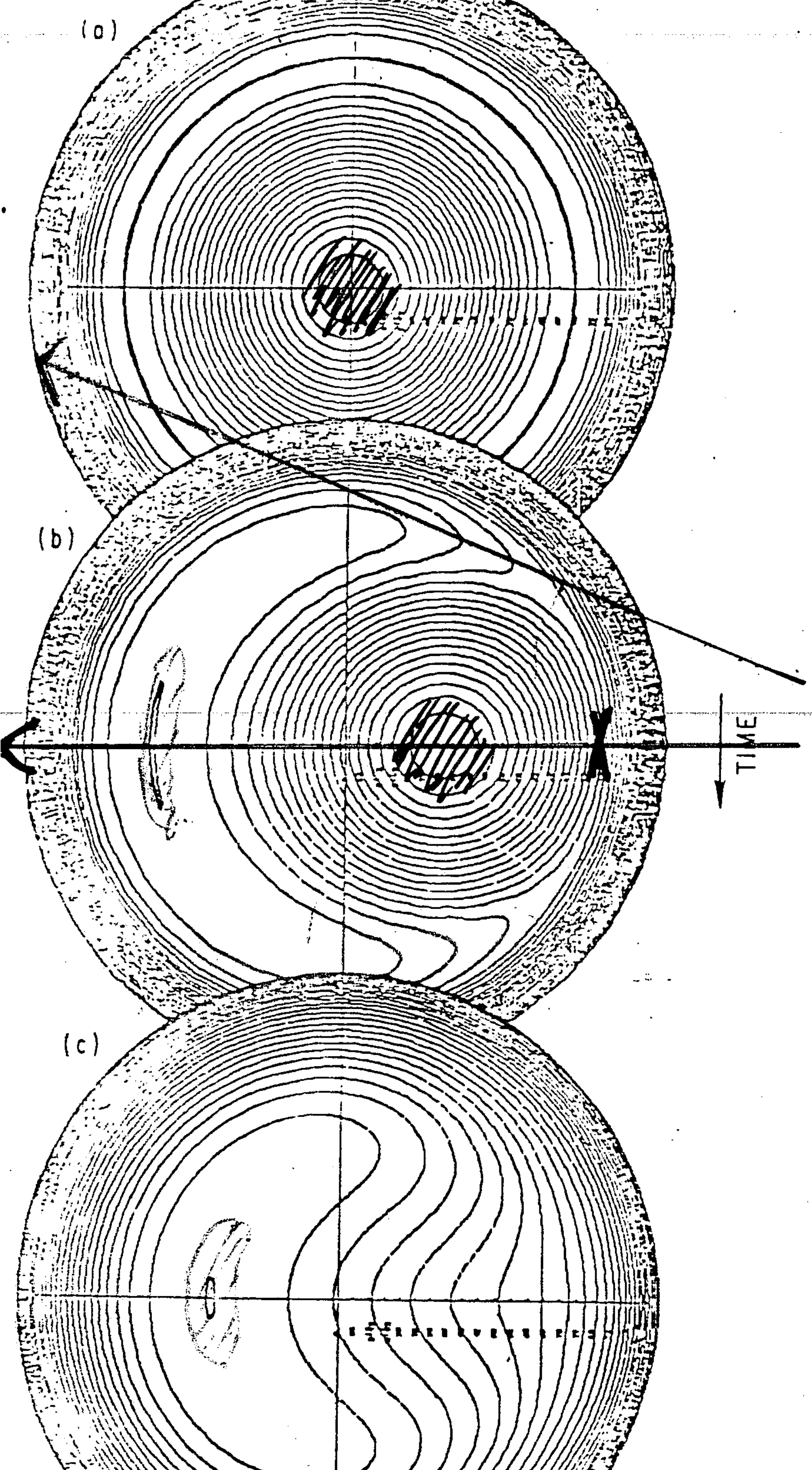

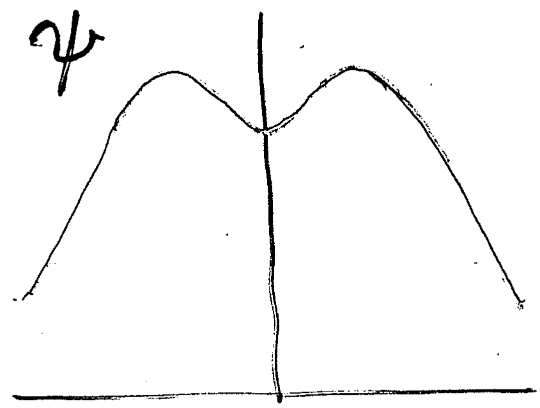

$$\frac{d\psi}{dt} = \eta J = \eta \nabla^2 \psi$$

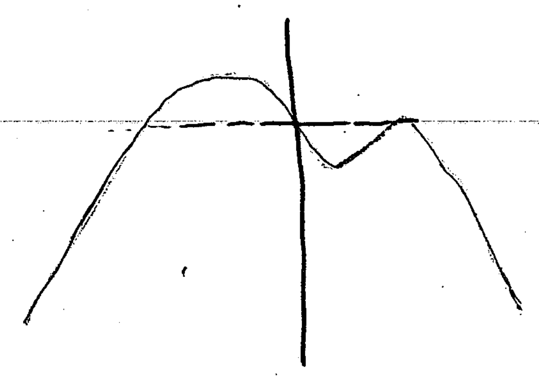

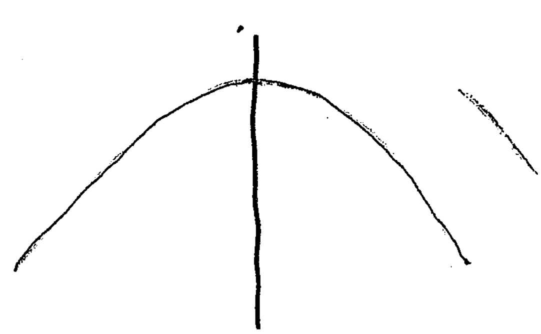

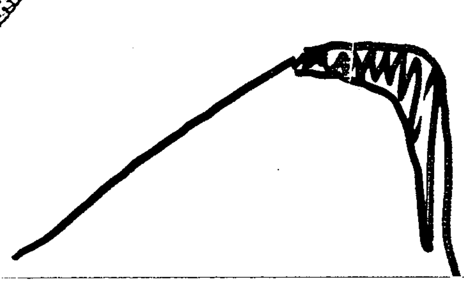

Fig. 7

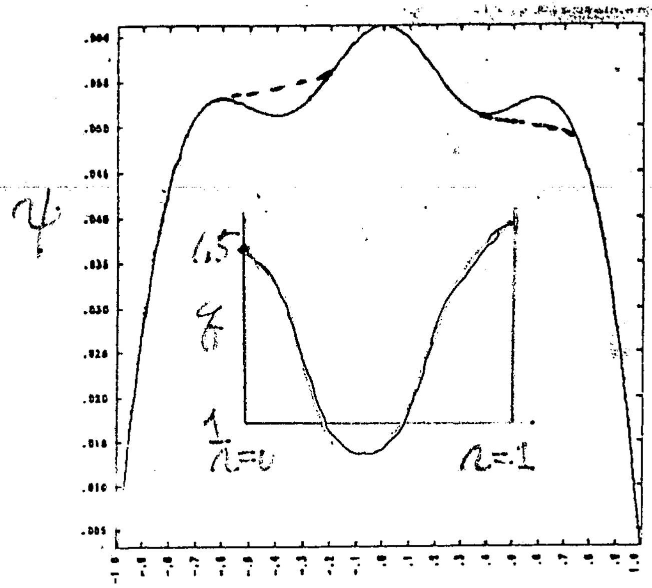

TIME= 0.00 SHIFT, SLPN, TC1= 0.400 0.601 0.300

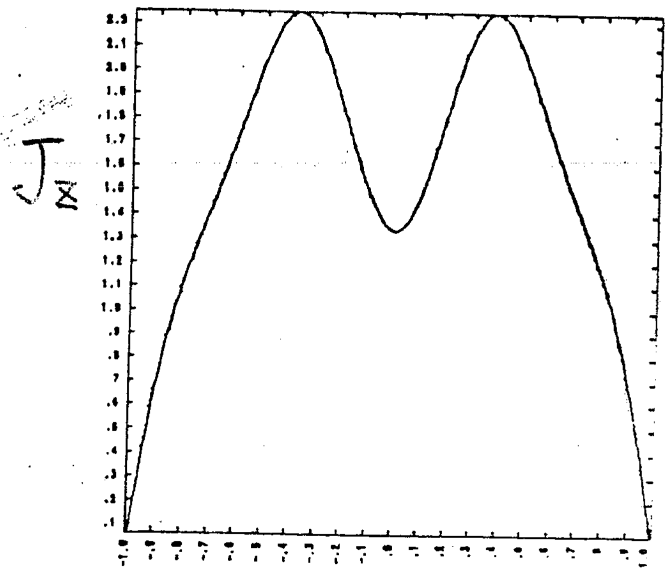

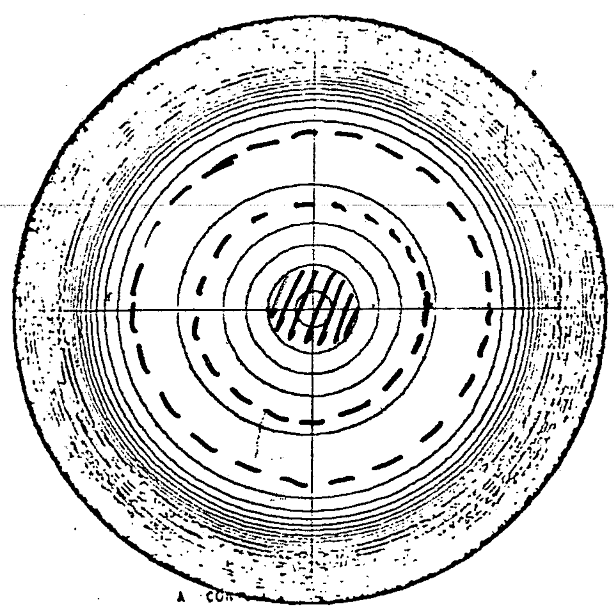

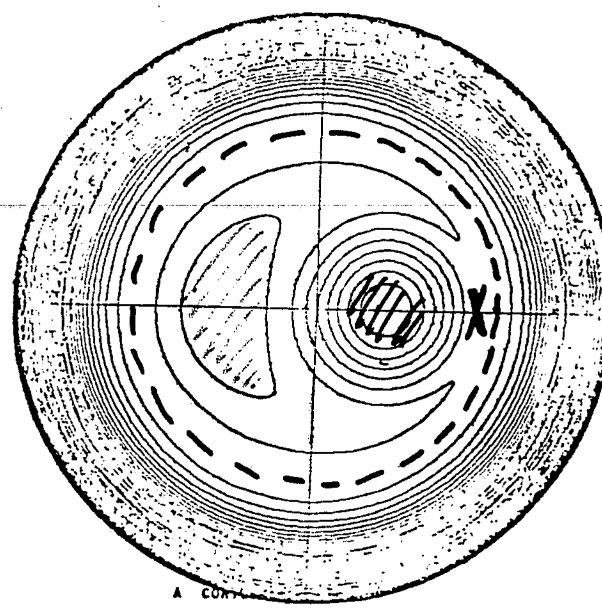

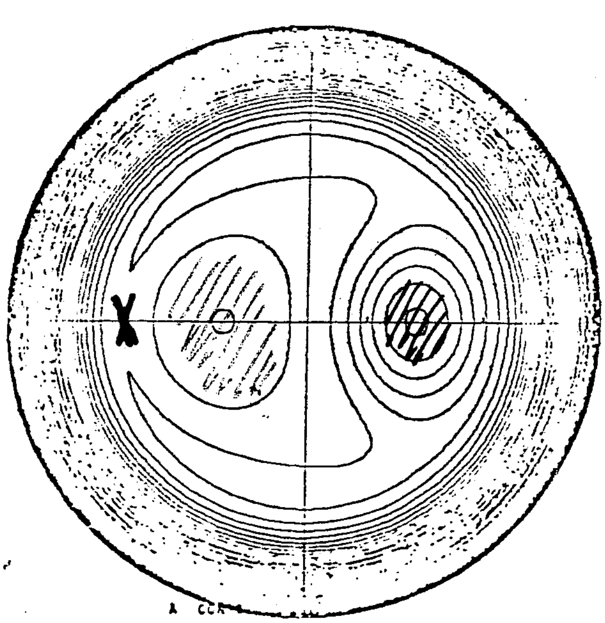

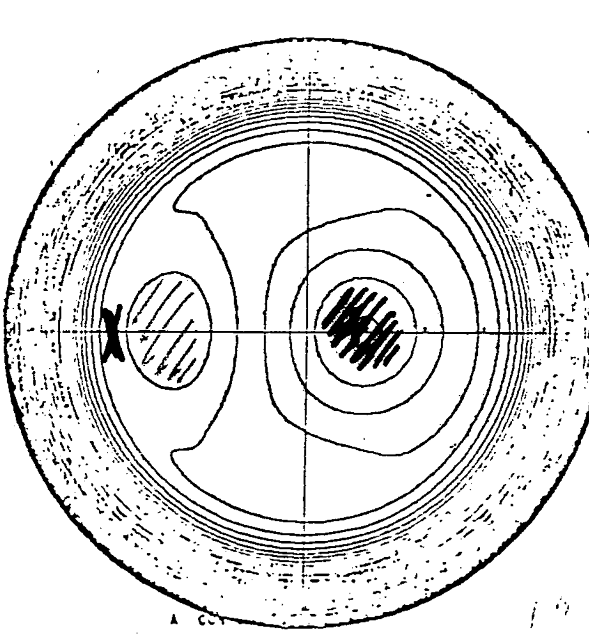

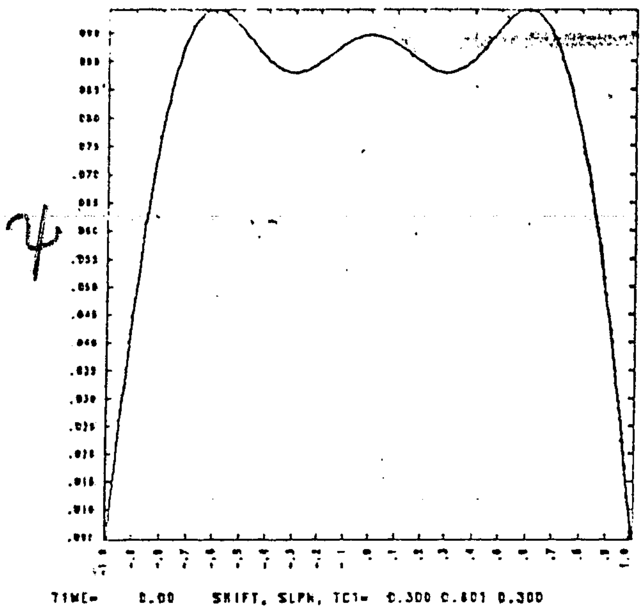

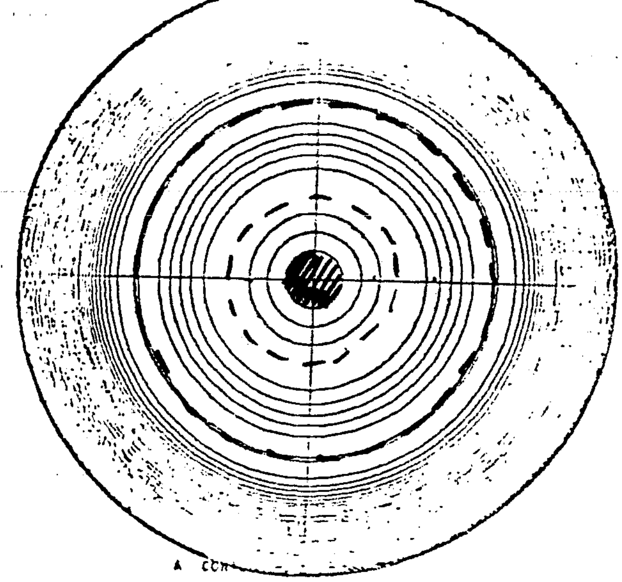

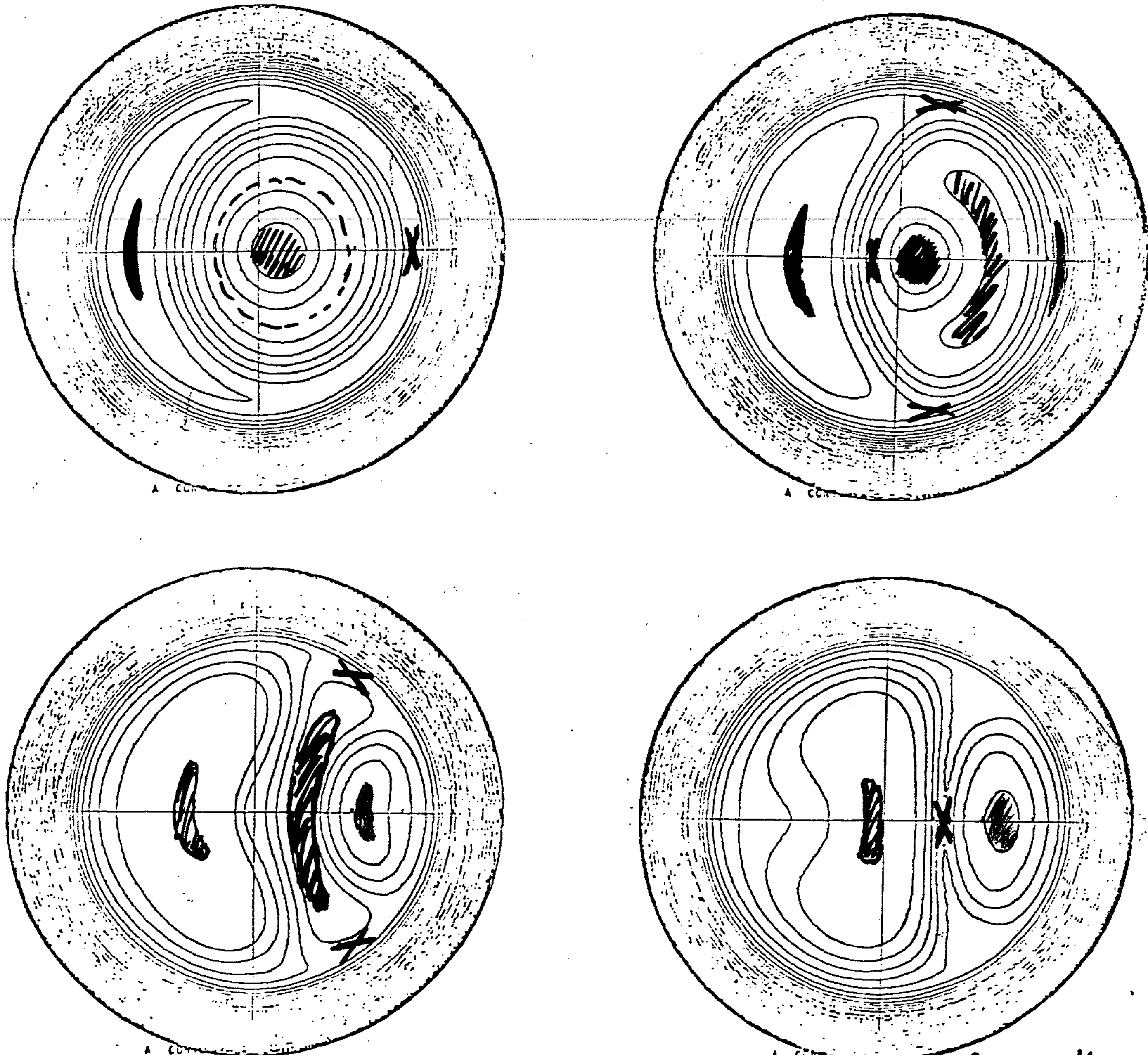

Singularities at x-points — $\dot{\psi}_s \sim \eta^{1/2}(1+M/q)^{-1/4}$

HALF COALESCENSE OF NONLINEAR M=1 MODE

R. PELLAT

ECOLE POLYTECHNIQUE

Half coalescence of N. linear m=1 mode

R PELLAT

- dynamic of the reconnection process unclear
- if the int. kink is linearly stable, origin of the current sheet?
- fast time scale of the disruption
- partial reconnection

⇒ ideal MHD mode at the origin?

- chain of magnetic island is unstable to an ideal MHD mode, leading to coalescence of the islands.

The m = n = 1 island is unstable to a half-coalescence motion, which destroys the up-down symmetry of the configuration.

let us start with standard δW.

$$2\delta W = \int d\tau \left(\underset{\sim}{Q}^2 - \underset{\sim}{j} \times \underset{\sim}{Q} \cdot \underset{\sim}{\xi} \right)$$

$$\underset{\sim}{Q} = \nabla \times (\underset{\sim}{\xi} \times \underset{\sim}{B})$$

helical deformations included

$s = \theta - hz$ $\qquad$ h pitch.

$\qquad\qquad\qquad\qquad$ $ha \ll 1$

$$\underset{\sim}{B}_\perp = \underset{\sim}{e}_z \times \nabla F$$

j_z function of $G = F - B_z h r^2/2$

$$\Delta F = j_z$$

by expansion in (ha), $k_\perp a \geq 1$

$\rightarrow$ $Q_z = 0$

$$\rightarrow \quad 2\delta W = \int d\tau \left\{ |\nabla_\perp \psi|^2 + \frac{dj_z}{dG} \psi \, \underset{\sim}{T} \cdot \underset{\sim}{\nabla} U \right\}$$

$$\underset{\sim}{\xi}_\perp = \underset{\sim}{e}_z \times \underset{\sim}{\nabla} U$$

$$\underset{\sim}{T} = \underset{\sim}{B}_\perp - h B_z r \, \underset{\sim}{e}_\theta$$

$\rightarrow$ Euler

Euler equation:

$$\underset{\sim}{B}\cdot\underset{\sim}{\nabla}\Delta\psi - \frac{dj_z}{d\psi}\,\underset{\sim}{T}\cdot\underset{\sim}{\nabla}\psi = 0$$

it is easy to prove that translations,

$\frac{\partial\psi}{\partial x,y}$ rotations are exact solutions of equation.

by derivation of equilibrium equation

D. EDERY; G LAVAL; R. PELLAT; J.L. SOULÉ

- phys. of fluids 19, 76, 260

then stability for internal kink modes in cylindrical discharges for different shapes:

q = 1

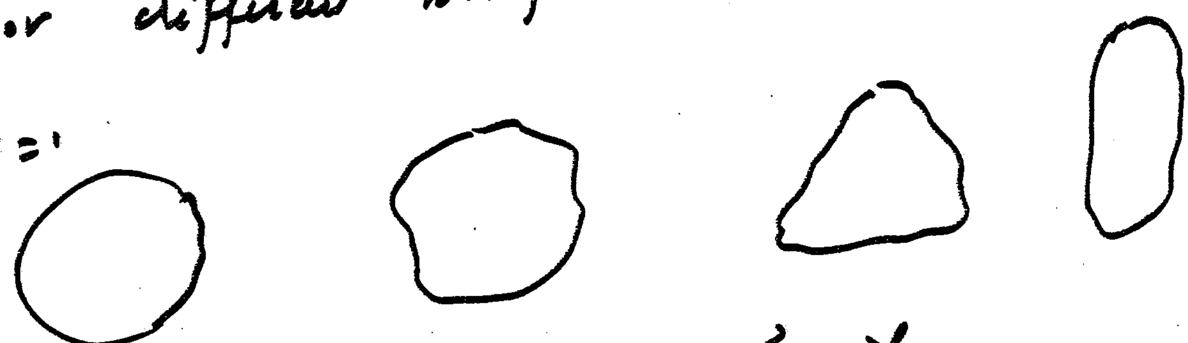

all corrections of order ε^2 if:

$$F = F_0 + \varepsilon F_1$$

□, Δ stabilizing

0 destabilizing.

. let us recall curvature effects.

cylindrical destabilizing $O\left(\frac{r}{R}\right)^2$

Shafranov.

toroidal stabilizing

if $\beta p \lesssim 1$ stable.

BUSSAC, PELLAT, EDERY, SOULÉ

Phys Rev. Lett. 35 (1875) 1638.

then non linear cylindrical.

Rosenbluth, Rutherford, Dagazian.

Park, White, Monticello, Jardin.

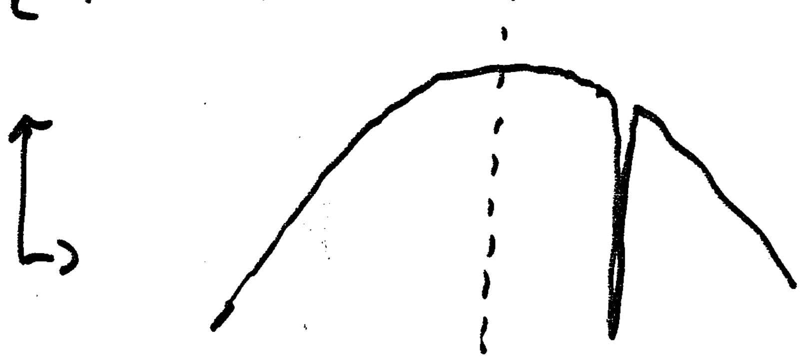

this is in numerical codes, but not true in toroidal.

. Now with resistivity.

Coppi, Galvao, Pellat, Rosenbluth, Rutherford
Sov. J. Plasma Phys. 2 (1976) 553

internal resistive mode. $\gamma \sim \eta^{1/3}$.
due to non constant ψ, $\delta W \sim O(\varepsilon^2)$

then numerical simulations.
+ "Kadomtsev theory"

previous talk.

Let us now speak of our recent approach:

I first come back to δW.

the idea is the following.

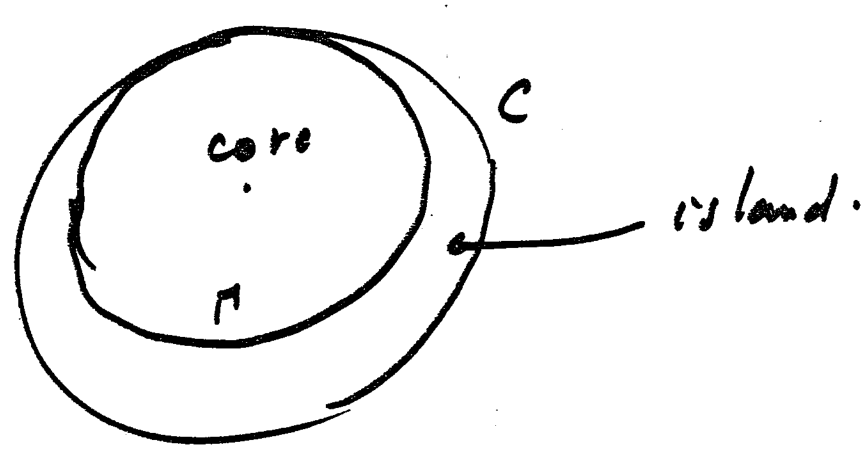

Γ has any shape.
C is for simplicity a circle.

let us compute δW.

inside the core we call ψ_e rotation about magnetic axis. Outside in the island, rotation about the center of C: ψ_R.

$$\psi_e = \underset{\sim}{B} \cdot \nabla U_e \qquad \psi_R = \underset{\sim}{B} \cdot \nabla U_R$$

$\|$ exact solutions apart from boundary conditions on Γ

One set, inside the core:

$$\psi_e + \psi_R + \psi_1$$

outside the island:

$$\psi_R + \psi_2$$

on Γ: $\quad \cancel{\psi_R} + \psi_1 = \psi_e + \cancel{\psi_R} + \psi_2$

by integration by parts:

$$2\,\delta W = \int d\tau \Big\{ \underbrace{\Big(|\nabla\psi_1|^2 - \frac{\partial J}{\partial \sigma}|\psi_1|^2 \Big)}_{\text{core}} + \underbrace{\Big(|\nabla\psi_2|^2 - \frac{\partial J}{\partial \sigma}\psi_2^2 \Big)}_{\text{island}} \Big\}$$

$$+ \int dA \Big\{ \psi_R \, \underset{\sim}{n} \cdot \underset{\sim}{\nabla} \psi_e - \psi_e \, \underset{\sim}{n} \cdot \underset{\sim}{\nabla} \psi_R + \underset{\sim}{n} \cdot \underset{\sim}{\nabla} \psi_e \, (\psi_e + 2\psi_1) \Big\}$$

if Γ is the circle we find the

result of :

Bussac, Pellat, Soulé and Tagger:

Physics letters, 105 A, 1,2. (1 October 84)

$$\lambda_H = \int dl\, \psi_R\, \underset{\sim}{n} \cdot \underset{\sim}{\nabla} \psi_e$$

because on Γ $\quad \psi_e = 0 \quad \psi_1 \equiv \psi_2 = 0$.

if non circular Γ:

corrections are all of order ε^2.

when our result of order $\beta\ (\sim \varepsilon)$.

Let us explain in more detail

our result for circular core.

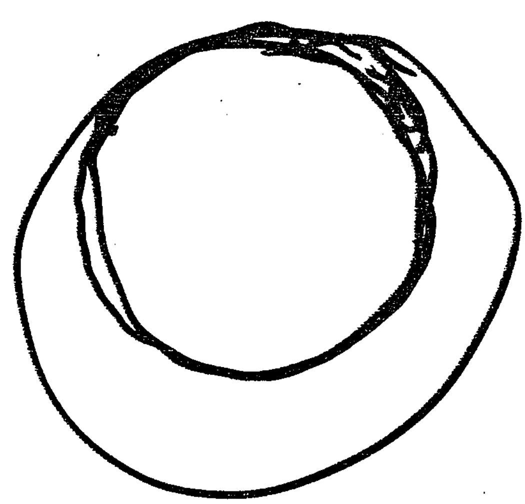

rotation:

$\xi = e_3 \times \nabla U_R$

U_R

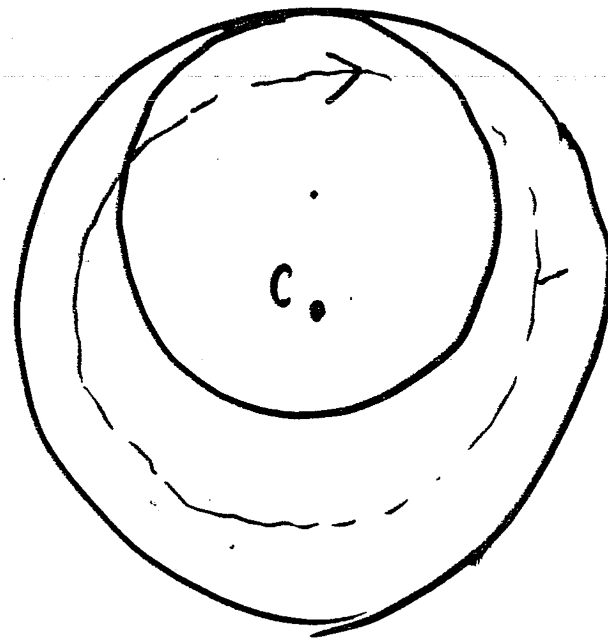

(1)

rotation

$\xi = e_3 \times \nabla U_e$

U_e

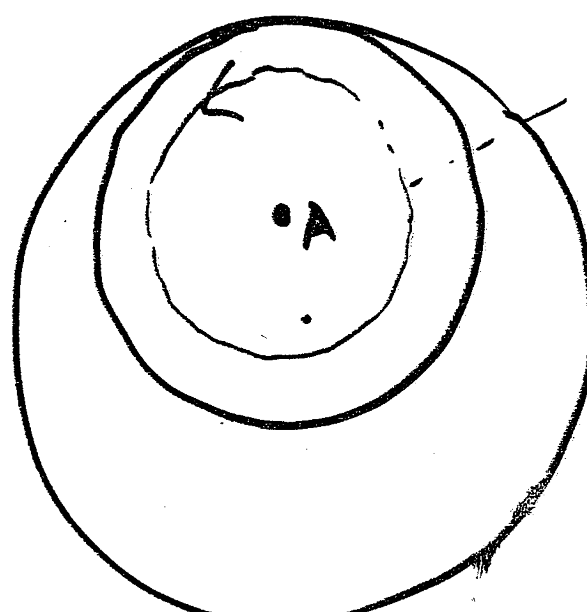

(2)

Equilibrium

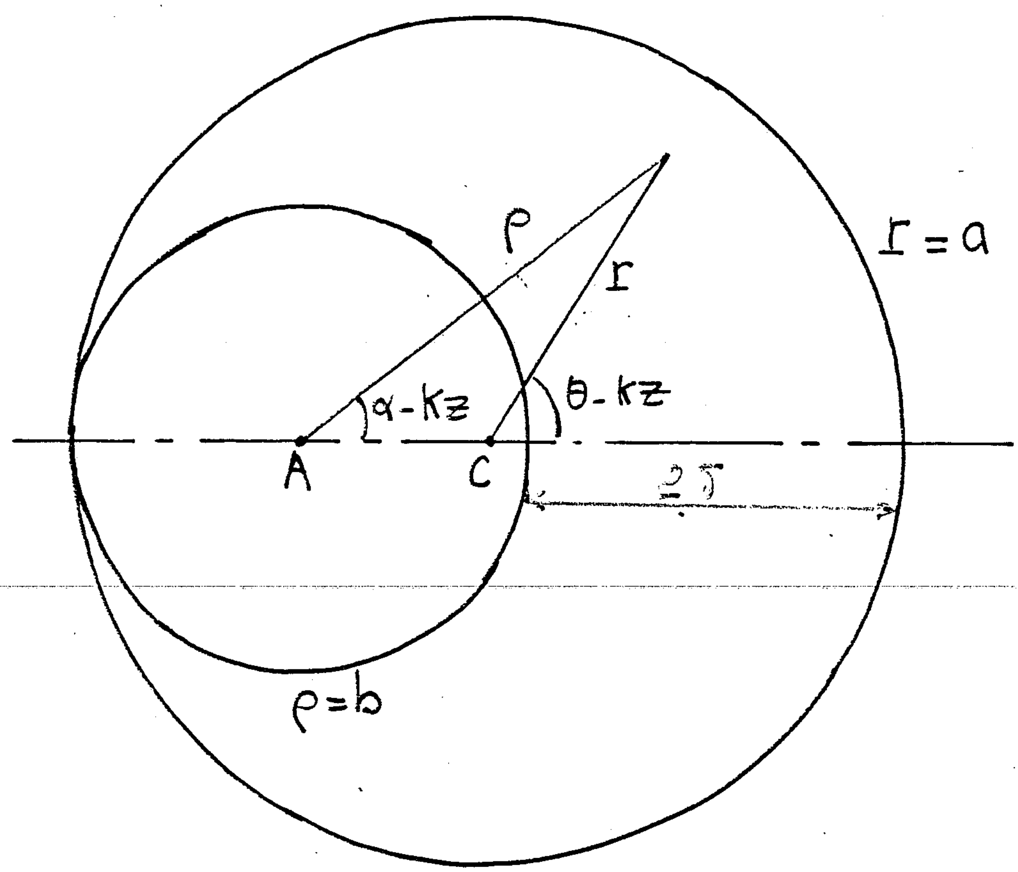

$$(r\,,\ \theta - kz) \qquad (\rho\,,\ \alpha - kz)$$

Separatrix $(\rho = b\ ,\ r = a)$

$$\vec{B} = B_0\,\vec{e}_z + k r\,B_0\,\vec{e}_\theta + \vec{B}^*$$

$$\vec{B}^* = \vec{e}_z \wedge \vec{\nabla} G\ (r, \theta - kz)$$

$$G\,(r, \theta - kz) = (r - a)(\rho - b)\,F(r, \rho)$$

inside the island, transverse solid rotation:

$$\xi = e_z \times \nabla U_i \qquad u_i = \frac{1}{2} r^2$$

displacement inside the core:

$$\xi = e_z \times \nabla U_c \qquad u_c = \frac{1}{2} r^2 - \frac{1}{2}\lambda(\rho^2 - b^2)$$

then $$\boxed{\delta W = \frac{1}{2}\lambda b \delta \int_0^{2\pi} d\alpha \, (B_s^*)^2 \cos(\alpha - kz)}$$

X point $\alpha - kz = 0$ $\qquad \delta = a - b$
island half width.

B_s^* : field at the inner separatrix.

to be a little bit more explicit:

$$n.\nabla\psi_e = \frac{\partial}{\partial\rho}(\rho B_\rho) = -\frac{\partial}{\partial\alpha}(B_\alpha)$$

$$rB_z = \Psi_R = k(r-a)\frac{\partial\rho}{\partial\theta}F = k(r-a)F\frac{(a-b)\sin\theta}{\rho}$$

with $r\sin\theta = \rho\sin\alpha$

$$\psi_R = \sin\alpha\,(a-b)(r-a)F = \frac{(a-b)}{\delta} B_\alpha \sin\alpha$$

then by integration by parts $\rightarrow \delta W$.

max of γ $\qquad \lambda = (a/b)^2$

$$\begin{cases} \lambda = 1 & \text{translation of the core} \\ \lambda = \dfrac{a}{b} & \text{core rolls along outer separatrix.} \end{cases}$$

$$\gamma \sim \frac{[1-q(0)]}{a} V_{Ap} \, \mu^{1/2}$$

$$B_\theta^* = [1-q(0)] \, k a B_0 \qquad V_{Ap}^2 = k^2 a^2 B_0^2/\rho$$

$$\mu = \frac{2a^2}{b(a+b)} \int_0^{2\pi} \left[- B_x^2/B_0^{*2} \right] \cos(\alpha - kz) \, d\alpha$$

$$\gamma \sim V_{Ap} \, \delta/a^2 \, (1-q(0)) \qquad \delta \text{ small}$$

$\gamma \propto$ island size. not $\delta^{1/2}$

it is an ideal $\{$ m=1 kink mode

with <u>one</u> <u>big</u> <u>difference</u> :

the finite island.

Why half coalescence.

Let us recall coalescence. attraction of currents

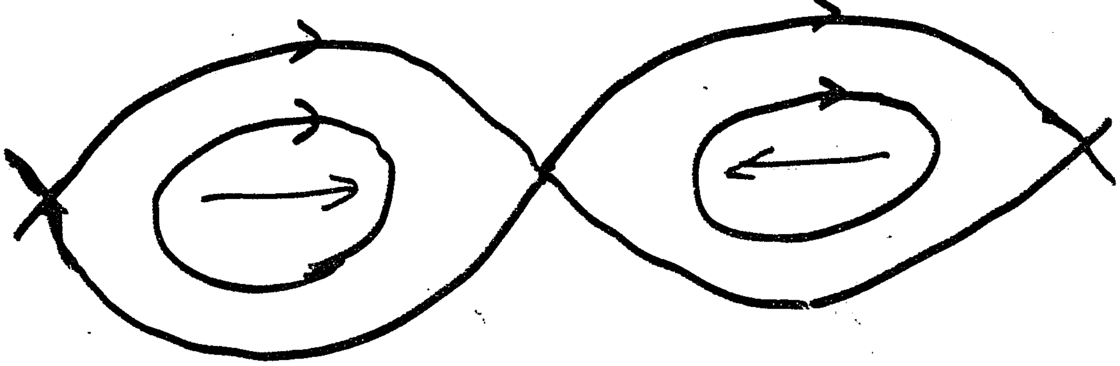

A. Bondeson Phys. Rev. Lett 51 1668 83
R. PELLAT for. J. Plasma φ 9 126 83
(Trieste meeting. June 82.).

difference:

$$\psi \sim \underbrace{\psi_k \sin kY}_{\text{not present for Bondeson}} + \alpha\left\{\psi_{\frac{k}{2}} \cos\frac{kY}{2} - \psi_{\frac{3k}{2}} \cos\frac{3kY}{2}\right\}$$

equivalent of translation.

two extremal $\begin{cases} \alpha \uparrow \infty \\ \alpha < 1 \text{ finite} \quad \underline{\text{true extremum}} \end{cases}$

. in fact half coalescence ~~is~~ is a one island instability

Let us comment about this "

it has a growth $\sim \left(\frac{\rho B}{B}\right)^{3/4} (\Delta')^{1/2}$

like Diamond's and al 3/2 mode

but it is not correct in true Rutherford growth because Rutherford current makes $\Delta' \equiv 0$ for MHD time scales. This instability can appear if one has faster modification of the outside Δ' than resistive Rutherford current can achieve.

In the case of the m=1 mode the few is due to the B modulation along the inner separatrix. If there is no such modulation then there is no source of energy but this modulation is a consequence of the island formation. ($B^{*}=0$ at X point)

For the half coalescence, there is repulsion of the two currents:

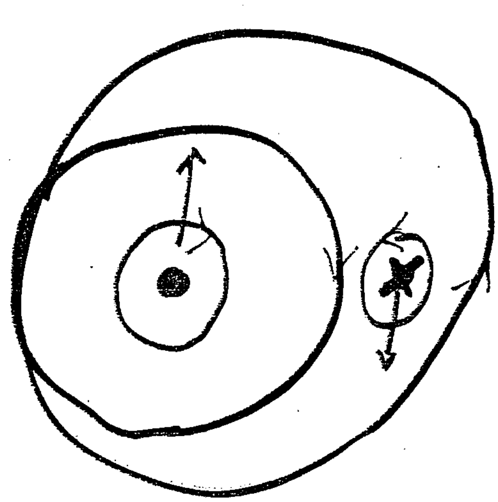

A SAWTOOTH OSCILLATION MODEL

T. JENSEN

GA TECHNOLOGIES

A SAWTOOTH OSCILLATION MODEL

BY TORKIL H. JENSEN + FRED W. MCCLAIN

GA TECHNOLOGIES INC. [BULL. AM. PHYS. SOC. 29 1370 (1984)]

~~RELAXATION PHAENOMENA IN~~:

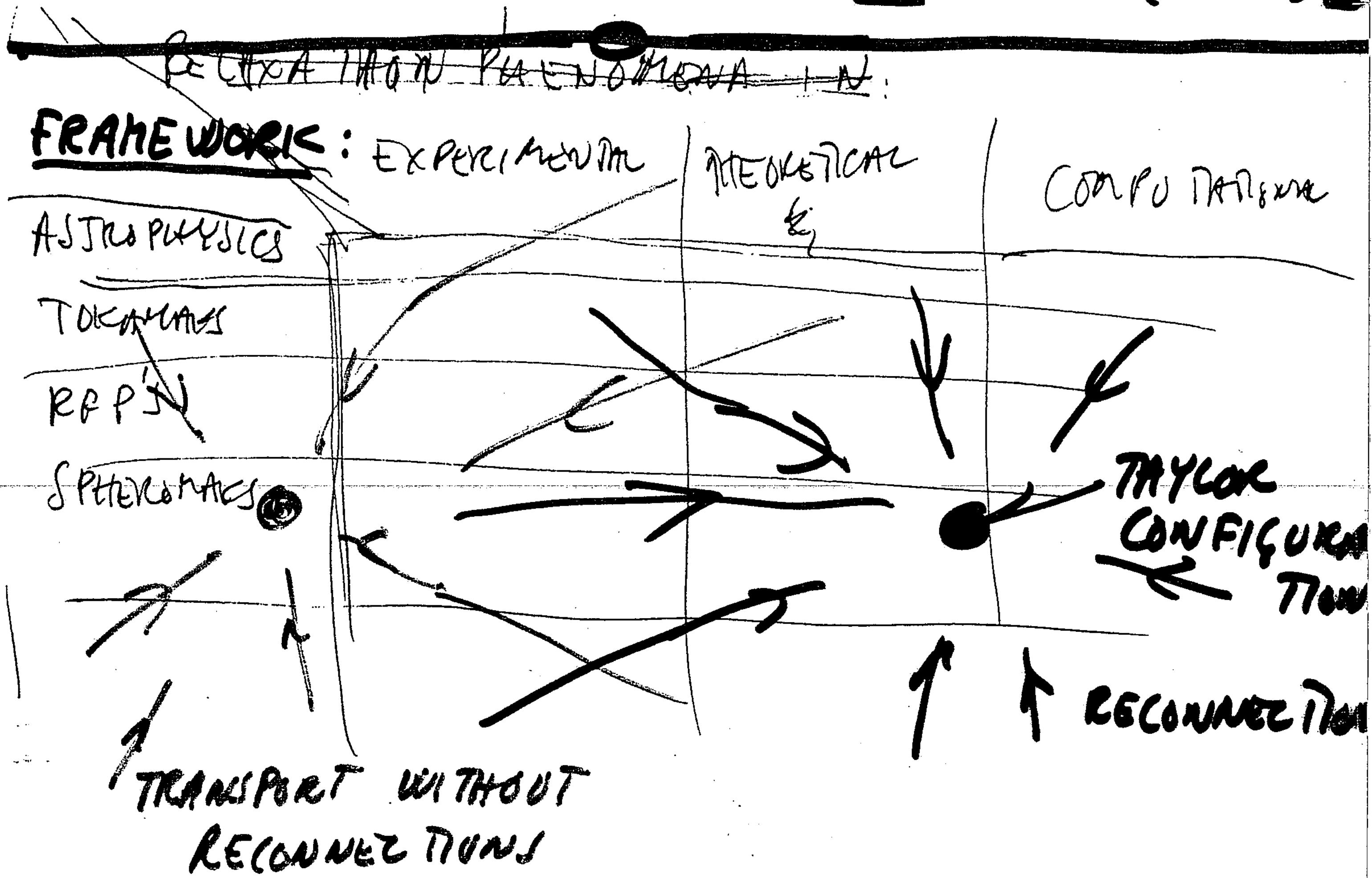

MULTIDIMENTIONAL CONFIGURATION PARAMETER SPACE

POSSIBLE RESULT OF CONTRADICTING TENDENCIES

- i) CONFIGURATION WITH $\partial/\partial t = 0$
- ii) SIMPLE FLUCTUATIONS (OSCILLATIONS)
- iii) COMPLICATED FLUCTUATIONS (TURBULENCE)

AIM OF THIS WORK:

A SIMPLE UNDERSTANDING OF THE SAWTOOTH OSCILLATION

—o—

WORK IS IN PROGRESS

MANY GUESSES NEEDED AT THIS TIME

ANALOGY : (RELAXATION OSCILLATOR)

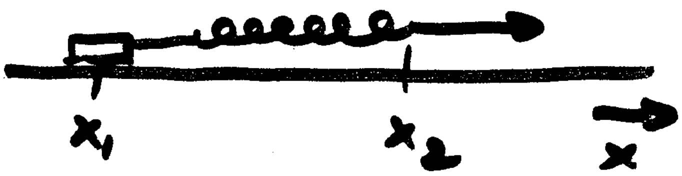

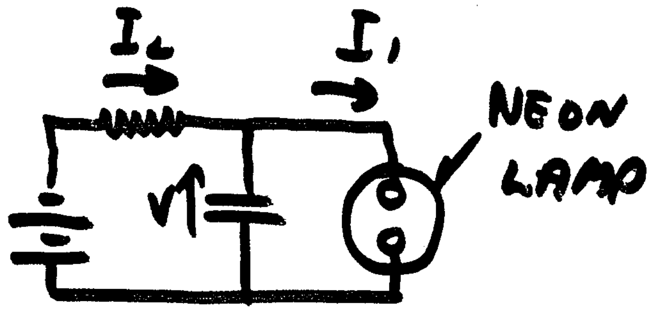

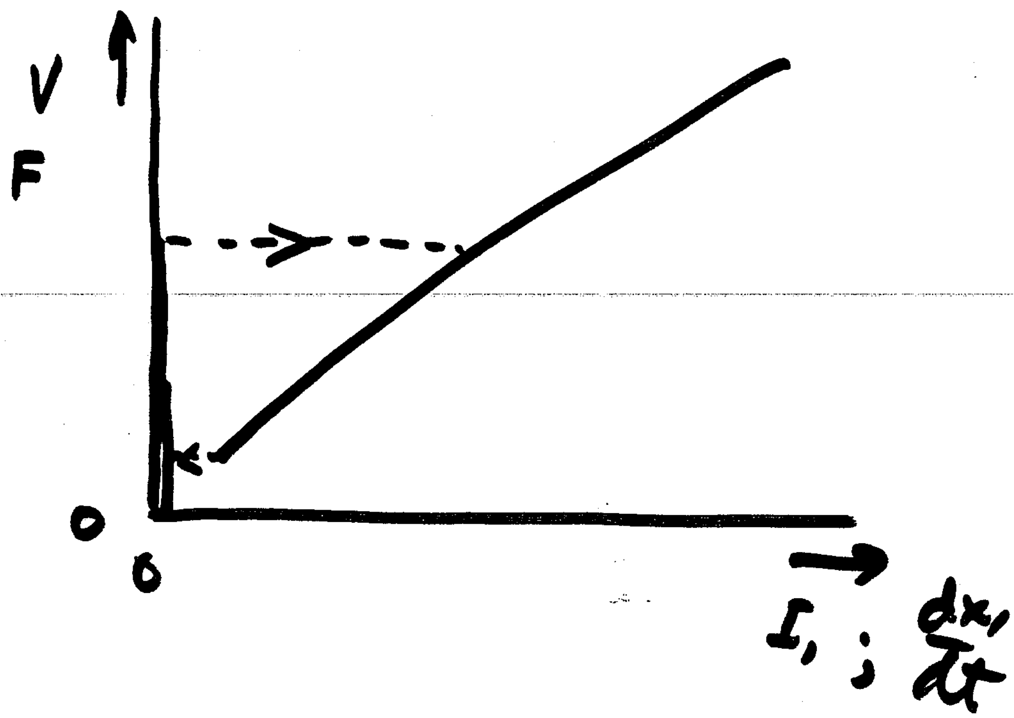

$$F\left(\frac{dx_1}{dt}\right) = E\,(x_2 - x_1) \quad ; \quad V(I_1) = \frac{1}{C}\left[\int I_L\,dt - \int I_1\,dt\right]$$

ARE SAWTOOTH OSCL. THAT SIMPLE ?

SIMPLIFYING ASSUMPTIONS:

i) RESISTIVE MHD

ii) HELICAL SYMMETRY $\left[(\hat{z} + k_z \hat{\theta}) \cdot \bar{\nabla} = 0\right]$; BOUNDARY: CIRCULAR X-SECTION CONDUCTOR.

iii) TOKAMAK ORDERING $((k_z)^2 \ll 1)$

iv) DESCRIPTION OF EQUIL. BY TWO PARAMETERS ONLY. (MAY INCLUDE EFFECT OF SOME TURBULENCE)

EQUILIBRIUM: $\bar{\nabla}^2 \psi + M\{\psi\} - 1 = 0 \; ; \; \psi_b = 0$

TWO PARAMETERS FOR DESCRIPTION OF M:

μ IS MAXIMUM CURRENT DENSITY $(\mu > 0)$

x IS PEAKEDNESS $0 < x < 1$

$$M_1 \equiv \frac{\mu}{x(2\psi_{sep} - \psi_{ol})} \left\{ \frac{K+1}{4}\left(\psi - \psi_{sep} + |\psi - \psi_{sep}|\right) + \frac{K-1}{2}(\psi - 2\psi_{sep}\right.$$

$$M \equiv \tfrac{1}{2}\left[M_1 + \mu - |\mu - M_1|\right]$$

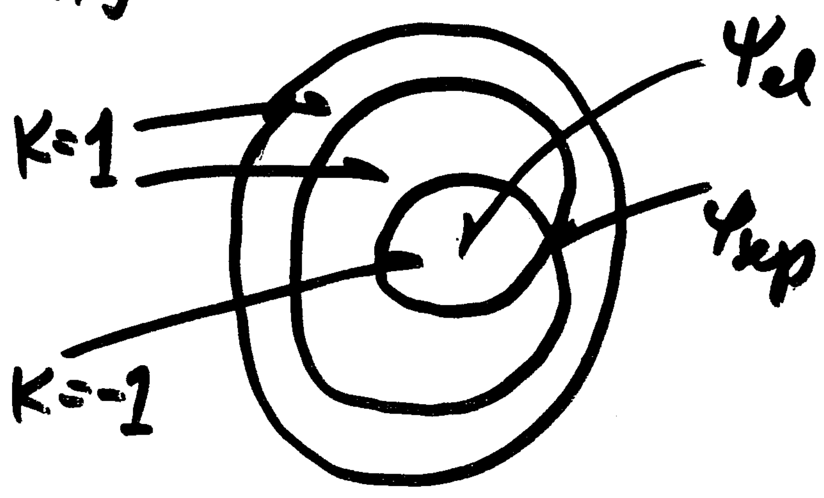

ψ_{ol} IS LARGEST ψ-VALUE AT MAGNETIC AXES.

ψ_{sep} IS SECOND LARGEST ψ-VALUE AT MAGNETIC AXES.

TRANSPORT WITHOUT RECONNECTION: 4

(FOR CONSTANT CURRENT)

$$\frac{d\mu}{dt} > 0 \qquad \frac{d\chi}{dt} > 0 \quad \text{(THERMAL INSTABILITY)}$$

TRANSPORT SLOW. EQUIL.

SOLUTIONS TO EQUILIBRIUM PROBLEM:

i) WHEN $\mu < 1$, $\nabla^2\psi > 0$, ONE MAGNETIC AXIS, ONE SOLUTION, AXISYMMETRIC, $q > 1$

ii) WHEN $\mu > 1$ MANY SOLUTIONS

1 SOLUTION WITH 1 MAGNETIC AXIS ($q_0 < 1$)

GUESS:

- 2 SOLUTIONS WITH 3 MAGNETIC AXES { UP-DOWN SYM / ASYM.
- MANY SOLUTIONS WITH MANY MAGNETIC AXES.

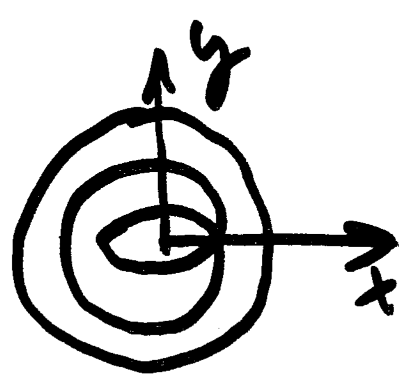

UP-DOWN SYM.: $\psi(x,y) = \psi(x,-y)$

ASYMMETRIC: $\psi(x,y) \neq \psi(x,-y)$

STABILITY:

[redacted]

— o —

ASSUMPTION: CONSIDER ONLY PERTURBATIONS OF SAME HELICAL SYMMETRY AS EQUILIBRIUM $\left[(\hat{z} + h_n\hat{\theta})\cdot\nabla = 0\right]$

FORMALISM*) FOR STABILITY:

STABLE IF LOWEST EIGENVALUE, λ_0, IS POSITIVE

$$\boxed{D^2\varphi_\nu + DM\{\varphi_\nu\} - \langle DM\{\varphi_\nu\}\rangle + \lambda_\nu\varphi_\nu = 0\,,}$$

$$\varphi_{\nu B} = 0\,;\quad DM\{\varphi_\nu\} \equiv \lim_{\varepsilon\to 0}\frac{1}{\varepsilon}\left[M\{\psi+\varepsilon\varphi_\nu\} - M\{\psi\}\right]$$

$$\langle S\rangle \equiv \oint \frac{S\,d\ell}{|D\psi|} \Big/ \oint \frac{d\ell}{|D\psi|}\,.$$

INCLUDES STABILITY AGAINST:

i) SLOW RESISTIVE MODES $(\gamma \propto \eta)$

ii) TEARING MODES $(\gamma \propto \eta^{k})$

iii) KINK (IDEAL) MODES $(\gamma \propto \eta^{0})$

*) JENSEN + THOMPSON, J. PLASMA PHYS. 19 227 (1978)

6

INSTABILITY OF UP-DOWN SYMMETRIC 3-AXES EQUIL.!

EQUIL: $\psi(x,y) = \psi(x,-y)$

DIFFERENTIATE EQUIL. EQ. W.R.T. y:

$$D^2 \frac{\partial\psi}{\partial y} + DM\left\{\frac{\partial\psi}{\partial y}\right\} = 0$$

NOTE: $\frac{\partial\psi}{\partial y} = 0$ ON SURFACE INSIDE BOUNDARY.

COMPARE TO STABILITY EIGENVALUE PROBLEM WITH $\varphi = \partial\psi/\partial y$.

BECAUSE OF SYMMETRY, $\langle DM\{\frac{\partial\psi}{\partial y}\}\rangle = 0$

SO → MARGINALLY STABLE ($\lambda = 0$) WHEN φ FORCED TO VANISH INSIDE BOUNDARY

→ UNSTABLE WHEN $\varphi = 0$ ON BOUNDARY.

SEE ALSO: BUSSAC, PELLAT, SOULE + TAGGER, INT. CONF. ON. PLASMA PHYS., LAUSANNE 1984

— o —

ARGUMENT ALSO HOLDS FOR 1-AXIS EQUIL. WHEN $\mu > 1$ ($q_0 < 1$)

→ KRUSKAL LIMIT.

(6A)

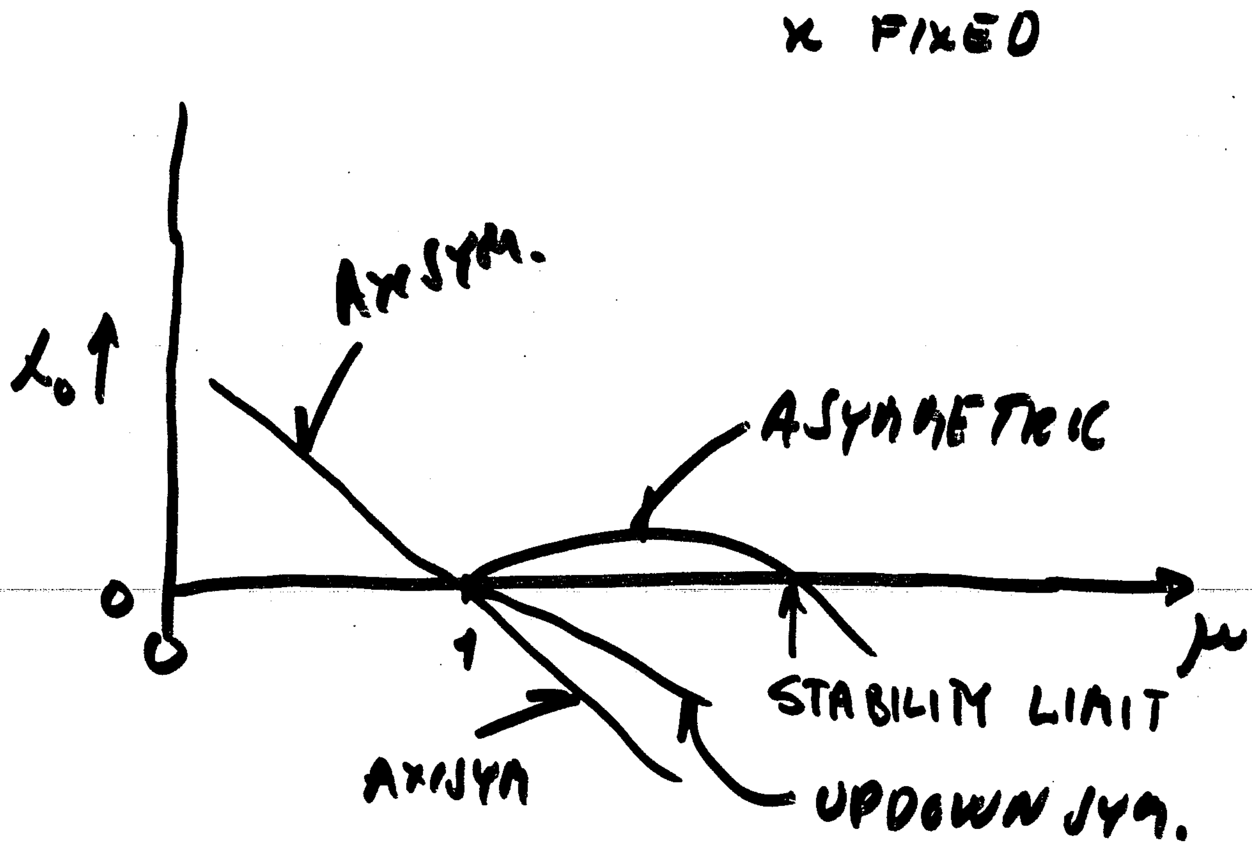

x FIXED
AXISYM.
λ_0
ASYMMETRIC
0
0
1
μ
STABILITY LIMIT
AXISYM
UPDOWN SYM.

7

WE ASSUME THERE EXISTS STABLE 3-AXIS EQUILIBRIA.

THEY MUST BE ASYMMETRIC.

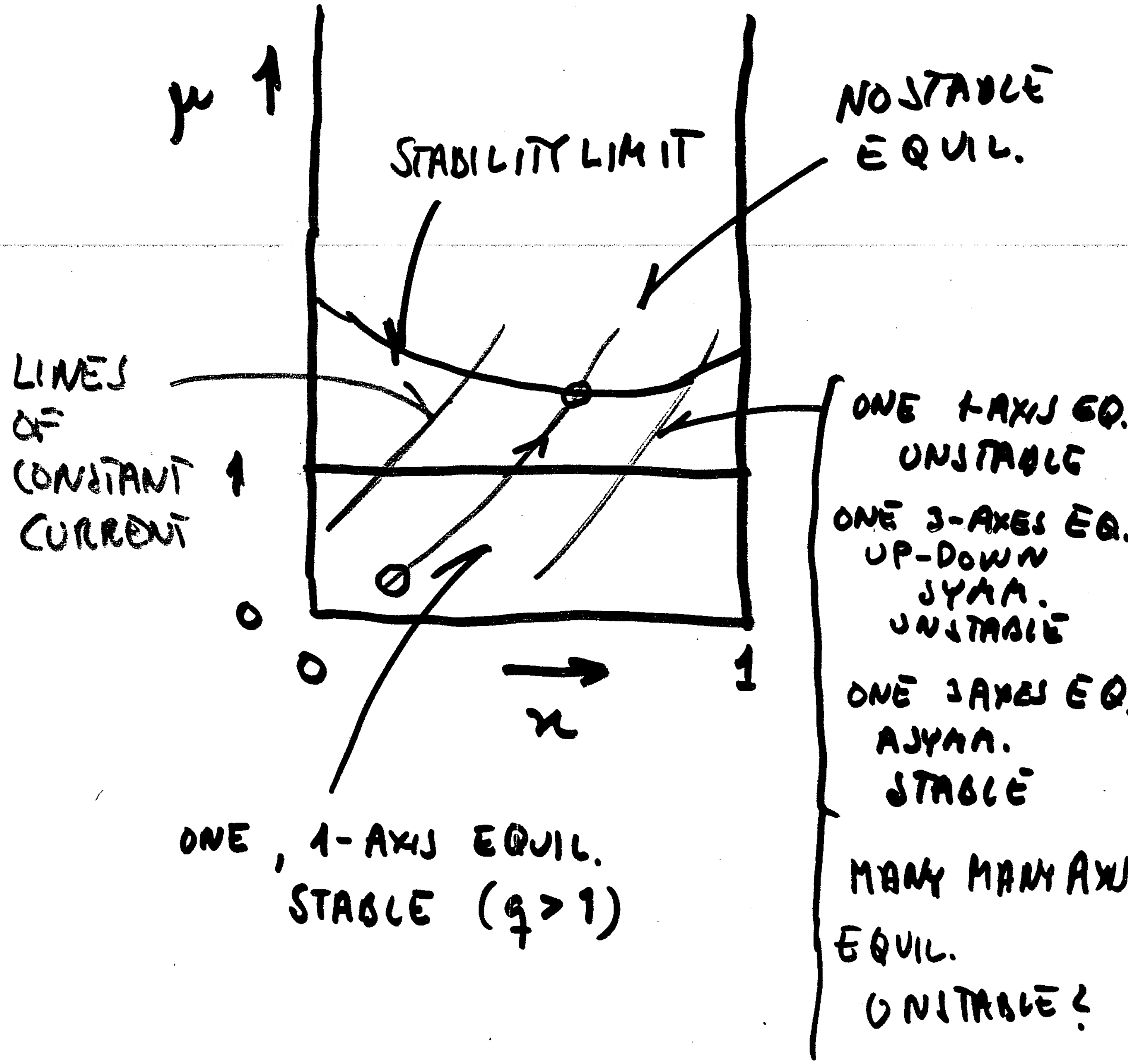

NATURE OF INSTABILITY:

SIMILAR TO DROPLET-ELLIPSE MODE OBSERVED IN DOUBLETS.

— o —

NONLINEAR EFFECT *):

i) ALWAYS NONLINEARLY DESTABILIZED (→ EXPLOSIVE)

ii) SPECIFIC DIRECTION

GUESS: THIS INSTABILITY BRINGS EQUILIBRIUM BACK TO 1-AXIS EQUIL. (INNER ISLAND DISAPPEARS).

SINCE $\psi(A)$ IS CONSERVED WE CAN ESTIMATE γ, μ OF RESULTING 1-AXIS EQUILIBRIUM.

*) JENSEN + MCCLAIN, J. PLASMA PHYS. 28 495 (1982)

9

THIS IS VERY CLOSE TO RELAXATION OSCILLATOR.

FOR GIVEN I WE CAN FIND BOTH μ_{MAX} AND μ_{MIN}.

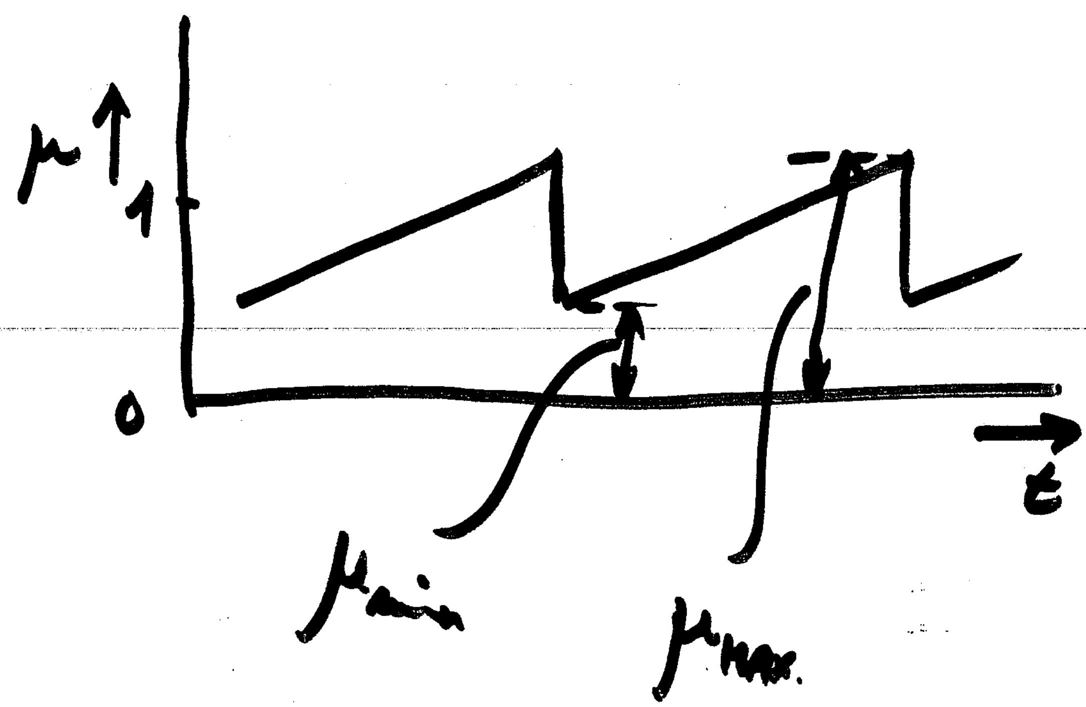

μ HAS PROBABLY A MONOTONIC RELATIONSHIP TO SOFT X-RAY INTENSITY OBSERVED IN TOKAMAKS.

(10)

NUMERICAL EFFORT:

i) MAKE AN EQUILIBRIUM CODE

INPUT: μ, x, NO OF AXES

IN PROGRESS

ii) MODIFY STABILITY CODE

iii) MAKE SURE "DIRECTION" OF NONLINEAR INSTABILITY HAS RIGHT SIGN.

EXPECTED EASY.

SOFT X-RAY IMAGING OF TRANSIENT AND DOUBLE SAWTEETH ON TEXT

S. KIM

UNIVERSITY OF TEXAS AT AUSTIN
FUSION RESEARCH CENTER

Soft X Ray Imaging of Transient and Double Sawteeth on TEXT

S.B. Kim
University of Texas at Austin
Austin, Texas 78712

US-JAPAN Workshop on Magnetic Reconnection
Austin, Texas

December 10 - 13, 1984

TEXT Integrated MHD Diagnostic System

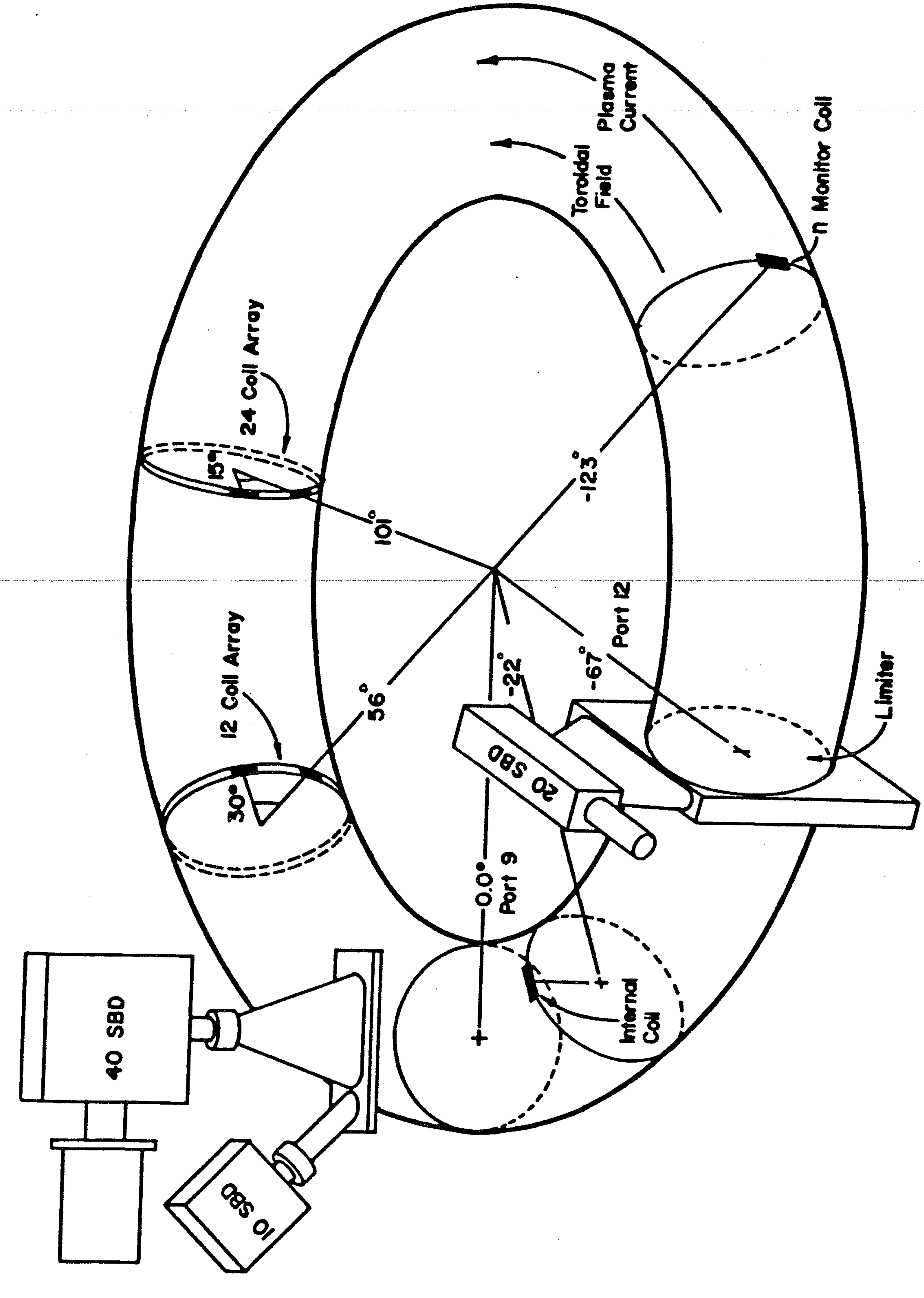

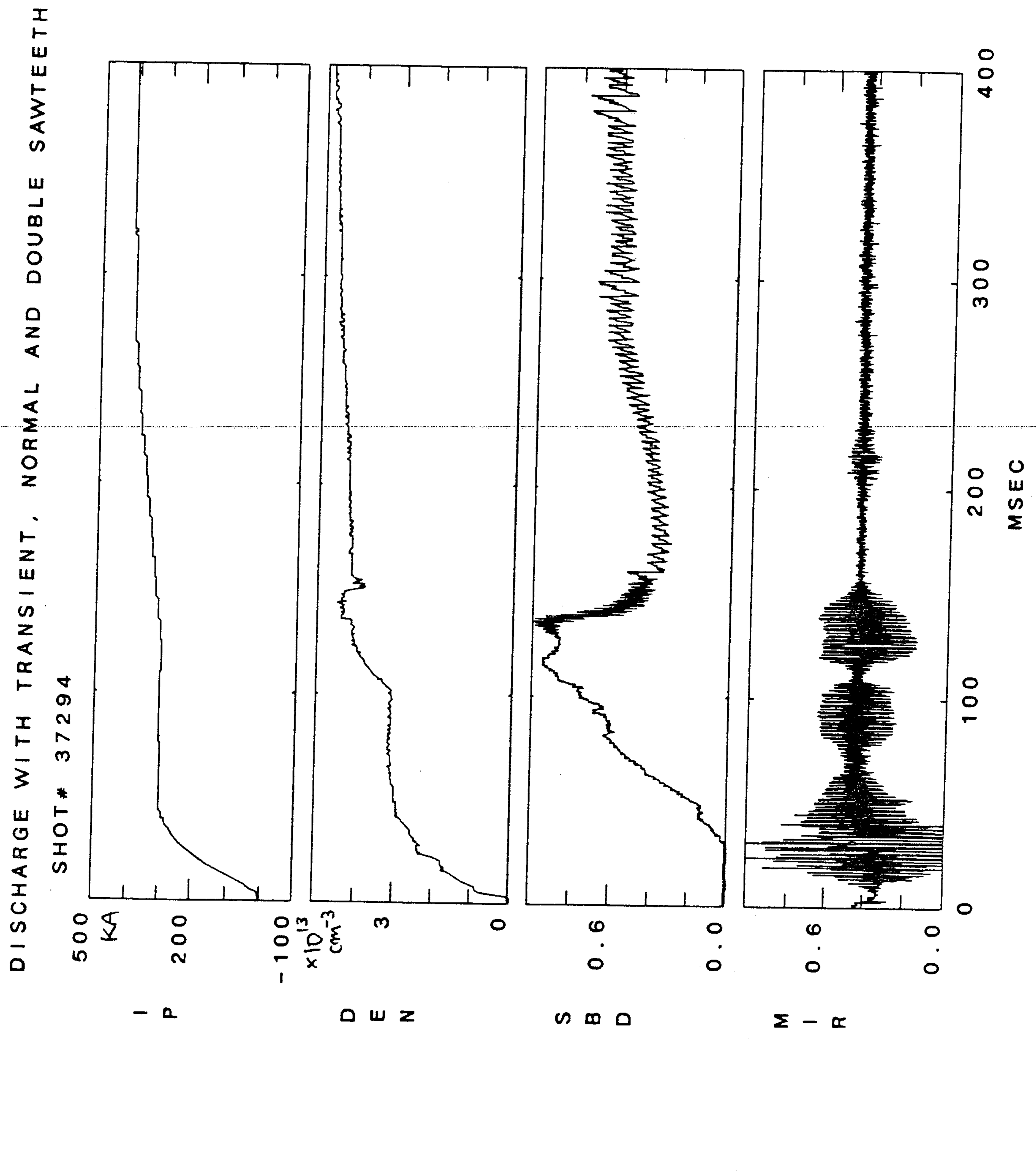
DISCHARGE WITH TRANSIENT, NORMAL AND DOUBLE SAWTEETH
SHOT# 37294
500
KA
200
-100
×10^13 cm^-3
3
0
0.6
0.0
0.6
0.0
IP
DEN
SBD
MIR
0
100
200
300
400
MSEC

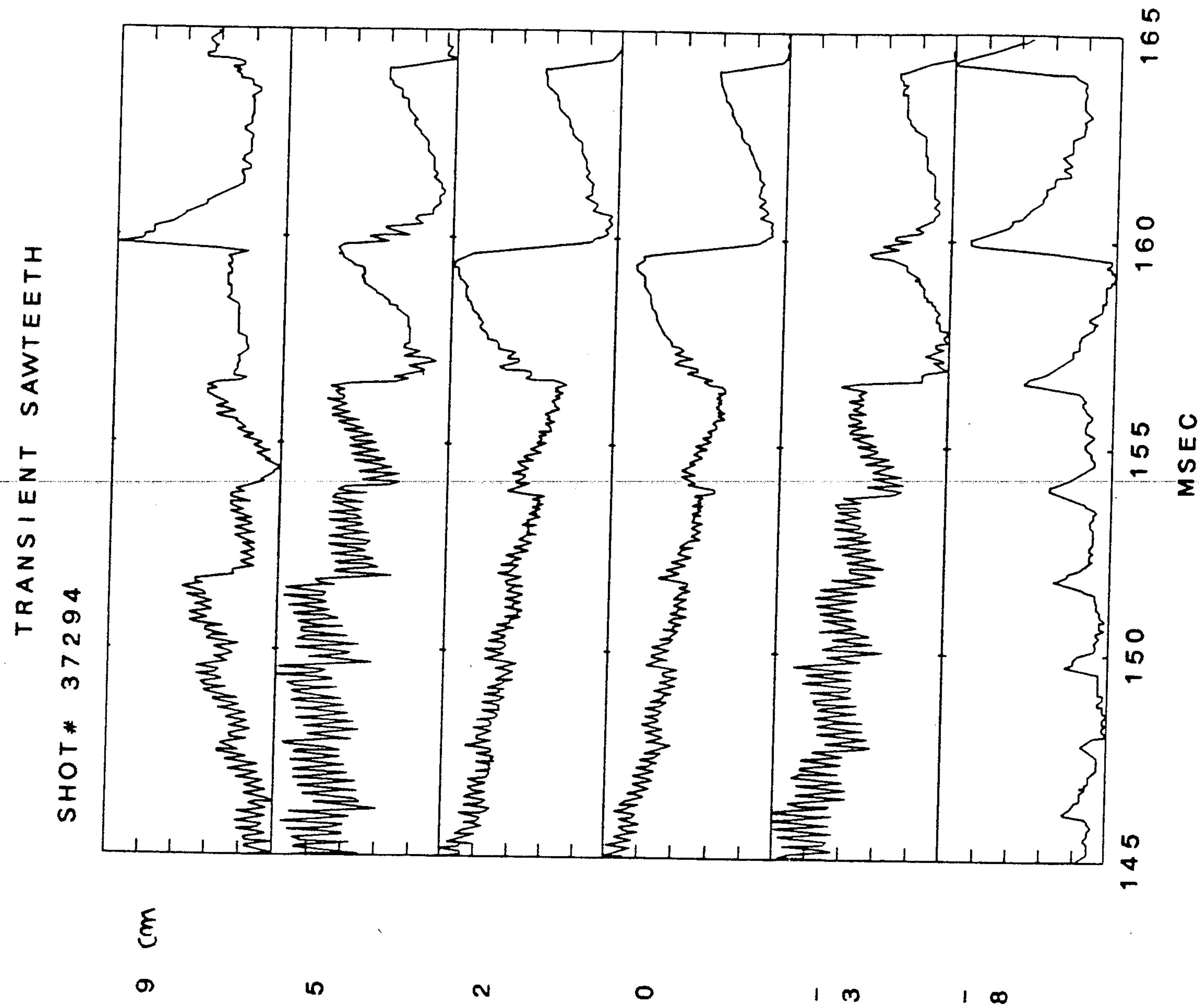
TRANSIENT SAWTEETH
SHOT# 37294
9 cm
5
2
0
- 3
- 8
145
150
155
160
165
MSEC

RELATIVE AMPLITUDE PROFILES OF TRANSIENT AND NORMAL SAWTEETH

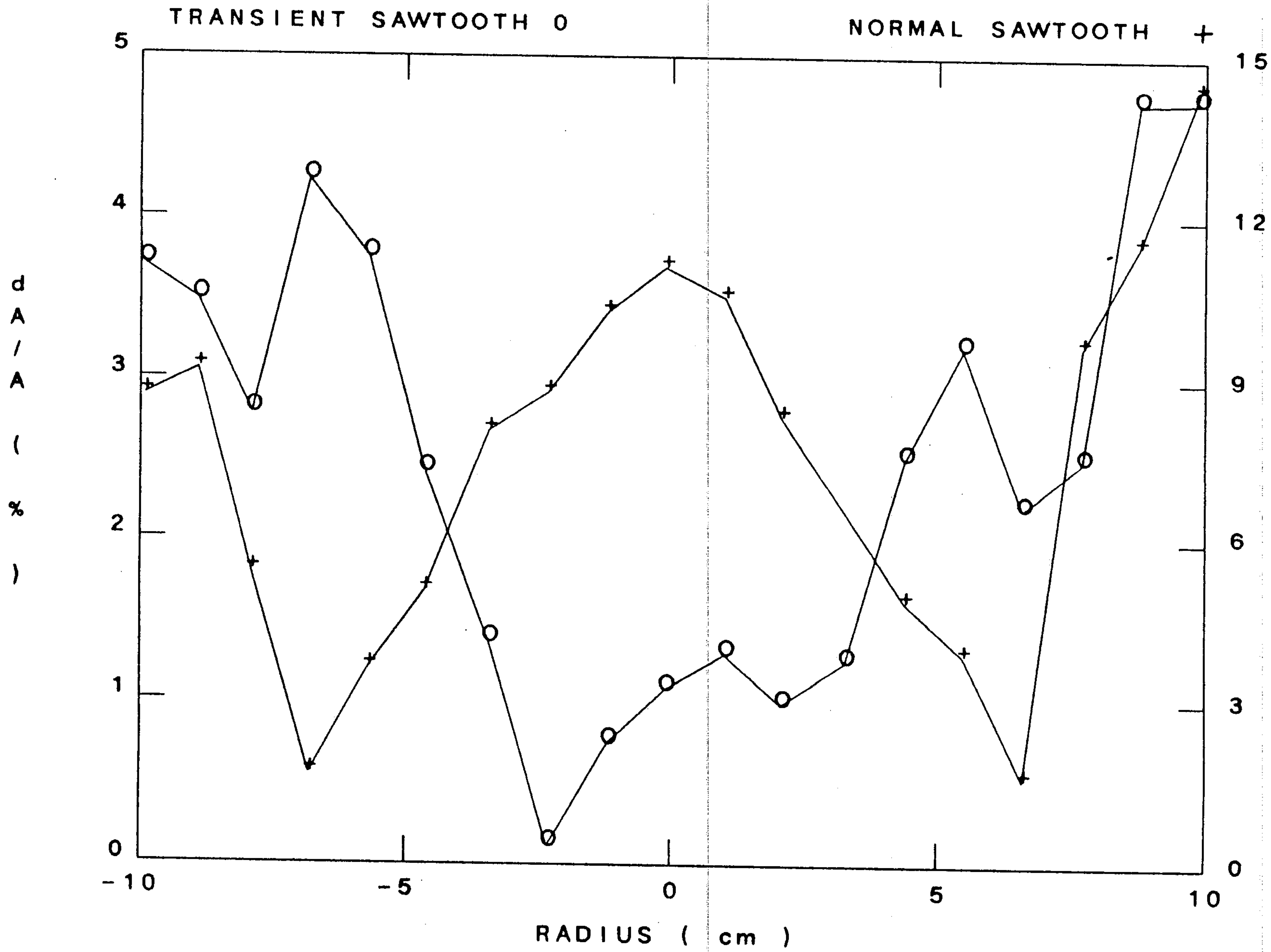

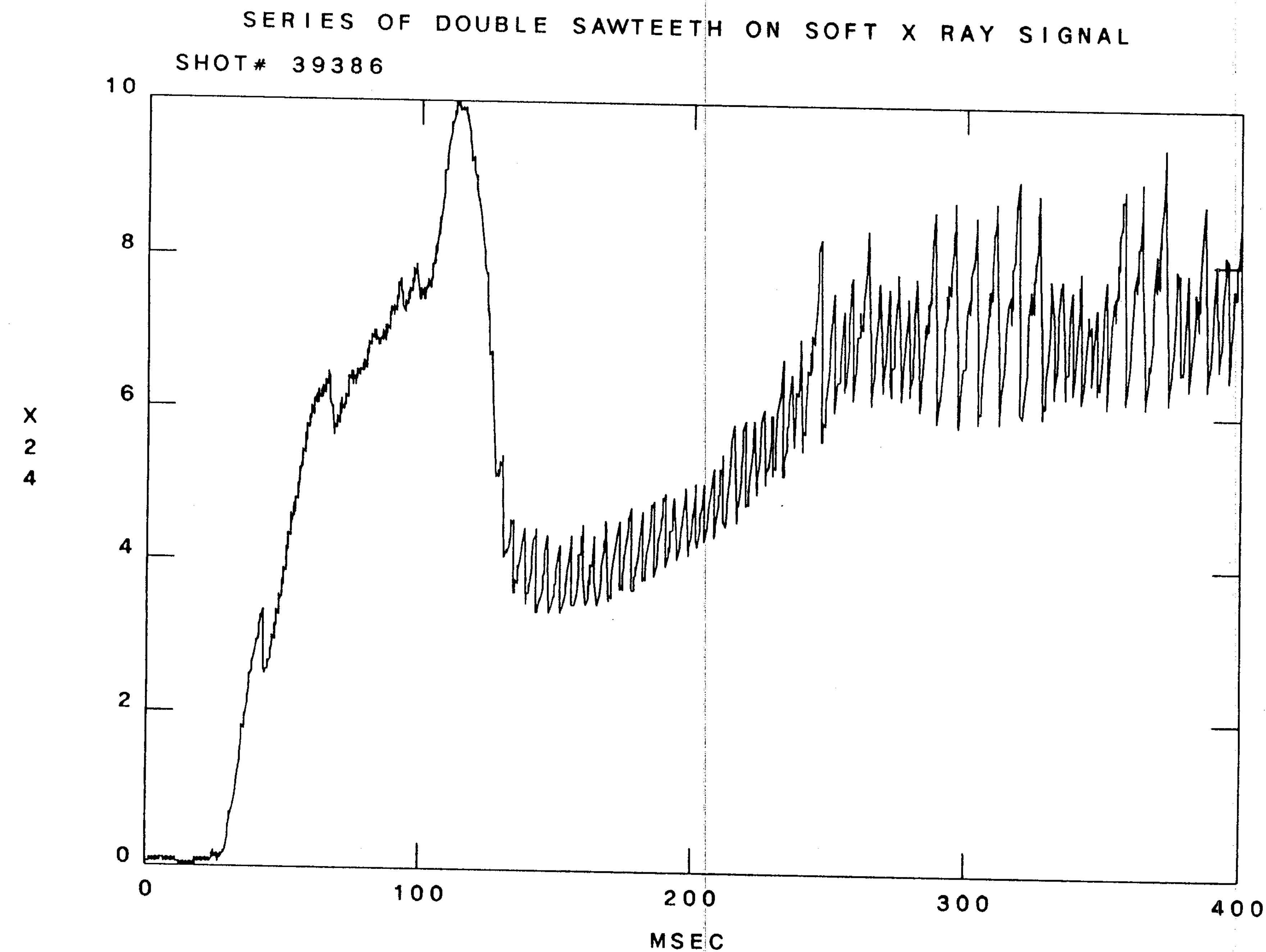
SERIES OF DOUBLE SAWTEETH ON SOFT X RAY SIGNAL
SHOT# 39386
X
2
4
0
2
4
6
8
10
0
100
200
300
400
MSEC

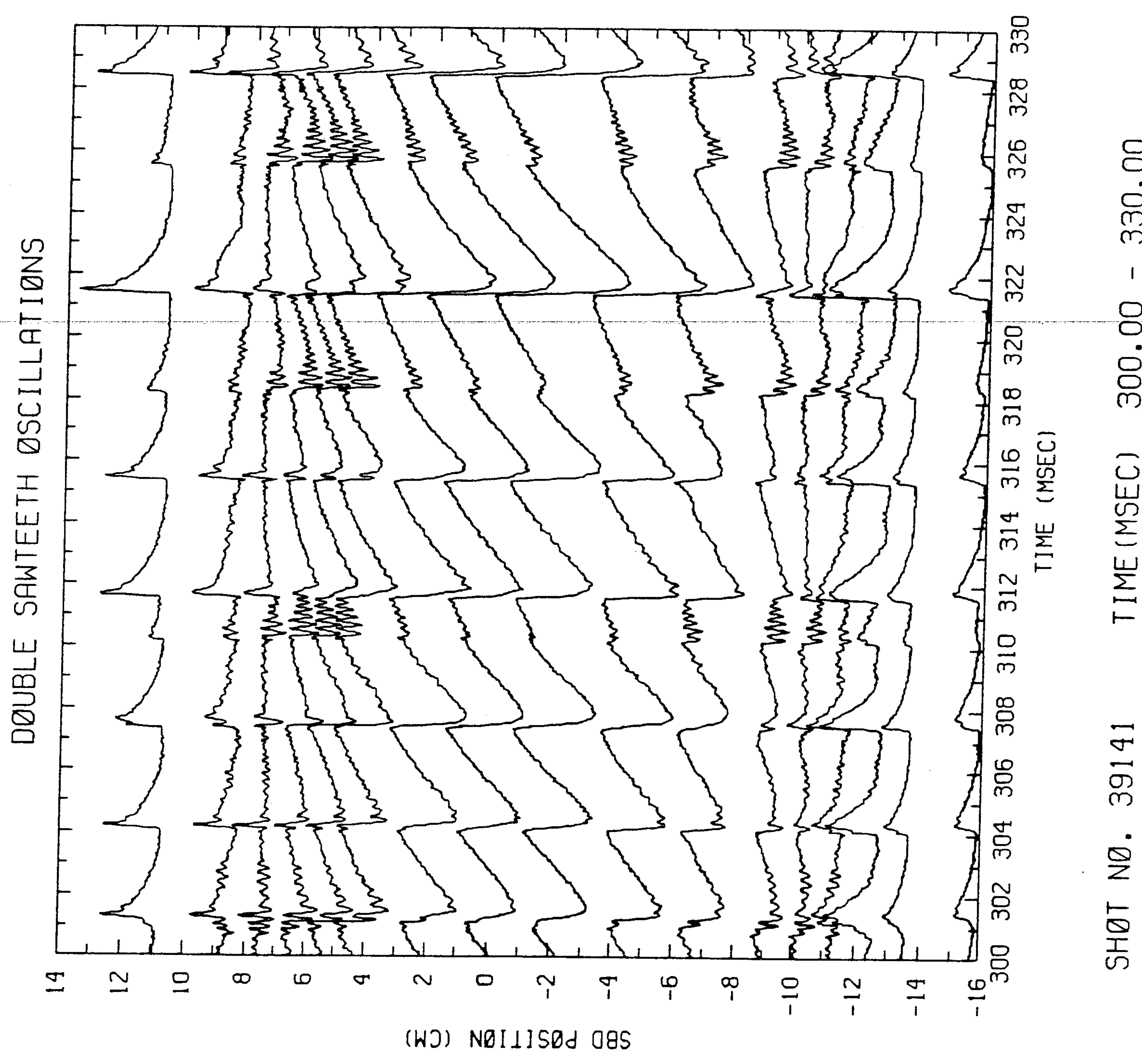
DØUBLE SAWTEETH ØSCILLATIØNS
SBD PØSITIØN (CM)
14
12
10
8
6
4
2
0
-2
-4
-6
-8
-10
-12
-14
-16
300
302
304
306
308
310
312
314
316
318
320
322
324
326
328
330
TIME (MSEC)
SHØT NØ. 39141 TIME(MSEC) 300.00 - 330.00

DOUBLE SAWTEETH ON RADIOMETER

SHOT# 58199 r = 5 cm

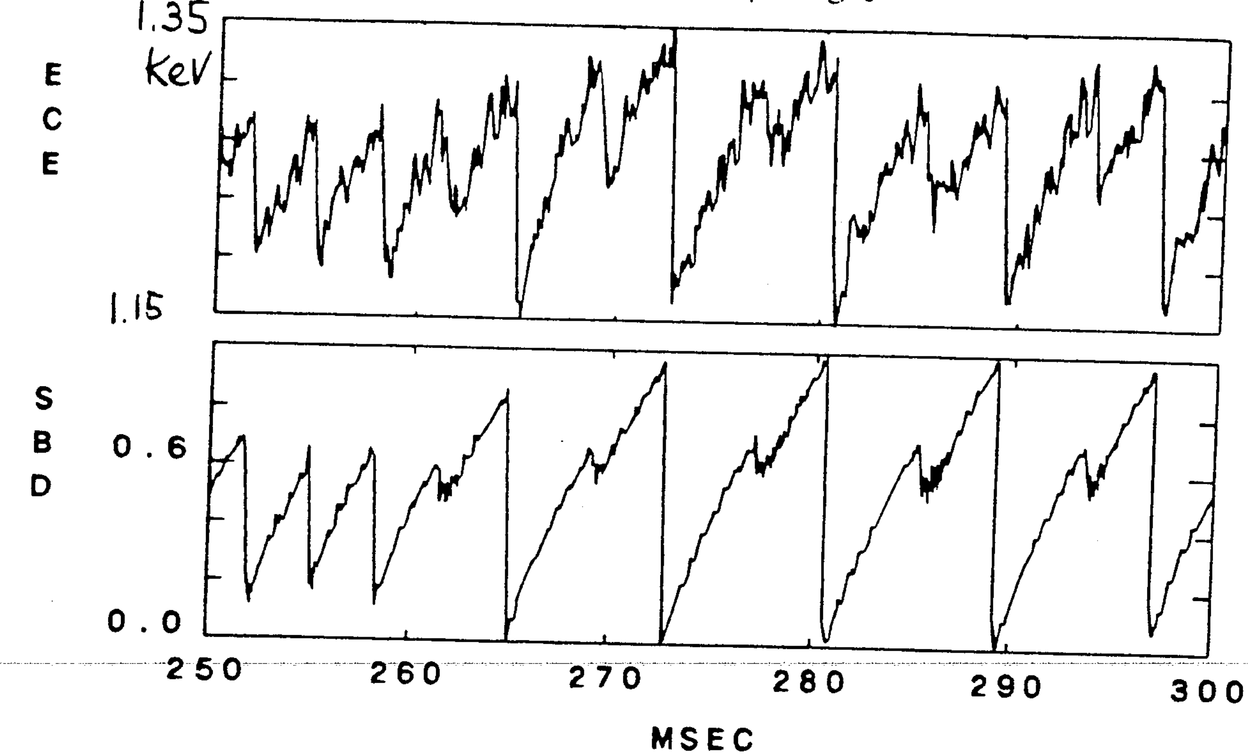

SHOT# 58213 r = 19 cm

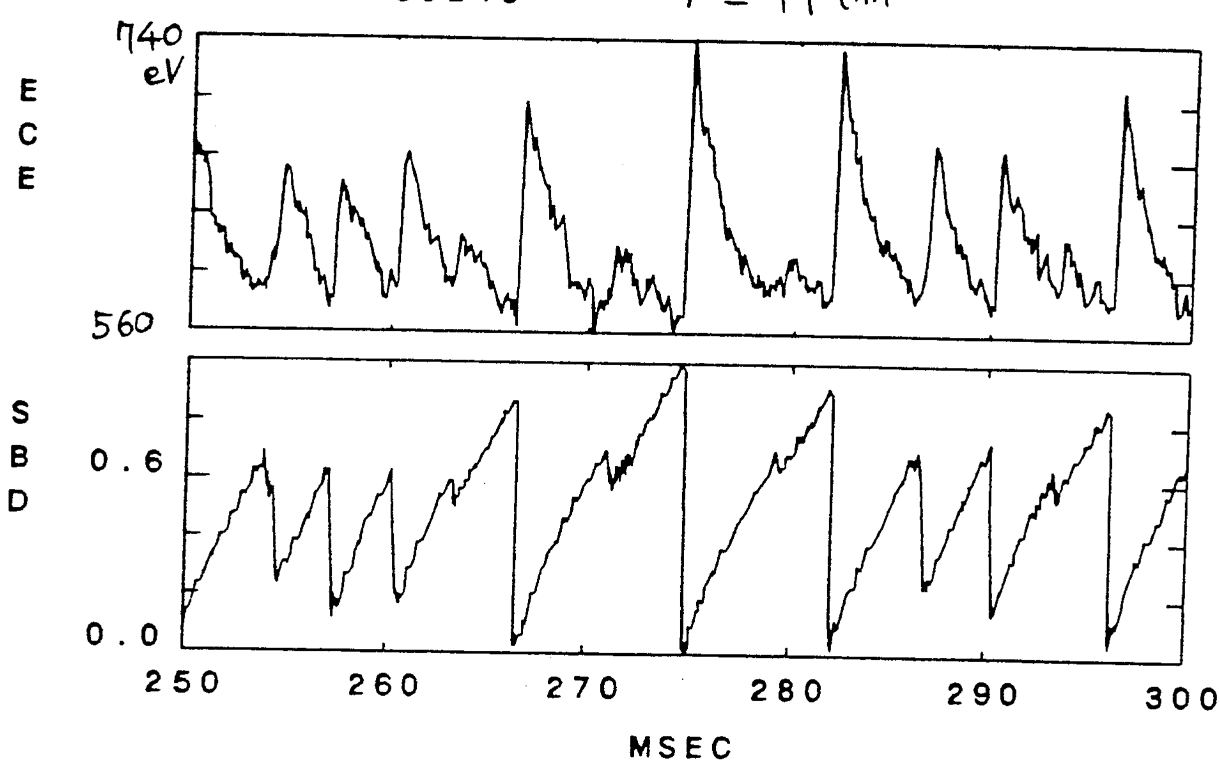

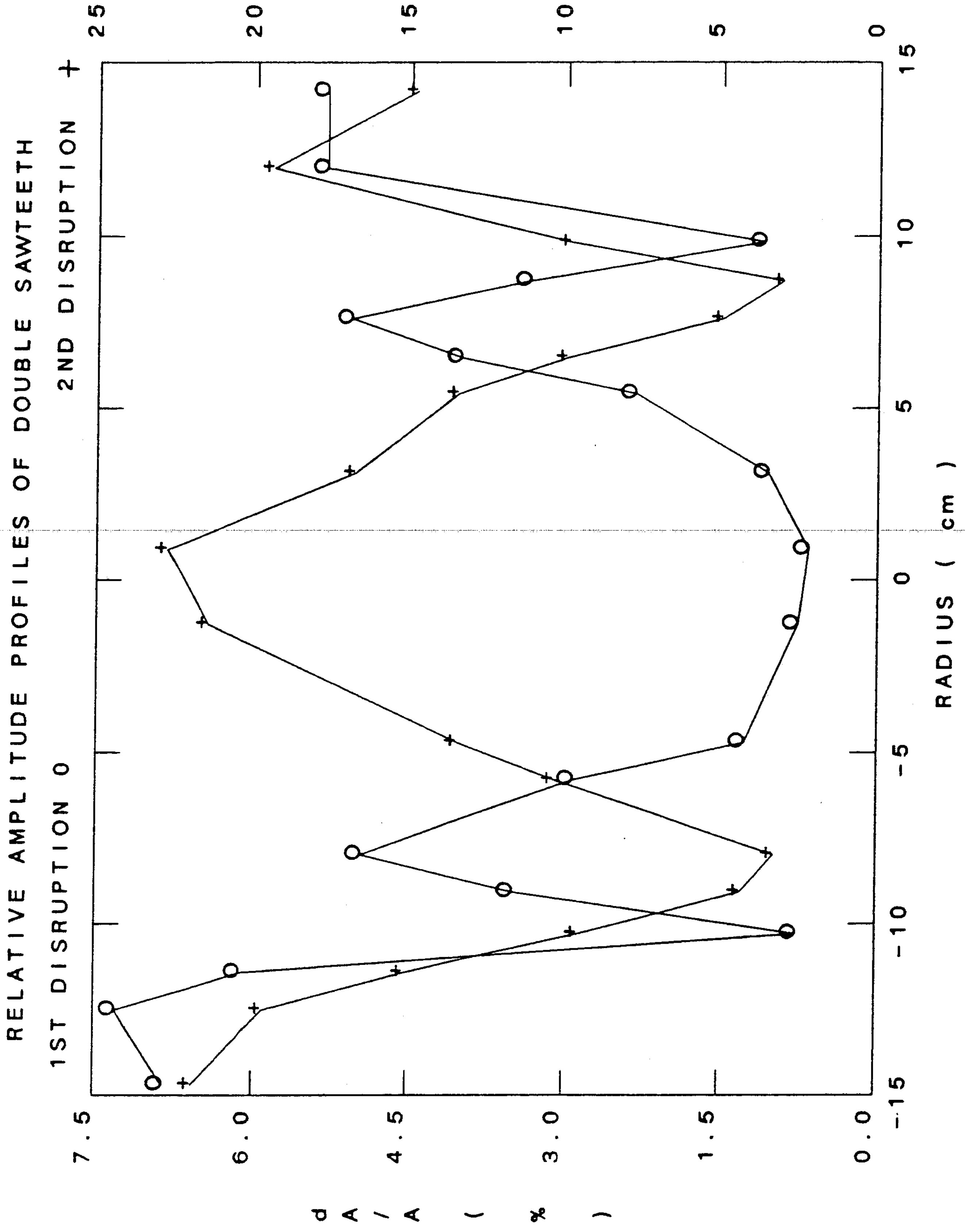
RELATIVE AMPLITUDE PROFILES OF DOUBLE SAWTEETH
1ST DISRUPTION O
2ND DISRUPTION +
dA/A (%)
0.0
1.5
3.0
4.5
6.0
7.5
0
5
10
15
20
25
RADIUS (cm)
−15
−10
−5
0
5
10
15

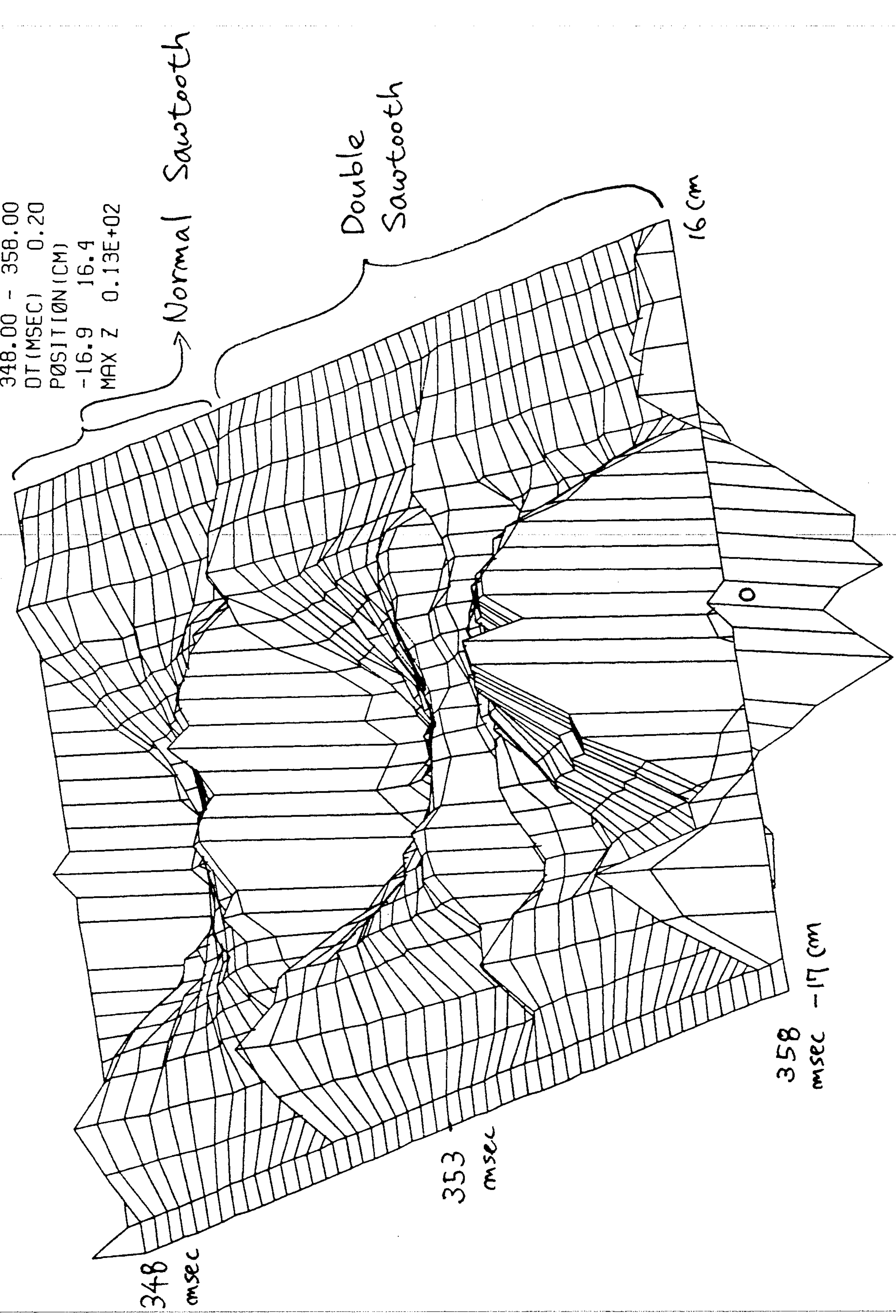
SHØT 39386
TIME(MSEC)
348.00 - 358.00
DT(MSEC) 0.20
PØSITIØN(CM)
-16.9 16.4
MAX Z 0.13E+02
Normal Sawtooth
Double Sawtooth
16 cm
0
348 msec
353 msec
358 msec
-17 cm

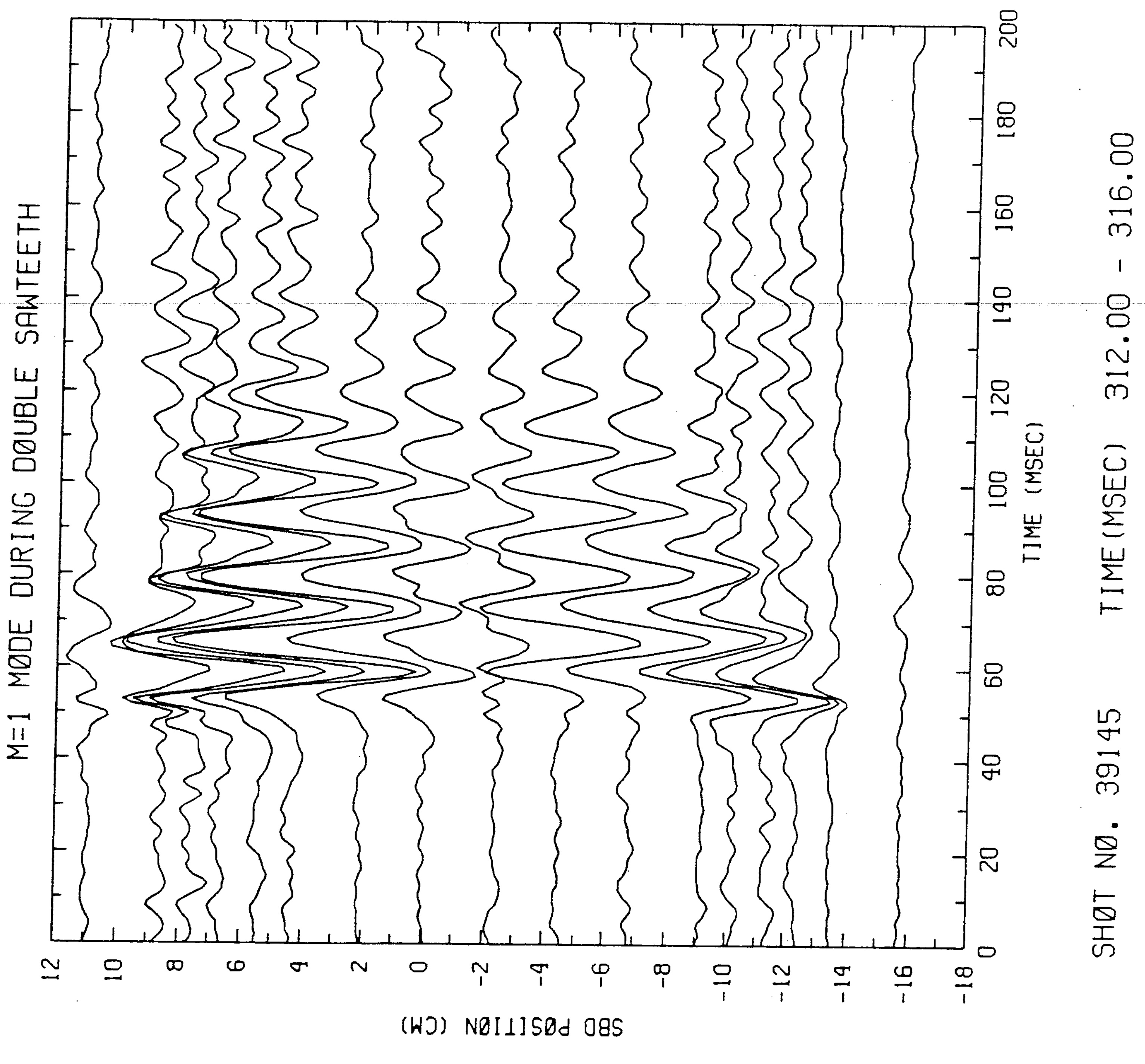
M=1 MØDE DURING DØUBLE SAWTEETH
SBD PØSITIØN (CM)
TIME (MSEC)
SHØT NØ. 39145
TIME(MSEC) 312.00 - 316.00

M-1 AMD M-2 MODE COUPLINGS DURING DOUBLE SAWTEETH

SHOT# 58671

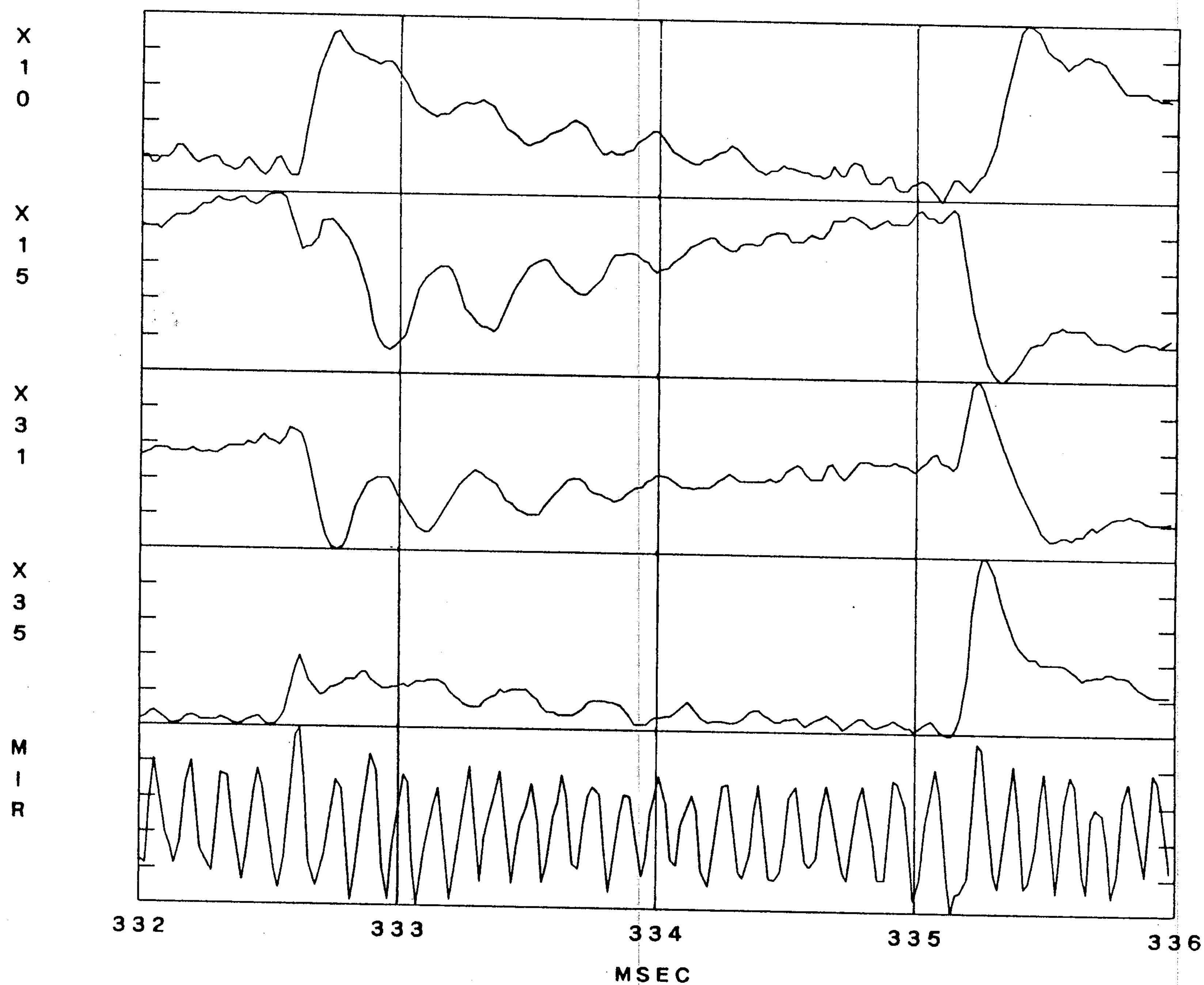

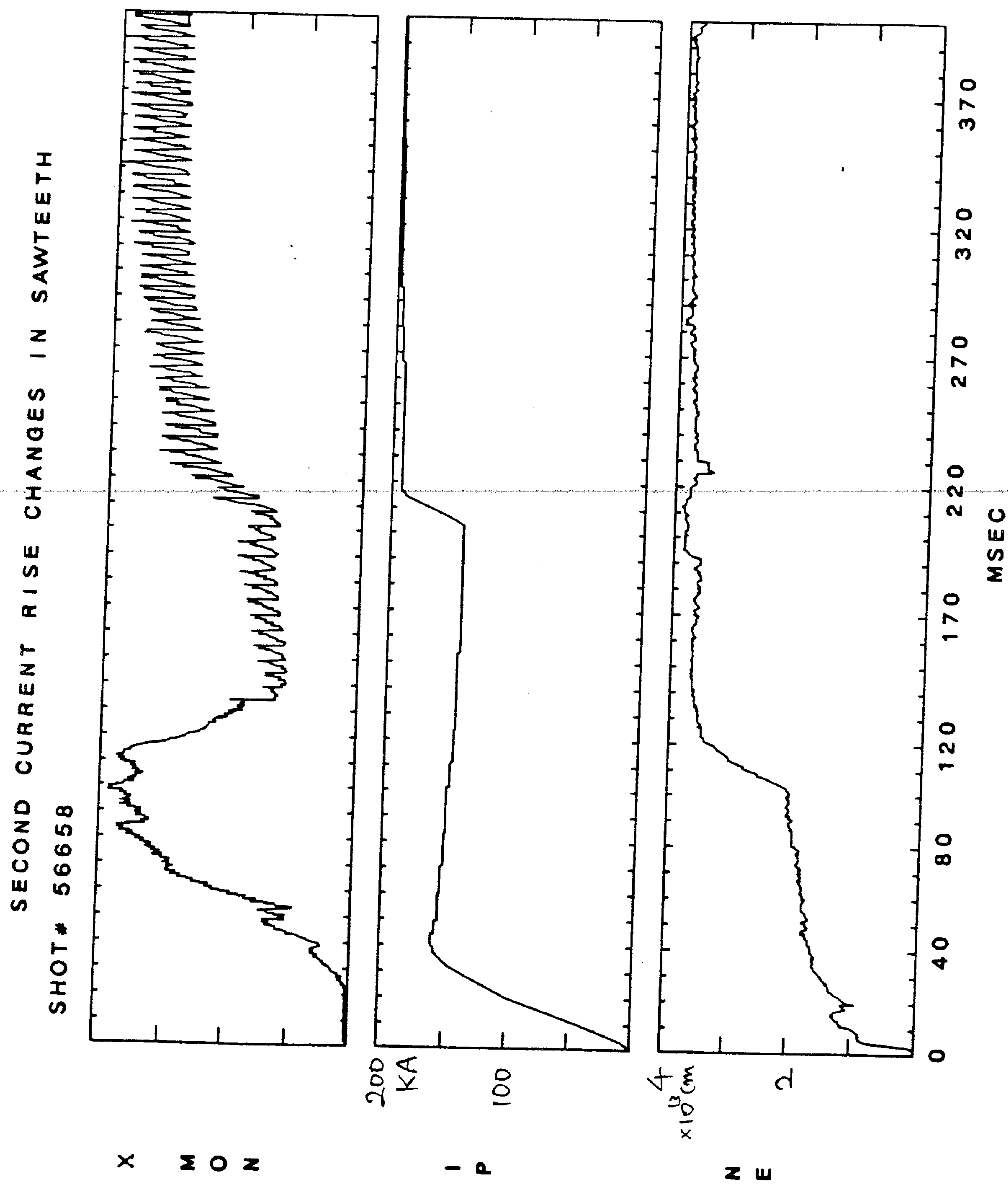
SECOND CURRENT RISE CHANGES IN SAWTEETH
SHOT# 56658
X MON
I P
200 KA
100
N E
4 ×10^13 cm
2
0
40
80
120
170
220
270
320
370
MSEC

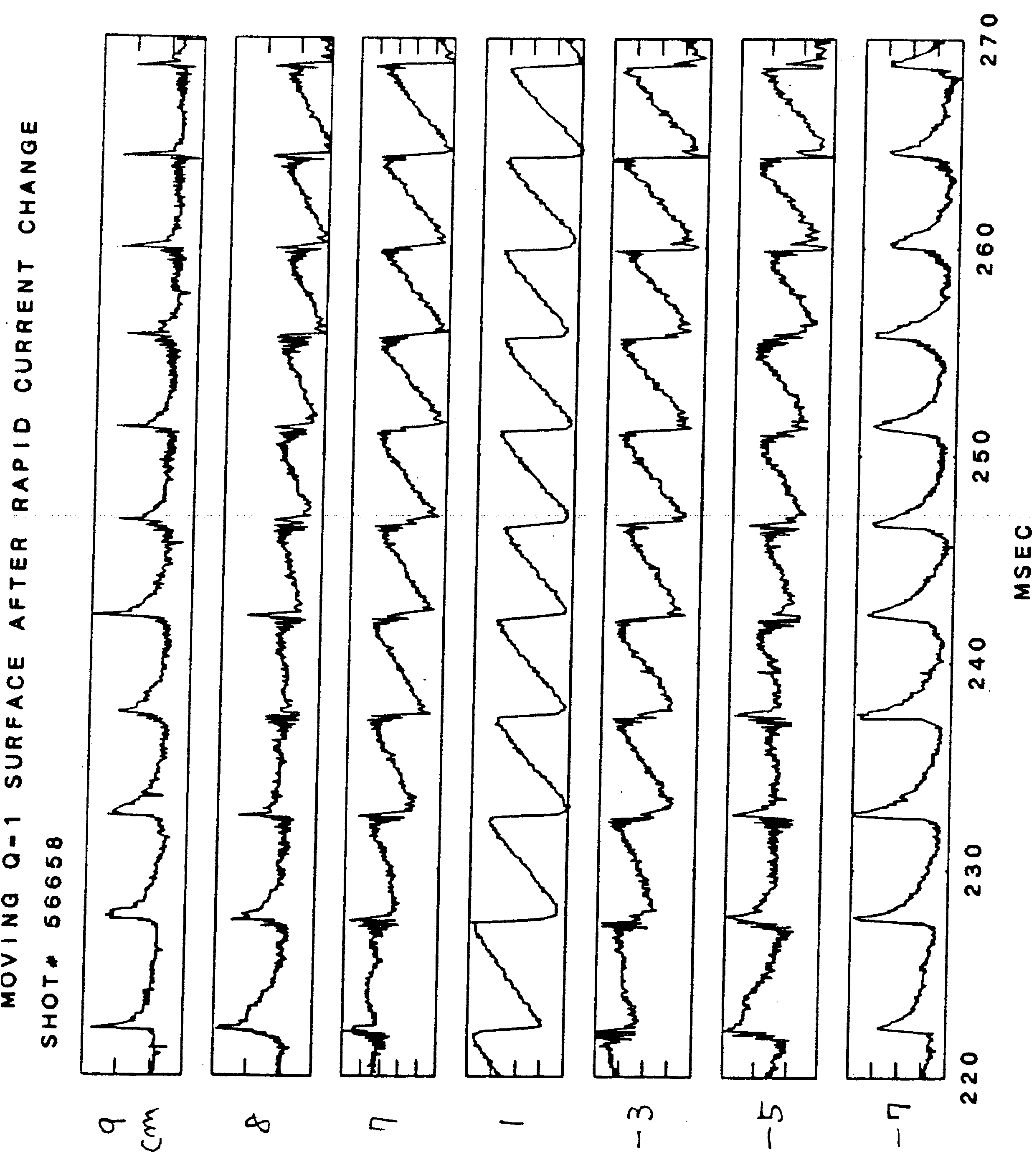
MOVING Q=1 SURFACE AFTER RAPID CURRENT CHANGE
SHOT# 56658
9
cm
8
7
1
-3
-5
-7
220
230
240
250
260
270
MSEC

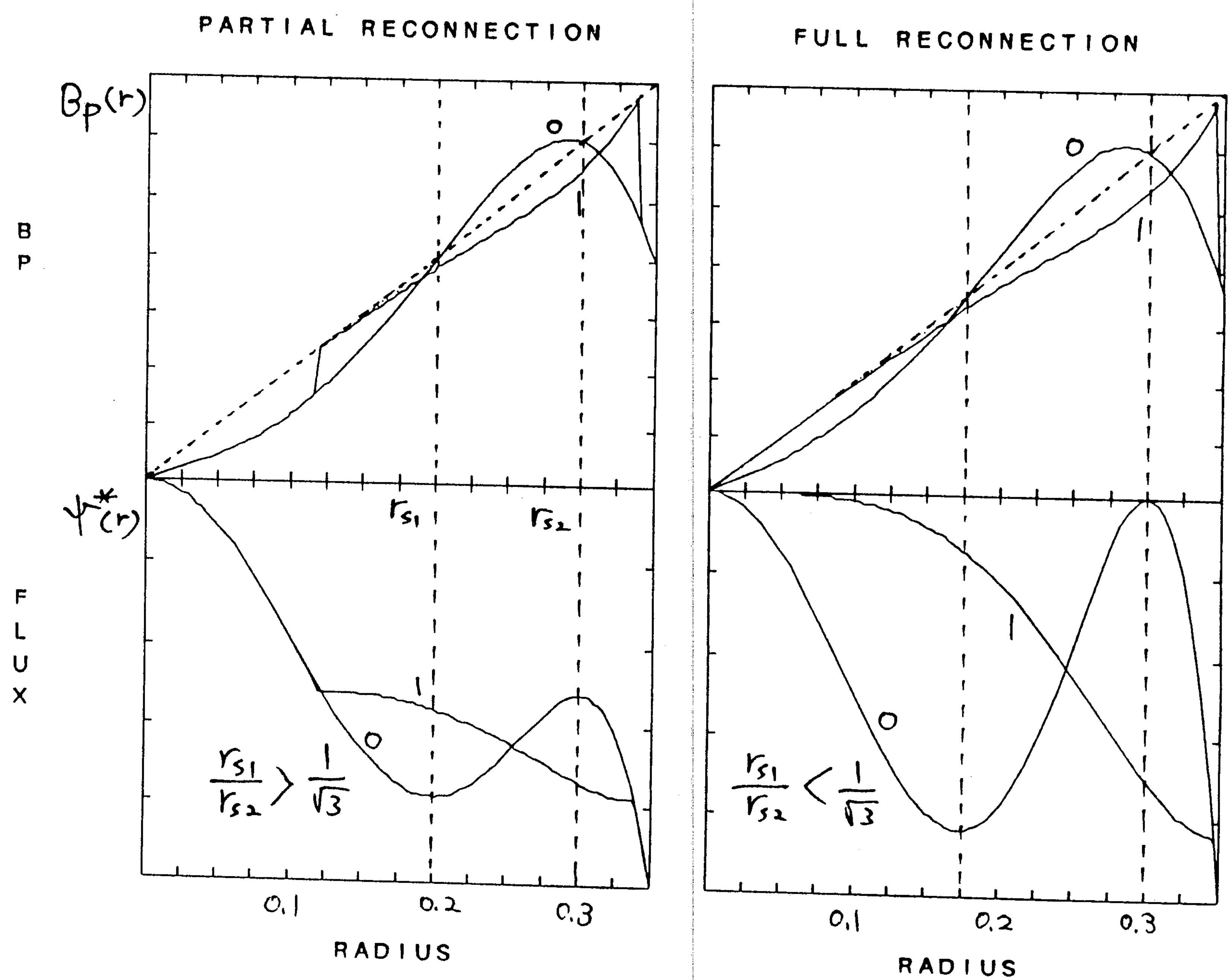

$$B_{po}(r) = \frac{r}{R} B_T + \alpha r (r^2 - r_{s1}^2)(r^2 - r_{s2}^2) \qquad \psi^*(r) \equiv \frac{B_T}{R} \int r \left(\frac{1}{q(r)} - 1 \right) dr$$

Summary

- Observed relative amplitude profiles of the transient sawteeth and the double sawteeth are consistent with partial reconnection model assuming hollow current profile.

- Because less heat is released to outside r_s during the 1st disruption of a double sawteeth, inside r_s is superheated and outside r_s is supercooled, which results in huge 2nd disruption ($dA/A \geqslant 20$ %).

- Two m=1 mode were observed during double sawteeth.

- Radiation loss due to impurity near the center of the plasma and anomalous current penetration may be responsible for a hollow current profile.

HALF COALESCENCE OF THE M=1 ISLAND IN TOKAMAKS

A. AYDEMIR

UNIVERSITY OF TEXAS AT AUSTIN
INSTITUTE FOR FUSION STUDIES

HALF-COALESCENCE of the $m=1$ ISLAND IN TOKAMAKS

A. AYDEMIR
INSTITUTE for FUSION STUDIES
UNIVERSITY of TEXAS

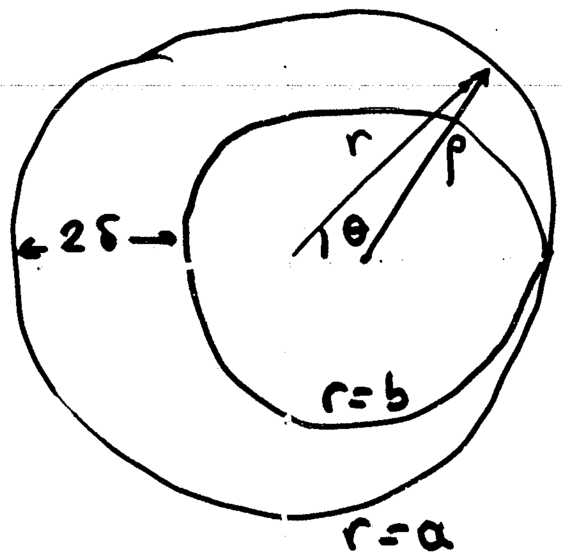

$$\delta = a - b$$

$$\rho^2 = \delta^2 + r^2 - 2\delta r \cos\theta$$

Perturbation:

Core: $r < a, \quad \rho < b$

$$\phi = \frac{r^2}{2} - \frac{\lambda}{2}(\rho^2 - b^2)$$

Island: $r < a, \quad \rho > b$

$$\phi = \frac{r^2}{2}$$

$$\underline{v} = \hat{z} \times \nabla\phi$$

$$\underline{v}_\perp = \hat{\theta}\, r(1-\lambda) \qquad (m=n=0)$$

$$+\ \hat{r}\{-\lambda\delta \sin\theta\} \qquad (m=1\ , n=1)$$

$$+\ \hat{\theta}\left[-\lambda\,\delta \cos\theta\right]$$

$m=1\ , n=1$ piece of $\underline{v}_\perp$:

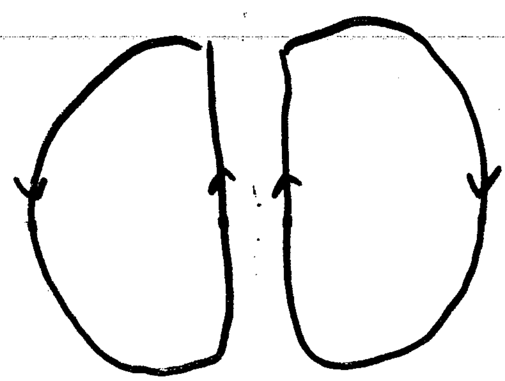

$\underline{v}_\perp$

SYMMETRIC

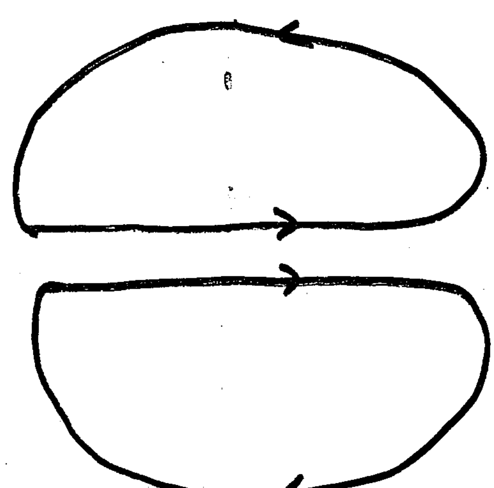

$\underline{B}'$

ANTI-SYMMETRIC

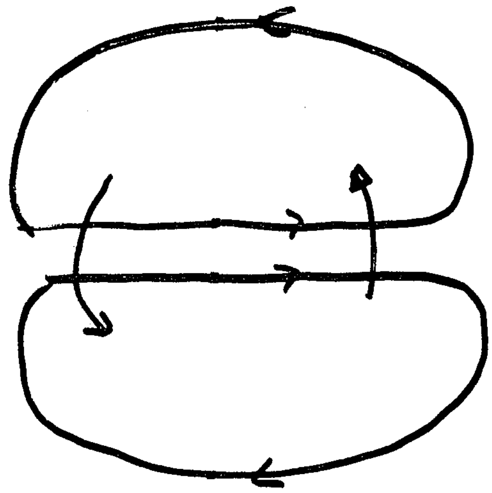

ANTI-SYMMETRIC PERTURBATION

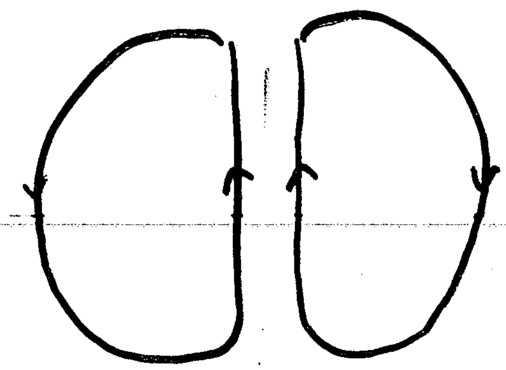

B ISLAND IN "EQUILIBRIUM".

SOURCE of FREE-ENERGY IS THE ATTRACTIVE POTENTIAL BETWEEN THE TWO DIPOLE-FIELDS.

$$\frac{\partial v'}{\partial t} = \underline{J}' \times \underline{B}_0 + \underline{J}_0 \times \underline{B}' \quad [m=1]$$

$$+ \underline{J}' \times \underline{B}_{IS} + \underline{J}_{IS} \times \underline{B}' \quad [m=0]$$

J_0, $\underline{B}_0$: $m=0$, $n=0$

J_{IS}, B_{IS} : $m=1$, $n=1$ [EQUILIBRIUM ISLAND]

$\underline{J}'$, $\underline{B}'$: $m=1$, $n=1$ [PERTURBATION]

TWO PROCESSES :

i) $m=1$ TEARING

ii) IDEAL ROTATIONAL INSTABILITY

If $B_{IS} \sim \delta^2$, then $\gamma_{ROT} \sim \delta^2$?

"EQUILIBRIUM" for the Linear Calculations

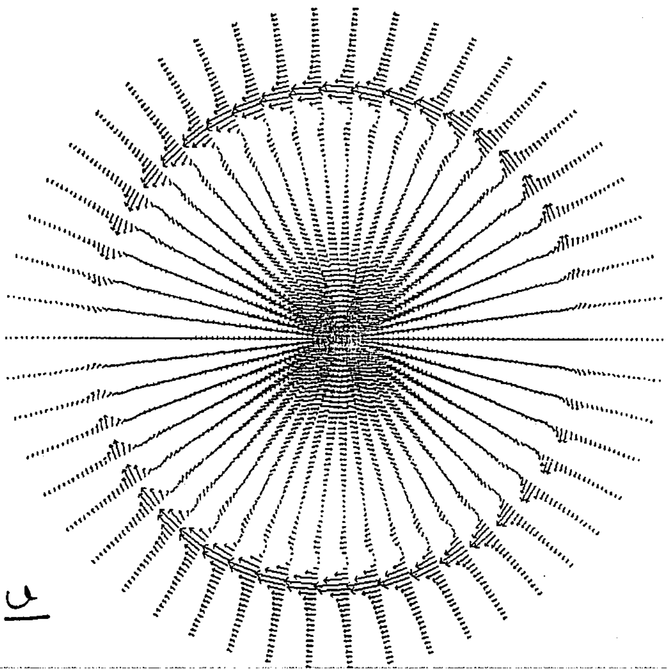

17:45:50 11/30/84 T =5.65E+02 ZETA= 0.00
VELOCITY MAX= 1.03E-05

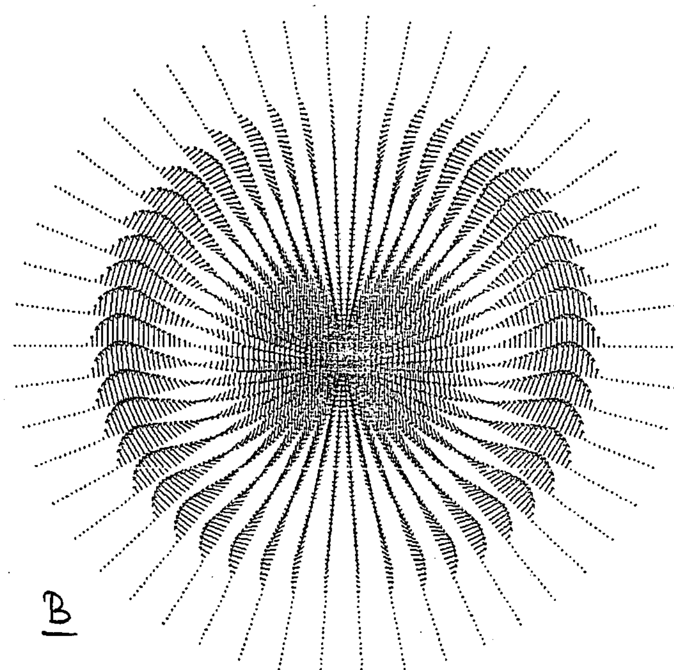

17:45:50 11/30/84 T =5.65E+02 ZETA= 0.00
B-FIELD MAX= 4.39E-02

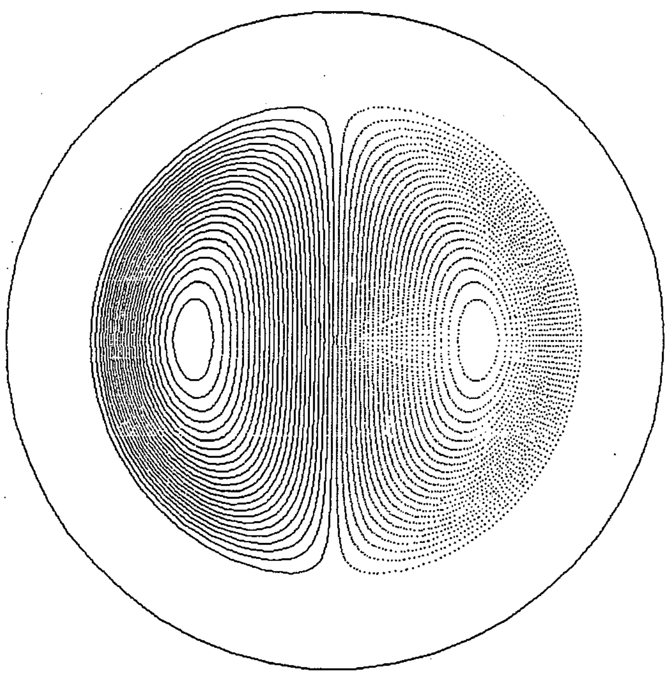

17:45:50 11/30/84 T =5.65E+02 ZETA= 0.00
MIN= -8.44E-03 MAX= 8.44E-03 M/N= 1/ 1
R(IN)= 6.54E-01 R(OUT)= 7.59E-01 W= 1.05E-01

PERTURBED HELICAL FLUX

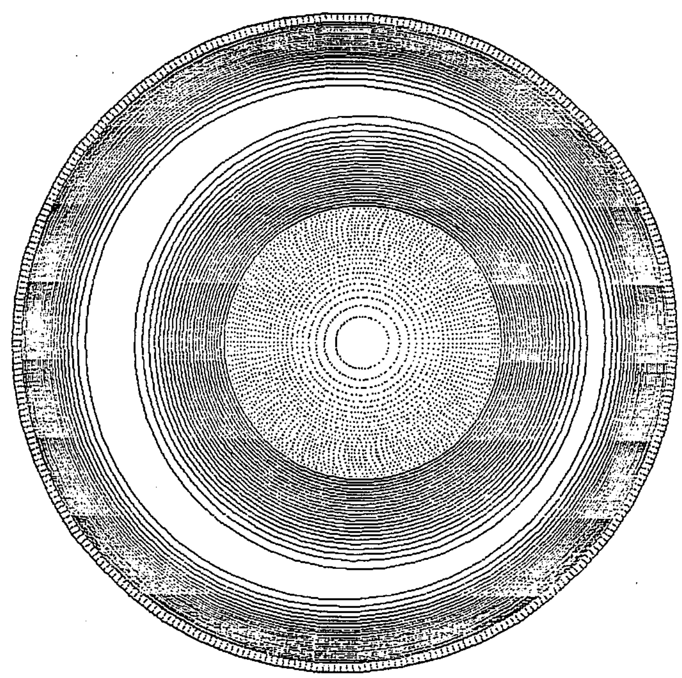

11:14:58 11/30/84 T =5.65E+02 ZETA= 0.00
MIN= -7.13E-04 MAX= 6.79E-02 M/N= 1/ 1
R(IN)= 0. R(OUT)= 0. W= 0.

TOTAL HELICAL FLUX

ANTI- SYMMETRIC PERTURBATION

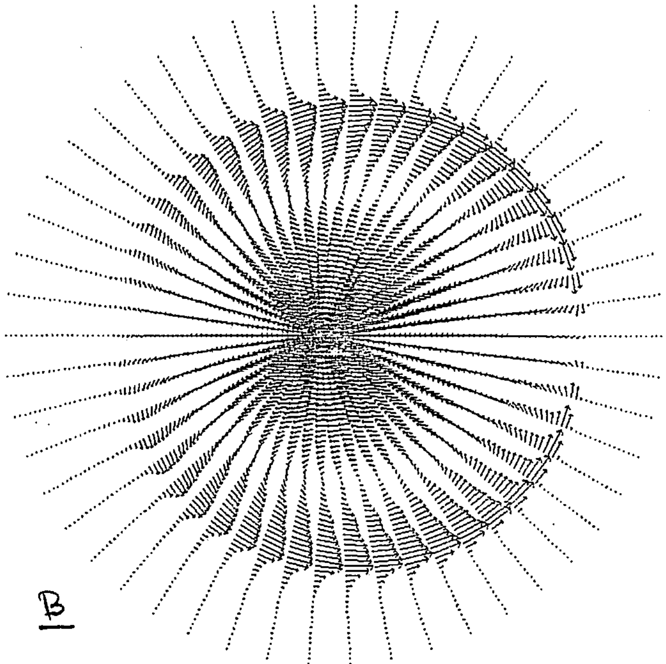

11:58:01 11/30/84 T =6.25E+02 ZETA= 0.00
B-FIELD MAX= 3.29E-04

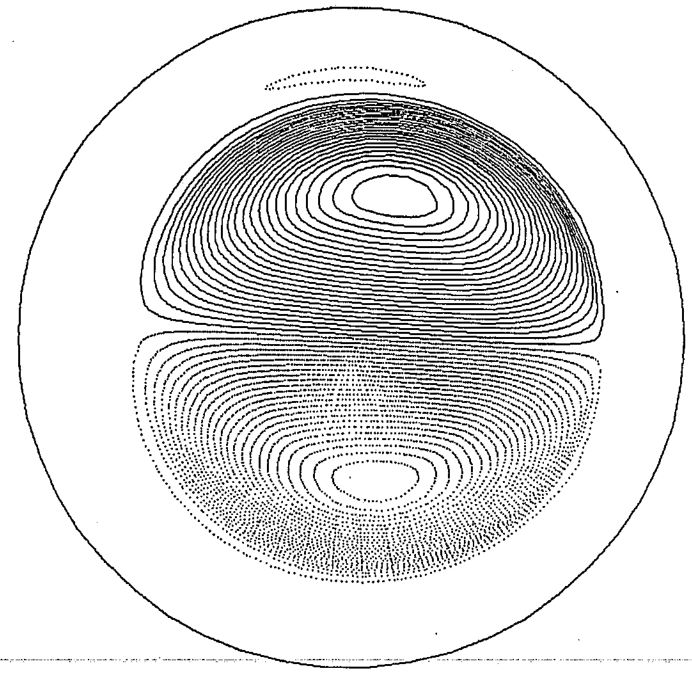

11:58:01 11/30/84 T =6.25E+02 ZETA= 0.00
MIN= -4.57E-05 MAX= 4.65E-05 M/N= 1/ 1
R(IN)= 6.28E-02 R(OUT)= 7.75E-01 W= 7.12E-01

t = 625

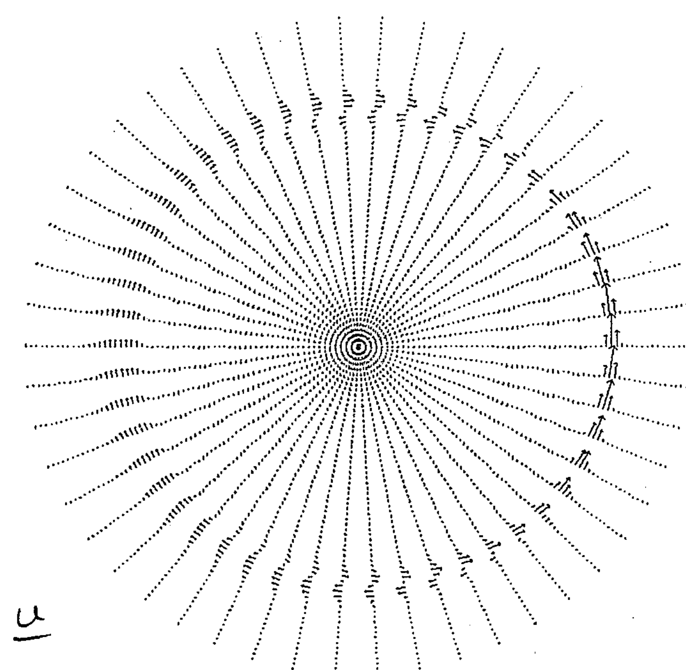

11:58:01 11/30/84 T =6.25E+02 ZETA= 0.00
VELOCITY MAX= 3.00E-04

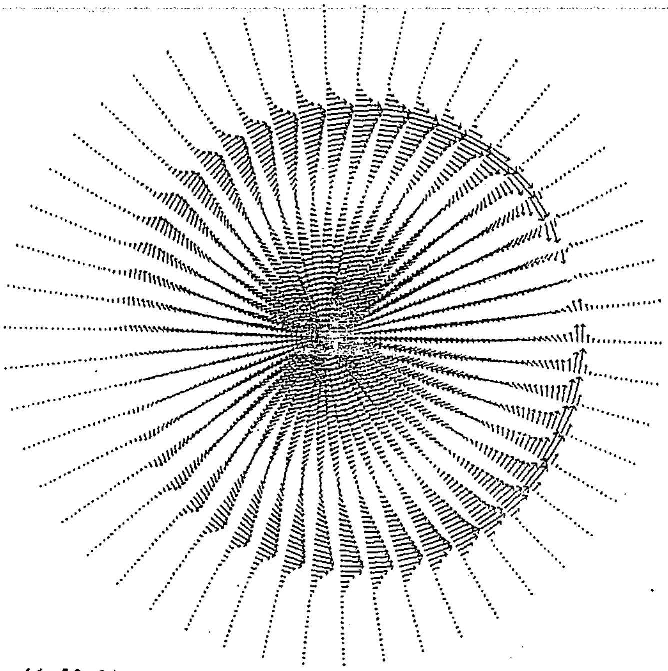

11:58:01 11/30/84 T =7.21E+02 ZETA= 0.00
B-FIELD MAX= 2.44E-02

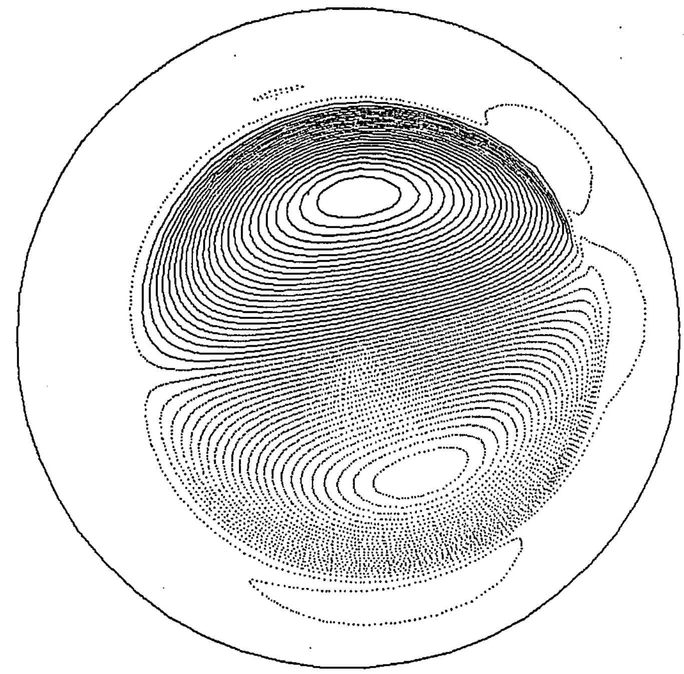

11:58:01 11/30/84 T =7.21E+02 ZETA= 0.00
MIN= -3.24E-03 MAX= 3.05E-03 M/N= 1/ 1
R(IN)= 5.24E-03 R(OUT)= 1.05E-01 W= 9.95E-02

t= 721

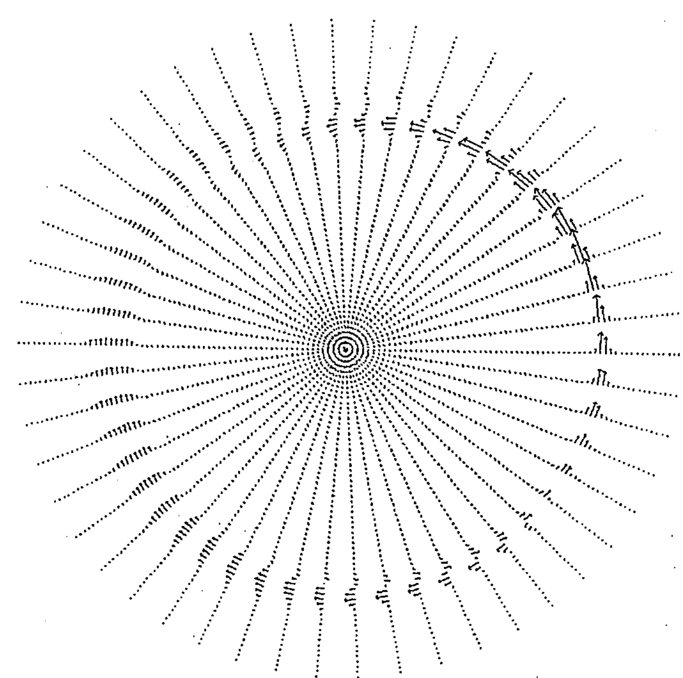

11:58:01 11/30/84 T =7.21E+02 ZETA= 0.00
VELOCITY MAX= 2.21E-02

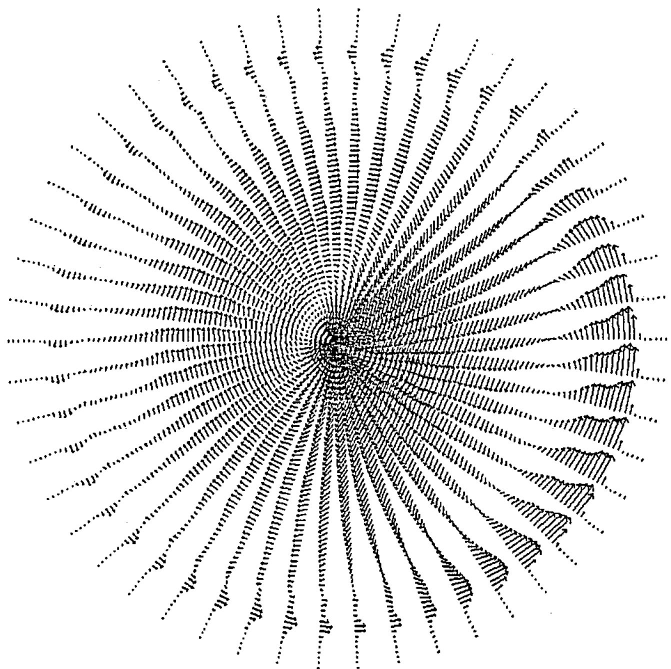

11:58:01 11/30/84 T =8.08E+02 ZETA= 0.00
B-FIELD MAX= 4.07E-01

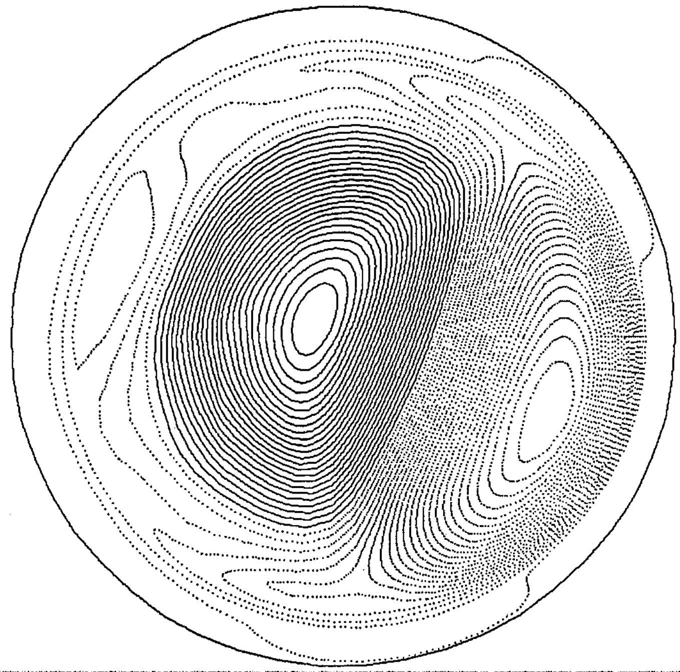

11:58:01 11/30/84 T =8.08E+02 ZETA= 0.00
MIN= -1.03E-01 MAX= 6.60E-03 M/N= 1/ 1
R(IN)= 5.24E-03 R(OUT)= 2.93E-01 W= 2.88E-01

t = 808

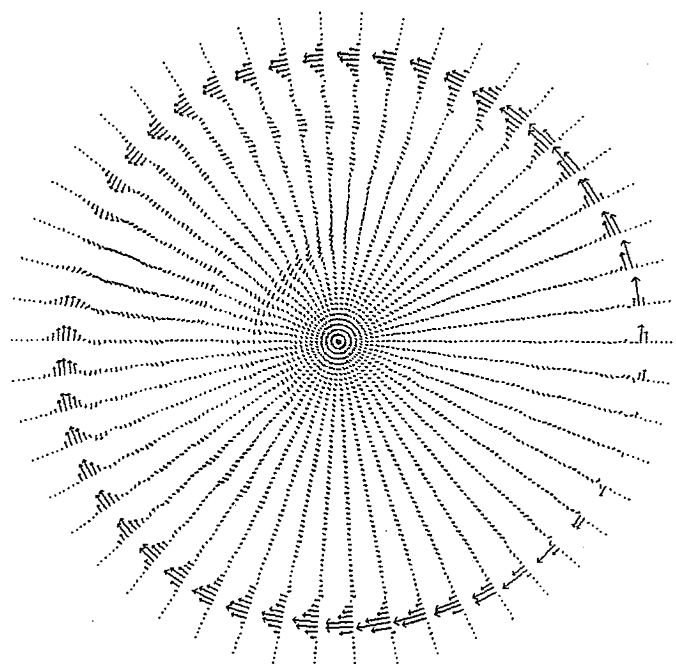

11:58:01 11/30/84 T =8.08E+02 ZETA= 0.00
VELOCITY MAX= 1.79E-01

INITIAL CONDITIONS
FOR THE NONLINEAR CALCULATION

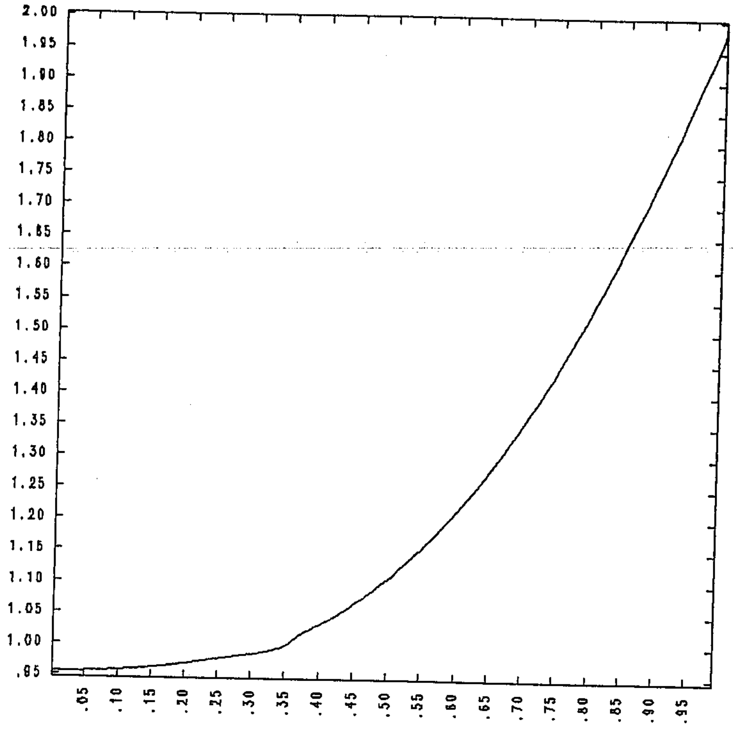

20:05:11 12/10/84 T=1.30E+02 MN= 0 Q-PROF

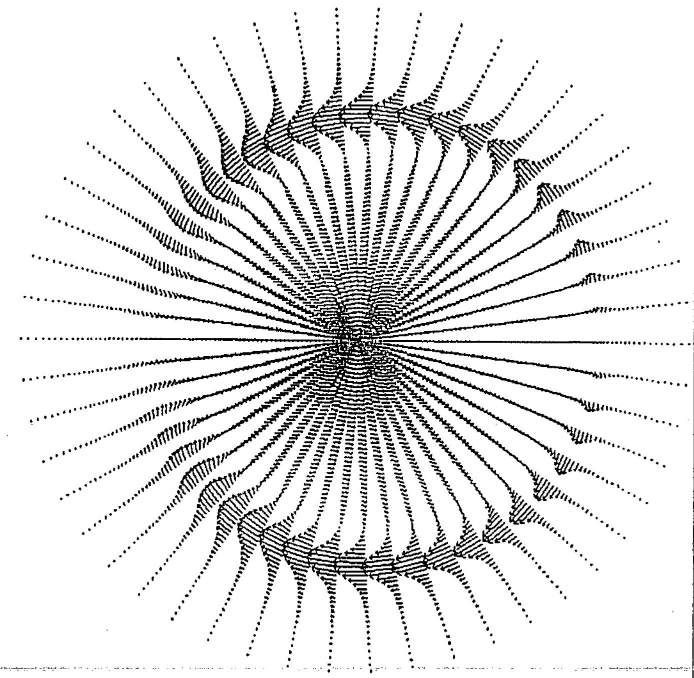

20:05:11 12/10/84 T =1.30E+02 ZETA= 0.00
VELOCITY MAX= 3.64E-03

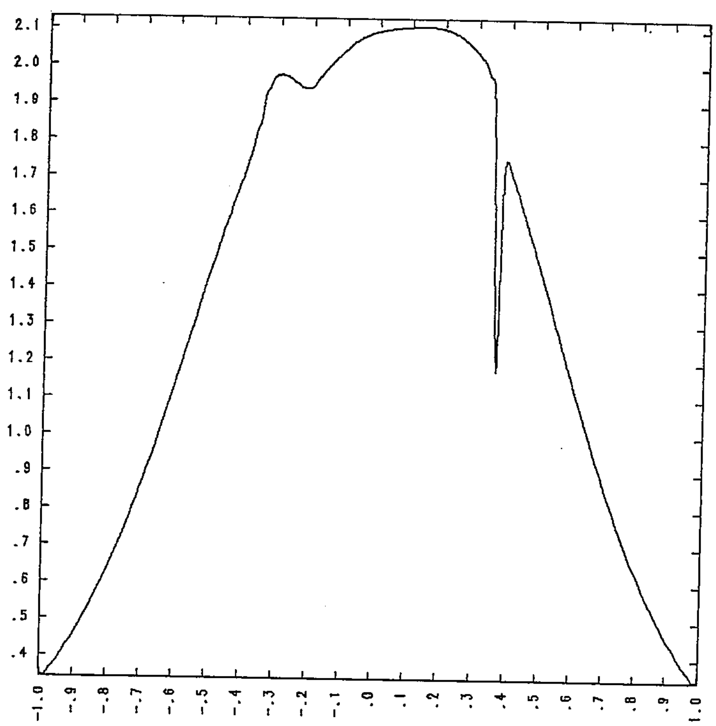

20:05:11 12/10/84 T=1.30E+02 MN= 0 TOR. CUR

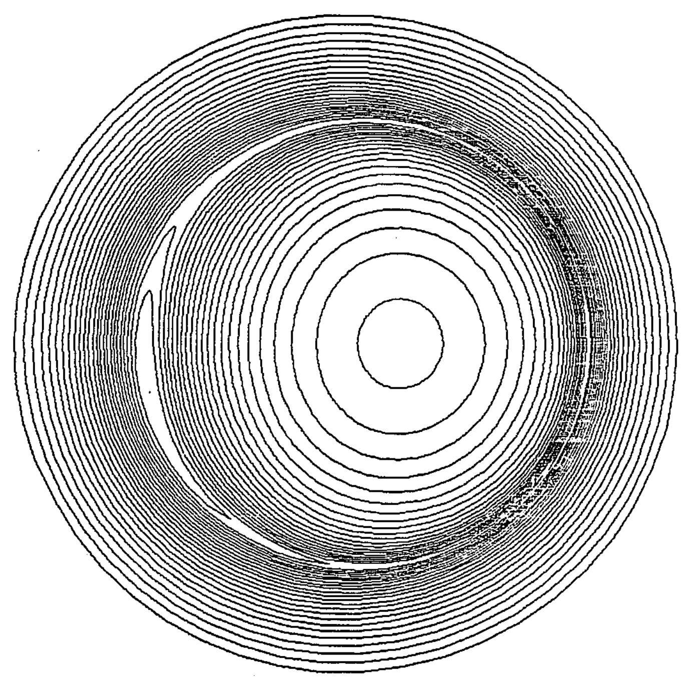

20:05:11 12/10/84 T =1.30E+02 ZETA= 0.00
MIN= -1.70E-03 MAX= 1.60E-03 M/N= 1/ 1
R(IN)= 2.77E-01 R(OUT)= 3.33E-01 W= 5.67E-02

ASYMMETRIC ISLAND

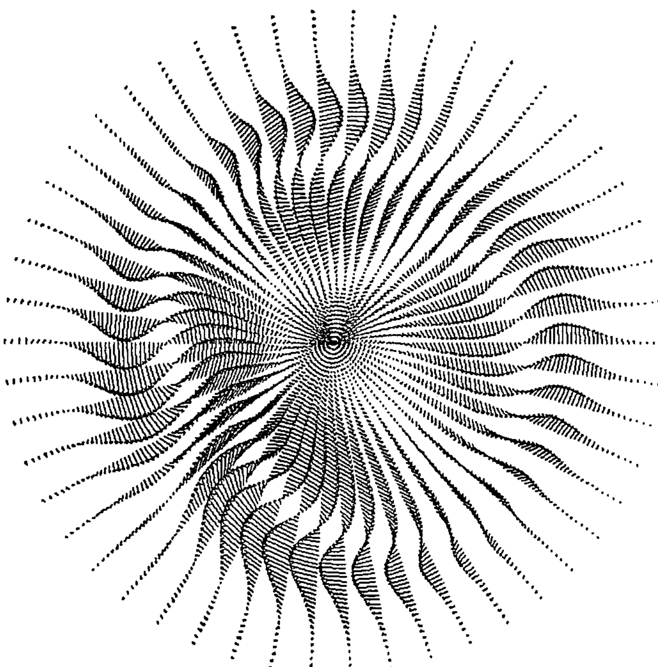

20:05:11 12/10/84 T =1.37E+02 ZETA= 0.00
VELOCITY MAX= 1.71E-02

t= 137

t= 137

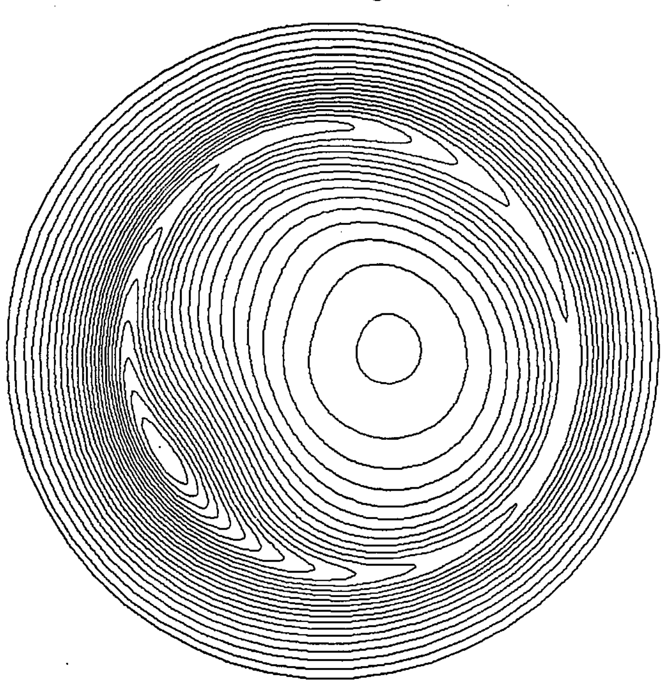

20:05:11 12/10/84 T =1.37E+02 ZETA= 0.00
MIN= -1.85E-03 MAX= 1.62E-03 M/N= 1/ 1
R(IN)= 2.27E-01 R(OUT)= 3.77E-01 W= 1.50E-01

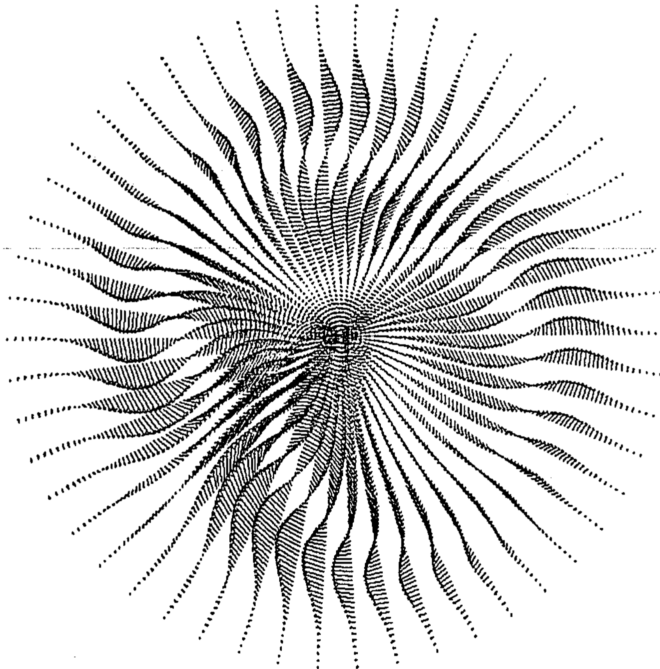

20:05:11 12/10/84 T =1.42E+02 ZETA= 0.00
VELOCITY MAX= 2.16E-02

$t = 142.$

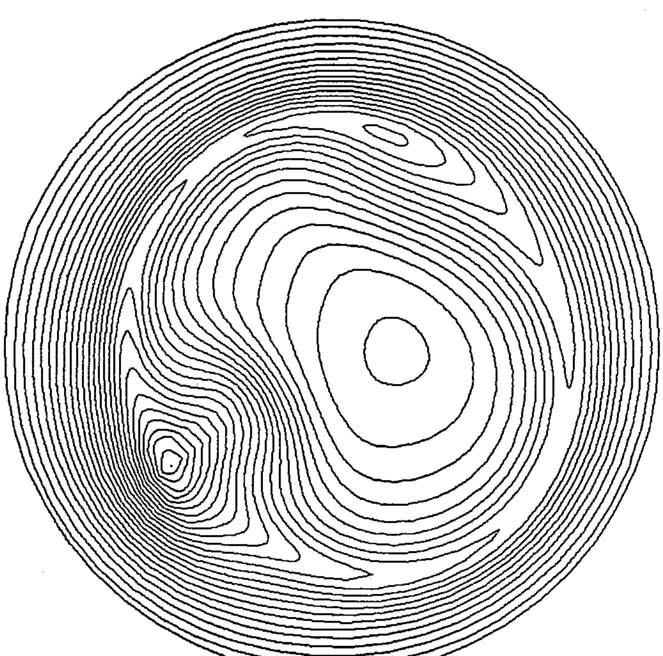

20:05:11 12/10/84 T =1.42E+02 ZETA= 0.00
MIN= -1.94E-03 MAX= 1.60E-03 M/N= 1/ 1
R⟨IN⟩= 1.97E-01 R⟨OUT⟩= 3.77E-01 W= 1.80E-01

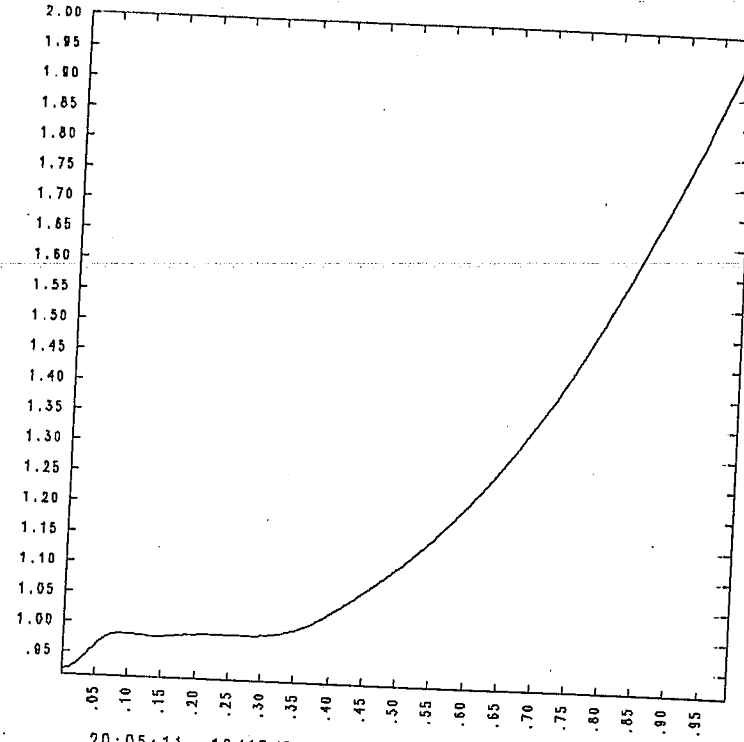

20:05:11 12/10/84 T=1.49E+02 MN= 0 Q-PROF

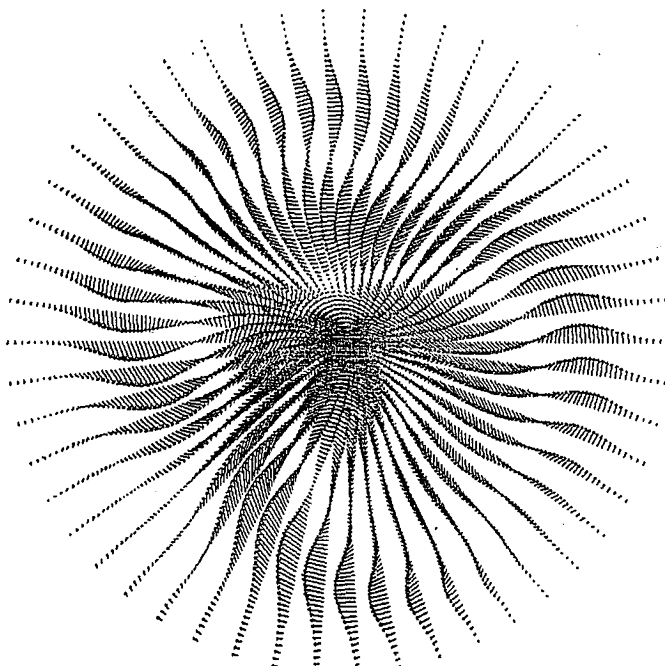

20:05:11 12/10/84 T =1.49E+02 ZETA= 0.00
VELOCITY MAX= 1.92E-02

t=149

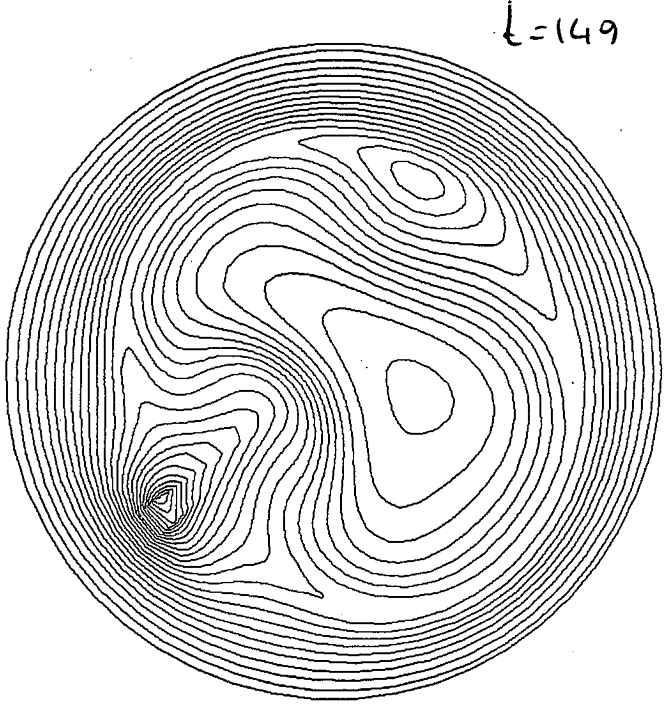

20:05:11 12/10/84 T =1.49E+02 ZETA= 0.00
MIN= -2.28E-03 MAX= 1.28E-03 M/N= 1/ 1
R(IN)= 7.33E-02 R(OUT)= 3.70E-01 W= 2.97E-01

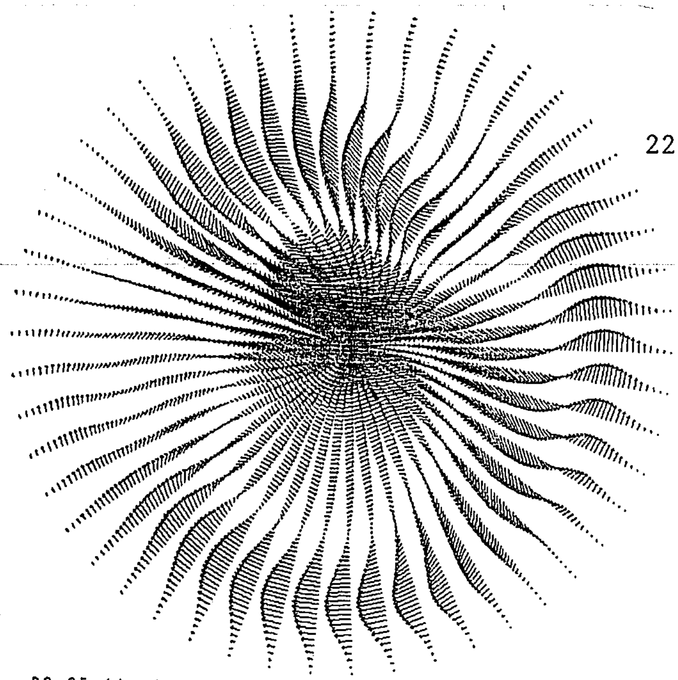

20:05:11 12/10/84 T =1.83E+02 ZETA= 0.00
VELOCITY MAX= 8.71E-03

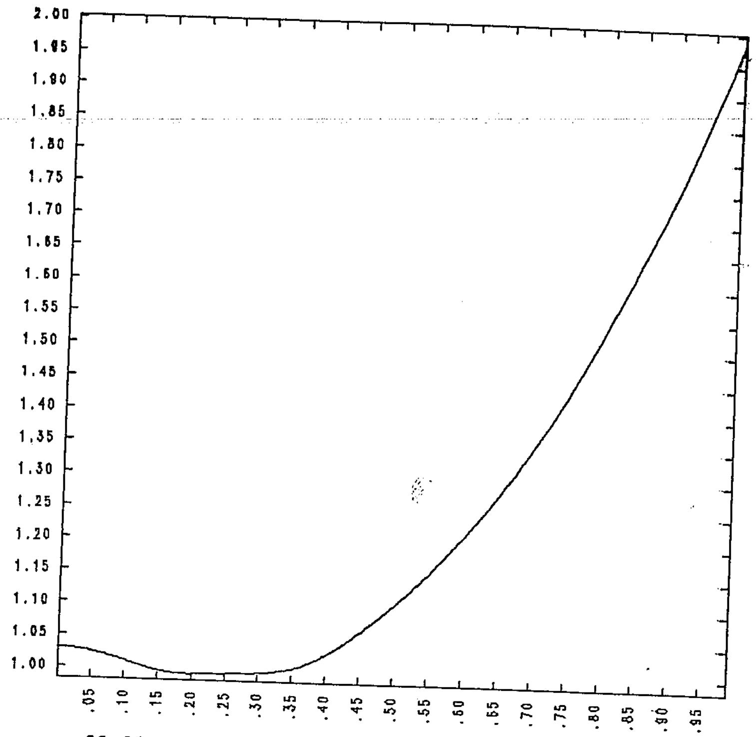

20:05:11 12/10/84 T=1.83E+02 MN= 0 Q-PROF

t = 183

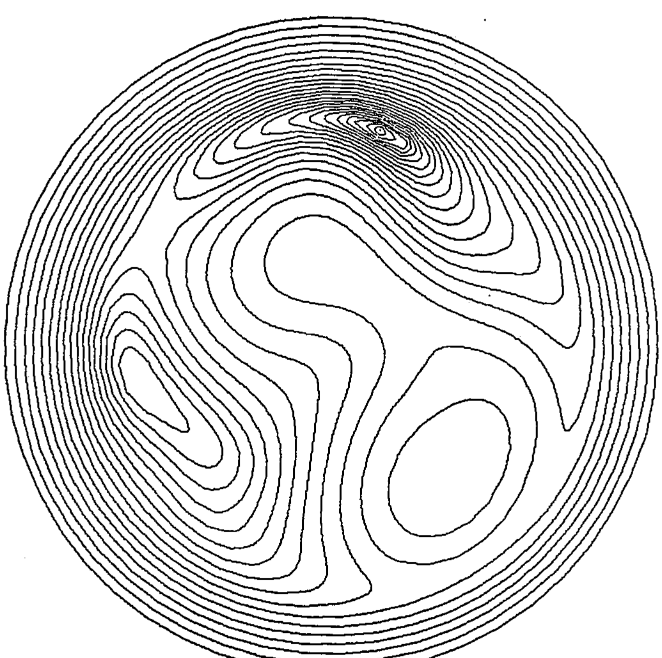

20:05:11 12/10/84 T =1.83E+02 ZETA= 0.00
MIN= -2.89E-03 MAX= 5.47E-04 M/N= 1/ 1
R(IN)= 3.33E-03 R(OUT)= 4.00E-01 W= 3.97E-01

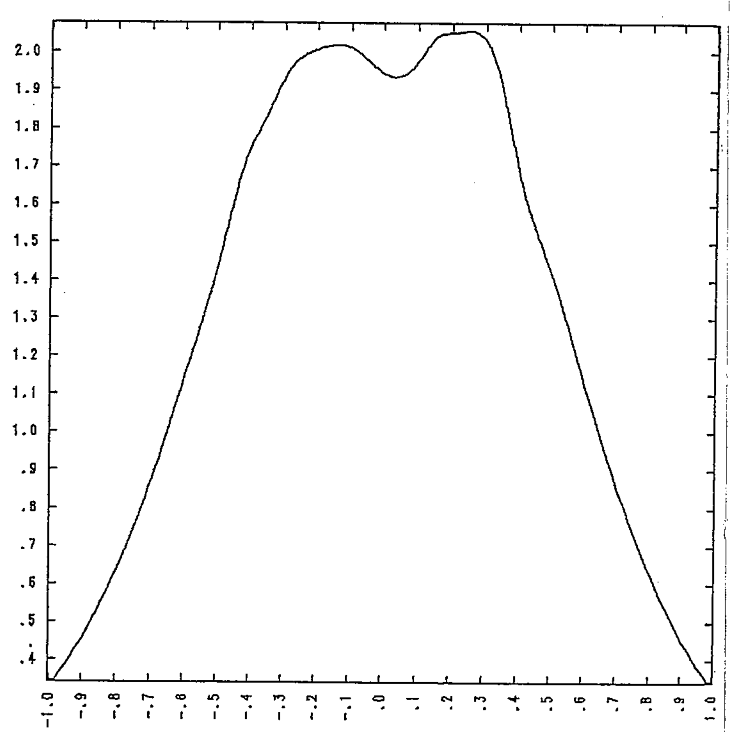

20:05:11 12/10/84 T=1.83E+02 MN= 0 TOR. CUR

FOR COMPARISON, A SYMMETRIC ISLAND EVOLVES TO THE FOLLOWING STATE.

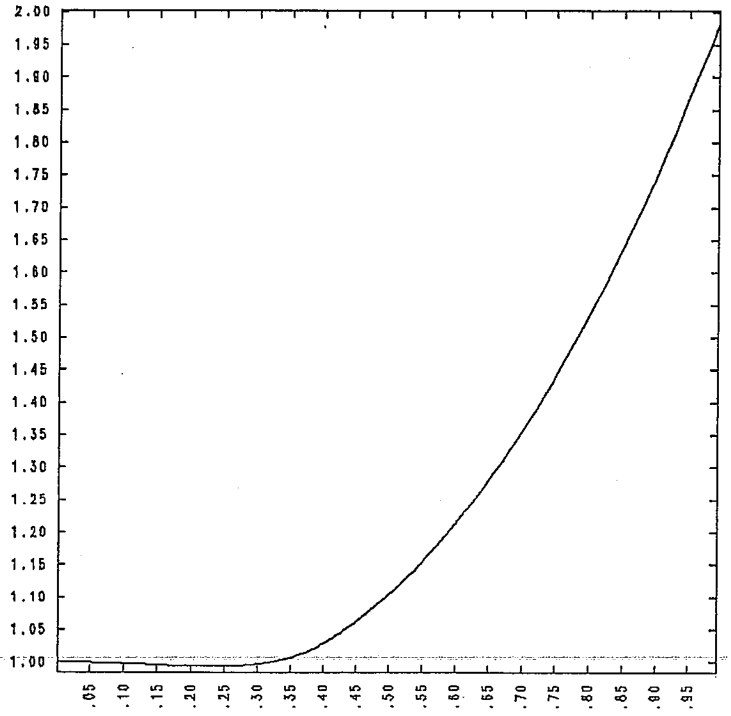

22:27:07 12/10/84 T=3.00E+02 MN= 0 Q-PROF

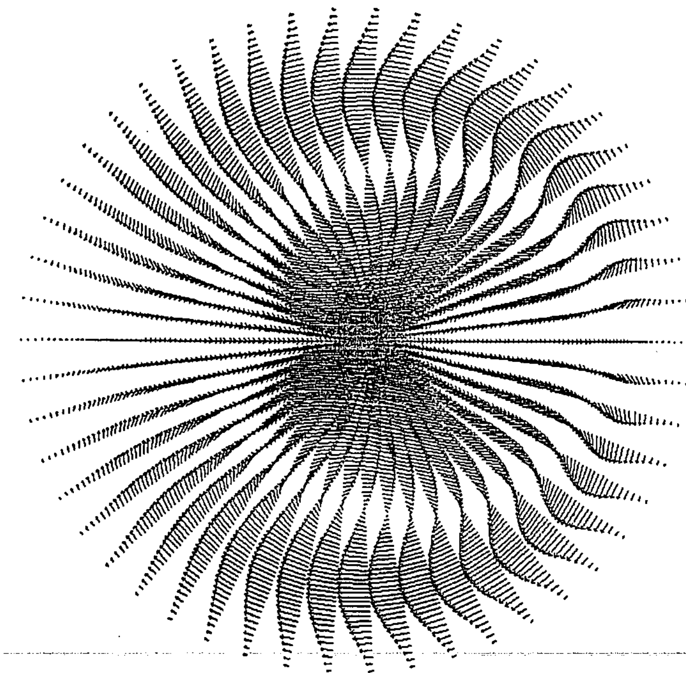

22:27:07 12/10/84 T =3.00E+02 ZETA= 0.00
VELOCITY MAX= 4.89E-03

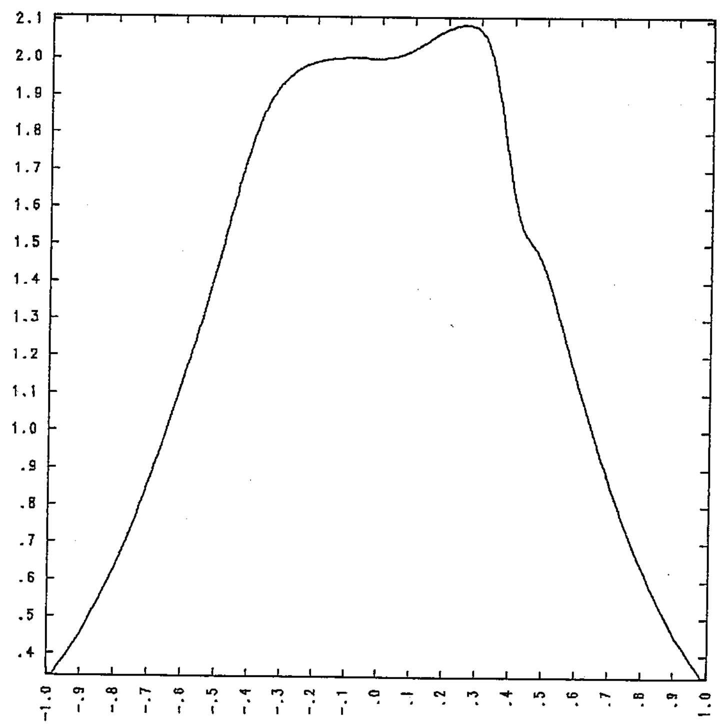

22:27:07 12/10/84 T=3.00E+02 MN= 0 TOR. CUR

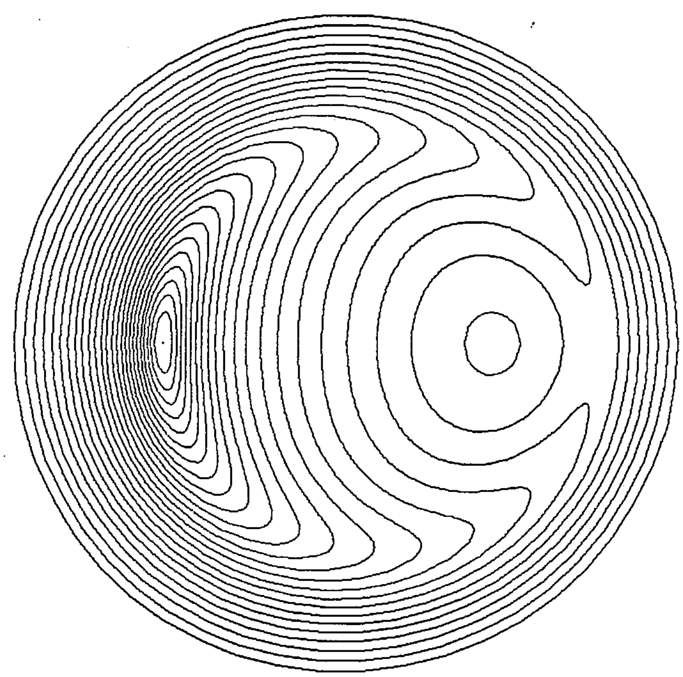

22:27:07 12/10/84 T =3.00E+02 ZETA= 0.00
MIN= -2.95E-03 MAX= 5.66E-04 M/N= 1/ 1
R(IN)= 3.33E-03 R(OUT)= 4.00E-01 W= 3.97E-01

$S_0 = 10^4$

KINETIC ENERGY HISTORIES

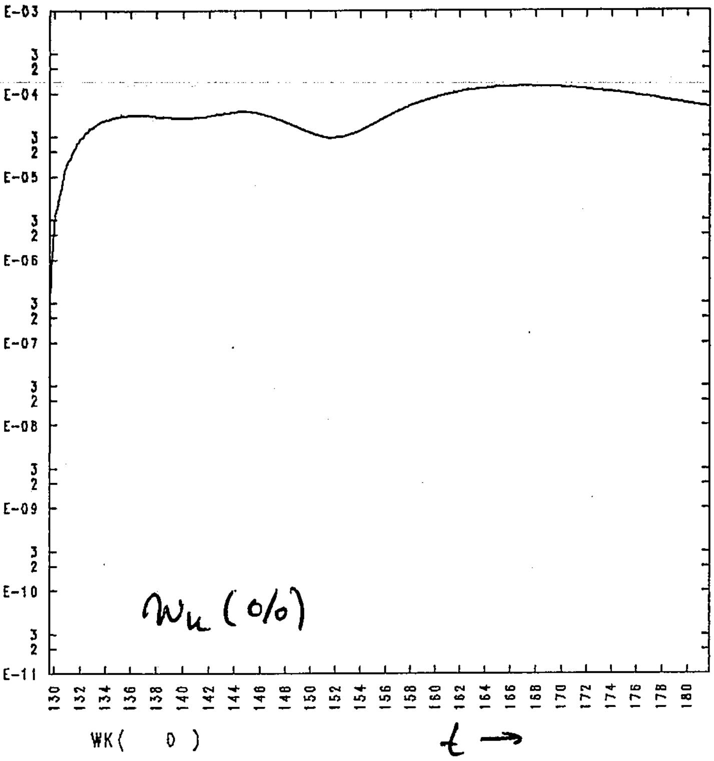

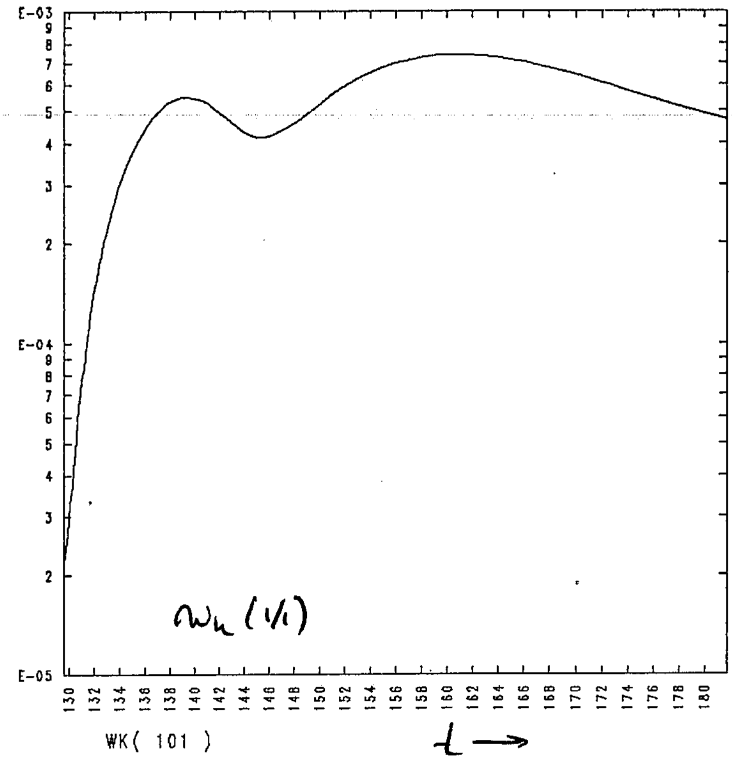

$S_0 = 10^5$

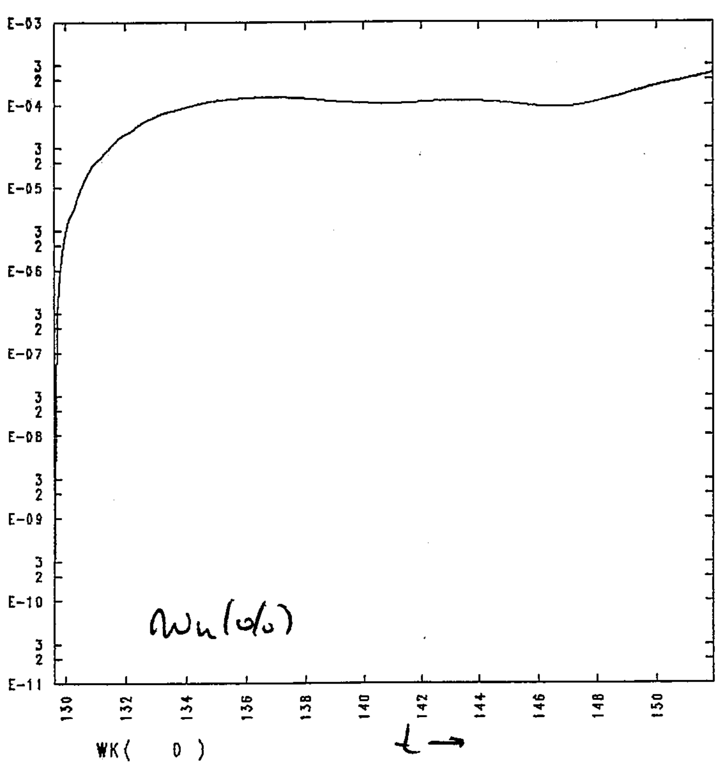

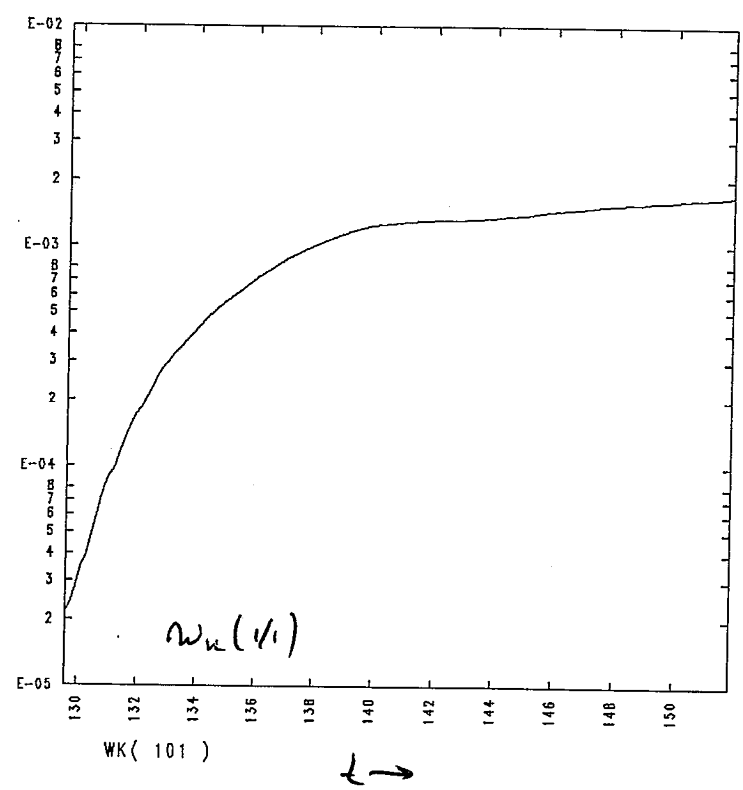

SYMMETRIC ISLAND

$S_0 = 10^4$

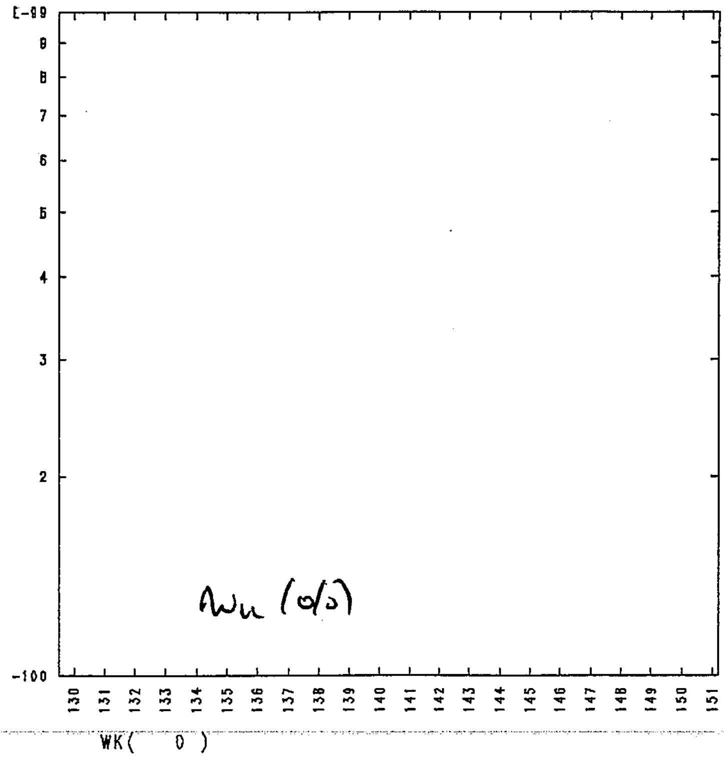

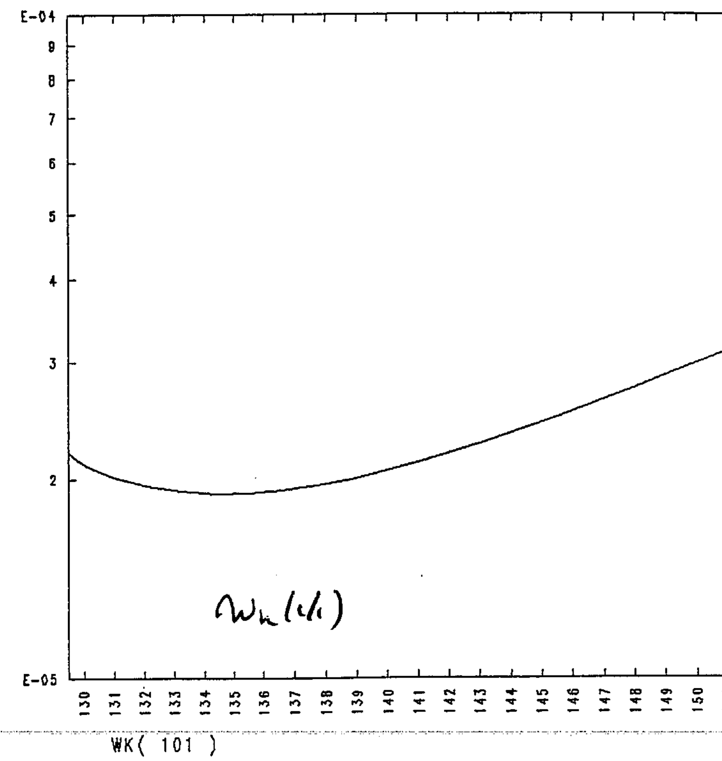

ARE VACUUM BUBBLES A CAUSE OF MAJOR DISRUPTIONS?

R. KLEVA

UNIVERSITY OF MARYLAND

ARE VACUUM BUBBLES A CAUSE OF MAJOR DISRUPTIONS?

R.G. KLEVA
J.F. DRAKE
D.A. BOYD
UNIVERSITY OF MARYLAND

IDEAL KINK INSTABILITY

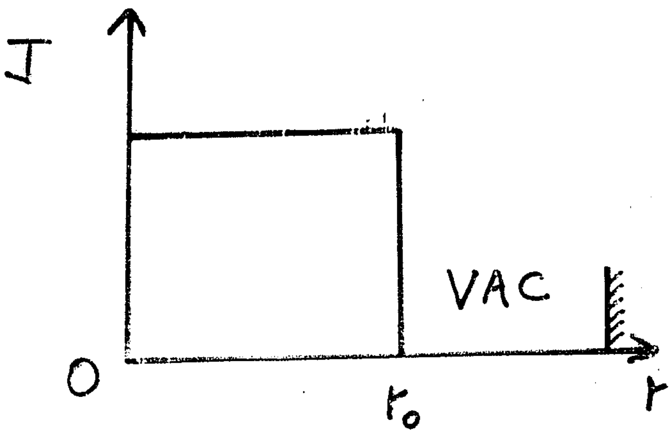

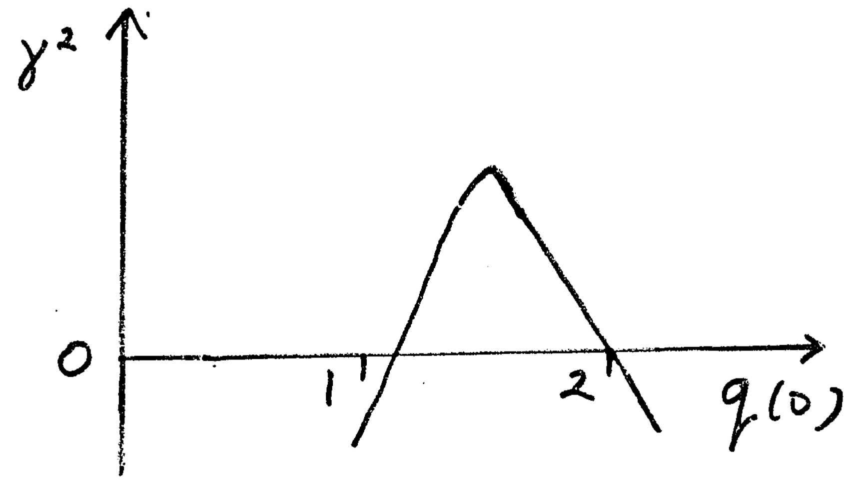

VACUUM BUBBLES

KADOMTSEV & POGUTSE

ROSENBLUTH, MONTICELLO, STRAUSS & WHITE

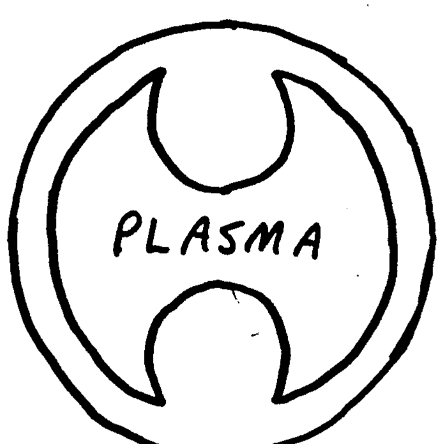

INCLUDING RESISTIVITY

$m=2$ TEARING MODE SATURATES BENIGNLY AT AN ISLAND WIDTH $W \lessapprox 0.4a$

MULTIPLE HELICITIES -

WADDELL, CARRERAS, HICKS & HOLMES

UNDER SOME CIRCUMSTANCES, THE ISLANDS OF THE 2/1, 3/2, 5/3, ... OVERLAP

$\longrightarrow$ FLUX SURFACES DESTROYED

OUR CONCLUSIONS

* WHEN $q(0) > 1.5$, THE $m=2$ TEARING MODE GROWS TO A VERY LARGE AMPLITUDE, ITS MAGNETIC ISLANDS ENCOMPASSING VIRTUALLY THE ENTIRE PLASMA CROSS SECTION.
* THESE VERY LARGE ISLANDS PRODUCED BY THE RESISTIVE TEARING MODE ARE RELATED TO THE VACUUM BUBBLES PRODUCED BY THE IDEAL KINK INSTABILITY.
* IS $q(0)$ LARGER THAN 1.5 DURING MAJOR DISRUPTIONS?

SCENARIO FOR MAJOR DISRUPTIONS

(1) MAGNETIC ISLANDS ASSOCIATED WITH MODES OF DIFFERENT HELICITIES OVERLAP

→ FLUX SURFACES DESTROYED

→ TEMPERATURE & CURRENT PROFILES FLATTENED

→ $q(0) > 1.5$

IF THE DISCHARGE RECOVERS AT THIS POINT

→ MINOR DISRUPTION

(2) ONCE $q(0) > 1.5$, THE ISLANDS OF THE $m=2$ TEARING MODE RAPIDLY GROW TO FILL THE CROSS SECTION

→ HOT CENTRAL PLASMA EXPELLED TO EDGE

→ DISCHARGE TERMINATES

* THIS SCENARIO IS SUPPORTED BY EXPERIMENTAL OBSERVATIONS OF TWO-STAGE DISRUPTIONS

REDUCED RESISTIVE MHD

OHM'S LAW

$$-\frac{\partial \psi}{\partial t} - \underline{B}\cdot\underline{\nabla}\varphi = \eta J$$

VORTICITY EQUATION

$$\frac{d}{dt} W = \underline{B}\cdot\underline{\nabla} J + \mu \nabla_\perp^2 W$$

AMPERE'S LAW

$$\nabla_\perp^2 \psi = -J$$

WHERE
$$W = \nabla_\perp^2 \varphi = \hat{z}\cdot\underline{\nabla}\times\underline{V}$$
$$\underline{B} = \hat{z} - \hat{z}\times\underline{\nabla}\psi$$
$$\underline{V} = \hat{z}\times\underline{\nabla}\varphi$$

UNITS

$$t/\tau_A \rightarrow t \quad , \quad \tau_A \equiv R/c_A$$
$$a\nabla_\perp \rightarrow \nabla_\perp \quad , \quad R\frac{\partial}{\partial z} \rightarrow \frac{\partial}{\partial z}$$

EQUILIBRIUM

$$q(r) = q(0)\left[1 + \left(\frac{r}{r_0}\right)^{2\lambda}\right]^{1/\lambda}$$

$$r_0^{-2\lambda} \equiv \left[\frac{q(1)}{q(0)}\right]^{\lambda} - 1$$

$$q(1) = 3.4$$

$$\lambda = 4$$

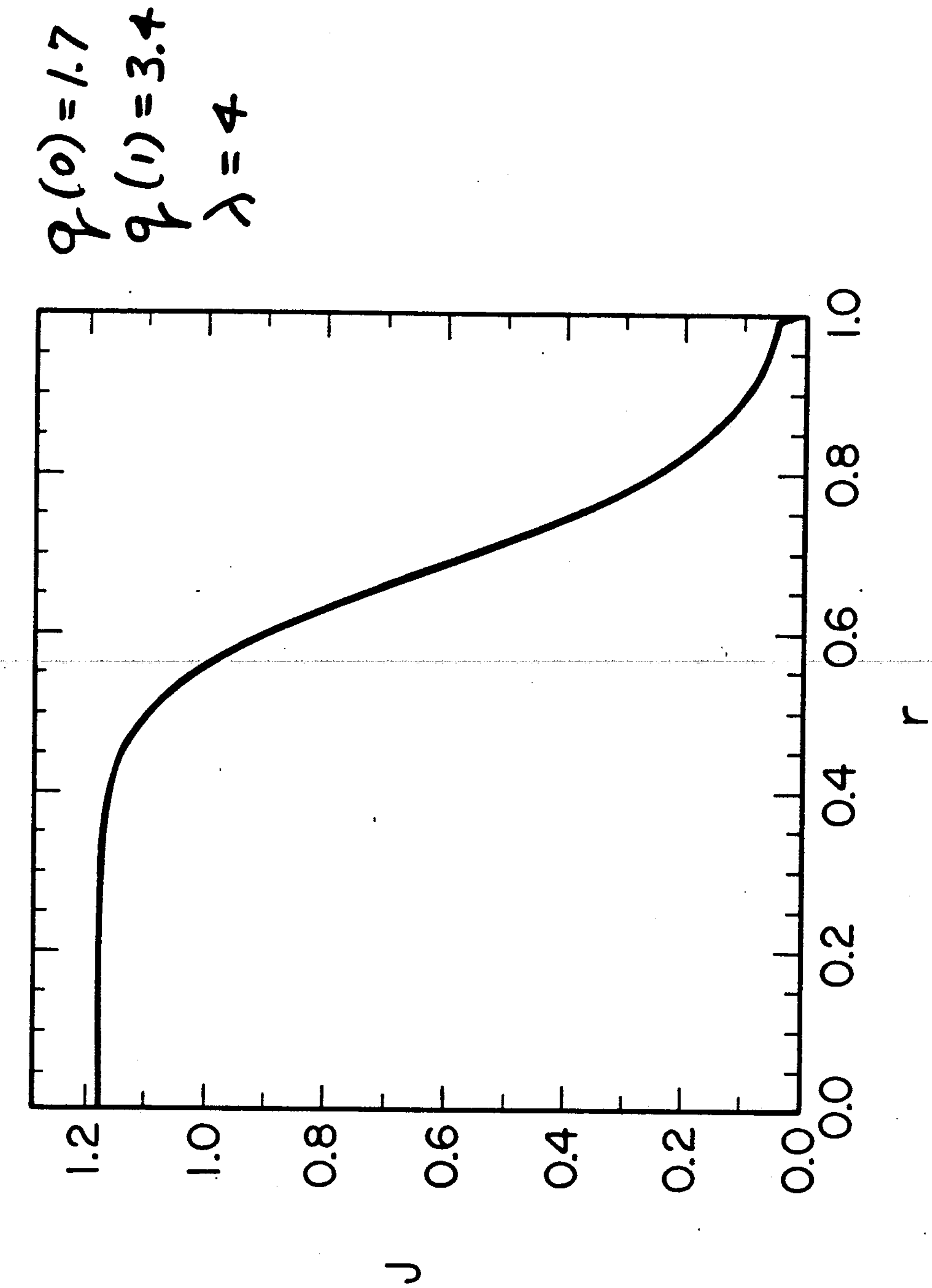
q(0) = 1.7
q(1) = 3.4
λ = 4
J
r
0.0
0.2
0.4
0.6
0.8
1.0
1.2

RESISTIVITY

1) $\eta(r) = \dfrac{\eta}{J(r)}$

2) $\dfrac{\partial \eta}{\partial t} + \underline{V} \cdot \underline{\nabla} \eta = K_{\parallel} \underline{B} \cdot \underline{\nabla} \underline{B} \cdot \underline{\nabla} \eta + K_{\perp} \nabla_{\perp}^{2} \eta$

NUMERICAL SIMULATION

$$\psi, \varphi, \eta \sim e^{i(m\theta - nz)}$$

$$\frac{m}{n} = 2$$

UP TO 60 HARMONICS RETAINED

200 RADIAL GRID POINTS

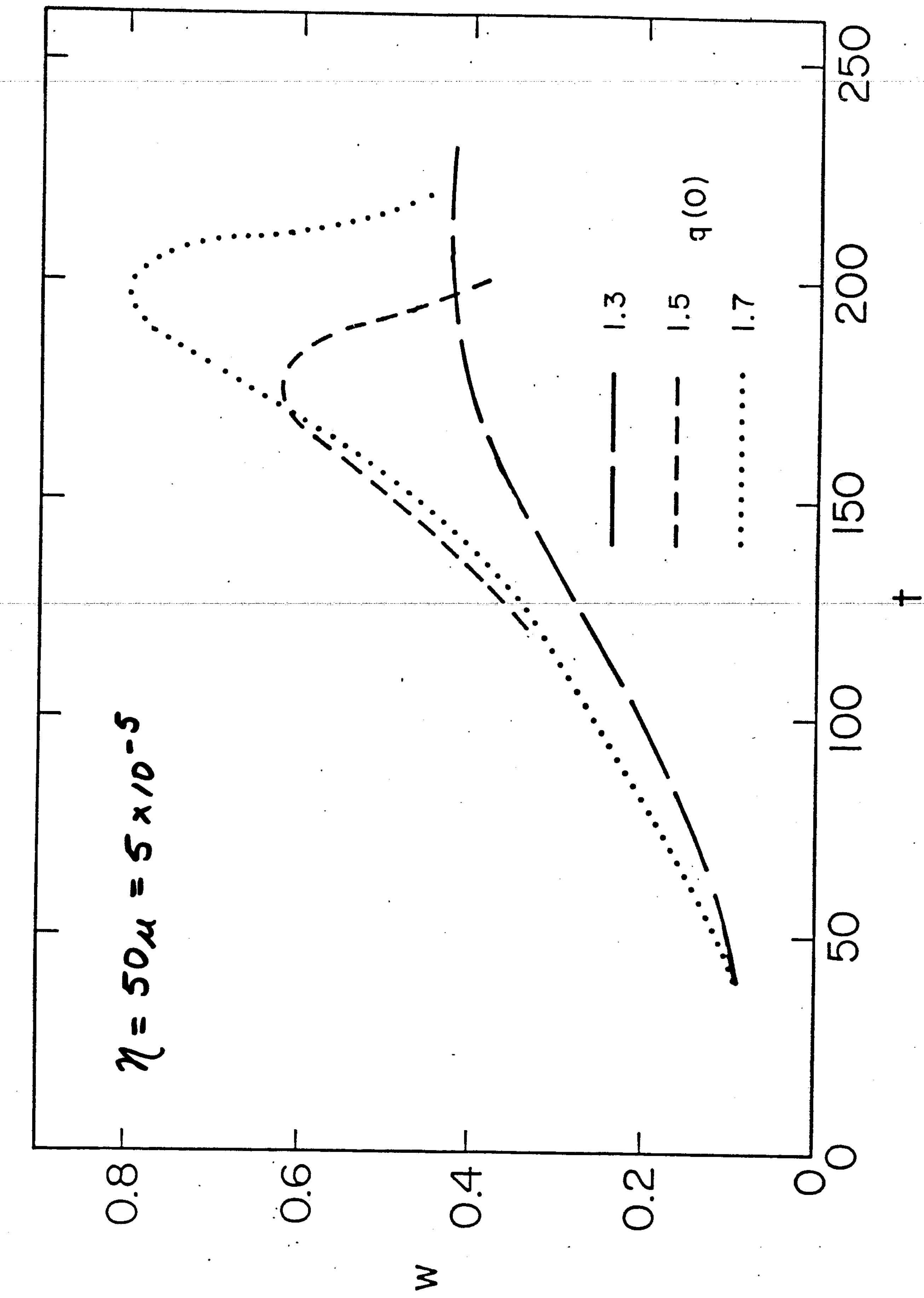
η = 50μ = 5 × 10⁻⁵
q(0)
1.3
1.5
1.7
w
0.8
0.6
0.4
0.2
0
t
0
50
100
150
200
250

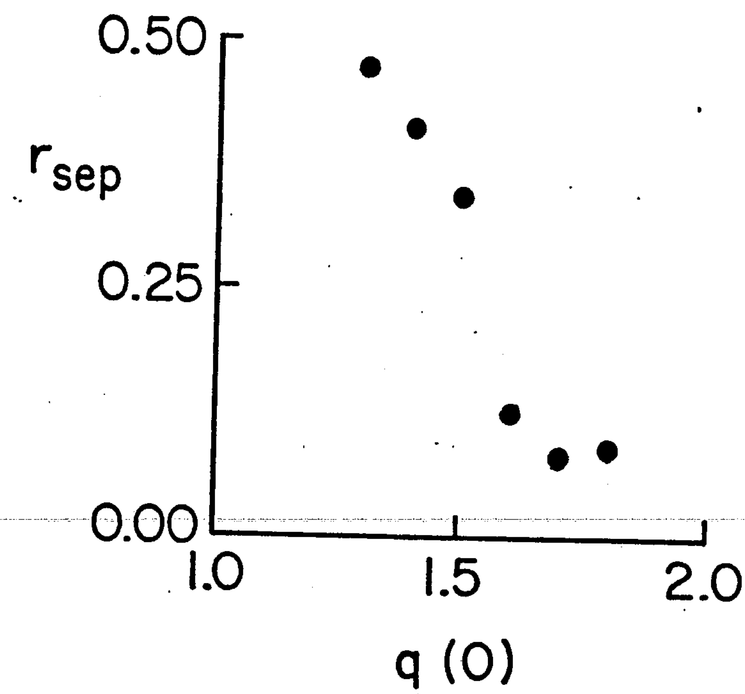

* ISLAND ABRUPTLY PENETRATES TO THE CENTER WHEN $q(0) > 1.5$

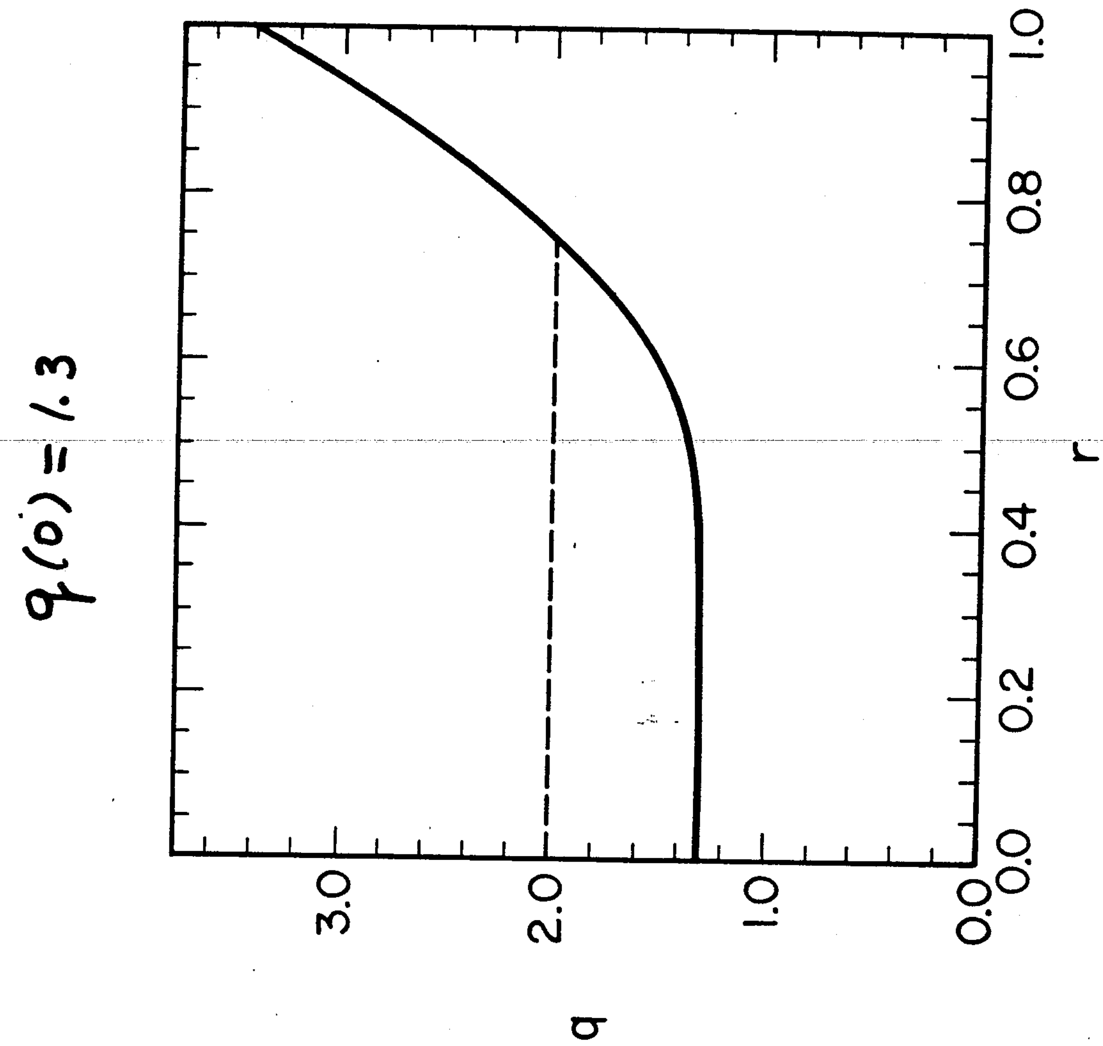
q(0) = 1.3
q
3.0
2.0
1.0
0.0
r
0.0
0.2
0.4
0.6
0.8
1.0

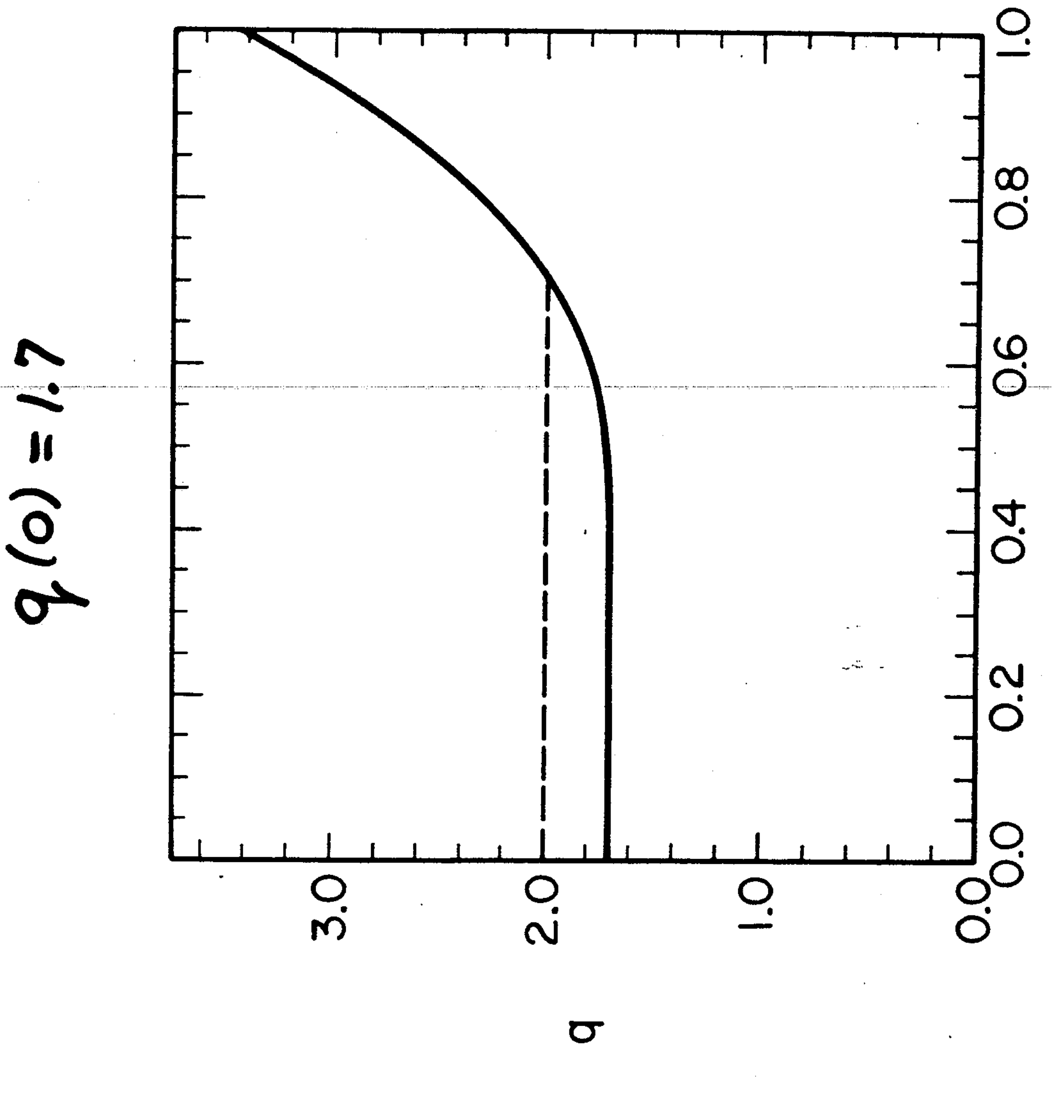
q(o) = 1.7
q
0.0
1.0
2.0
3.0
r
0.0
0.2
0.4
0.6
0.8
1.0

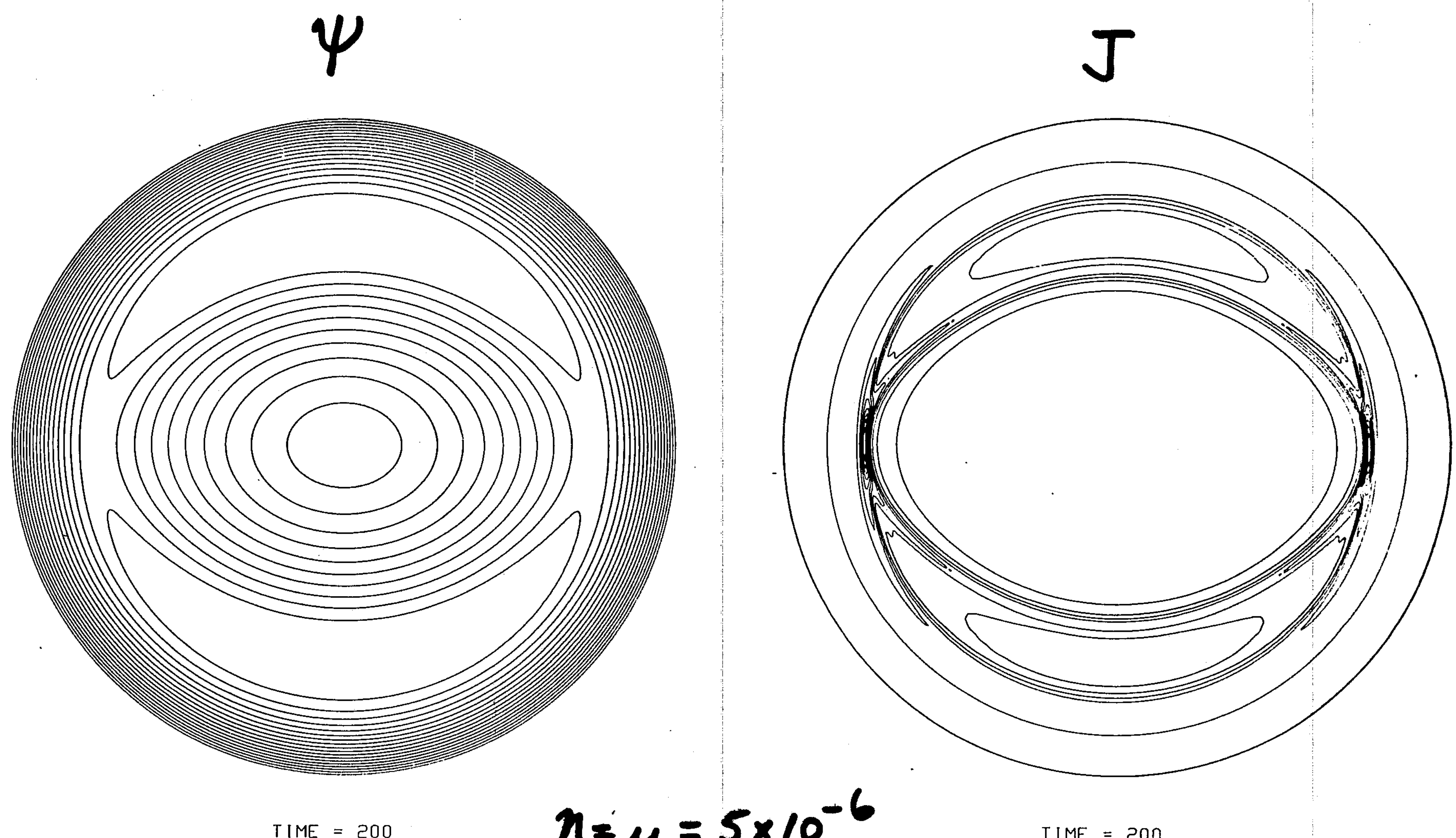

$\eta = \mu = 5\times10^{-6}$

ψ

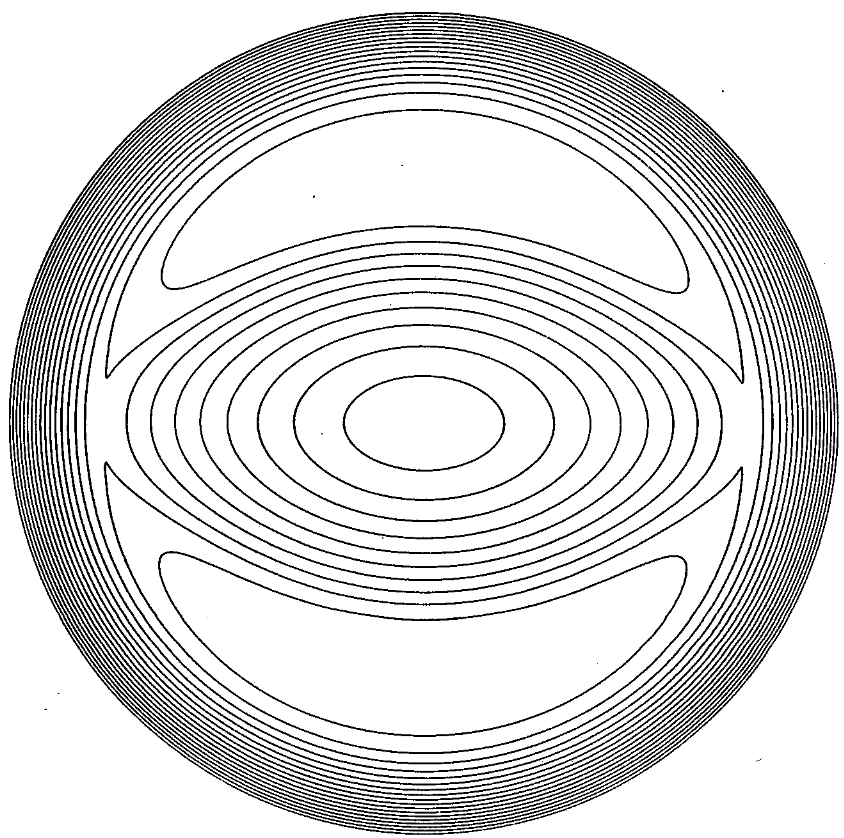

TIME = 250

J

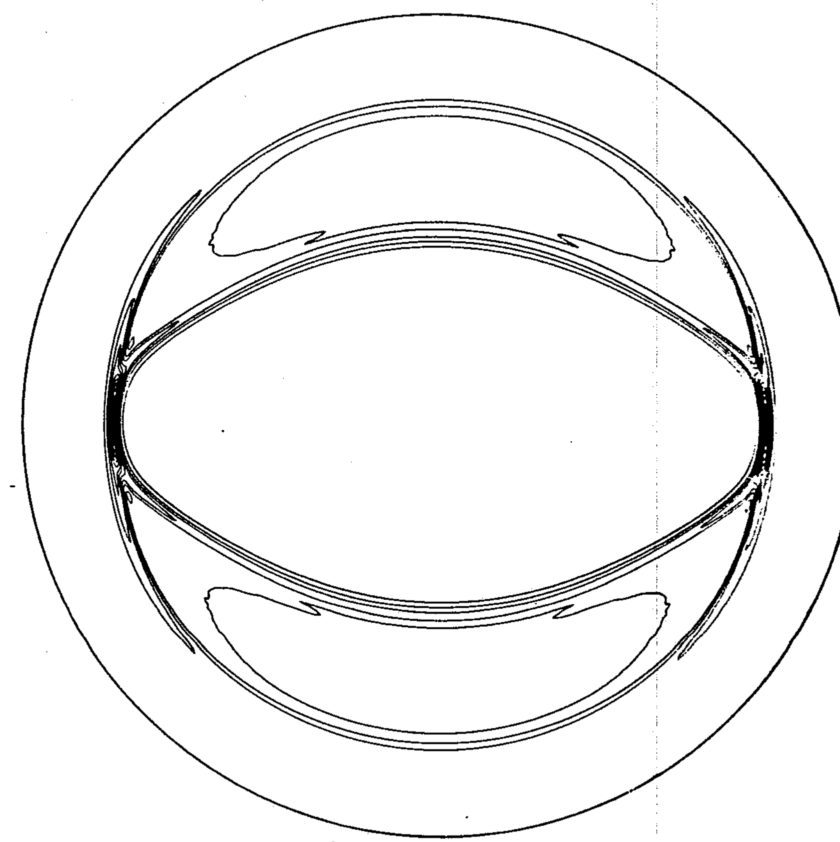

TIME = 250

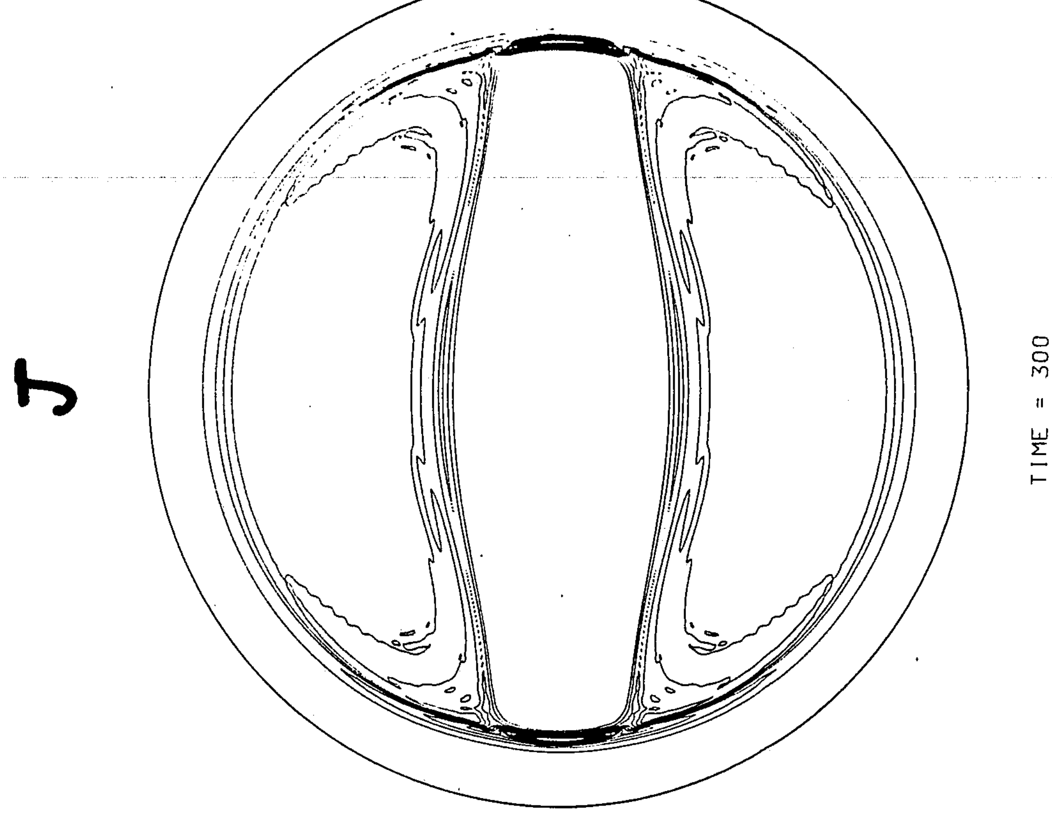
J
TIME = 300

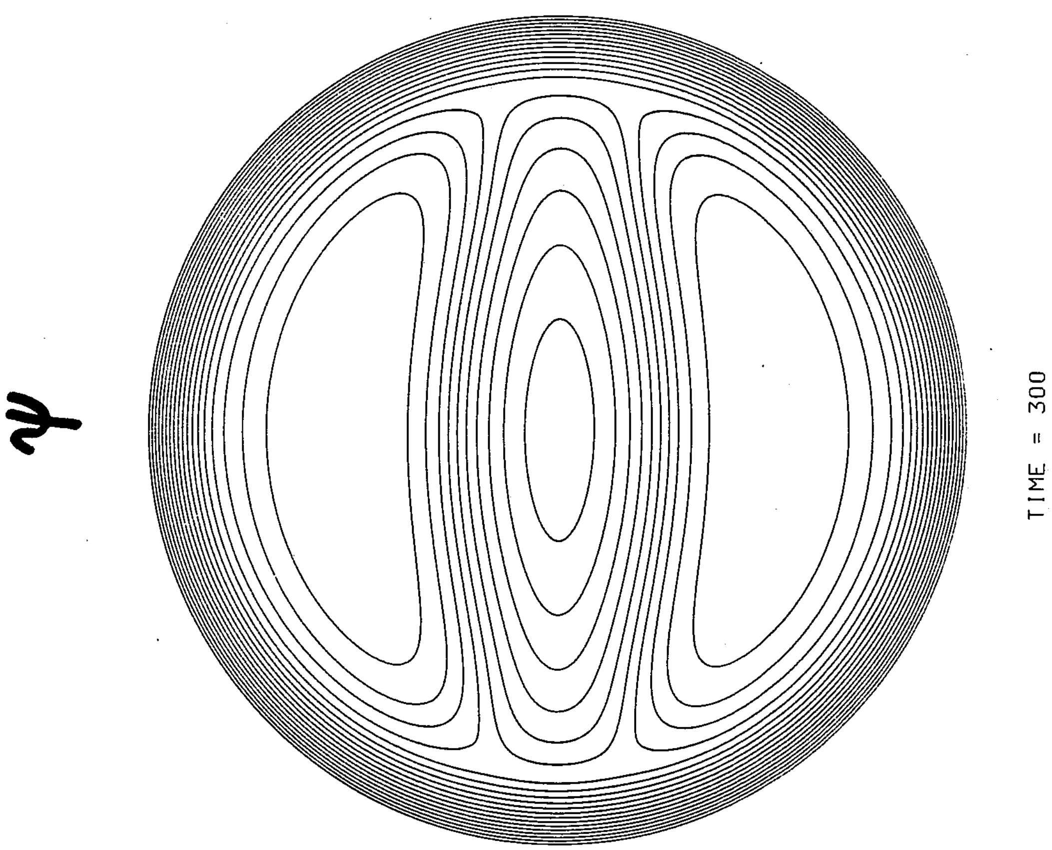
ψ
TIME = 300

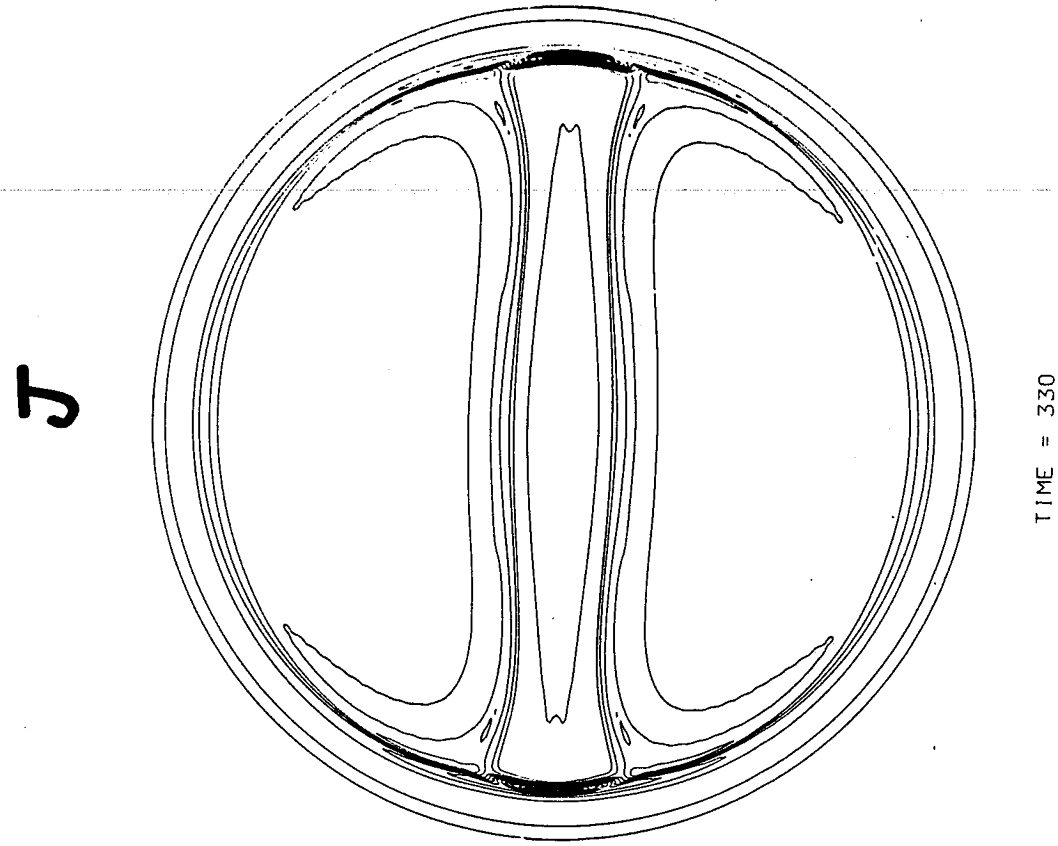
J
TIME = 330

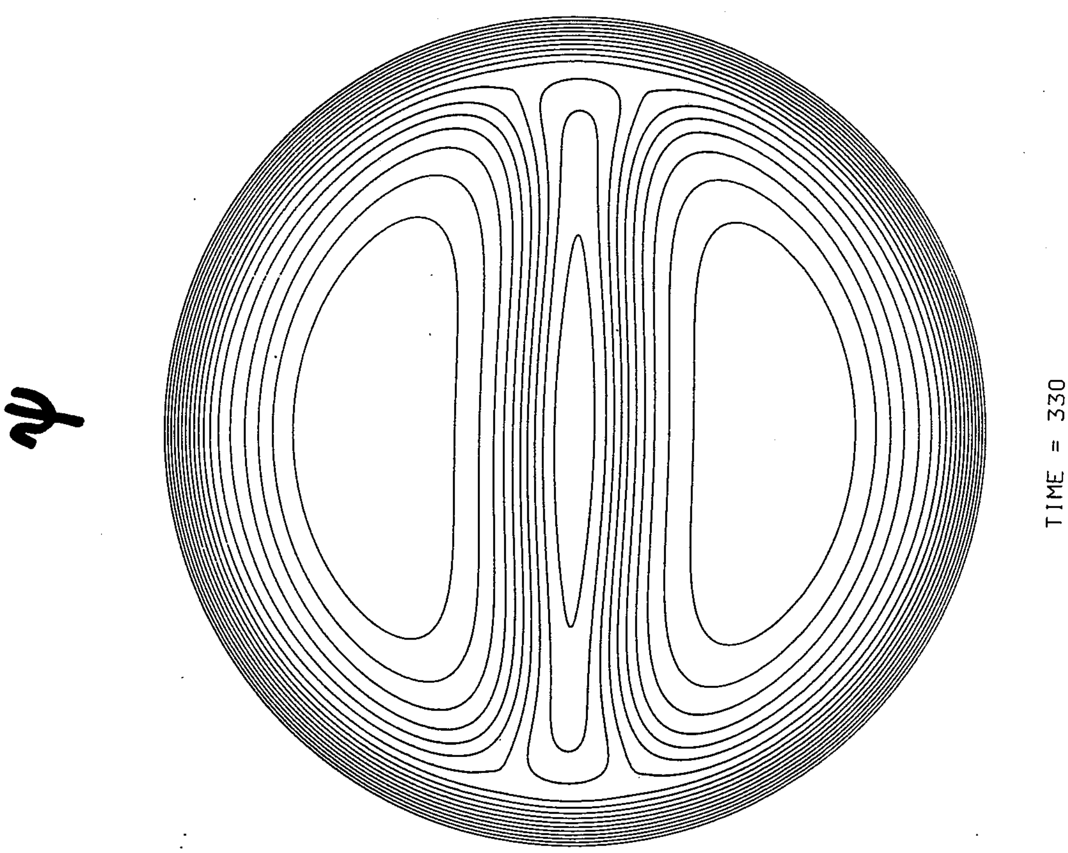
ψ
TIME = 330

ψ

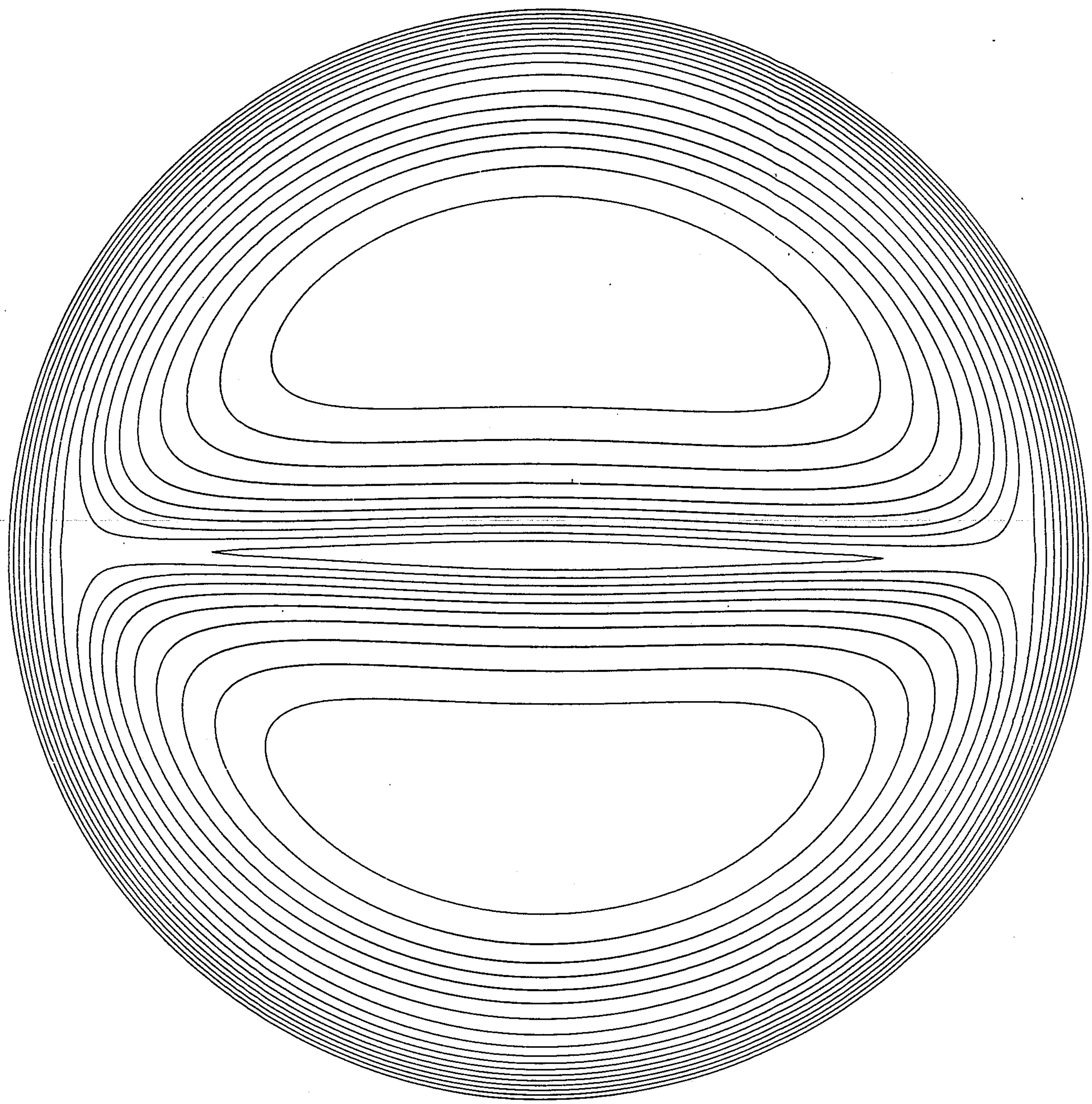

TIME = 351

J

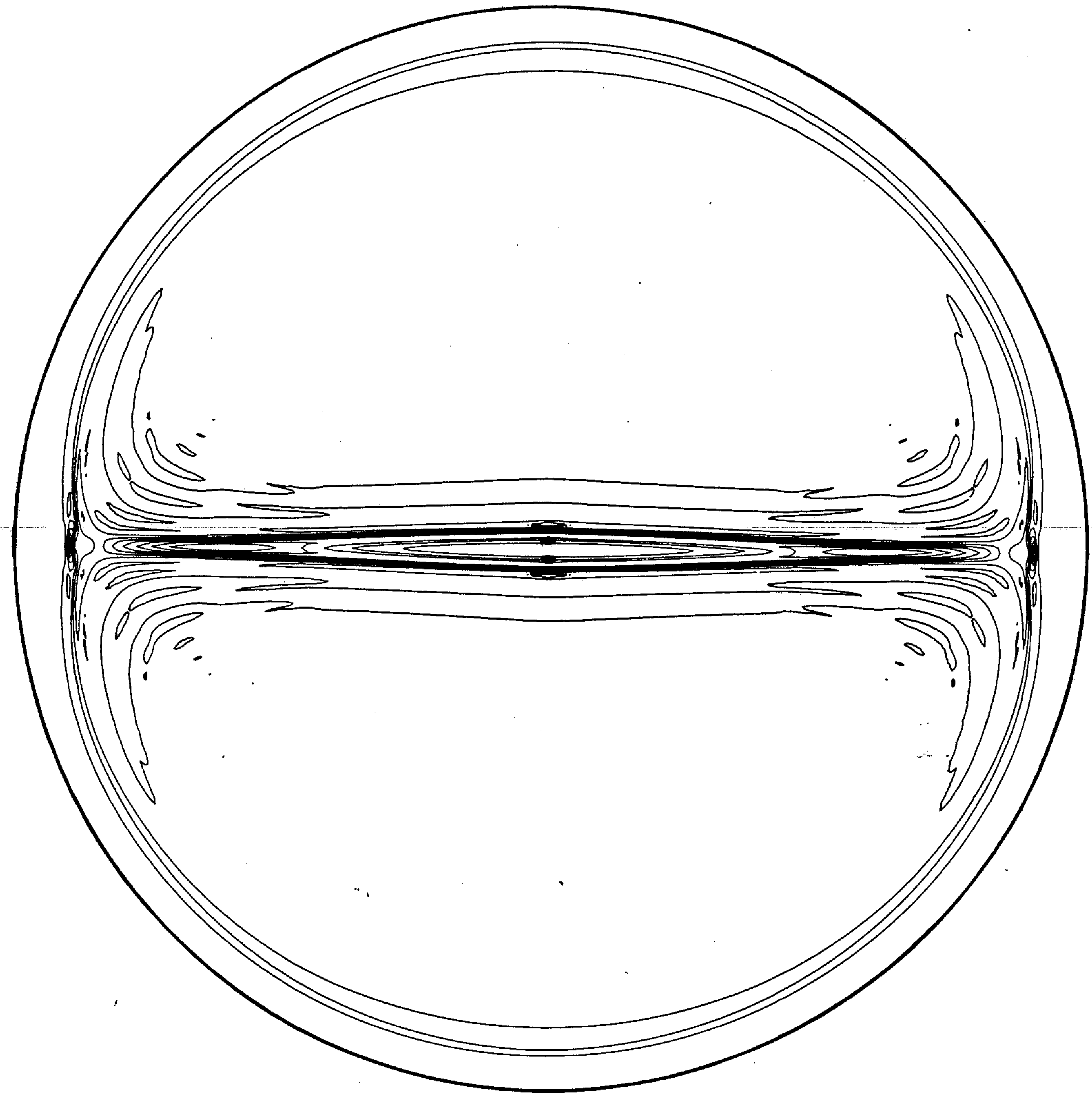

TIME = 351

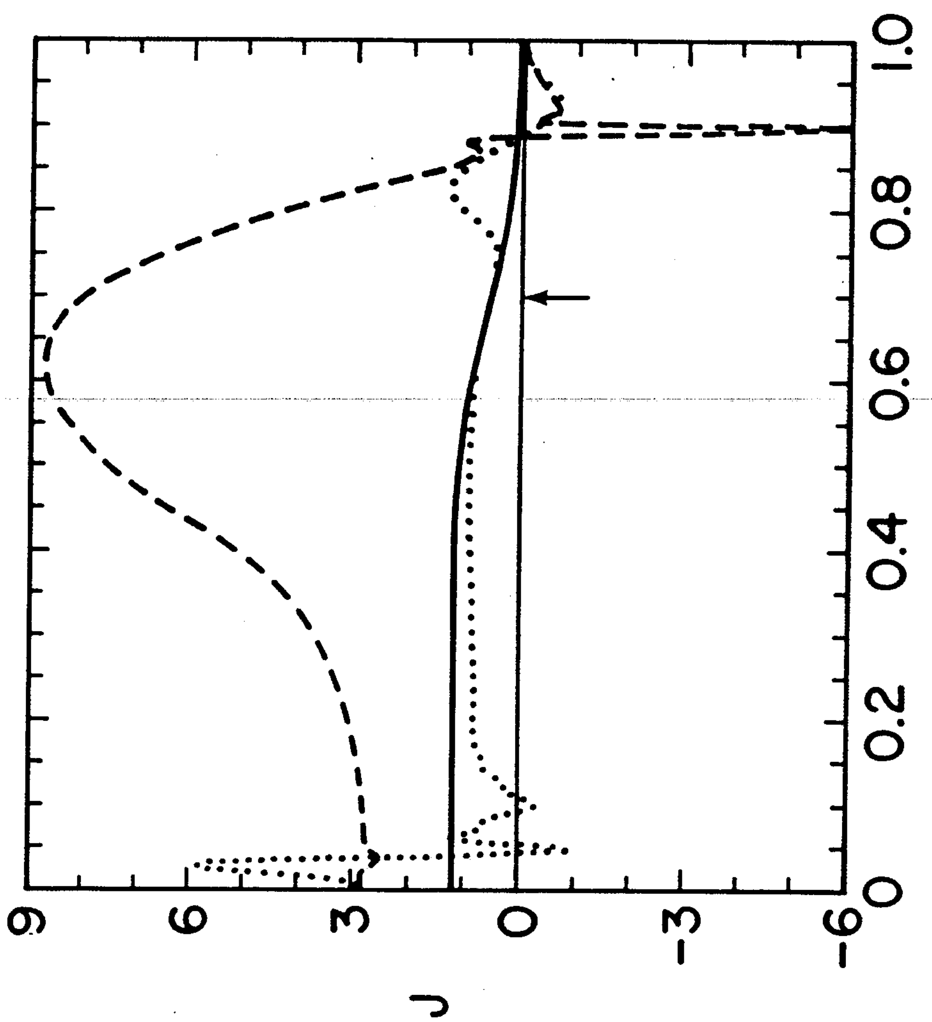
J
9
6
3
0
-3
-6
r
0
0.2
0.4
0.6
0.8
1.0

DOUBLING TIME τ

η	τ
5×10^{-5}	60
5×10^{-6}	100

$\Longrightarrow$

$$\tau \sim \eta^{-0.2}$$

IDEAL KINK

$$q(r) = q(0)\left[1 + \left(\frac{r}{r_0}\right)^{2\lambda}\right]^{1/\lambda}$$

$$r_0^{-2\lambda} \equiv \left[\frac{q(1)}{q(0)}\right]^{\lambda} - 1$$

$$J(r) = \frac{2}{q(r)}\left[\frac{q(0)}{q(r)}\right]^{\lambda}$$

$\lambda \to \infty$, $J(r) \to$

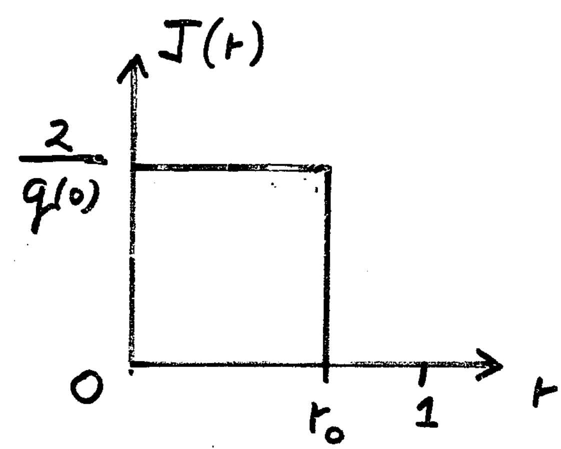

$$\eta(r) \sim \frac{1}{J(r)}$$

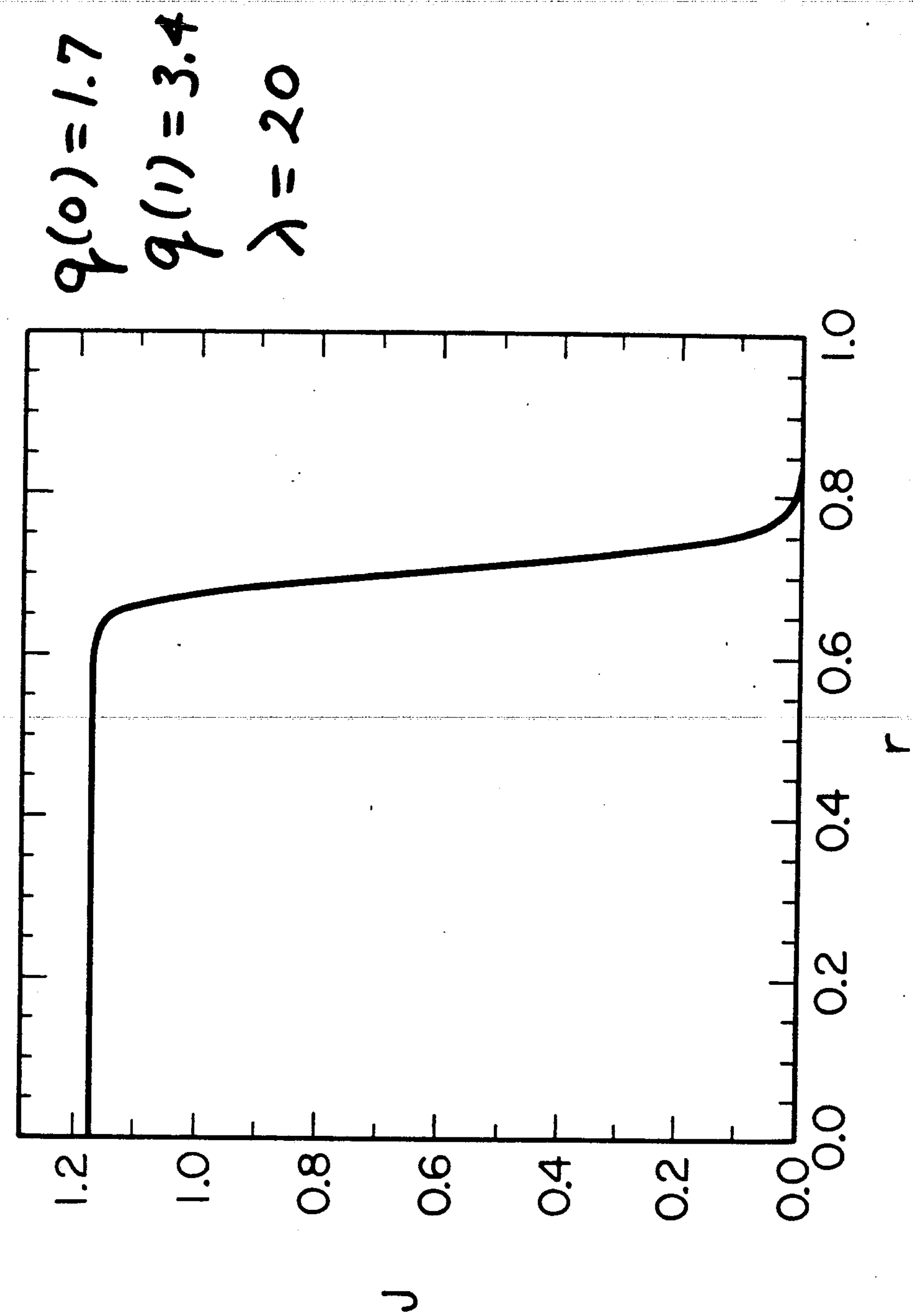

q(0) = 1.7
q(1) = 3.4
λ = 20
J
r
0.0
0.2
0.4
0.6
0.8
1.0
1.2

ψ

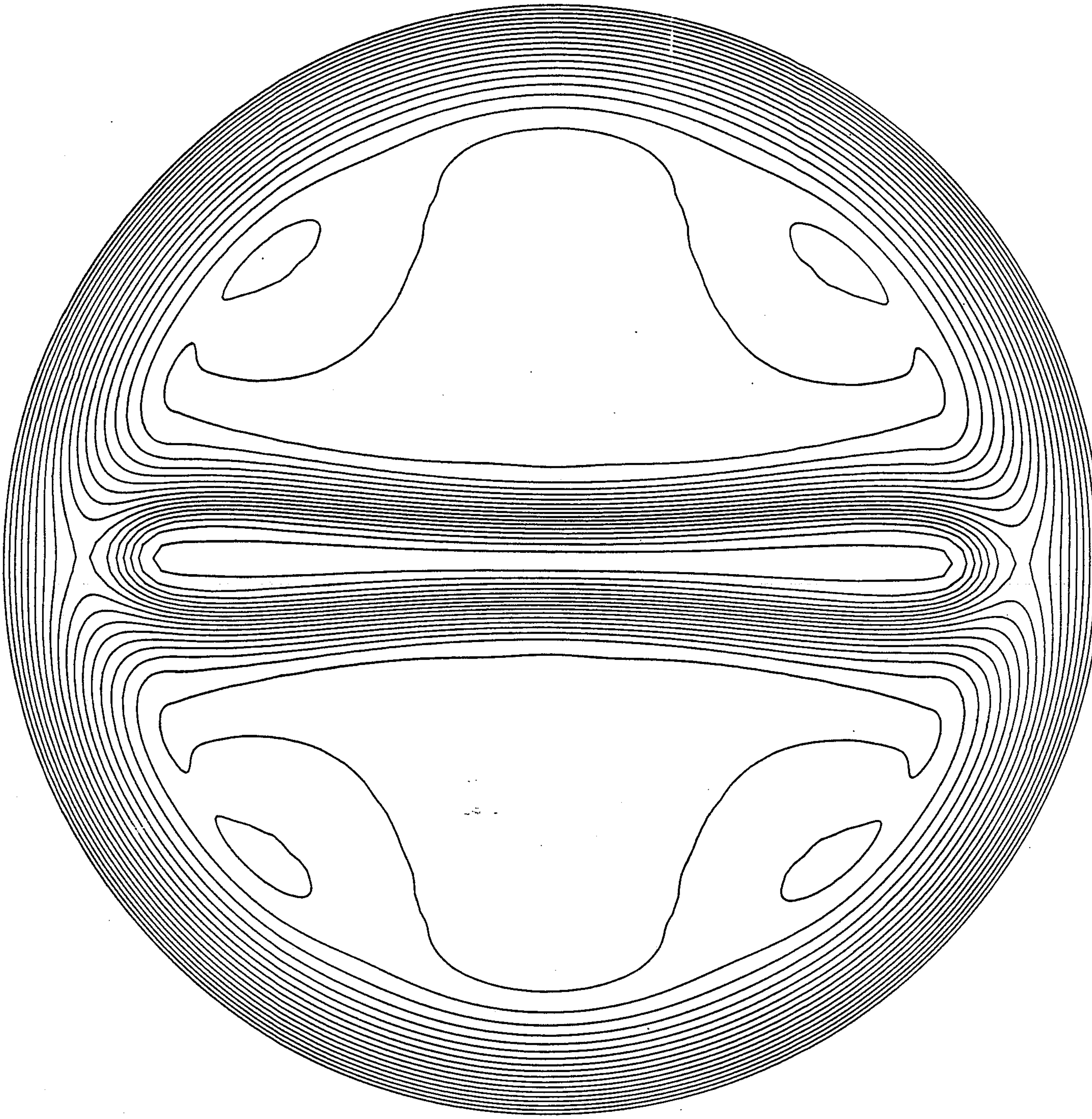

$t = 60$

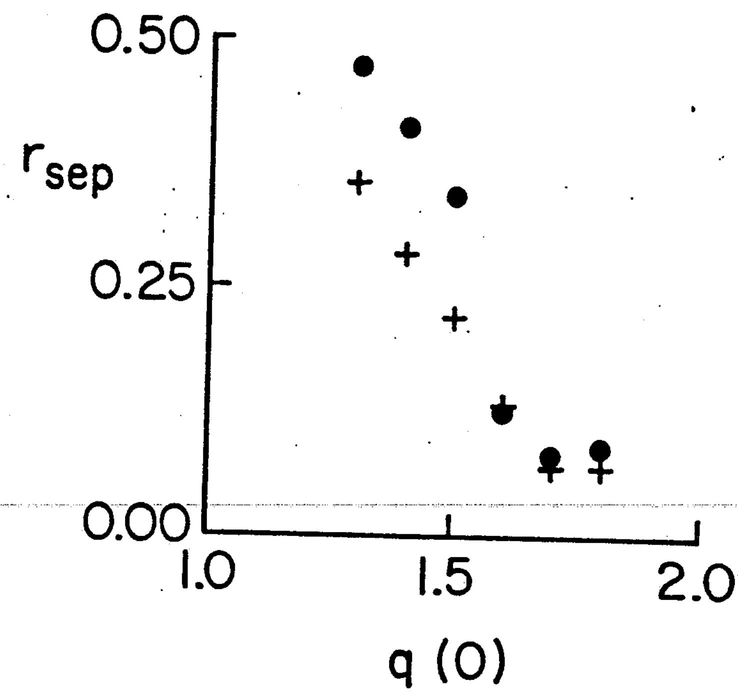

● RESISTIVE
+ IDEAL

* SATURATION OF RESISTIVE AND IDEAL CASES IS THE SAME WHEN $q(0) > 1.5$

SELF-CONSISTENT η EVOLUTION

$$\frac{\partial \eta}{\partial t} + \underline{V} \cdot \underline{\nabla} \eta = K_{\parallel} \underline{B} \cdot \underline{\nabla} \underline{B} \cdot \underline{\nabla} \eta + K_{\perp} \nabla_{\perp}^{2} \eta$$

$$\eta(r, t=0) = \frac{\eta}{J(r)} \qquad , \ \eta = 5 \times 10^{-5}$$

$$K_{\parallel} = 1$$

$$K_{\perp} = 10^{-5}$$

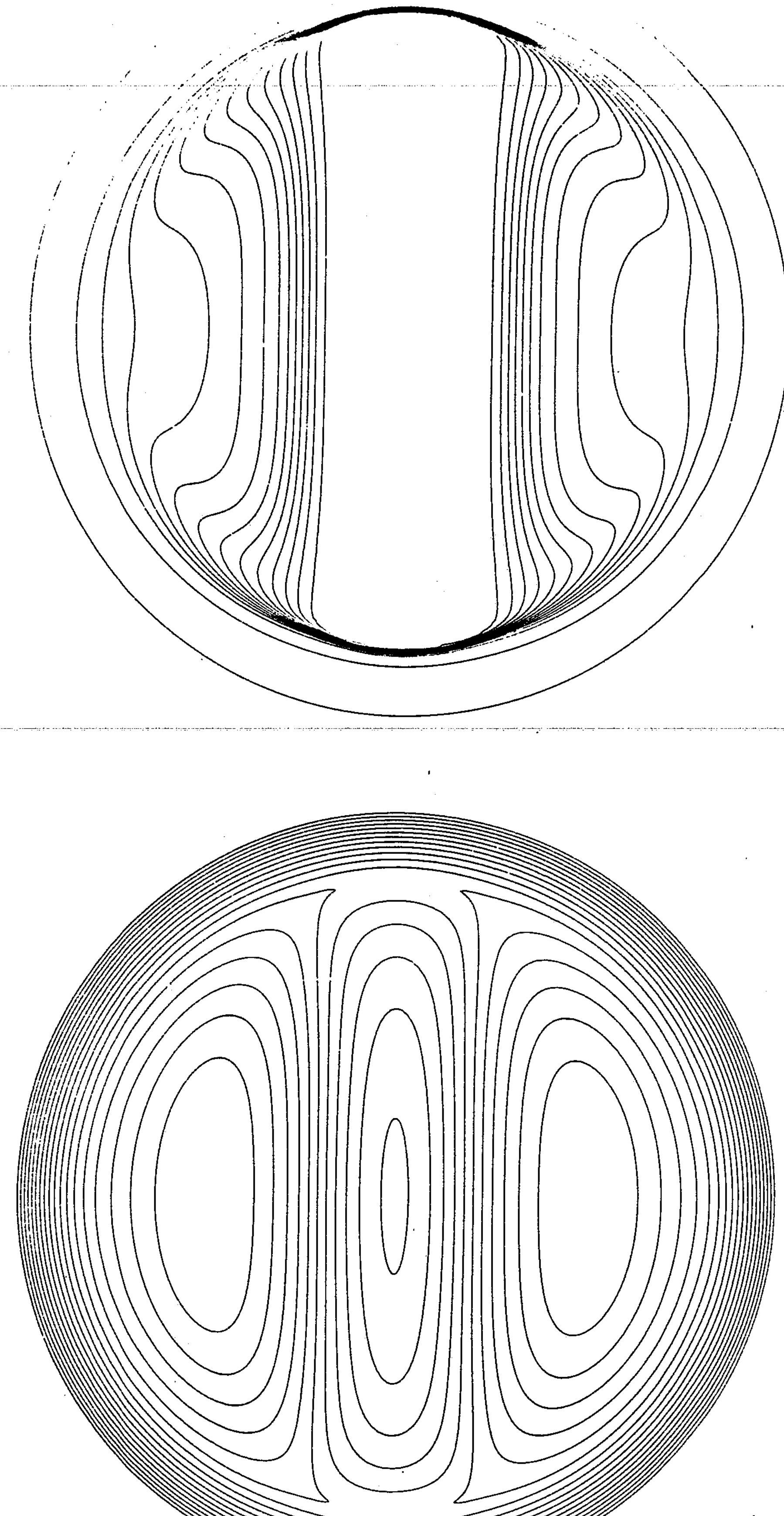

130

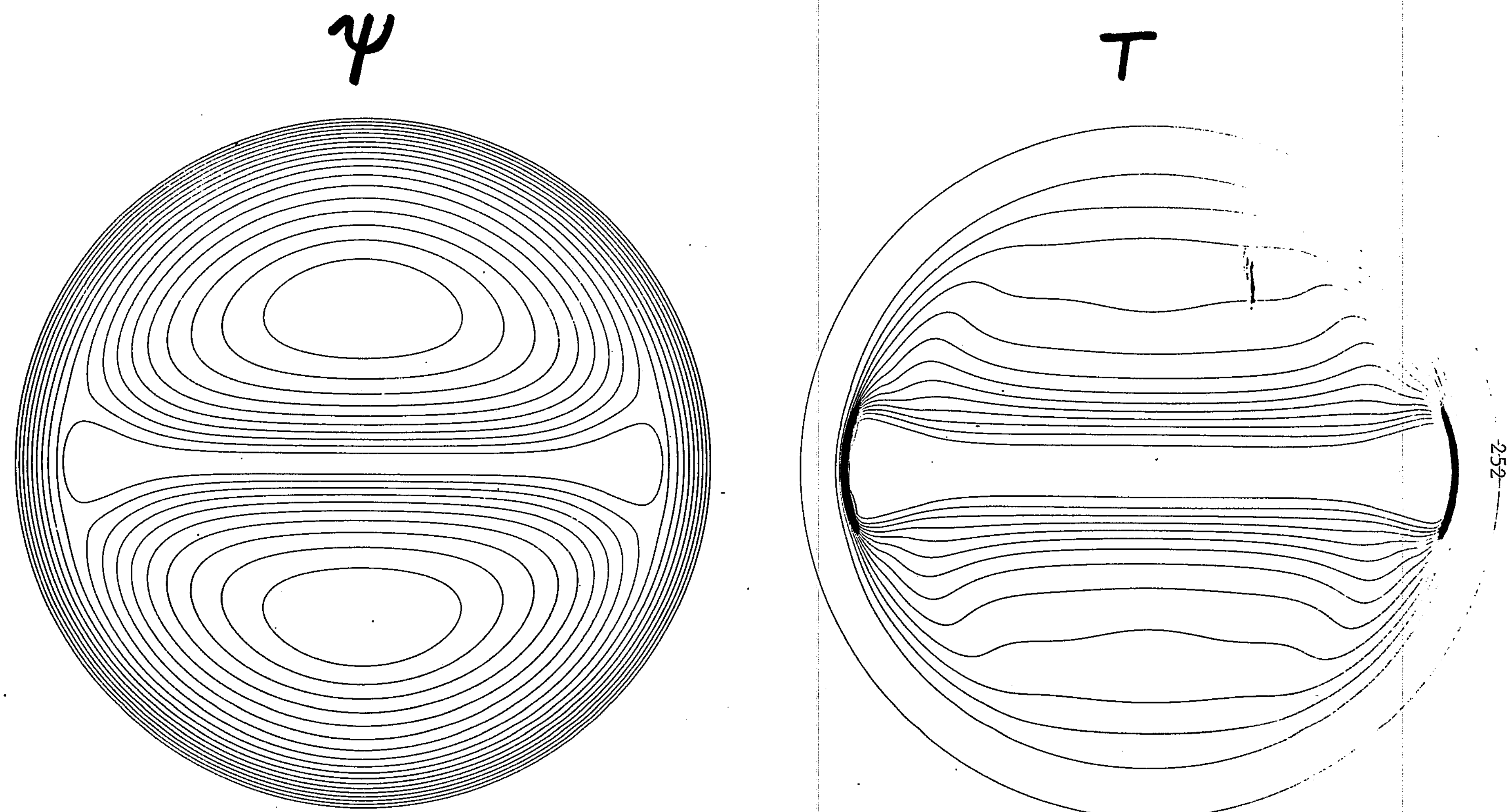

156

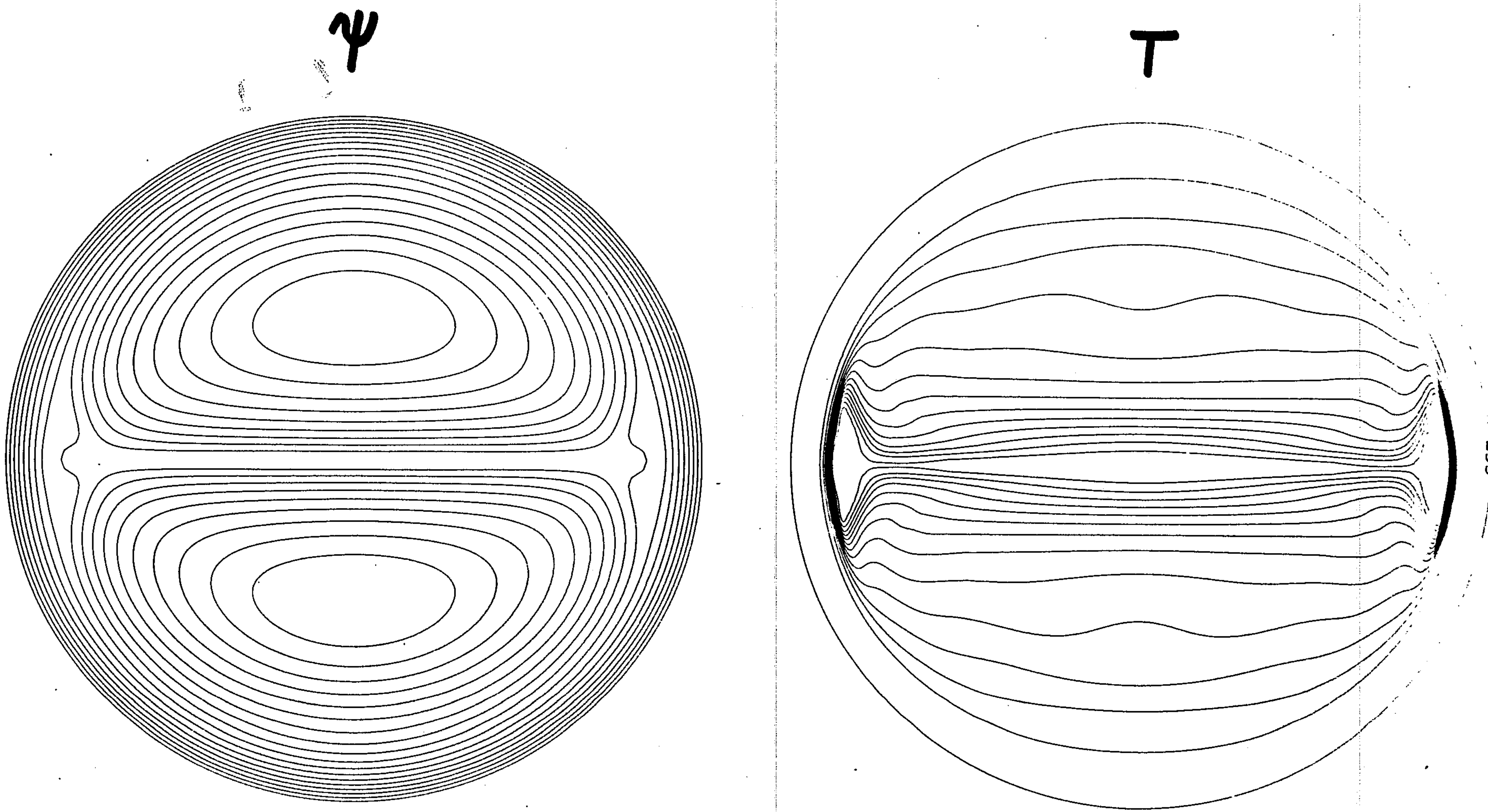

166

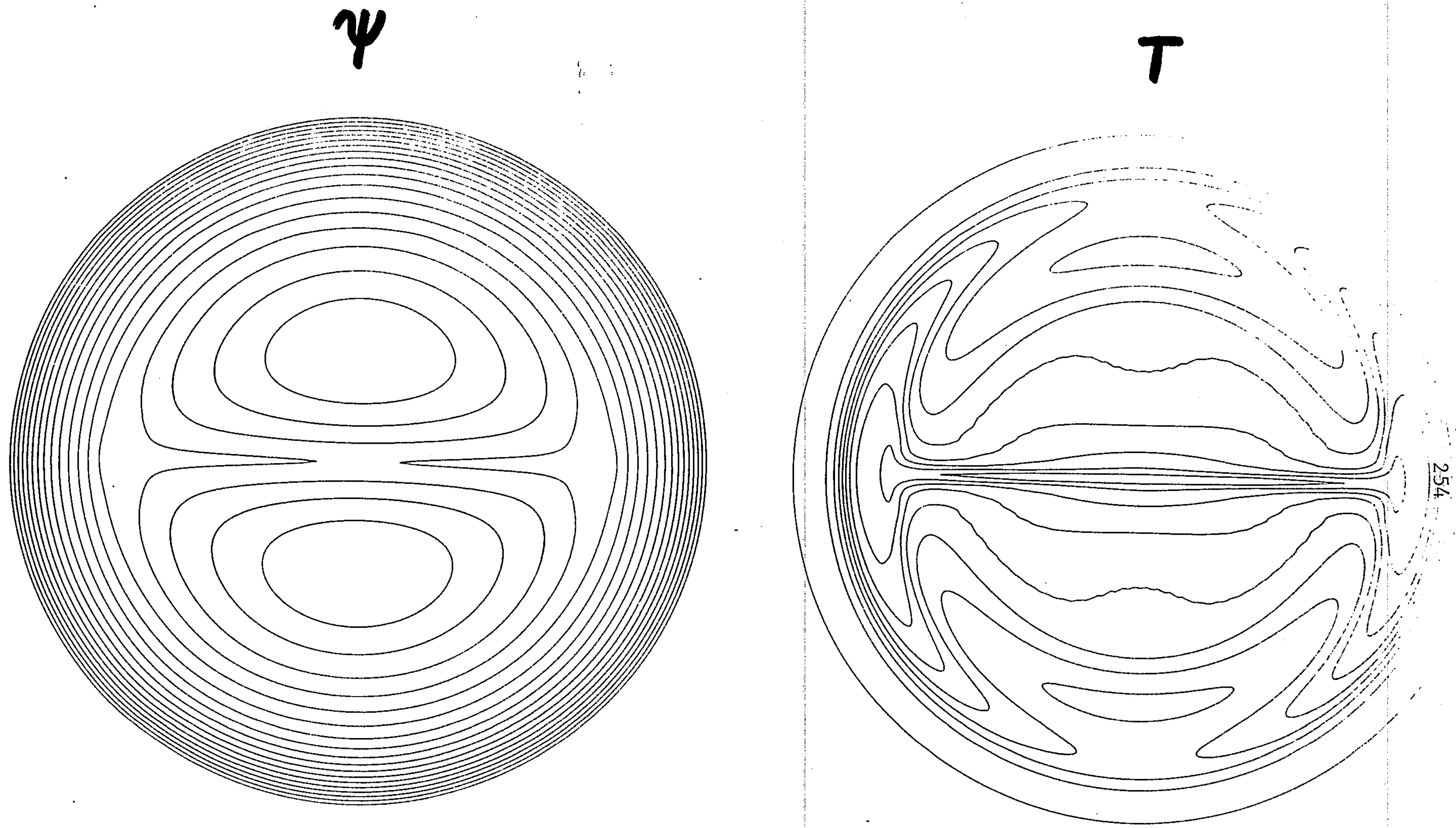

225

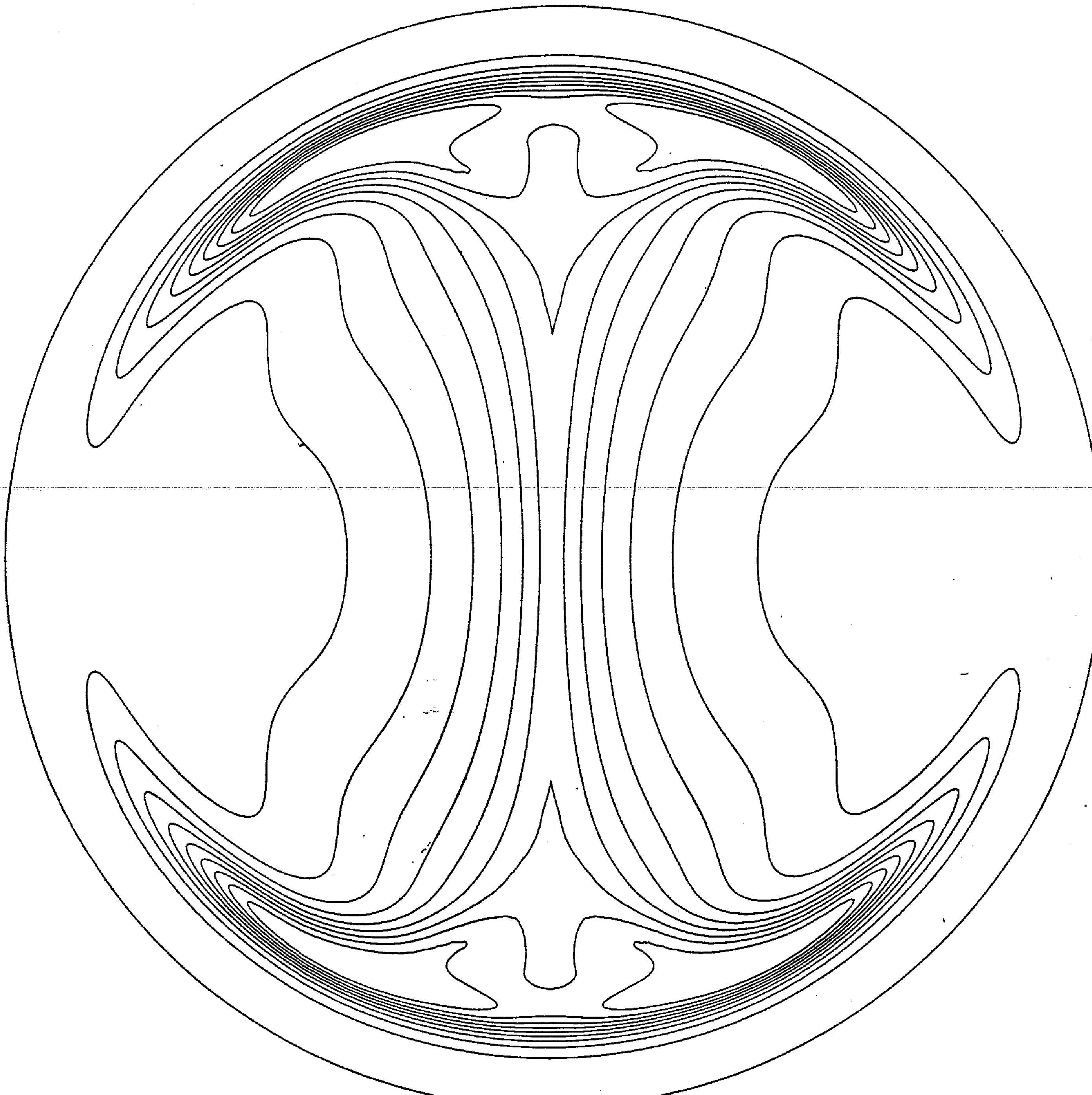

$K_{\parallel} = 0$

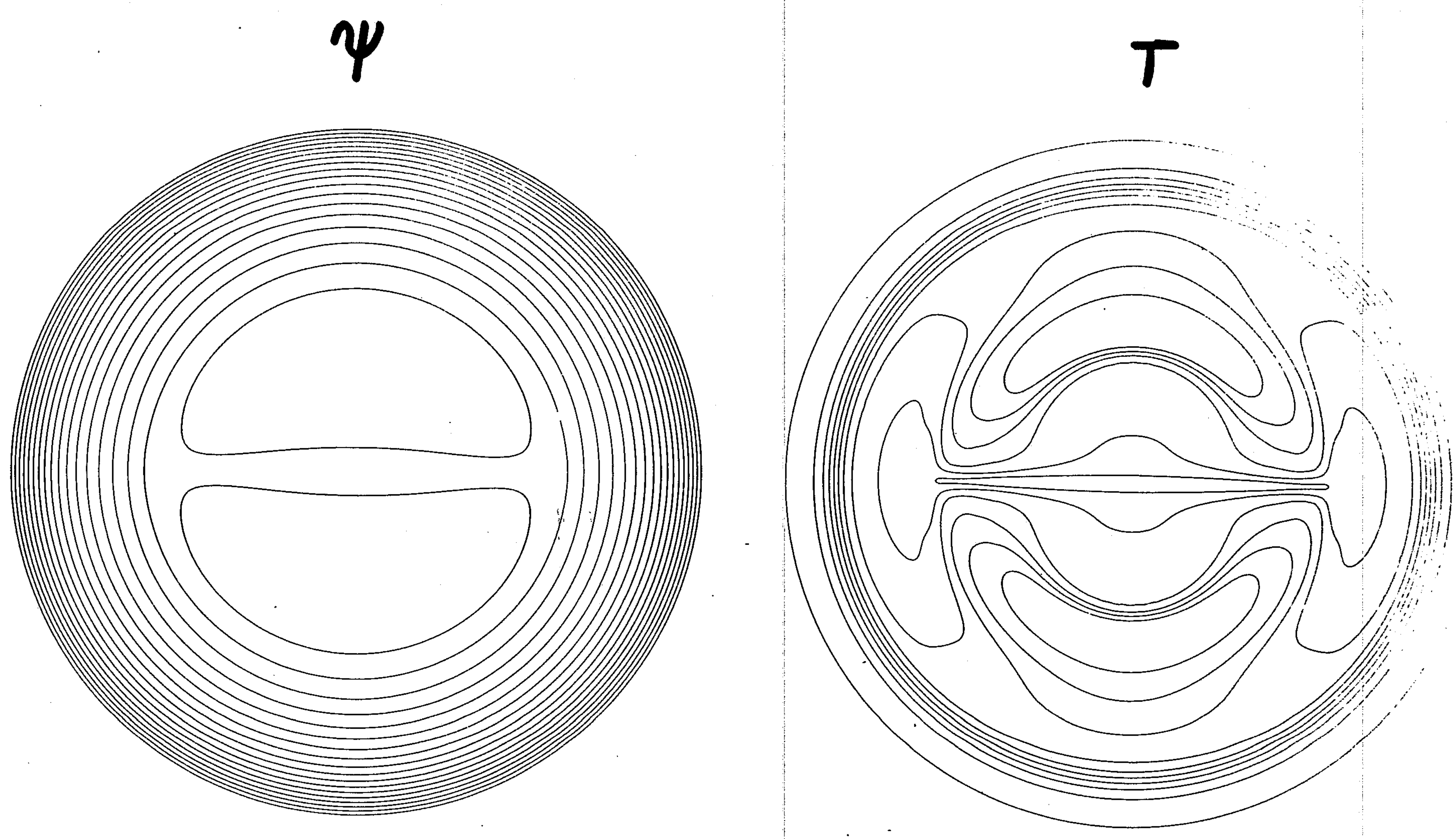

280

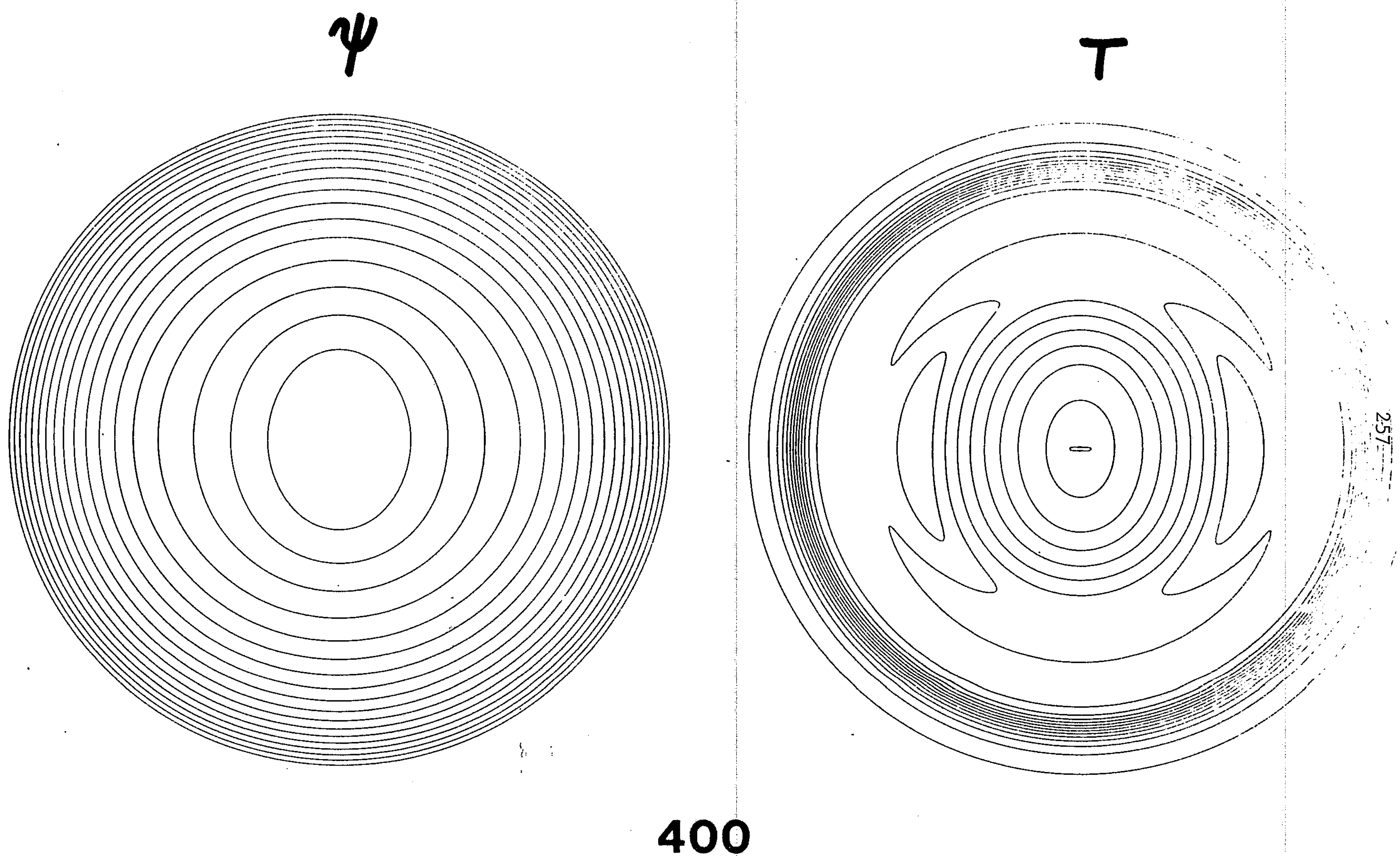
ψ
T
400

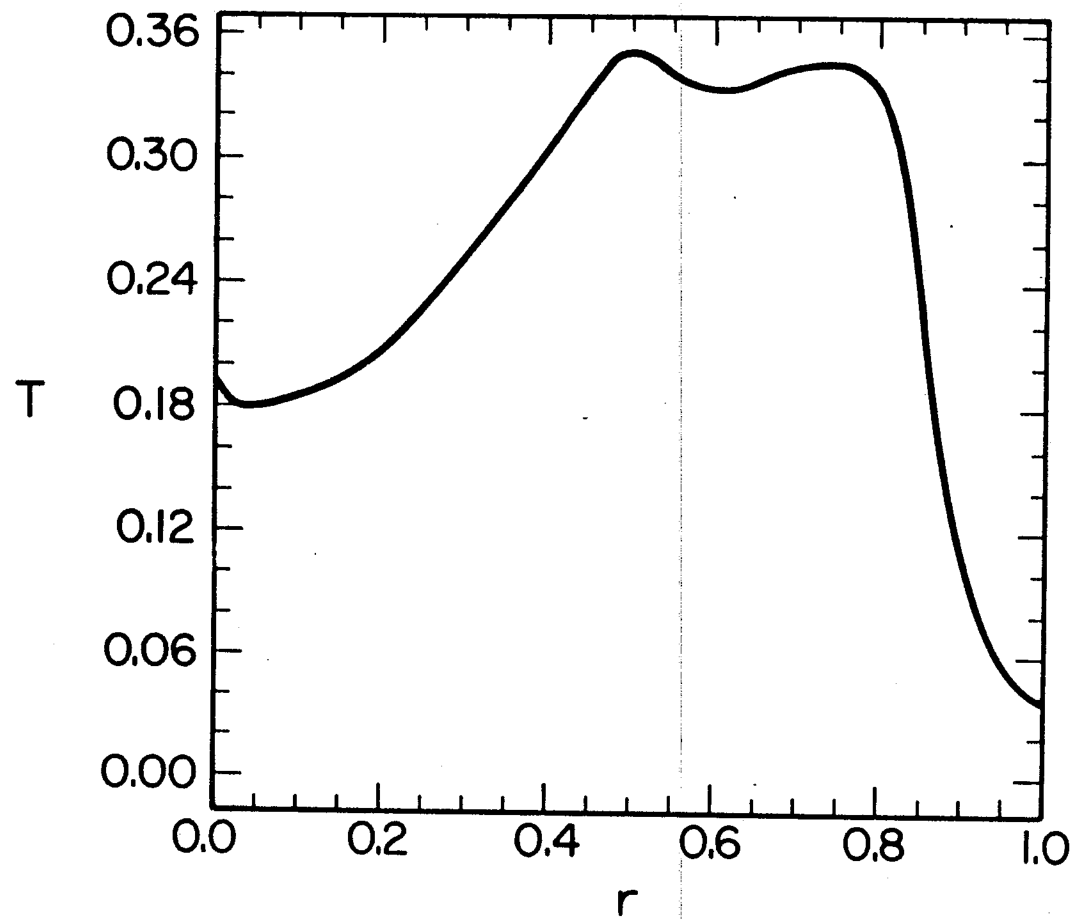

* CENTRAL TEMPERATURE HAS DROPPED BY A FACTOR OF SIX

m = 2 SAWTEETH

* REGION INSIDE SEPARATRIX HAS $q \simeq 2$ AFTER RECONNECTION.

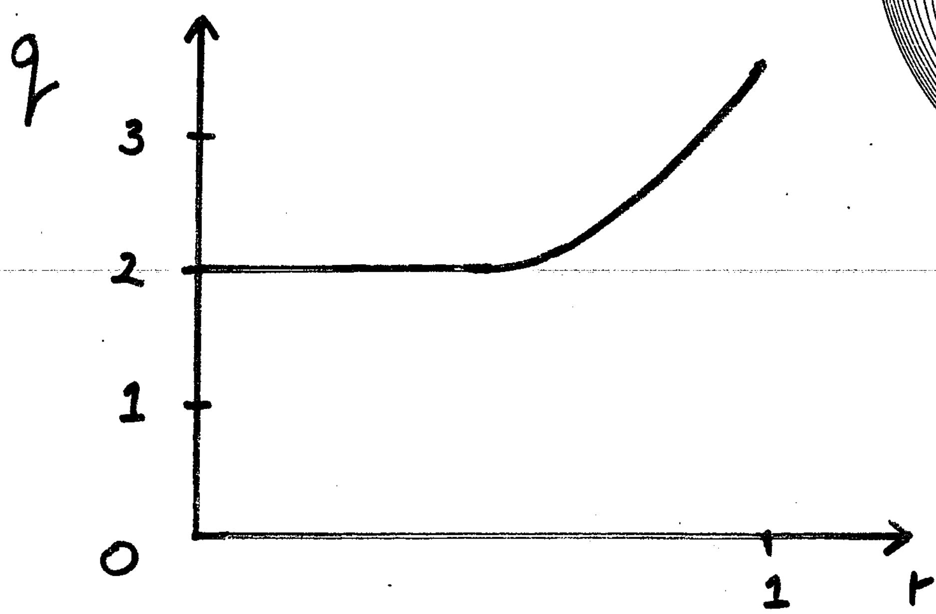

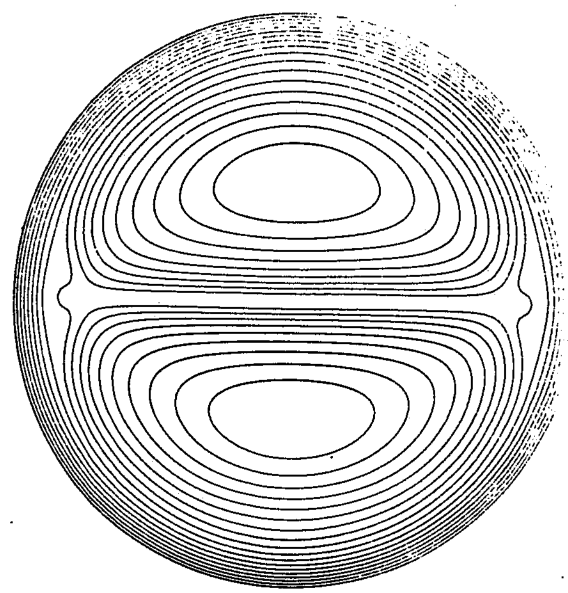

* OHMIC HEATING LOWERS q BELOW 2; LARGE ISLANDS GROW AGAIN

$\longrightarrow$ m = 2 SAWTEETH

EXPERIMENTAL EVIDENCE

T-4 MIRNOV & SEMENOV, IAEA (1976)

20 MAJOR DISRUPTIONS IN NEARLY IDENTICAL DISCHARGES

TWO STAGE DISRUPTIONS :

① PRE-DISRUPTION : INTERACTION OF $m = 2$ AND $m = 1$ PERTURBATIONS RESULTS IN A RADIAL EXPANSION AND FLATTENING OF CURRENT AND TEMPERATURE PROFILES. $q(0)$ RISES ABOVE 1.5.

② DISRUPTION PER SE : DEVELOPMENT OF $m = 2$ PERTURBATION IN FLATTENED CURRENT PROFILE ; EXPANSION OF COLUMN TO THE WALL

PDX -

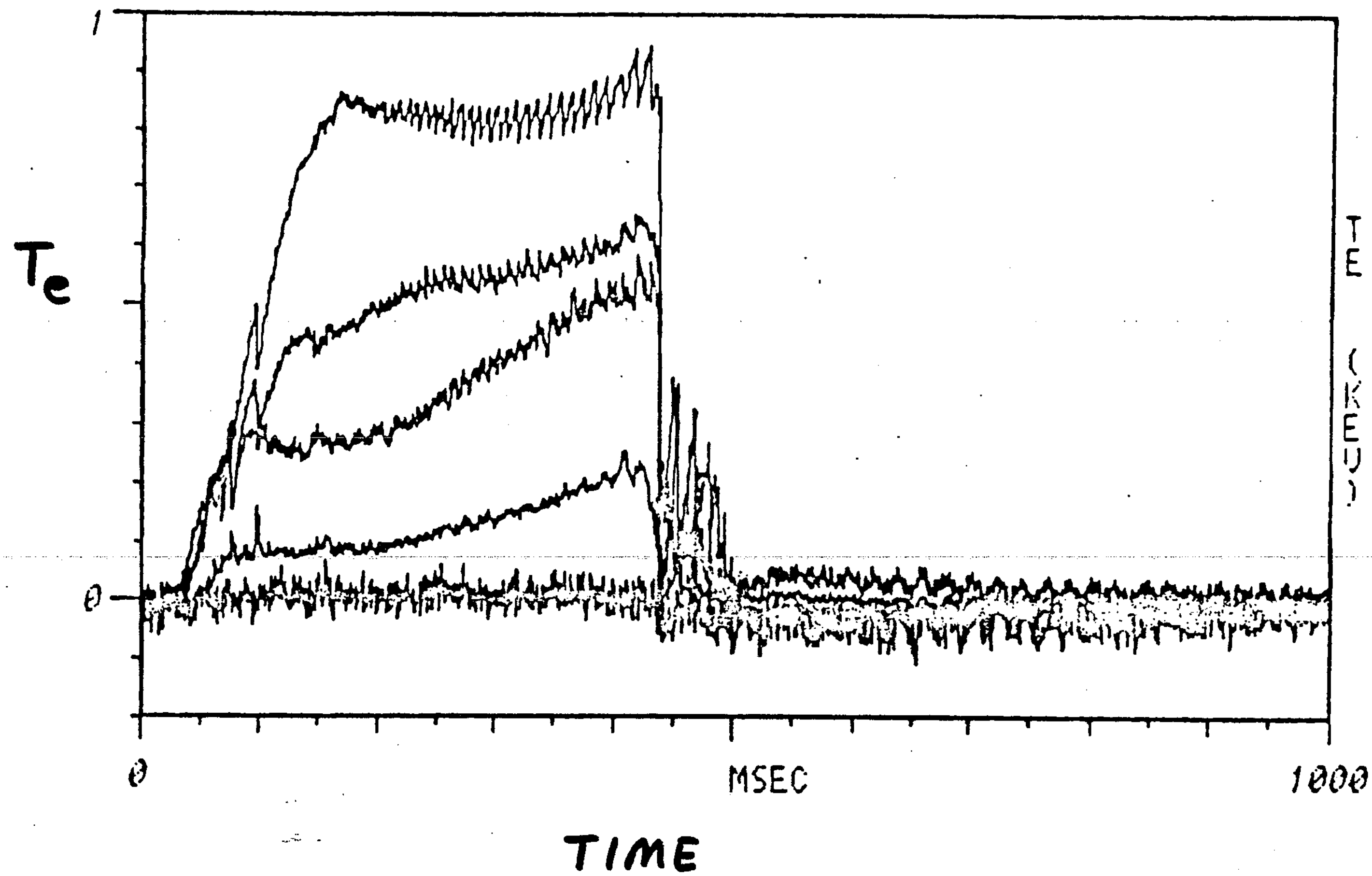

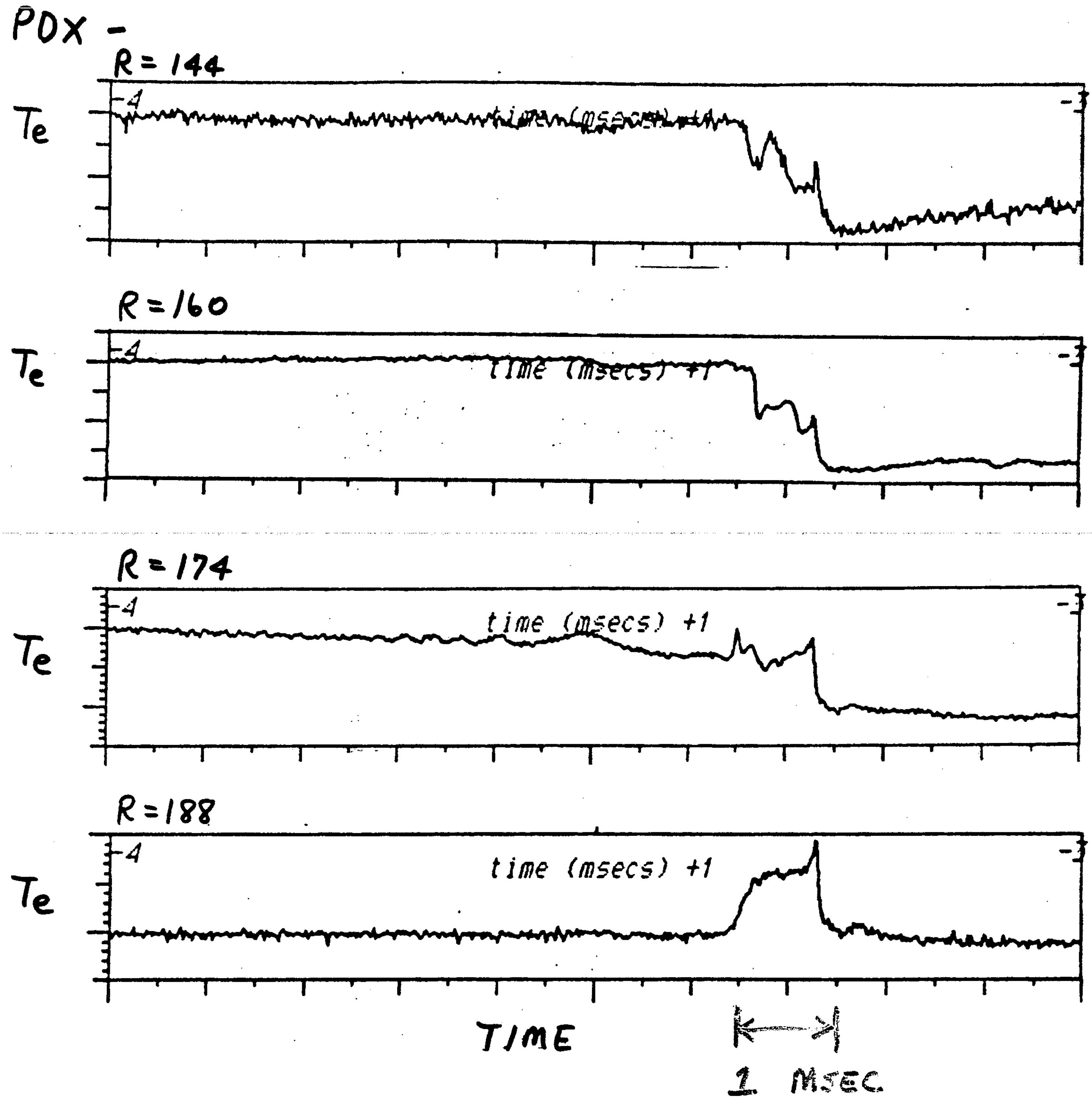
PDX -
R = 144
Te
-4
time (msecs) +1
R = 160
Te
-4
time (msecs) +1
R = 174
Te
-4
time (msecs) +1
R = 188
Te
-4
time (msecs) +1
TIME
1 MSEC

TFR -

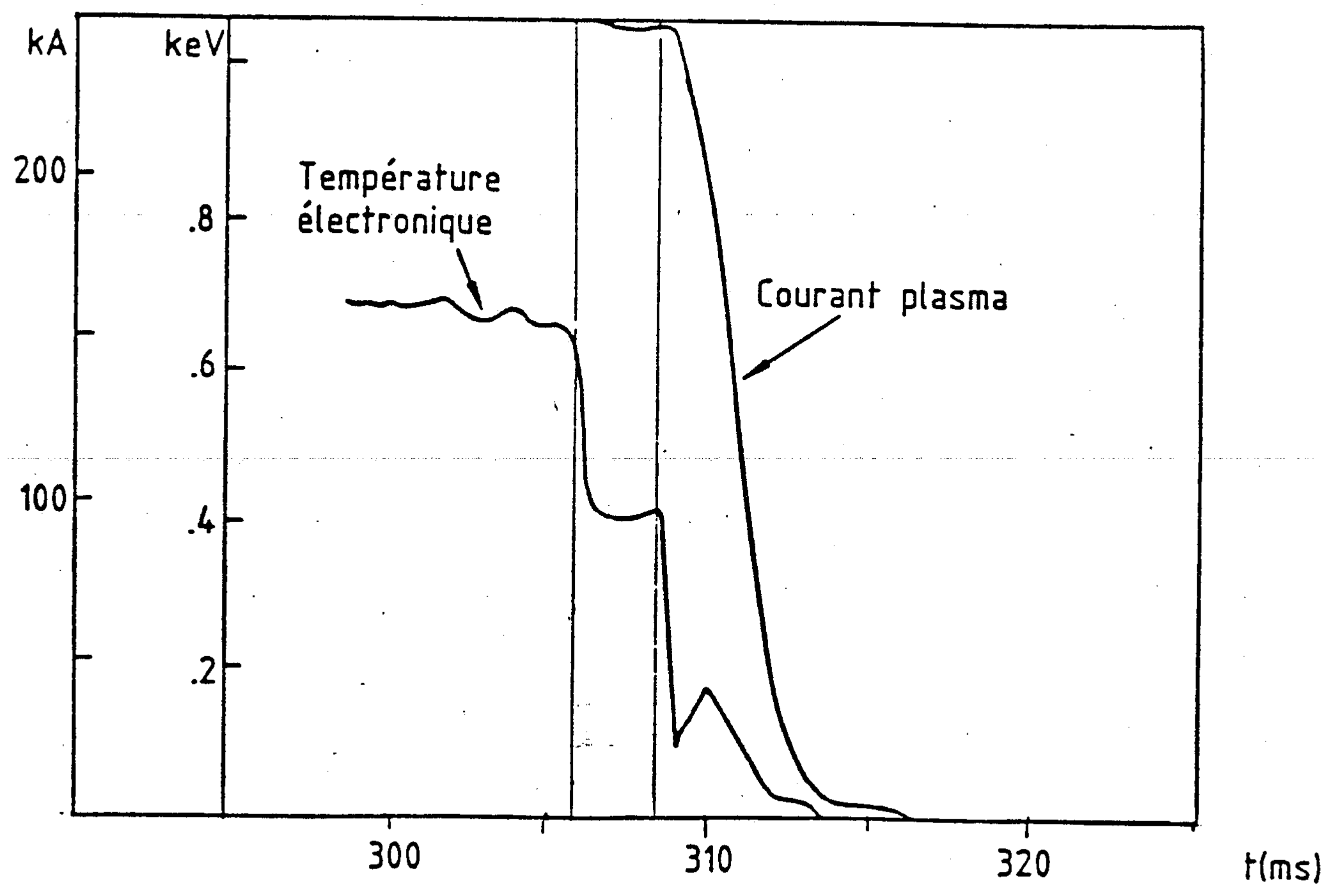

- L. LAURENT

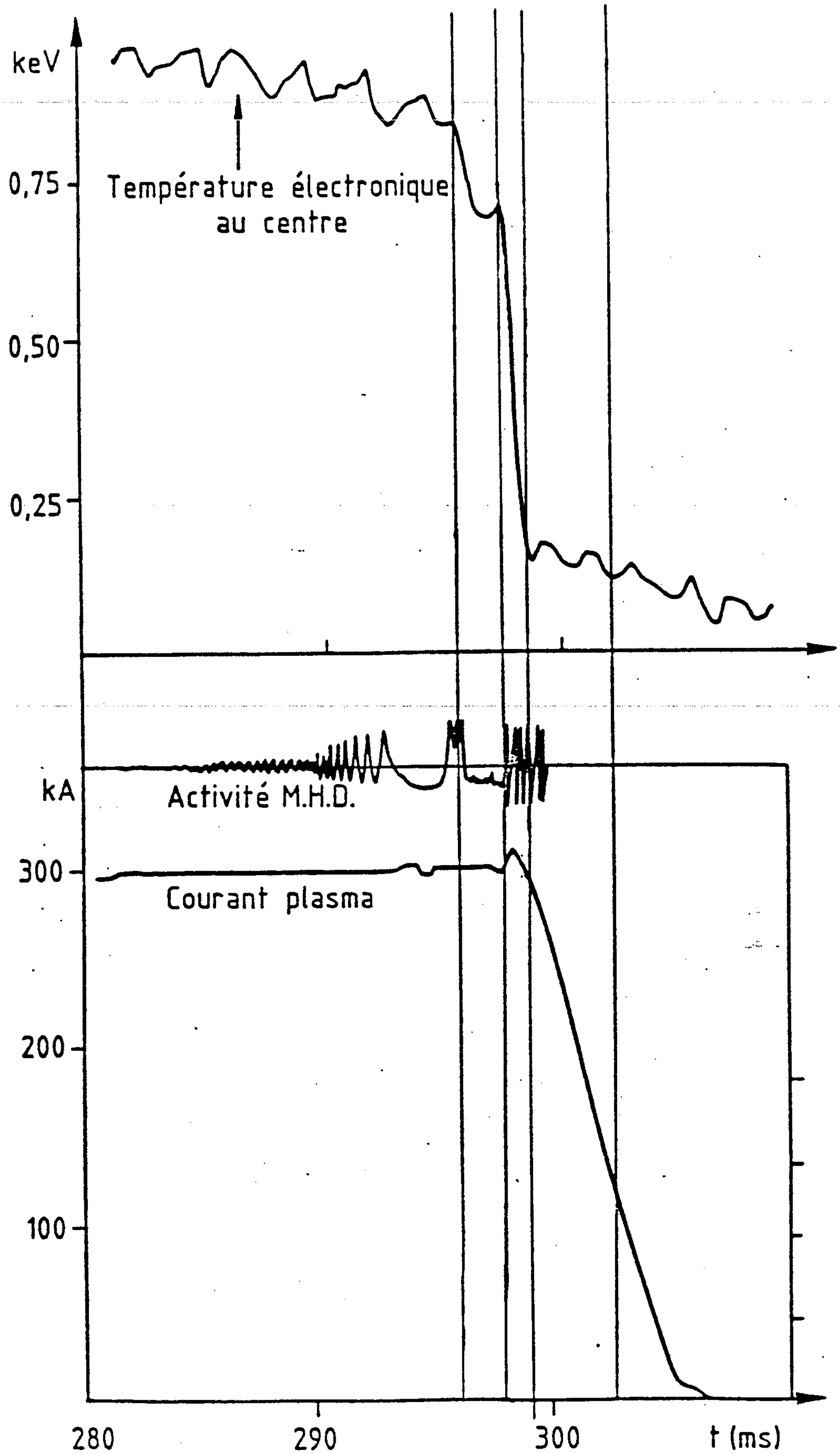
keV
0,75
0,50
0,25
Température électronique
au centre
kA
300
200
100
Activité M.H.D.
Courant plasma
280
290
300
t (ms)

JIPP T-II TOKAMAK

TSUJI, ET AL. (1983)

* DURING MAJOR DISRUPTIONS, THE DOMINANT MODE IS $m/n = 2/1$ MODULATED BY A WEAKER 1/1 MODE WHEN THE 2/1 AMPLITUDE BECOMES LARGE.

* NO 3/2 MODE IS DETECTED DURING MAJOR DISRUPTIONS. THE 3/2 MODE IS ONLY DETECTED DURING PARTIAL (MINOR) DISRUPTIONS IN WHICH THE CENTRAL REGION OF THE DISCHARGE IS NOT AFFECTED.

JIPP TII -

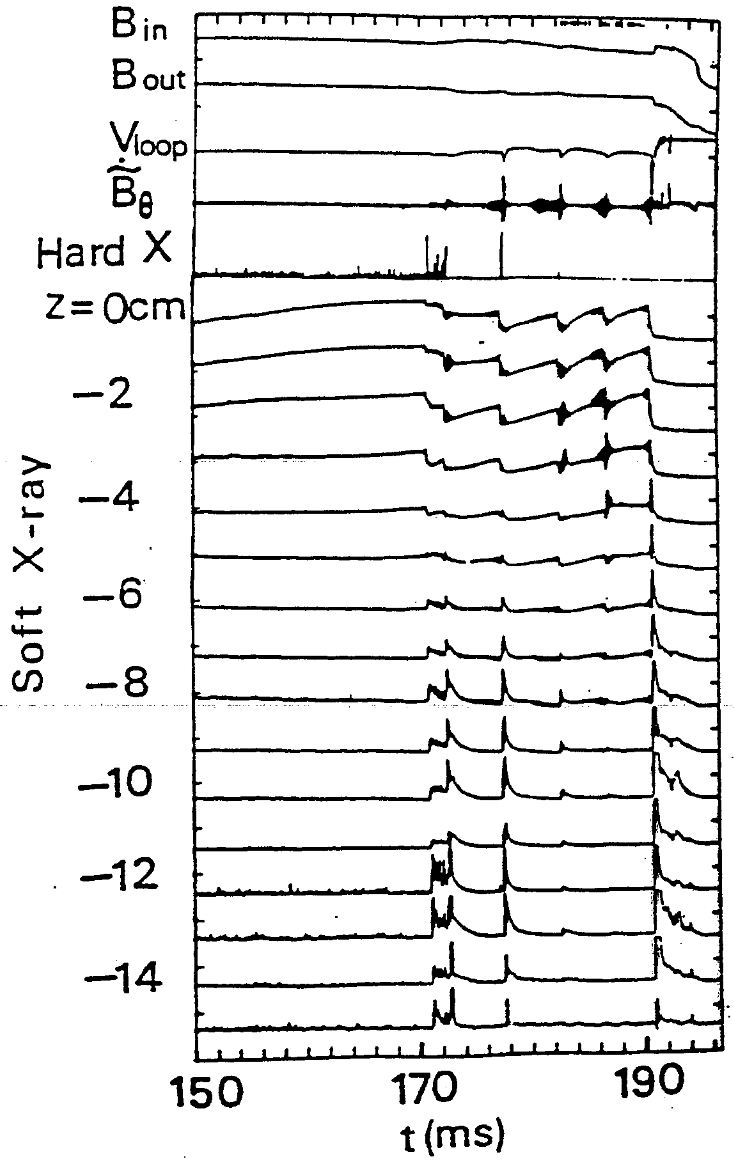

- TSUJI, ET AL.

SUMMARY

* WHEN $q(0) > 1.5$, $m=2$ MAGNETIC ISLANDS GROW TO A VERY LARGE AMPLITUDE ENCOMPASSING VIRTUALLY THE ENTIRE PLASMA CROSS SECTION.
* THESE VERY LARGE ISLANDS ARE RELATED TO THE VACUUM BUBBLES FORMED DURING THE NONLINEAR DEVELOPMENT OF THE IDEAL KINK INSTABILITY.
* AS A RESULT OF THE FORMATION OF THESE LARGE ISLANDS, THE HOT CENTRAL PLASMA IS CONVECTED OUT TO THE EDGE.

* OUR SCENARIO FOR MAJOR DISRUPTIONS IS SUPPORTED BY THE OBSERVATION OF TWO STAGE DISRUPTIONS ON SEVERAL TOKAMAKS.

* IF THIS SCENARIO IS CORRECT, THEN A POSSIBLE METHOD FOR AVOIDING MAJOR DISRUPTIONS IS TO STRONGLY HEAT AT THE CENTER (USING ECRH, FOR EXAMPLE) THEREBY DRIVING $q(0)$ DOWN.

ENERGY PRINCIPLE FOR TOROIDAL PLASMA WITH BOUNDARY

Y. KONDOH

GUNMA UNIVERSITY

1.

< Energy Principle for Toroidal Plasma with Boundary >

Y. Kondoh

Dept. of Electronic Engineering, Gunma Univ., Japan

- Generalized fundamental global invariant.
- Energy principle for plasma with ~~b~~ounday.
- Typical numerical results.

Refs. 3. Y. Kondoh, T. Amano, A. Nagata, K. Ogawa et al.; J. Phys. Soc. Jpn. <u>53</u> (1984) 3427.

4. Y. Kondoh; submitted to J. Phys. Soc. Jpn.

1. Y. Kondoh; Nucl. Fusion <u>21</u> (1981) 1607.

2. Y. Kondoh; Nucl. Fusion <u>22</u> (1982) 1372.

2.

papers on Energy Principle, Variational Principle, Relaxation ....

$$W = \int \left(\frac{B^2}{2\mu_0} + \frac{P}{\gamma - 1} \right) dV$$

$$W_m = \int \frac{B^2}{2\mu_0} dV.$$

- M.D. Kruskal, R.M. Kulsrud; Phys. Fluids 1 (1958) 265.
  ideal MHD. $\delta W = 0 \rightarrow \nabla p = \vec{j} \times \vec{B}$.
- I.B. Bernstein et al; Proc. R. Soc. London Ser. A244 (1958) 17.
  ideal MHD. $\delta^2 W > 0 \rightarrow$ ideal MHD stability.
- J. B. Taylor; Phys. Rev. Lett. 35 (1974) 1139.
  slightly resistive MHD $\rightarrow$ global invariant $K_0 = \int_{V_0} \vec{A} \cdot \vec{B} dV / \mu_0$.
  mag. energy $W_m \rightarrow$ minimum $\Rightarrow \mu_0 \vec{j} = \lambda_0 \vec{B}$.
- B. Kadomtsev; IAEA, 6th Conf. 1977, Vol. I, p.555.
  helical tearing mode $\rightarrow$ global invariant $K_\chi = \int \chi \, d\phi / \mu_0$.
  $W_m \rightarrow$ minimum $\Rightarrow \mu_0 \vec{j} = \lambda_0 \vec{B}$.
- A. Bhattacharjee et al; Phys. Fluids 25 (1982) 887.
  infinite sets of global invariants $K[\omega]$, $M[u]$, $S[v]$.
  $W \rightarrow$ minimum.
- J.W. Edenstrasser et al; Phys. Fluids 26 (1983) 500.
  $\delta K_0 = 0$, $\nabla p = \vec{j} \times \vec{B} \rightarrow W$ minimum. $\rightarrow$
- J. D. Jukes, • H. Oshiyama, • T. Tsukada et al. ----

Three unsophisticated questions ;

(I) Why do we obtain the same result of $\mu_0 \vec{j} = \lambda_0 \vec{B}$, starting from the two different global invariants K_0 and K_χ ?

(II) Why do we obtain the mininum-energy state of $\mu_0 \vec{j} = \lambda_0 \vec{B}$ which does not satisfy the experimental boundary condition of $\vec{j} = 0$ at the wall ?

(III) Are all the infinite set of global invariants $K[w]$, $M[u]$, and $S[v]$ new mutually independent, physically available, fundamental invariants ?

logical structure of the Taylor's theory on the minimum-energy state.

< 1st step > ideal MHD timescale $\Delta t(\mathrm{IMHD})$

$$(\text{initial state}) \to \overset{\text{vertual displacement}}{\vec{\xi}} \to (\text{final state})$$

local helicity $\Delta K_0^i = \Delta K_0^f$

< local invariant >

$\Downarrow$

global $K_0^i = K_0^f$

< global invariant >

< 2nd step > quasi-ideal MHD timescale $\Delta t(\mathrm{QIMHD})$.

slightly resistive. reconnection of field lines.

local $\Delta K_0^i \neq \Delta K_0^f$

global $K_0^i = K_0^f$ (conjecture)

< 3rd step > minimization of mag. energy W_m

under the global constraint $K_0^f = \text{const.}$

$\to \delta K_0^f = 0.$

$$\Rightarrow \delta W_m + \lambda_0 \delta K_0^f = 0 \quad \Rightarrow \mu_0 \vec{j} = \lambda_0 \vec{B}.$$

Kadomtsev's model

2nd step global $K_\chi^{\,i} = K_\chi^{\,f}$

3rd step $\delta W_m + \lambda_0 \delta K_\chi^f = 0 \rightarrow \mu_0 \vec{j} = \lambda_0 \vec{B}$.

Question (I) ? (K_0, K_χ $\rightarrow \mu_0 \vec{j} = \lambda_0 \vec{B}$).

a common root

* Generalized fundamental global invariant

< 1st step > Δt (IMHD)

initial $\longrightarrow \vec{\xi} \longrightarrow$ final

local

poloidal flux $\psi^i = \psi^f$

toroidal flux $\phi^i = \phi^f$

between two neighbouring surface $\left\{ \begin{array}{l} d\psi^i = d\psi^f \\ d\phi^i = d\phi^f \end{array} \right.$

$\Big\}$ local invariants

$\Downarrow$ combinations of the local invariants

mutually independent local invariants

$d\psi$, $d\phi$, $\psi d\psi$, $\phi d\psi$, $\psi d\phi$, $\phi d\phi$, $\psi\phi d\psi$, $\psi\phi d\phi$, $d\phi d\psi$, $\psi d\psi d\phi$, -----

- higher order combinations $\longrightarrow$ poorer constancy

ex. $(\psi + \Delta\psi)/\psi = 1 + (\Delta\psi/\psi)$.

$(\psi + \Delta\psi)^2/\psi^2 = 1 + 2(\Delta\psi/\psi) + (\Delta\psi/\psi)^2$

- ex. $\psi^\alpha d\phi$ — dependent $\rightarrow \psi d\phi$

global invariant up to the 2nd order combination

$$\rightarrow K = \frac{1}{\mu_0}\int(a_1\psi d\phi + a_2\phi d\psi + a_3\psi d\psi + a_4\phi d\phi + a_5 d\psi + a_6 d\phi) \quad \text{— (1)}$$

(generalized fundamental global invariant)

$(a_1, \cdots, a_6)$: constants

* $K \supset K_0, K_\chi$

cylindrical model by Kadomtsev

$$\rightarrow \quad K_0 = \frac{1}{\mu_0}\int_{V_0}\vec{A}\cdot\vec{B}\,dV = \frac{2\pi R}{\mu_0}\int(\phi d\psi - \psi d\phi)$$

$$K_\chi = \frac{1}{\mu_0}\int(\psi - \alpha\phi)d\phi \quad : \alpha \equiv \frac{1}{R q_s} \, . \, q_s \equiv \frac{m}{n}.$$

$$\Rightarrow \begin{cases} K_0: & a_1 = -2\pi R,\; a_2 = 2\pi R,\; a_3 = a_4 = a_5 = a_6 = 0 \\ K_\chi: & a_1 = 1,\; a_4 = -\alpha,\; a_2 = a_3 = a_5 = a_6 = 0 \end{cases}$$

< 2nd step > Δt(QIMHD)

local $\quad \psi^i \neq \psi^f, \; \phi^i \underset{\neq}{=} \phi^f, \; d\psi^i \neq d\psi^f, \; d\phi^i \underset{\neq}{=} d\phi^f$

global $\quad K^i = K^f$ (conjecture)

< 3rd step > minimization of W_m subject to

$K^f = \text{const} \rightarrow \delta K^f = 0 \rightarrow \delta W_m + \lambda\,\delta K^f = 0$

using the cylindrical model by Kadomtsev

$$\underset{\text{Euler-Lagrange eqs.}}{\Longrightarrow} \quad \mu_0\vec{j} = \lambda_0\vec{B}\,, \qquad \lambda_0 \equiv \lambda(a_1 - a_2) \quad \text{— (2)}$$

arbitrary set of constants $(a_1, \cdots, a_6)$

$\Rightarrow$ minimum mag. energy state $\mu_0 \vec{j} = \lambda_0 \vec{B}$.

• $K \supset \left\{ \begin{array}{l} \text{global invariants on mag. fluxes} \\ \text{for various types of relaxation process} \end{array} \right.$

Question (II) ? ($\vec{j} = 0$ at the wall)

< 2nd step >

✓ implicit assumption of $\underbrace{\text{slightly plasma}}$ resistive
in whole area inside the wall in Δt (QIMHD).

resistivity η of plasma $\to \infty$ near the wall
because of the plasma-wall interaction

$\Rightarrow$ slightly resistive MHD timescale Δt (RMHD)
(more realistic definition)

in Δt (RMHD)

$\psi, \phi, d\psi, d\phi$ near the wall

$\to \left\{ \begin{array}{l} \text{are no longer conserved.} \\ \text{do not contribute to the global invariant.} \end{array} \right.$
because of resistive decay.

ex.

$$\frac{dK_0}{dt} = \left(-2\int_{V_0} \eta \vec{j} \cdot \vec{B} \, dV + \phi_W V_\zeta - \psi_W V_\theta \right) / 2\mu_0$$

$\eta \to \infty$ near the wall.

global $K_f^i \Rightarrow K_f^f$ with contribution functions $f_{\eta i}(\psi, \phi)$

where

$$K_f^f = \frac{1}{\mu_0}\int \left(\underline{f_{\eta 1}} a_1 \psi d\phi + \underline{f_{\eta 2}} a_2 \phi d\psi + \underline{f_{\eta 3}} a_3 \psi d\psi + \underline{f_{\eta 4}} a_4 \phi d\phi + \underline{f_{\eta 5}} a_5 d\psi + \underline{f_{\eta 6}} a_6 d\phi \right) \quad \text{— (3)}$$

boundary conditions on $f_{\eta i}$ $(i = 1, \cdots, 6)$

a thin but a finite layer of plasma-wall interaction just inside the wall

$$\rightarrow \quad f_{\eta i} = \frac{\partial f_{\eta i}}{\partial \psi} = \frac{\partial f_{\eta i}}{\partial \phi} = 0 \quad \text{at the wall} \quad \text{—(4)}$$

$$f_{\eta i} = 1 \quad \text{at the mag. axis} \quad \text{—(5)}$$

<3rd step>

minimization of W_m subject to $K_f^f = \text{const.}$

$(\delta K_f^f = 0)$

$$\Rightarrow \quad \delta W_m + \lambda_0 \delta K_f^f = 0$$

$$\Rightarrow \quad \mu_0 \vec{j} = \lambda^R(\psi, \phi) \vec{B} \quad \text{—(6)}$$

(Euler-Lagrange eqs.)

where

$$\lambda^R(\psi, \phi) = \lambda_0 \left\{ a_1 \left(f_{\eta 1} + \psi \frac{\partial f_{\eta 1}}{\partial \psi} \right) - a_2 \left(f_{\eta 2} + \phi \frac{\partial f_{\eta 2}}{\partial \phi} \right) - a_3 \psi \frac{\partial f_{\eta 3}}{\partial \phi} + a_4 \phi \frac{\partial f_{\eta 4}}{\partial \psi} - a_5 \frac{\partial f_{\eta 5}}{\partial \phi} + a_6 \frac{\partial f_{\eta 6}}{\partial \psi} \right\} \quad \text{—(7)}$$

(4)(5) → (6)(7)

$\Rightarrow$ { $\vec{j} = 0$ at the wall } is satisfied naturally!

Question (III) ? ($K[\omega]$, $M[u]$, $S[v]$)

< 1st step > in Δt(IMHD)

$$\left.\begin{array}{llll} \text{local} & \text{integrated} & \text{helicity} & dK = \int_V \vec{A}\cdot\vec{B}\,dV/\mu_0 \\ \text{"} & \text{"} & \text{mass} & dM = \int \rho\,dV \\ \text{"} & \text{"} & \text{entropy} & dS = \int s\,dV \end{array}\right\} \begin{array}{l}\text{between}\\ \text{two}\\ \text{mag.}\\ \text{surfaces}\end{array}$$

are all local invariants.

$$\rightarrow \left.\begin{array}{l} \omega(\psi,\phi)\,dK = \int \omega(\psi,\phi)\,\vec{A}\cdot\vec{B}\,dV/\mu_0 \\ u(\psi,\phi)\,dM = \int u(\psi,\phi)\,\rho\,dV \\ v(\psi,\phi)\,dS = \int v(\psi,\phi)\,s\,dV \end{array}\right\} \begin{array}{l}\text{local}\\ \text{invariants}\end{array}$$

$\because$ $\psi, \phi \rightarrow$ local invariants and const. on mag. surfaces

$$\Rightarrow \left.\begin{array}{l} K[\omega] = \frac{1}{\mu_0}\int_{V_0} \omega(\psi,\phi)\,\vec{A}\cdot\vec{B}\,dV \\ M[u] = \int u(\psi,\phi)\,\rho\,dV \\ S[v] = \int v(\psi,\phi)\,s\,dV \end{array}\right\} \begin{array}{l}\text{global invariants}\\ \text{in } \underline{\Delta t\text{(IMHD)}}\end{array}$$

$\Updownarrow$ < analogous arguments >

if independent quantities X and Y $\rightarrow$ invariants

then infinite set of $X^\alpha Y^\beta$ and/or $\omega(X,Y)$

$\Rightarrow$ invariants

Are they all <u>new mutually independent</u>, <u>fundamental</u>, <u>physically available invariants ?</u>

(X, Y, XY)

< 2nd step >

* higher order combinations $\longrightarrow$ poorer constancy

* $$\left.\begin{array}{l} K[w] \\ M[u] \\ S[v] \end{array}\right\} \xrightarrow{\text{dependent invariants on}} \left\{\begin{array}{l} K_0\,[w \equiv 1] \\ M_0\,[u \equiv 1] \\ S_0\,[v \equiv 1] \end{array}\right.$$

∘ in Δt (RMHD)

$$\begin{array}{ccccc} & & \text{constancy} & \text{wall effects} & \\ K[\omega] & < & K_0 & \longrightarrow & K_f^f \\ M[u] & < & M_0 & \longrightarrow & M_f^f \\ S[v] & < & S_0 & \longrightarrow & S_f^f \end{array} \left.\vphantom{\begin{array}{c}a\\a\\a\\a\end{array}}\right\} \text{with contribution functions } f$$

↳ not independent fundamental global invariants against K_0, M_0, S_0.

< 3rd step >

Bhattacharjee et al.

$$\delta W - \sum_{\alpha} \lambda_\alpha \delta K[w_\alpha] - \sum_{\alpha} \mu_\alpha \delta M[u_\alpha] - \sum_{\alpha} T_\alpha \delta S[v_\alpha] = 0.$$

$\alpha = 0, 1, 2, \cdots\cdots$ including K_0, M_0, S_0.

physically reasonable ?

or available ?

Energy Principle for Different Timescales

• in Δt(IMHD)

local constraint on mass (L.C.M.)

" " on entropy (L.C.E.)

" " on mag. fluxes (L.C.MG)

$\Rightarrow$ Kruskal & Kulsrud $\delta W = 0 \rightarrow \nabla p = \vec{j} \times \vec{B}$

Bernstein et al. $\delta^2 W > 0 \rightarrow$ ideal MHD stability

By <u>relaxing</u> the strongest constraints of the <u>three local constraints</u> <u>step by step</u> <u>to</u> <u>global constraints</u>

$\rightarrow$ • Δt(RMHD) for slightly resistive MHD timescale

L.C.MG $\longrightarrow$ global constraint on mag. fluxes (G.C.MG)

L.C.M $\dashrightarrow$ L.C.M.

L.C.E $\dashrightarrow$ L.C.E.

minimization of $W = \int \left(\frac{B^2}{2\mu_0} + \frac{p}{\gamma - 1} \right) dV$ subject to (G.C.MG), (L.C.M), (L.C.E.)

$$\Rightarrow \quad \vec{j} = \frac{\lambda^R(\psi)}{\mu_0} \vec{B} + \frac{\nabla\theta \times \nabla p}{\vec{B} \cdot \nabla\theta}$$

Euler-Lagrange eqs. equilibrium state

Partially Relaxed State (P.R.S.)

→ o $\Delta t(Tu)$ for turbulent plasma timescale

G.C.MG ---→ G.C.MG

L.C.M. ⟶ G.C.M.

L.C.E. ⟶ G.C.E. global.

$$\delta W = 0 \Rightarrow \vec{j} = \frac{\lambda^{tu}(\psi)}{\mu_0}\vec{B} + \frac{\nabla\theta \times \nabla P}{\vec{B}\cdot\nabla\theta}$$

(P.R.S.)

→ o $\Delta t(Tr)$ for plasma transport timescale

(G.C.MG.), (G.C.M.), (G.C.E.)

and in MHD equilibrium state in the sence of time average (semilocal constraint)

$$\left(\vec{j} = \frac{\lambda^{X}(\psi)}{\mu_0}\vec{B} + \frac{\nabla\theta \times \nabla P}{\vec{B}\cdot\nabla\theta}, \quad X = R \text{ or } tu \right)$$

$$\delta W = 0 \Rightarrow \vec{j} = \frac{\lambda^{tr}(\psi)}{\mu_0}\vec{B} + \frac{\nabla\theta \times \nabla P}{\vec{B}\cdot\nabla\theta}$$

$\left.\begin{array}{l} p = nkT \\ \rho = mn \end{array}\right)$ $T = T_{ax} f_s^{tr}(\psi)$ $f_s^{tr}(\psi)$: contribution function on entropy.

$$\rho = (kT_{ax} f_s^{tr}/m)^{\gamma-1} \exp\left(\frac{\gamma}{\gamma-1} - \frac{m\chi f_m^{tr}}{kT_{ax} f_s^{tr}}\right).$$

$$p = (kT_{ax} f_s^{tr}/m)^{\gamma} \exp\left(\frac{\gamma}{\gamma-1} - \frac{m\chi f_m^{tr}}{kT_{ax} f_s^{tr}}\right).$$

$f_m^{tr}(\psi)$: contribution function on mass.

relaxation by the helical tearing mode with single helicity ($q_s = m/n$) [Kadomtsev].

$\rightarrow \quad f_\eta(\chi) \sim \chi/\chi_0 \quad \begin{cases} \chi = 0 & \text{at the wall} \\ \chi = \chi_0 & \text{: mag. axis} \end{cases}$

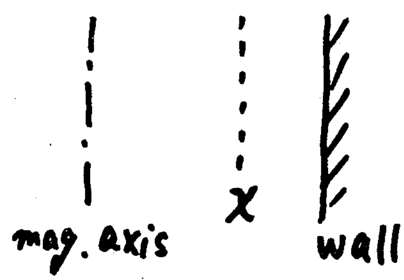

larger $\chi \Rightarrow \{ f_\eta(\chi) \rightarrow 1 \}$

$$\Rightarrow \quad \lambda^R(\chi) = \lambda_0 \, \chi/\chi_0$$

PRSM. $\quad \vec{j} = \dfrac{\lambda^R(\chi)}{\mu_0} \vec{B} + \dfrac{\nabla\theta \times \nabla P}{\vec{B} \cdot \nabla\theta}$

numerical procedure $\rightarrow$ ref. 1
(cylindrical approximation).

Suydam criterion [in Δt(IMHD)].
$\rightarrow$ finite β

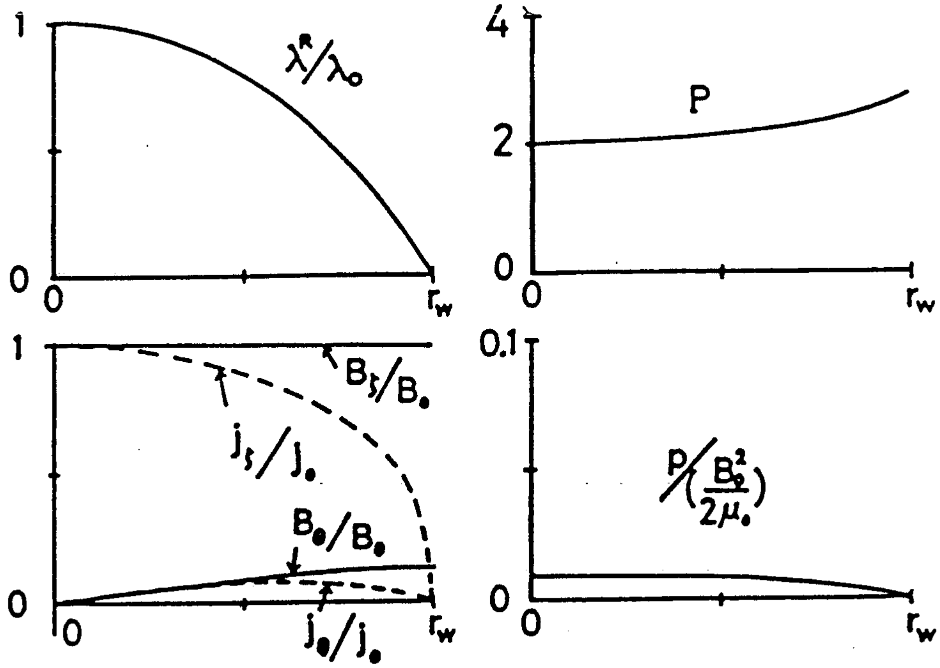

Fig.1 A typical numerical result of Tokamak-like equilibria stable with respect to the Suydam criterion. $\lambda_0 r_w$ = 0.34. q_s = m/n = 1/1. β_{ax}(at the magnetic axis) = 0.008.

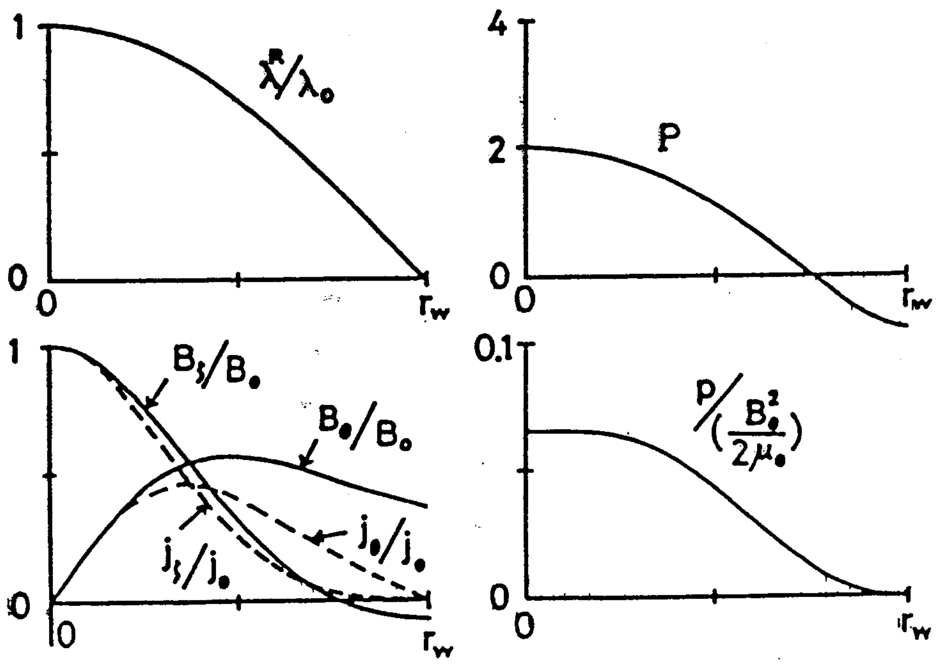

Fig.2 A typical numerical result of RFP equilibria stable with respect to the Suydam criterion. $\lambda_0 r_w$ = 4.16. q_s = 1/10. β_{ax} = 0.067.

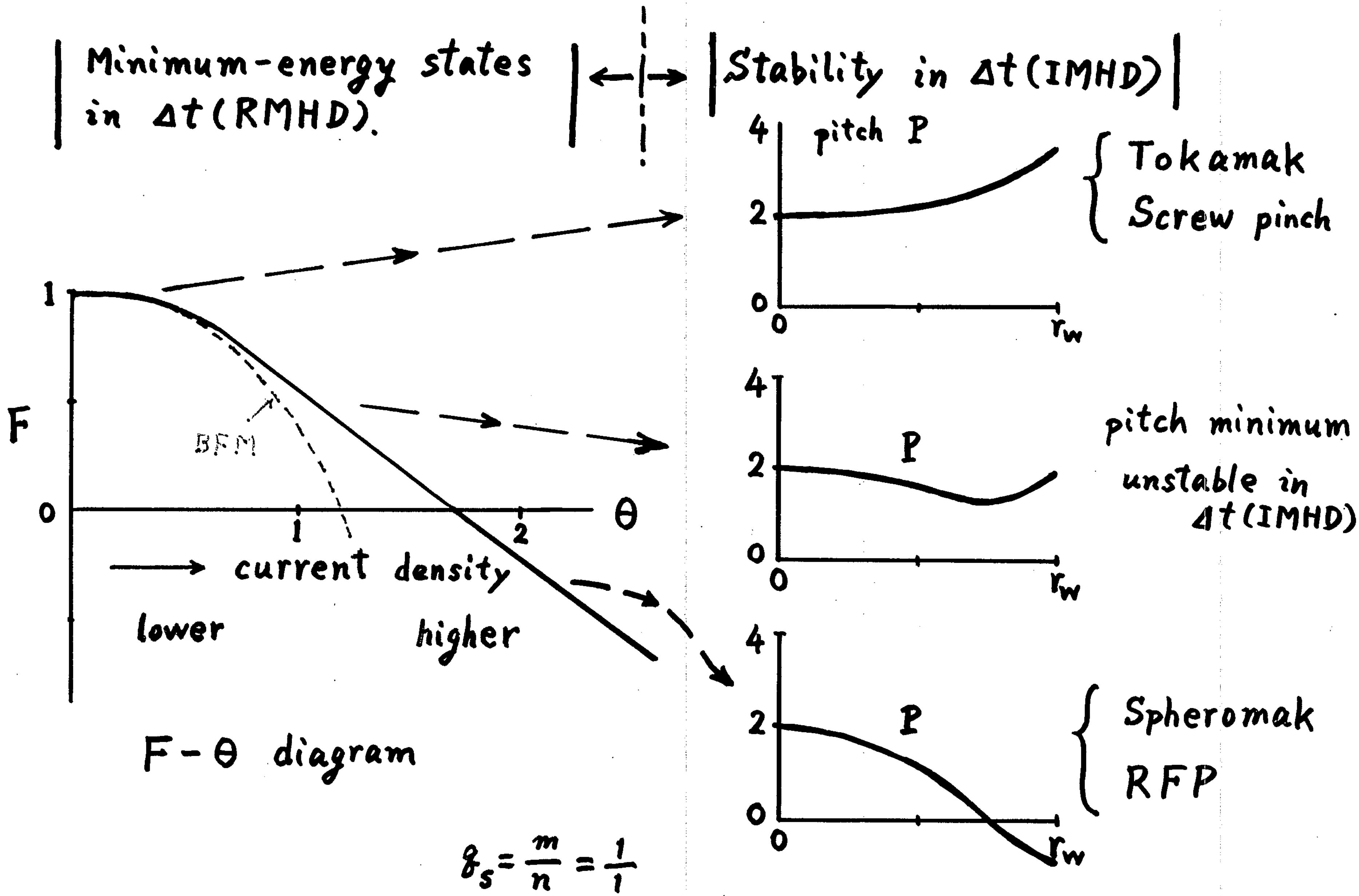
Minimum-energy states in Δt(RMHD).
Stability in Δt(IMHD)
F
1
0
Θ
1
2
BFM
current density
lower
higher
F-Θ diagram
$q_s = \frac{m}{n} = \frac{1}{1}$
pitch P
4
2
0
0
r_w
Tokamak
Screw pinch
P
pitch minimum
unstable in Δt(IMHD)
P
Spheromak
RFP

• marginally Suydam stable

PRSM(I) : $\bar{\lambda}(\psi) = \lambda_0[1-(\psi_0-\psi/\psi_0)^2]$

PRSM(II) : $\bar{\lambda}(\psi) = \lambda_0[1-(\psi_0-\psi/\psi_0)^4]$

PRSM(III) : $\bar{\lambda}(\psi) = \lambda_0$

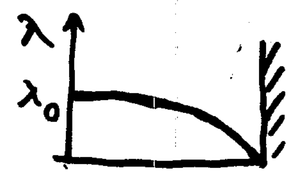

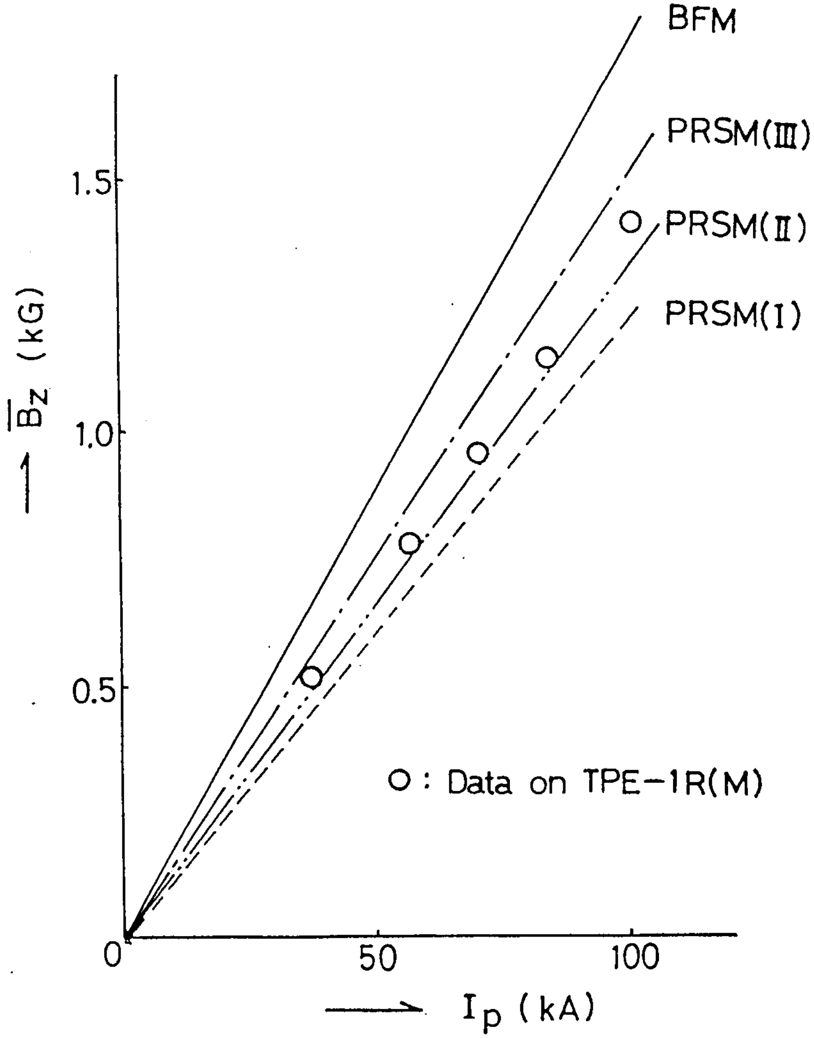

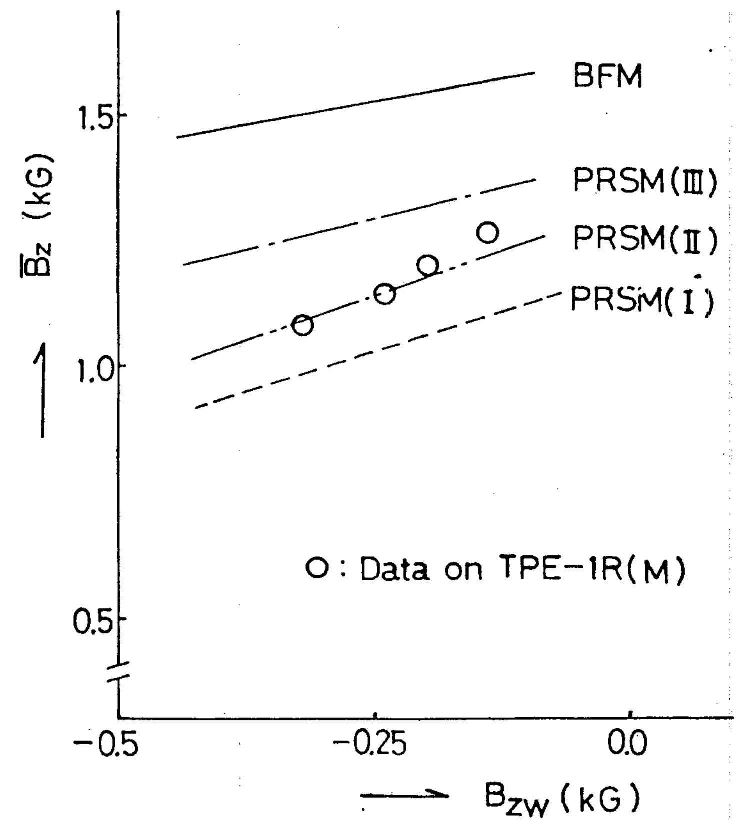

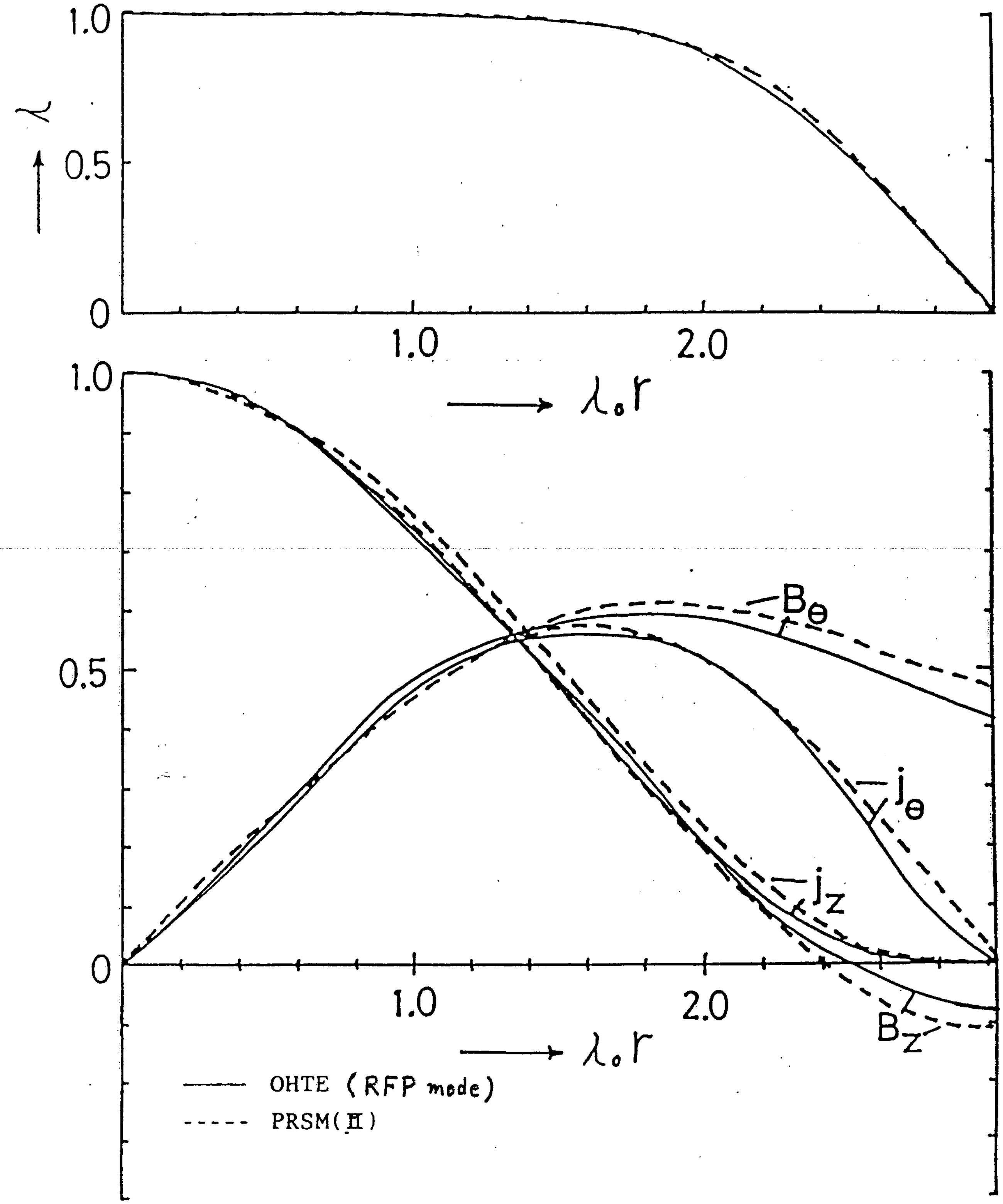

comparison between OHTE and PRSM(II).

o marginally stable with respect to the Suydam criterion.

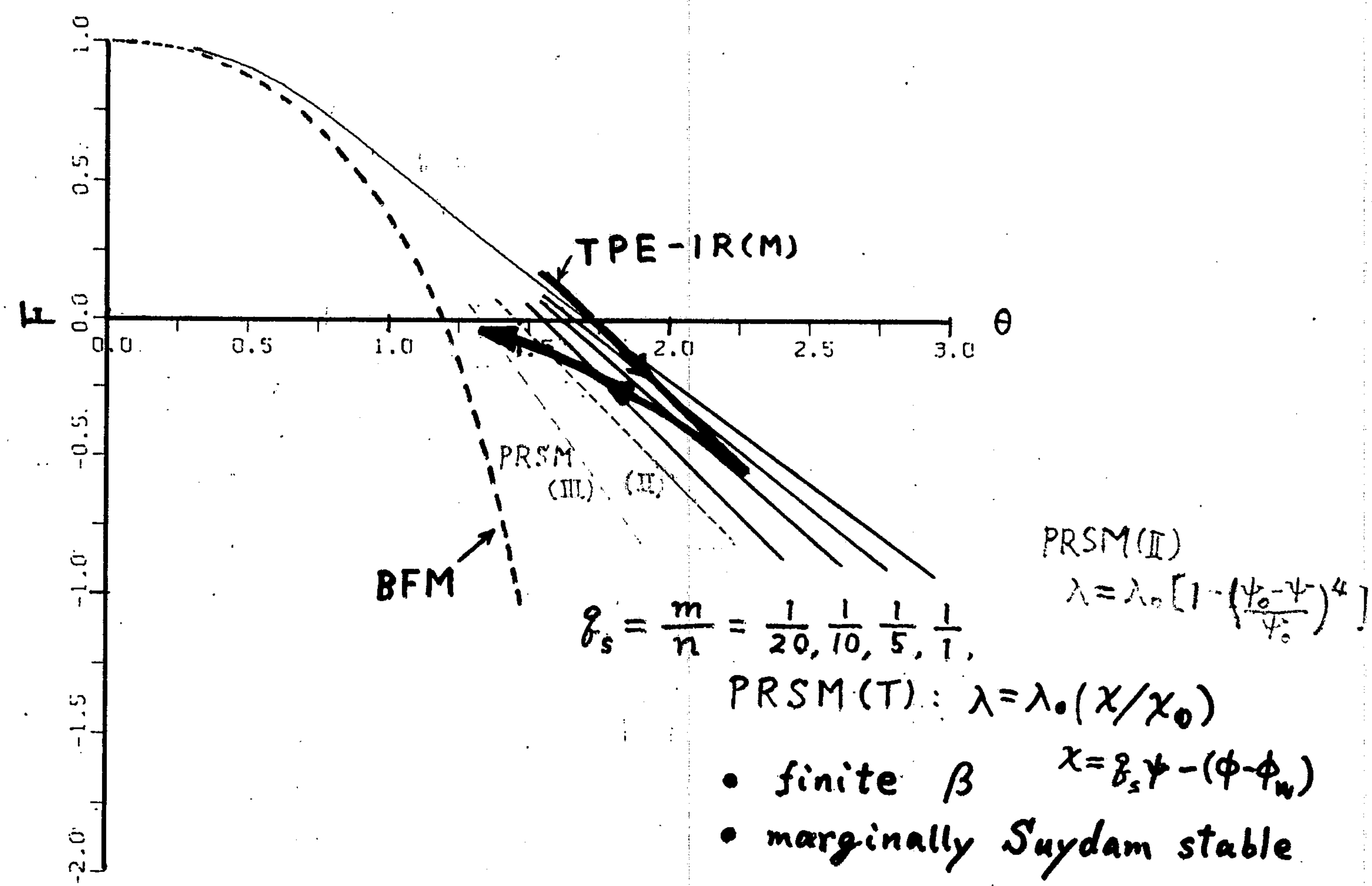

F-THETA DIAGRAM

Conclusions

(1) The generalized fundamental global invariant K includes both the two global invariants, K_0 by Taylor and K_χ by Kadomtsev.

(2) The minimum-magnetic-energy state under the generalized global invariant K is proved to become the same state of $\mu_0 \mathbf{j} = \lambda_0 \mathbf{B}$.

(3) When the plasma-wall interaction is taken into account in the global constraints on magnetic fluxes, the resultant minimum-energy state is proved to satisfy naturally the experimental boundary condition of $\mathbf{j} = 0$ at the wall.

(4) Energy principles for three timescales of $\Delta t(\mathrm{RMHD})$, $\Delta t(\mathrm{Tu})$, and $\Delta t(\mathrm{Tr})$ lead to the same vector form of equilibrium equations used in the partially relaxed state model (PRSM).

(5) Numerical results by the PRSM agree fairly well with experimental data on the two typical RFP experiments.

It should be noted that the present theory of energy principles is available not only to the RFP plasma but also to the plasma in the Tokamak and other toroidal devices.

SPHEROMAK AND MAGNETIC RECONNECTION

T. HAYASHI

HIROSHIMA UNIVERSITY

Spheromak and Magnetic Reconnection

T. Hayashi and T. Sato
(Hiroshima Univ.)

Reconnection in spheromak { formation, relaxation, instability

1. Tilting Instability
   Magnetic Reconnection
   (simulation
   (experiment (Princeton S-1, proto S-1/C , Movie)

2. Relaxation
   $n = 2, 3, 4$
   (simulation
   (experiment

formation

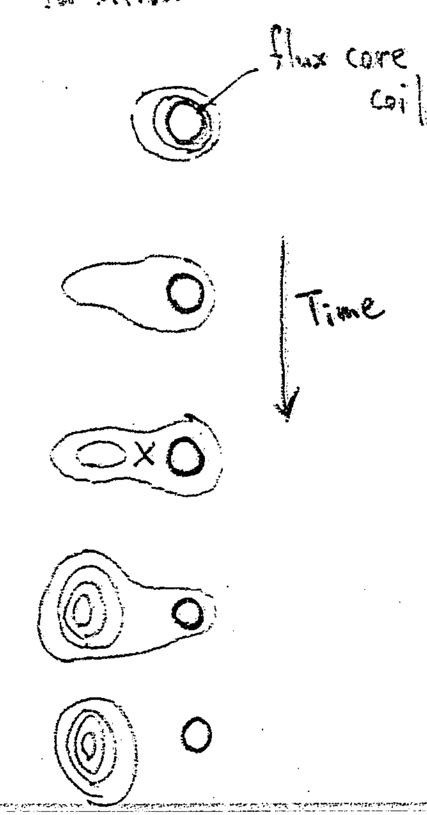

Simulation #84T0310

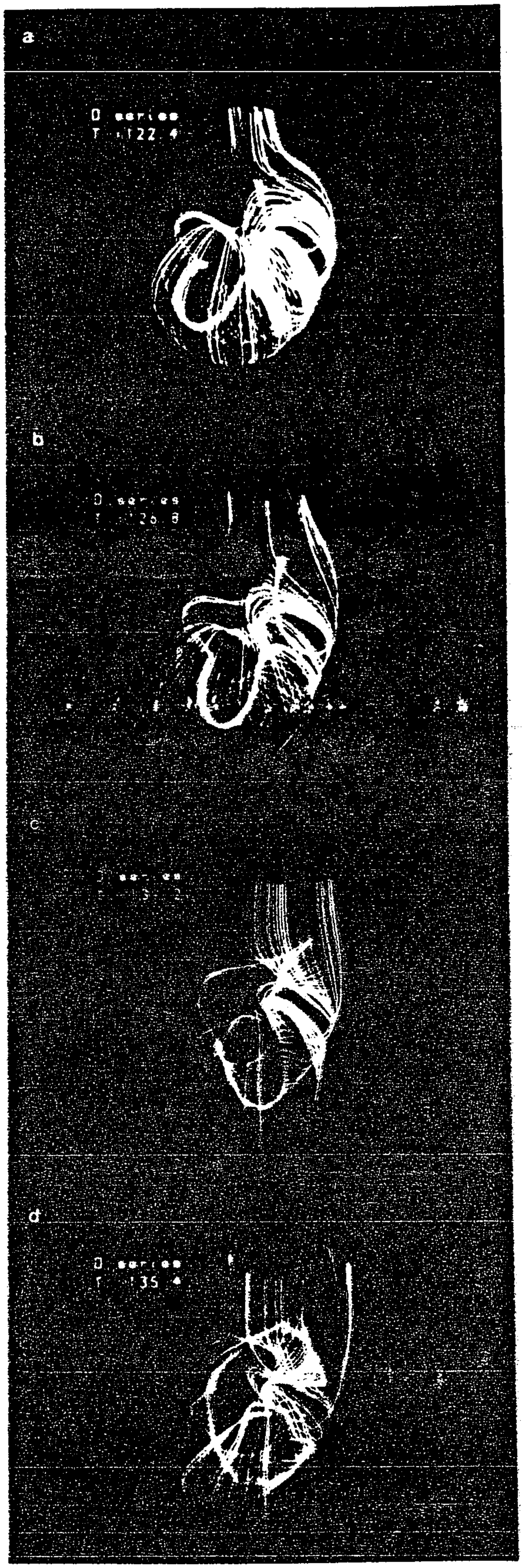

Experiment #84T0309

(a) T=28

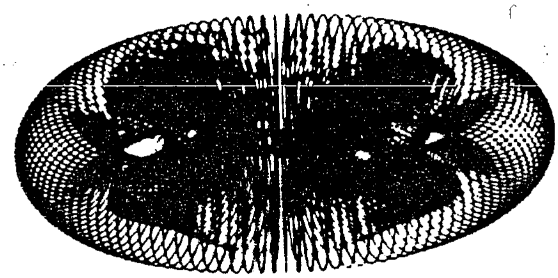

(b) T=40

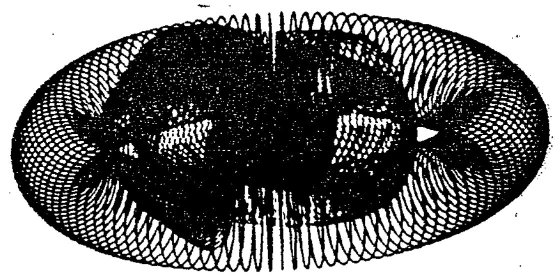

(c) T=56

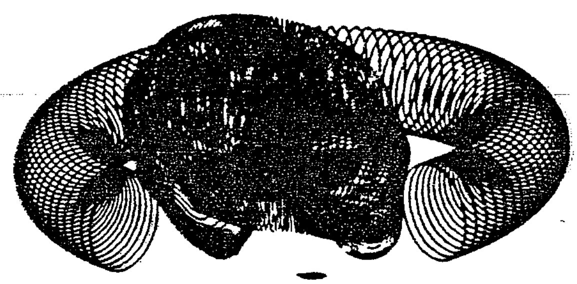

(d) T=64

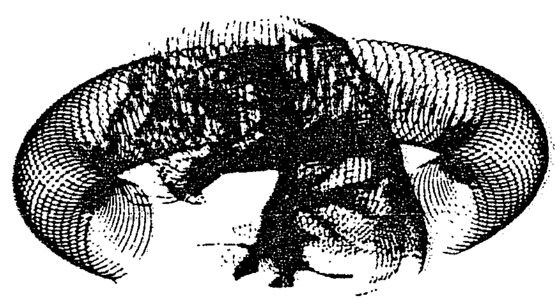

(e) T=72

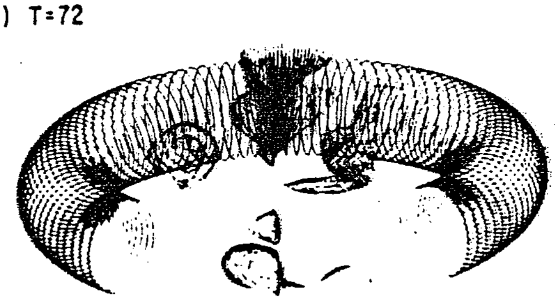

experimental method

Proto S-1/C

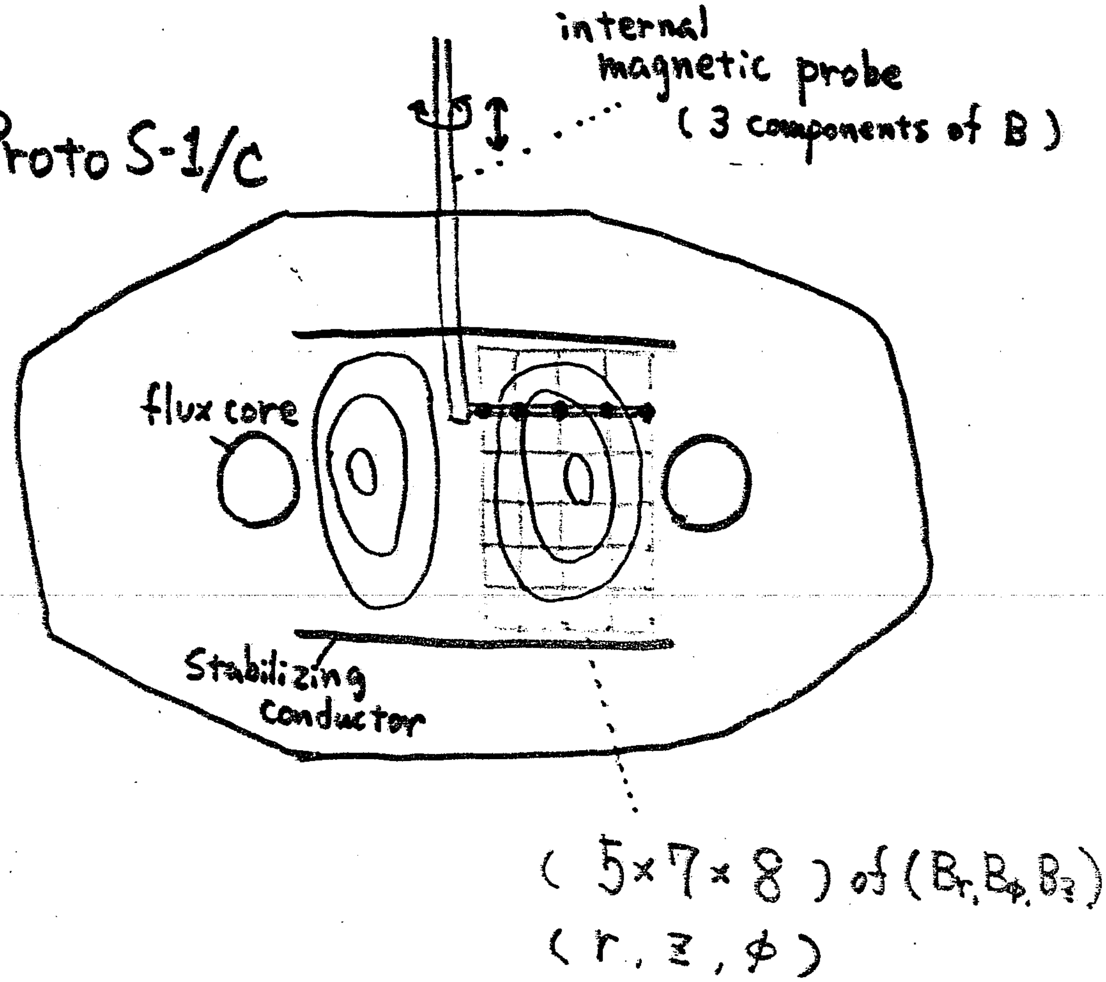

movie (slide)

Contours of magnitude of B_t

750~800 G

550~700 G

(formation stage
~
tilting instability stage

293

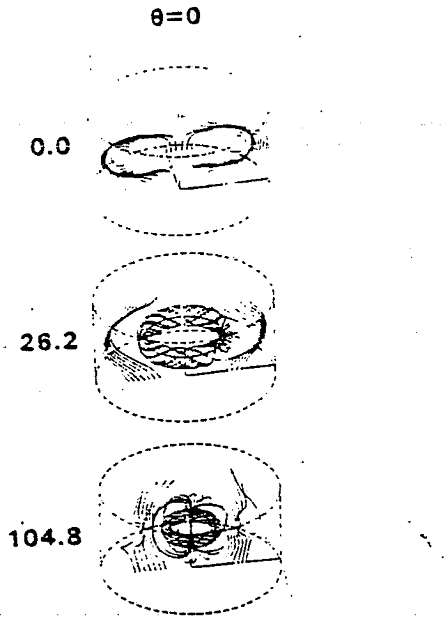

FIG. 2. Magnetic field line trajectories in formation stage of spheromak.

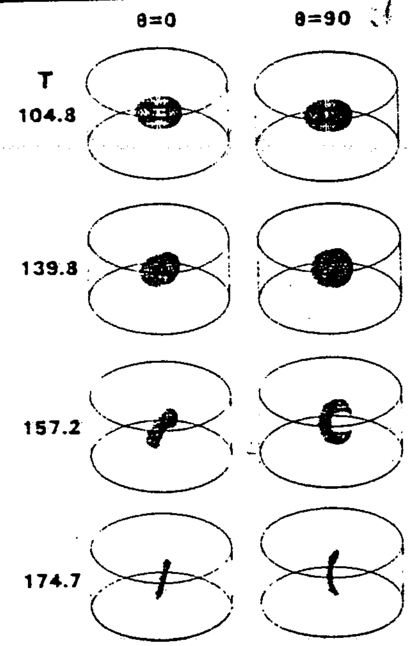

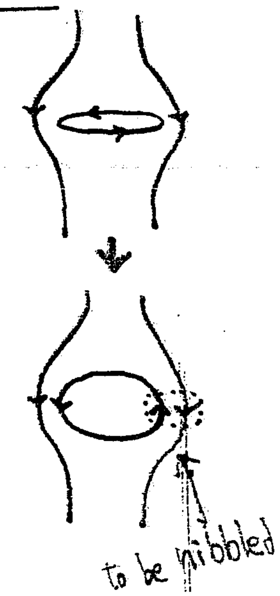

FIG. 3. A three-dimensional display of spheromak tilting and disruption. Plotted are the contours of the azimuthal component ($B_\theta = 1$ kG). The left column is the view seen from the direction of the tilt axis ($\theta = 0$) and the right one is the view from $\theta = 90°$. Note the asymmetric deformation.

$\psi_p{}^c = -0.3 + 0.5 \sin(\pi T/44)$ Wb where T is normalized by the Alfvén transit time τ_A which is approximately 2.3 μsec and r is the radial distance of a core surface point. We note, however, that ψ_p is so programmed that the toroidal-flux core current is crowbarred at -100 kA once it reduces to -100 kA (the crowbar time was roughly $35\tau_A$ in our case). The wall of the vacuum vessel is assumed to be a conductor so that the perpendicular magnetic field component is fixed at the wall. The simulation domain (r, θ, z) is divided into $37 \times 16 \times 37$ meshes.

First, we show the formation stage of the spheromak. Figure 2 shows some field line trajectories at three different times. It is seen that a thin closed magnetic surface (torus) formed just inside the flux core develops into a fat torus (spheromak) with a gradual movement of the magnetic axis toward the central axis. The formation is completed at about $90\tau_A$ and the created spheromak keeps its shape thereafter. We have continued the run until $140\tau_A$ but it is found that its shape is maintained without any appreciable change. This indicates that the numerical diffusion time is much longer than $50\tau_A$.

With this success in creating a spheromak, we then go on to study the tilting instability. We have applied a small $n = 1$ tilting perturbation at $T = 105$. With intent to see the dynamic behavior of the spheromak in response to the perturbation,

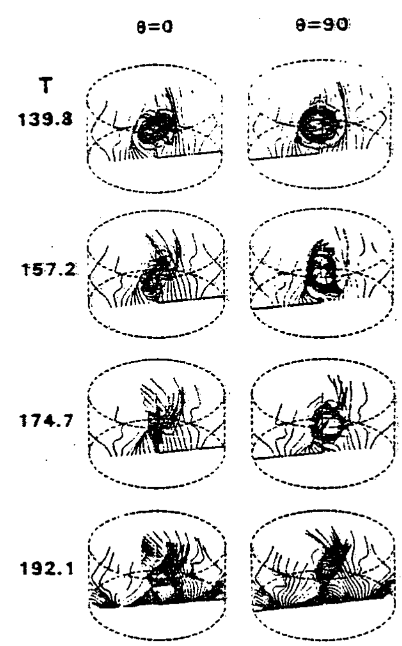

FIG. 4. Magnetic field line trajectories in tilting stage seen from $\theta = 0$ (left) and $\theta = 90°$ (right). Note reconnection of the spheromak field with the vertical field.

#84T0311

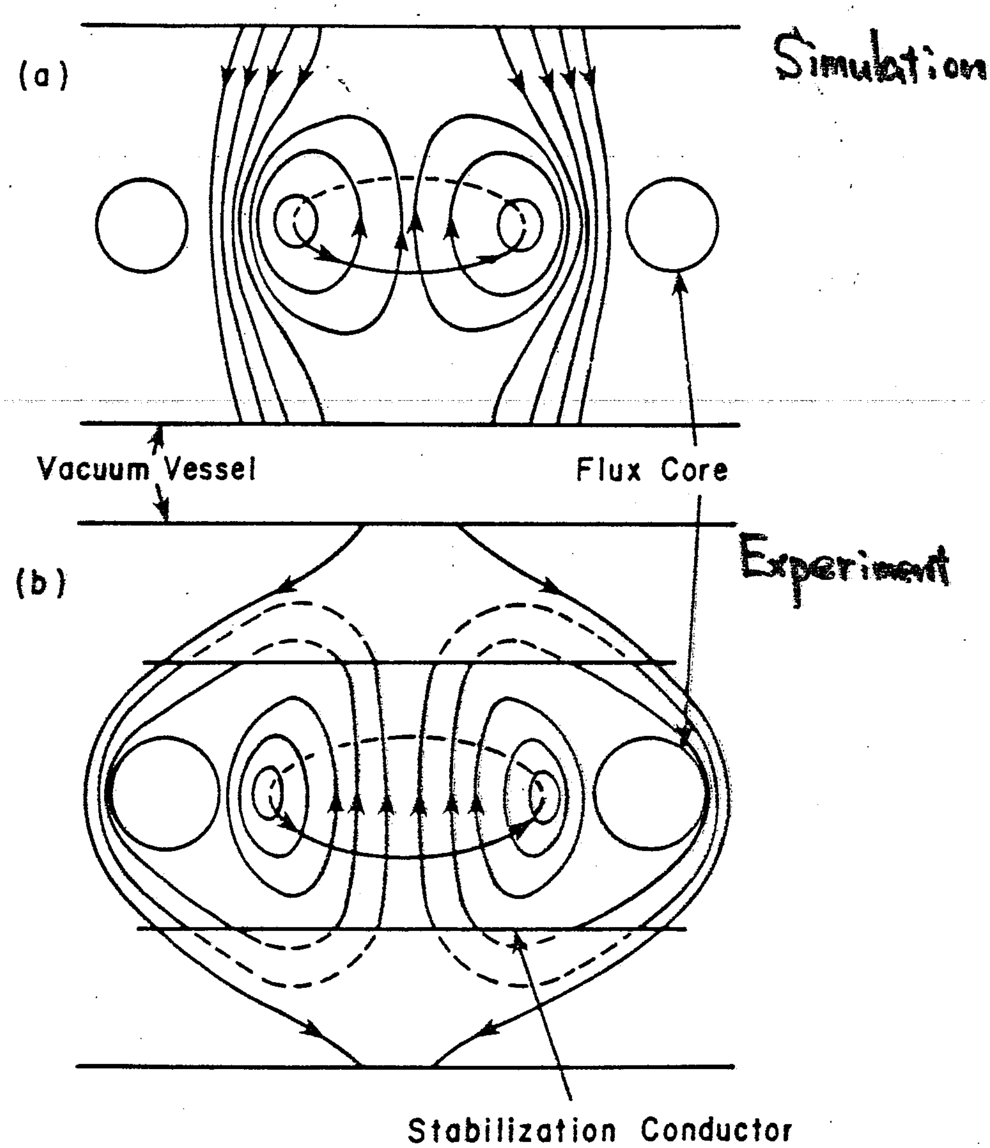
Simulation
(a)
Vacuum Vessel
Flux Core
Experiment
(b)
Stabilization Conductor

Magnetic Reconnection

	forced reconnection	Tearing mode
system	open	closed
boundary	B v	(wall)
drive	forced	spontaneous
reconnection rate	boundary condition (indep. of η) $\gg$	internal condition (η)

B v

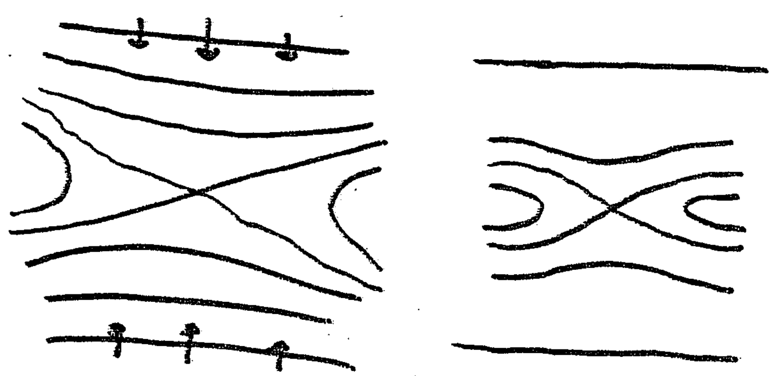

In the tilting case,
the external flow is caused by tilting motion, etc.

$$(\text{S.P.} \quad \dot{\psi} \sim \frac{B_y^{\frac{3}{2}}\, \eta^{\frac{1}{2}}}{\rho^{\frac{1}{4}}\, l^{\frac{1}{2}}})$$

- Order estimation of the reconnection time scale

a minor radius $\quad a \sim 1$

v inflow speed $\quad \langle v \rangle \sim 0.01\ (V_A)$

$B_{\parallel}$ antiparallel component of B $\quad \langle B_{\parallel} \rangle \sim 0.05$

T time scale

$\psi \sim a \langle B_{\parallel} \rangle$

$\dot{\psi} \sim \langle v \rangle \langle B_{\parallel} \rangle \Leftarrow$ forced reconnection

$$T \sim \frac{\psi}{\dot{\psi}} \sim \frac{a}{\langle v \rangle} \sim \frac{1}{0.01}$$

$$\sim 100\ (\tau_A)$$

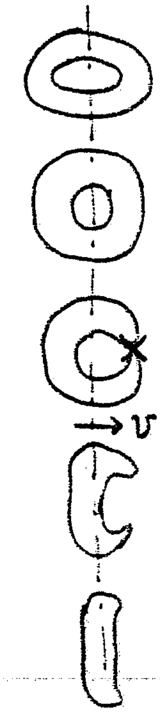

- $S \sim 5000$ (corresponding to Spitzer resistivity with $\sim 20\,eV$)

[$S_{numerical} \sim S$?]

- Estimation of j in current layer

$$j \sim \frac{\langle v \rangle \langle B_{\parallel} \rangle}{\eta} \quad (\eta = \tfrac{1}{S})$$

$\sim 2 \qquad$ cf. $j_{torus} \sim 10$

- $S \sim 50000$, $S \sim 5000$ } Simulation result ↓ Similar Time Scale (However, $S_{numerical}$ might be concealing the physics.)

$S \sim 500$ — decay (shrink) + tilt

Typical Spheromak with a flux hole
(created by numerical simulation)

POLOIDAL ψ_p - - - - -
MAX= 0.21089 MIN= -3.8540E-2
TOROIDAL B_T ——
MAX= 0.89071 MIN= -0.89071
T = 52.40

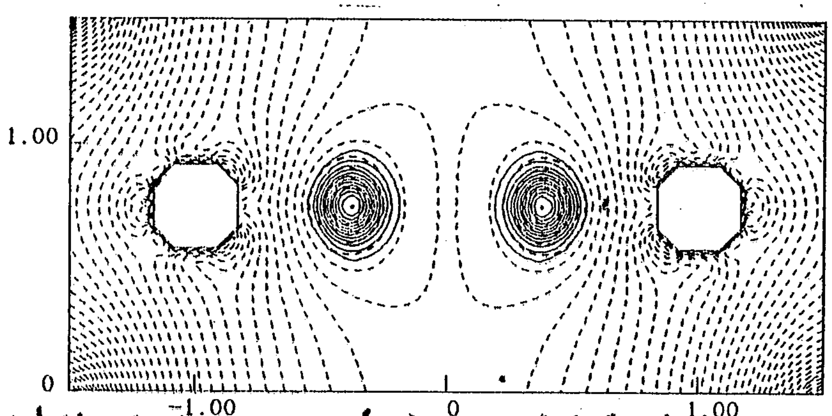

The substantial amount of the toroidal field which was supplied from the flux core is contained in the spheromak.

BPHI, BZ B_T —— B_p - - - - - T = 52.40
MAX= 0.89071 MIN= -2.1073E-2
0,66274 -0.47089

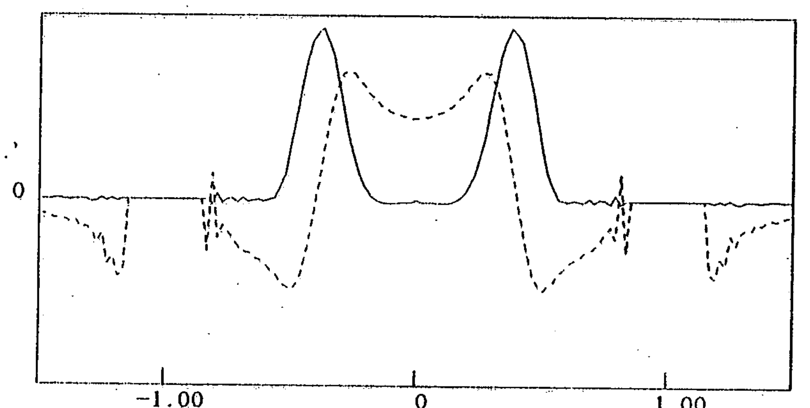

The existence of a flux hole can be clearly seen. It turns out that the aspect ratio R/a is about 2.0 in this example.

J POLOID J_p
T = 52.4043
MAX= 7.2555

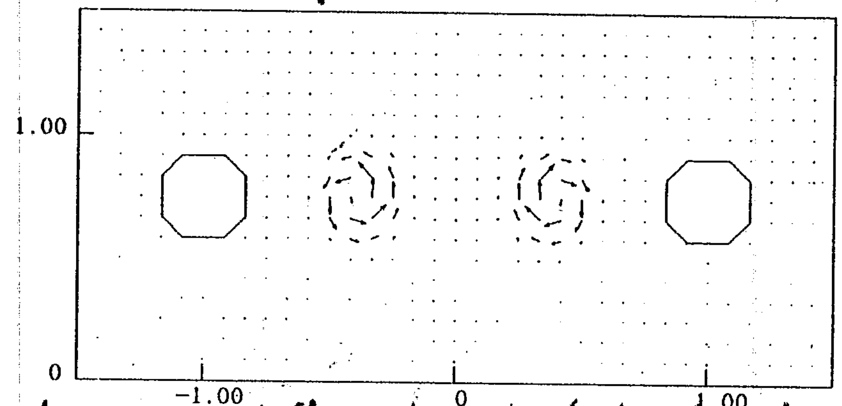

The plasma current flows only inside of the spheromak torus. So a vacuum-like magnetic field is realised outside the torus.

JPHI, JZ J_T —— J_p - - - - - T = 52.40
MAX= 13.436 MIN= -5.3066
8.6739 -6.5245

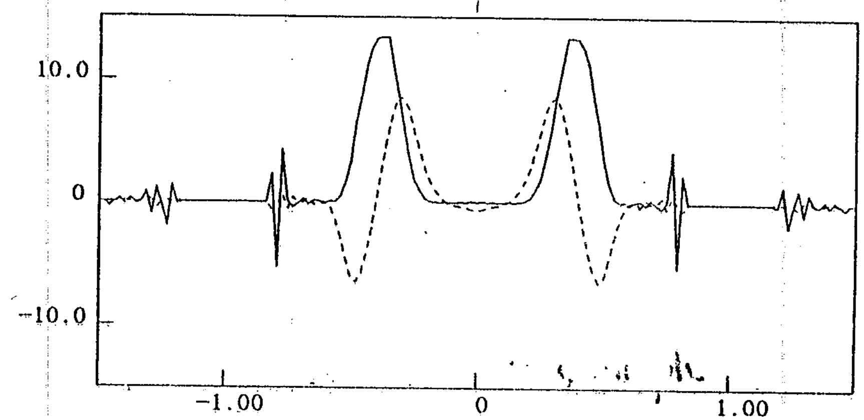

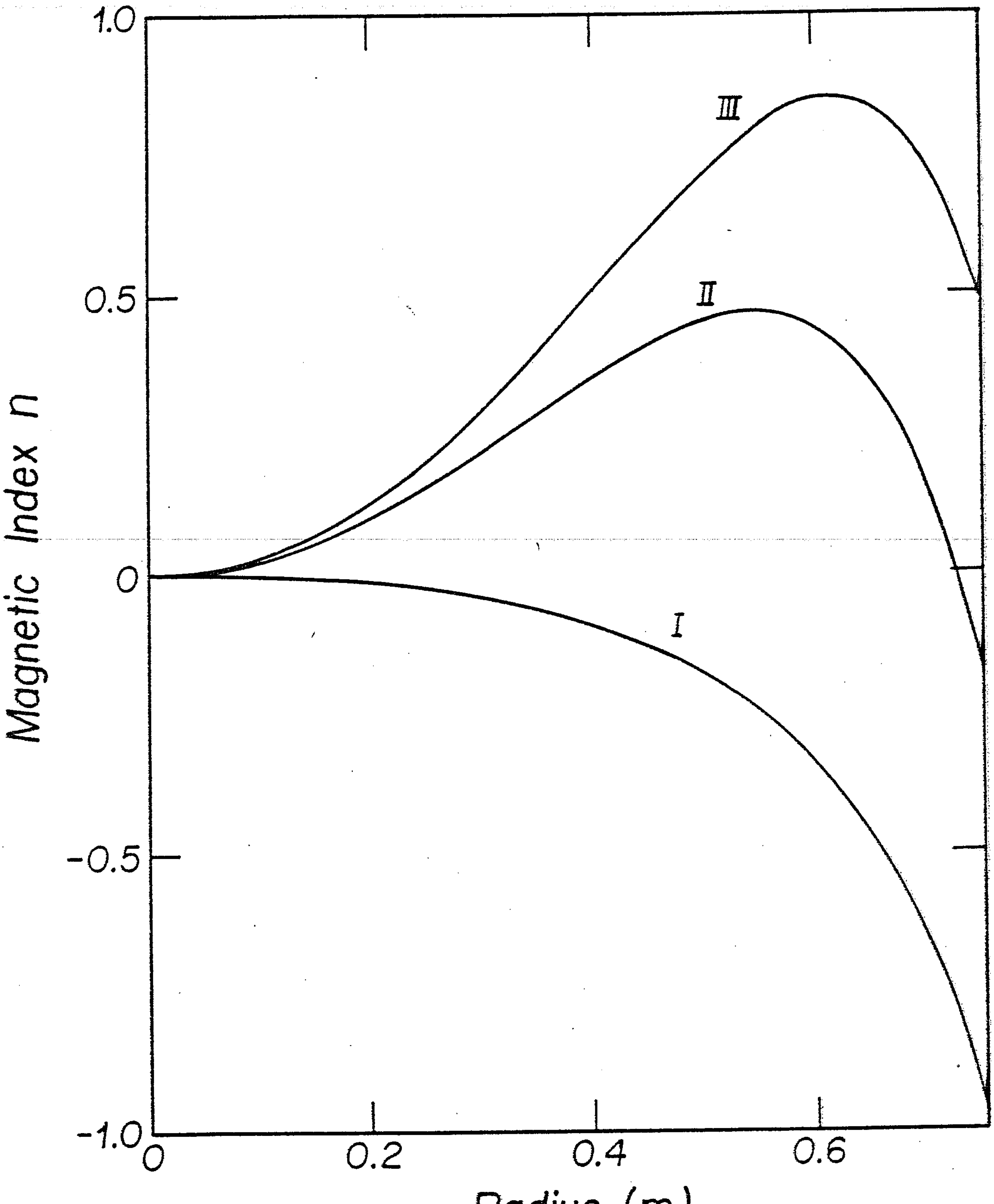

1.0
0.5
0
-0.5
-1.0
Magnetic Index n
III
II
I
0
0.2
0.4
0.6
Radius (m)

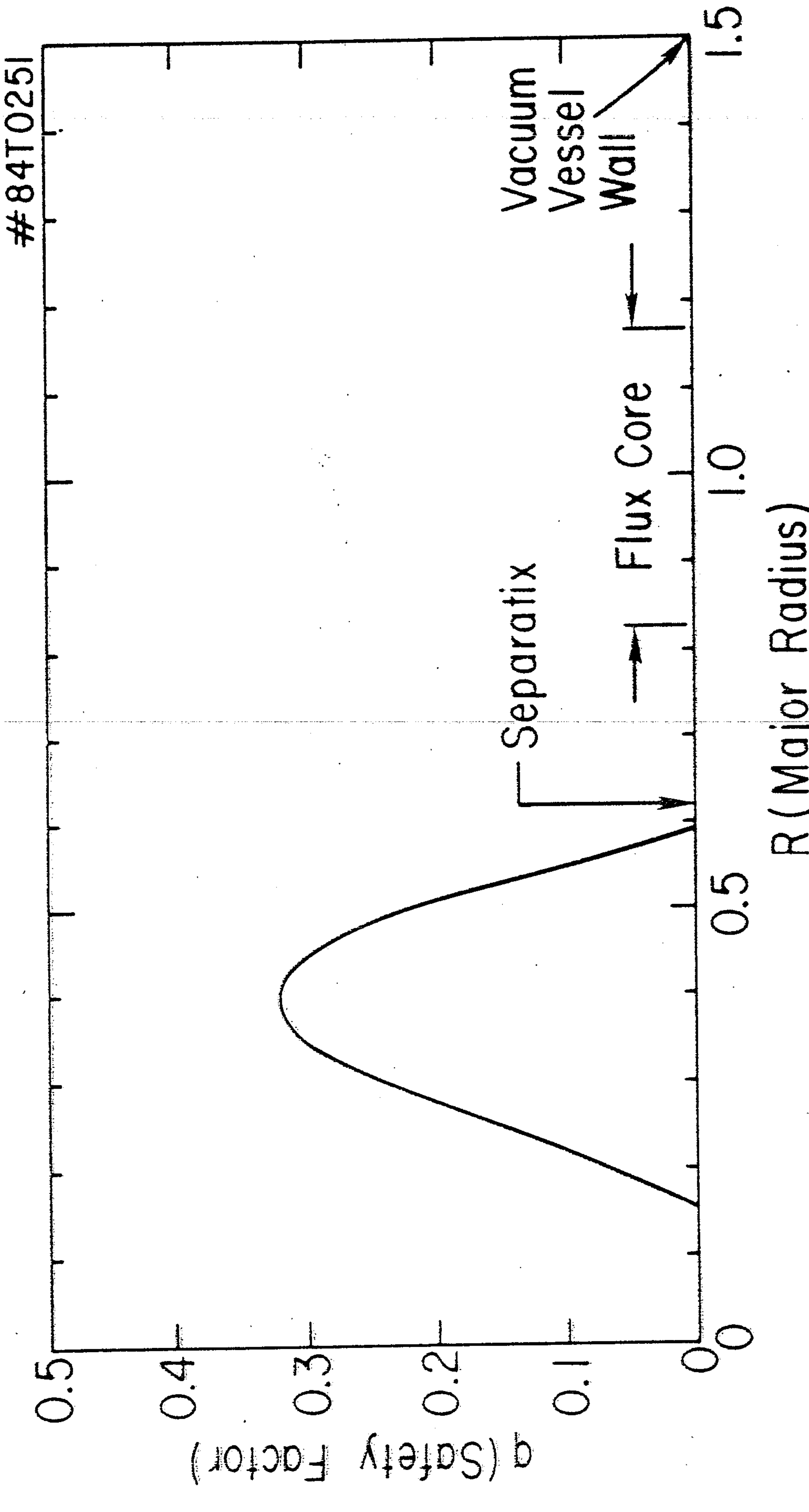
#84T0251
q (Safety Factor)
0.5
0.4
0.3
0.2
0.1
0
0
0.5
1.0
1.5
R (Major Radius)
Separatix
Flux Core
Vacuum
Vessel
Wall

T. Hayashi
ex 3310

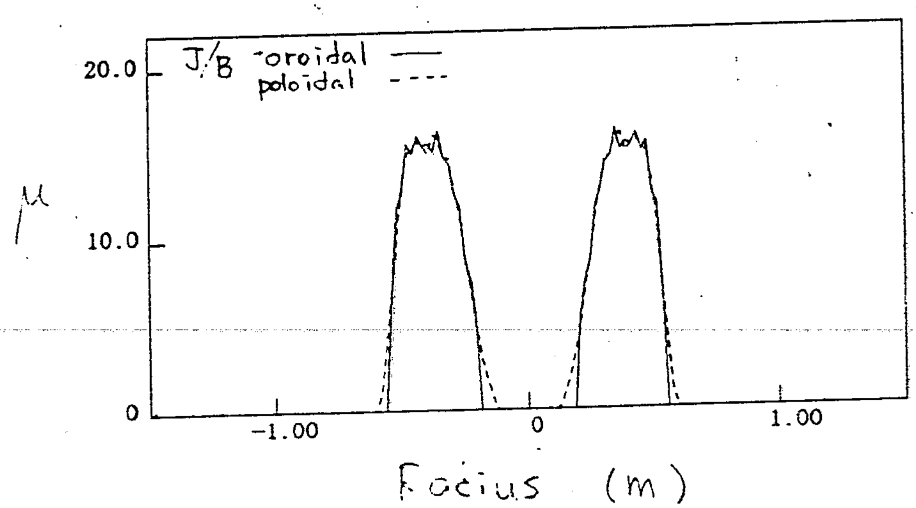

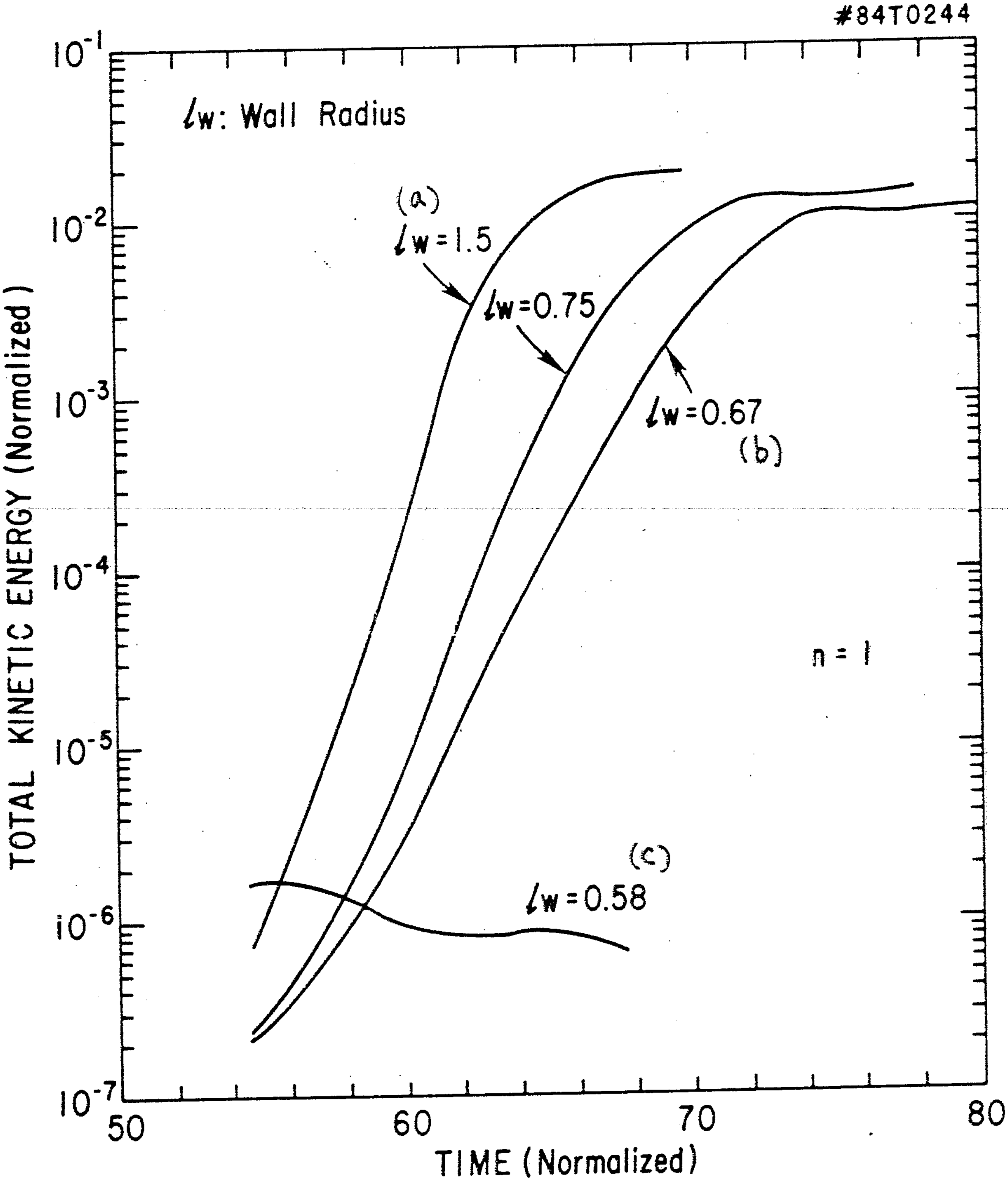
#84T0244
ℓ_w: Wall Radius
(a)
ℓ_w = 1.5
ℓ_w = 0.75
ℓ_w = 0.67
(b)
n = 1
(c)
ℓ_w = 0.58
10^{-1}
10^{-2}
10^{-3}
10^{-4}
10^{-5}
10^{-6}
10^{-7}
50
60
70
80
TIME (Normalized)
TOTAL KINETIC ENERGY (Normalized)

\# 84X1460

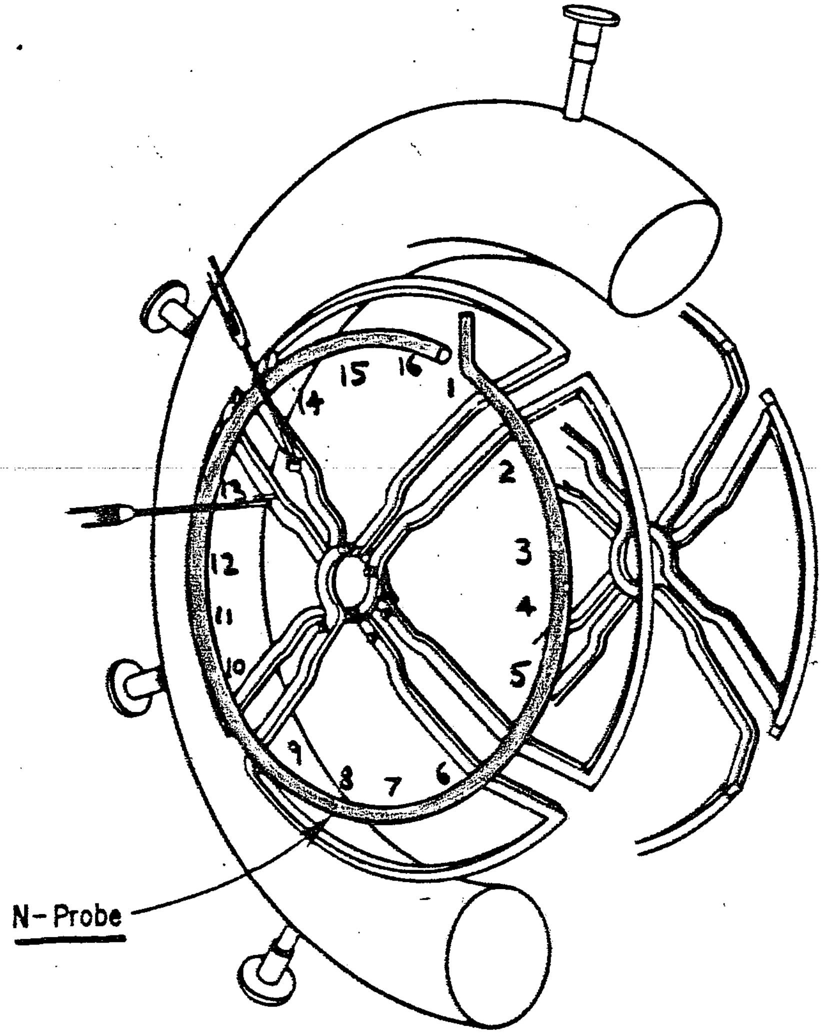

COIL SYSTEM & S-1 FLUX-CORE

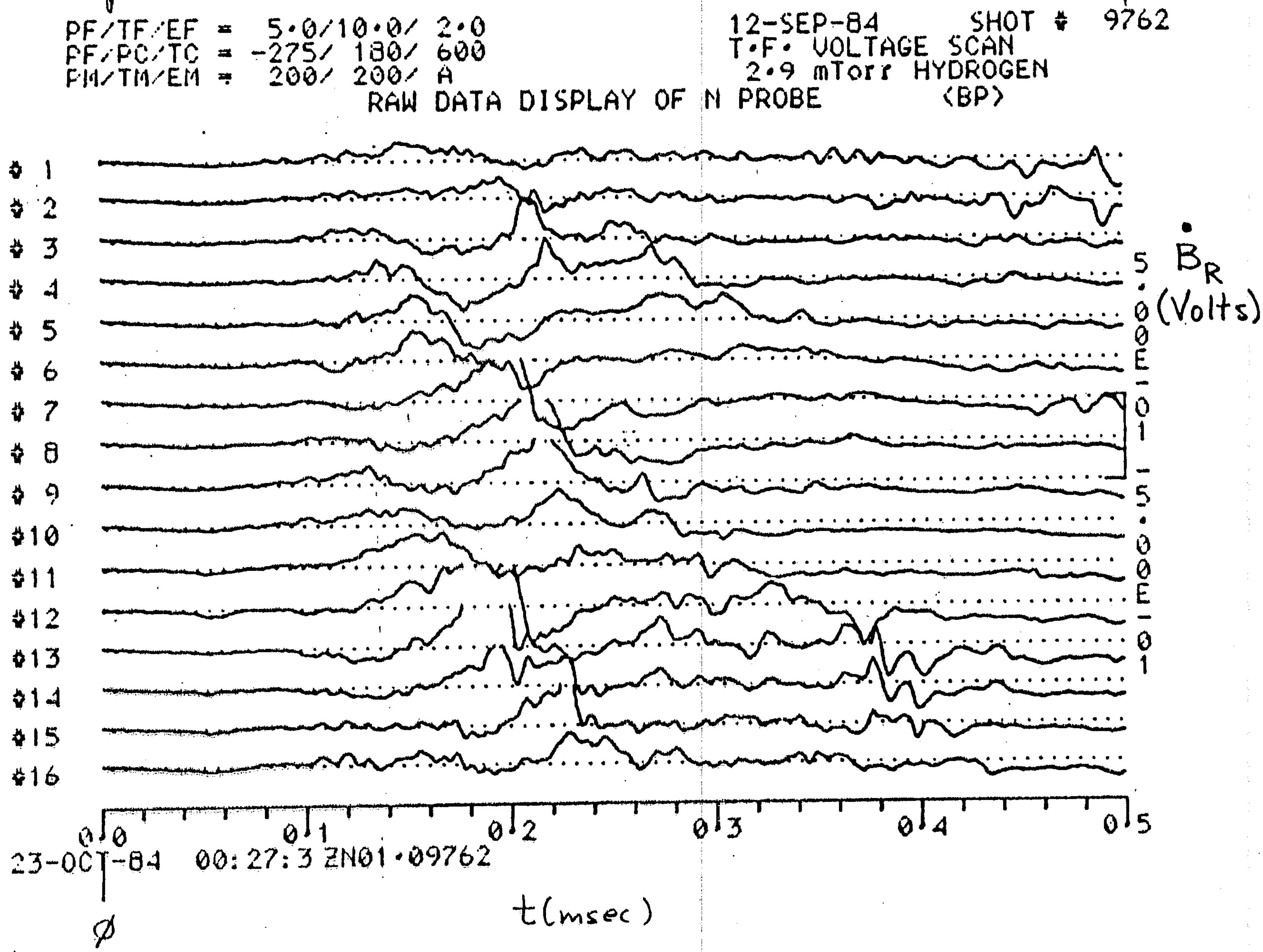
PF/TF/EF = 5·0/10·0/ 2·0
PF/PC/TC = -275/ 180/ 600
FM/TM/EM = 200/ 200/ A
12-SEP-84 SHOT # 9762
T·F· VOLTAGE SCAN
2·9 mTorr HYDROGEN
RAW DATA DISPLAY OF N PROBE <BP>
1
2
3
4
5
6
7
8
9
#10
#11
#12
#13
#14
#15
#16
5·000E-01
5·000E-01
$\dot{B}_R$ (Volts)
0·0
0·1
0·2
0·3
0·4
0·5
23-OCT-84 00:27:3 ZN01·09762
ϕ
t(msec)

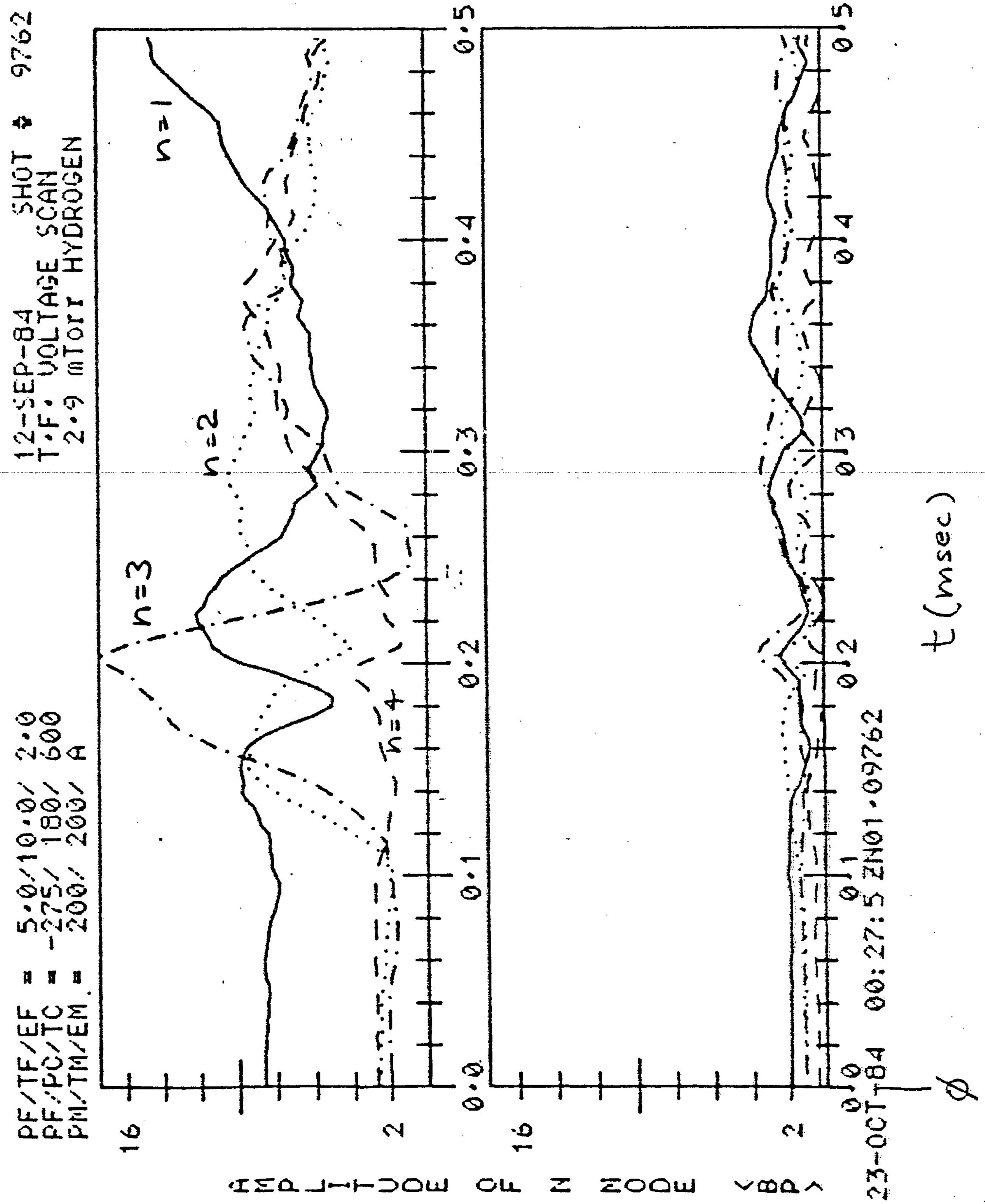
PF/TF/EF = 5.0/10.0/ 2.0
PF/PC/TC = -275/ 180/ 600
PM/TM/EM = 200/ 200/ A
12-SEP-84 SHOT # 9762
T.F. VOLTAGE SCAN
2.9 mTorr HYDROGEN
AMPLITUDE OF N MODE (ARB)
16
2
0.0
0.1
0.2
0.3
0.4
0.5
n=1
n=2
n=3
n=4
23-OCT-84 00:27:5 ZN01.09762
t (msec)

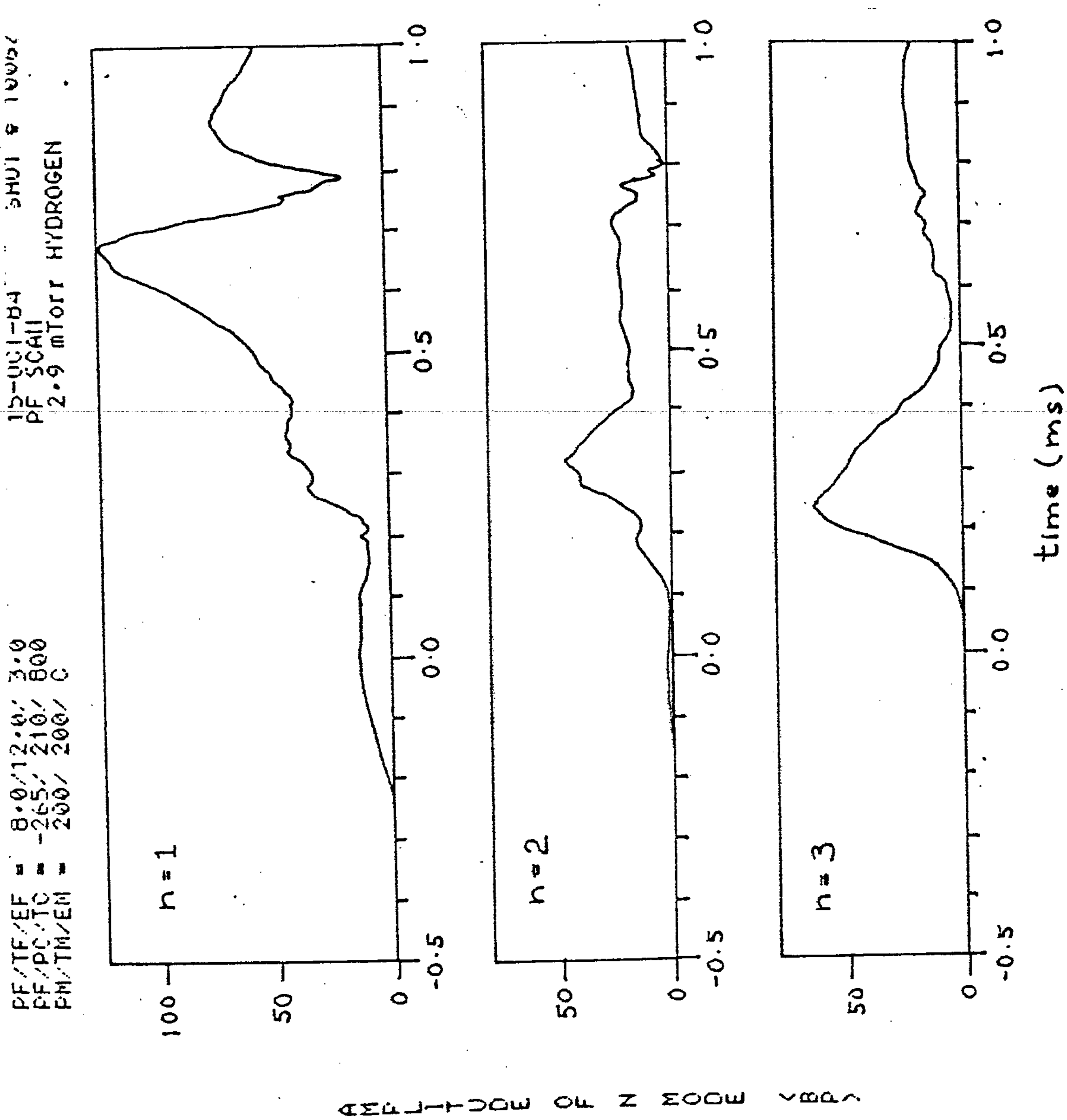
PF SCAN
2.9 mTorr HYDROGEN
n = 1
n = 2
n = 3
time (ms)

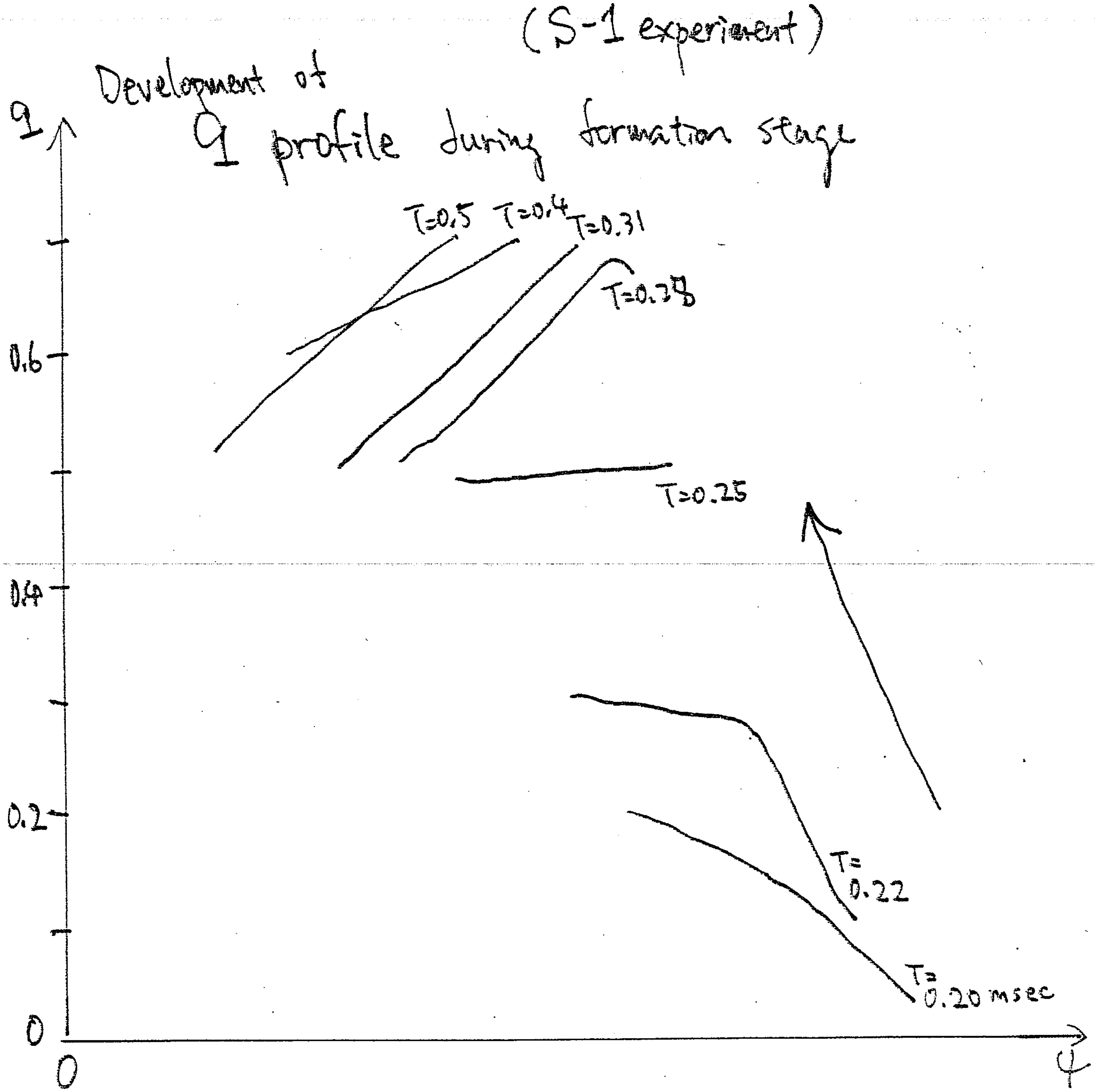
(S-1 experiment)
Development of
q profile during formation stage
q
0.6
0.4
0.2
0
0
ψ
T=0.5
T=0.4
T=0.31
T=0.28
T=0.25
T=
0.22
T=
0.20 msec

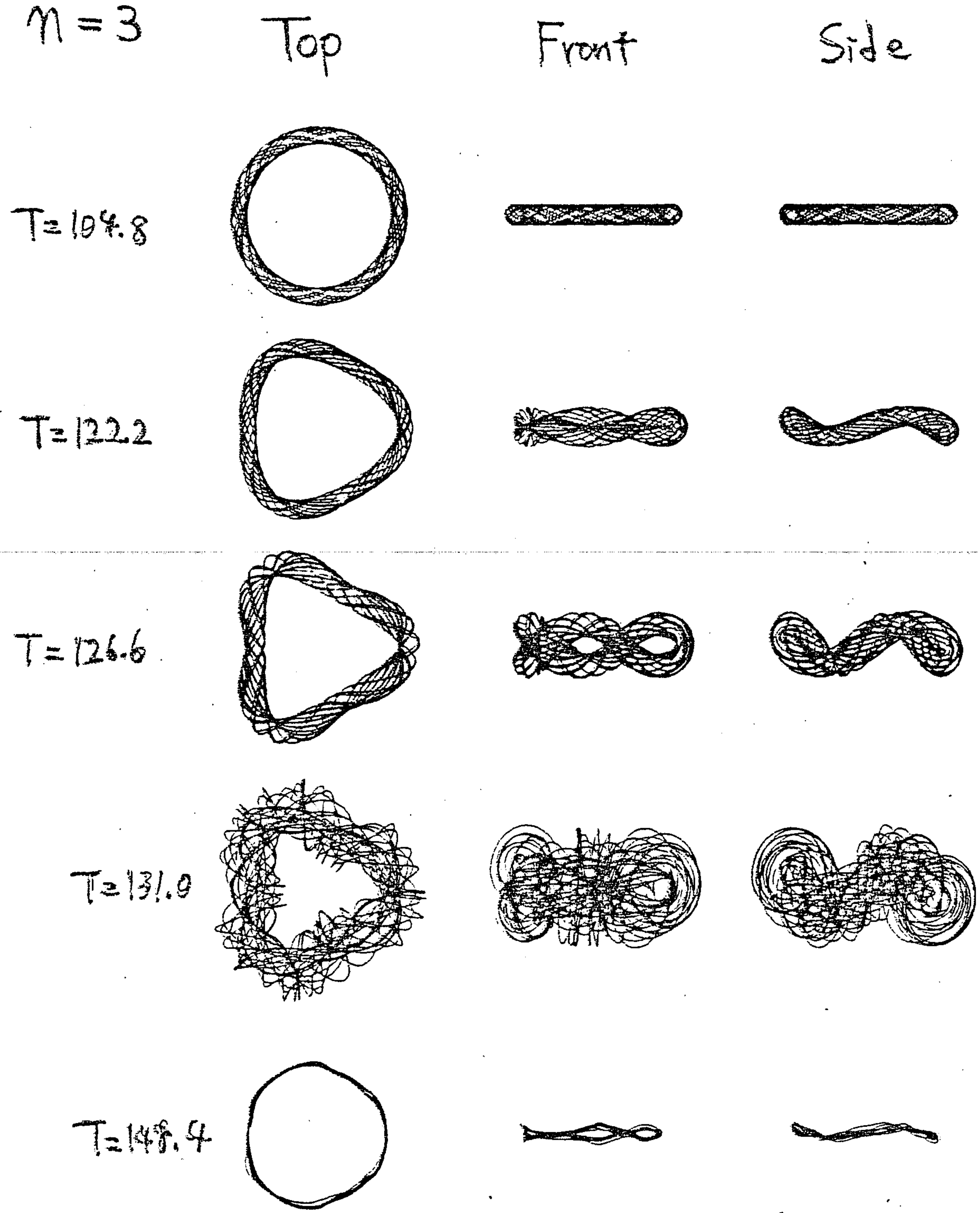
n = 3
Top
Front
Side
T=104.8
T=122.2
T=126.6
T=131.0
T=148.4

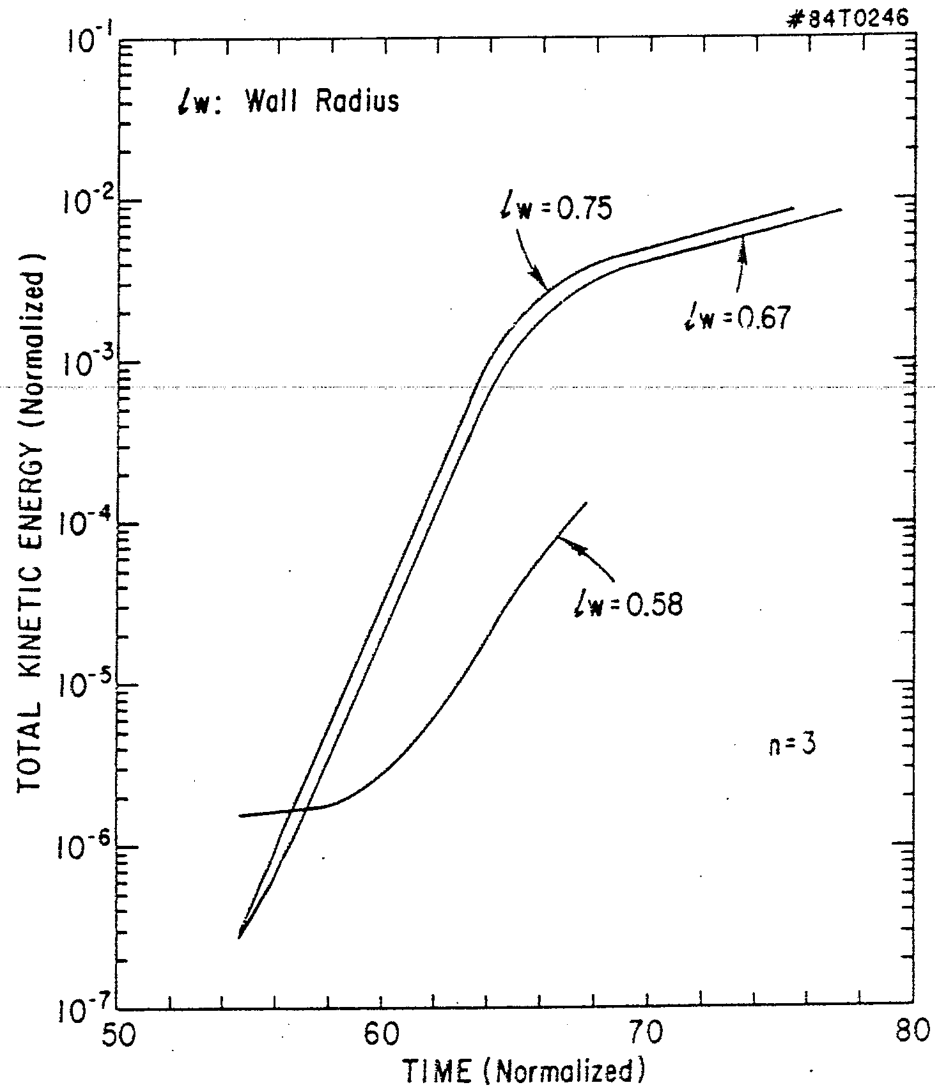
#84T0246
lw: Wall Radius
lw = 0.75
lw = 0.67
lw = 0.58
n=3
TOTAL KINETIC ENERGY (Normalized)
TIME (Normalized)
10^-1
10^-2
10^-3
10^-4
10^-5
10^-6
10^-7
50
60
70
80

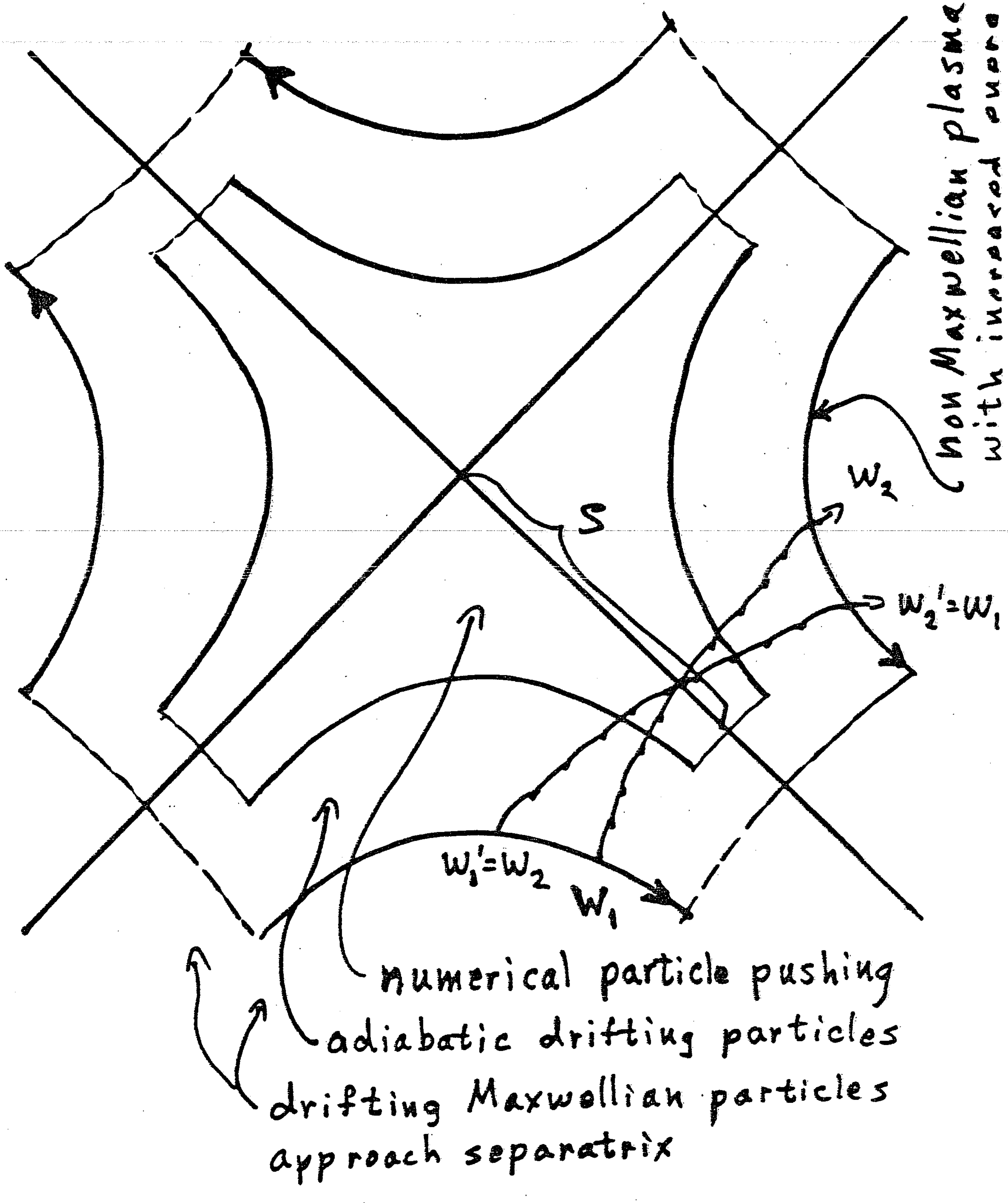
non Maxwellian plasma
with increased
S
W2
W2'=W1
W1'=W2
W1
numerical particle pushing
adiabatic drifting particles
drifting Maxwellian particles
approach separatrix

Model:

1) steady state
2) kinetic ions and electrons
3) collisionless
4) no resistivity imposed
5) drifting Maxwellian approaches separatrix
6) low β, may be extended easily to high β

Fields:

$$\bar{E} = E_0 \hat{z} \quad , \quad E_0 \equiv \text{constant}$$

$$\bar{B} = B'(x\hat{y} + y\hat{x}) = -\nabla\phi$$

$$\phi = -B'xy \quad , \quad B' \equiv \text{constant} \left(\begin{array}{c} < 0 \\ \text{in sketch} \end{array} \right)$$

$$\psi = -\tfrac{1}{2} B'(x^2 - y^2)$$

Define "guiding center" as a point where $v_z = 0$.

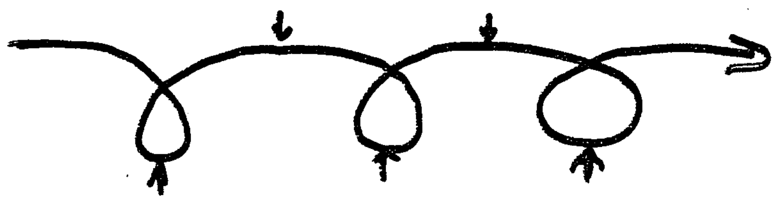

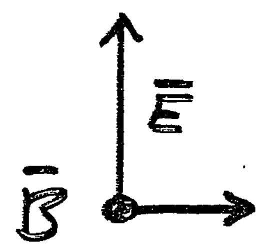

$$v_d = \frac{\bar E \times \bar B}{B^2}$$

$$\bar A = \Psi(x, y)\,\hat z$$

$$\bar E = -\nabla \phi = E_0 \hat z - \nabla f(x, y)$$

$$\bar p = m\bar v + q\bar A$$

$$H = \frac{1}{2m}(p - qA)^2 + q\phi$$

$$\dot p_z = -\frac{\partial H}{\partial z} = qE_0$$

$$m v_z = qE_0(t - t_0) - q\Psi(x, y)$$

The "guiding center" moves with the $v_z = 0$ surfaces.

ie $\quad x^2 - y^2 = -\frac{2}{B'}E_0(t - t_0)$

The guiding center may have $v \to \infty$ but the particle never does.

Power transferred to plasma near the X point

$$P = \iint f(W_1)(W_2 - W_1)\,\bar{v} \cdot d\bar{S}\, d^3v$$

where

S is a position on the separatrix

$\bar{v}$ is velocity of particle crossing S

W_1 is kinetic energy of particle referred to Maxewellian entry point

W_2 is kinetic energy of particle leaving vicinity of separatrix

When adiabatic invariants $\mu = W_\perp / B$ and $J = \int v_{\parallel} \cdot dl_{\parallel}$ break down near the X point, $W_1 \neq W_2$.

Analytic indication that P is positive:

By symmetry, every orbit of a particle entering with W_1 and leaving with W_2 has a corresponding orbit with $W_1' = W_2$ and $W_2' = W_1$

$$
\begin{aligned}
x' &= -y & v_{sx}' &= v_{sy} \\
y' &= -x & v_{sy}' &= v_{sx} \\
z' &= -z & v_{sz}' &= v_{sz} \\
t' &= -t & &
\end{aligned}
$$

The power integral may be rewritten

$$P = \frac{1}{2}\iint \left[f(W_1) - f(W_2)\right](W_2 - W_1)\,\bar{v}\cdot d\bar{s}\,d^3v$$

$$\simeq \frac{-1}{2}\iint f'(\tilde{W})\,(W_2 - W_1)^2\,\bar{v}\cdot d\bar{s}\,d^3v$$

$$\simeq \frac{1}{2kT}\iint f(\tilde{W})\,(W_2 - W_1)^2\,\bar{v}\cdot d\bar{s}\,d^3v$$

$$\underline{\underline{P > 0}} \qquad \tilde{W} \equiv (W_1 + W_2)/2$$

Comments:

- The X point acts as a scattering center. The reconnection process is reversable and appears to cause no entropy increase. Particles leaving the separatrix are not precisely Maxwellian. They are slightly more "ordered" than those approaching the separatrix. To keep entropy fixed there must be a net energy gain.

- Axial current in the nonadiabatic region near the X point is $I \simeq P/E_0$

- $I \underset{\sim}{\propto} n$

- As I increases the X point becomes oblique

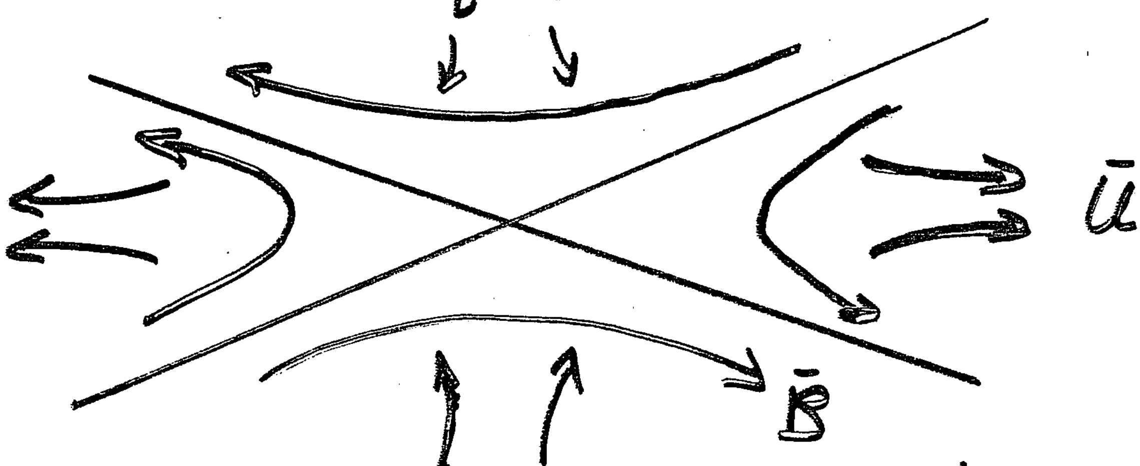

The convenient symmetry is lost.

- There are no shocks.

Conclusions:

- A model of driven reconnection in a collisionless nonresistive plasma has been developed.

- It has been shown analytically that energy is transferred from fields to the plasma.

- Plasma heating has been verified by a computer model, to be published.

- The reconnection mechanism described here will influence the rate of island formation for the Field Reversed Theta Pinch.

- A similar mechanism with $B_z \neq 0$ will affect reconnection in other devices

- There is no simple vacuum limit when $B_z \neq 0$

BUBBLE FORMATION DUE TO SURFACE TEARING MODES

G. KURITA

J. A. E. R. I.

Bubble Formation due to Surface Tearing Mode

G. Kurita, M. Azumi,
T. Tuda, T. Tsunematsu,
T. Takizuka, Y. Tanaka*
and T. Takeda

JAERI

* on leave from Fujitsu Limited

Purpose

To re-investigate the bubble formation due to free boundary mode precisely, taking into account of the finite plasma resistivity.

Method

The vacuum region is replaced by a highly resistive plasma, "pseudo-vacuum" model, to avoid the difficulty of tracing the plasma surface position precisely.

Basic Equations

$$\frac{\partial U_{m/n}}{\partial t} = [U, \phi]_{m/n} + [J, \psi]_{m/n}$$

$$\frac{\partial \psi_{m/n}}{\partial t} = [\psi, \phi]_{m/n} + \sum_{\substack{m=m'+m'' \\ n=n'+n''}} \eta_{m'/n'} J_{m''/n''} - E^{\omega}_{m/n}$$

$$\frac{\partial \eta_{m/n}}{\partial t} = [\eta, \phi]_{m/n}$$

$$[\psi, \phi]_{m/n} = \sum_{\substack{m=m'+m'' \\ n=n'+n''}} \frac{m'}{r}\left(\psi_{m'/n'} \frac{\partial \phi_{m''/n''}}{\partial r} - \phi_{m'/n'} \frac{\partial \psi_{m''/n''}}{\partial r}\right)$$

$$J_{m/n} = \Delta \psi_{m/n}$$

$$U_{m/n} = \vec{\nabla} \cdot (\rho_0 \vec{\nabla} \phi_{m/n})$$

Numerical Method

to advance Ψ eq. without numerical instability.

For this two-dimensional diffusion eq.

$$\frac{\partial \hat{\Psi}(r,\theta)}{\partial t} = \hat{\eta}(r,\theta)\,\Delta\hat{\Psi}(r,\theta),$$

the numerical stability condition is

$$\hat{\eta}(r,\theta) > 0 \quad \text{for all } (r,\theta).$$

To satisfy this condition, we introduce new variable $S_{m/n}$, and solve

$$\frac{\partial S_{m/n}}{\partial t} = [S, \Phi]_{m/n}$$

instead of η eq., and calculate $\hat{\eta}(r,\theta)$ by assuming

$$\hat{\eta}(\hat{S}) \equiv \hat{\eta}(\hat{S}_{t=0}) \;:\; \hat{S}_{t=0} = r$$

for all θ. Then we can obtain

$$\eta_{m/n} \,(= \frac{1}{2\pi}\int_{-\pi}^{\pi} \hat{\eta}(r,\theta)\cos m\theta \, d\theta$$

Shaping Function

$$J(r) = f_J(r)\, S_J(r)$$

$$P(r) = f_P(r)\, S_P(r)$$

$$\eta(r) = f_\eta(r)\, S_\eta^{-1}(r)$$

$$f_i(r) = \begin{cases} (1.-C_a)\left[1.-\left(\frac{r}{a}\right)^{2C_b}\right]^{C_c} + C_a \;; & r \le a \\ C_a \;; & r > a \end{cases}$$

$$S_i(r) = \begin{cases} S_i(a-C_\gamma) \;; & r < a - C_\gamma \\ (1.-C_\alpha)\left[\frac{1}{2} + \frac{1}{\pi}(\tan^{-1}x - \beta x)\right] + C_\alpha \;; & a - C_\gamma \le r \le a + C_\gamma \\ S_i(a+C_\gamma) \;; & r > a + C_\gamma \end{cases}$$

$$x = \pi \cdot \frac{r-a}{C_\beta}, \quad \beta = \frac{1.}{1.+x_\gamma^2}$$

$$x_\gamma = \pi \cdot C_\gamma / C_\beta$$

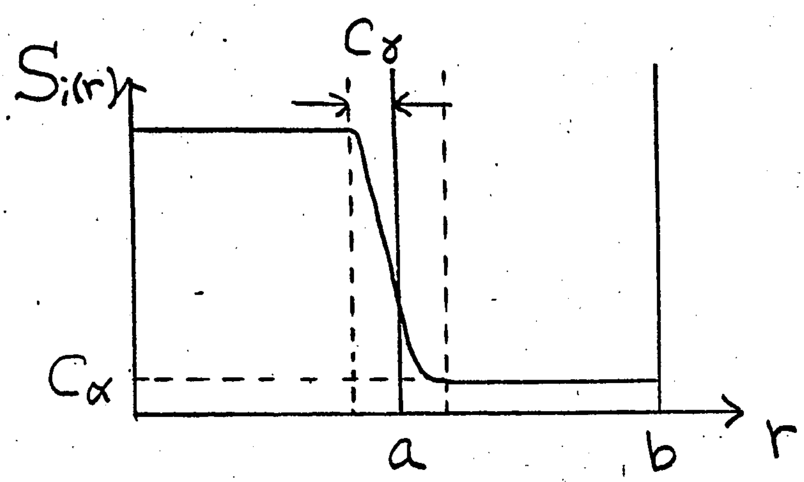

Linearised Equations

$$\gamma \vec{\nabla} \cdot (\rho_0 \vec{\nabla} \phi) = F \Delta \psi - \frac{m}{r} \frac{dJ_0}{dr} \psi$$

$$\gamma \psi = - F \phi + \eta_0 \Delta \psi + \eta J_0$$

$$\gamma \eta = - \frac{m}{r} \frac{d\eta_0}{dr} \phi$$

$$F = \frac{1}{q} (m - nq)$$

$\frac{\partial}{\partial t} \longrightarrow \gamma$: growth rate

subscript 0 : equilibrium quantity

q : safety factor

Effect of External Density

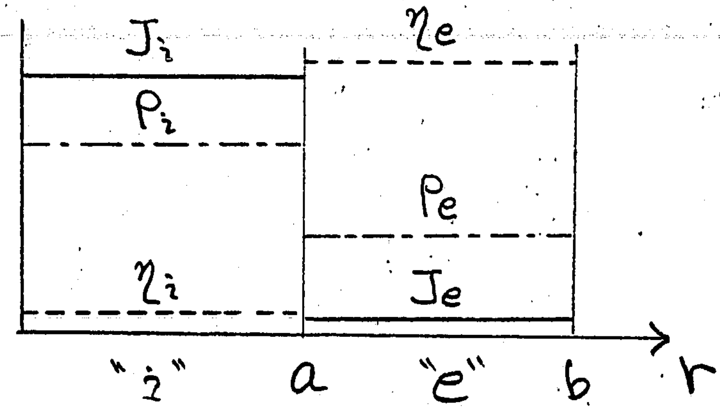

$J_e / J_i \ll 1$

$\eta_i / \eta_e \ll 1$

- Internal Solutions
$$\begin{cases} \psi_i = r^m \\ \phi_i = -\dfrac{\gamma}{F_i} \psi_i \end{cases}$$

- External Solutions
$$\begin{cases} \psi_e = \hat{\psi}_e \left(r^m - b^{2m} r^{-m} \right) \\ \phi_e = \hat{\phi}_e \left(r^m - b^{2m} r^{-m} \right) \end{cases}$$

- Boundary Condition
  - $\phi_i = \phi_e \,|_{r=a}$
  - $\psi_i = \psi_e \,|_{r=a}$
  - $\gamma \left[\rho \dfrac{d\phi}{dr} \right]_{a-\delta}^{a+\delta} = F_a \left[\dfrac{d\psi}{dr} \right]_{a-\delta}^{a+\delta} - \dfrac{m}{a} \psi_a \left[J \right]_{a-\delta}^{a+\delta}$

$$\gamma^2 = \left[1. + \frac{\rho_e}{\rho_i} \frac{1. + (a/b)^{2m}}{1. - (a/b)^{2m}} \right]^{-1} \gamma^2_{\text{analy.}}$$

$$\gamma^2_{\text{analy.}} = \frac{2}{\rho_i q_{\delta a}^2} \left(m - n q_{\delta a} \right) \left[1. - \frac{m - n q_{\delta a}}{1 - (a/b)^{2m}} \right]$$

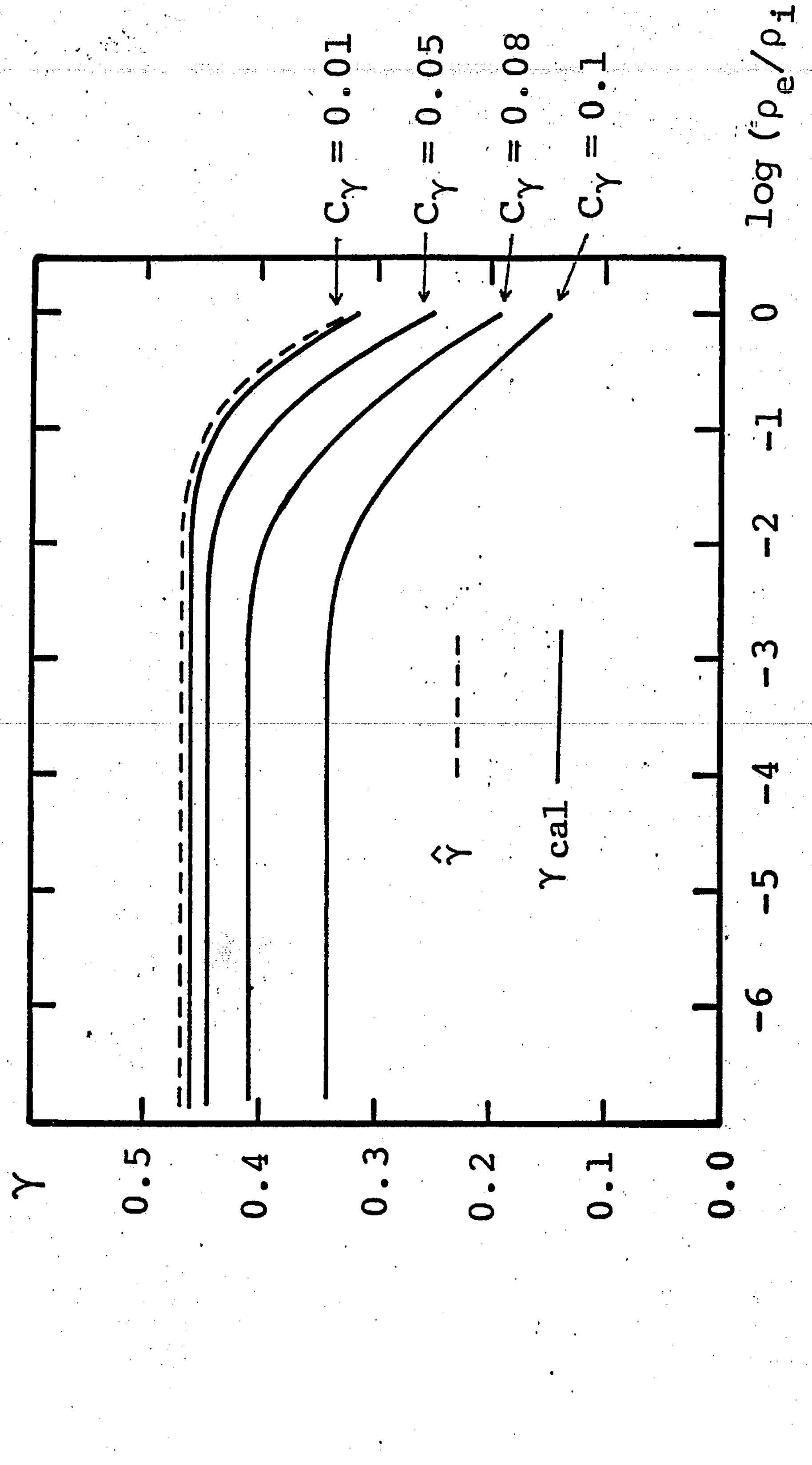
$C_\gamma = 0.01$
$C_\gamma = 0.05$
$C_\gamma = 0.08$
$C_\gamma = 0.1$
$\log(\rho_e/\rho_i)$
0
−1
−2
−3
−4
−5
−6
$\hat{\gamma}$
γ_{cal}
γ
0.5
0.4
0.3
0.2
0.1
0.0

Effect of External Resistivity

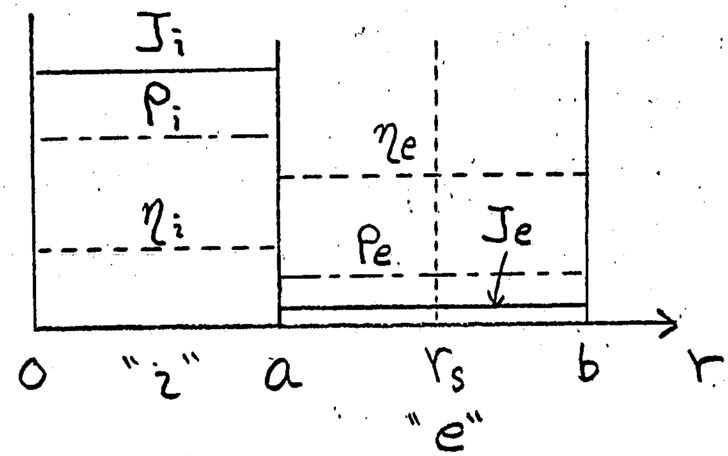

$J_e/J_i \ll 1$

$\rho_e/\rho_i \ll 1$

$$\left[1.-\left(\frac{r_s}{b}\right)^{2m}\right]\left[1-\left(\frac{a}{r_s}\right)^{2m}\right]\frac{q_{\delta a}^2}{2}\gamma^{13/5}$$

$$+\beta\left[1-\left(\frac{a}{b}\right)^{2m}\right]\frac{q_{\delta a}^2}{2}\gamma^2$$

$$+(m-nq_{\delta a})\left[1-\left(\frac{r_s}{b}\right)^{2m}\right]\left[m-nq_{\delta a}-1+\left(\frac{a}{r_s}\right)^{2m}\right]\gamma^{5/4}$$

$$+\beta(m-nq_{\delta a})\left[m-nq_{\delta a}-1+\left(\frac{a}{b}\right)^{2m}\right]=0$$

$$\beta=\frac{2m}{r_s}\left[\frac{q_\delta'^2 m^2}{32 q_\delta^4 \rho_e}\right]^{1/4}\eta_e^{3/4}$$

$$\beta \gg 1 \longrightarrow \gamma^2=\gamma^2_{analy.}$$

$$\beta \ll 1 \longrightarrow \gamma=\frac{1}{2}\left[\frac{q_\delta'^2 m^2}{q_\delta^4\rho_e}\right]^{1/5}\Delta'^{4/5}\eta_e^{3/5}$$

$$\Delta'=-\frac{2m}{r_s}\frac{1}{1-(r_s/b)^{2m}}\frac{m-nq_{\delta a}-1+(a/b)^{2m}}{m-nq_{\delta a}-1+(a/r_s)^{2m}}$$

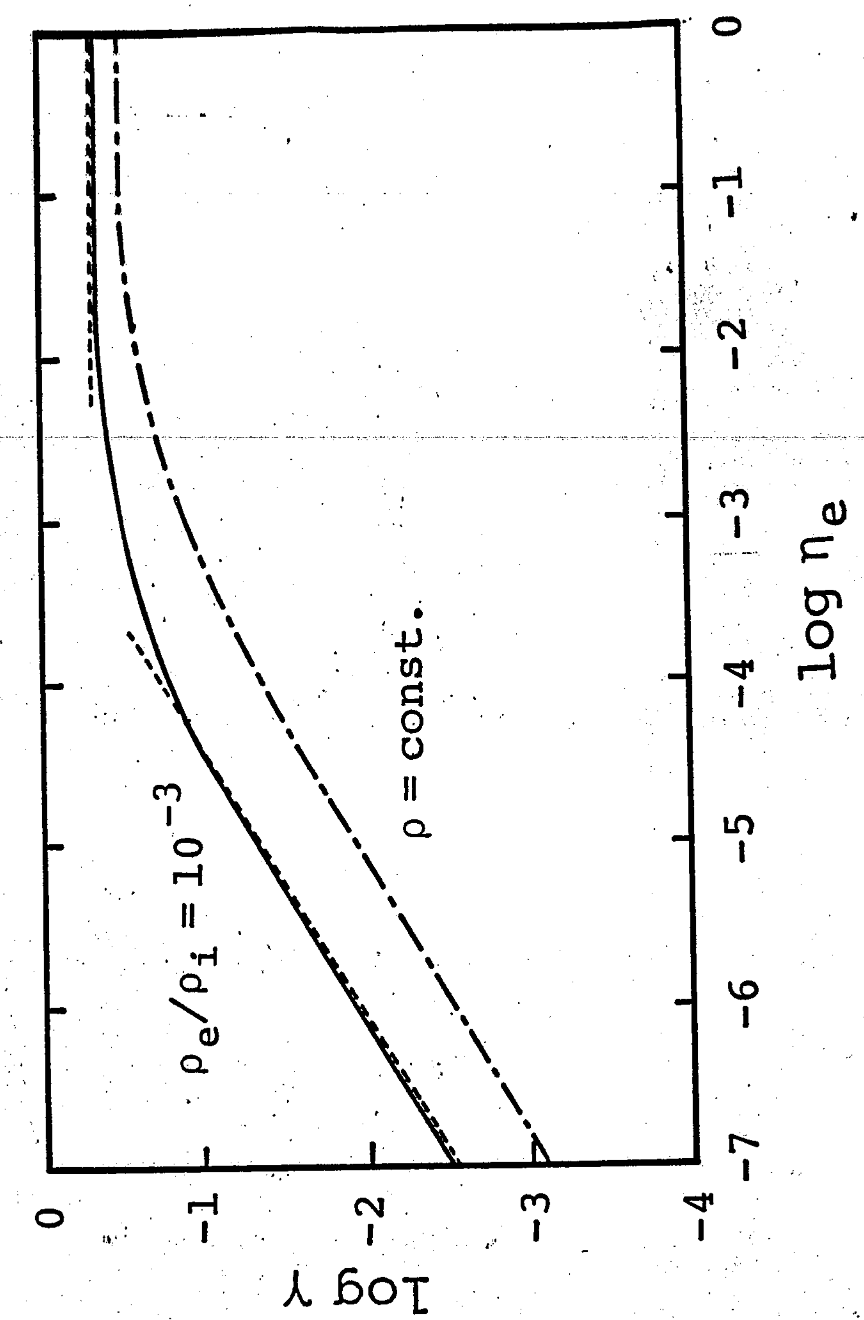

ρe/ρi = 10^-3
ρ = const.
log ηe
log γ

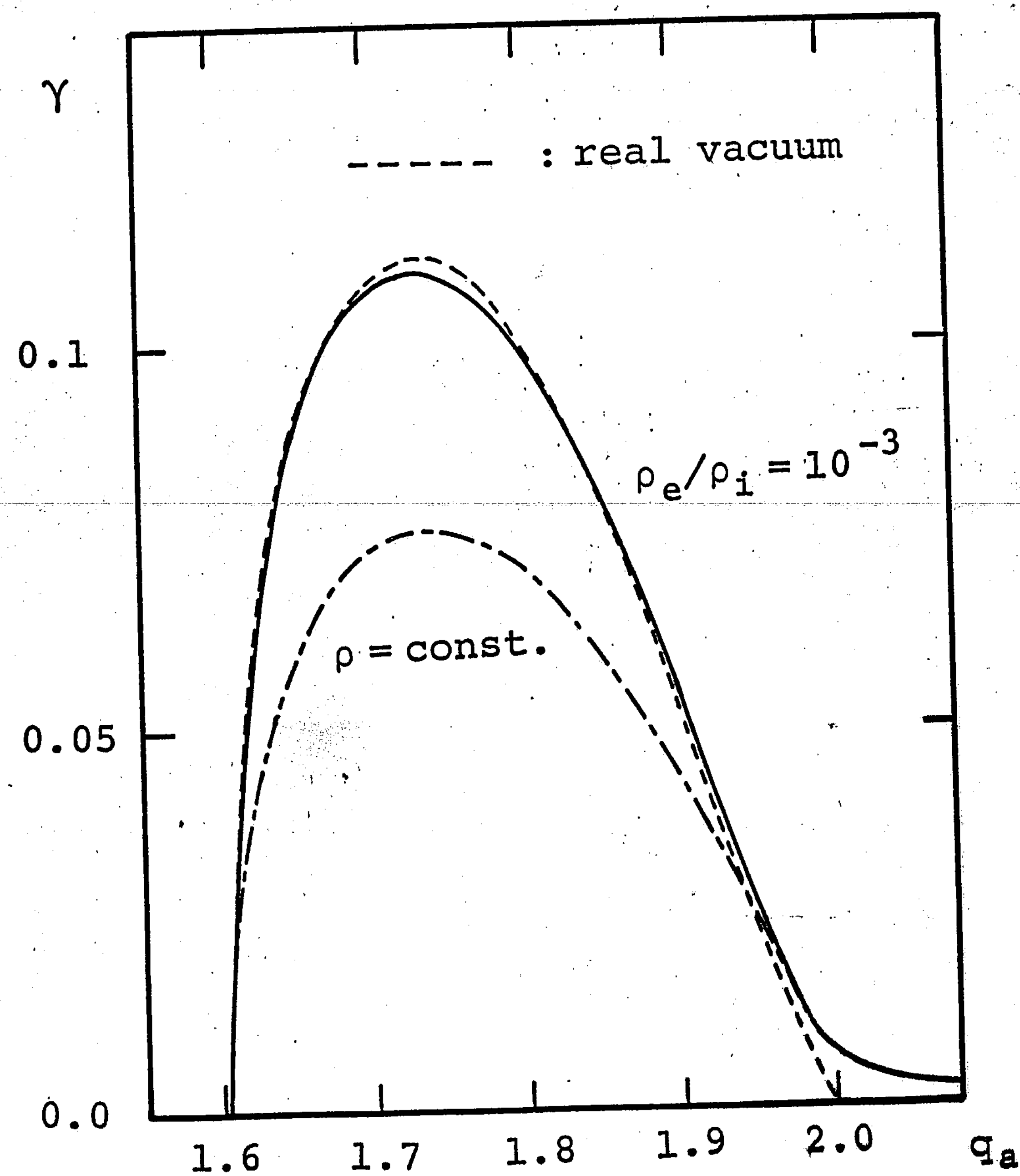
γ
----- : real vacuum
0.1
0.05
0.0
$\rho_e/\rho_i = 10^{-3}$
ρ = const.
1.6
1.7
1.8
1.9
2.0
q_a

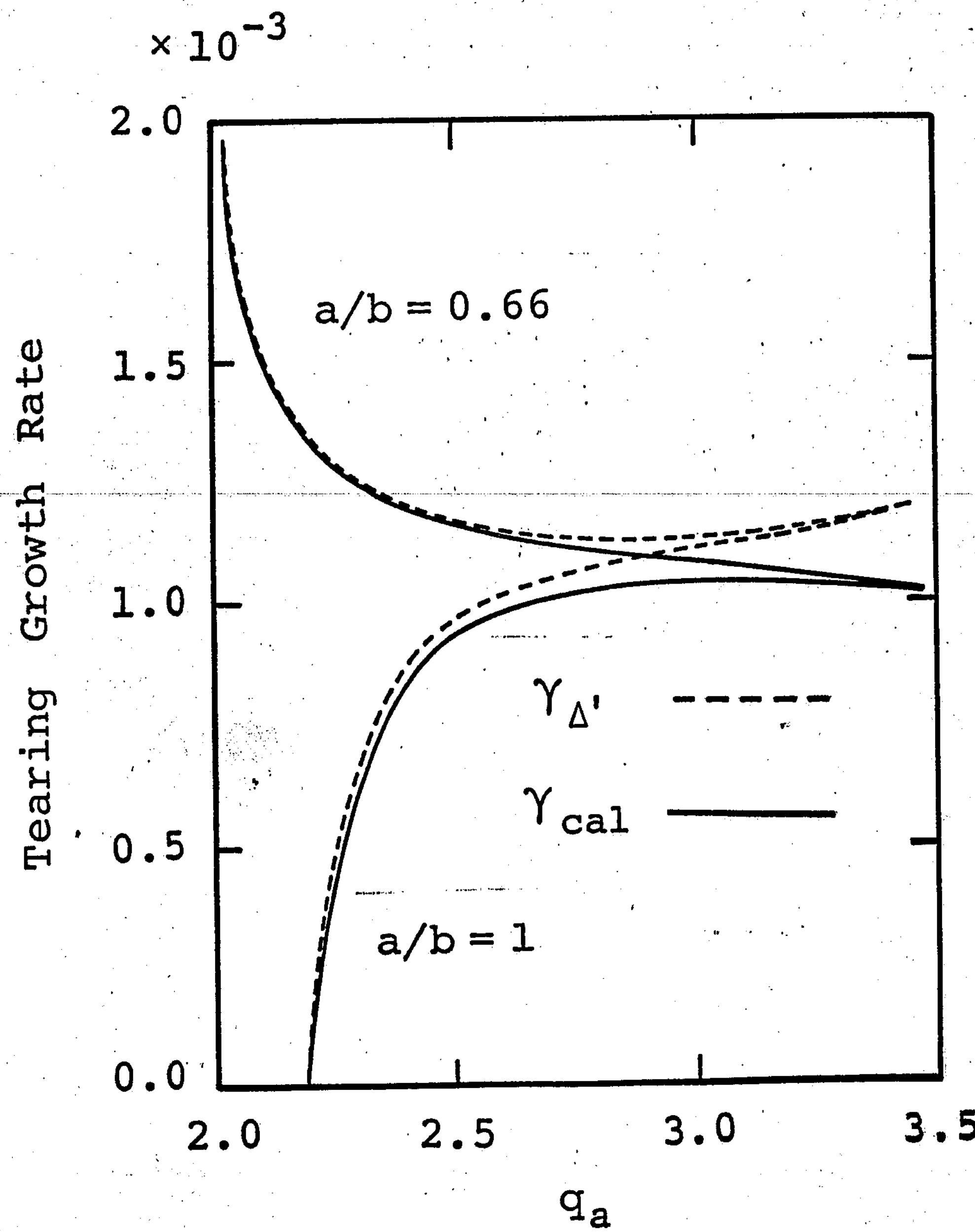
× 10^-3
2.0
1.5
1.0
0.5
0.0
Tearing Growth Rate
a/b = 0.66
a/b = 1
γ_Δ'
γ_cal
2.0
2.5
3.0
3.5
q_a

Parameters of nonlinear calculation

- $\rho_i = \rho_e = 1.$
- $\eta(0) = 1. \times 10^{-6}$, $\eta(b) = 1.$

  $$(\eta(r) = E/J(r))$$
- $a/b = 0.66$
- 201 equal spacing radial mesh
- 24 Fourier components
- Single helicity

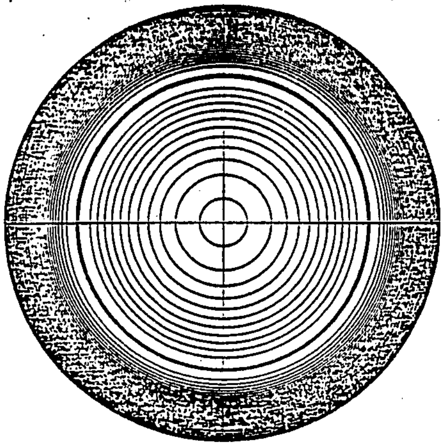

t= 2.5

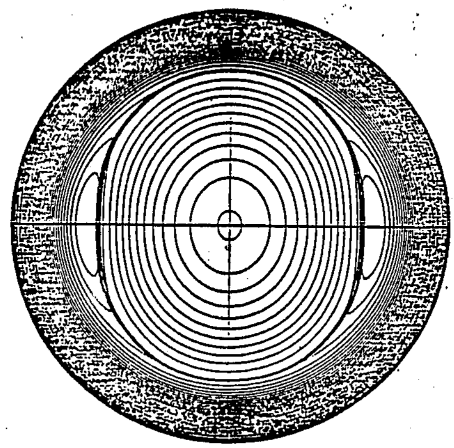

t= 25.0

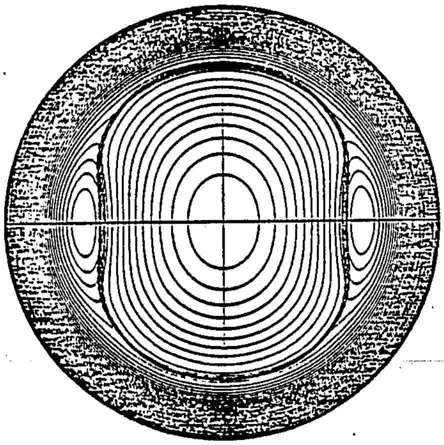

t= 27.5

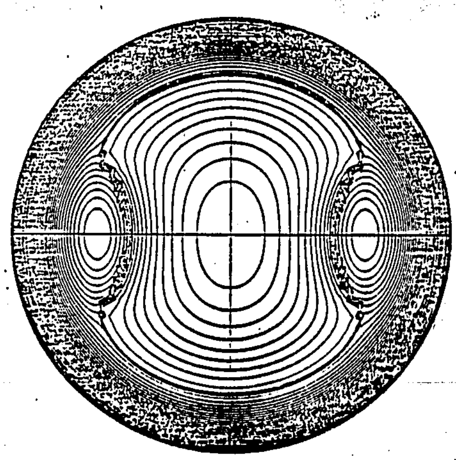

t= 30.0

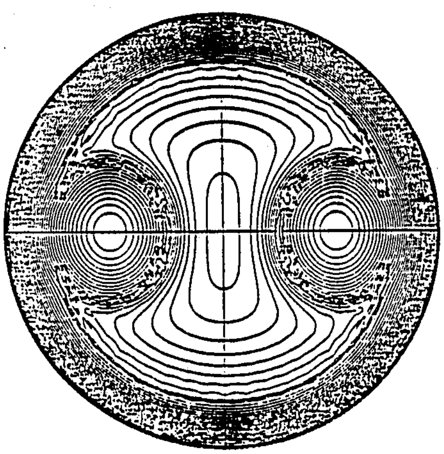

t= 35.0

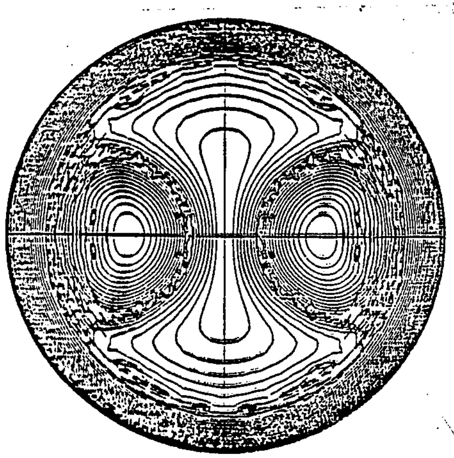

t= 40.0

$J(r) = J_0(1.-r^{20})$ $\qquad q_a = 1.95$

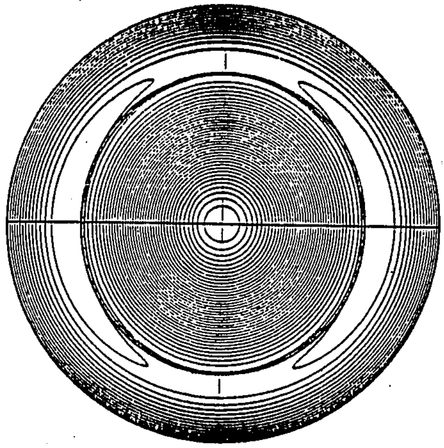

t= 2.5

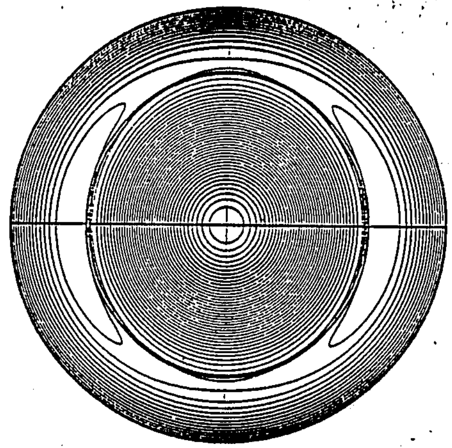

t= 10.0

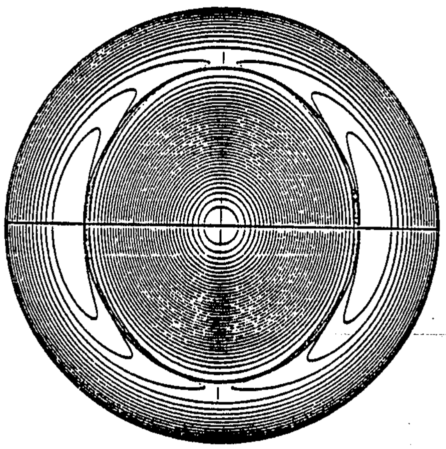

t= 20.0

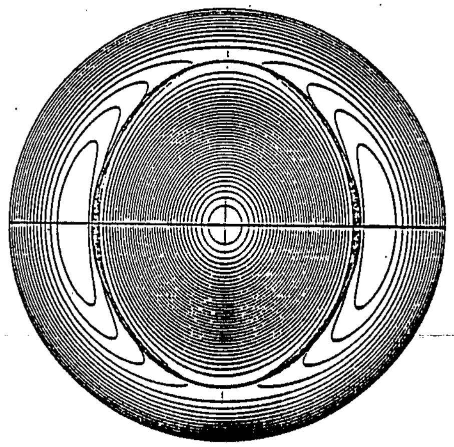

t= 30.0

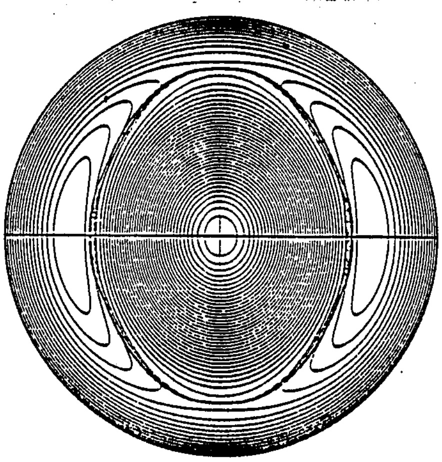

t= 40.0

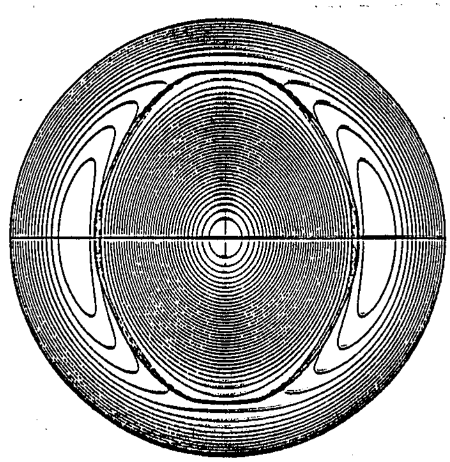

t= 45.0

$J(r) = J_0(1.-r^2)$ $\qquad q_a=1.64$

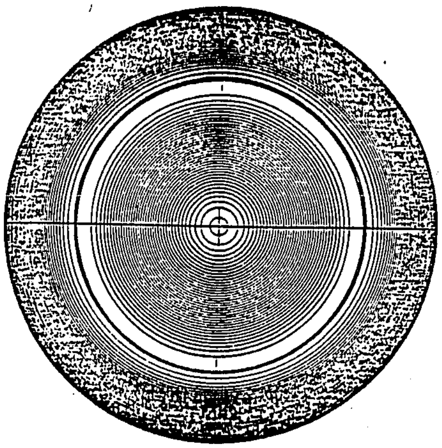

t= 2.5

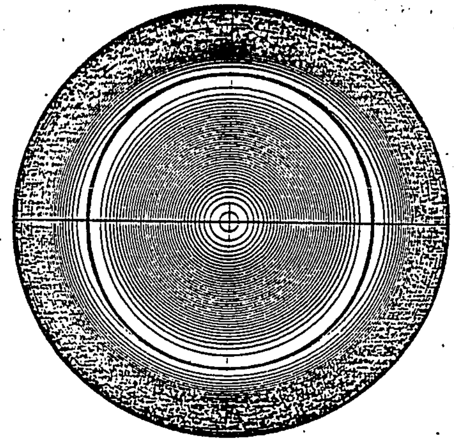

t= 30.0

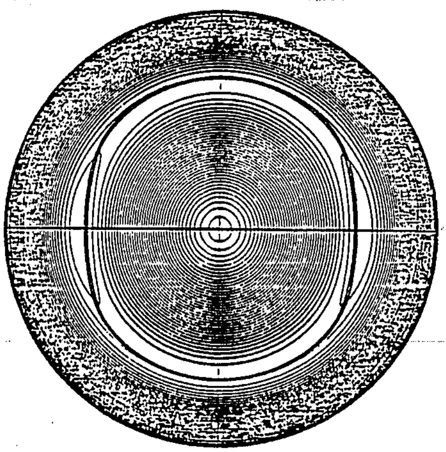

t= 40.0

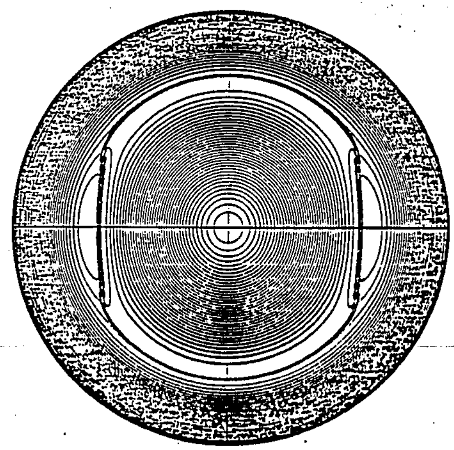

t= 45.0

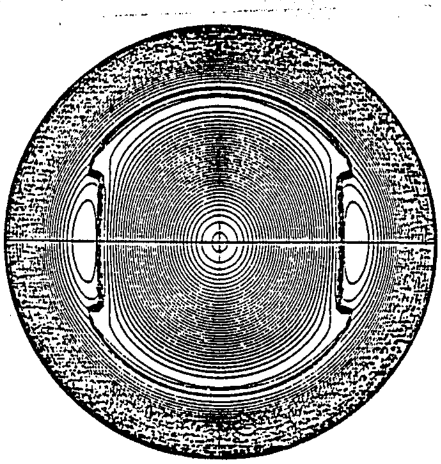

t= 50.0

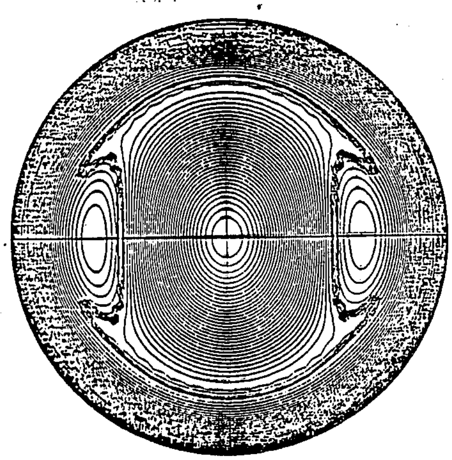

t= 57.5

$J(r) = J_0(1.-r^2)$ $q_a = 2.05$

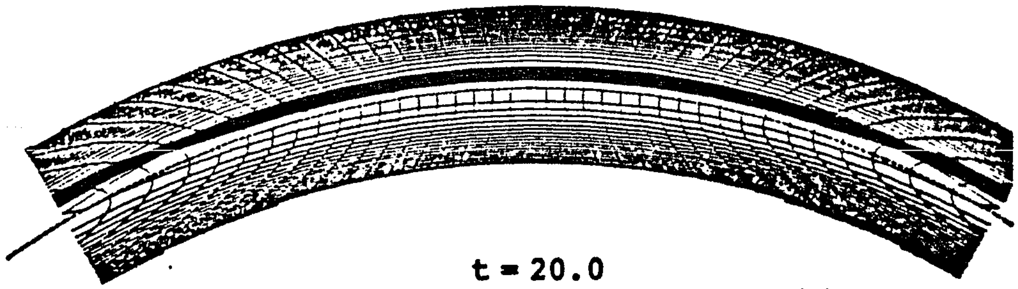

t = 20.0

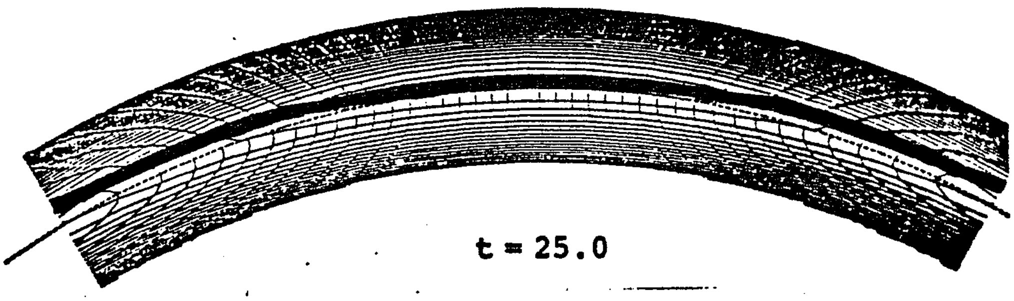

t = 25.0

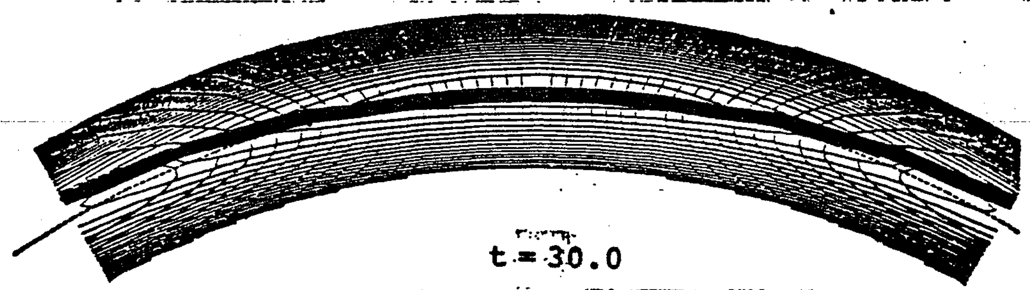

t = 30.0

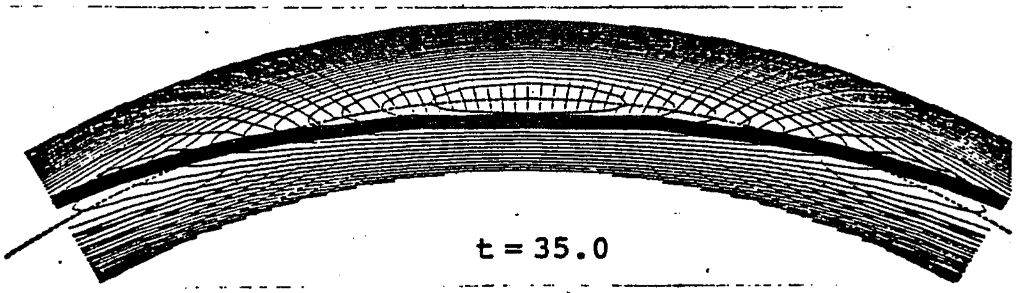

t = 35.0

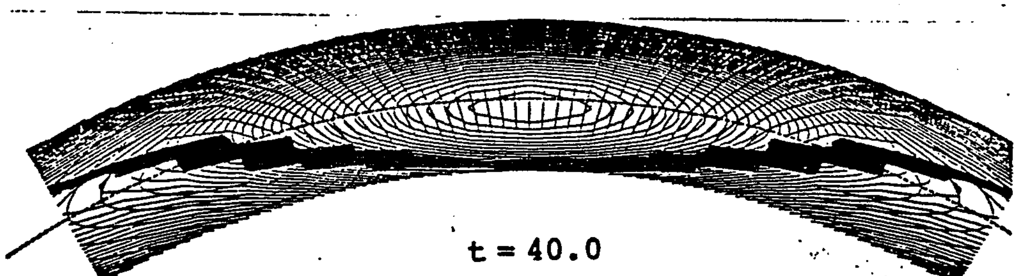

t = 40.0

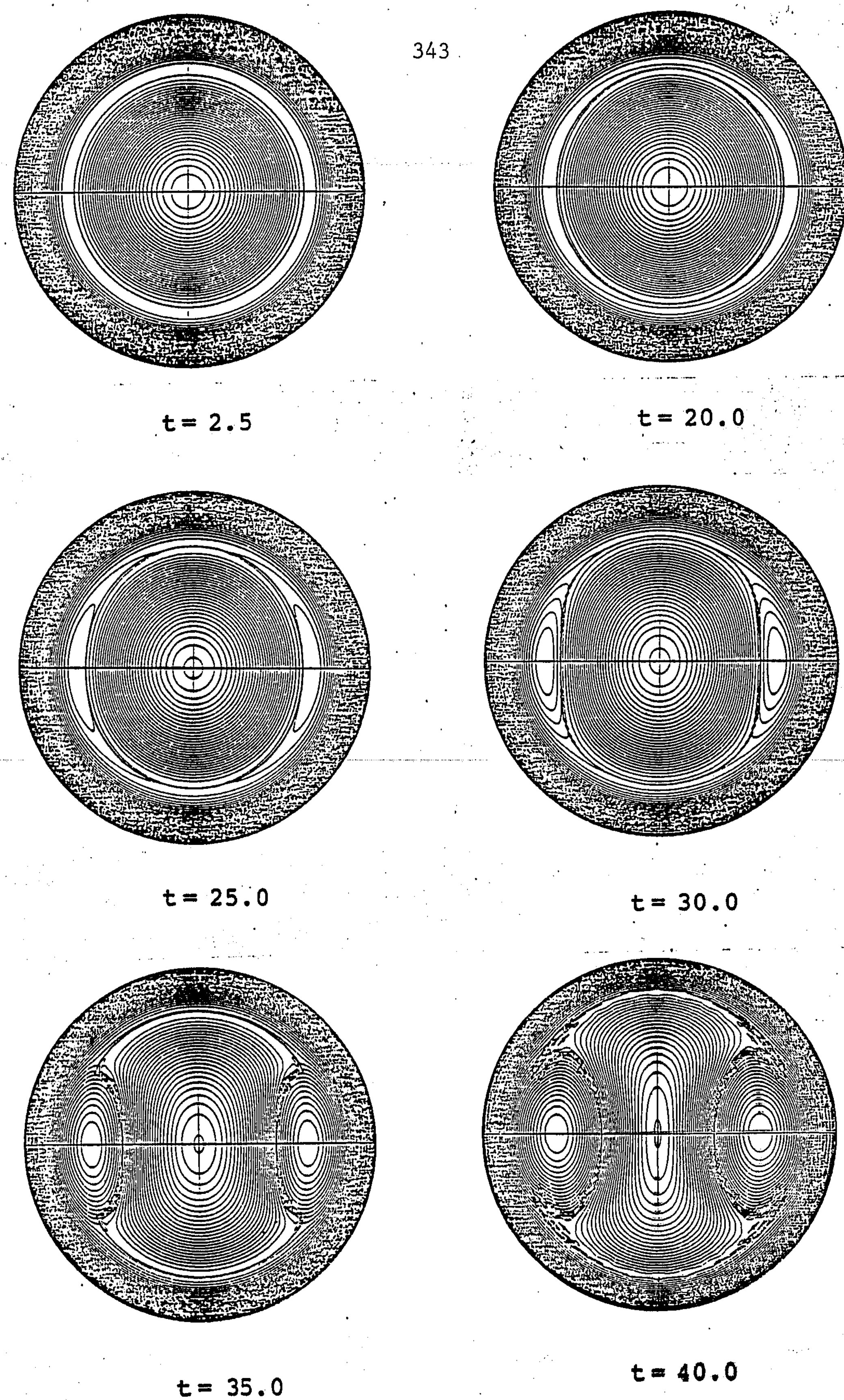

$$J(r) = J_0(1.-r^{10})^2 \qquad q_a = 1.90$$

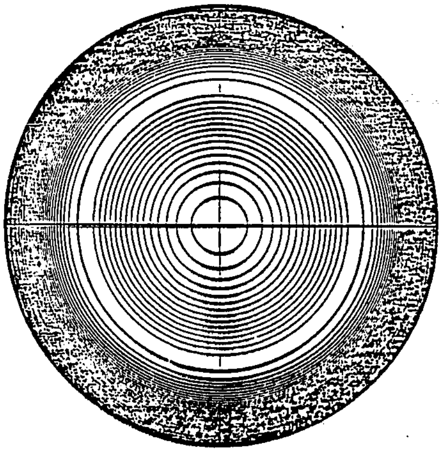

t= 2.5

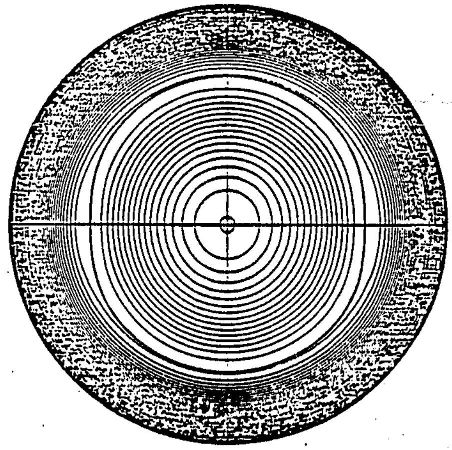

t= 35.0

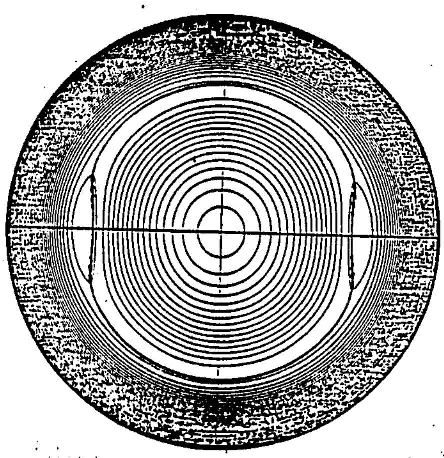

t= 40.0

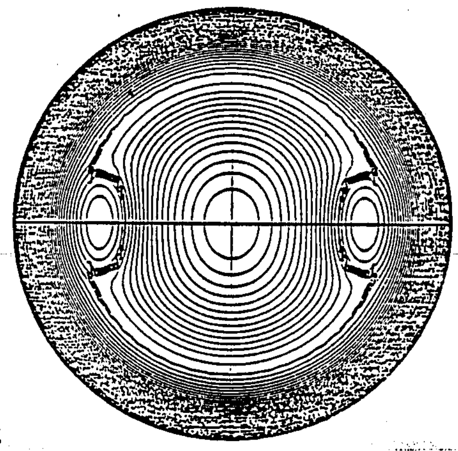

t= 45.0

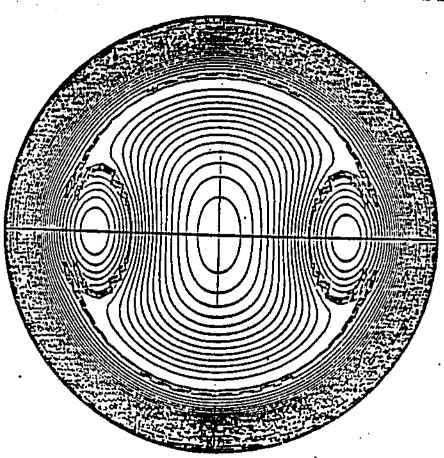

t= 50.0

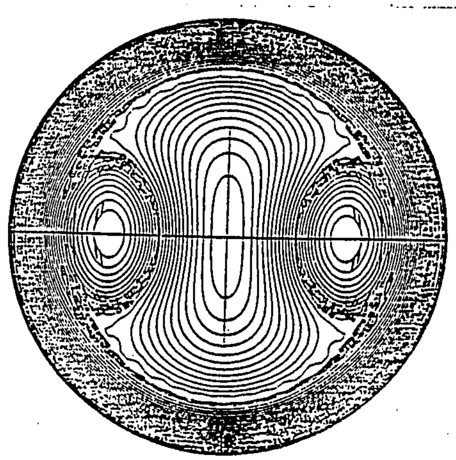

t= 57.5

$J(r) = J_0(1.-r^{10})^2$ $\quad q_a = 2.10$

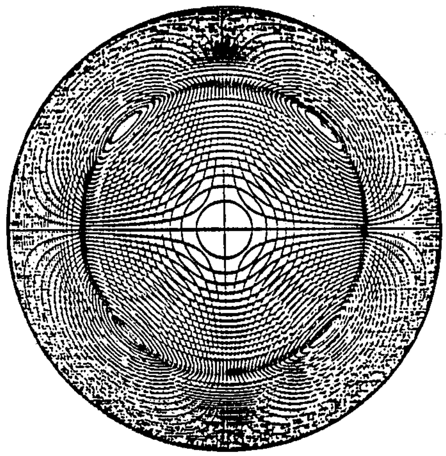

t= 2.5

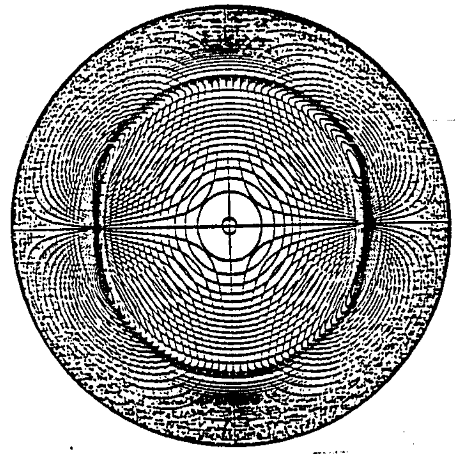

t= 35.0

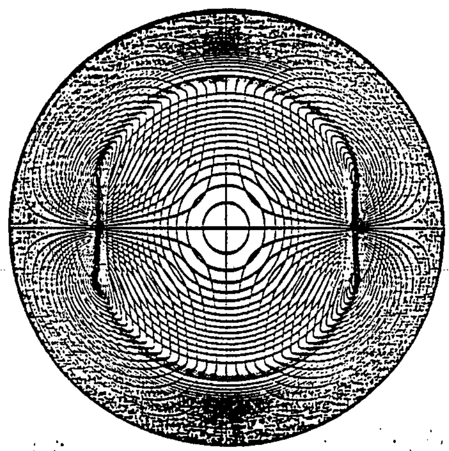

t= 40.0

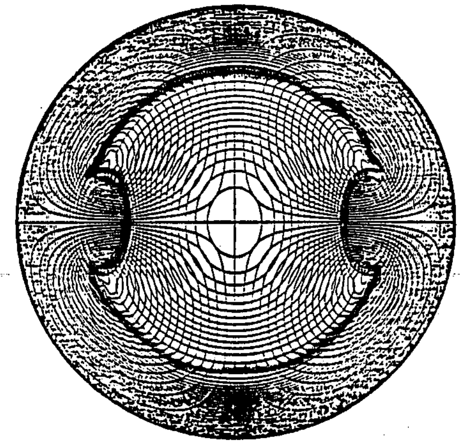

t= 45.0

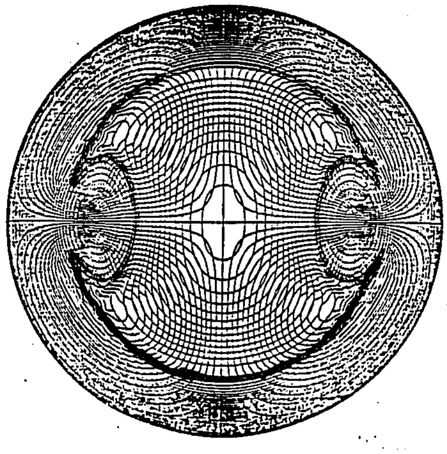

t= 50.0

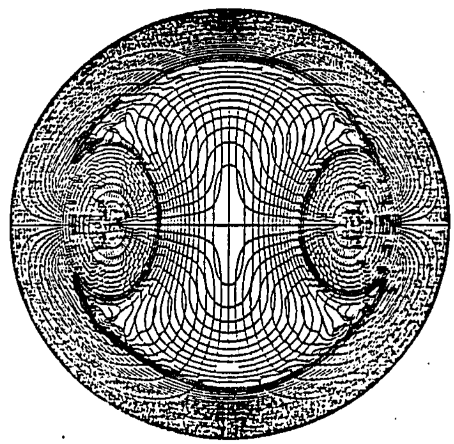

t= 57.5

$J(r) = J_0(1.-r^{10})^2$ $\quad$ $q_a = 2.10$

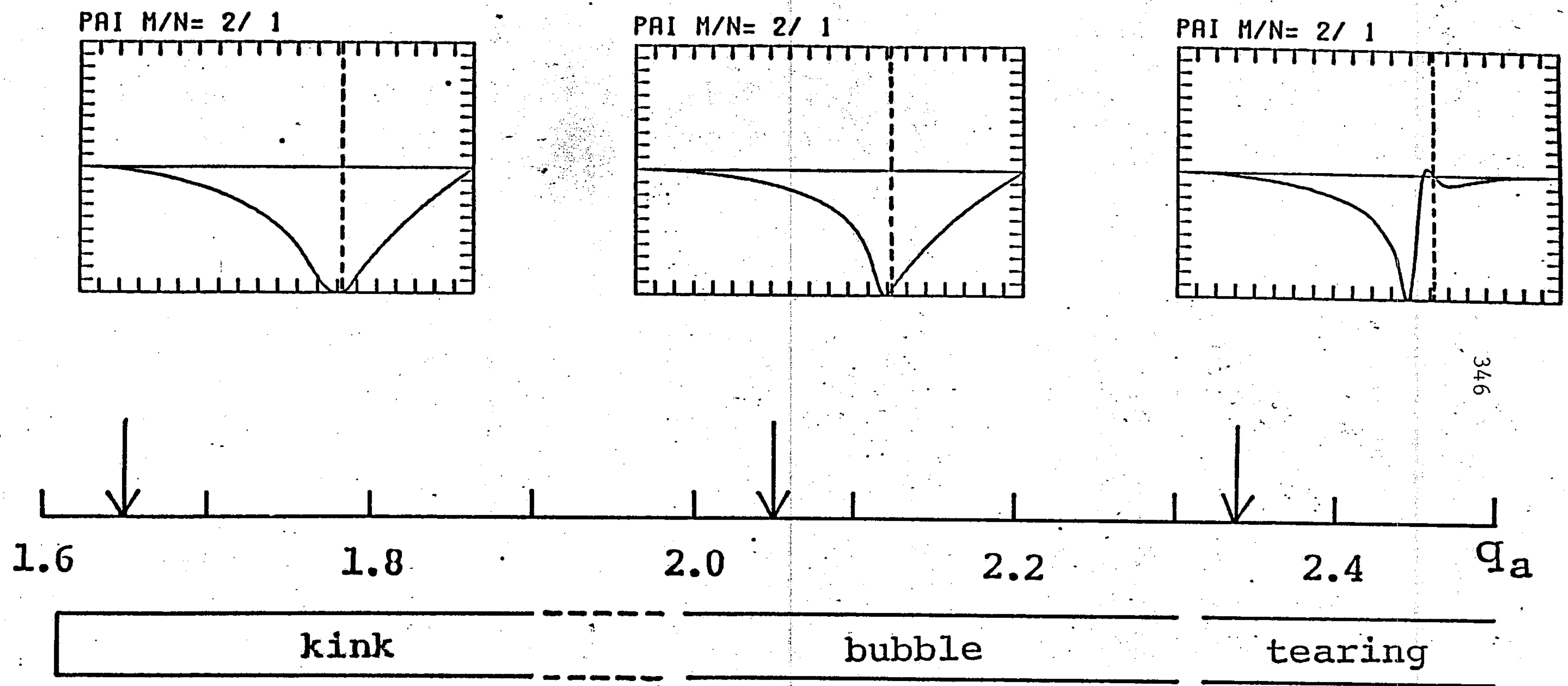
PAI M/N= 2/ 1
PAI M/N= 2/ 1
PAI M/N= 2/ 1
1.6
1.8
2.0
2.2
2.4
q_a
kink
bubble
tearing

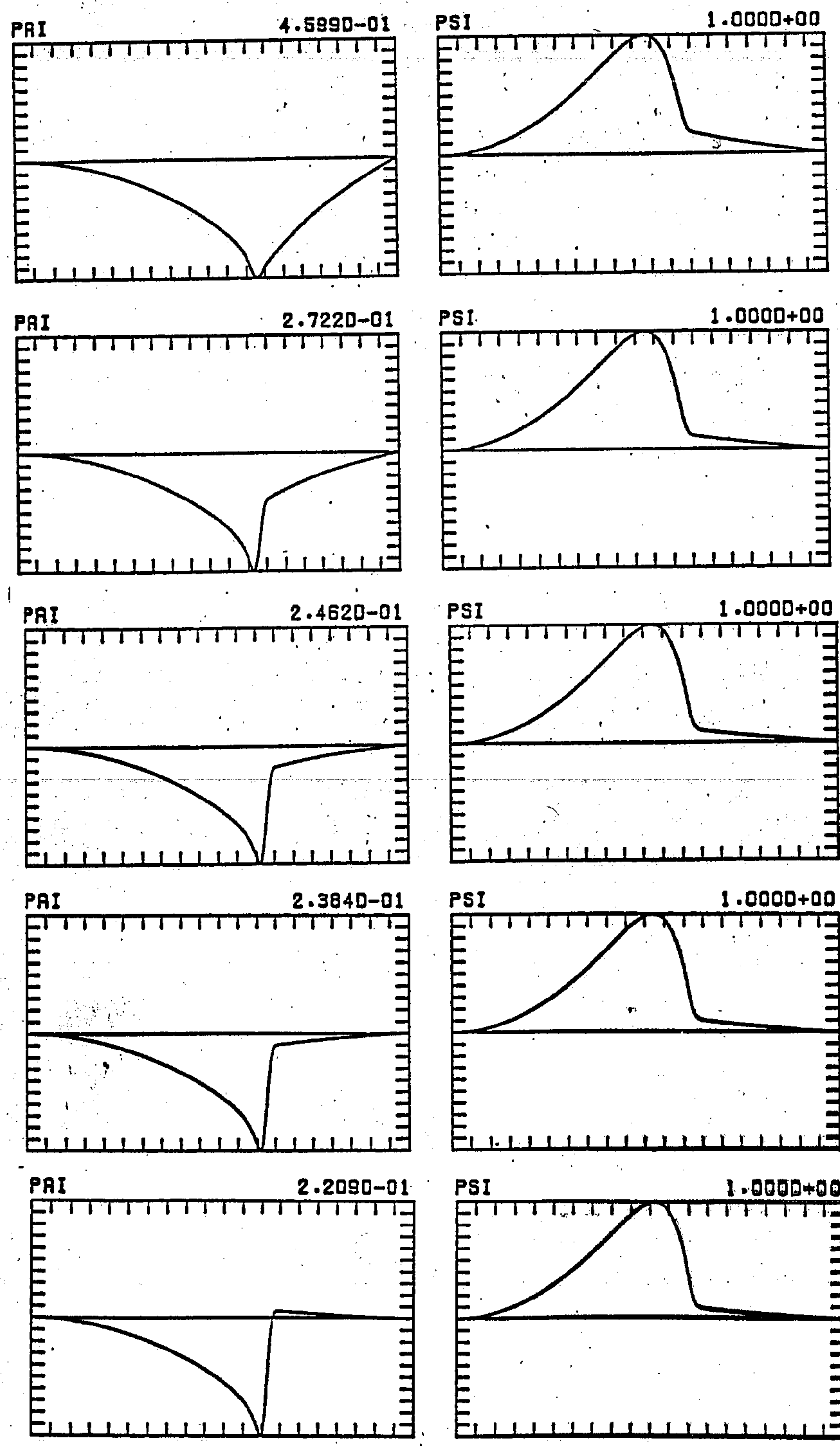

$q_a = 2.123$

$q_a = 2.193$

$q_a = 2.216$

$q_a = 2.227$

$q_a = 2.289$

$$J(r) = J_0(1.-r^{10})^2$$

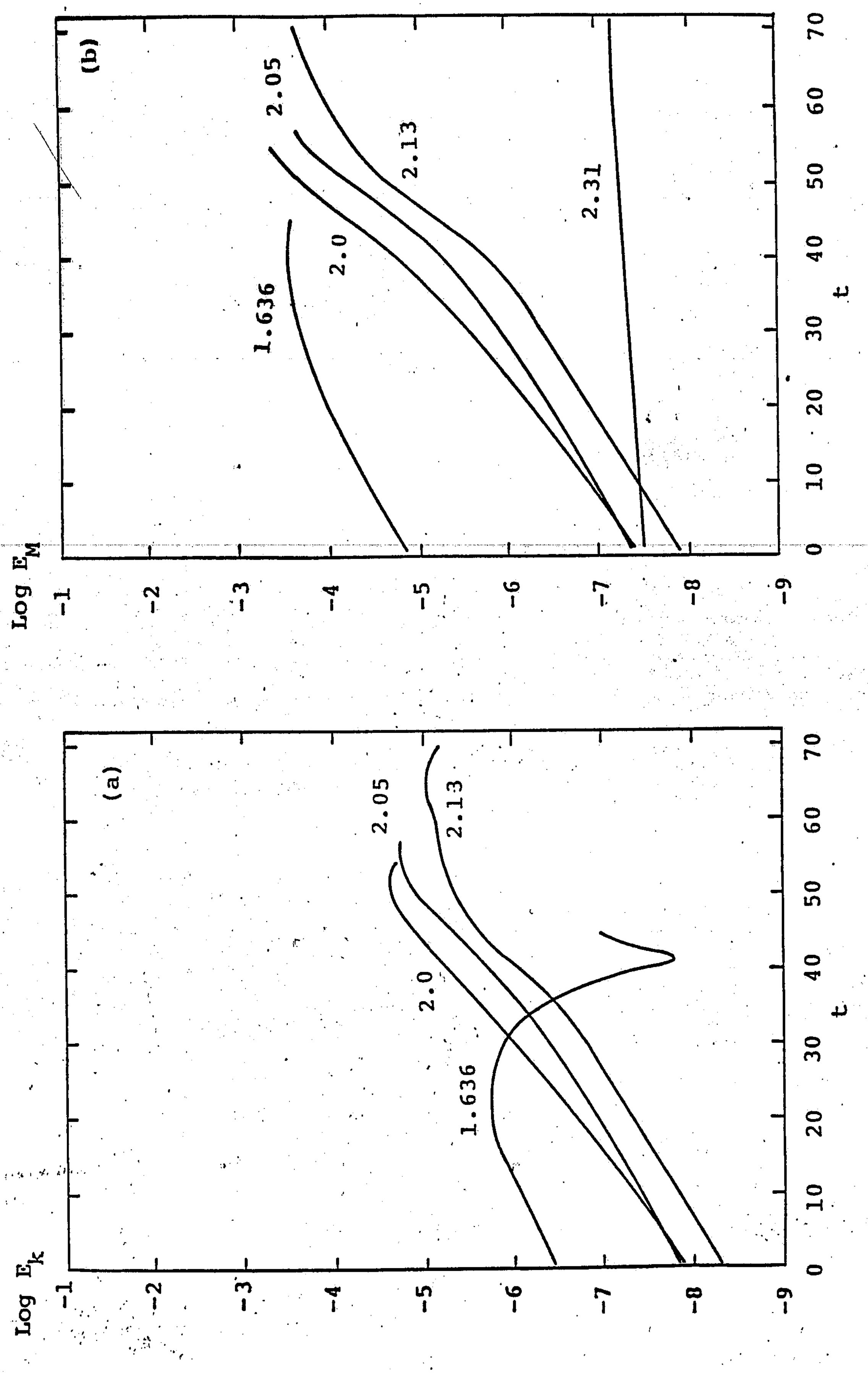

(b)
Log E_M
2.05
2.13
2.0
1.636
2.31
t
(a)
Log E_k
2.05
2.13
2.0
1.636
t

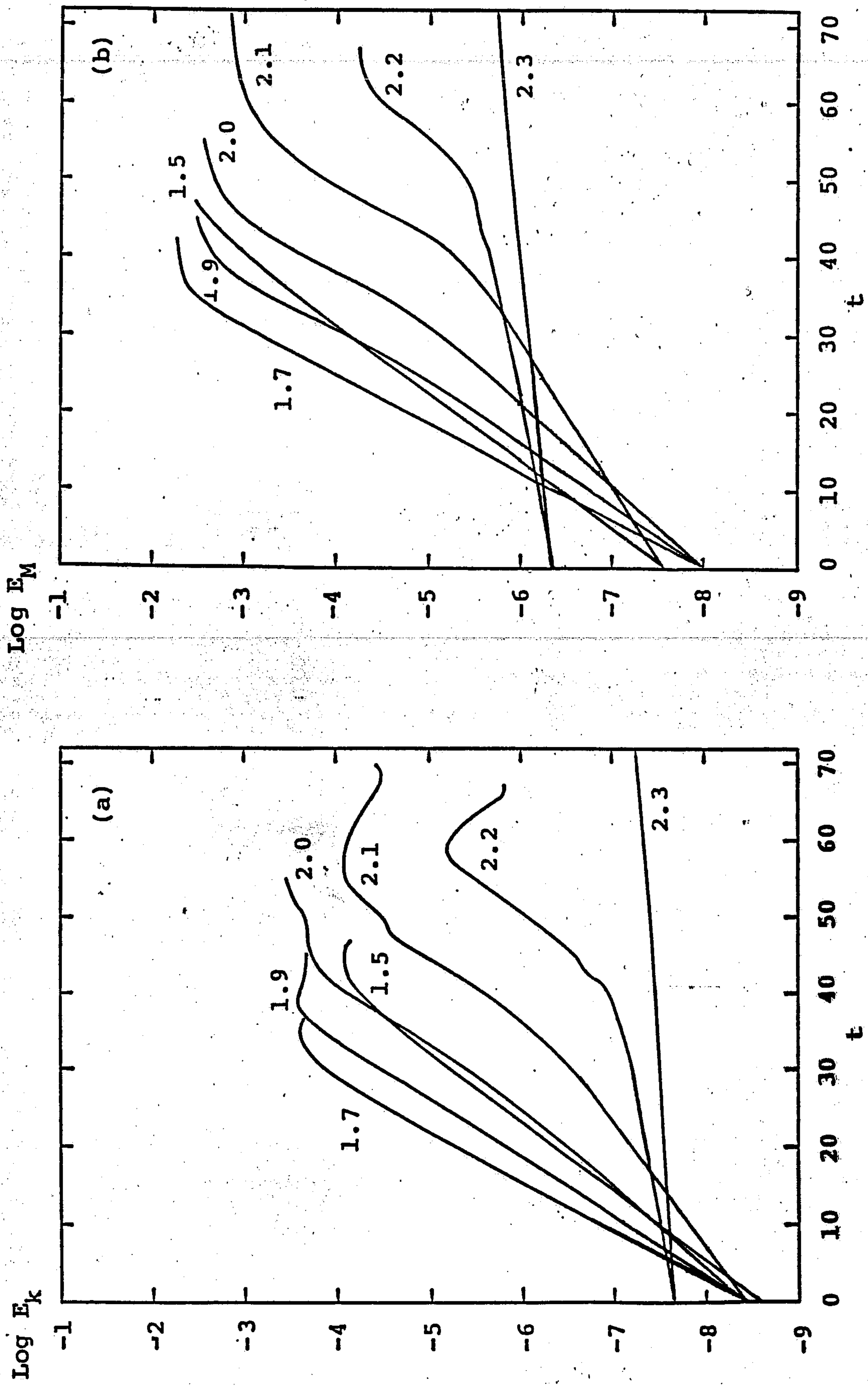
(a)
Log E_K
t
1.5
1.7
1.9
2.0
2.1
2.2
2.3
(b)
Log E_M
t
1.5
1.7
1.9
2.0
2.1
2.2
2.3

Mechanism of this bubble formation

1. The change of the profile of stream function from tearing eigenfunction to the surface tearing one as q_a decreases.
2. The plasma boundary moves inward due to this plasma flow, while the rational surface remains at the initial position. And the axis of magnetic island comes out to the vacuum region.
3. The mode grows like the kink mode but with rescricted range of poloidal angle in the vacuum region and forms the bubble.

Summary

The bubble is formed for q_a neary equal to 2. Therefore, it is a candidate of the major disruption in the discharge with $q_a \cong 2$. In order to understand the relation between the bubble formation and the major disruption, however, we need to take into account of the interaction between the surface current and the material limiter resulting from the bubble formation.

This problem remains for future study.

REVERSE FLOW VORTICES AND CURRENT SHEETS IN NONLINEAR TEARING

R. STEINOLFSON

UNIVERSITY OF CALIFORNIA AT IRVINE

REVERSE FLOW VORTICES AND CURRENT SHEETS IN NONLINEAR TEARING

R. S. Steinolfson - UC Irvine

I. Introduction

A. Typical aspects of the solar flare

- Energy "release" of 10^{30-32} ergs on time scale of $10-10^3$ sec.
- Observable consequences: Radiation (UV, X-ray, γ-ray), Energetic particles, coronal disruptions, Mass ejections.
- Magnetic configurations:

Magnetic loop or Arcade

Susceptible to instabilities:

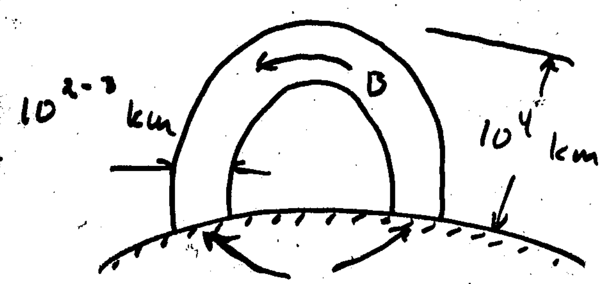

B fixed in photosphere - many modes stabilized

Driven Reconnection:

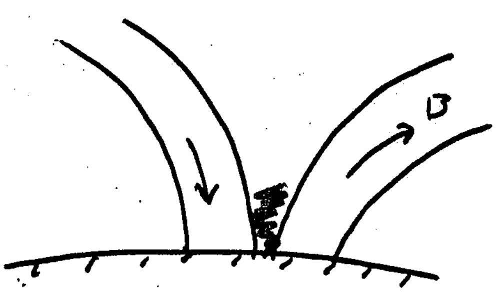

Loop merging due to convective motion

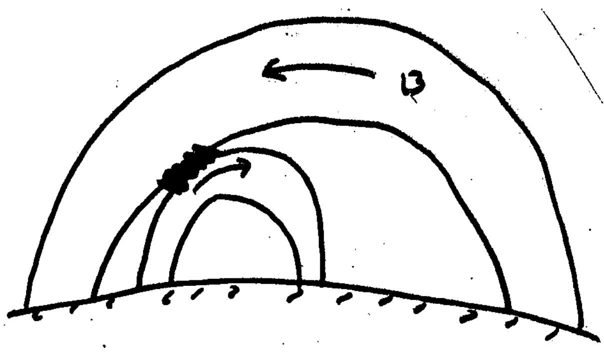

Emerging Flux

- Physical parameters:

$T \approx 1\text{-}2 \times 10^6$ K ≈ 150 ev, $\quad n = 10^{9-10}$ cm^{-3}

$B \approx 10$ G, $\quad$ scale $= a = 10^7$ cm

$S = 10^{10-11}$, $\quad \beta \approx 0.01\text{-}0.1$, $\quad ka \approx 0.1$

B. Energy conversion process

A reasonable scenario is as follows:

- Flare energy stored in stressed (nonpotential) coronal magnetic fields.
- Magnetic reconnection responsible for conversion process.
- Reconnection occurs in nonlinear phase of tearing instability.

Two questions regarding this approach

1. Does the tearing mode saturate early in nonlinear regime; i.e., is the required energy converted?
2. Is the process fast enough?

   <u>Problem:</u> <u>1 growth time</u> of tearing instability (classical resistivity) $\approx$ <u>1 day</u>. Need several growth times.

C. Present study

- Saturation properties (constant ψ vs. long wavelength)
- Energy conversion
- Behavior of physical properties in nonlinear mode.

II. Model

MHD equations: incompressible, η = const., $\nu = 0$, slab geometry

$$\nabla \times \left[\rho_0 \frac{d\vec{v}}{dt} - \frac{1}{4\pi} (\nabla \times \vec{B}) \times \vec{B} \right] = 0,$$

$$\frac{\partial \vec{B}}{\partial t} - \nabla \times \left(\vec{v} \times \vec{B} - \frac{c^2 \eta}{4\pi} \nabla \times \vec{B} \right) = 0.$$

$$\vec{v} = \nabla \phi \times \hat{e}_z, \quad \vec{B} = \nabla \psi \times \hat{e}_z$$

Initial field: $\vec{B}_0 = B_\infty \left[\tanh\left(\frac{y}{a}\right) \hat{e}_x + \operatorname{sech}\left(\frac{y}{a}\right) \hat{e}_z \right]$

where a = shear scale

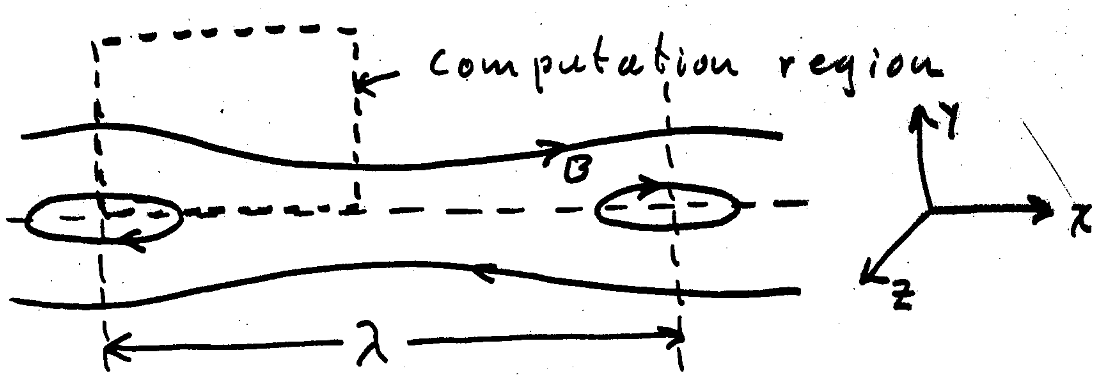

Initial disturbance: Linear tearing mode with magnitude ∋ linear, nonlinear terms ~ equal.

Parameters (Nondimensionalize w.r.t. a, $\frac{a}{\tau_h}$, B_∞)

$$S = \frac{\tau_r}{\tau_h} \; ; \quad \tau_r = \frac{4\pi a^2}{c^2 \eta} \; , \quad \tau_h = \frac{a\sqrt{4\pi \rho_0}}{B_\infty}$$

$$\alpha = ka = \frac{2\pi a}{\lambda}$$

III. Integrated behavior

Linear Dispersion Relation

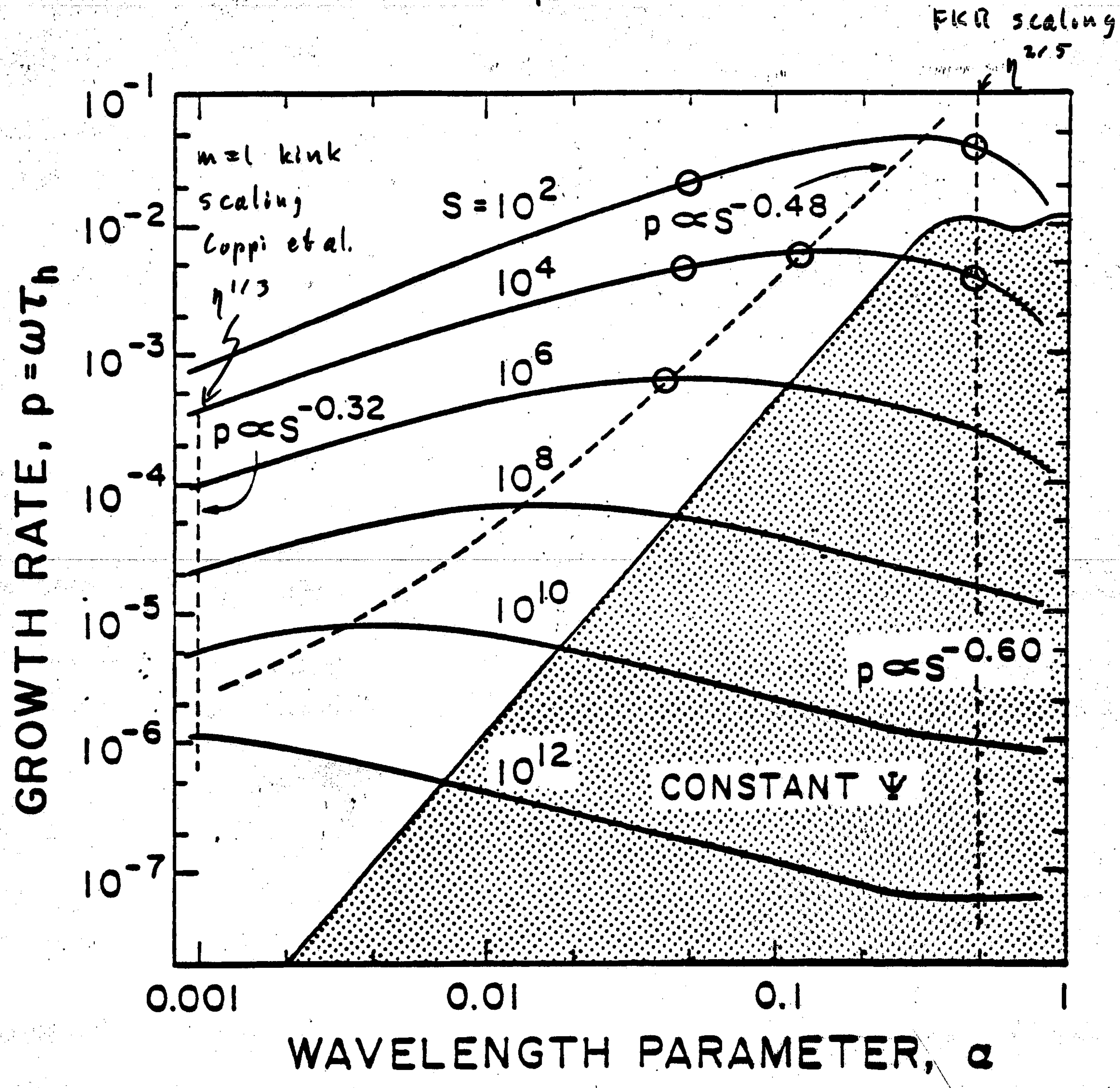

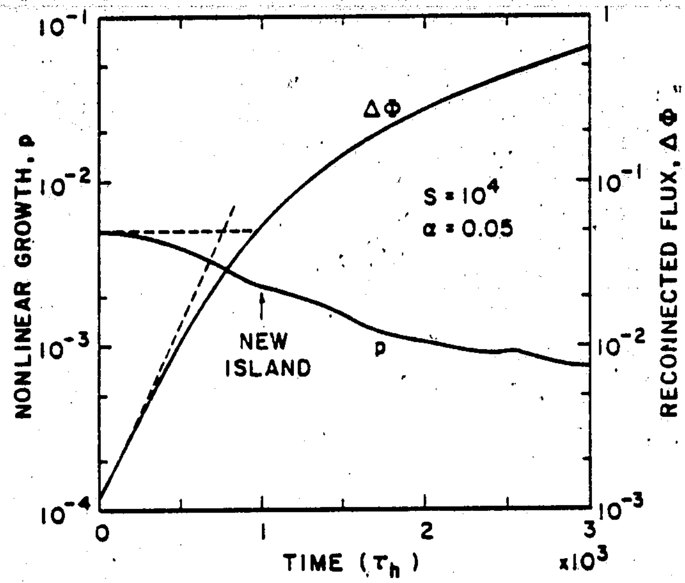

Long Wavelength

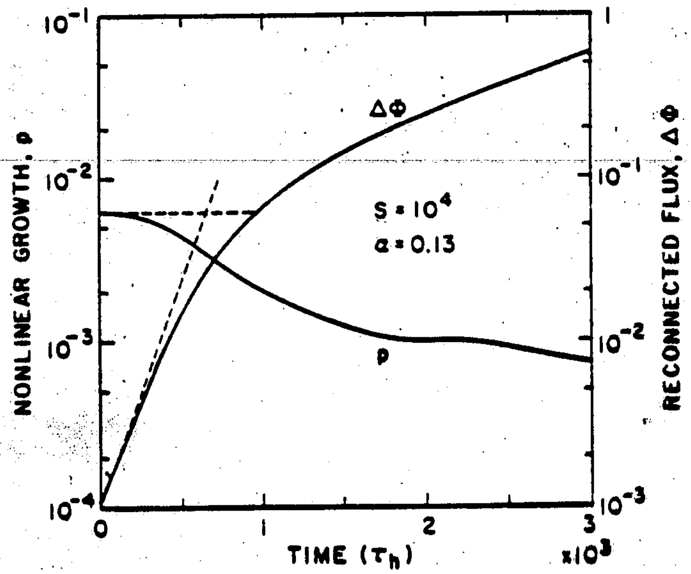

Maximum Linear Growth

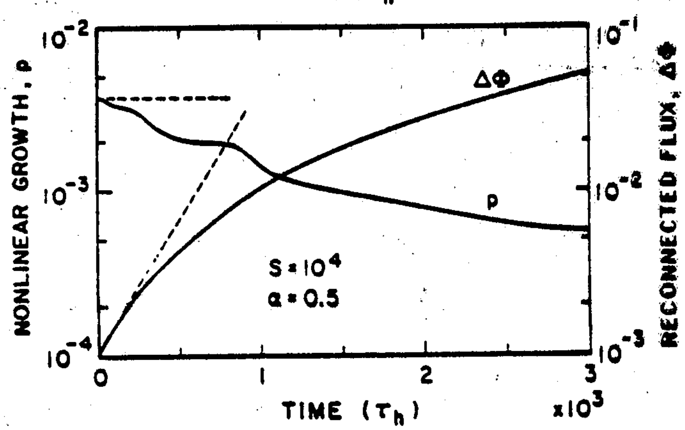

Constant ψ

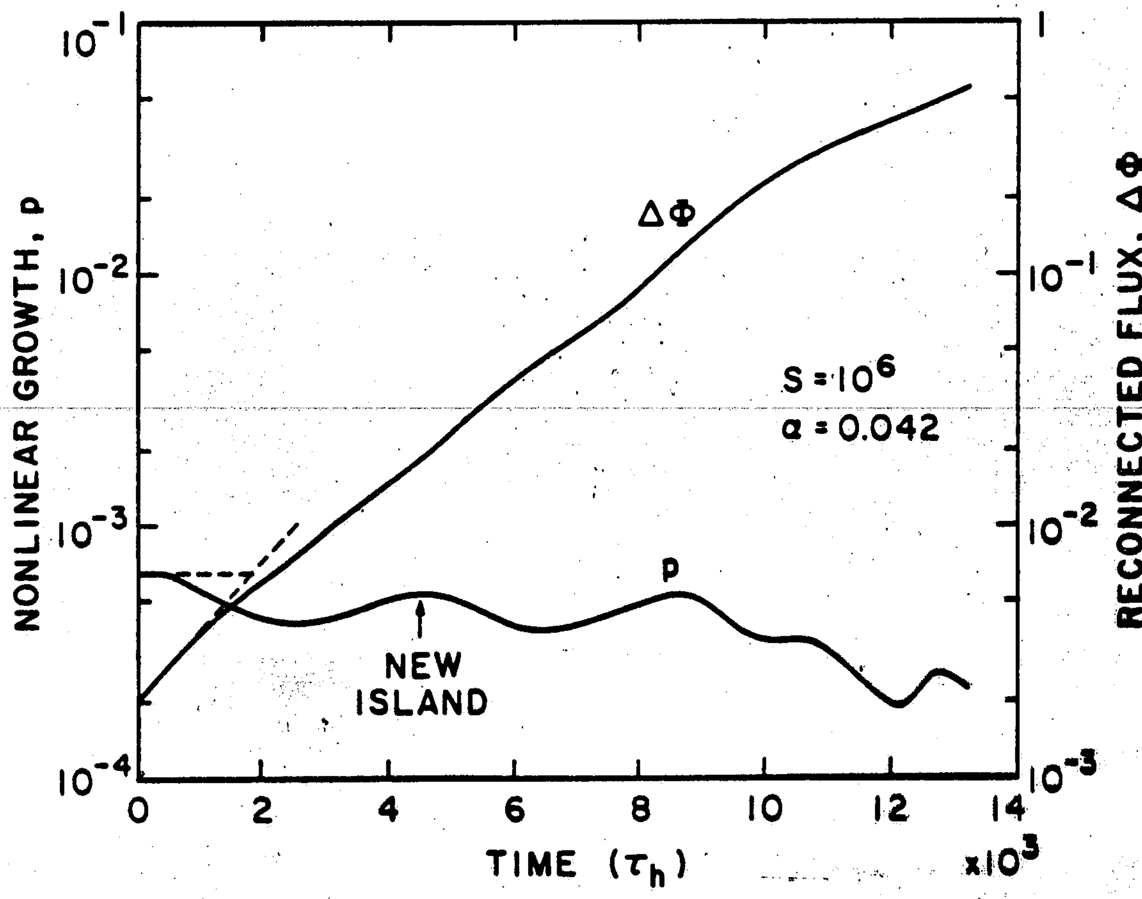
10^{-1}
10^{-2}
10^{-3}
10^{-4}
NONLINEAR GROWTH, p
1
10^{-1}
10^{-2}
10^{-3}
RECONNECTED FLUX, ΔΦ
ΔΦ
p
$S = 10^6$
$\alpha = 0.042$
NEW
ISLAND
0
2
4
6
8
10
12
14
TIME (τ_h)
$\times 10^3$

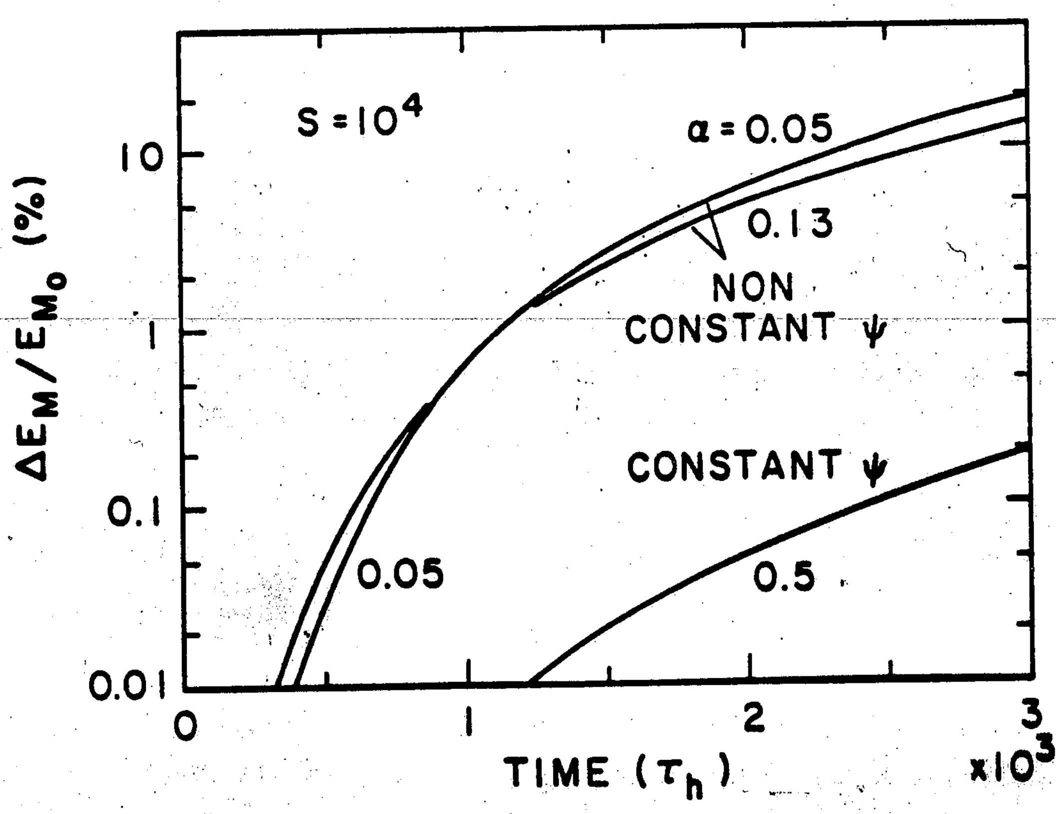
S = 10^4
α = 0.05
0.13
NON CONSTANT ψ
CONSTANT ψ
0.05
0.5
ΔE_M/E_M0 (%)
10
1
0.1
0.01
0
1
2
3
TIME (τ_h)
x10^3

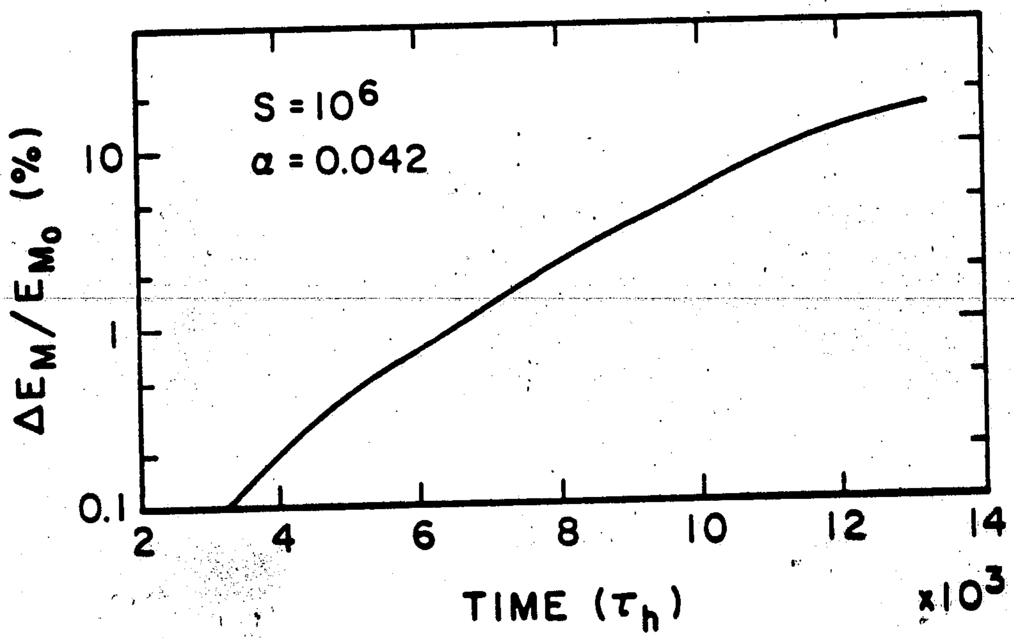

S = 10^6
α = 0.042
ΔE_M/E_M0 (%)
10
1
0.1
2
4
6
8
10
12
14
TIME (τ_h)
x10^3

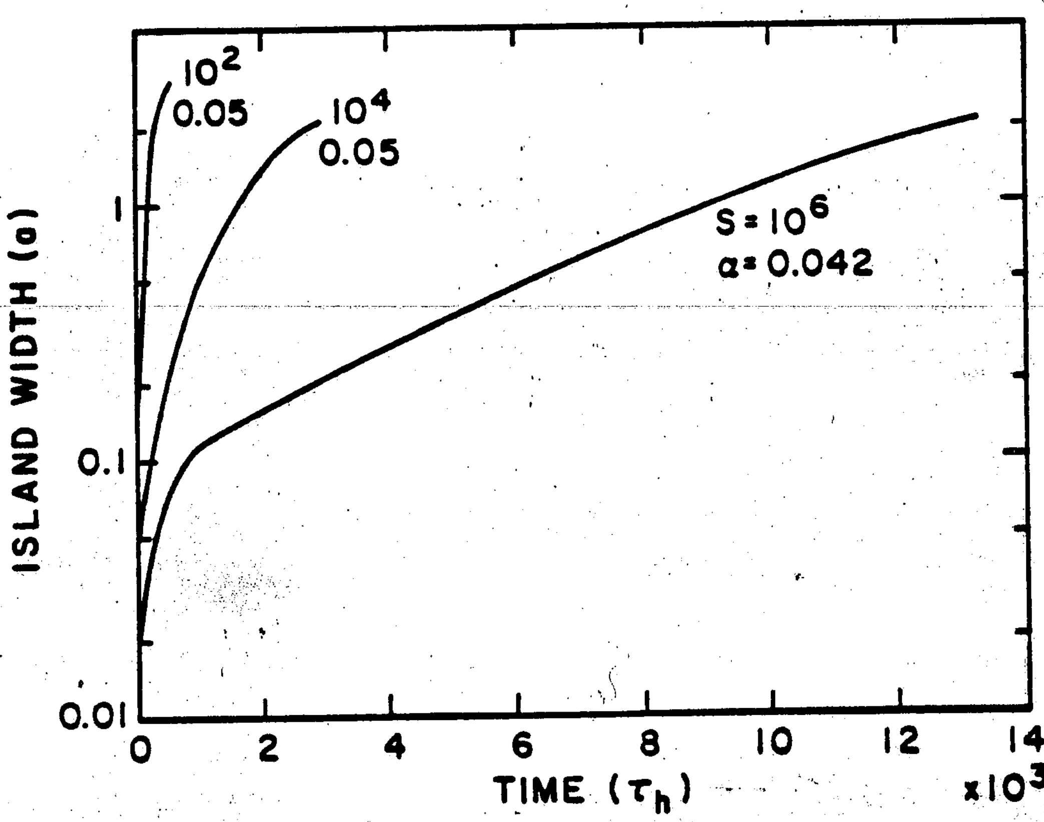

ISLAND WIDTH (a)
TIME (τh)
x10^3
0.01
0.1
1
0
2
4
6
8
10
12
14
10^2
0.05
10^4
0.05
S = 10^6
α = 0.042

$S = 10^4$

		Nonconstant ψ $\alpha = 0.05$	Constant ψ $\alpha = 0.5$	
Evolution time		15	11	τ_e
		116	119	sec
Energy release		1.2×10^8	3.8×10^5	ergs cm^{-2}
Energy source	(x)	90	100	%
	(z)	10	–	%
Energy budget	M_y	8	49	%
	M_z	0	3	%
	$K_x + K_y + K_z$	< 0.05	< 0.09	%
	thermal	92	48	%
$(J_{\parallel} / J_0)_{max}$		25	2	
$(E_{\parallel} / E_0)_{max}$		8×10^{-4}	6×10^{-5}	

IV. Spatial Structure

Temporal sequence-of-events in nonlinear evolution

1. X-point ⇒ current sheet (all parameter space)
2. Reverse flow vortex (all except $S = 100,\ a = 0.5$)
3. Second island or bifurcation ($S \gtrsim 10^3$, nonconstant ψ)

- Question: What's going on in these simulations?
- Requirements on numerics in order to simulate this behavior (not present in all nonlinear tearing computations).

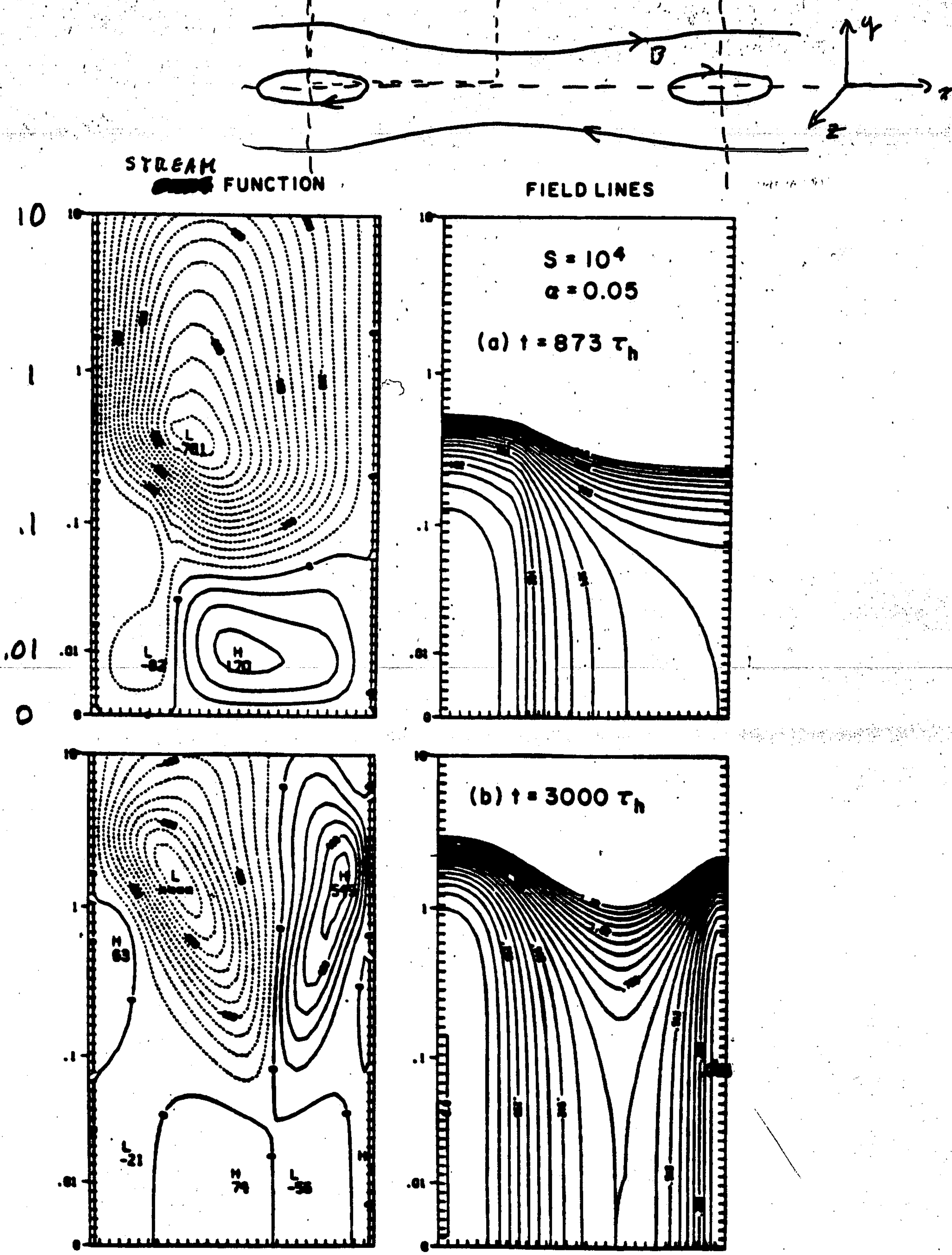
B
y
x
z
STREAM
[redacted] FUNCTION
FIELD LINES
10
1
.1
.01
0
S = 10^4
α = 0.05
(a) t = 873 τ_h
(b) t = 3000 τ_h

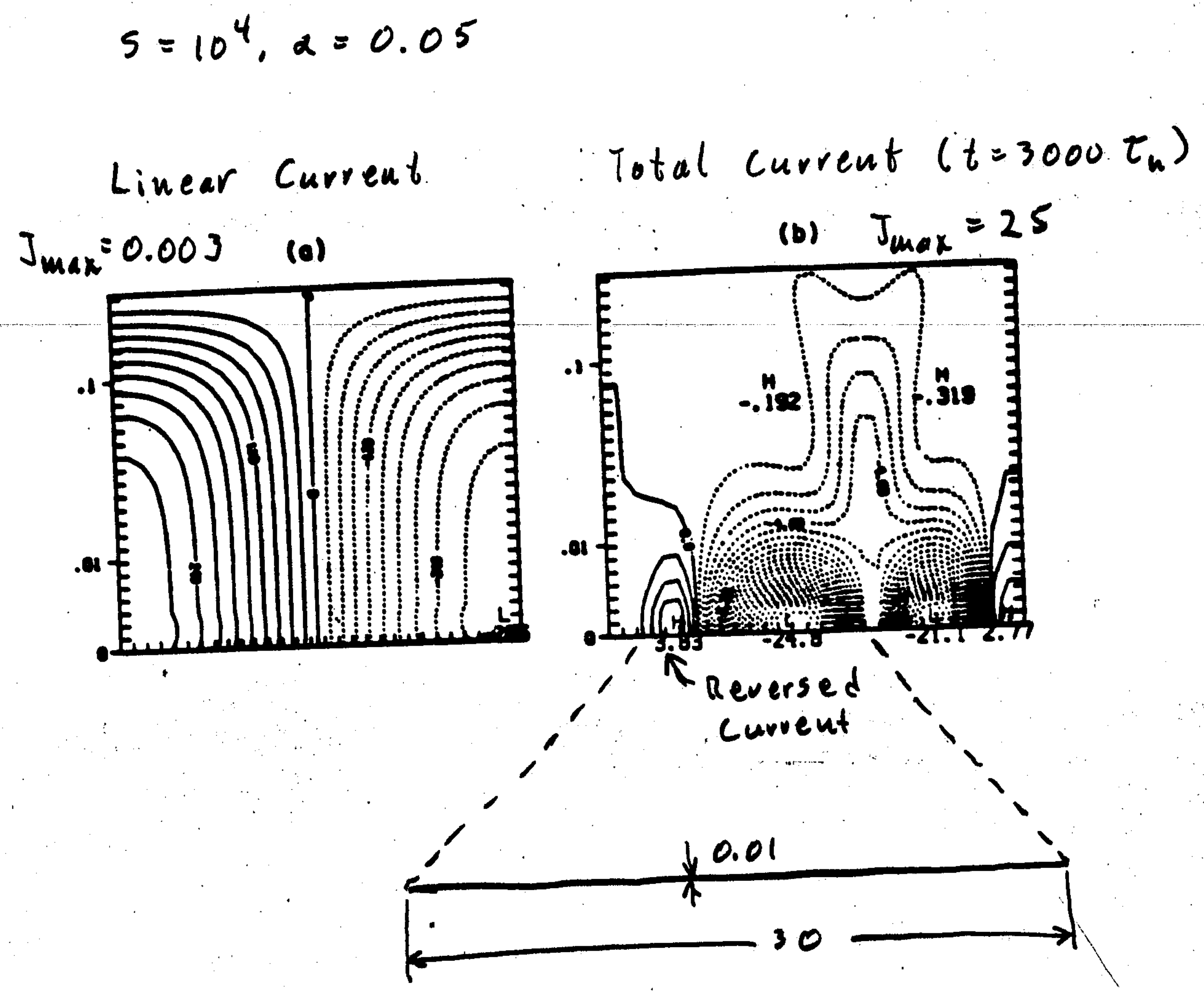
S = 10⁴, α = 0.05
Linear Current
Jmax = 0.003
(a)
Total current (t = 3000 τh)
(b)
Jmax = 25
.1
.01
0
H
-.192
H
-.319
3.83
-24.8
-21.1
2.77
Reversed Current
0.01
30

Current sheet formation

Syrovatskii's result: Current sheets form at time of variation of a Frozin-in magnetic field containing a neutral line or X-point (ideal MHD, $\nabla p = 0$)

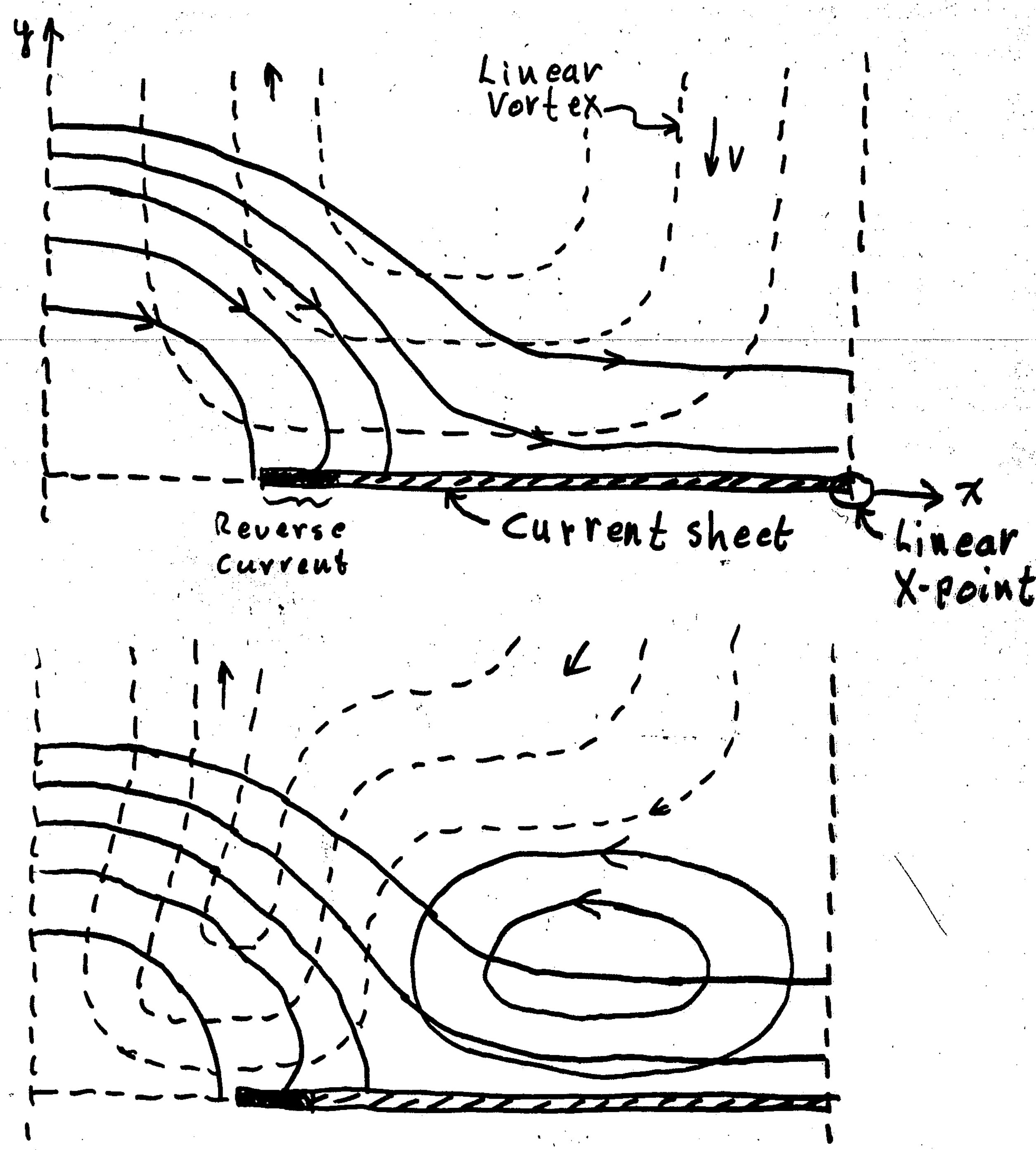

X-component of momentum equation-

$$\rho \frac{\partial v_x}{\partial t} = -\rho v_x \frac{\partial v_x}{\partial x} - \boxed{\rho v_y \frac{\partial v_x}{\partial y}} - \frac{1}{c} B_y J_z - \frac{\partial P}{\partial x}$$

Formation of reverse vortex

X-component of induction equation-

$$\frac{\partial B_x}{\partial t} = \frac{\partial}{\partial y}\left(v_x B_y - v_y B_x - \eta J_z \right)$$

Formation of second island

Note: • Nonlinear effect (terms not present in linear solution)
• Relevant terms contain y-derivatives ($\perp$ to current sheet)

Numerical resolution requirement: At $S = 10^4$, current sheet thickness ≈ 0.01. Use $\Delta y \approx 0.05$ near $y = 0$.

Result - No current sheets, reverse flow vortices, second islands

Conclusion - Fine numerical resolution essential. Approximately 2 orders of magnitude smaller than linear tearing layer thicknes.

Linear Tearing Mode

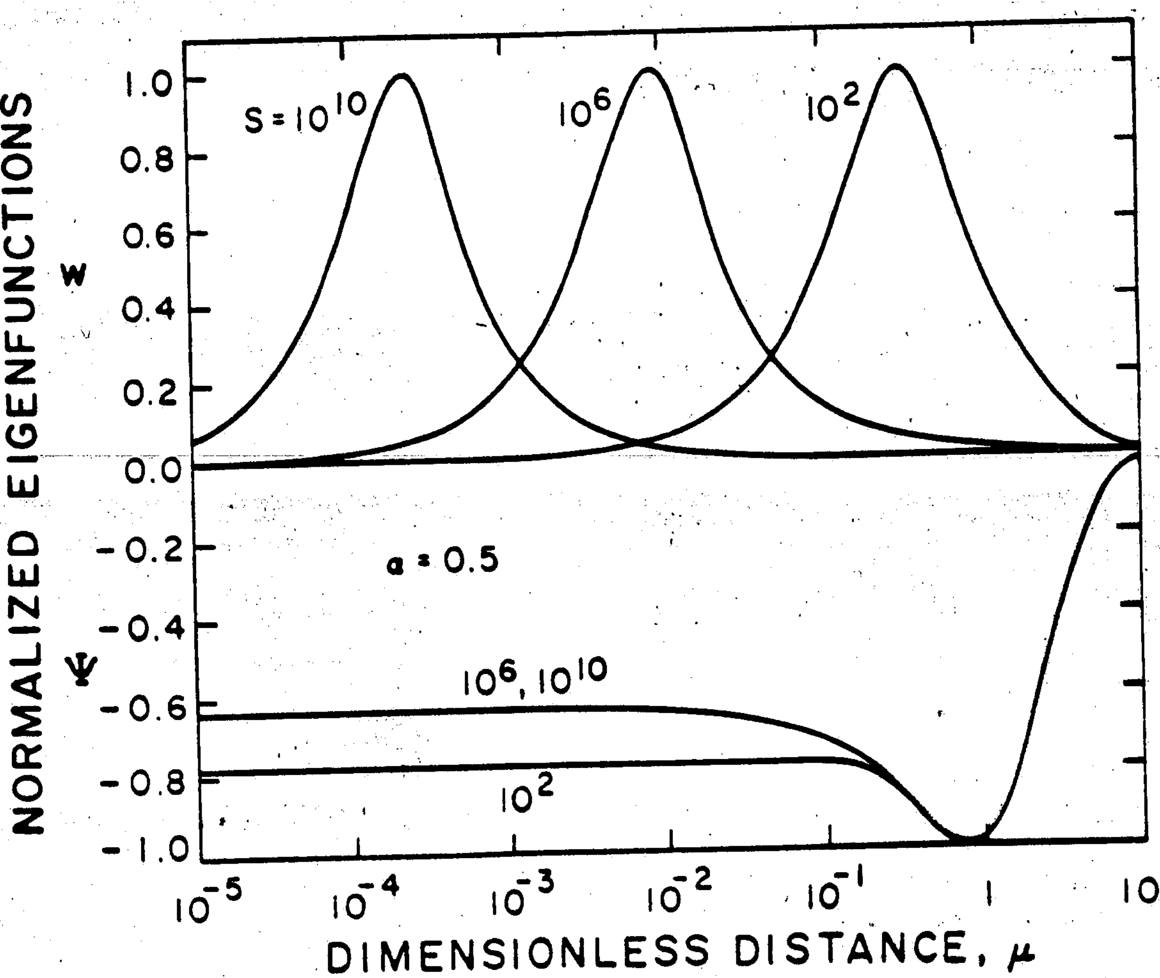

Possible alternative explanation for reverse vortices:
Build-up of back pressure due to symmetry conditions at center of island.

Result - Outflow in early stages. However, eventually obtain behavior as for symmetry conditions - with virtually no outflow.

Conclusion - Behavior governed by physics in tearing layer rather than by boundary conditions (for this case).

LIE TRANSFORM APPROACH TO DRIFT-RESONANT INTERACTIONS IN FLUID AND PLASMA TURBULENCE

B. McNAMARA

LAWRENCE LIVERMORE NATIONAL LAB

LIE TRANSFORM APPROACH TO DRIFT-RESONANT INTERACTIONS IN FLUID AND PLASMA TURBULENCE

BRENDAN McNAMARA, LLNL, US-JAPAN WORKSHOP ON MAGNETIC RECONNECTION, IFS. DEC. 1984.

- A Dominant Mechanism for generating high wave-number modes at the onset of turbulence is the drift-resonant interaction of a few large scale modes.

- RESONANT COUPLING BETWEEN $\underline{K}$ AND LARGE $\underline{K}'$ IS LIKE

$$\epsilon\, V_{\underline{K}} \cdot \frac{V_{K'}}{d^2_{K'}} \cdot \left\{ a_K \sqrt{\epsilon} \left(\frac{k_1'}{k_1} + 1 \right) \right\}^{1/k_1 \omega_D \sqrt{\epsilon}}$$

BUT MODE-MODE COUPLING IS LIKE $\epsilon^{[K'/K]}$

- BENARD CONVECTION DISPLAYS ISLANDS LIKE $\underline{B}$ IN TOKAMAK
- LIE TRANSFORM PRIMER
- RESONANT INTERACTIONS OF COUPLED OSCILLATORS
- 'PINBALL' MODEL OF DIFFUSION WITH MANY RESONANCES 'RFP ?'
- LIE TRANSFORM APPROACH TO REDUCED MHD TURBULENCE.

BULL. AM. PHYS. SOC., NOVEMBER 1984.
WORK BEGUN AT CULHAM LABORATORY, 1983, WITH J. B. TAYLOR, J. A. CONNOR, et al.

BENARD CONVECTION PROBLEM

(WAYNE ARTER, CULHAM '83)

J FLUID MECH, '83/84

$$\underline{u} = \frac{d\underline{X}}{dt} = \nabla \times \nabla \times f\, \hat{z} \qquad f = \cos x \cos y \sin z + \epsilon(\cos 2x + \cos 2y)\sin 2z$$

$$= f_1 + \epsilon f_2$$

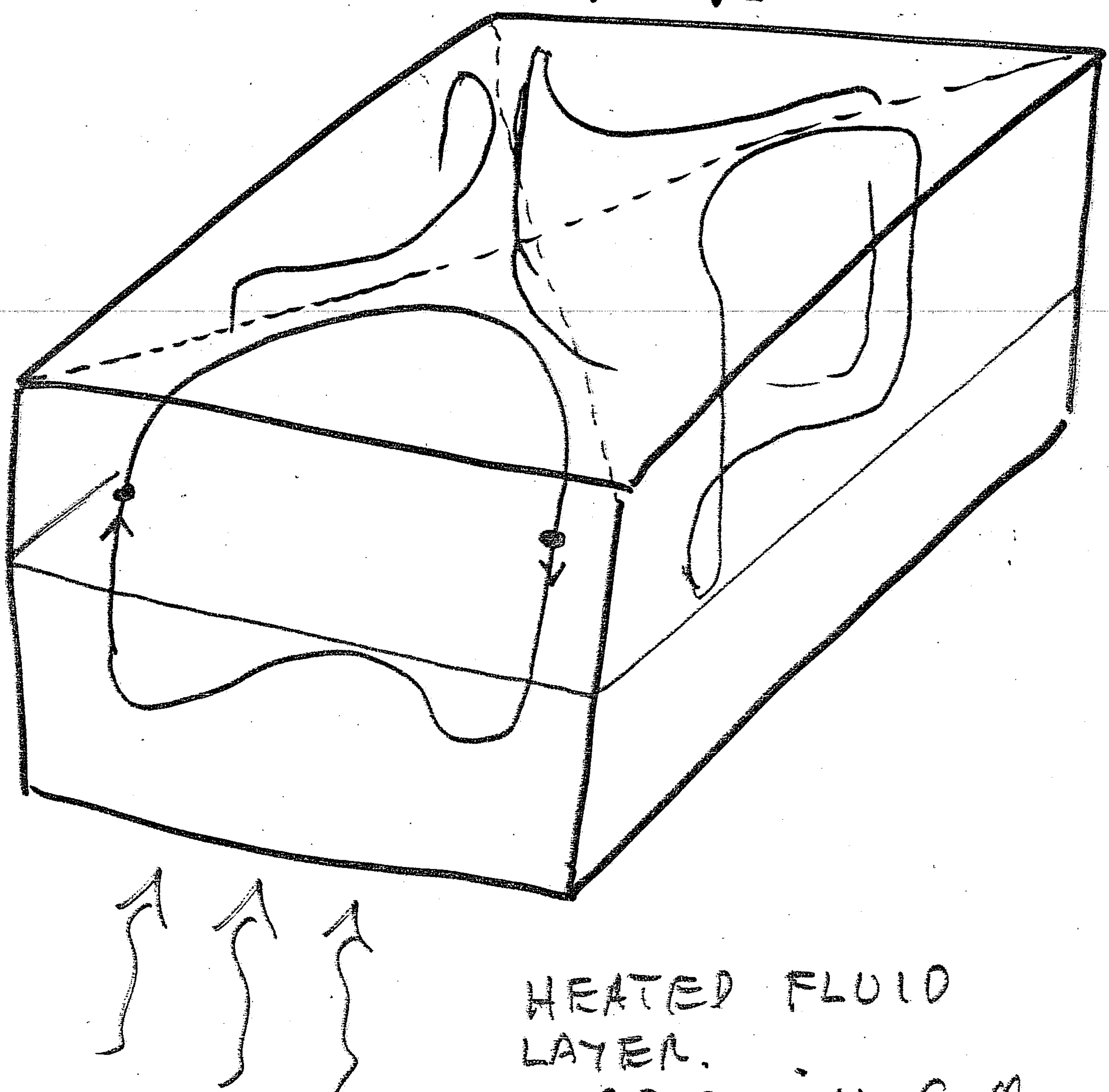

HEATED FLUID LAYER.

∞ 2D Periodic Cells.

(14.)

FLOW LINE SURFACE OF SECTION
AT $\epsilon = .1$

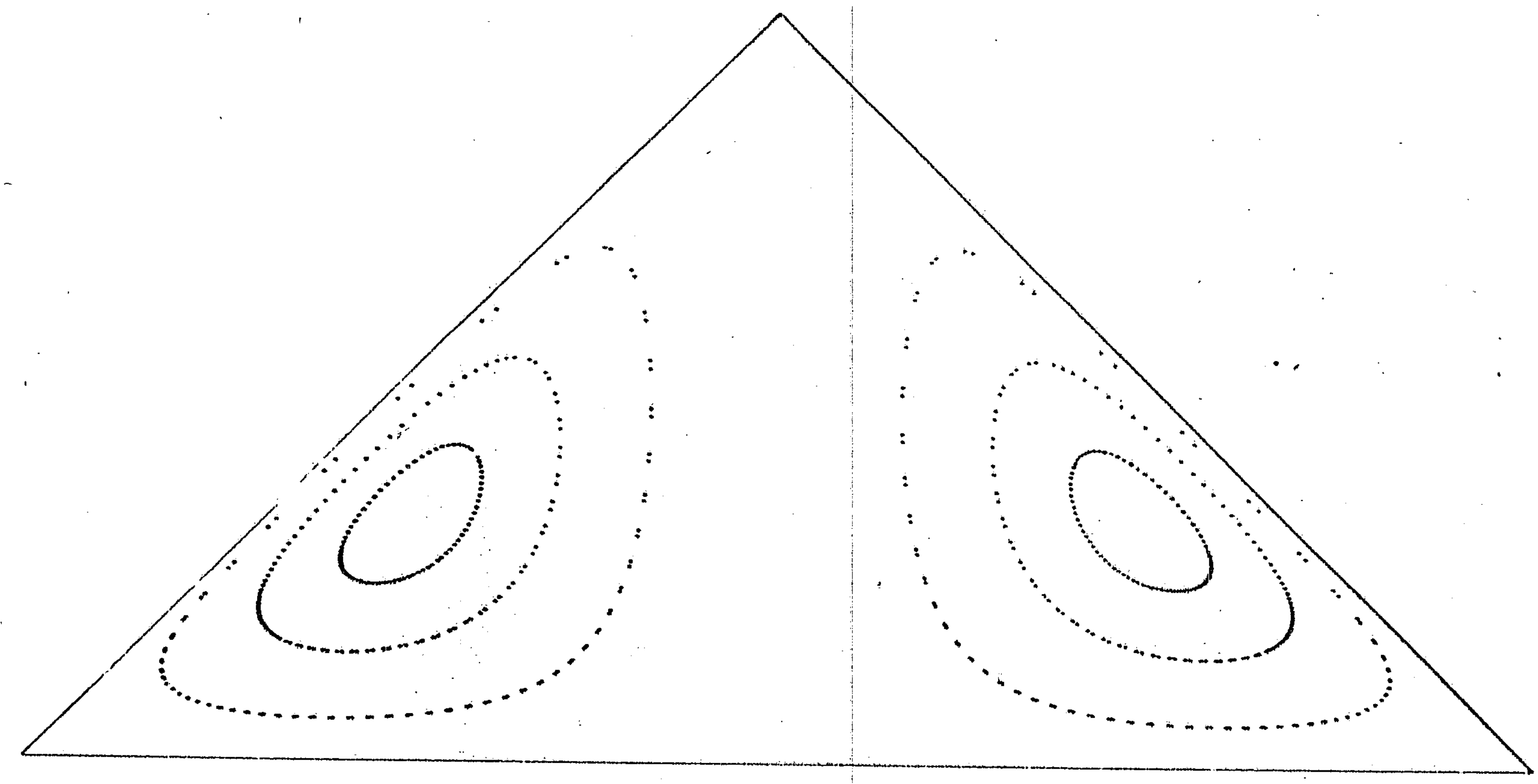

Spit

(5)

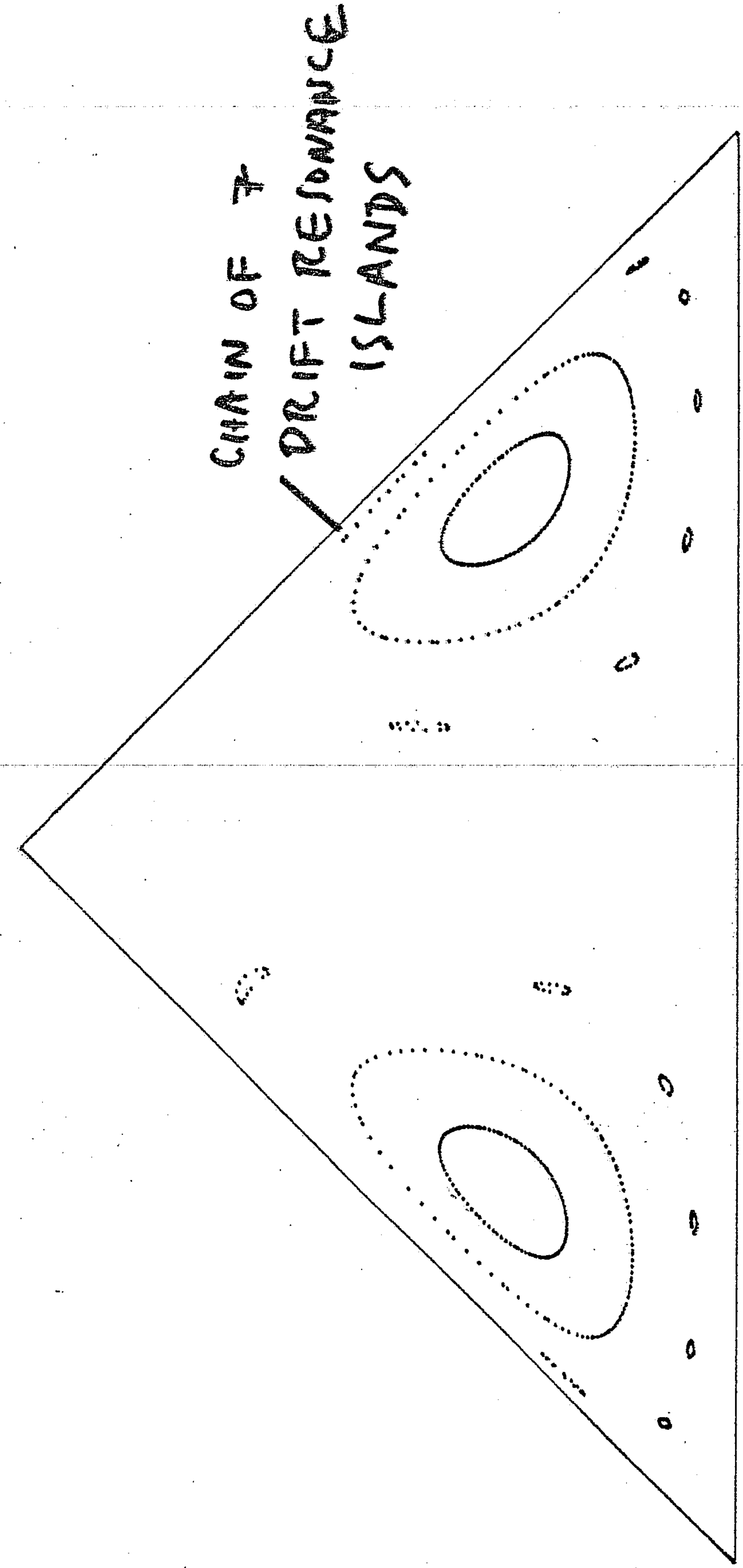

16

FLOW LOOKS
STOCHASTIC

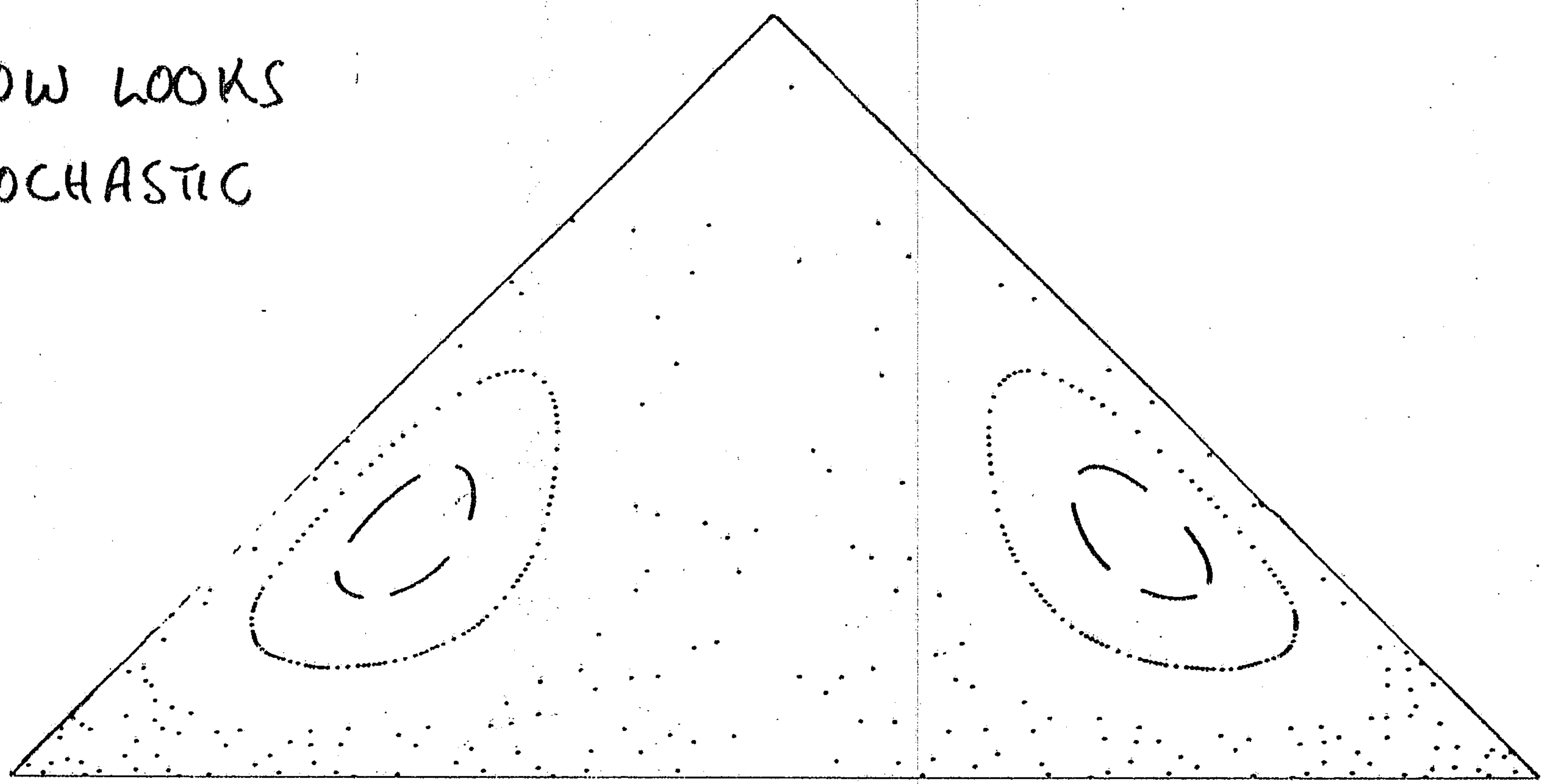

(17)

REGULAR MOTION NEAR O-POINT ONLY.
BUT NOTE REMNANTS OF DRIFT SURFACES

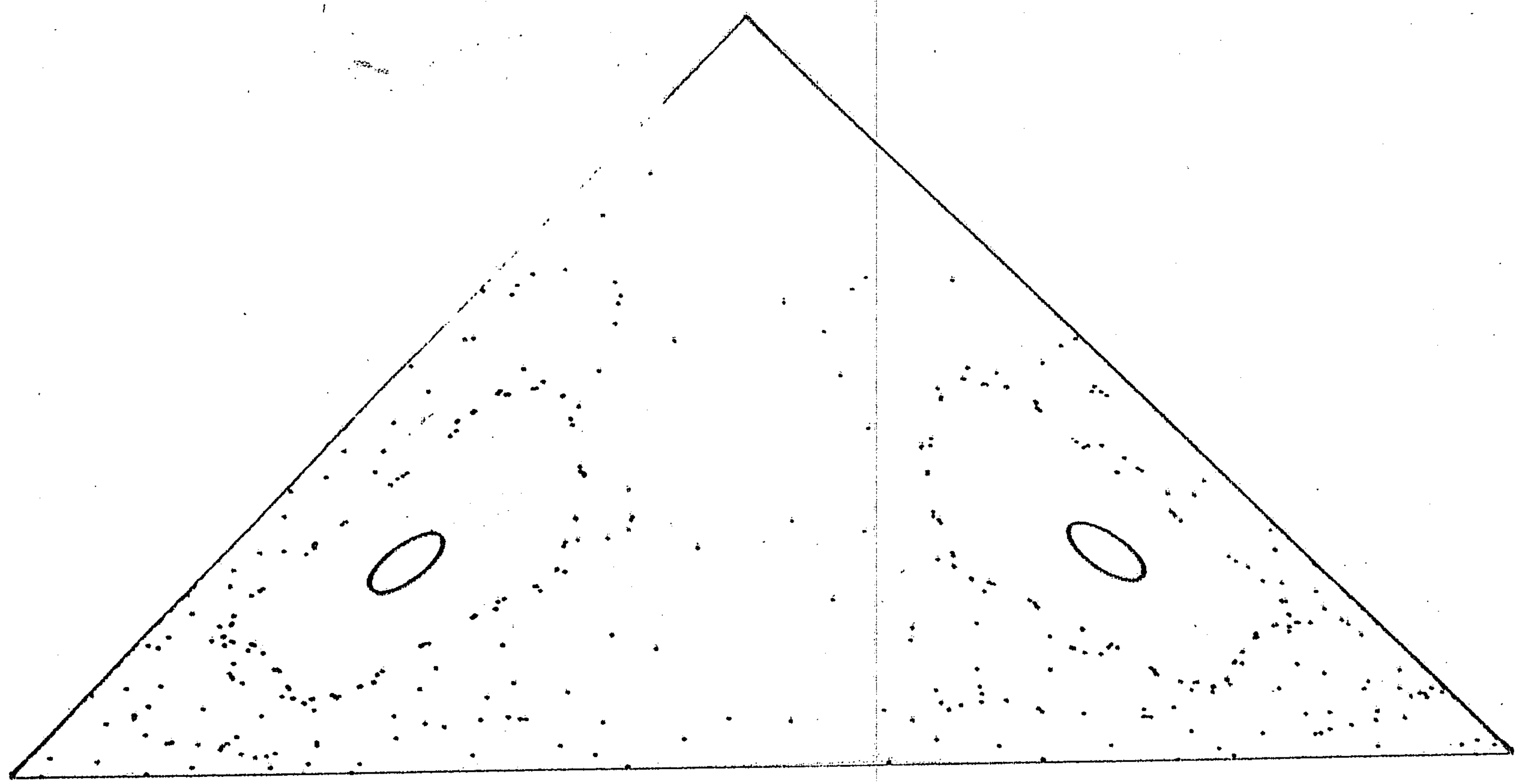

HAMILTONIAN FOR FLUID FLOW.

B.M. BOGHOSIAN, B. McNAMARA, DYNAMICS DAYS, LA JOLLA, 1985.

COMPARE

$$\nabla \cdot \underline{u} = 0 \qquad \frac{\partial f}{\partial t} + [H, f] = 0$$

CONSERVES —

$$F = \iint_A u_z \, dx\, dy \qquad J = \oint_C p \, dq$$

IDENTIFY CANONICAL VARIABLES AS

$$p = \int u_z \, dy \qquad q = x \qquad t = z$$

$$\therefore \; p = 2\cos x \sin y \sin z + 4\epsilon\left(y\cos 2x + \tfrac{1}{2}\sin 2y\right)\sin 2z$$

FROM EQNS. OF MOTION

$$\frac{dp}{dz} = -\frac{\partial H}{\partial x} \qquad \frac{dx}{dz} = \frac{\partial H}{\partial p} \equiv \frac{u_x}{u_z}$$

THEN

$$H = \int u_x \, dy = -\sin x \sin y \cos z - 2\epsilon y \sin 2x \cos 2z$$

OR

$$\boxed{H \equiv -\frac{p}{2}\frac{\tan q}{\tan t} + \epsilon h_1(p, q, t)}$$

(5)

THE BASIC LIE TRANSFORM

$$\mathcal{L} = e^{\epsilon[\hat{H}_1,\ ]}$$

$$\mathcal{L}^{-1} = e^{-\epsilon[\hat{H}_1,\ ]}$$

EASY INVERSE

DEFINITIONS

ORBIT OPERATOR $[H_0,\ ]$

AVERAGE OP. $\bar{H}_1 = \oint H_1\, dq_1$

PROPOGATOR $\hat{H}_1 = \int (H_1 - \bar{H}_1)\, dq_1 \Big/ \frac{\partial H_0}{\partial P_1}$

AND $[H_0, \hat{H}_1] = H_1 - \bar{H}_1$

RESULT OF APPLYING OPERATOR

$$\mathcal{L}\cdot H = \left(1 + \epsilon[\hat{H}_1\ ] + \frac{\epsilon^2}{2}[\hat{H}_1[\hat{H}_1\ ]] + \cdots\right)\cdot(H_0 + \epsilon H_1)$$

$$= H_0 + \epsilon H_1$$
$$+ \epsilon[\hat{H}_1, H_0]$$
$$+ \frac{\epsilon^2}{2}[\hat{H}_1, [\hat{H}_1, H_0]] + \epsilon^2[\hat{H}_1, H_1] + \cdots$$

$$= H_0 + \epsilon\bar{H}_1 + \frac{\epsilon^2}{2}[\hat{H}_1, H_1 + \bar{H}_1] + \cdots$$

REPEAT PROCESS TO GET $O(\epsilon^n)$ TRANSFORM

B. McNAMARA. J. MATH. PHYS. 19 2154. (1978)

RESONANT PERTURBATION OF COUPLED OSCILLATORS IN A SHEARED SYSTEM

$$H = H_A(p_1) + p_2 - \epsilon \sum_{K'} V_{K'} \cos(k_1' q_1 - k_2' q_2)$$

$$= \underbrace{H_A(p_1) + p_2 - \epsilon V_K \cos(K \cdot Q)}_{\substack{K^{TH} \text{ ISLAND CHAIN WHEN} \\ k_1 H_A' - k_2 = 0}} - \epsilon \underbrace{\sum{}^{*} V_{K'} c_{K'}}_{\substack{\text{OSCILLATES} \\ \text{NEAR } K^{TH} \text{ CHAIN.}}}$$

$V_{nK} \equiv 0$ for simplicity.

LIE TRANSFORM GENERATOR TO AVERAGE Σ^*

$$\mathcal{L} = e^{-\epsilon[\hat{\Sigma}^*, \,]} \qquad \hat{\Sigma}^* \equiv \sum{}^{*} \frac{V_{K'} S_{K'}}{k_1' H_A' - k_2'} \equiv \sum{}^{*} \frac{V_{K'} S_{K'}}{d_{K'}}$$

ALL $d_{K'} \neq 0$.

THEN

$$\mathcal{L} \cdot H = H_A + p_2 - \epsilon V_K c_K$$
$$- \frac{\epsilon^2}{2} \sum_{K''}{}^{+} \sum_{K'}{}^{*} \left(c_{K'} c_{K''} \frac{V_{K'}}{d_{K'}} [V_{K''}, K' \cdot Q] + s_{K'} s_{K''} V_{K''} \left[\frac{V_{K'}}{d_{K'}}, K'' \cdot Q\right] \right)$$
$$+ O(\epsilon^3)$$

Σ^{+} includes $2V_K$, Σ^* has no V_K.

ϵ^2 TERM IS LEADING PART OF EFFECT ON K^{TH} CHAIN OF $(K;K')$ INTERACTIONS AND (K',K'') MODE COUPLING.

SECONDARY ISLANDS.

TRANSFORM TO FRAME OF K

TRANSFORM TO FRAME OF $\underline{K}^{TH}$ CHAIN

$$Q_1 = k_1 q_1 - k_2 q_2 \qquad Q_2 = q_2$$

WHEN

$$c_{K'} c_{K''} \rightarrow \cos\left(\frac{(k_1' + k_1'')}{k_1} Q_1 + Q_2\left(\frac{k_2}{k_1}(k_1' + k_1'') - (k_2' + k_2'') \right)\right)$$

THEN TRANSFORM TO DRIFT COORDS. ON THE ISLAND.

$$Q_1 \doteq a\sqrt{\epsilon}\cos Q_D \qquad \text{(Actually an elliptic fn. of } \Theta_D\text{).}$$

SO

$$c_{K'} c_{K''} \rightarrow \sum_m J_m\left(a\sqrt{\epsilon}.(k_1' + k_1'')/k_1\right)\cos(mQ_D - LQ_2)$$

RESONANCE CONDITION

$$m\omega_D\sqrt{\epsilon} = k_2' + k_2'' - \left(\frac{k_2}{k_1}\right)(k_1' + k_1'') \qquad \neq 0$$

REQUIRE m TO BE AS SMALL AS POSSIBLE,

$$m \sim 1/k_1\omega_D\sqrt{\epsilon} \qquad \text{INDEPENDENT OF } K', K''$$

$$\text{SO} \quad J_m \sim \left(a\sqrt{\epsilon}\,\frac{k_1' + k_1''}{k_1}\right)^{\frac{1}{k_1\omega_D\sqrt{\epsilon}}}$$

RESONANT COUPLING TO HIGH MODE K' IS

$$\boxed{\epsilon^2\left(\frac{V_{K'}}{d_{K'}^2}\right) V_K \left(a\sqrt{\epsilon}\left(\frac{k_1'}{k_1} + 1\right)\right)^{1/k_1\omega_D\sqrt{\epsilon}}}$$

COUPLING DIAGRAM

NOTE: ANY MODE, $\underline{K}'$, GIVES ∞ NUMBER OF DRIFT RESONANCES AT K^{th} CHAIN.

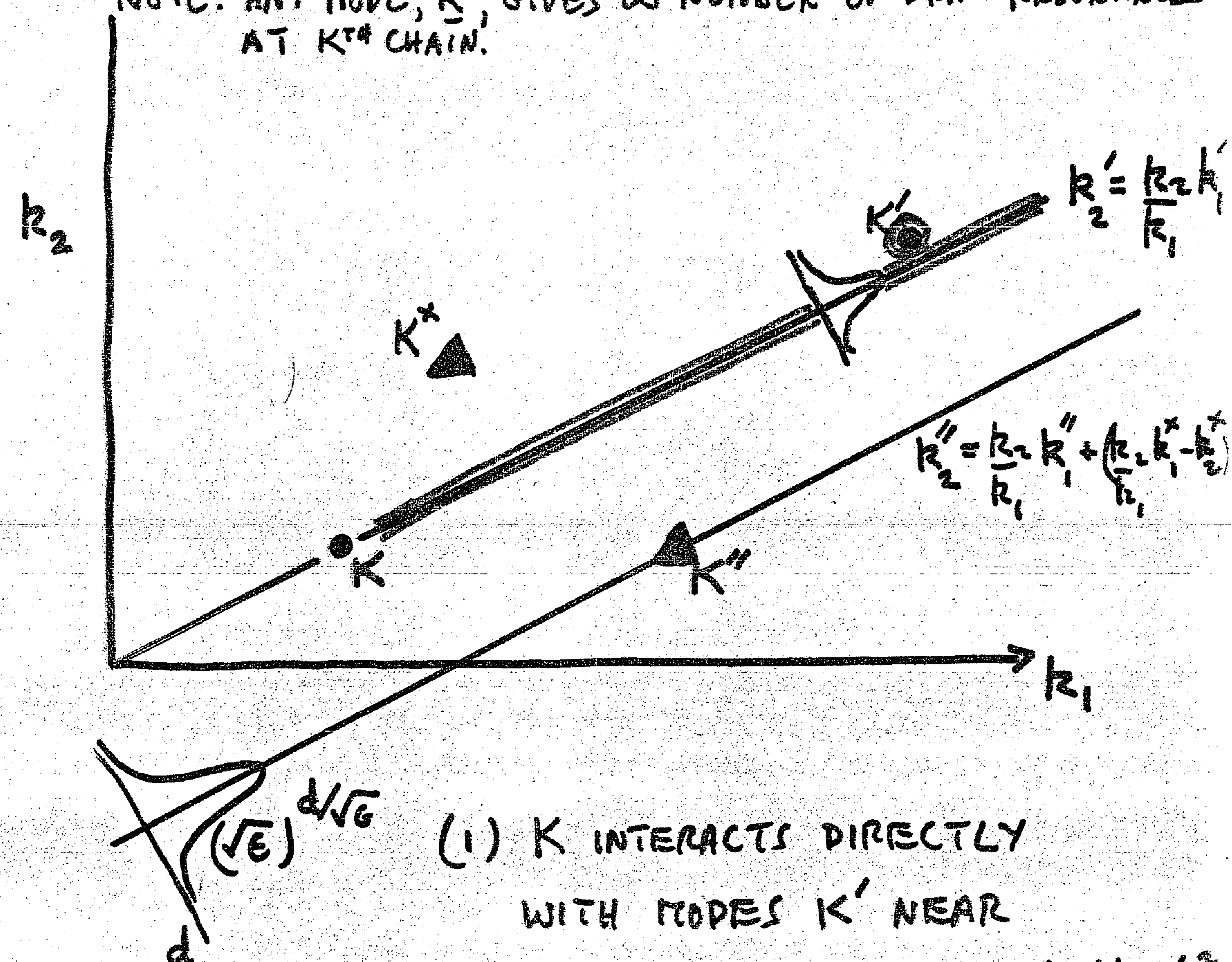

(1) K INTERACTS DIRECTLY WITH MODES K' NEAR RESONANCE LINE. $V_K V_{K'}/d_{K'}^2$

(2) K^x AND K'' BEAT AT ISLAND $V_{K^x} V_{K''}/d_{K''}^2$

$\therefore$ PERTURBATION THEORY FINDS RESONANCE ONLY WHEN $\underline{K}' = nK + mK''$, COUPLING $\sim \epsilon^{n+m}$

LIE TRANSFORM OF LIOUVILLE EQN. (10)

$$\frac{\partial f}{\partial t} + [H, f] = 0 \qquad f = f(\underline{x}, \dot{\underline{x}}, t)$$

INTRODUCE CONJUGATE PAIR $(\mathcal{E}, t)$, ENERGY & TIME

$$K = \mathcal{E} - H \equiv 0$$

THEN, IN EXTENDED PHASE SPACE,

$$[K, f] = 0$$

LIE TRANSFORM

$$\mathcal{L}\cdot[K, f] \equiv [\mathcal{L}\cdot K, \mathcal{L}\cdot f] = 0$$

OR
$$[K_0 + \epsilon\bar{K}_1 + \frac{\epsilon^2}{2}[\hat{R}_1, K_1 + R_1] + \cdots, f(P, Q, T)] = 0$$

'PINBALL MACHINE' DIFFUSION MODEL (3)

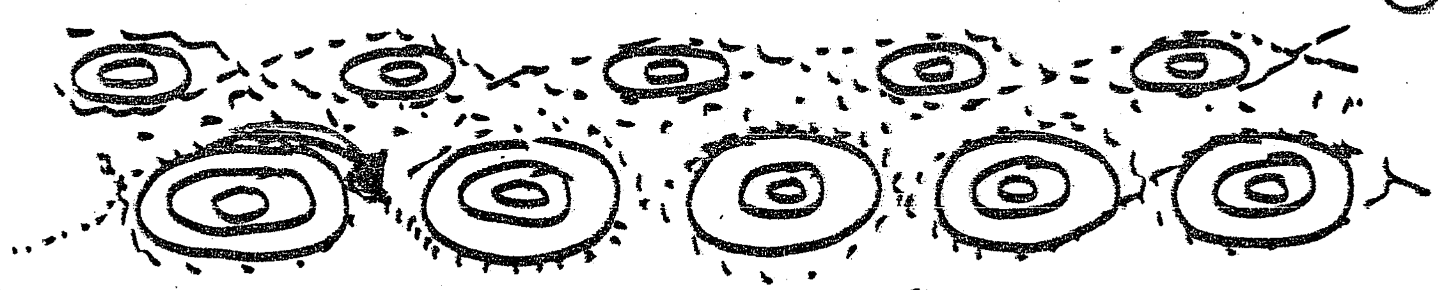

QUASILINEAR THEORY GIVES

$$[K_0 + \epsilon^2 K_2, f] = 0 \qquad f = f_0 + \tilde{f}$$

DIFFUSION IN J-SPACE:

$$[K_0, f_0] - \epsilon^4 \langle [K_2, [\oint_{\text{SEP-X}} K_2, f_0]\rangle = 0$$

TOKAMAK DISRUPTIONS

HISTORY OF TEARING MODE GROWTH

1961 (1) LINEAR PHASE. GROWS LIKE $e^{\gamma t}$

$$\gamma \sim O(\eta^{3/5})$$

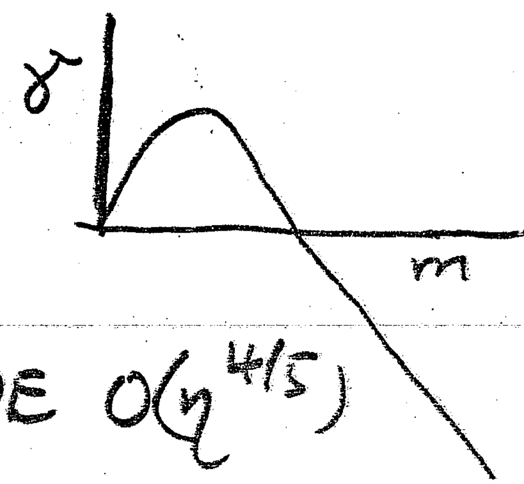

1973 (2) RUTHERFORD PHASE,

SATURATES AT AMPLITUDE $O(\eta^{4/5})$

GROWS LIKE $(\eta t)^2$

1979 (3) DISTORTION OF EQUILIBRIUM DESTABILISES OTHER MODES

(4) INTERACTION OF ALL MODES → EXPLOSIVE DISRUPTION.!!

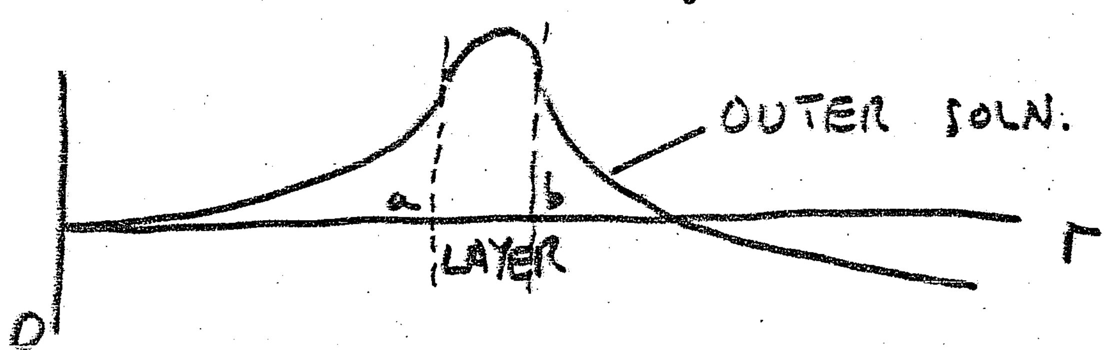

$$\Delta' = \left[\frac{1}{\psi}\frac{\partial \psi}{\partial r}\right]_a^b$$

REDUCED MHD TEARING MODE EQNS

$$\frac{\partial \psi}{\partial t} - \eta \nabla_\perp^2 \psi = \underline{B} \cdot \nabla \phi \qquad \underline{B} = B_z \hat{z} + \nabla \psi \times \hat{z}$$

$$\frac{\partial u}{\partial t} + \underline{V} \cdot \nabla u = \underline{B} \cdot \nabla (\nabla_\perp^2 \psi) \qquad u = \nabla_\perp^2 \phi$$

$$\underline{V} = \nabla \phi \times \hat{z}$$

The reduced resistive magnetohydrodynamic equations for a current-carrying magnetofluid in a sheared slab are:

$$\begin{aligned} \frac{\partial \psi_{\mathbf{k}}}{\partial t} &+ \Bigg\{\Bigg[\frac{\partial}{\partial r}\Bigg(\sum_{\mathbf{k}'}(-ik'_y)\phi_{-\mathbf{k}'}\psi_{\mathbf{k}''}\Bigg) - ik_y \sum_{\mathbf{k}'} \frac{\partial \phi_{-\mathbf{k}'}}{\partial r}\psi_{\mathbf{k}''}\Bigg] \\ &- \Bigg[\frac{\partial}{\partial r}\Bigg(\sum_{\mathbf{k}'}(-ik'_y)\psi_{-\mathbf{k}'}\phi_{\mathbf{k}''}\Bigg) - ik_y \sum_{\mathbf{k}'} \frac{\partial \psi_{-\mathbf{k}'}}{\partial r}\phi_{\mathbf{k}''}\Bigg]\Bigg\} \\ &= -ik_\parallel \phi_{\mathbf{k}} + \eta \nabla_\perp^2 \psi_{\mathbf{k}}, \end{aligned} \tag{47}$$

and

$$\begin{aligned} \frac{\partial}{\partial t}(\nabla_\perp^2 \phi_{\mathbf{k}}) &+ \Bigg\{\Bigg[\frac{\partial}{\partial r}\Bigg(\sum_{\mathbf{k}'}(-ik'_y)\phi_{-\mathbf{k}'}\nabla_\perp^2\phi_{\mathbf{k}''}\Bigg) - ik_y \sum_{\mathbf{k}'} \frac{\partial \phi_{-\mathbf{k}'}}{\partial r}\nabla_\perp^2\phi_{\mathbf{k}''}\Bigg] \\ &- \Bigg[\frac{\partial}{\partial r}\Bigg(\sum_{\mathbf{k}'}(-ik'_y)(\nabla_\perp^2\phi_{-\mathbf{k}'})\phi_{\mathbf{k}''}\Bigg) - ik_y \sum_{\mathbf{k}'} \Bigg(\frac{\partial}{\partial r}\nabla_\perp^2\phi_{-\mathbf{k}'}\Bigg)\phi_{\mathbf{k}''}\Bigg] \\ &= -ik_\parallel \nabla_\perp^2 \psi_{\mathbf{k}} + ik_y \frac{dJ_0(r)}{dr}\psi_{\mathbf{k}} + \Bigg[\frac{\partial}{\partial r}\Bigg(\sum_{\mathbf{k}'}(-ik'_y)\psi_{-\mathbf{k}'}\nabla_\perp^2\psi_{\mathbf{k}''}\Bigg) - ik_y \sum_{\mathbf{k}'} \frac{\partial \psi_{-\mathbf{k}'}}{\partial r}\nabla_\perp^2\psi_{\mathbf{k}''} \\ &- \Bigg[\frac{\partial}{\partial r}\Bigg(\sum_{\mathbf{k}'}(-ik'_y)\nabla_\perp^2\psi_{-\mathbf{k}'}\psi_{\mathbf{k}''}\Bigg) - ik_y \sum_{\mathbf{k}'} \frac{\partial}{\partial r}(\nabla_\perp^2\psi_{-\mathbf{k}'})\psi_{\mathbf{k}''}\Bigg]\Bigg\}. \end{aligned}$$

 DIAMOND, HAZELTINE, AN, CARRERAS, HICKS.

RECONNECTION

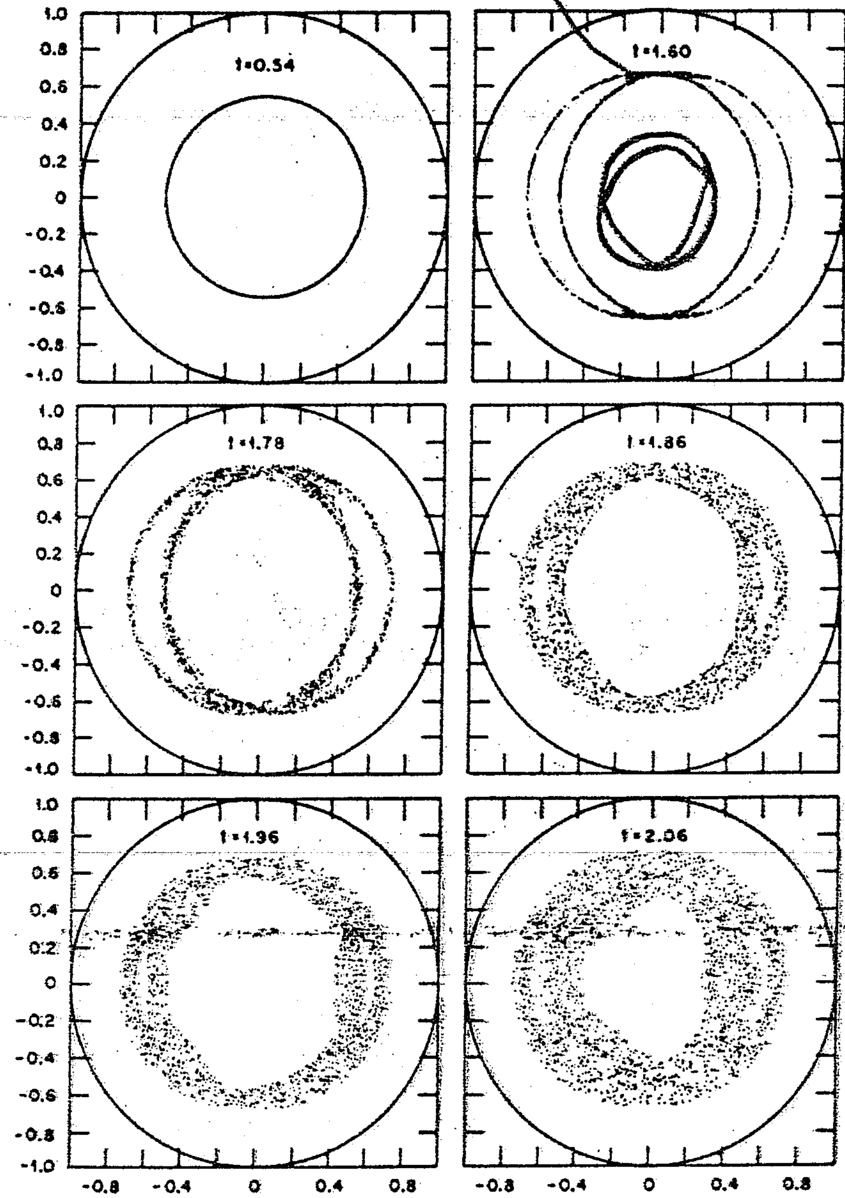

MAGNETIC SURFACES FOR 2:1 MODE IN PRESENCE OF 3:2 AND OTHERS.

FIG. 11. Intersection of a single-magnetic field line with the poloidal plane $\zeta=0$. The field line goes through the point $r=0.54a$, $\theta=0$, and $\zeta=0$. The times are the same as in Fig. 8.

at the end of the calculation (see Fig. 13).

The presence of large spikes in the toroidal current density profile suggests that effects such as parallel electron viscosity could be very important.[20] A numerical calculation by Welter and Biskamp[10] including this effect did not show any qualitative change in the results, only an acceleration in time scale.

The nonlinear process just described does not change much when the resistivity is kept constant in time instead of being permitted to evolve. There is a slightly faster development of the nonlinear interaction when the resistivity is allowed to change in time, with values of $\overline{\chi}_\parallel$ and $\overline{\chi}_\perp$ close to the experimental values. This effect can be clearly seen in Fig. 14, which shows the plot of the time evolution of the 2/1, 3/2, and 5/3 island widths taken from two numerical calculations differing only in the way the resistivity evolves. The observed increase in speed is of the same order as the increase in linear growth rates already mentioned in Sec. III (see Fig. 3).

The perpendicular electron thermal conductivity $\overline{\chi}_\perp$ does not have much influence on the nonlinear process when the classical value for the perpendicular transport coefficient is used.[21] Using an anomalous value for $\overline{\chi}_\perp$, smoother temperature profiles can be obtained during the calculation. Figure 15 compares, for a fixed time, the current density and temperature profiles for two different values of $\overline{\chi}_\perp$ ($\overline{\chi}_\perp=0.05$ and $\overline{\chi}_\perp=5.0$, respectively). The effect of $\overline{\chi}_\perp$ on the current profile is not as noticeable as it is on the temperature profile, but there is a clear tendency for the smallest scale length fluctuations in the current density profile to disappear as $\overline{\chi}_\perp$ is increased.

Finally, another point to consider is the effect of the initial conditions on the nonlinear evolution, i.e., the effect of changing the initial island widths $W_I^{2/1}$ and $W_I^{3/2}$ for the ($m=2; n=1$) and ($m=3; n=2$) modes, respectively. This is illustrated in Figs. 16(a) and 16(b), where the nonlinear growth rates of two modes are plotted as functions of time for different initial condi-

RENORMALISED TURBULENCE EQNS.

In deriving Eq. (97), contributions added in m' were dropped; thus, the renormalized reduced magnetohydrodynamic equations for a long-wavelength tearing mode instability in the presence of fully developed, densely packed turbulence are

$$\gamma_{\mathbf{k}} \psi_{\mathbf{k}} + ik_{\parallel} \phi_{\mathbf{k}} = (D_{\mathbf{k}}^{A} + \eta) \frac{\partial^2 \psi_{\mathbf{k}}}{\partial x^2}. \tag{98}$$

$$\gamma_{\mathbf{k}} \frac{\partial^2 \phi_{\mathbf{k}}}{\partial x^2} + ik_{\parallel} \frac{\partial^2 \psi_{\mathbf{k}}}{\partial x^2} = a_{\mathbf{k}} \frac{\partial^2 \phi_{\mathbf{k}}}{\partial x^2}, \tag{99}$$

$$D_{\mathbf{k}}^{A} = \sum_{\mathbf{k}'} \frac{k_y'^2}{\gamma''} |\phi_{\mathbf{k}'}|^2, \tag{100}$$

and

$$a_{\mathbf{k}} = \sum_{\mathbf{k}'} \frac{\Delta_{\mathbf{k}'}' \delta(x'')}{\gamma''} \frac{m^2}{m''^2} k_y'^2 |\psi_{\mathbf{k}'}|^2. \tag{101}$$

Because the case of interest is one characterized by high levels of fluid turbulence, $D_{\mathbf{k}}^{A} \gg \eta$, the collisional resistivity is neglected hereafter. Equations (98) and (99) admit two classes of solution. The first class corresponds to a tearing instability triggered by the anomalous ohmic diffusivity $D_{\mathbf{k}}^{A}$, with the dispersion relation

$$\gamma_{\mathbf{k}}^5 = (\sqrt{2}/3)^4 (\Delta_{\mathbf{k}}')^4 (D_{\mathbf{k}}^{A})^3 (k_y/L_s)^2. \tag{102}$$

Because $D_{\mathbf{k}}^{A} \simeq (\gamma'')^{-1}$ and $\gamma'' \simeq \gamma_{\mathbf{k}}$, the anomalous tearing mode growth rate is

EXPLOSIVE GROWTH RATE

$$\gamma_{\mathbf{k}} = [(\sqrt{2}/3)\Delta_{\mathbf{k}}']^{1/2} (\hat{D})^{3/8} (k_y/L_s)^{1/4}, \tag{103}$$

where

$$\hat{D} = \sum_{\mathbf{k}} k_y'^2 |\phi_{\mathbf{k}'}|^2. \tag{104}$$

The turbulently broadened tearing layer width is

$$\lambda_{\mathbf{k}} = (L_s/k_y)^{1/2} \hat{D}^{1/4}, \tag{105}$$

where $\gamma_{\mathbf{k}} > a_{\mathbf{k}}$ is required for consistency with the neglect of $a_{\mathbf{k}}$ in the calculation of the growth rate. Note that while the anomalous ohmic diffusivity accelerates the tearing mode growth, $\Delta_{\mathbf{k}}' > 0$ is still required for instability. The mode

LIE TRANSFORM OF REDUCED MHD EQNS.

AS WITH FLUID FLOW, $\nabla\cdot\underline{B}=0$ SUGGESTS HAMILTONIAN FORMULATION.

$$\underline{B} = B_0\hat{z} + \nabla\psi_0(r)\times\hat{z} + \nabla\psi_1\times\hat{z}$$

FIELD LINES FOLLOW

$$H = B_0\mathcal{E} + \psi_0 + \psi_1 = H_0 + \psi_1$$

WITH

$$p \equiv \frac{B_0 r^2}{2} \qquad q \equiv \theta \qquad (\mathcal{E}, z) \text{ CONJUGATE}$$

SO

$$\underline{B}\cdot\nabla J \equiv [H, J]$$

$$\frac{dq}{dt} = \frac{\partial H}{\partial p} = \frac{1}{rB_0}\frac{\partial H}{\partial r} = \frac{1}{rB_0}\frac{\partial\psi}{\partial r} \equiv \frac{1}{B_0}\frac{d\theta}{dz}$$

$$\frac{dz}{dt} = \frac{\partial H}{\partial\mathcal{E}} = B_0$$

LIE TRANSFORM OPERATOR ON M^{TH} RESONANCE IS

$$\mathcal{L} = \exp[\hat{\psi}_1^*, \;]$$

$$\hat{\psi}_1^* = \sum_{m'\neq m} \frac{\psi_{m'}\, e^{i(m'\theta + k'z)}}{i(m'q + k')}$$

TRANSFORM MOMENTUM EQN

$$\mathcal{L}\cdot\left(\underline{B}\cdot\nabla J = \frac{dU}{dt}\right)$$

$$\equiv \left[H_0 + \psi_M + \tfrac{1}{2}\left[\hat{\psi}_1^*, \psi_1 + \psi_M\right], J\right] = \mathcal{L}\cdot\frac{dU}{dt}$$

And

$$\left[H_0 + \psi_M, J\right] = \frac{\partial H_D}{\partial I}\frac{\partial J}{\partial q_D} = \Omega_D \frac{\partial J}{\partial q_D}$$

IS THE ANGLE DERIVATIVE OF J AROUND THE ISLAND AND

$$\Omega_D \sim O\left(\sqrt{|\psi_1|}\right)$$

TOKAMAK

WITH $\psi_1 = \psi_2(r,t)\cos(2\theta - z) + \psi_3\cos(3\theta - 2z)$

$$\Omega_D \frac{\partial J}{\partial q_D} + \left[\frac{6\psi_2'\psi_3}{rB_0^2}\left(\cos(\theta - z) + \cos(5\theta - 3z)\right), J\right] = \mathcal{L}\cdot\frac{dU}{dt}$$

FINAL RESONANT MODE COUPLING EQN IS

$$\oint \frac{dq_D}{\Omega_D}\left(\left[H_2, J\right] - \mathcal{L}\cdot\frac{dU}{dt}\right) = 0$$

COUPLES 2 MODES TO MANY LARGE $\underline{M}$ MODES!

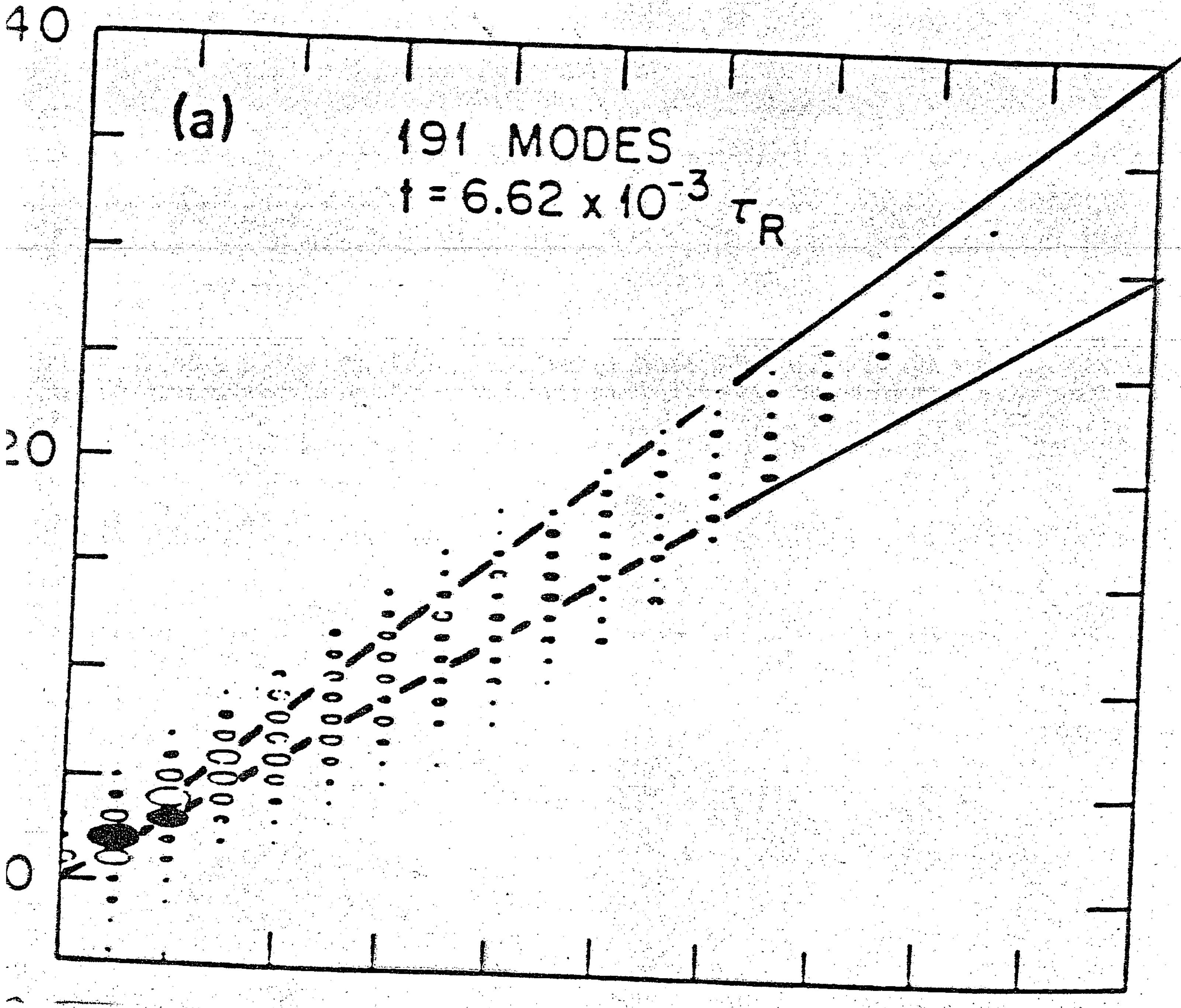
40
(a)
191 MODES
$t = 6.62 \times 10^{-3}\ \tau_R$
20
0

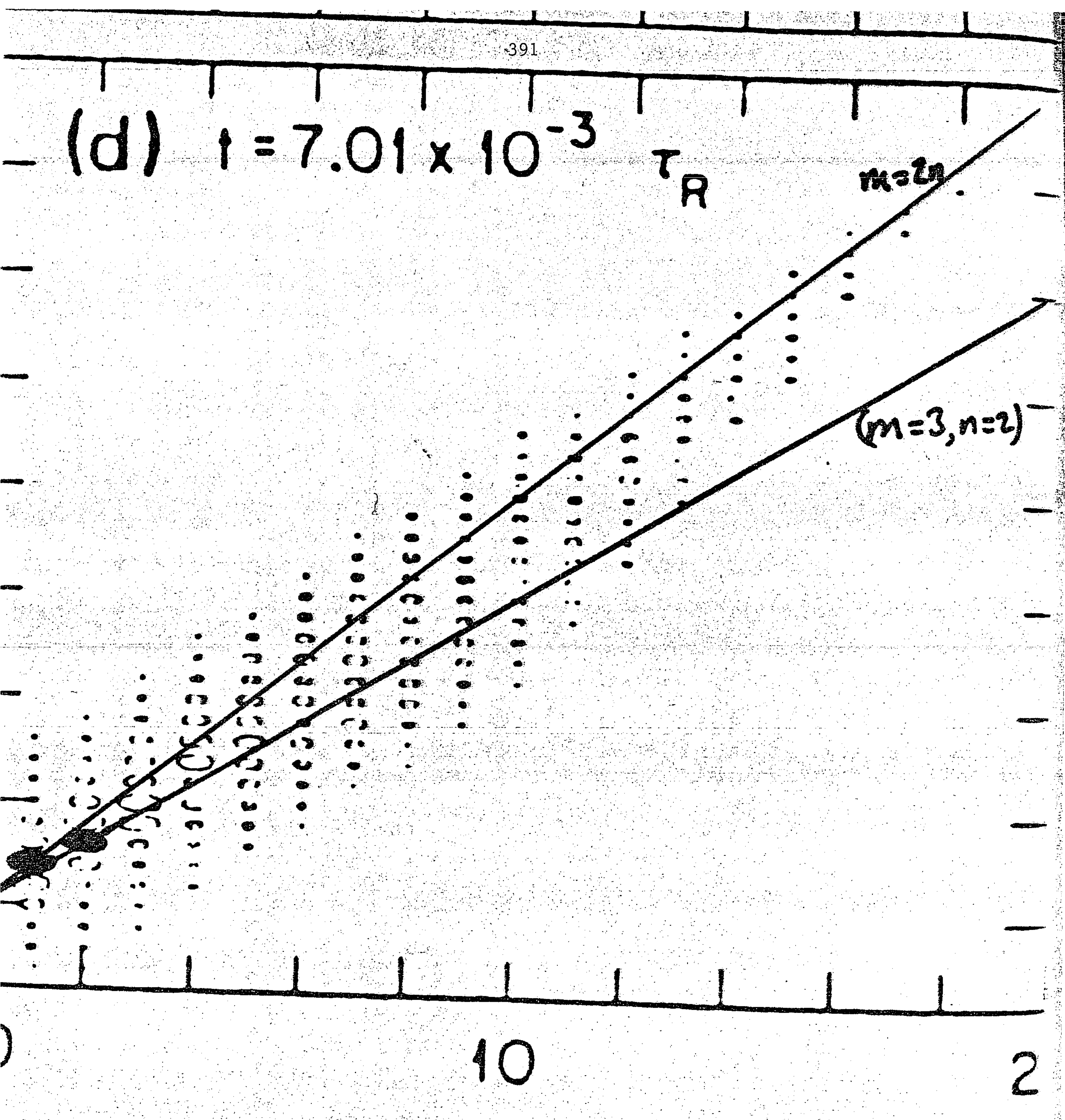

(m=2, n=1) Island filled with many modes!
(m=3, n=2) Initialised at lower amplitude.

rate of the ($m = 3$; $n = 2$) mode is calculated, and its value can be compared with the nonlinear growth rate of this mode (Fig. 3). The agreement is good. It is also important to investigate the correlation of this anomalous growth with the buildup of the high-m fluid turbulence under various cir-

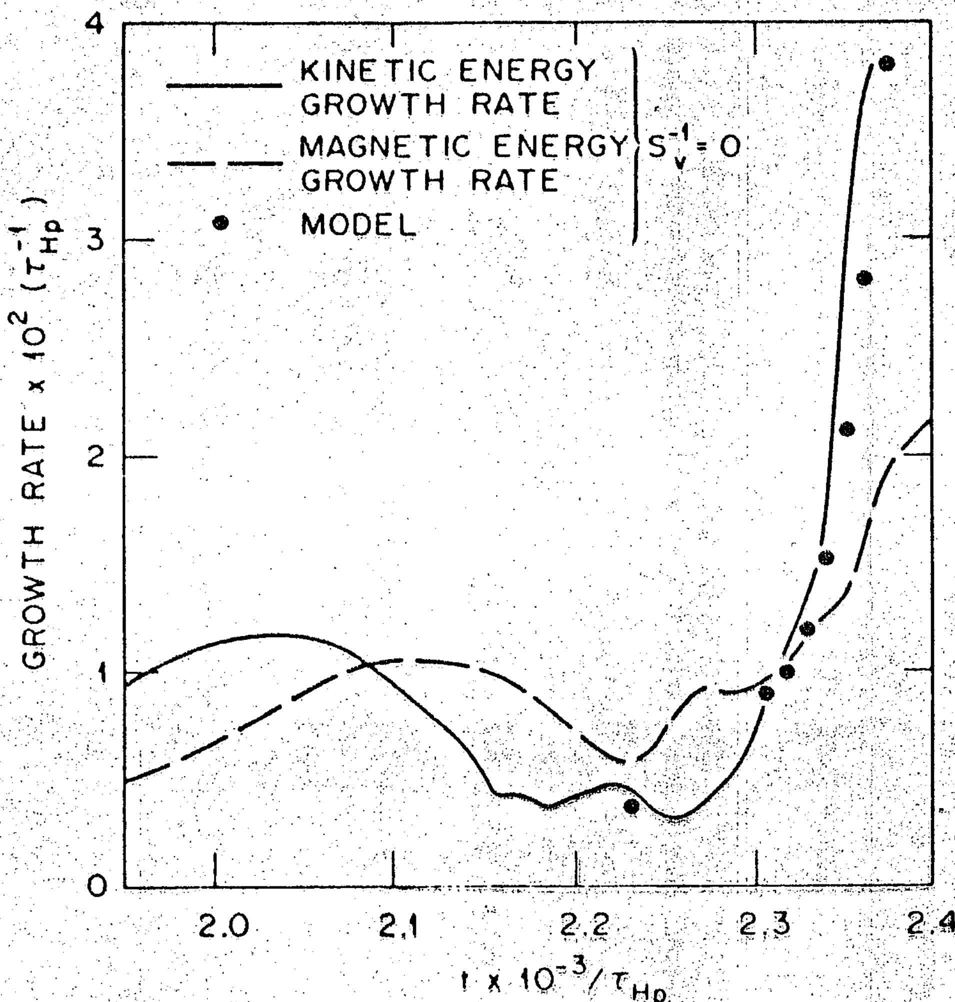

FIG. 3. The growth rate of the ($m = 3$; $n = 2$) mode as obtained from the model is compared with the calculation. Same case as in Fig. 2.

and voltage trace for the sa
compared. It shows that the t
the same as the anomalous g
calculation and confirms the t

In the last phase of th
high-k modes are being gene
about the numerical validi

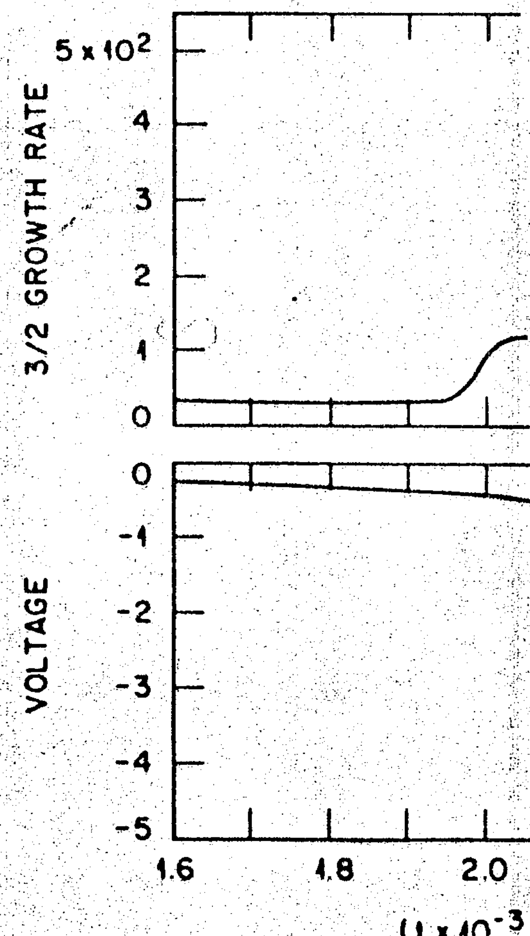

FIG. 5. Same case as Figs. 2 and 3:
mode kinetic energy; (b) voltage trace

CONCLUSIONS

* DYNAMICS OF PARTICLES, FLUID FLOW LINES, MAGNETIC FIELD LINES ALL SHOW STOCHASTIC MOTION WHEN 2 ORMORE MODES OF LOW MODE # INTERACT

* LIE TRANSFORM DEVELOPS DRIFT EQNS. FOR ISLAND INTERACTION WHICH ARE LARGE, $O(\sqrt{\epsilon})^{1/\sqrt{\epsilon}}$

* LIE TRANSFORMS CAN BE APPLIED TO FLUID EQNS. TO GIVE NEW, LARGE COUPLINGS BETWEEN MODES.

RESISTIVE DYNAMICS OF MAGNETIC ISLANDS WITH CURVATURE AND PRESSURE

M. KOTSCHENREUTHER

INSTITUTE FOR FUSION STUDIES

INTRODUCTION

Curvature and pressure are very important in the linear stability of resistive instabilities.Glasser, Greene and Johnson found it resulted in a LARGE CRITICAL Δ'_c for instability in tokamaks.

Rutherford considered the nonlinear theory of tearing modes driven by Δ'.

Here we compute the nonlinear evolution including interchange effects.

We compute a Grad-Shafranov equation to descibe MHD equilibria in the island vicinity.We then derive the resistive evolution.

We focus attention on the region near the rational surface, $q_0=m/n$.

Matching to exterior region introduces Δ'.

Islands are taken to be thin to make problem tractable.

Nonlinear islands grow more slowly than linear instabilities. So

1) Neglect inertia
2) Assume sound wave propagation along B causes $B\cdot\nabla p=0$

Make expansion in aspect ratio ϵ

Local pressure profile is found by assuming large diffusion and given sources deep in plasma interior (e.g. ohmic heating, etc.)

Islands described by resistive MHD

$$\nabla j_{\parallel} = -B \cdot \nabla p \times \nabla (1/B^2)$$

$$\underline{j} \times \underline{B} = \nabla p$$

$$E_{\parallel} = \eta j_{\parallel}$$

We employ flux coordinates

$$B_0 = \nabla \chi \times \nabla (q(\chi)\theta - \varphi)$$

Define angle which follows the island: $\alpha = \theta - \varphi / q_0$

Define averaging operator to separate out resonant and non-resonant parts

$$\bar{f}(\chi,\alpha) = \oint d\varphi\, f(\chi,\alpha,\varphi) \Big/ \oint d\varphi$$

$$\tilde{f} = f - \bar{f}$$

The average vorticity equation is crucially important. Define

$$[A,C] = \nabla\varphi \cdot \nabla A \times \nabla C$$

$$h = -1/B_0^2 + 2p/B_0^4$$

$$B_0 + B_1 = \nabla\varphi \times \nabla\psi$$

$$Q = j_\parallel / B$$

The total helical flux, $\psi_h = \bar{\psi} - \int d\chi\, q/q_0$ is an important quantity, since it acts as a flux function in the island vicinity (e.g. $p = p(\psi_h)$). The averaged vorticity equation is

$$[\psi_h, \bar{Q}] = [\bar{p}, \bar{h}] + \overline{[\tilde{p}, \tilde{h}]} - \overline{[\tilde{\psi}, \tilde{Q}]}$$

Eq(1)

Without pressure or curvature,
Eq(1) implies

$$Q = Q(\psi_h)$$

which is a central element of Rutherfords analysis.Interchange effect modify this.

The first term gives the effect of normal curvature, the others the geodesic curvature.

To compute the latter terms ,we make an expansion for thin islands.

This is similar to the approximation of localization near a rational surface used by Glasser,Greene,and Johnson.

Computation of the nonresonant terms proceeds similarly to linear theory,since the magnetic non-linearity is negligible for them. The result has the form

$$\overline{[\tilde{p},\tilde{h}]}-\overline{[\tilde{\Psi},\tilde{I}]}=[\bar{p},h_g]$$

which makes the solution of Eq(1) very simple

$$Q = Q_*(\Psi_h)+G_1\,\partial p(\Psi_h)/\partial\Psi_h$$

where $G_1 = \overline{h}+h_g$, and Q_* is an arbitrary function needed to specify the current on a flux surface. G_1 is proportional to the curvature expression E+F given by Glasser et. al. .

To obtain a Grad-shafranov equation for $\overline{\Psi}$,we take the average of Ampere's Law.For thin islands,this is

$$\frac{\partial^2}{\partial \chi^2}\overline{\Psi} = \overline{\nabla\chi^{-2}}\,\bar{Q} + \overline{\widetilde{\nabla\chi}^{-2}\,\tilde{Q}}$$

We then obtain

GRAD-SHAFRANOV EQUATION

$$\frac{\partial^2}{\partial \chi^2}\Psi_h = Q_*(\Psi_h) + (\chi - \chi_R)(G_1 + G_2)\frac{\partial p(\Psi_h)}{\partial \Psi_h}$$

Where G_1+G_2 is proportional to the expression in the Mercier stability criterion $D_I < 1/4$, $D_I = E+F+H$

$Q_*(\Psi_h)$ is determined by Ohm's Law. As in Rutherford,we define the flux average $\langle\ \ \rangle$ over a surface of constant Ψ_h .Then

$$\langle \partial\Psi_h/\partial t\rangle = Q_*(\Psi_h)$$

This determines J_*.The Grad-Shafranov equation can then be solved with two conventional approximations:

1)One harmonic dominates in the perturbed flux,so

2)The "constant ψ" appxoximation holds in the island interior.This requires that E+F be small.

Far from the island,Eq(2) gives

$$\Psi \sim C_1(\chi-\chi_R)^{-\frac{1}{2}+\sqrt{\frac{1}{4}-D_I}} + C_2(\chi-\chi_R)^{-\frac{1}{2}-\sqrt{\frac{1}{4}-D_I}}$$

which are the Mercier solutions.

The finite β generalization of Δ' is

$$\Delta'_* = \frac{C_{2+}}{C_{1+}} - \frac{C_{2-}}{C_{1-}}$$

ISLAND WIDTH EVOLUTION

When matched to the exterior, we obtain the evolution of ψ. This is most clearly written in terms of the island width $\Delta\chi$

$$\frac{k_1}{\eta}\frac{\partial \Delta\chi}{\partial t} =$$

$$\Delta'_{*}\,\Delta\chi^{s} + k_2\,\frac{E+F}{\Delta\chi}$$

Where $s = -1 + \sqrt{1-4D_I}$, $k_2 \cong 6.3$

The finite β generalization of Δ' is

$$\Delta'_* = \frac{C_{2+}}{C_{1+}} - \frac{C_{2-}}{C_{1-}}$$

When matched to the exterior, we obtain the evolution of ψ. This is most clearly written in terms of the island width $\Delta\chi$

$$\frac{k_1}{\eta}\frac{\partial}{\partial t}\Delta\chi =$$

$$\Delta'_* \Delta\chi^{s_1} + k_2 \frac{(E+F)}{\Delta\chi}$$

where $k_2 \cong 6.3$, $s_1 = -1 + \sqrt{1-4D_I}$

The driving term for magnetic free energy was given by Rutherford (for $\beta \to 0$).

The interchange driving term is stabilizing for good curvature, but decreases in relative importance as $\Delta\chi$ increases. The two are comparable when

$$\Delta'_* \, \Delta\chi^{\sqrt{1-4D_I}} = K_2(E+F)$$

Eq (3)

This is the nonlinear generalization of the concept of Δ'_c.

There are several similarities between the linear results of Glasser. et. al. and those above.

1)For islands just barely into the nonlinear regime,with widths of order the linear theory resistive layer,the Δ' required for growth according to Eq(3) agrees with the critical Δ' of linear theoy.

Since the influence of pressure decreases as the island grows,a tearing mode in a region of good curvature which has $\Delta' > \Delta'_C$ is not stabilized in this nonlinear regime.

2) Only E+F contributes to the resistive evolution,despite the fact that the pressure drive for the ideal MHD case is E+F+H.This agrees with linear theory when E+F and H is small.

ALSO,note that Eq(3) gives the saturated island width for a resistive interchange instability (when $\Delta'<0$).Of course,the dynamics if two islands overlap is not described by the present calculation.

RELAXATION OF TOROIDAL PLASMAS

A. BHATTACHARJEE

Columbia University

RELAXATION OF TOROIDAL PLASMAS

A. Bhattacharjee, Columbia University

A. H. Glasser, LANL

Other Co-workers (chronologically)

R. L. Dewar, PPPL, Australian National University

D. A. Monticello, PPPL

M. S. Chance, PPPL

J. C. Wiley, FRC, University of Texas

A. Khare, PPP, India

J. E. Sedlak, IFS

Review of basic ideas

1 Ideal plasmas characterised by denumerably infinite number of invariants

$$\frac{\partial \bar{B}}{\partial t} - \nabla \times (\bar{v} \times \bar{B}) = 0$$

$$\frac{\partial \bar{A}}{\partial t} - \bar{v} \times \bar{B} + \nabla \alpha = 0$$

$$\Leftrightarrow \quad \frac{dK}{dt} = 0 \ ; \quad K = \int_V d\tau \, \frac{\bar{A}.\bar{B}}{2}$$

over every volume V bounded by field-lines (Moffatt, 1969)

2 Taylor's conjecture (1974)

For small departures from ideal behaviour

$$K_0 = \int_{V_0} d\tau \, \frac{\bar{A}.\bar{B}}{2}$$

is the only remaining invariant. Plasma relaxes to minimum-energy state consistent with the invariance of K_0 and total toroidal flux

Thus, minimising

$$W = \int_{V_0} d\tau \left[\frac{B^2}{2} + \frac{p}{\gamma - 1} \right]$$

subject to conservation of K_0, and toroidal flux,

$$\delta W - \lambda_0 \, \delta K_0 = 0$$

$$\Rightarrow \quad \vec{J} = \lambda_0 \vec{B} \, , \quad \nabla p = 0$$

Comments

(1) Mechanism for conservation of K_0 ?

(2) Model not generally good for tokamaks : predicts disrupted profiles

(3) Taylor states: overkill for internal modes
$\sigma = \vec{J} \cdot \vec{B} / B^2 = \lambda_0 =$ constant ;
unstable with wall removed from plasma ;
always force-free.
Bear little resemblance to "optimised profiles" in fusion devices

Yet, Taylor's model is an undeniably attractive theoretical model for relaxation in RFP's

Might the basic idea be extended to understand relaxation in tokamaks or stellarators ?

3. Ideal MHD (Kruskal and Kulsrud, 1958)

$$\bar{B} = \nabla\chi \times \nabla\Psi + \nabla\Phi \times \nabla\theta$$

$$\bar{A} = \Phi \nabla\theta - \Psi \nabla\chi$$

Under ideal variations

$$\delta\Psi = -\bar{\xi}\cdot\nabla\Psi, \quad \delta\Phi = q(\Psi)\,\delta\Psi$$

$$K[w_\alpha] = \int_V d\tau \; w_\alpha(\Psi,\Phi)\,\frac{\bar{A}\cdot\bar{B}}{2}$$ is conserved

for every volume V bounded by field lines

Equivalent to the class of invariants due to Moffatt

4. Quasi-ideal MHD (Kadomtsev, Monticello, 1975)

$m=1, n=1$ resistive internal kink

$$K_\alpha = \int_{V_0} w_\alpha(\chi)\,\frac{\bar{A}\cdot\bar{B}}{2}\,d\tau$$

$$\chi = q_s\Psi - \Phi\,; \quad q_s \equiv \text{pitch of the mode}$$

Further arguments (Bhattacharjee, Dewar, Monticello, 1980, 1982) show $w_\alpha(\chi) = \chi^\alpha$, where α is a positive integer

Ad hoc truncation

$\alpha = 0, 1$

$$K_0 = \int_{V_0} d\tau \, \frac{\bar{A}.\bar{B}}{2} \, , \quad K_1 = \int_{V_0} d\tau \, \chi \, \frac{\bar{A}.\bar{B}}{2}$$

Examine consequences of the simplest modification to Taylor's truncation procedure

$$\bar{J} = \left(\lambda_0 + \frac{3\lambda_1}{2} \chi\right) \bar{B}$$

Examine solutions for which $\bar{J} = 0$ on wall

$$\bar{J} = \lambda_0 \left(1 + \frac{\chi}{\Phi_p}\right) \bar{B}$$

$\Phi = \Phi_p$ on boundary

Equilibrium solutions obtained by scanning in λ_0.

Quasi-ideal model of reconnection (Kadomtsev, 1973 Monticello)

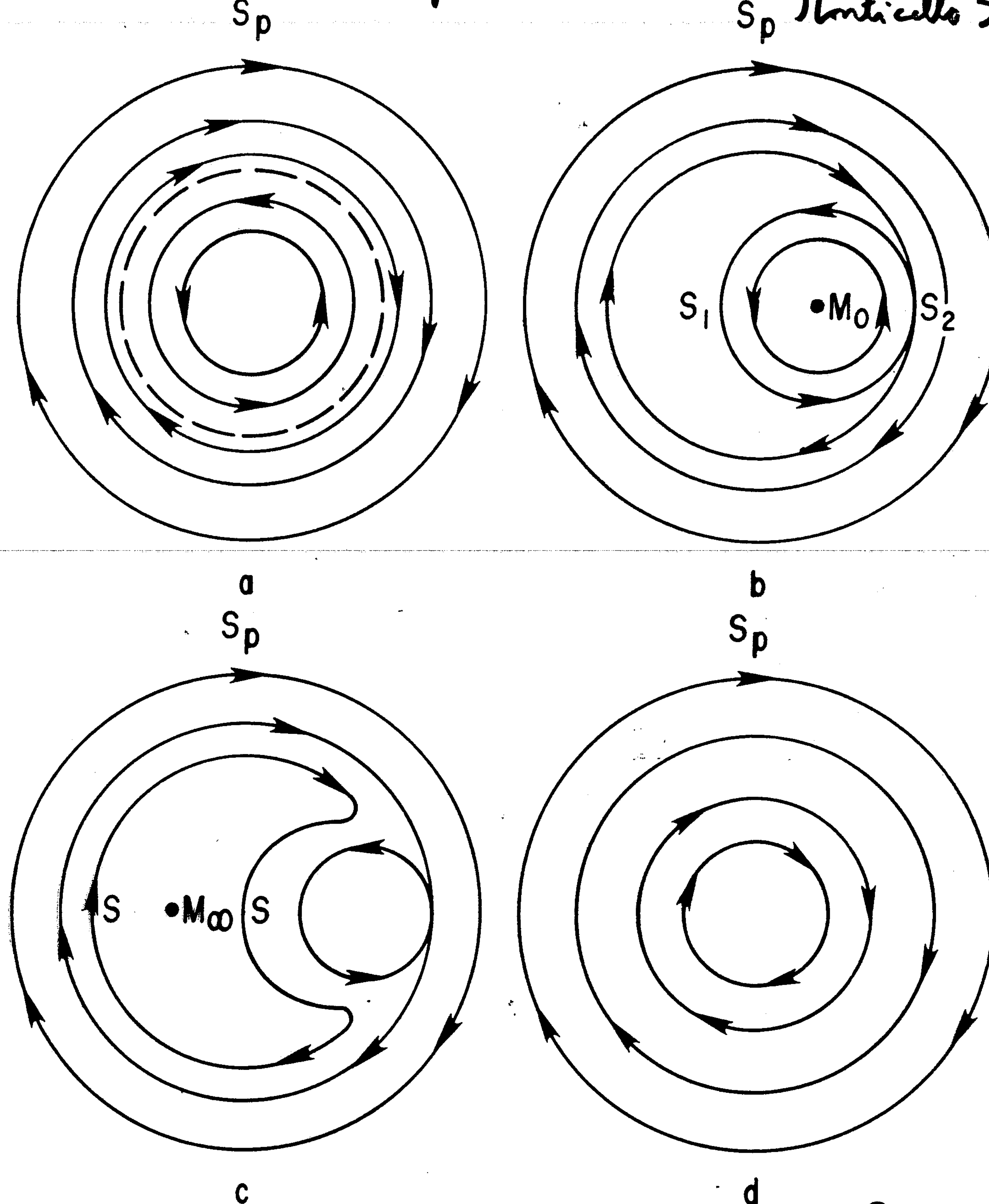

Contours of auxiliary field ($B_\theta - \frac{r B_z}{R q_s}$)

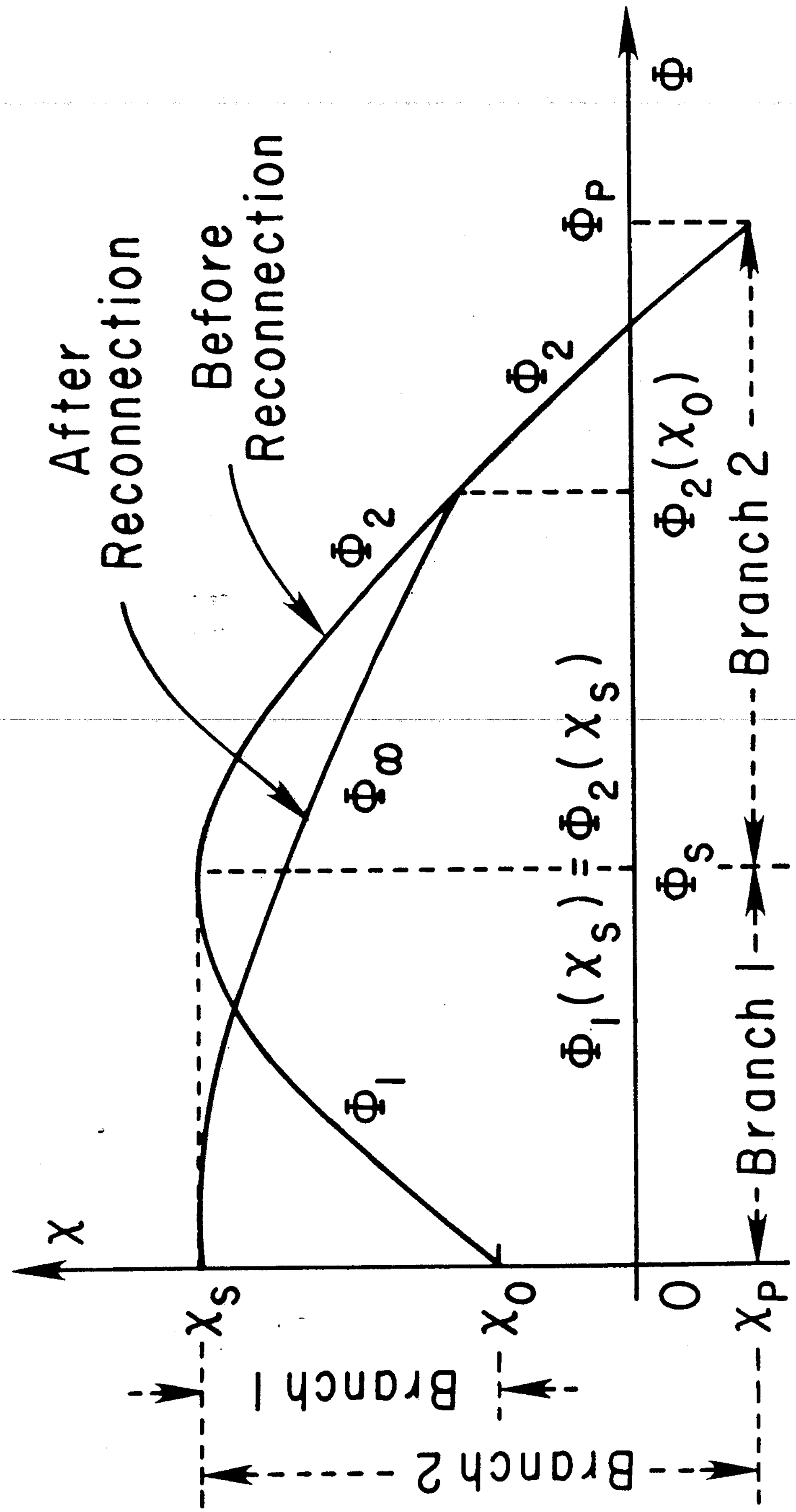
After Reconnection
Before Reconnection
Φ
Φ_P
Φ_2
$\Phi_2(X_0)$
Φ_2
Φ_∞
$\Phi_1(X_S) = \Phi_2(X_S)$
Φ_S
Φ_1
Branch 2
Branch 1
X
X_S
X_0
0
X_P
Branch 1
Branch 2

Estimate of decay rates

$$K_\alpha = \int d\tau \, \chi^\alpha \frac{\bar{A}\cdot\bar{B}}{2}$$

$$\frac{dK_\alpha}{dt} = \frac{1}{2}\int d\tau \left[\chi^\alpha \left\{ \frac{\partial \bar{A}}{\partial t}\cdot \bar{B} + \frac{\partial \bar{B}}{\partial t}\cdot \bar{A} \right\} + \bar{A}\cdot\bar{B} \, \frac{\partial \chi^\alpha}{\partial t} \right]$$

$$\frac{\partial \bar{B}}{\partial t} - \nabla \times (\bar{v}\times\bar{B}) = -\eta \, \nabla\times\bar{J}$$

$$\frac{\partial \bar{A}}{\partial t} - \bar{v}\times\bar{B} = -\eta \bar{J} + \nabla\alpha$$

$$\frac{dK_\alpha}{dt} = \int_{V_0} d\tau \left[-\eta \bar{J}\cdot\bar{B}\, \chi^\alpha + \frac{\bar{A}\cdot\bar{B}}{2}\frac{D\chi^\alpha}{Dt} - \frac{\eta \bar{J}}{2}\cdot(\nabla\chi^\alpha \times \bar{A}) \right]$$

Also

$$W = \int_{V_0} d\tau \, \frac{B^2}{2}$$

$$\frac{dW}{dt} = \int_{V_0} d\tau \left[-\eta J^2 - \frac{D}{Dt}\left(\tfrac{1}{2}\rho v^2\right) \right]$$

Park, Monticello and White (1984)

$$\tau_K^{-1} \equiv \frac{1}{K_\alpha}\frac{dK_\alpha}{dt} \sim -\eta(\alpha+1)$$

$$\tau_W^{-1} \equiv \frac{1}{W}\frac{dW}{dt} \sim -\eta \frac{L}{\delta}$$

L : macroscopic length
δ : singular layer width

$$\tau_K^{-1}/\tau_W^{-1} \sim \frac{\delta}{L}(\alpha+1) \sim \eta^{1/2}$$

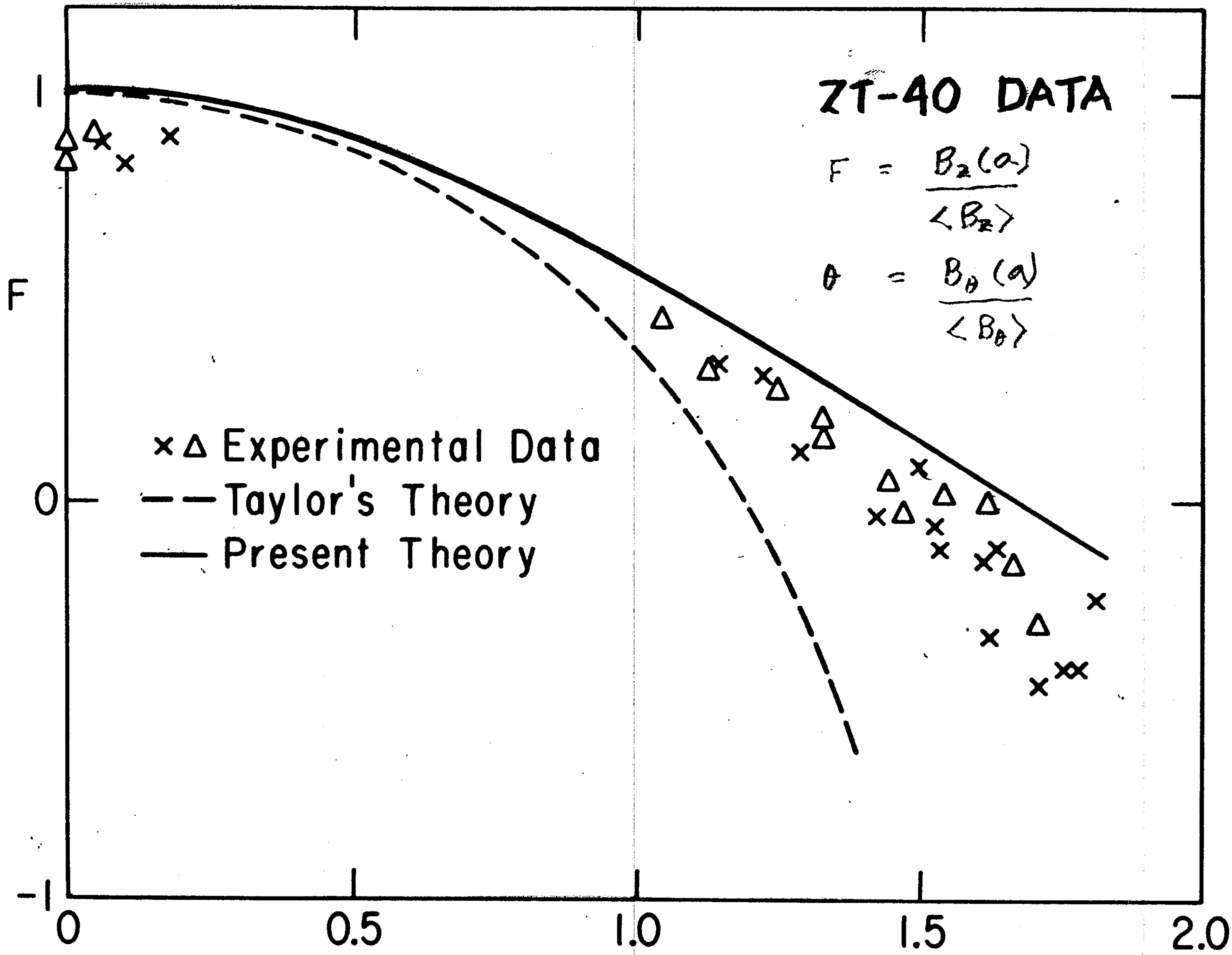

Courtesy: D. Baker, LASL

Energy Principle with Global Invariants

Extremise $W = \int_{V_0} d\tau \, \frac{B^2}{2}$ subject to the

invariance of $K_\alpha = \int_{V_0} d\tau \, \chi^\alpha \frac{\bar{A} \cdot \bar{B}}{2}$

$$\delta W - \sum_\alpha \lambda_\alpha \delta K_\alpha = 0$$

$$\Rightarrow \quad \vec{J} = \sum_\alpha \frac{\lambda_\alpha (\alpha + 2)}{2} \chi^\alpha \bar{B}$$

$$\sigma = \frac{\bar{J} \cdot \bar{B}}{B^2} = \sum_\alpha \lambda_\alpha \frac{(\alpha+2)}{2} \chi^\alpha$$

Consider equilibrium in periodic cylinder, with dependence only on r

$$\frac{d\sigma}{dr} = \sum_\alpha \lambda_\alpha \frac{(\alpha+2)}{2} \frac{d\Phi}{dr} (q_s - q)$$

$$= 0 \quad \text{if} \quad q_s = q$$

In the final state, model <u>predicts</u> that if the rational surface for the mode falls within the plasma, the parallel current will flatten itself at that surface. Or, the rational surface may be eliminated from within the plasma

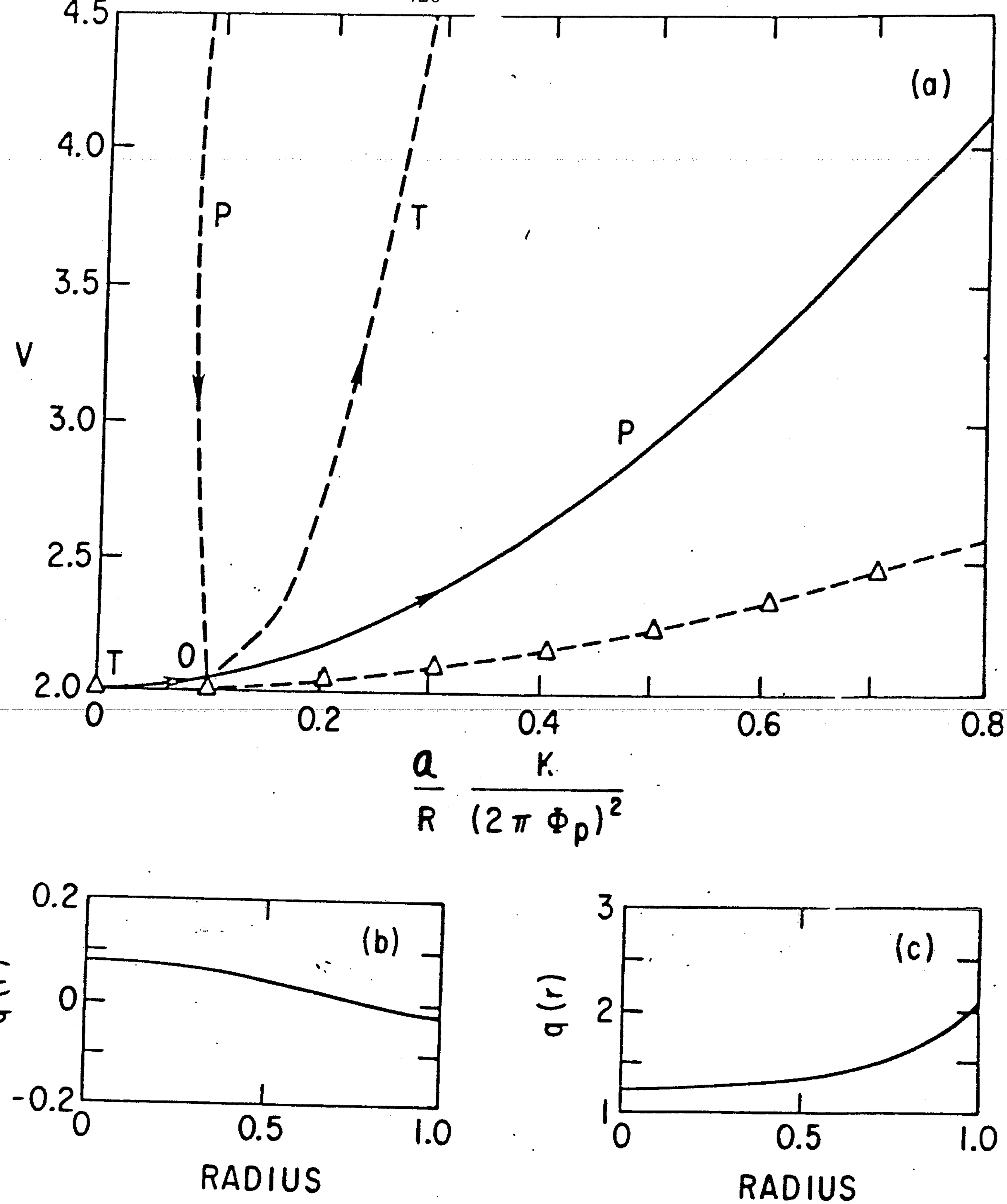

Fig. 1(a) Energy of equilibria in present theory compared with energy of Taylor states (marked by Δ). Arrows indicate direction of increasing λ. Labels P and T distinguish pinchlike and tokamaklike equilibria. Dashed lines indicate unstable equilibrium (energy stationary, but not minimum). (b) Typical q-profile on the stable P-branch. (c) Typical q-profile on the stable T-branch.

$$V \equiv 2WaR^{-1}(2\pi\Phi_p)^{-2}$$

STABILITY OF RELAXED STATES

Ideal and resistive stability of relaxed states are examined by integrating Newcomb's equation, and computing Δ'.

Have found completely stable (stable w.r.t. internal modes) tokamaklike solutions with $q\,(\text{center}) \simeq 1$, $q\,(\text{edge}) \lesssim 1.3$

RFP branch usually unstable to some $m = 1$, large n instability

Wisconsin RFP (Sprott, Prager, Kerst)

Proposed q-scaling studies from tokamak to RFP branch.

Have found transition region to be usually unstable in this model

STABLITY OF TOKAMAK BRANCH

ARATIO= 5.000 QS= 1.000 LAMDAO= 9.000 BETAO= 1.000e-04
PSIO=-4.693e-01 PHIA= 4.911e-01

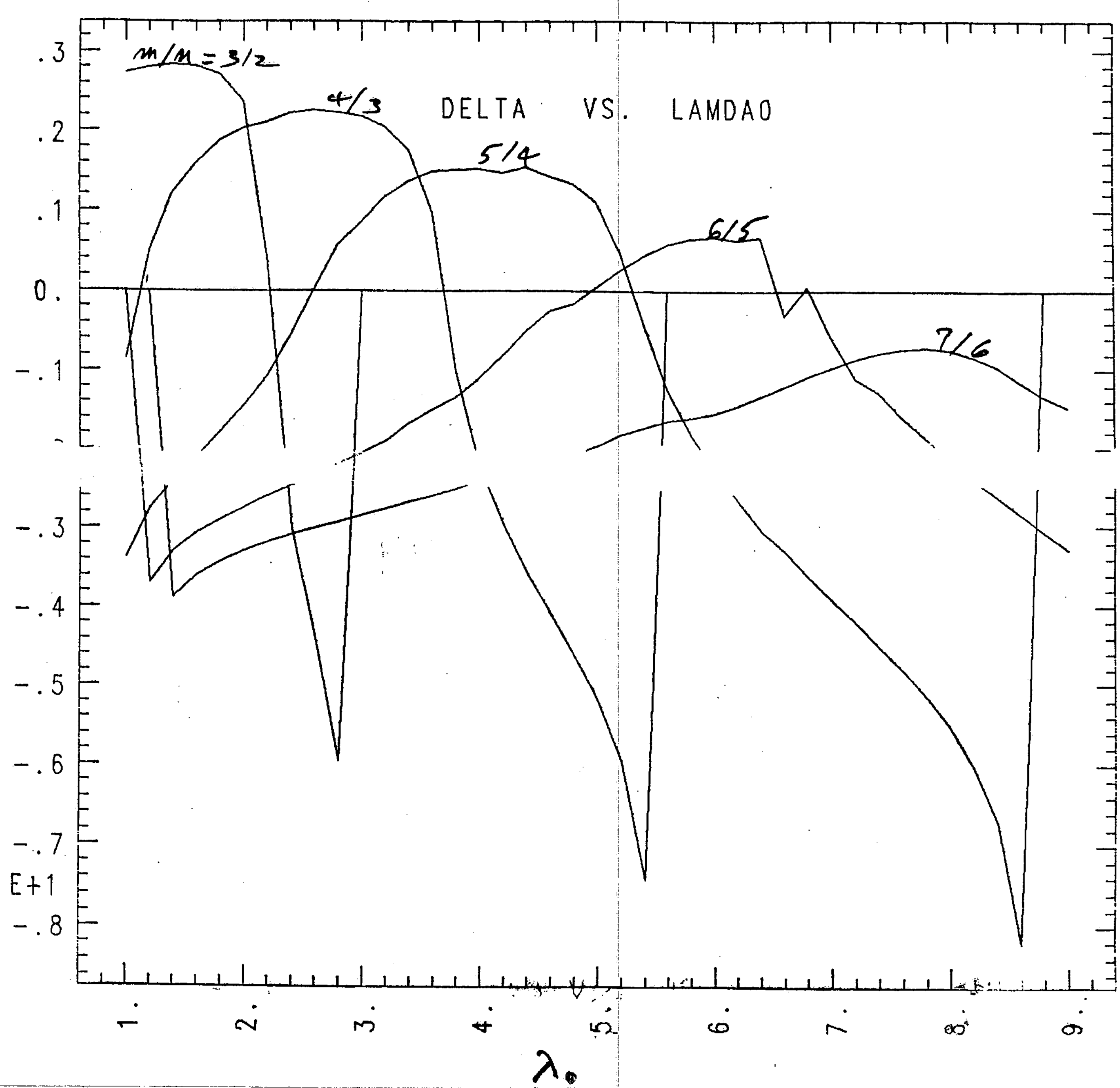

STABLE TOKAMAK PROFILE

ARATIO= 5.000 QS= 1.000 LAMDAO= 9.000 BETAO= 1.000e-04
PSIO=-4.693e-01 PHIA= 4.911e-01

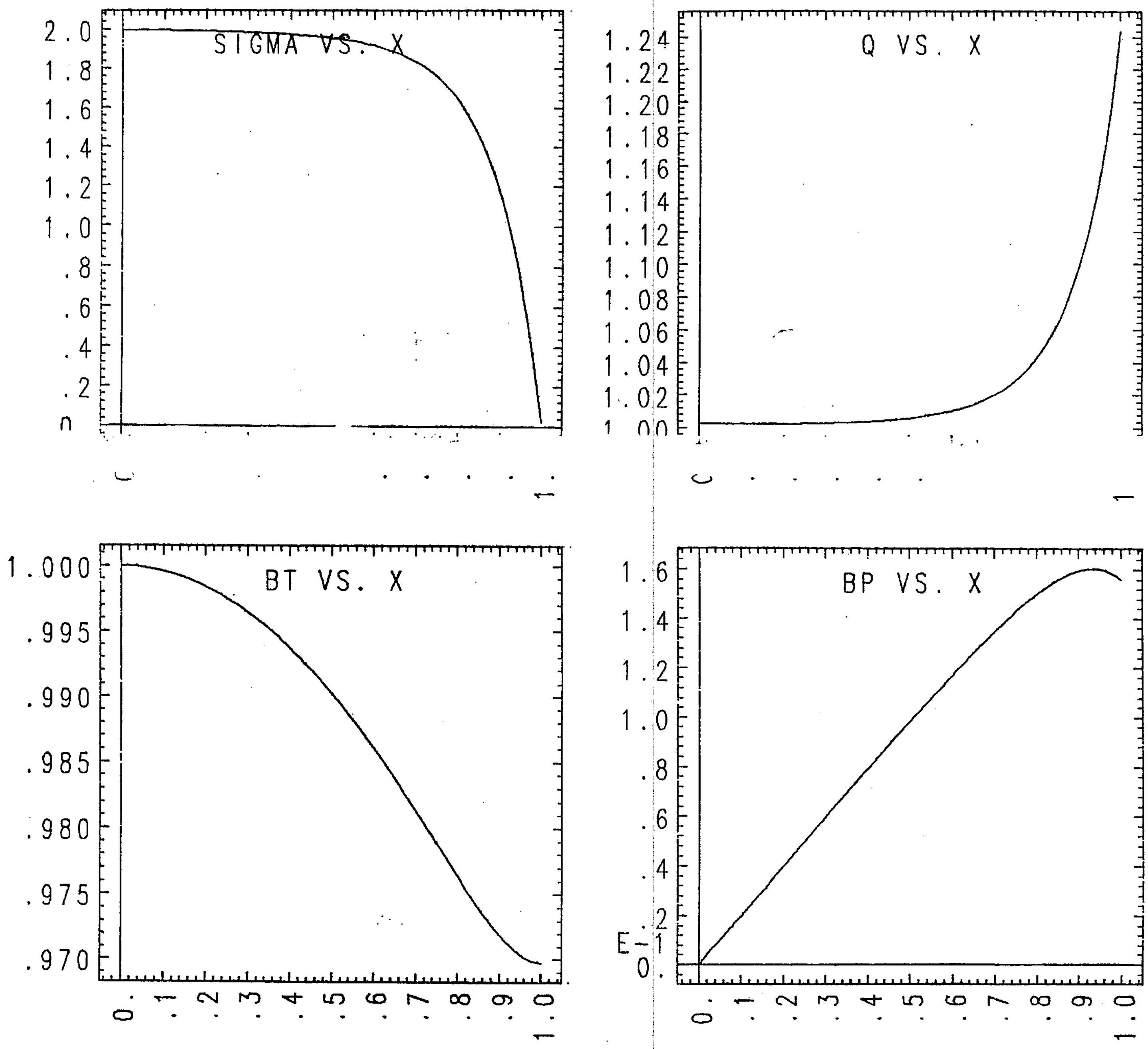

UNSTABLE RFP PROFILE

ARATIO= 5.000 QS= 1.000 LAMDA0=-0.200 BETA0= 1.000e-03
PSI0=-1.964e+00 PHIA= 7.324e-02

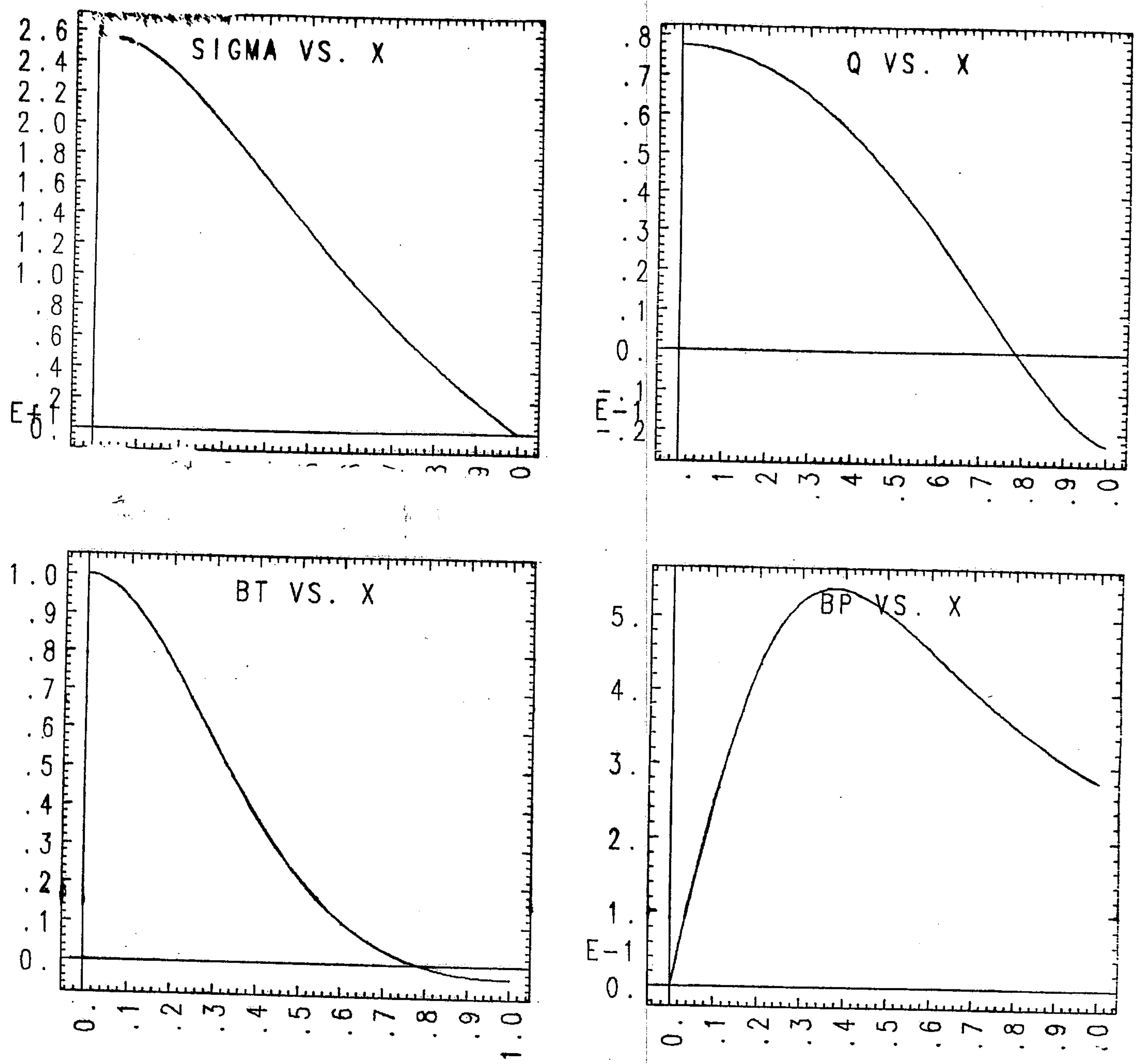

TRANSITION REGION BETWEEN TOKAMAK AND RFP BRANCH

ARATIO= 5.000 QS= 1.000 LAMDA0=-0.300 BETA0= 1.000e-03
PSI0=-2.024e+00 PHIA= 1.258e-01

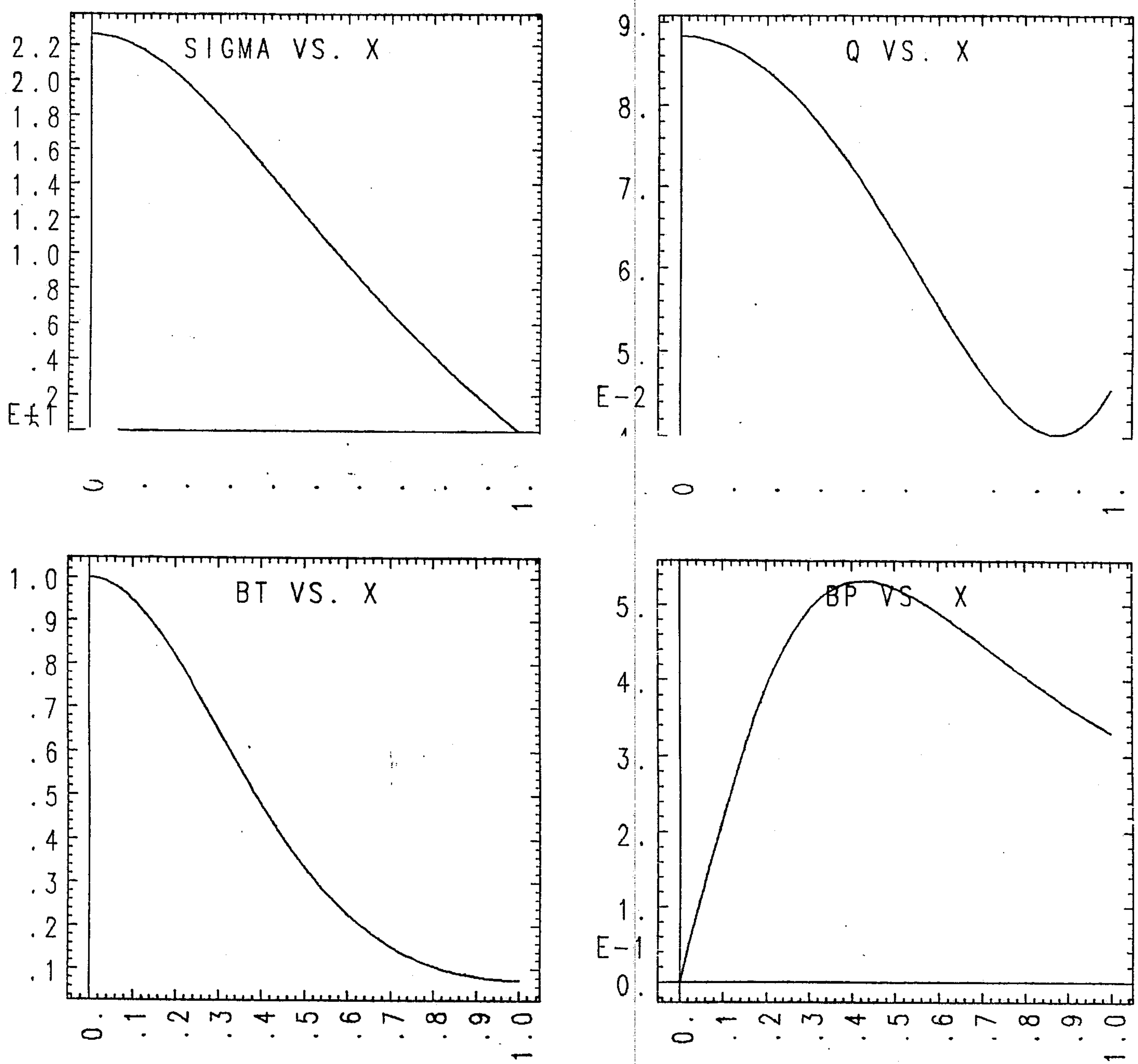

SECOND VARIATION OF FREE ENERGY

$$F = W - \sum_{\alpha} \lambda_\alpha K_\alpha$$

$\delta F = 0$ equilibrium

$\delta^2 F > 0$ sufficient conditions for ideal and resistive stability

In particular, have shown in a straight cylinder that if variations are restricted to the ideal class, then $\delta^2 F$ reduces to Newcomb's form (Bhattacharjee and Dewar, 1982)

Connection to resistive stability needs to be made more precise

Sufficient conditions for stability thus obtained without resolving the singular region of ideal theory.

FINITE PRESSURE EQUILIBRIA

Taylor states force-free even in the presence of finite pressure ; $\vec{J} = \lambda_0 \vec{B}$, $\nabla p = 0$

Consider resistive interchanges, with global invariants

$$K_\alpha = \int d\tau\, \chi^\alpha \frac{\vec{A}.\vec{B}}{2}$$

$$S_\alpha = \int d\tau\, \chi^\alpha \frac{\rho}{\gamma - 1} \ln\left(\frac{p}{\rho^\gamma}\right)$$

$$M_\alpha = \int d\tau\, \chi^\alpha \rho$$

$$\delta W - \sum_\alpha \left[\lambda_\alpha \delta K_\alpha + \mu_\alpha \delta M_\alpha + T_\alpha \delta S_\alpha\right] = 0$$

$\Rightarrow$

$$\vec{J} = \sum_\alpha \frac{\lambda_\alpha(\alpha+2)}{2} \chi^\alpha \vec{B} - p'(\chi)\left(\nabla\Psi . \nabla\theta \times \nabla\chi\right)^{-1} \times \nabla\Psi \times \nabla(q_s\theta - \chi)$$

$$p = \rho \sum_\alpha T_\alpha \chi^\alpha$$

$$\rho \sum_\alpha \mu_\alpha \chi^\alpha = \frac{\rho}{\gamma - 1}\left[\gamma - \ln\left(\frac{p}{\rho^\gamma}\right)\right] \sum_\alpha T_\alpha \chi^\alpha$$

Truncation $\alpha = 0$

$$\bar{J} = \lambda_0 \bar{B}, \quad p = \rho T_0, \quad \rho = \text{constant}$$

Inclusion of total mass and total entropy as global constraints still gives Taylor states

$\alpha = 0, 1$

$$\bar{J} = \left(\lambda_0 + \frac{3\lambda_1}{2}\chi\right)\bar{B} - (\nabla\Phi \cdot \nabla\theta \times \nabla\chi)^{-1}\, p'(\chi)\, \nabla\Phi \times \nabla(q_s\theta - \chi)$$

$p = p_0 \exp(p_1 \chi)$, p_0 and p_1 are constants

$\frac{dp}{dr} = 0$ at $q = q_s$, independent of the level of truncation

APPLICATION TO PROFILE OPTIMISATION FOR 2-D AND 3-D EQUILIBRIA

1 Choose a dynamical model, e.g., resistive internal modes, resistive interchanges

2 Construct global invariants

3 Energy Principle with Global Invariants then specifies automatically so-called "free" functions such as currnt and pressure.

States expected to have robust stability

Implemented for axisymmetric states (Bhattacharjee and Wiley, 1982)

May be a reasonable way to go for stellarator equilibria, particularly in those cases for which perfect surfaces may not exist

SUMMARY

1 Have constructed a thermodynamic model, in the spirit of Taylor, to understand relaxation in tokamaks

2 For a tearing mode of single helicity, imposition of additional constraints has given realistic profiles. Furthermore, a subset of these profiles have been shown to be ideally and resistively stable

3 Model allows the construction of finite beta equilibria, with non-zero gradients

4 Method may have useful applications for profile optimisation for 2-D and 3-D equilibria.

STATISTICAL PROPERTIES OF MHD TURBULENCE

J. MIZUSHIMA

SAGAMI INSTITUTE OF TECHNOLOGY

NO. 1
US-JAPAN W. P.
10-13 DECEMBER 89

Statiscal properties of MHD turbulence

Jiro Mizushima

① Mechanism of turbulent dynamo

with helicity

M. Steenbeck, F. krause & K. H. Rädler (1966)

A. Pouquet, U. Frish & J. Léorat (1976)

② Phenomenological theory of MHD turbulence

without helicity

R. H. Kraichnan (1965)

Y. Saito, J. Mizushima & N. Futami (1985)

③ Modified zero-fourth cumulant approximation for MHD turbulence

without helicity

Y. Saito, J. Mizushima & N. Futami (1985)

Methods to study Ordinary (N.S.) turbulence

more assumptions

- Theoretical Methods
  - Phenomenological argument — Kolmogorov
  - Closure theory
    - EDQNM approximation — Orszag, Frisch et al.
    - DIA — Kraichnan
    - MZFC approximation — Tatsumi, Kida & Mizushima
  - Numerical Simulation
    - LED ~~Smagorinsky~~
    - Orszag

less assumptions

- Experimental Methods

- Observational Methods

(1) Mechanism of turbulent dynamo

Can large-scale magnetic fields be generated when E^V and H^V are injected?

M. Steenbeck, F. Krause & K. H. Rädler (1966)

A. Pouquet, U. Frisch & J. Léorat (1976)

Large-scale	Middle-scale	Small-scale
M-energy	M-energy	M-energy
M-helicity	negative M-helicity	positive M-helicity
iv inverse cascade	i α-effect	ii Alfrén effect
		V-energy
	V-energy	iii Cascade
	V-helicity	
	injected	

(i) α-effect : middle- or Large-scale magnetic fields generation by V-helicity
(Residual helicity $H^R = H^V - k^2 H^M$)

(ii) Alfrén effect : equipartition of $E^V(k)$ and $E^M(k)$ by b_0

(iii) Cascade : Stretching of Vortex lines

(iv) inverse cascade : inverse cascade of M-helicity
cf. Two-dimensional N.S. turbulence

② Phenomenological theory of MHD turbulence

ⓘ NS turbulence

Kolmogorov's Theory A.N. Kolmogorov (1941)

$$E(k) \sim \frac{l^3}{t^2} \qquad (2.1)$$

energy dissipation rate

$$\epsilon \sim \frac{l^2}{t^3} \qquad (2.2)$$

$$k \sim \frac{1}{l} \qquad (2.3)$$

if $E(k)$ is expressed only by ϵ and k, dimensional analysis leads

$$E(k) = K \epsilon^{2/3} k^{-5/3} \qquad (2.4)$$

ⓘⓘ MHD turbulence

R. H. Kraichnan (1965)

$$\epsilon \propto (b_0 k)^{-1} \qquad (2.5)$$

$$\epsilon = A^2 b_0^{-1} [E(k)]^2 k^3 \qquad (2.6)$$

$$\frac{3}{2} b_0^2 = \int_0^\infty E^M(k)\,dk \qquad (2.7)$$

$$E^V(k) = E^M(k) = K (\epsilon b_0)^{1/2} k^{-3/2} \qquad (2.8)$$

(iii) Extension of Kolmogorov's theory to decaying NS Turbulence.

T. Tatsumi, S. Kida & J. Mizushima
(1978)

three assumptions

1. $E(k,t)/E_0 = t^{-\beta} F(k/t^{\delta})$ (2.9)

   at $k \sim k_E$ and inertial subrange and $k \gg 1$

2. $E(k,t)/E_0 = A_a k^a$ (2.10)

   at $k \ll 1$

3. $E(k,t) = K \epsilon(t)^{2/3} k^{-5/3}$ (2.11)

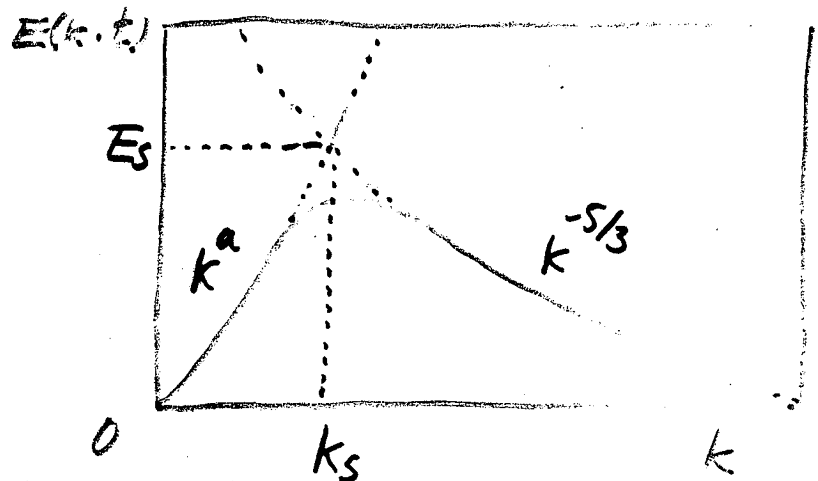

intersection

$$E_s = A_a k_s^a = K \epsilon(t)^{2/3} k_s^{-5/3} \quad (2.12)$$

$$\left.\begin{aligned} k_s &= \epsilon(t)^{3/(3a+5)} \\ E_s &= \epsilon(t)^{2a/(3a+5)} \end{aligned}\right\} \quad (2.13)$$

$$\mathcal{E}(t) \propto t^{-b} \quad (2.14)$$

$$\epsilon(t) = -\frac{d\mathcal{E}(t)}{dt} \propto t^{-(b+1)} \quad (2.15)$$

$$\left.\begin{aligned} k_s &\propto t^{-2(b+1)/(3a+5)} \\ E_s &\propto t^{-2a(b+1)/(3a+5)} \end{aligned}\right\} \qquad (2.16)$$

$$\beta = 2a(b+1)/(3a+5), \quad \delta = -2(b+1)/(3a+5) \qquad (2.17)$$

$$\mathcal{E}(t) = \int_0^\infty E(k,t)\,dk = E_0 k_0 t^{-\beta+\delta} \int_0^\infty F(\xi)\,d\xi$$

$$\propto t^{-2(a+1)(b+1)/(3a+5)} \qquad (2.18)$$

comparing (2.18) and (2.14)

$$b = 2(a+1)/(a+3) \qquad (2.19)$$

$$\beta = \frac{2a}{a+3}, \qquad \delta = -\frac{2}{a+3} \qquad (2.20)$$

when $a=2$

$\mathcal{E}(t) \propto t^{-6/5}$: case of Birkoff's invariant exists (2.21)

when $a=4$

$\mathcal{E}(t) \propto t^{-10/7}$: case of Loitsiansky's invariant exists (2.22)

No. 6

(iv) Extension of Kraichnan's theory to decaying MHD turbulence without helicity

Y. Saito, J. Mizushima & N. Futami
(1985)

three assumptions

1. $E^V(k.t)/E_0 = E^M(k.t)/E_0 \equiv E(k.t)/E_0$

$$= t^{-\beta} F(k/t^{\delta}) \qquad (2.23)$$

at $k \sim k_E$ and inertial subrange and $k \gg 1$

2. $E(k.t)/E_0 = A_a k^a$

at $k \ll 1$ (2.24)

3. $E(k.t) = K[\epsilon(t) b_0(t)]^{1/2} k^{-3/2}$ (2.25)

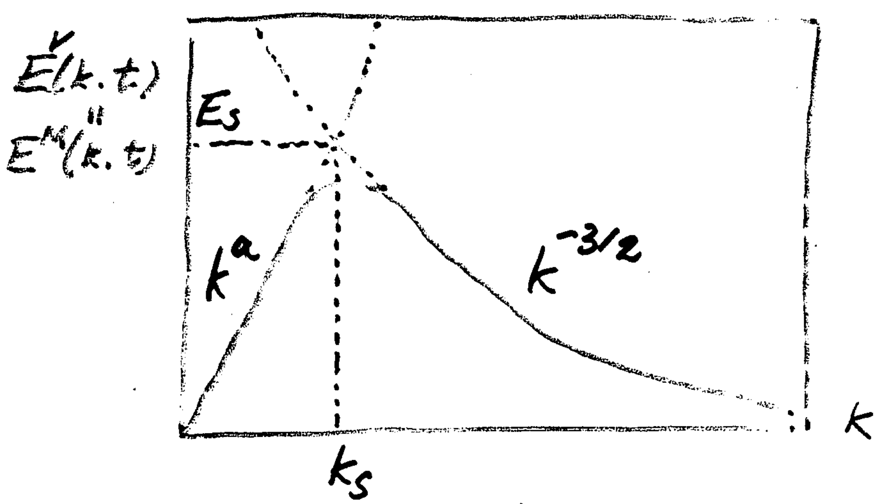

$$\mathcal{E}(t) \propto t^{-b}, \quad b_0(t) \propto t^{-b/2} \qquad (2.26)$$

$$\epsilon(t) = -\frac{d\mathcal{E}(t)}{dt} \propto t^{-(b+1)}$$

$$\left.\begin{array}{l} k_S(t) \propto t^{-(3b+2)/2(2a+3)} \\ E_S(t) \propto t^{-a(3b+2)/2(2a+3)} \end{array}\right\} \qquad (2.27)$$

NO. 7

$$\beta = a(3b+2)/2(2a+3), \quad \alpha = -(3b+2)/2(2a+3) \tag{2.28}$$

$$\mathcal{E}(t) = \int_0^\infty E(k,t)\,dk = E_0 k_0 t^{-\beta+\delta} \int_0^\infty F(\xi)\,d\xi$$

$$\propto t^{-(a+1)(3b+2)/2(2a+3)} \tag{2.29}$$

comparing (2.29) with (2.26)

$$b = 2(a+1)/(a+3)$$

$$\beta = \frac{2a}{a+3}, \quad \delta = -\frac{2}{a+3} \tag{2.30}$$

(2.30) is the same with (2.20) for NS turbulence

$$\frac{\partial \mathbf{u}}{\partial t} + (\mathbf{u}\cdot\nabla)\mathbf{u} = -\nabla p + \nu\,\Delta\mathbf{u} + (\mathbf{b}\cdot\nabla)\mathbf{b} \,, \tag{3.1}$$

$$\frac{\partial \mathbf{b}}{\partial t} + (\mathbf{u}\cdot\nabla)\mathbf{b} = (\mathbf{b}\cdot\nabla)\mathbf{u} + \lambda\,\Delta\mathbf{b} \,, \tag{3.2}$$

$$\nabla\cdot\mathbf{u} = 0 \,, \tag{3.3}$$

$$\nabla\cdot\mathbf{b} = 0 \,, \tag{3.4}$$

$$\begin{aligned}\left(\frac{\partial}{\partial t} + \nu k^2\right)\hat{v}_i(\mathbf{k},t) = & -ik_l\Delta_{ij}(\mathbf{k})\int_{\mathbf{p}+\mathbf{q}=\mathbf{k}} d\mathbf{p}\,d\mathbf{q}\;\hat{v}_l(\mathbf{p},t)\hat{v}_j(\mathbf{q},t) \\ & + ik_l\Delta_{ij}(\mathbf{k})\int_{\mathbf{p}+\mathbf{q}=\mathbf{k}} d\mathbf{p}\,d\mathbf{q}\;\hat{b}_l(\mathbf{p},t)\hat{b}_j(\mathbf{q},t) \,,\end{aligned} \tag{3.5}$$

$$\begin{aligned}\left(\frac{\partial}{\partial t} + \lambda k^2\right)\hat{b}_i(\mathbf{k},t) = & -ik_l\delta_{ij}\int_{\mathbf{p}+\mathbf{q}=\mathbf{k}} d\mathbf{p}\,d\mathbf{q}\;\hat{v}_l(\mathbf{p},t)\hat{b}_j(\mathbf{q},t) \\ & + ik_l\delta_{ij}\int_{\mathbf{p}+\mathbf{q}=\mathbf{k}} d\mathbf{p}\,d\mathbf{q}\;\hat{b}_l(\mathbf{p},t)\hat{v}_j(\mathbf{q},t) \,,\end{aligned} \tag{3.6}$$

where

$$\Delta_{ij}(\mathbf{k}) = \delta_{ij} - \frac{k_i k_j}{k^2} \quad \text{and} \quad k = |\mathbf{k}| \,. \tag{3.7}$$

$$\left.\begin{aligned} E^V(k,t) &= 2\pi k^2 \langle \hat{\mathbf{v}}(\mathbf{k},t)\cdot\hat{\mathbf{v}}^*(\mathbf{k},t)\rangle \,, \\ E^M(k,t) &= 2\pi k^2 \langle \hat{\mathbf{b}}(\mathbf{k},t)\cdot\hat{\mathbf{b}}^*(\mathbf{k},t)\rangle \,. \end{aligned}\right\} \tag{3.8}$$

No. 9

$$\frac{\partial E^V(k,t)}{\partial t} + 2\frac{k^2}{R}E^V(k,t)$$

$$= \frac{R}{2}\int_{p+q=k} dpdq\{\frac{1-\exp[-(k^2+p^2+q^2)t/R]}{k^2+p^2+q^2}[k^2E^V(p,t) - p^2E^V(k,t)]$$

$$\times E^V(q,t)\frac{1}{q}(xy+z^3)$$

$$+ \frac{1-\exp[-(k^2+\gamma p^2+\gamma q^2)t/R]}{k^2+\gamma p^2+\gamma q^2}[k^2E^M(p,t) - p^2E^V(k,t)]$$

$$\times E^M(q,t)\frac{1}{q}z(1-y^2)\}, \tag{3.9}$$

$$\frac{\partial E^M(k,t)}{\partial t} + 2\gamma\frac{k^2}{R}E^M(k,t)$$

$$= \frac{R}{2}\int_{p+q=k} dpdq\{\frac{1-\exp[-(\gamma k^2+\gamma p^2+q^2)t/R]}{\gamma k^2+\gamma p^2+q^2}[k^2E^M(p,t) - p^2E^M(k,t)]$$

$$\times E^V(q,t)\frac{k}{pq}(1-y^2)$$

$$+ \frac{1-\exp[-(\gamma k^2+p^2+\gamma q^2)t/R]}{\gamma k^2+p^2+\gamma q^2}[k^2E^V(p,t) - p^2E^M(k,t)]$$

$$\times E^M(q,t)\frac{k^2}{p^2q}z(1-y^2)\}, \tag{3.10}$$

The kinetic and magnetic energies

$$\mathcal{E}^V(t) = \frac{1}{2}\langle|\mathbf{u}(\mathbf{x},t)|^2\rangle = \int_0^\infty E^V(k,t)dk ,$$
$$\mathcal{E}^M(t) = \frac{1}{2}\langle|\mathbf{b}(\mathbf{x},t)|^2\rangle = \int_0^\infty E^M(k,t)dk . \tag{3.11}$$

The kinetic and magnetic enstrophies

$$\Omega^V(t) = \langle(\partial u_1/\partial x_1)^2\rangle = \int_0^\infty k^2E^V(k,t)dk ,$$
$$\Omega^M(t) = \langle(\partial b_1/\partial x_1)^2\rangle = \int_0^\infty k^2E^M(k,t)dk . \tag{3.12}$$

Taylor's micro-scales of the kinetic and magnetic fields

$$\lambda^V(t)^2 = \langle u_1{}^2\rangle/\langle(\partial u_1/\partial x_1)^2\rangle = 5\mathcal{E}^V(t)/\Omega^V(t) ,$$
$$\lambda^M(t)^2 = \langle b_1{}^2\rangle/\langle(\partial b_1/\partial x_1)^2\rangle = 5\mathcal{E}^M(t)/\Omega^M(t) . \tag{3.13}$$

The micro-scale Reynolds numbers

$$\left.\begin{aligned} R_\lambda^V(t) &= \langle u_1{}^2\rangle\lambda^V(t)R = [\tfrac{2}{3}\mathcal{E}^V(t)]^{1/2}\lambda^V(t)R , \\ R_\lambda^M(t) &= \langle b_1{}^2\rangle\lambda^M(t)R = [\tfrac{2}{3}\mathcal{E}^M(t)]^{1/2}\lambda^M(t)R , \end{aligned}\right\} \tag{3.14}$$

@ Initial conditions

$$\left.\begin{aligned} E^V(k,0) &= C^VF(k) , \\ E^M(k,0) &= C^MF(k) , \end{aligned}\right\} \tag{3.15}$$

where

$$\left.\begin{aligned} F(k) &= \beta_a k^a \exp(-\alpha_a k^2) , \\ \alpha_a &= \frac{a+1}{10} , \quad \beta_a = 3\left(\frac{a+1}{10}\right)^{\frac{a+1}{2}} / \Gamma\left(\frac{a+1}{2}\right) , \end{aligned}\right\} \tag{3.16}$$

No. 11

Table I. The values of the parameters for the present numerical integrations.

	R	P_r	a	C^V	C^M
CASE I	800	1	2	1.0	0.1
CASE II	800	1	2	1.0	1.0
CASE III	800	1	4	1.0	0.1
CASE IV	800	1	4	1.0	1.0

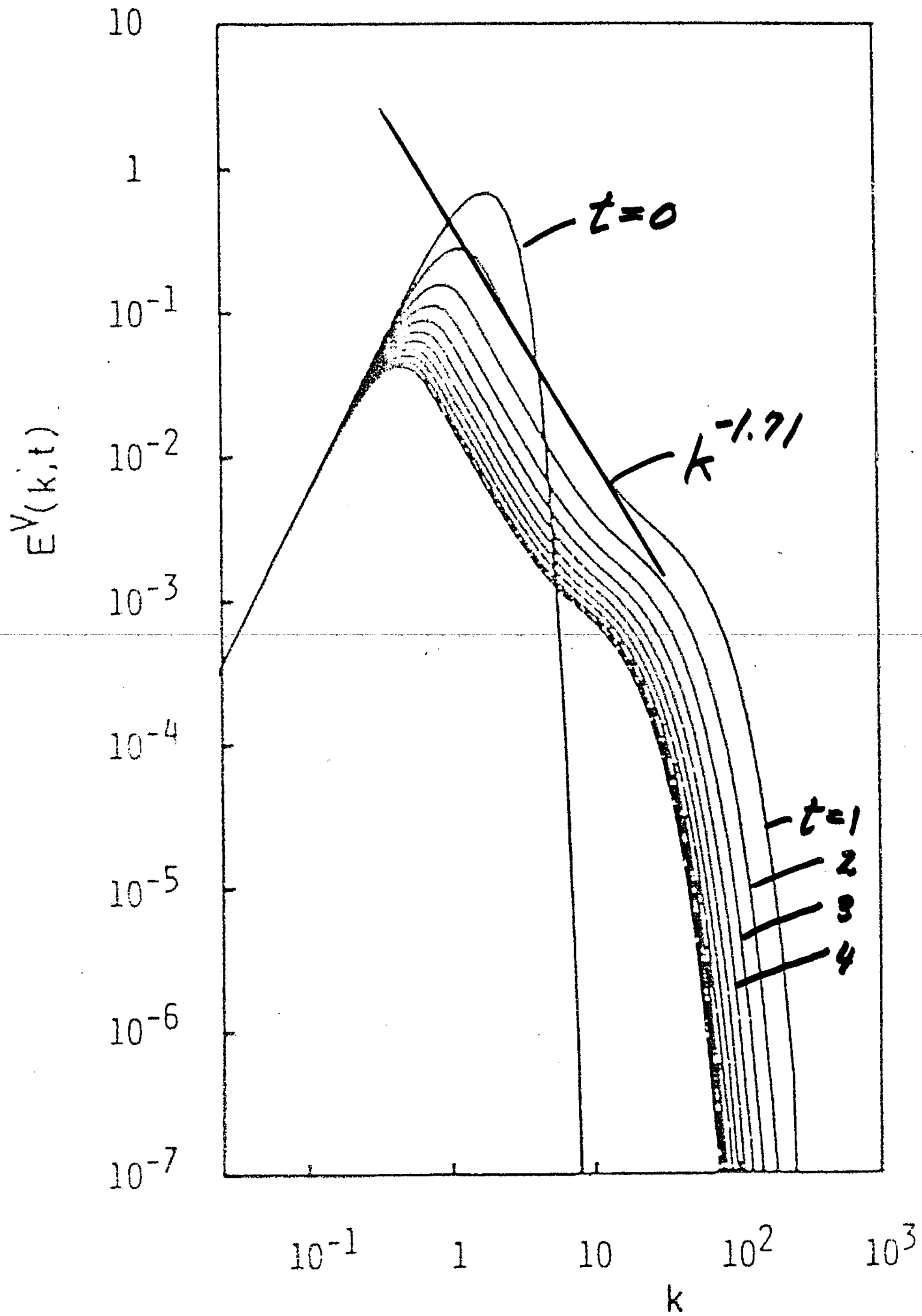

Fig.2 The time evolutions of the kinetic and magnetic energy spectra for cases III and IV.

(a) $E^V(k,t)$ for case III.

No. 14

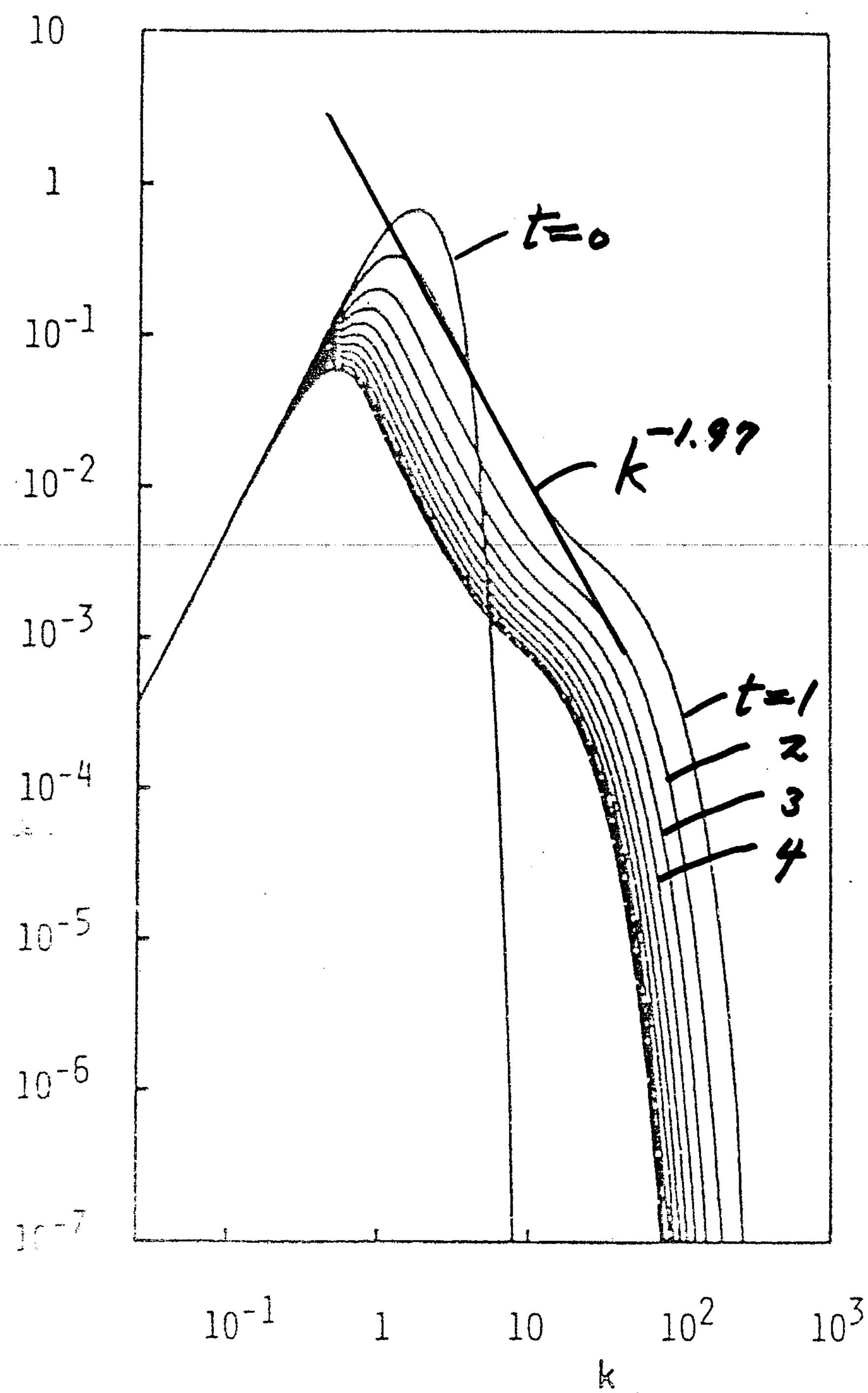

(b) $E^M(k,t)$ for case III.

No. 15

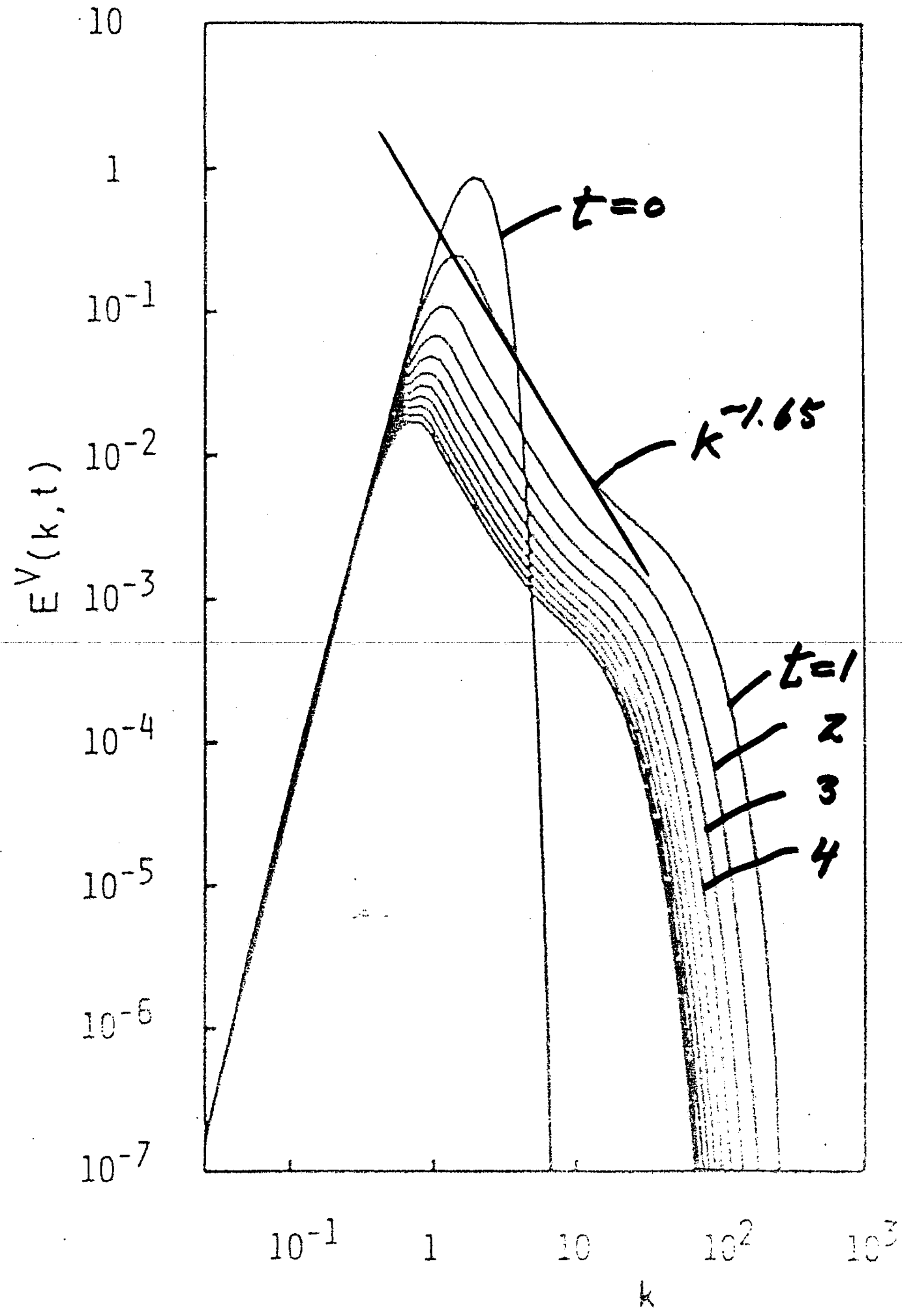

(c) $E^V(k,t)$ for case IV.

NO. 16

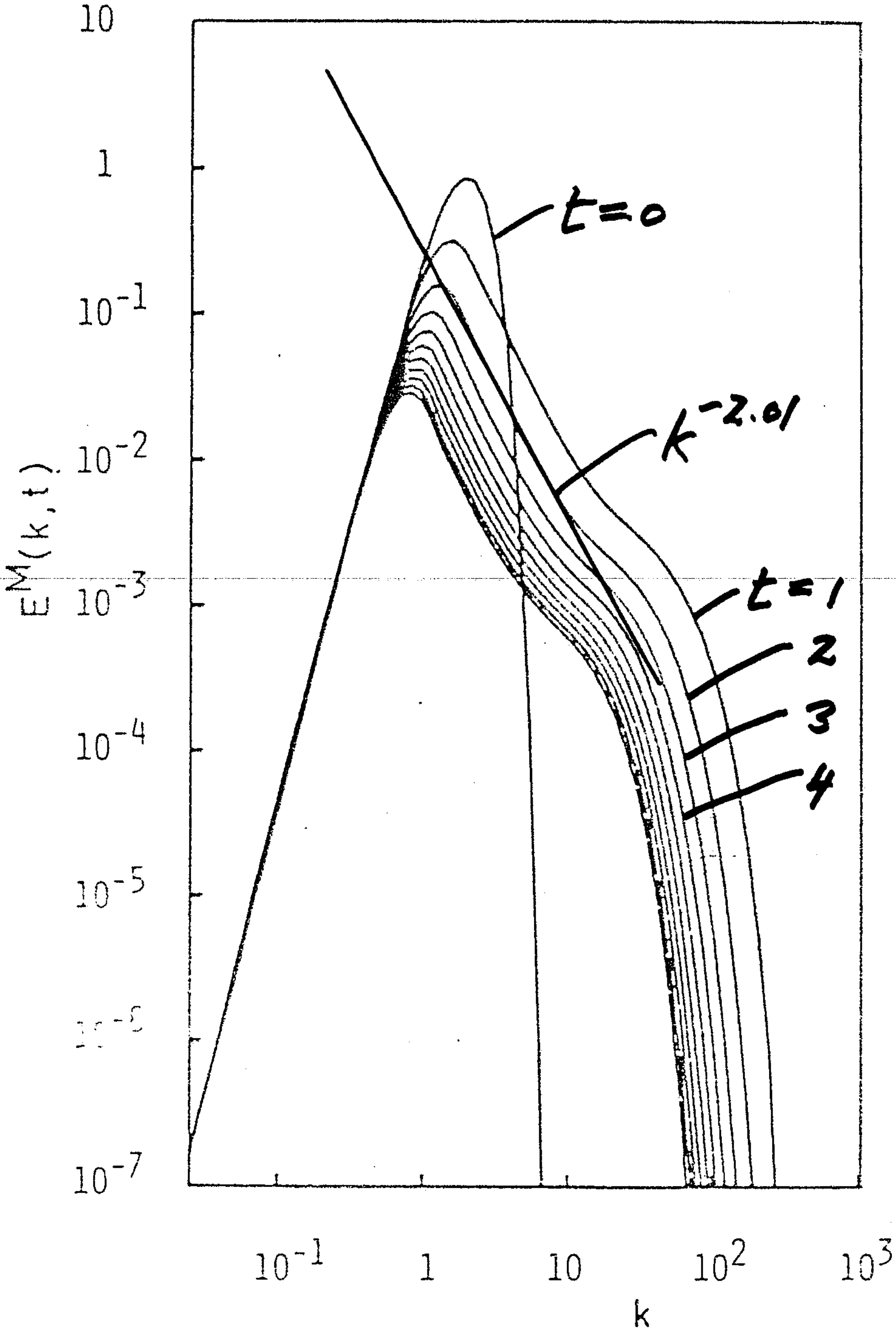

(d) $E^M(k,t)$ for case IV.

No. 1

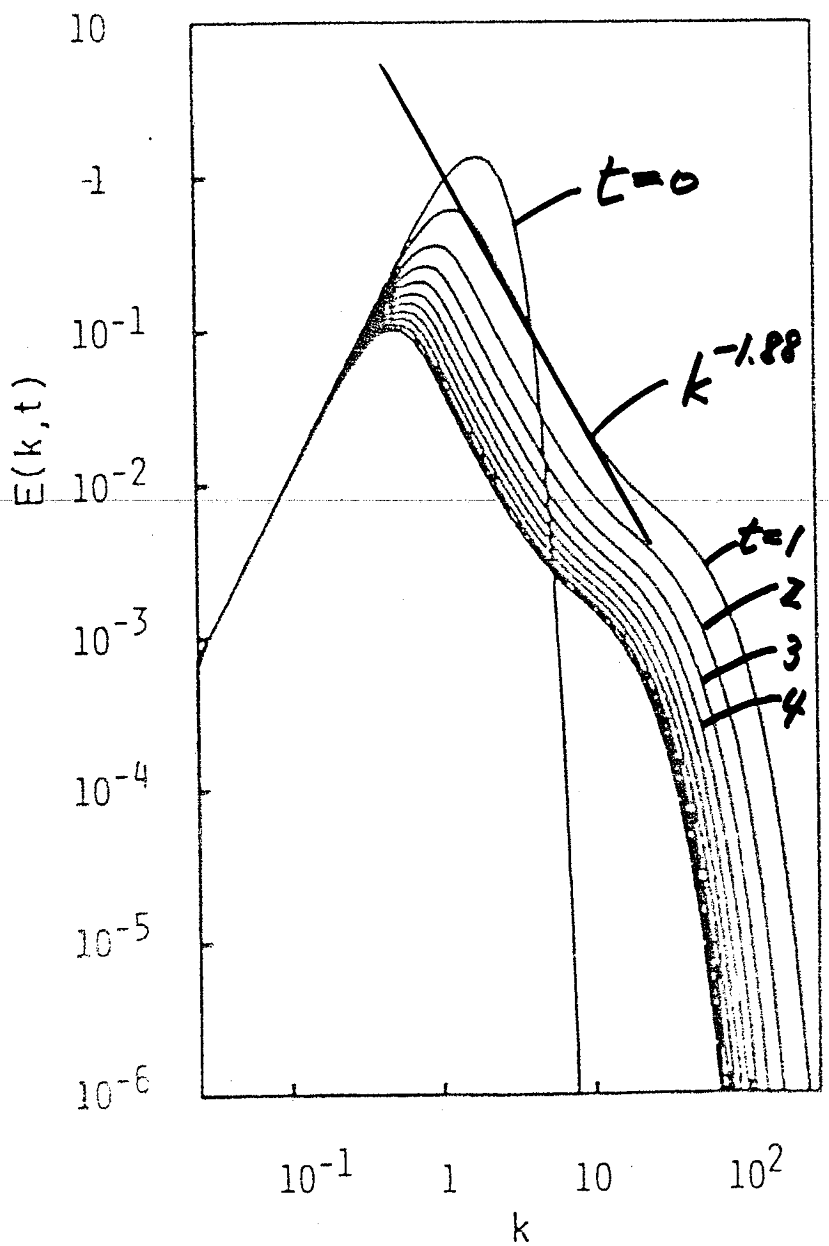

Fig.3. The total energy spectra E(k,t) for cases III and IV.

(a) E(k,t) for case III.

NO. 18

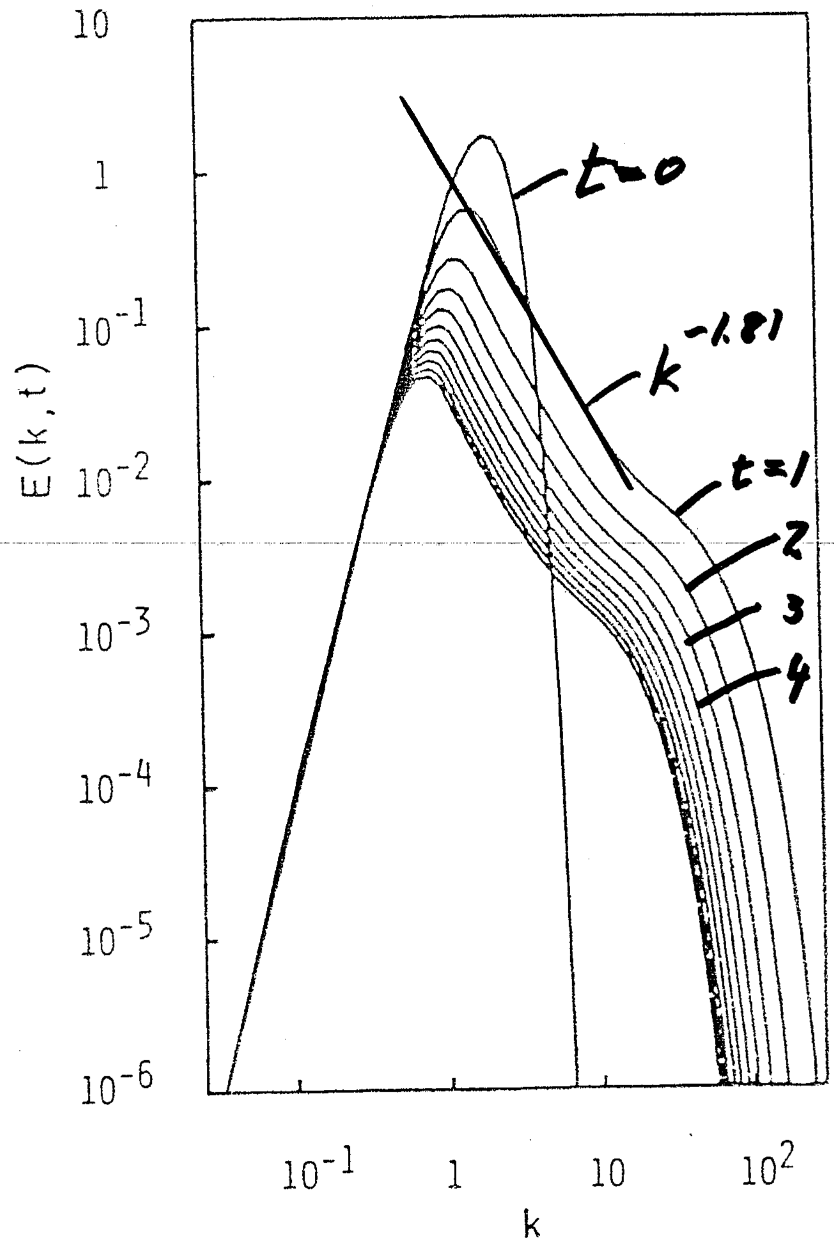

(b) E(k,t) for case IV.

Ne. 19

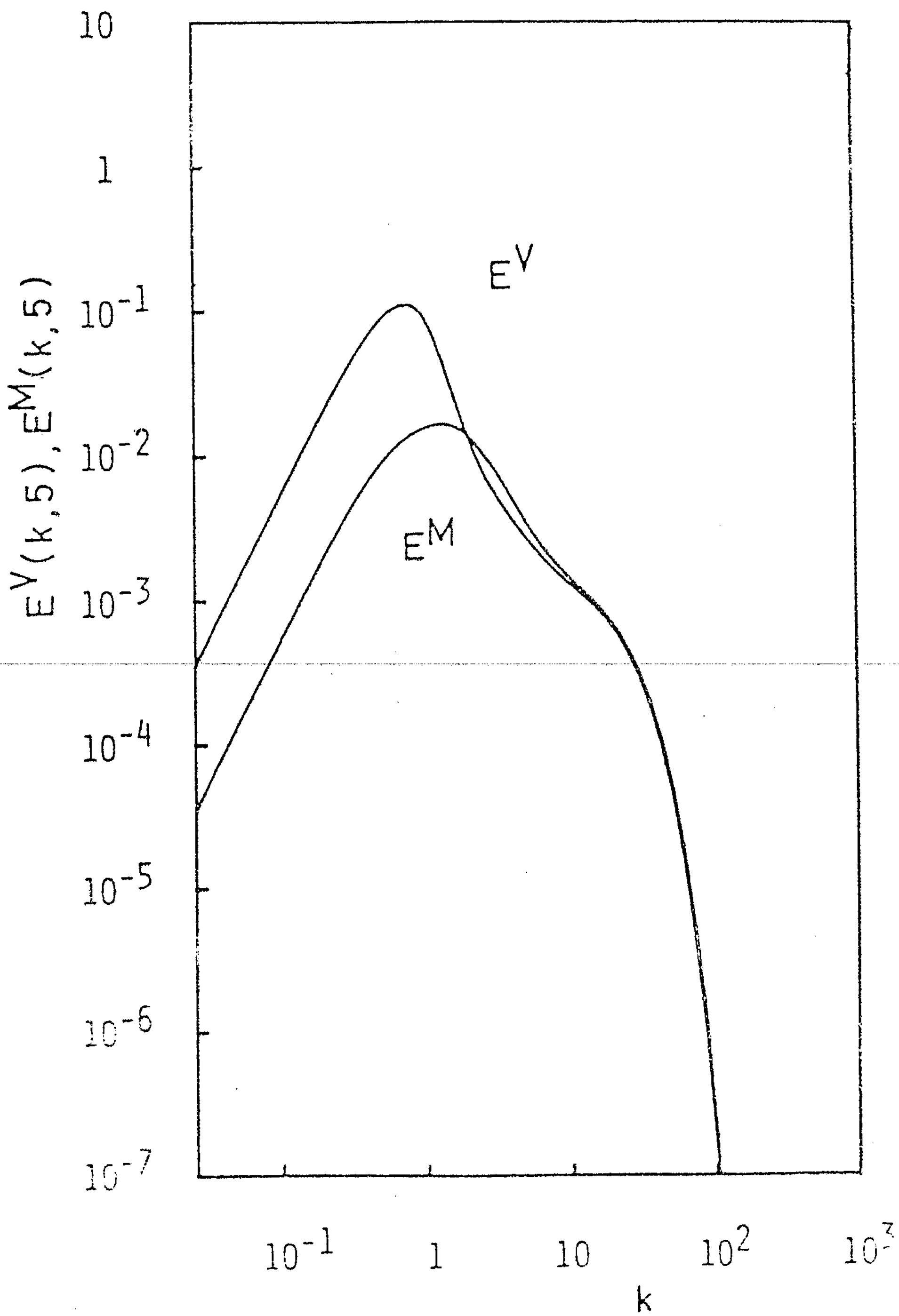

Fig.4. The energy spectra $E^V(k,t)$ and $E^M(k,t)$ at t=5 for cases I and II.

(a) $E^V(k,5)$ and $E^M(k,5)$ for case I.

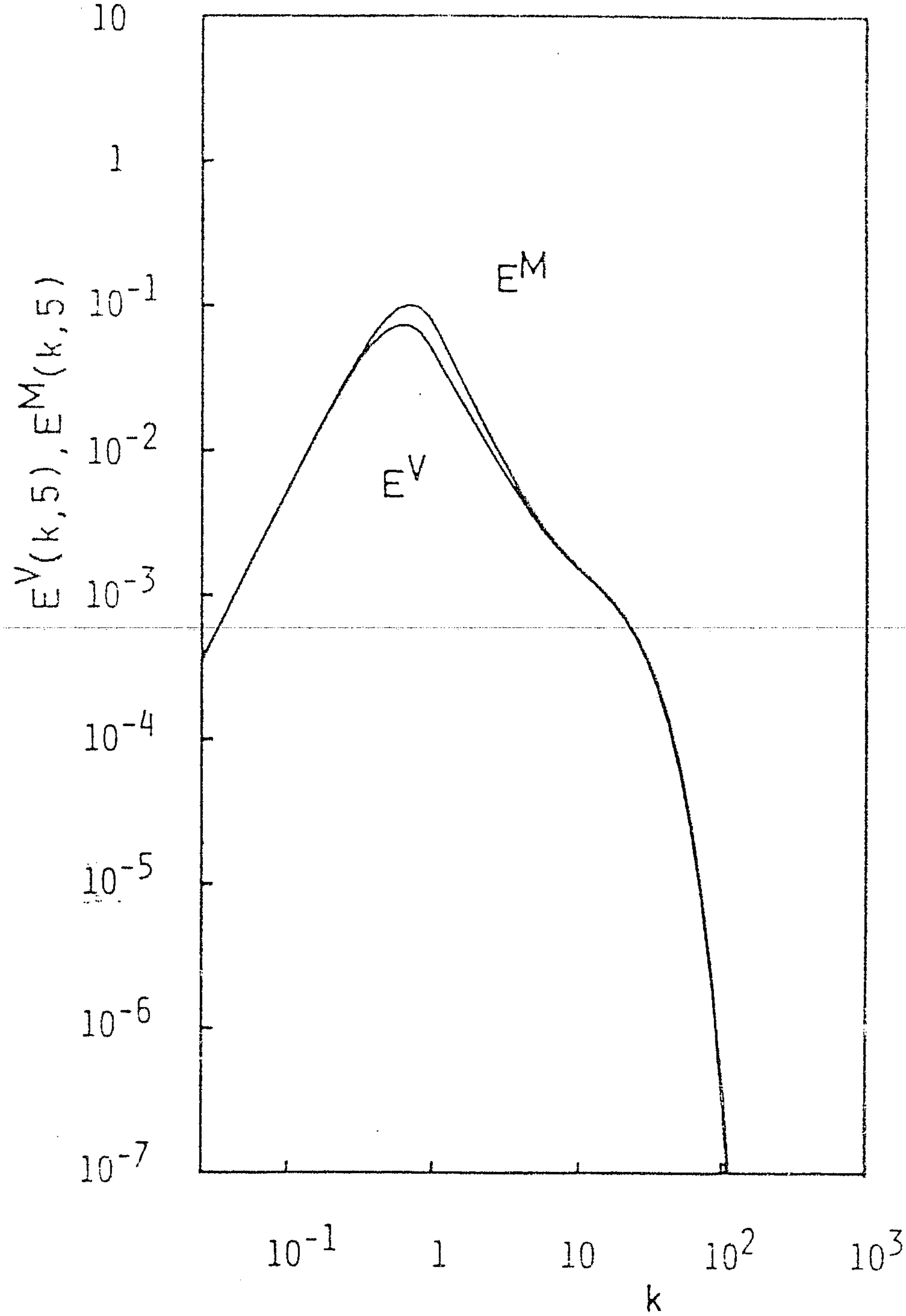

(b) $E^V(k,5)$ and $E^M(k,5)$ for case II.

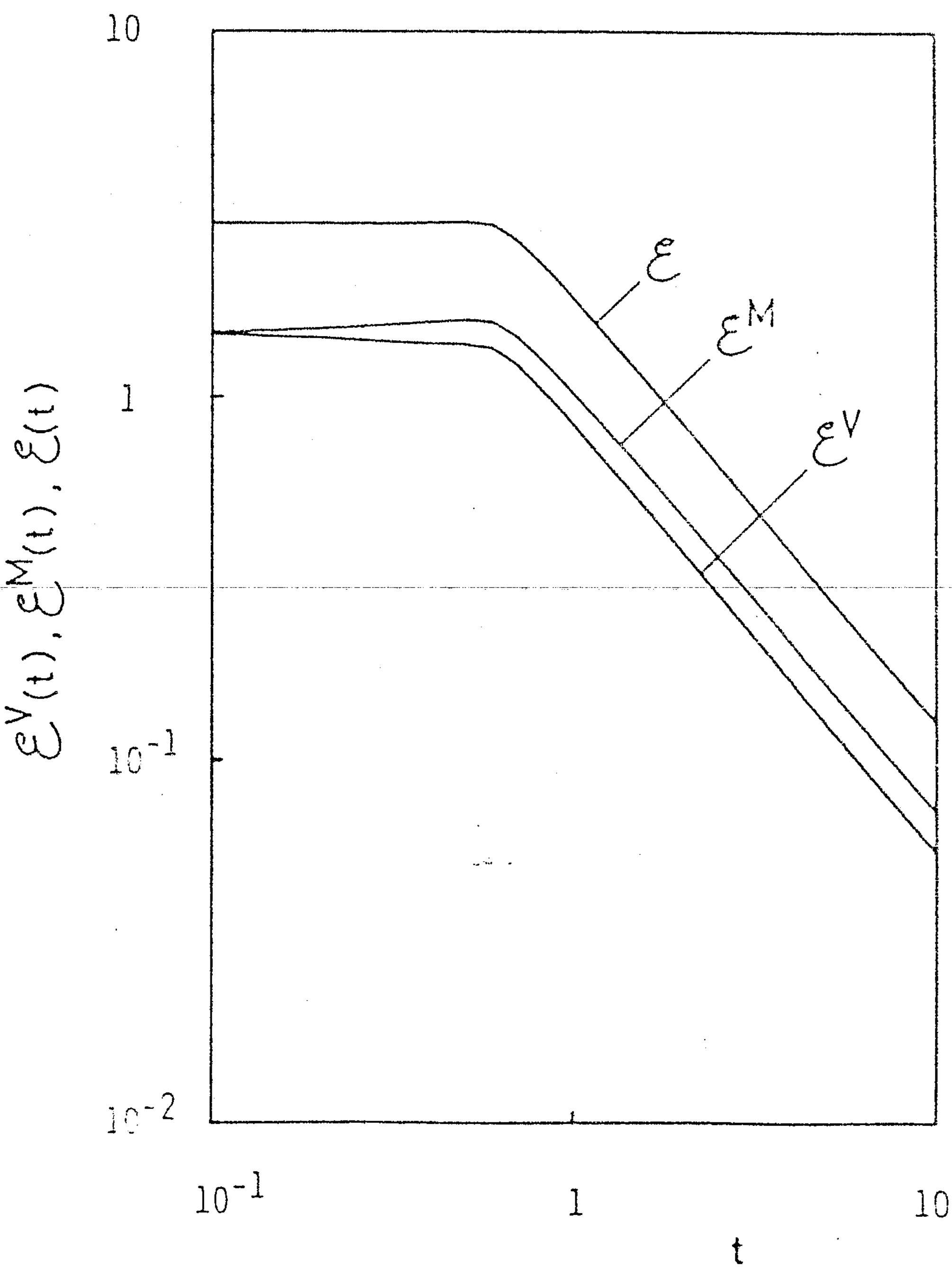

Fig. [illegible] The decays of the kinetic, magnetic and total energies, i.e. $\mathcal{E}^V(t)$, $\mathcal{E}^M(t)$ and $\mathcal{E}(t)$ for cases II and IV.

(a) $\mathcal{E}^V(t)$, $\mathcal{E}^M(t)$ and $\mathcal{E}(t)$ for case II.

No. 22.

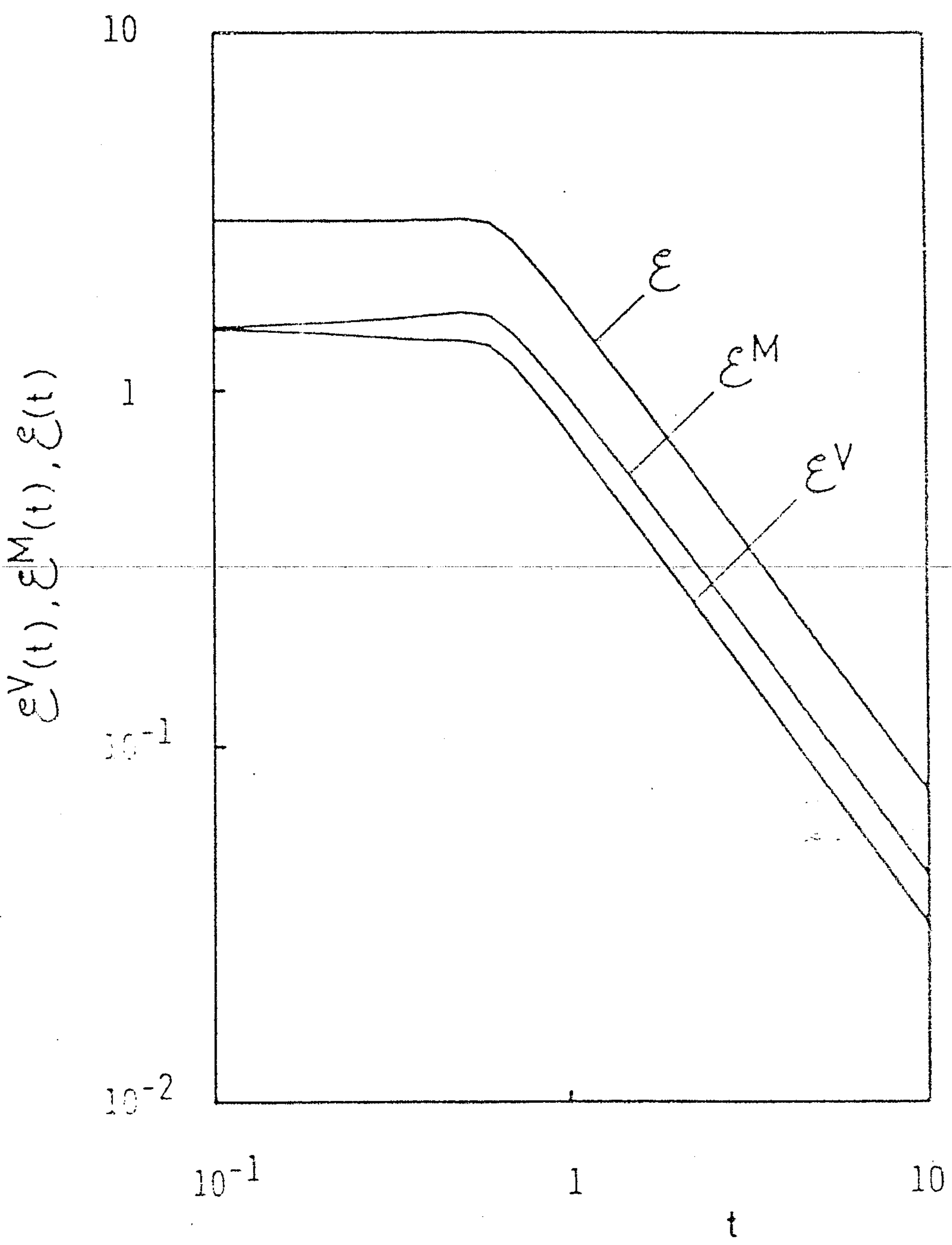

(b) $\mathcal{E}^V(t)$, $\mathcal{E}^M(t)$ and $\mathcal{E}(t)$ for case IV.

NC. 23

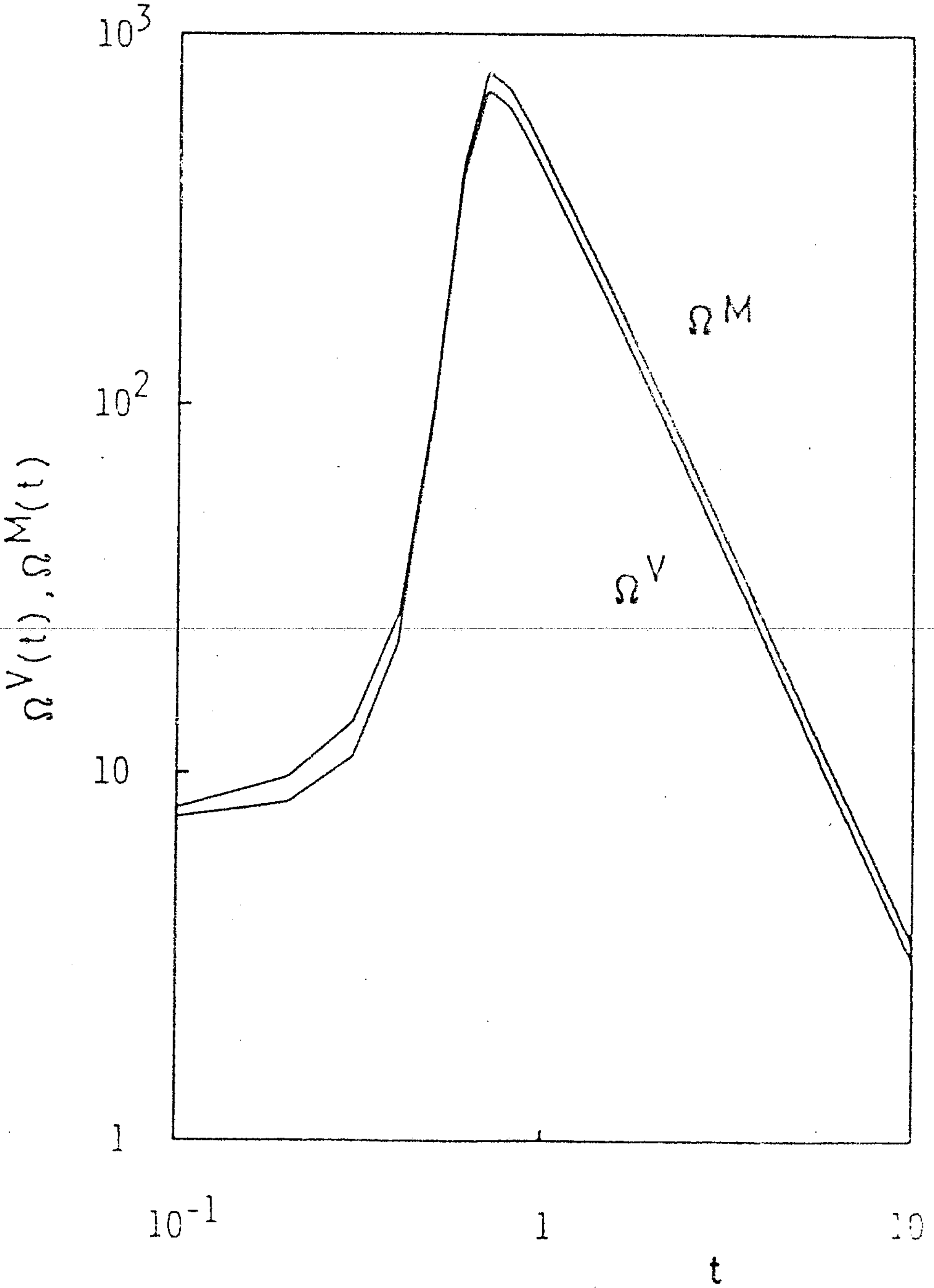

Fig.6.7 The time dependences of the enstrophy $\Omega^V(t)$ and $\Omega^M(t)$ for cases III and IV.

(a) $\Omega^V(t)$ and $\Omega^M(t)$ for case III.

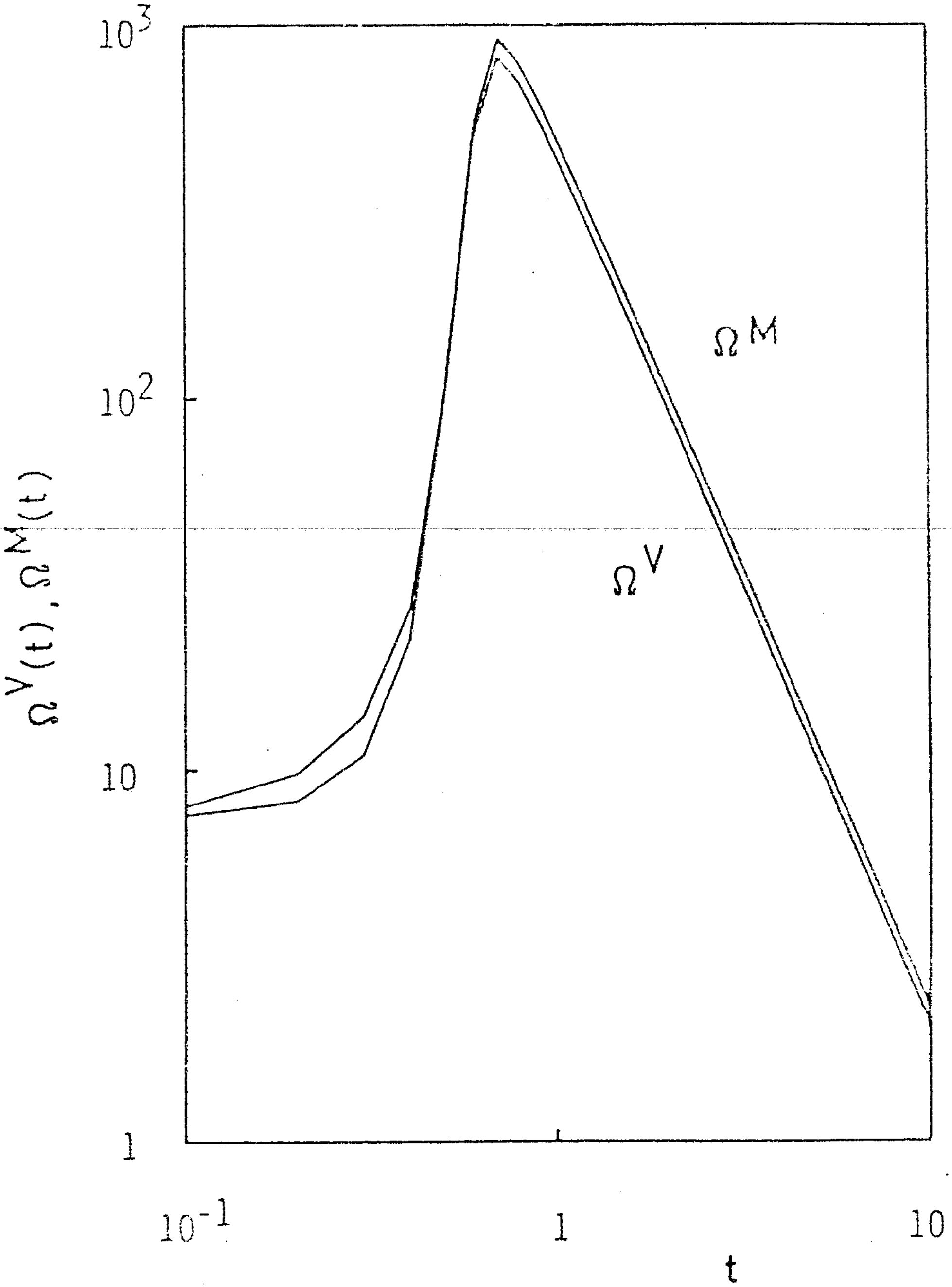

(b) $\Omega^V(t)$ and $\Omega^M(t)$ for case IV.

Nc. 25

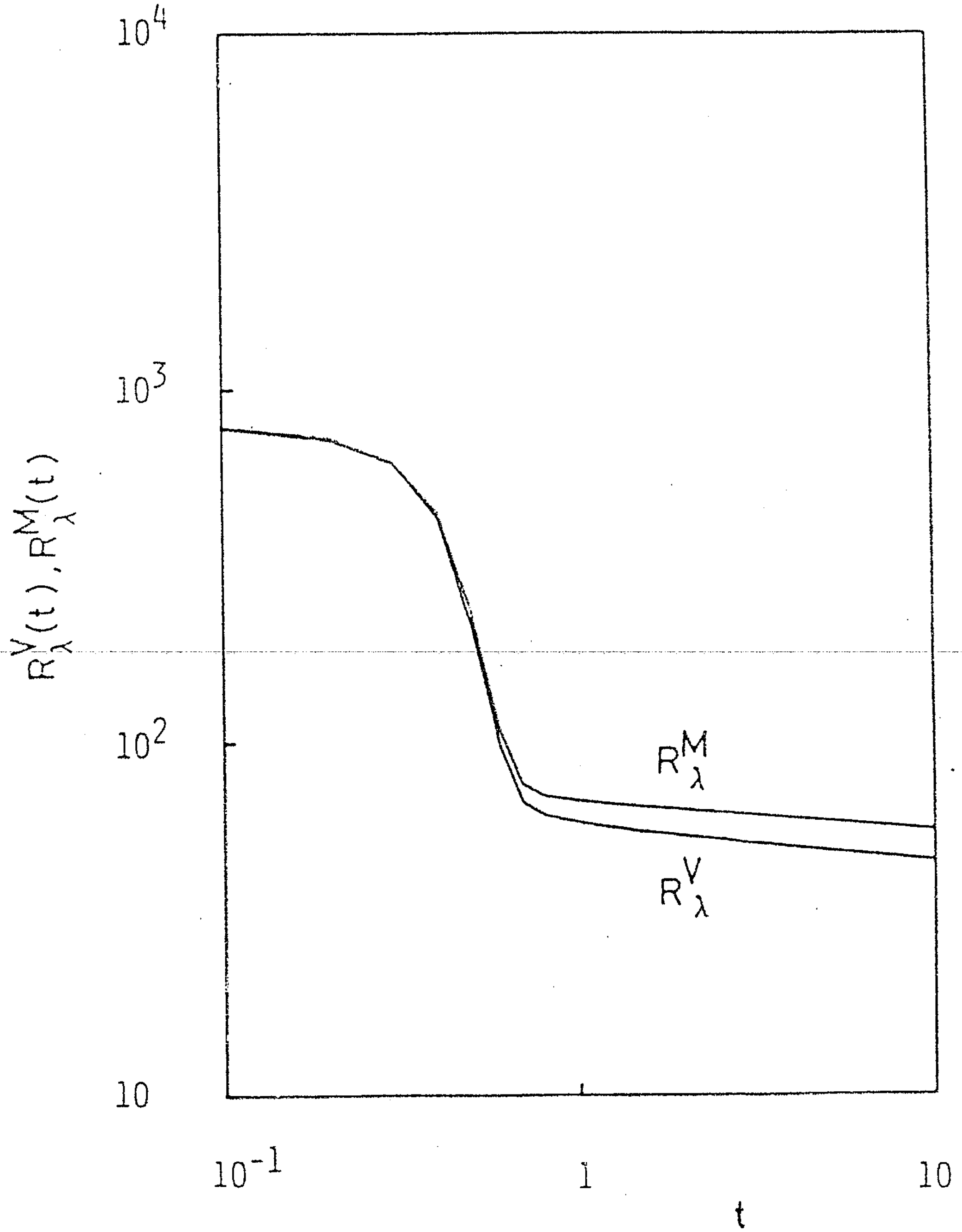

Fig.7. The time developments of the micro scale Reynolds number $R^V_\lambda(t)$ and $R^M_\lambda(t)$ for cases III and IV.

(a) $R^V_\lambda(t)$ and $R^M_\lambda(t)$ for case III.

nc. 2f

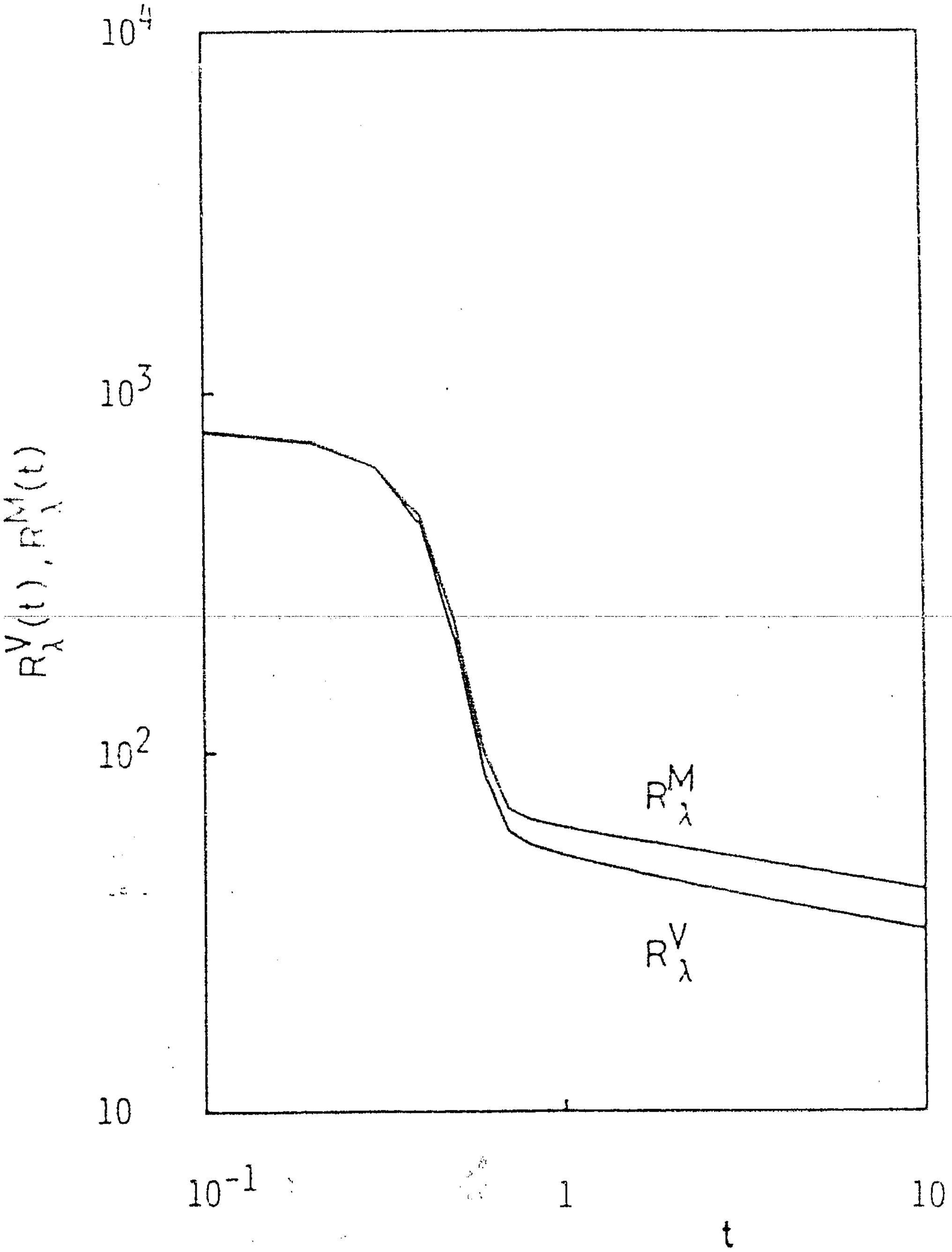

(b) $R_\lambda^V(t)$ and $R_\lambda^M(t)$ for case IV.

NO. 12

Table II. The power indexes of the energy decay law, $\mathcal{E}^V(t) \propto t^{-b^V}$, $\mathcal{E}^M(t) \propto t^{-b^M}$ and $\mathcal{E}(t) \propto t^{-b}$.

	a	b^V	b^M	b
Eq. (2.16)	2	1.2	1.2	1.2
CASE I	2	1.19	1.15	1.19
CASE II	2	1.17	1.17	1.17
Eq. (2.16)	4	1.43	1.43	1.43
CASE III	4	1.40	1.34	1.38
CASE IV	4	1.36	1.34	1.36

$\langle V \times b \rangle \simeq \alpha B$

RELAXATION, TURBULENCE, AND DYNAMO ACTION IN DRIVEN SYSTEMS

D. SCHNACK

SCIENCE APPLICATIONS, INC.

RELAXATION, TURBULENCE, AND DYNAMO ACTION IN DRIVEN SYSTEMS.

D. Schnack
SAI La Jolla

Driven System

A magnetoplasma system with external reservoirs of energy and flux

Examples

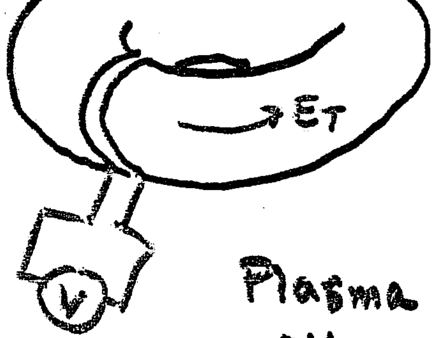

or

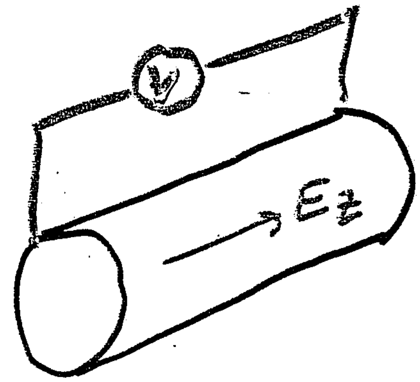

Plasma confinement experiment with applied voltage.

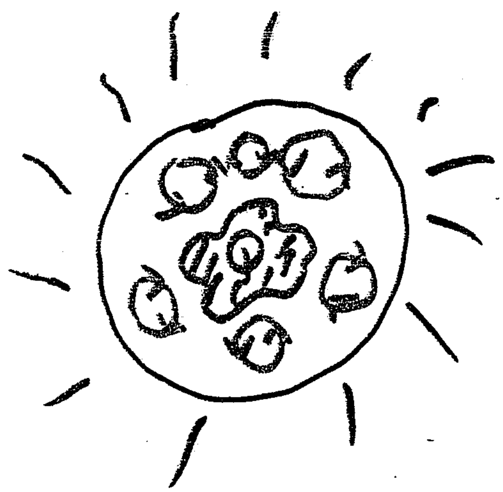

Convective heating from within (stars, earth)

differential rotation

or

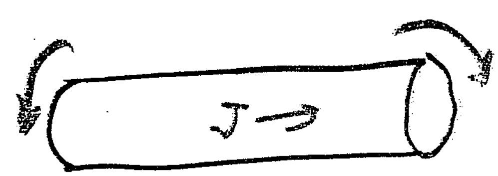

Corona loop driven by ~~differential~~ rotation at feet.

Many Driven Systems Exhibit anomalously long lifetimes:

- Terrestrial and Solar Magnetic Fields
- Positive (non-reversed) toroidal flux in RFP.
- Spheromak (d.c.)

How do such systems evolve?

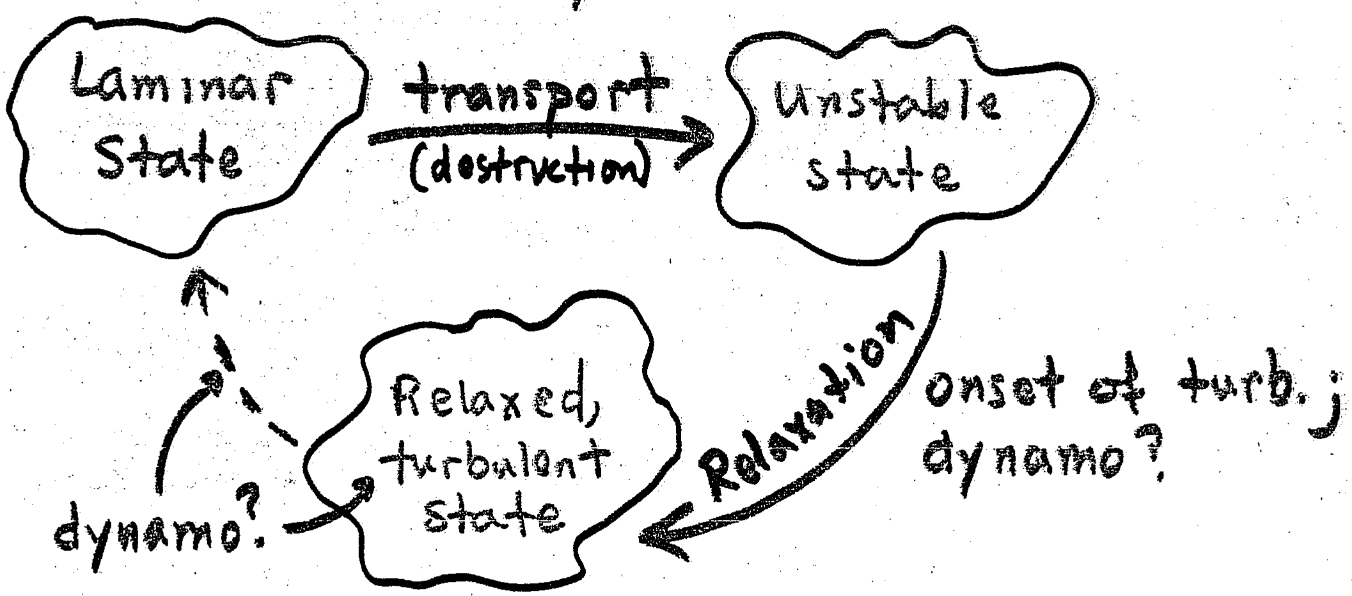

- Is there such a separation between transport, instability, relaxation, and turbulence?
- Does the loop close?
- Properties of each step. (Relaxation, instab., turb.)
- What is responsible for dynamo?

CODES FOR RELAXATION, DYNAMO, AND TURBULENCE STUDIES

SPECTR3 - fully compressible

INCOMPR - incompressible

NOTSOINC - (0,0) compressible; (m,n) incompressible

ALL HAVE:

- Resistive MHD
- "Primitive" equations
- 3-D cylindrical geometry
- Pseudo-spectral (θ, z); dealiased
- Finite difference (r)
- Explicit, leap-frog advection (except NOTSOINC, where (0,0) is implicit)
- Implicit resistive diffusion.

- NUMERICAL EXPERIMENTS.
- GUIDE TO ANALYTIC UNDERSTANDING.

RELAXATION

The tendency of non-ideal magnetoplasma systems to spontaneously minimize energy subject to constraints.

- Taylor hypothesis (Resistive plasma $\Rightarrow$ reconnection $\Rightarrow$ topology breaking)

  $W = \int B^2 dv \;,\; K = \int \underline{A} \cdot \underline{B}\, dv \;,\; \frac{W}{K} \to \min.$

  - Is K an invarient?
  - Is K the proper invarient?
  - Is K the only invarient?

- Transport processes increase W/K (Caramana, et.al. 1983)

  What mechanisms cause W/K to decrease?

  - Instabilities?
  - Turbulence?

- Interplay between <u>transport</u> and <u>relaxation</u>.

- Effect of <u>relaxation</u> on <u>confinement</u>.

RELAXATION DUE TO MHD INSTABILITIES (RFP)

(onset of turbulence)

- Plasma driven away from $(W/K)_{min}$ by transport.

- Resistive modes ⇒ reconnection ⇒ relaxation

- Many modes unstable
  - $m=1$, $|n| \gg 1$
  - resonant
  - non-resonant

- Single helicity evolution
  - 2 reconnection phases
  - $q(0)$ lowered, then raised

- 3-D evolution
  - $m=1$ saturation affected by other modes
  - mode coupling to $m=0, 2$
  - reconnection ⇒ stochasticity

- W/K minimized during growth and saturation of modes.

m=1, n=-11 single helicity

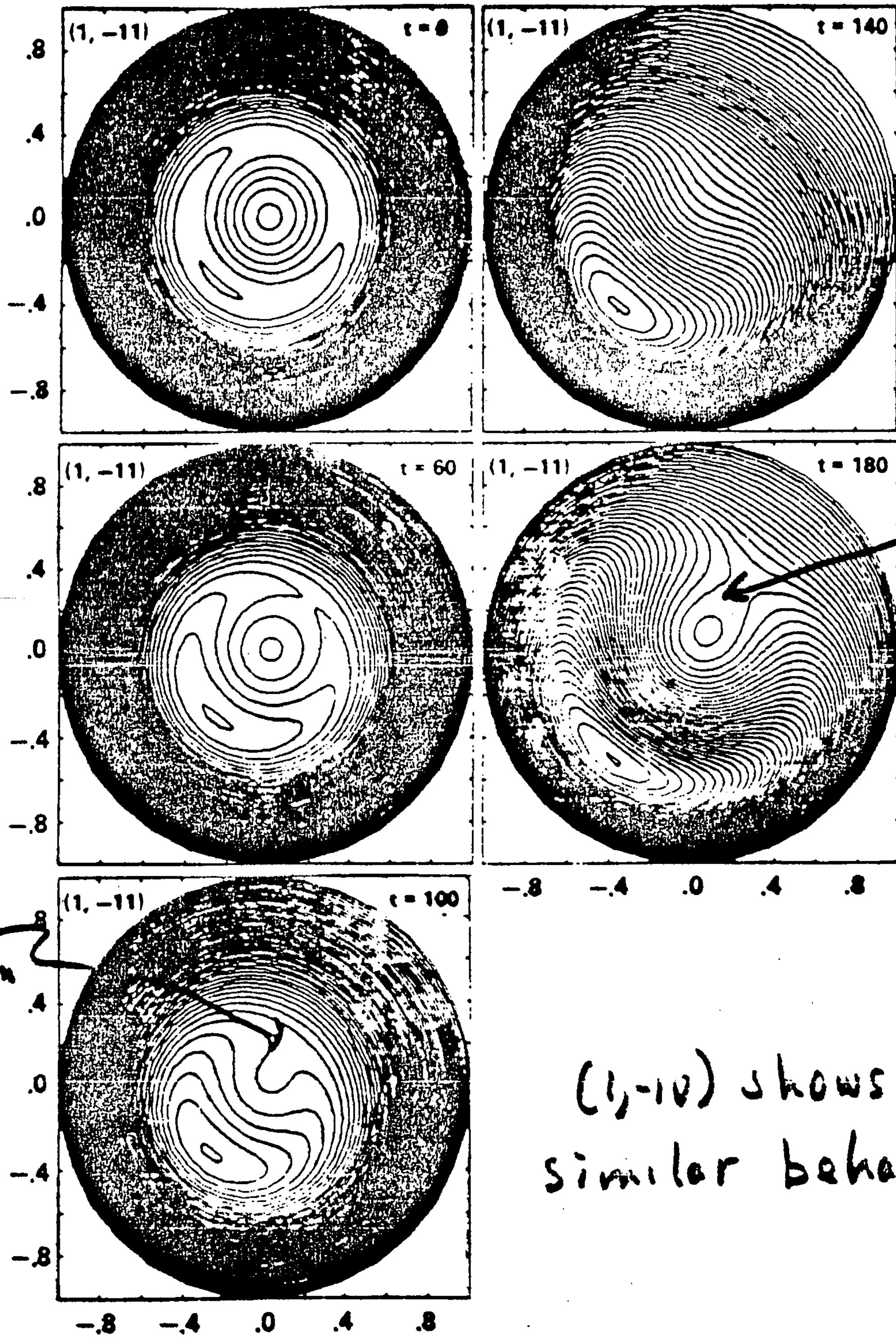

"second reconnection"

first "reconnection"

(1,-10) shows similar behavior.

m=1, n=-11 3-D SIMULATION

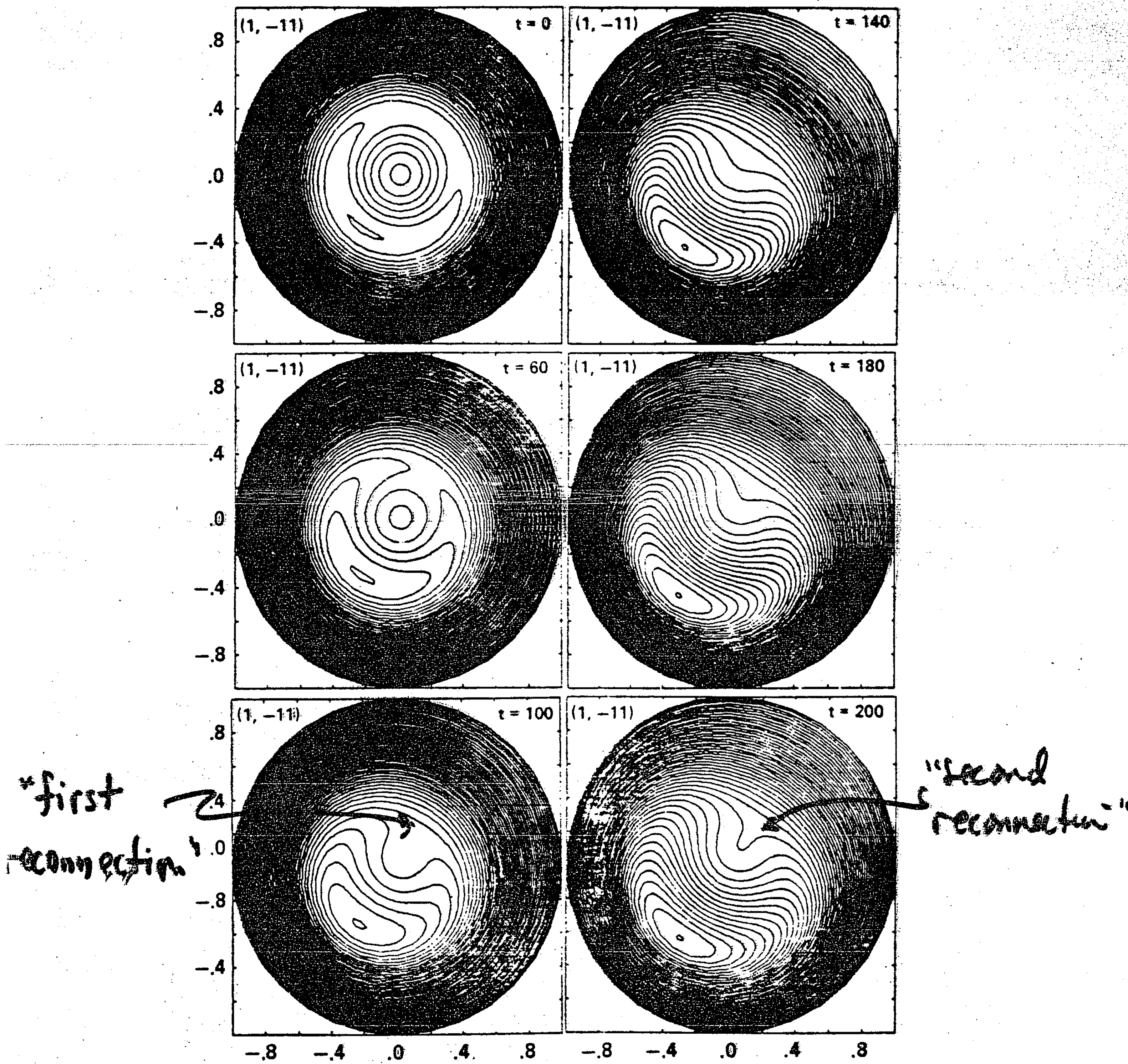

- Growth retarded
- Second reconnection begins

m=1, n=-10 3-D SIMULATION

note "bounce"

"first reconnection"

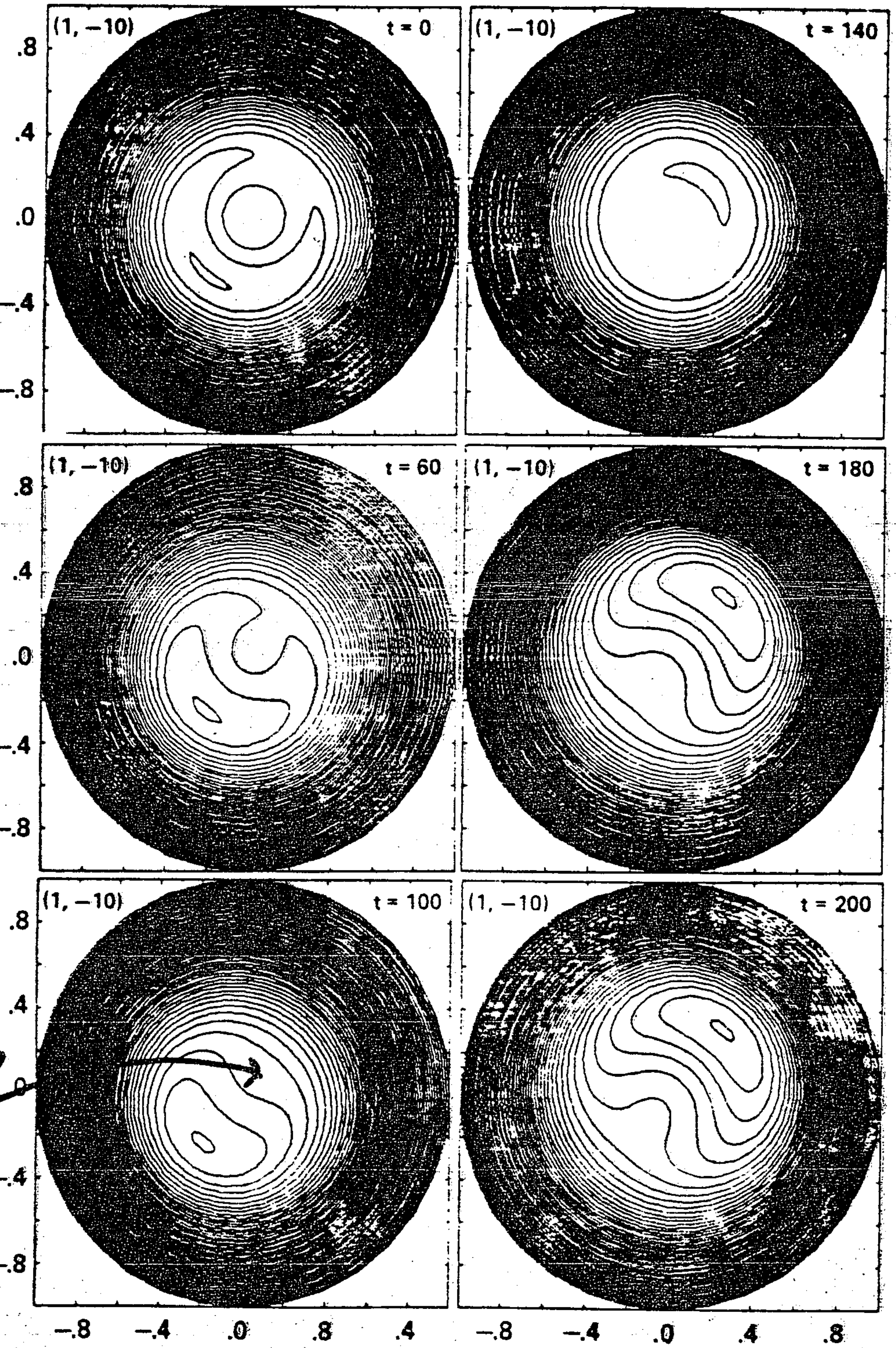

• No second reconnection ⟸

• "Bounce" at t ≈ 120

(1,−10)   resonant
(1,−11)   modes

Non-resonant modes show rapid rise of q(0):

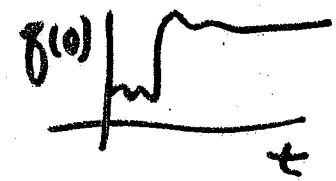

first reconnection

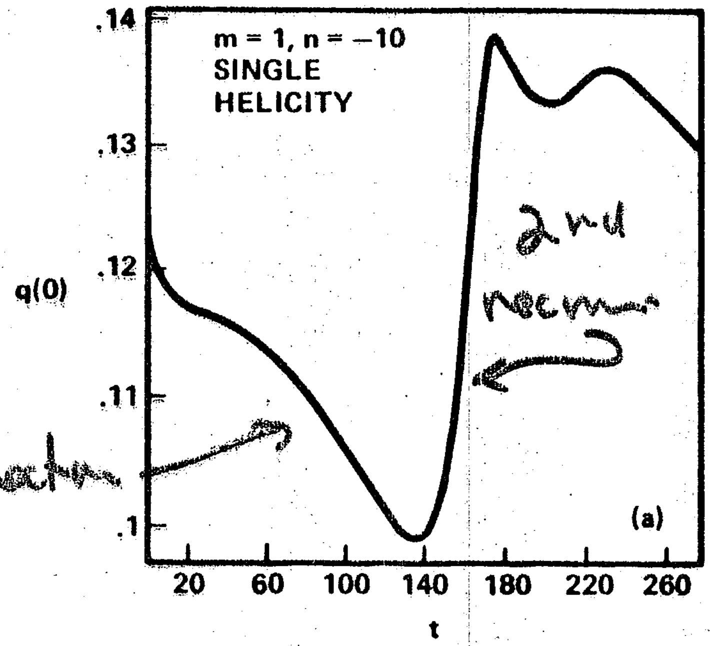

2nd reconn.

first reconn.

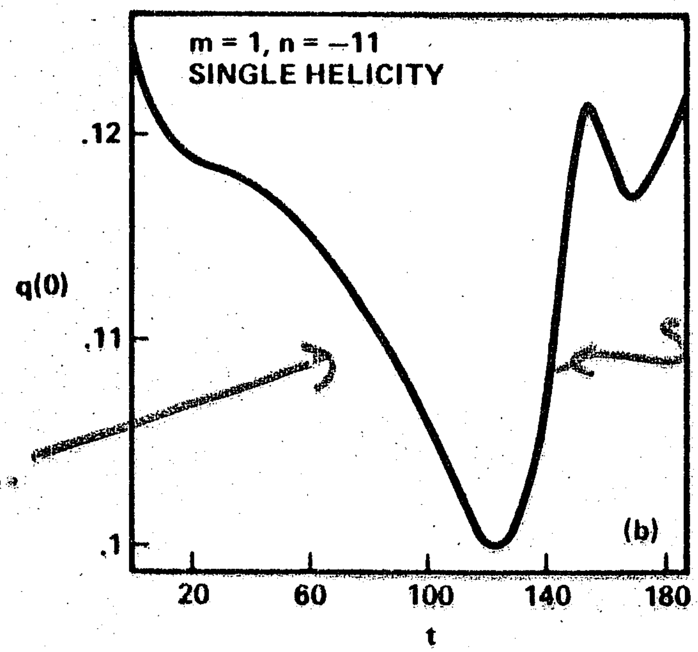

2nd reconn.

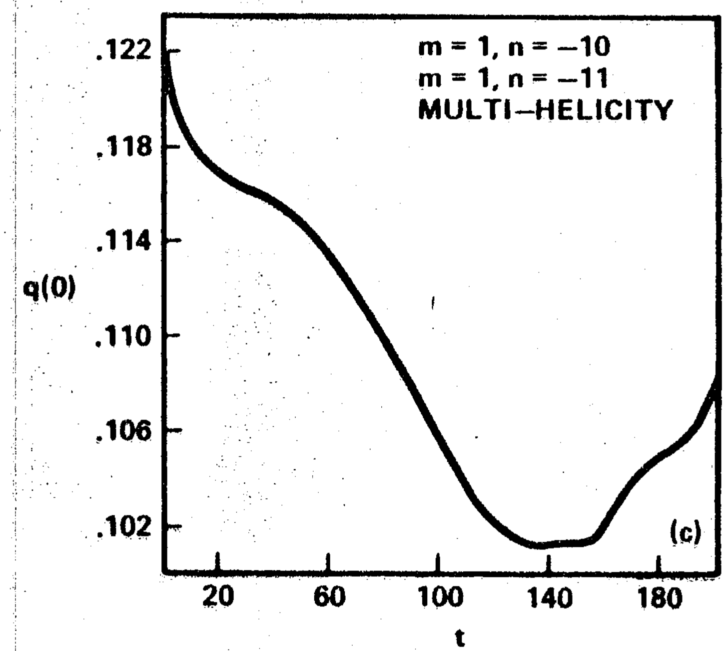

slower rate of rise

COMPARISON OF SINGLE-HELICITY AND THREE-DIMENSIONAL RESULTS

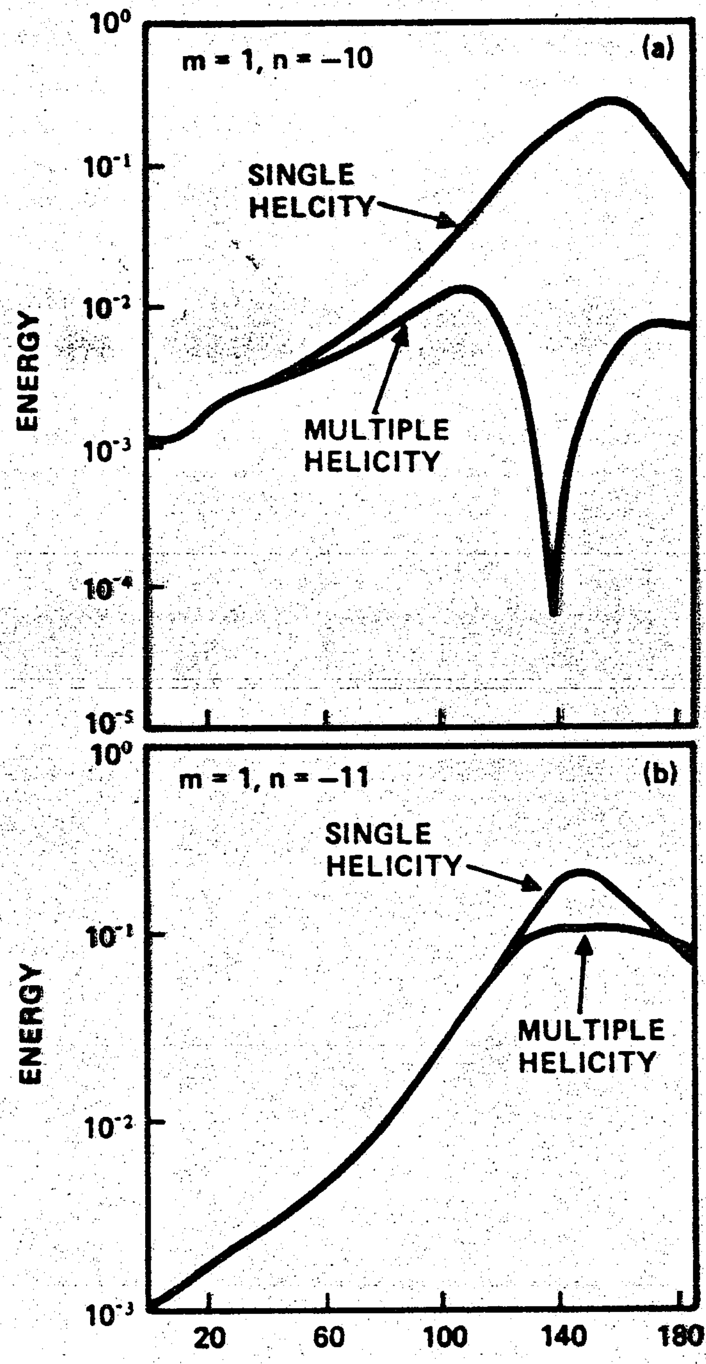

- Saturates at lower level ~~the~~ in 3D than single helicity
- Energy drain to m=0, m=2
- Agreement with Holmes, et. al. APS, LA (1983)

$N_r = 65$, $N_\theta = 8$, $N_z = 64$

3-D SIMULATION — LOW (H)

Field line plots - surfaces of section

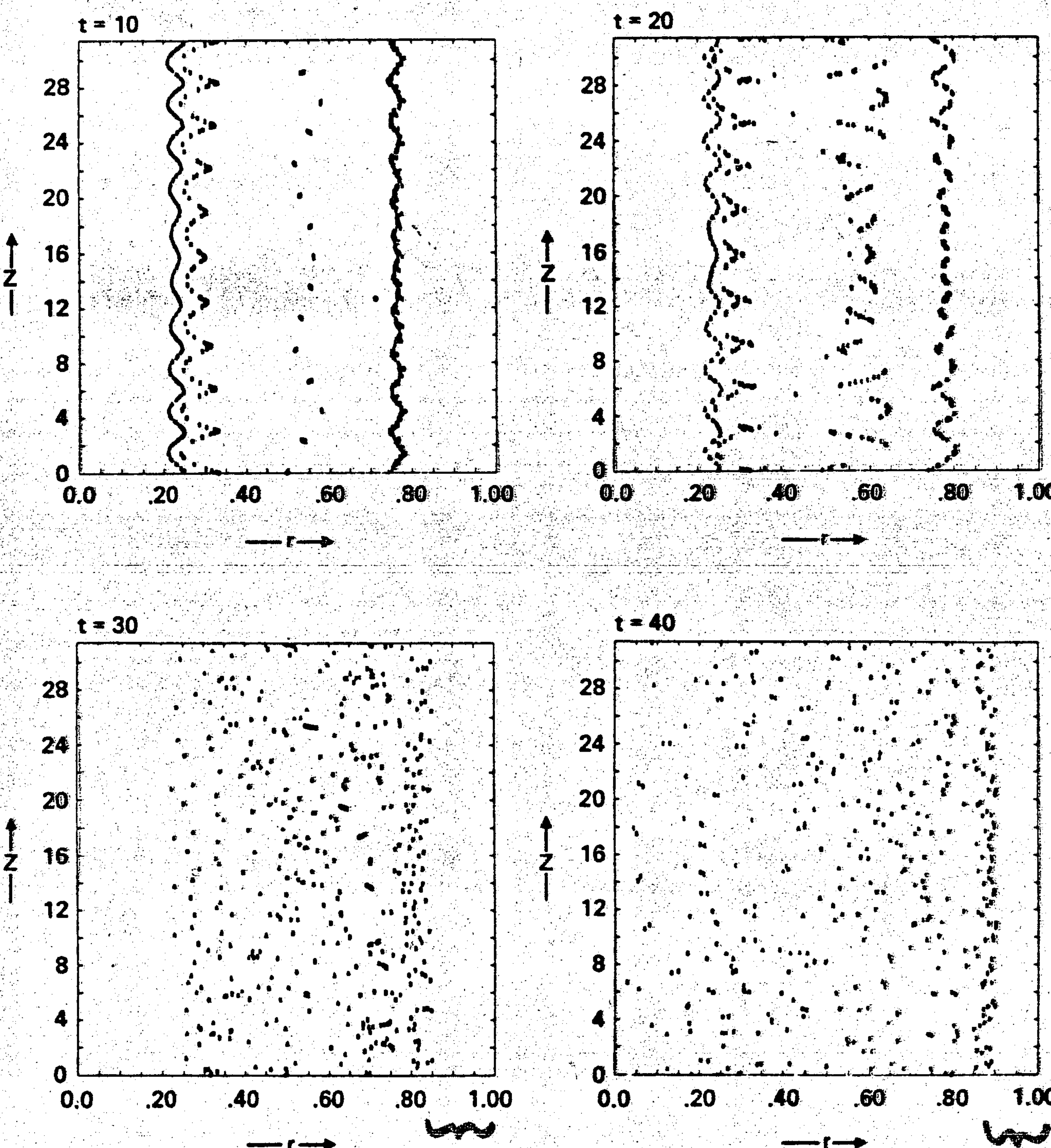

Flux surfaces remain

3-D SIMULATION - HIGH Θ

Field line plots

Confinement lost

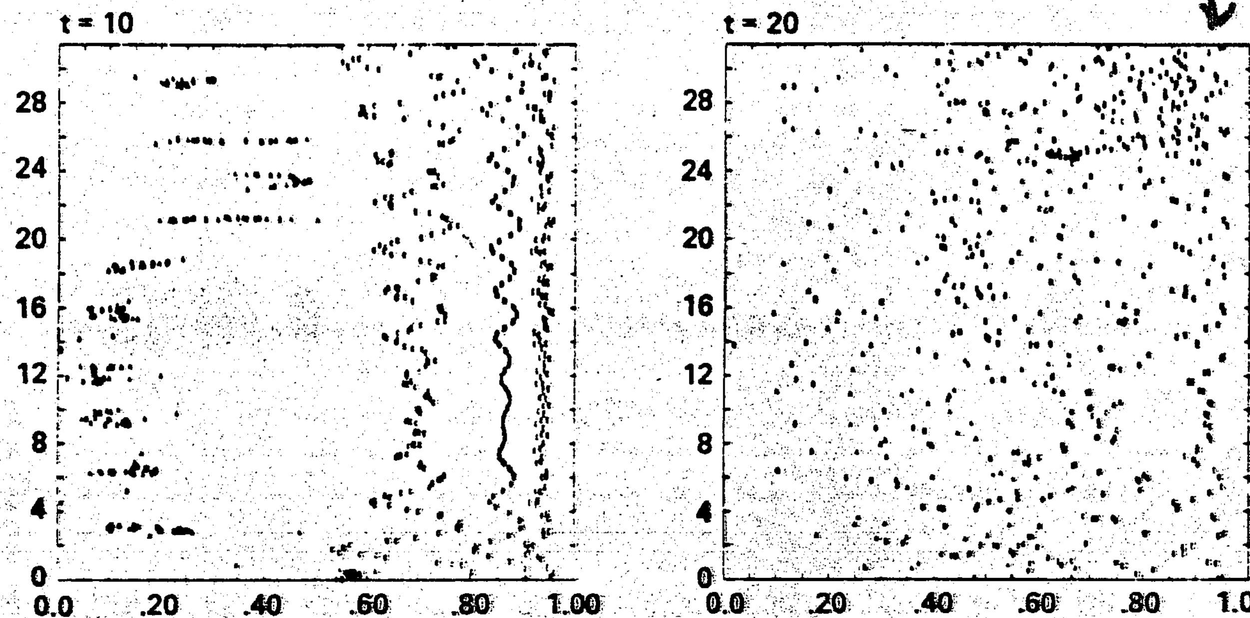

"leak" toroidally localized

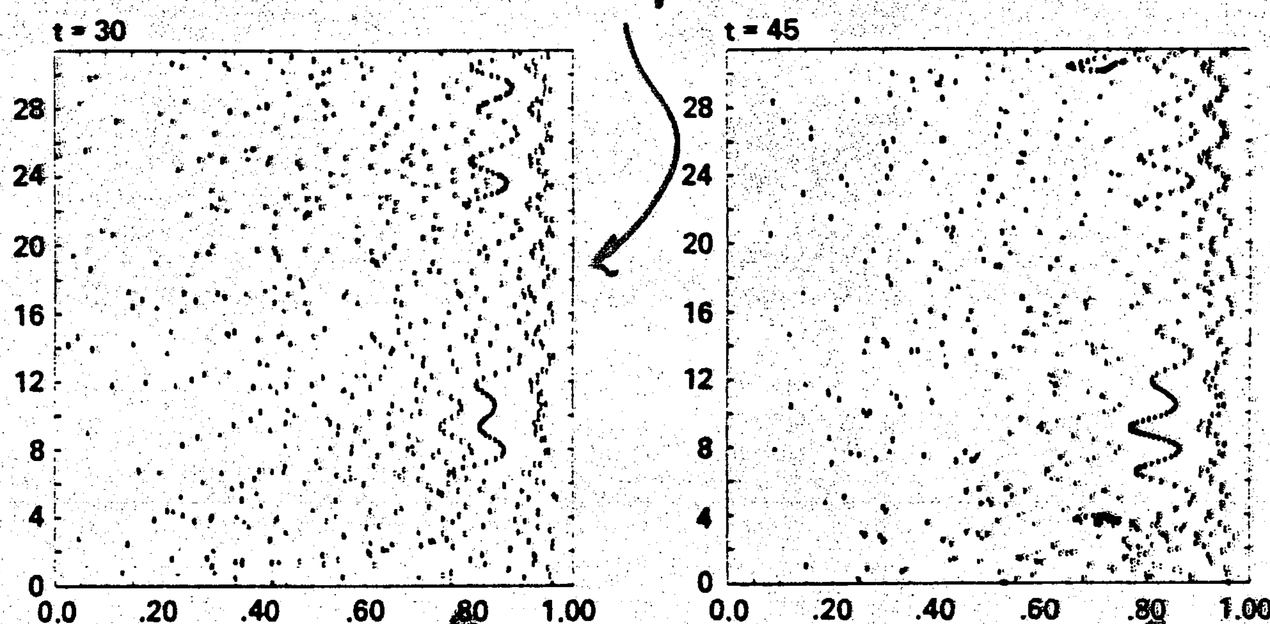

rehealing of surfaces

3-D SIMULATION – LOW ④
m=0 magnetic islands.

Small m=0 cannot interact with m=1

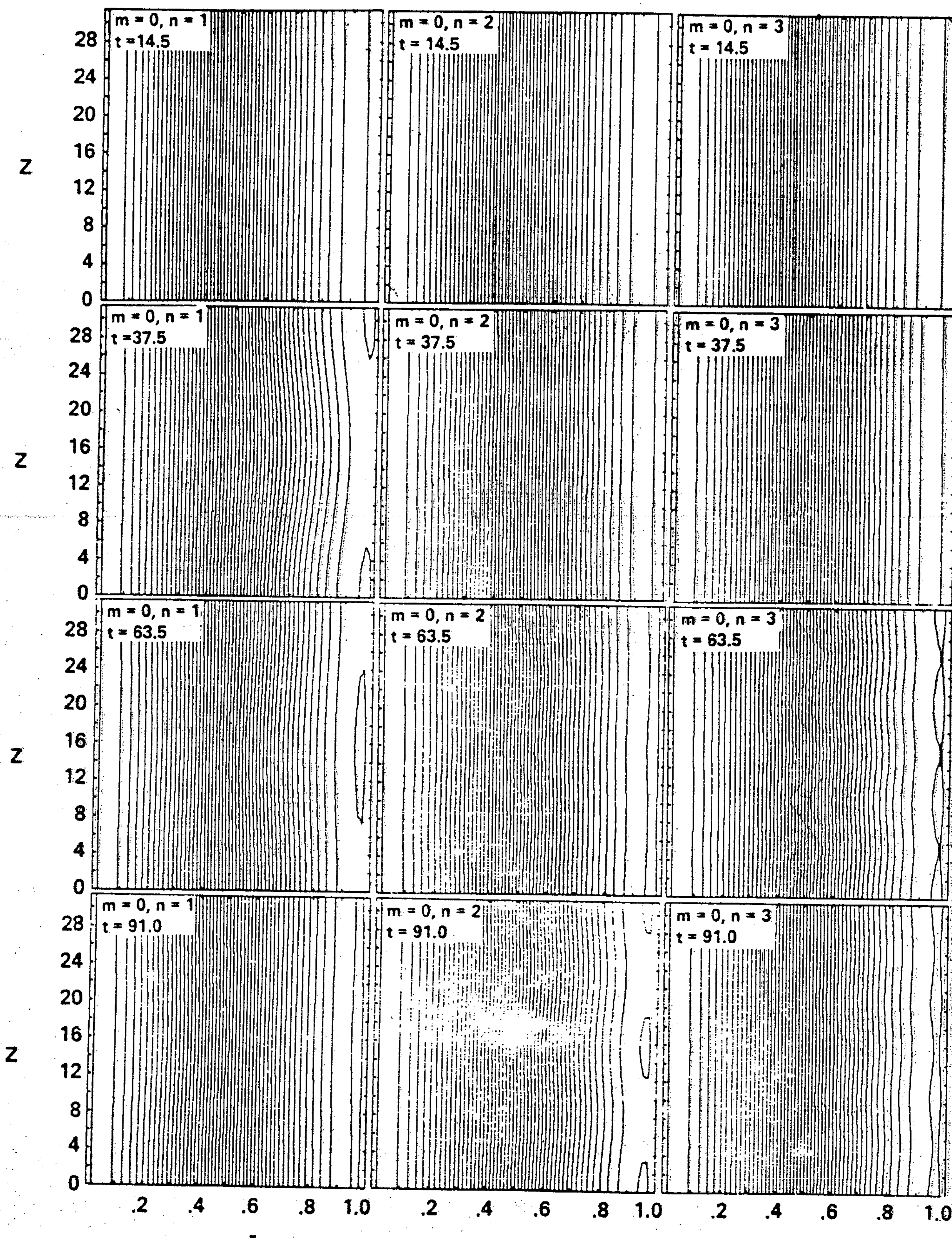

3-D SIMULATION - HIGH

m=0 magnetic islands

large m=0 can interact with m=1

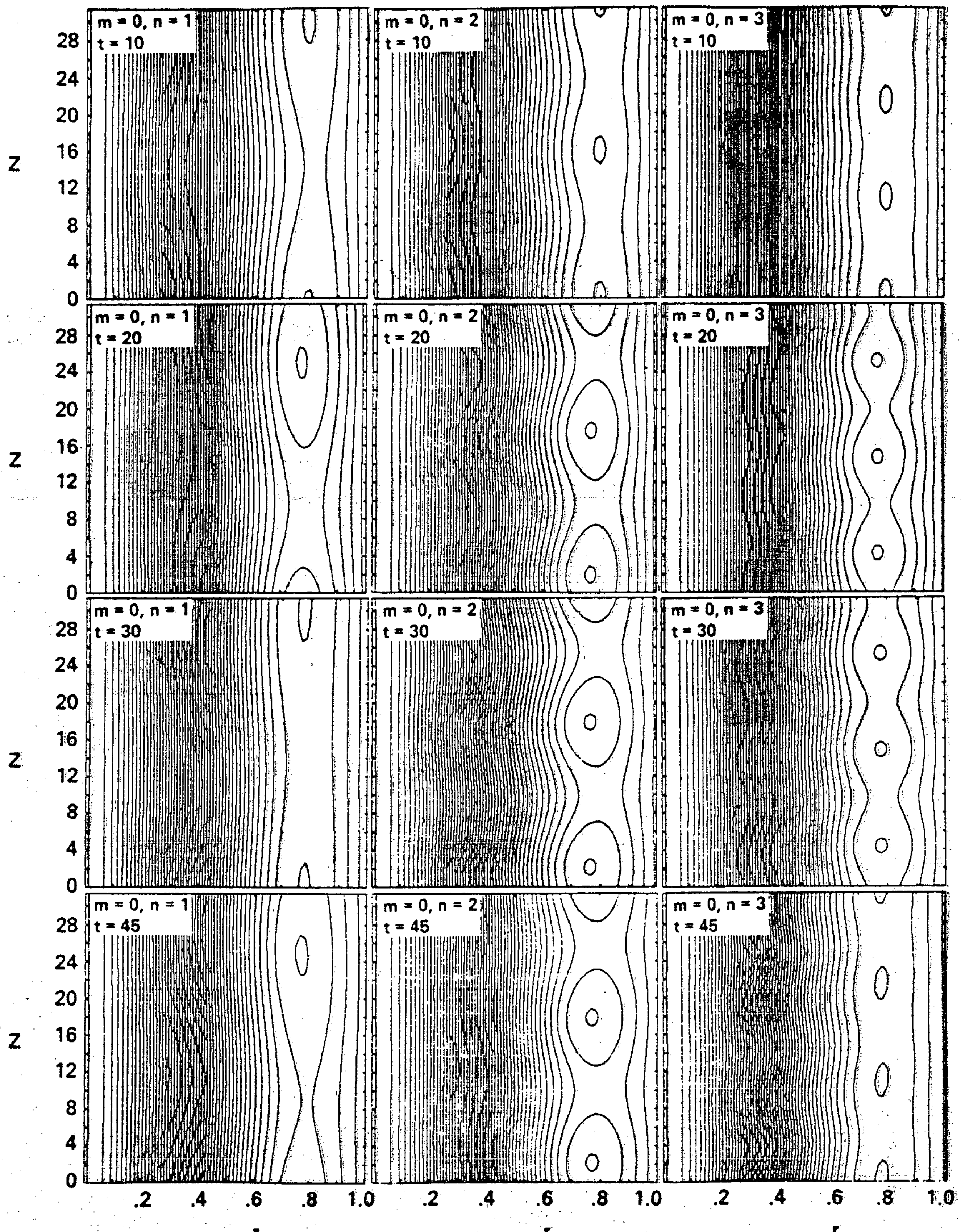

RADIAL MAGNETIC ENERGY VS. TIME

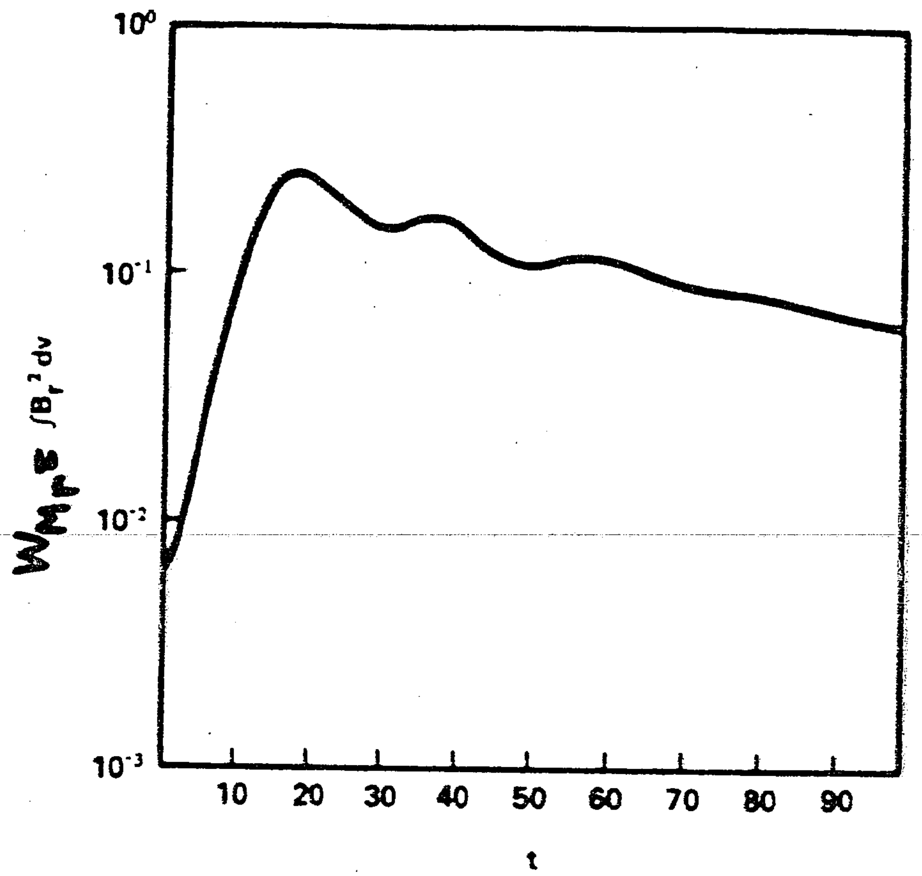

Fig. 9. Energy in the radial component of the magnetic field as a function of time for the high-β case.

(MAGNETIC ENERGY)/HELICITY VS TIME

WM/K .VS TIME

$W_M = W_{M_r} + W_{M_\theta} + W_{M_z}$

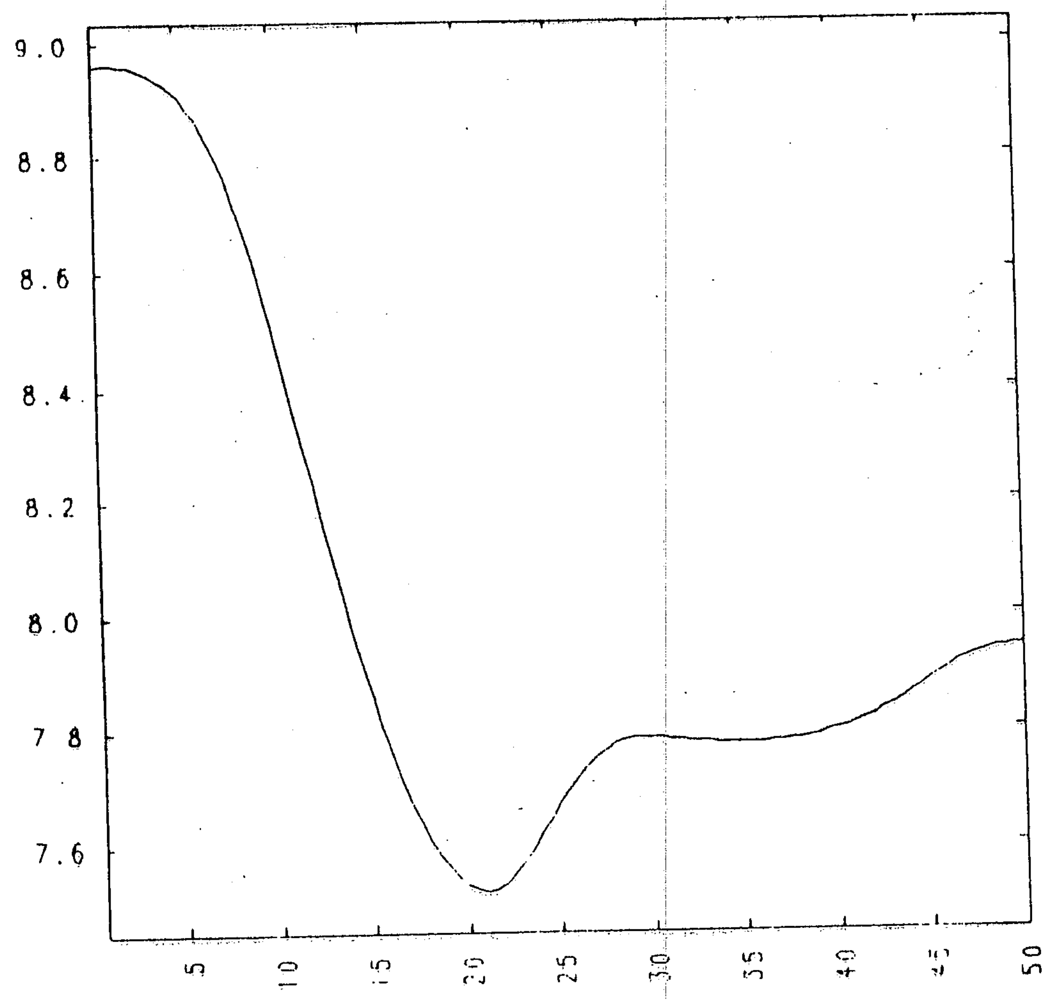

$\frac{W_M}{K}$

t/τ_A

(TOTAL ENERGY)/HELICITY vs. TIME

(WM+WK)/K VS TIME

$W_K = \int \rho v^2 d^3\underline{r}$

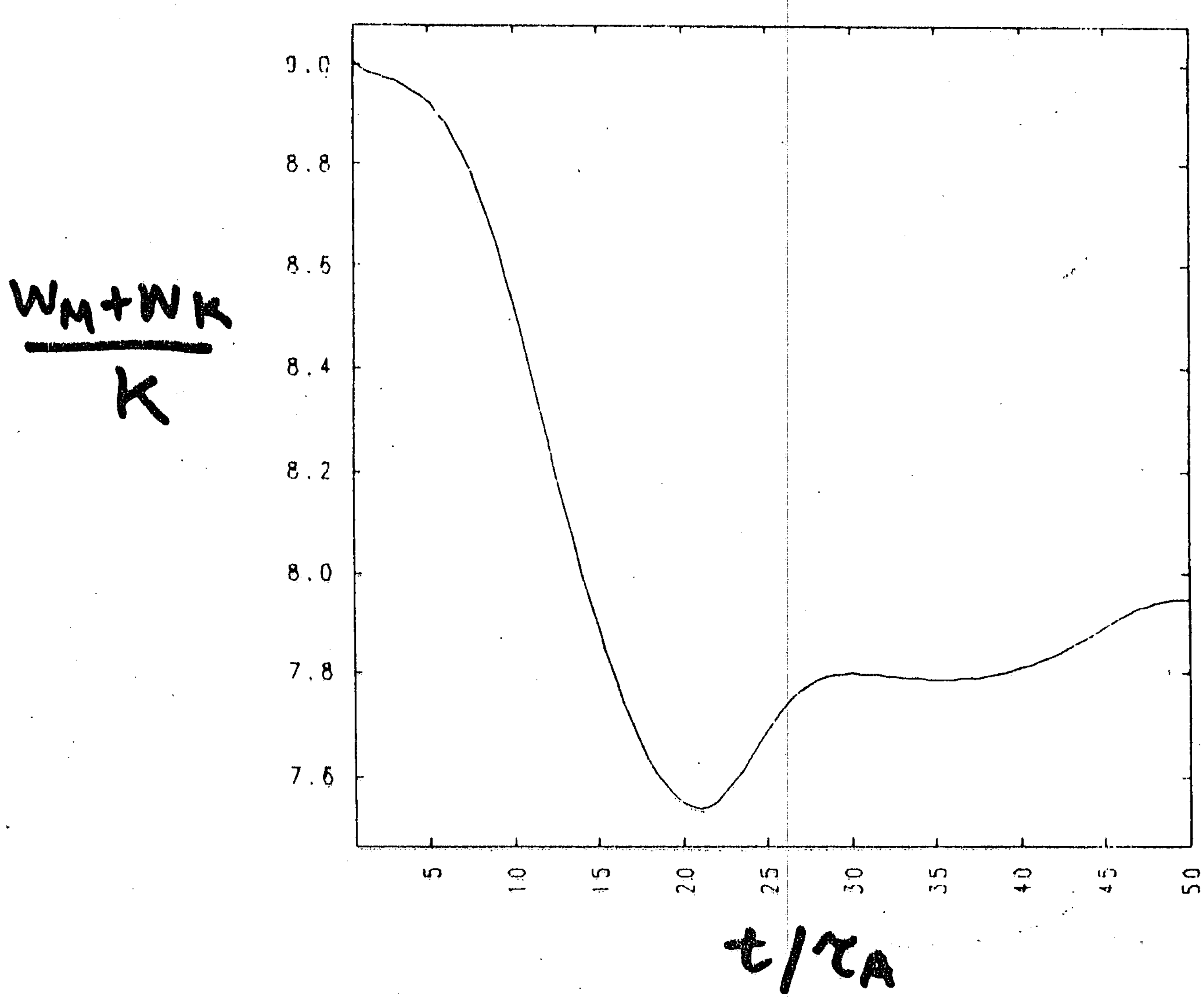

COMMENTS

1. W/K minimized during nonlinear growth of resistive MHD modes.
$\Rightarrow$ relaxation due to instabilities.

2. Process of relaxation from an unstable ("bad") state to a stable ("good") state causes destruction of flux surfaces, i.e., you don't get something for nothing.

DYNAMO ACTION

The observed continuous conversion of externally supplied poloidal flux into toroidal flux so as to maintain a non-trivial "steady-state" in the presence of resistive diffusion.

Example: RFP

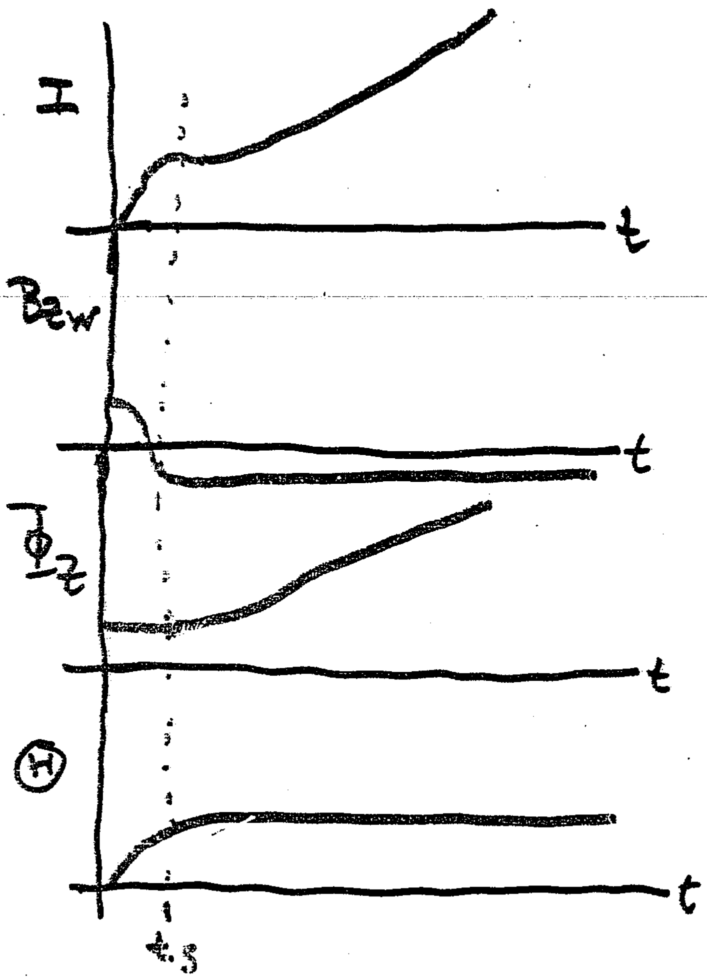

For $t > t_s$, only negative Φ_z can be taken from, or given to, external circuit.

- Requires reconnection to "lock in" toroidal flux.
- Cannot be modeled with transport (Caramana & Baker)
- Relationship to relaxation, turbulence, and instability?
- Compressible or Incompressible?
- Role of boundaries, and boundary conditions.
- Continuous, or "quantized"?

FLUX GENERATION DURING 3-D SIMULATION

- 3-D evolution of modes,

  $\Theta_0 = 1.77$, $\underline{\underline{\varepsilon = .2}}$

  $N_r = 65$, $N_\theta = 8$, $N_z = 65$

- Flux generation during growth phase; diffusion after saturation.

- $\langle E_\theta \rangle$ vs. r during growth phase, and after saturation.

- Relaxation: W/K decreases during growth phase, slow increase after saturation.

STRUCTURE OF "DYNAMO" ELECTRIC FIELD

- Flux change inside field reversal surface:

$$\dot{\underline{\Phi}}(r_v) = -r_v \int_0^{2\pi} E_\theta(r_v)\, d\theta$$

$$= -r_v \langle E_\theta(r_v) \rangle$$

where:

$$\langle E_\theta(r_v)\rangle = \underbrace{\eta \langle J_\theta \rangle}_{\text{diffusion}} - \underbrace{\langle \underline{v} \times \underline{B} \rangle_\theta}_{\text{fluctuations}}$$

For

$$\boxed{\dot{\underline{\Phi}}(r_v) \geq 0 \;\Rightarrow\; \langle E_\theta(r_v) \rangle \leq 0}$$

i.e., $\delta E_\theta = -\langle \underline{v} \times \underline{B} \rangle_\theta$ cancels resistive diff.

Examine time evolution and radial structure of $\langle E_\theta(r) \rangle$ during nonlinear evolution of unstable RFP.

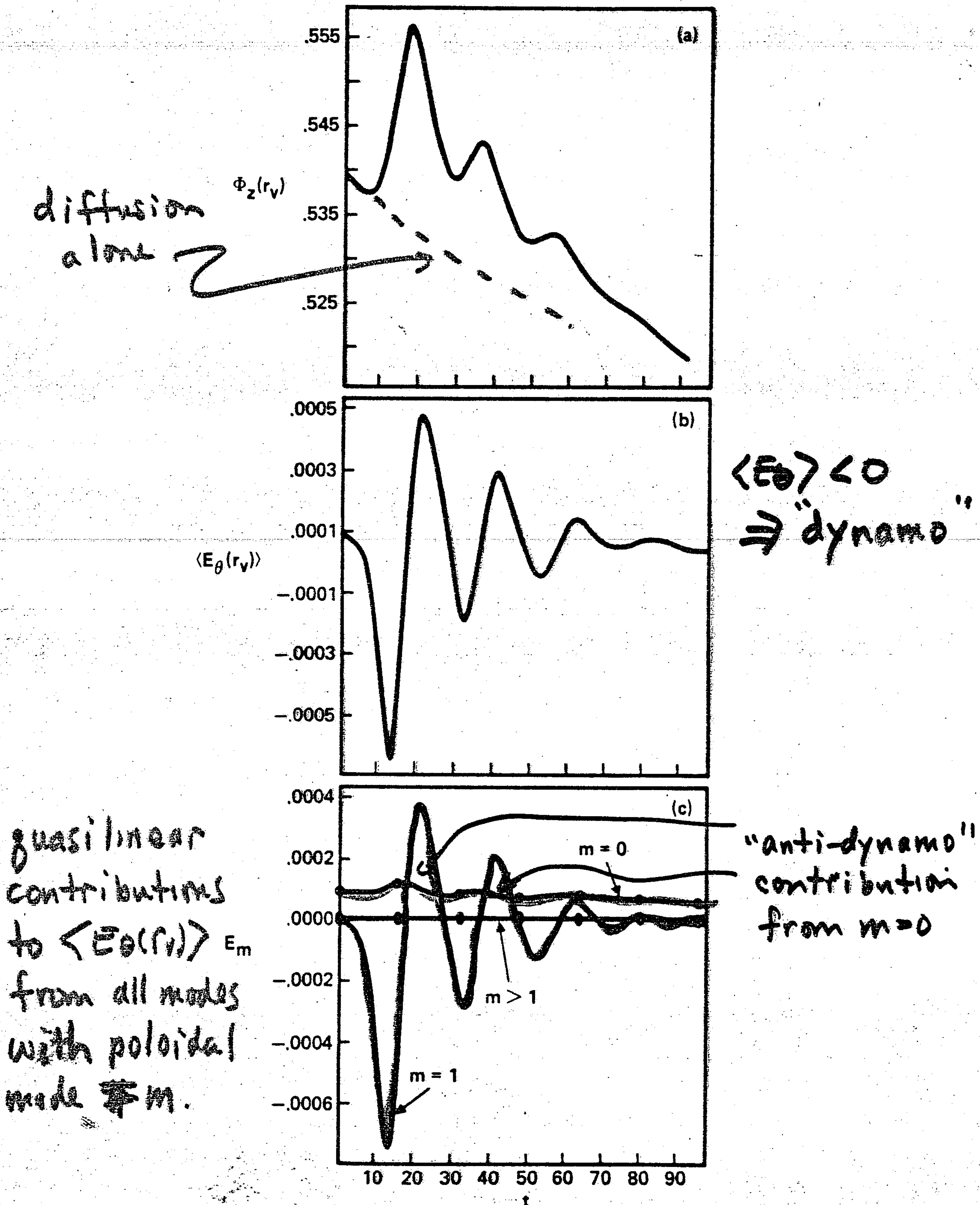
(a)
.555
.545
.535
.525
$\Phi_z(r_v)$
diffusion alone
(b)
.0005
.0003
.0001
−.0001
−.0003
−.0005
$\langle E_\theta(r_v)\rangle$
$\langle E_\theta\rangle < 0$
⇒ "dynamo"
(c)
.0004
.0002
.0000
−.0002
−.0004
−.0006
E_m
m = 0
m > 1
m = 1
10 20 30 40 50 60 70 80 90
t
quasilinear contributions to $\langle E_\theta(r_v)\rangle$ from all modes with poloidal mode # m.
"anti-dynamo" contribution from m=0

E-THETA VS RADIUS M= 0 N- 0 TIME= 5.00185E+00

$t=5$

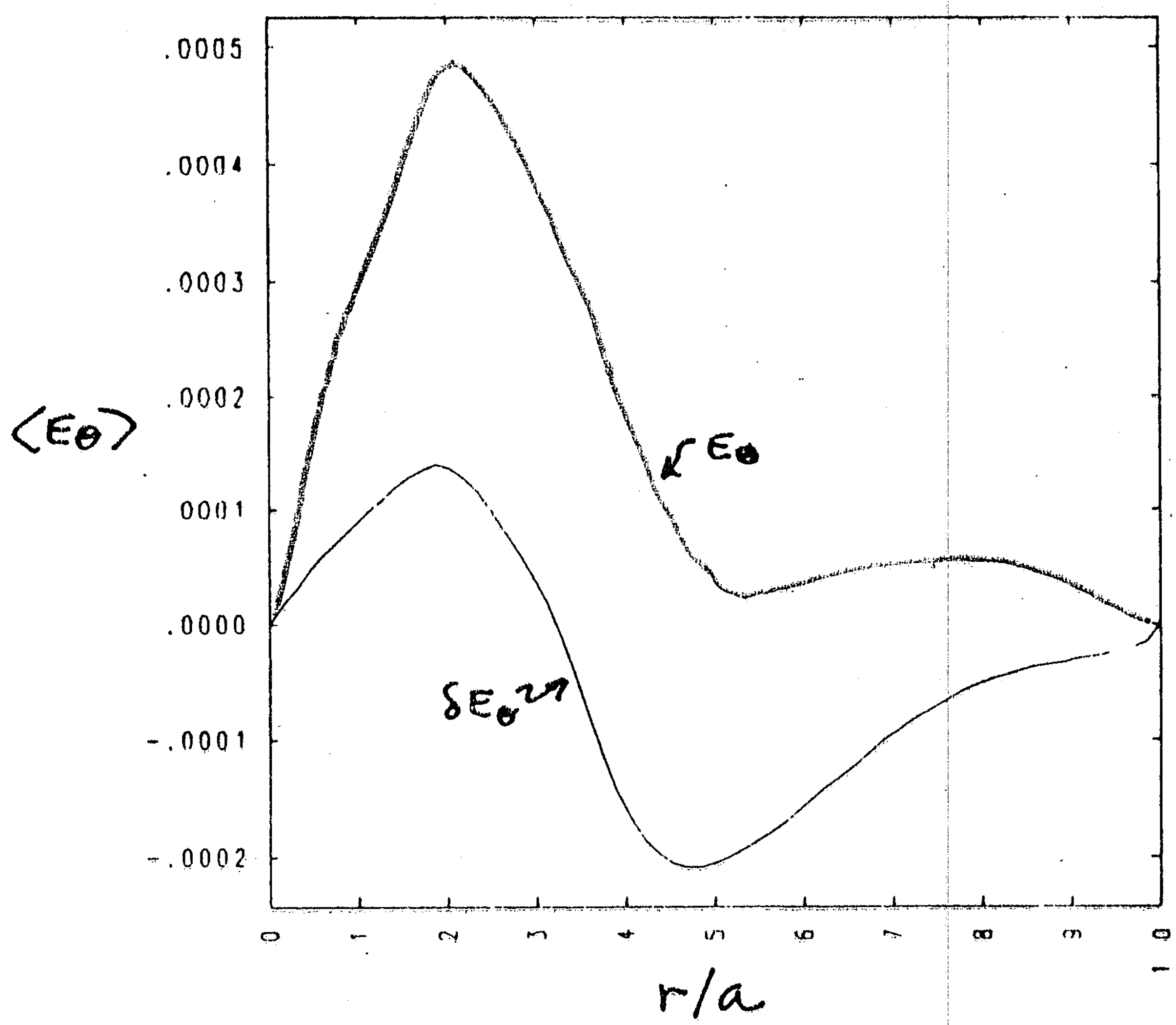

$\delta E_\theta = -\langle \underline{v} \times \underline{B} \rangle_\theta$

$E_\theta = \eta \langle J_\theta \rangle + \delta E_\theta$

E-THETA VS RADIUS M- 0 N- 0 TIME= 1.40030E+01

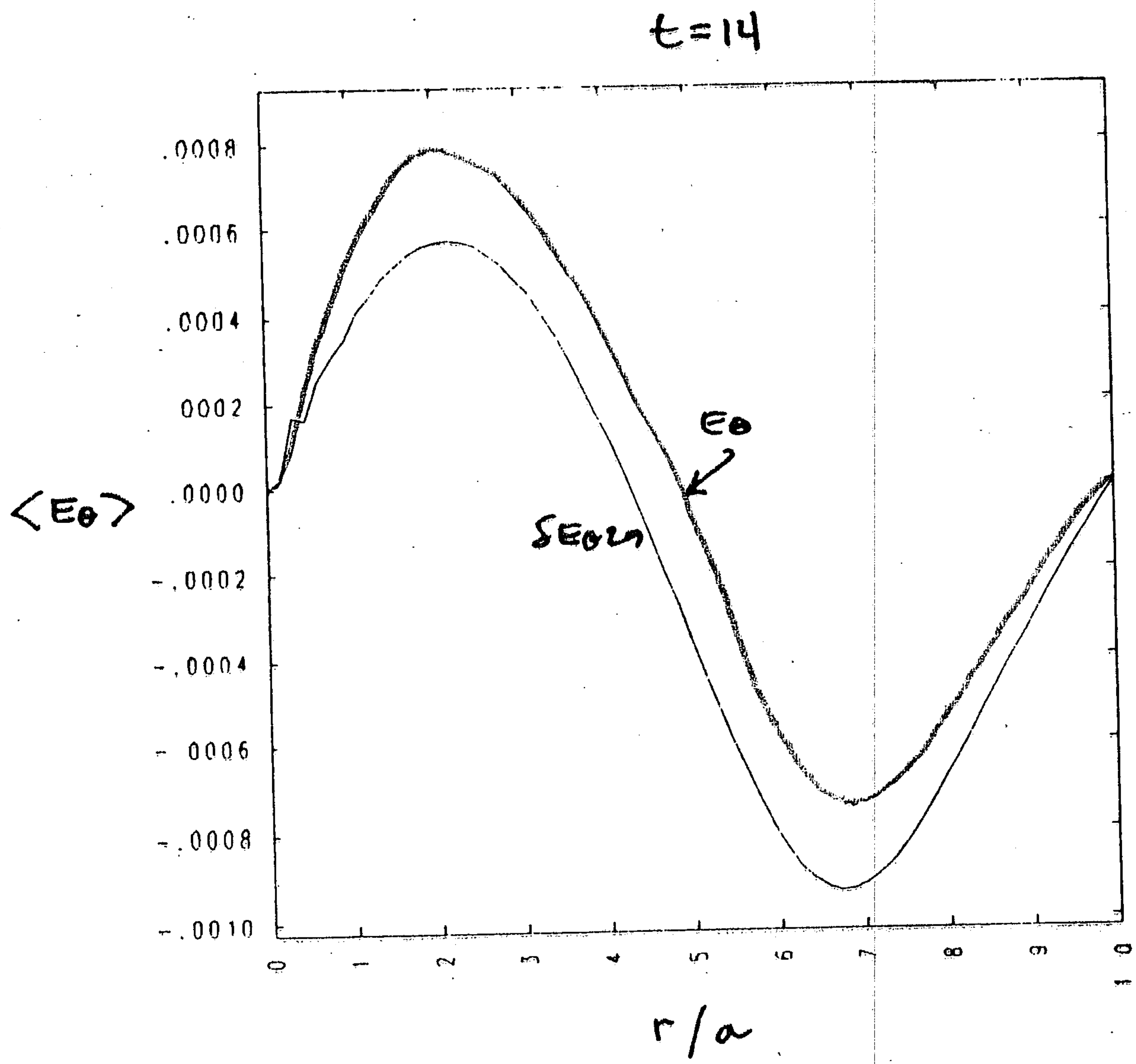

$\delta E_\theta = -\langle \underline{v} \times \underline{B} \rangle_\theta$

$E_\theta = \eta \langle J_\theta \rangle + \delta E_\theta$

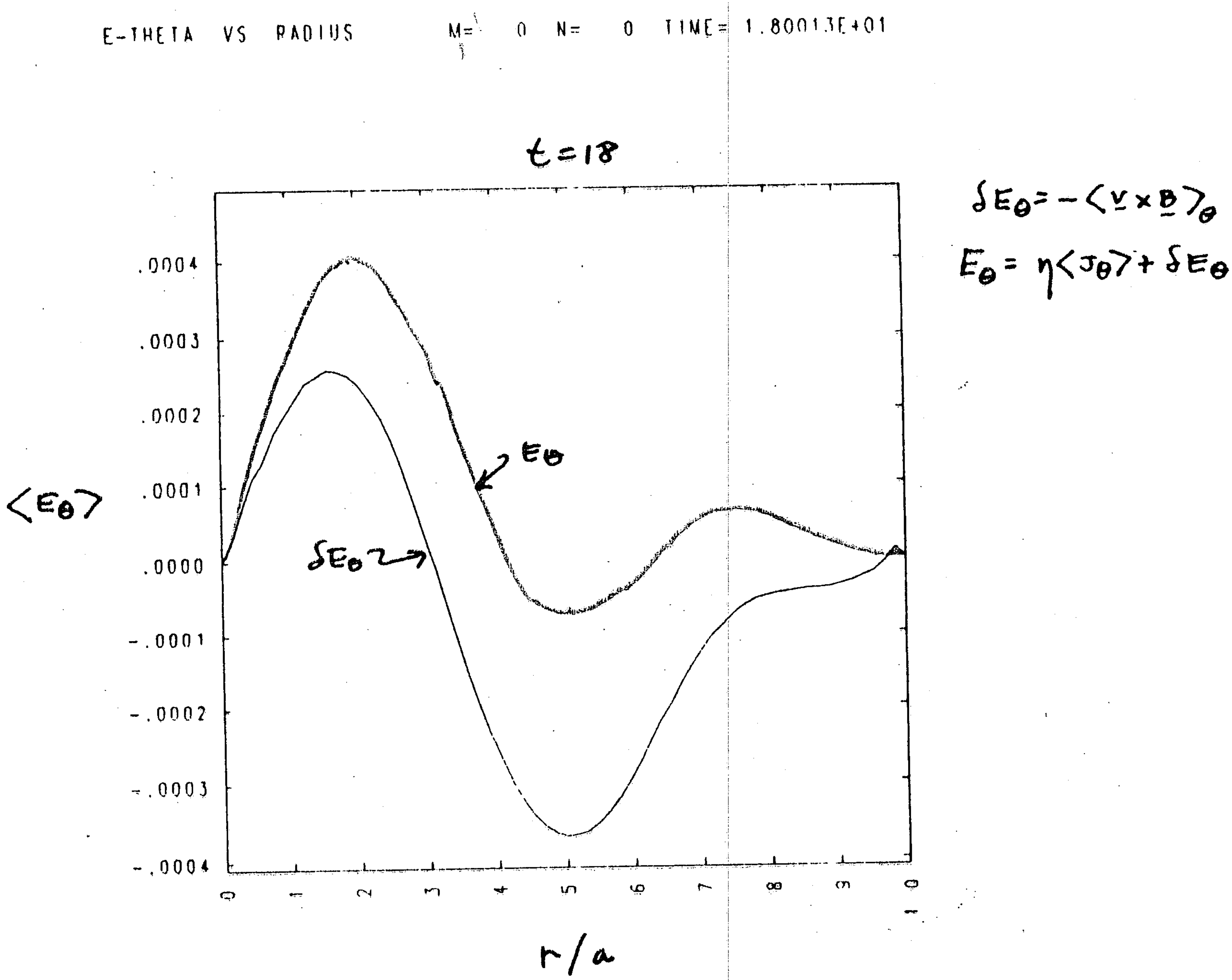

E-THETA VS RADIUS M= 0 N= 0 TIME= 1.80013E+01
t=18
.0004
.0003
.0002
.0001
.0000
-.0001
-.0002
-.0003
-.0004
0
.1
.2
.3
.4
.5
.6
.7
.8
.9
1.0
r/a
⟨E_θ⟩
E_θ
δE_θ
δE_θ = −⟨v × B⟩_θ
E_θ = η⟨J_θ⟩ + δE_θ

E-THETA VS. RADIUS M= 0 N= 0 TIME= 2.00031E+01

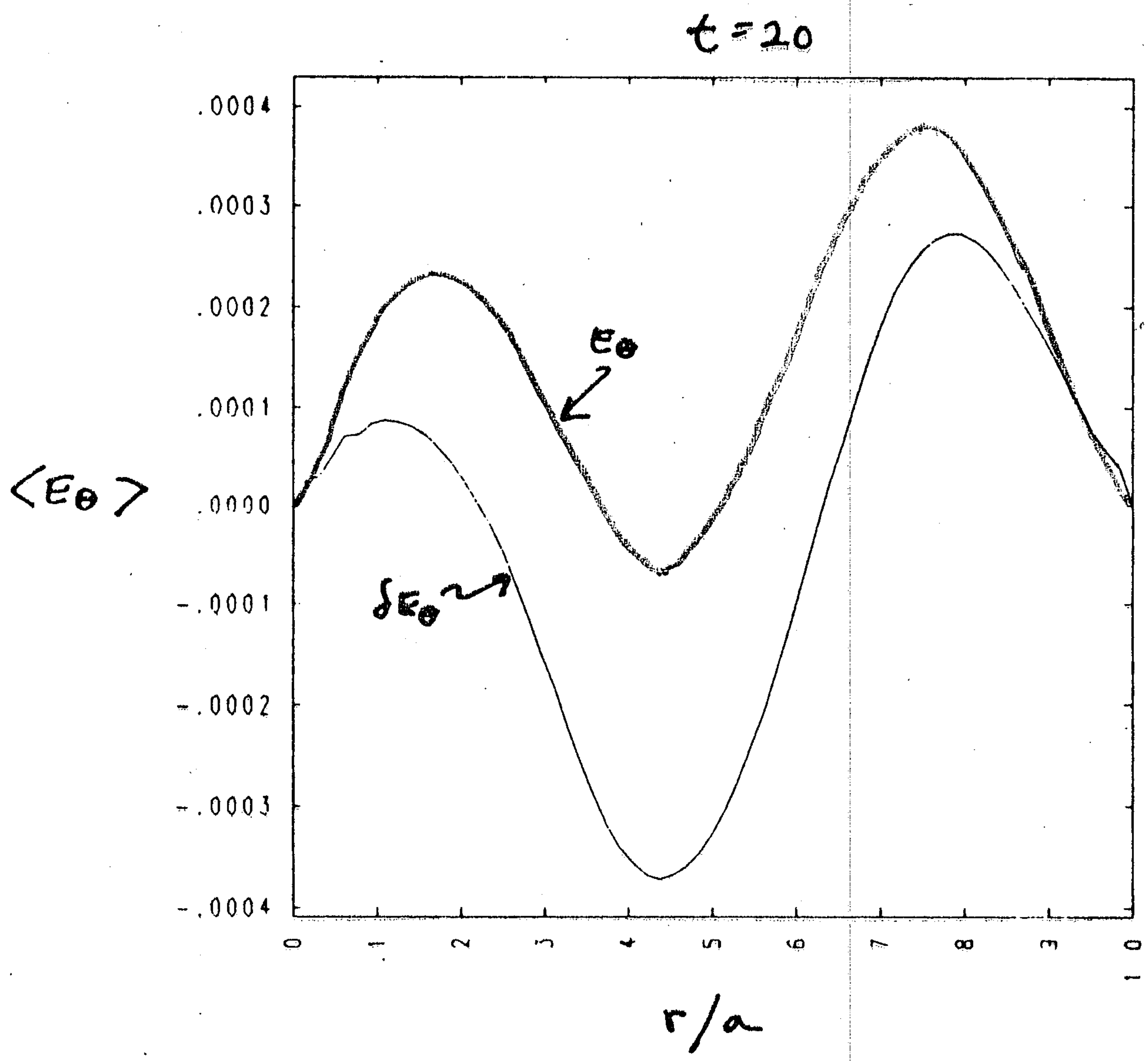

$\delta E_\theta = -\langle \underline{v} \times \underline{B} \rangle_\theta$

$E_\theta = \eta \langle J_\theta \rangle + \delta E_\theta$

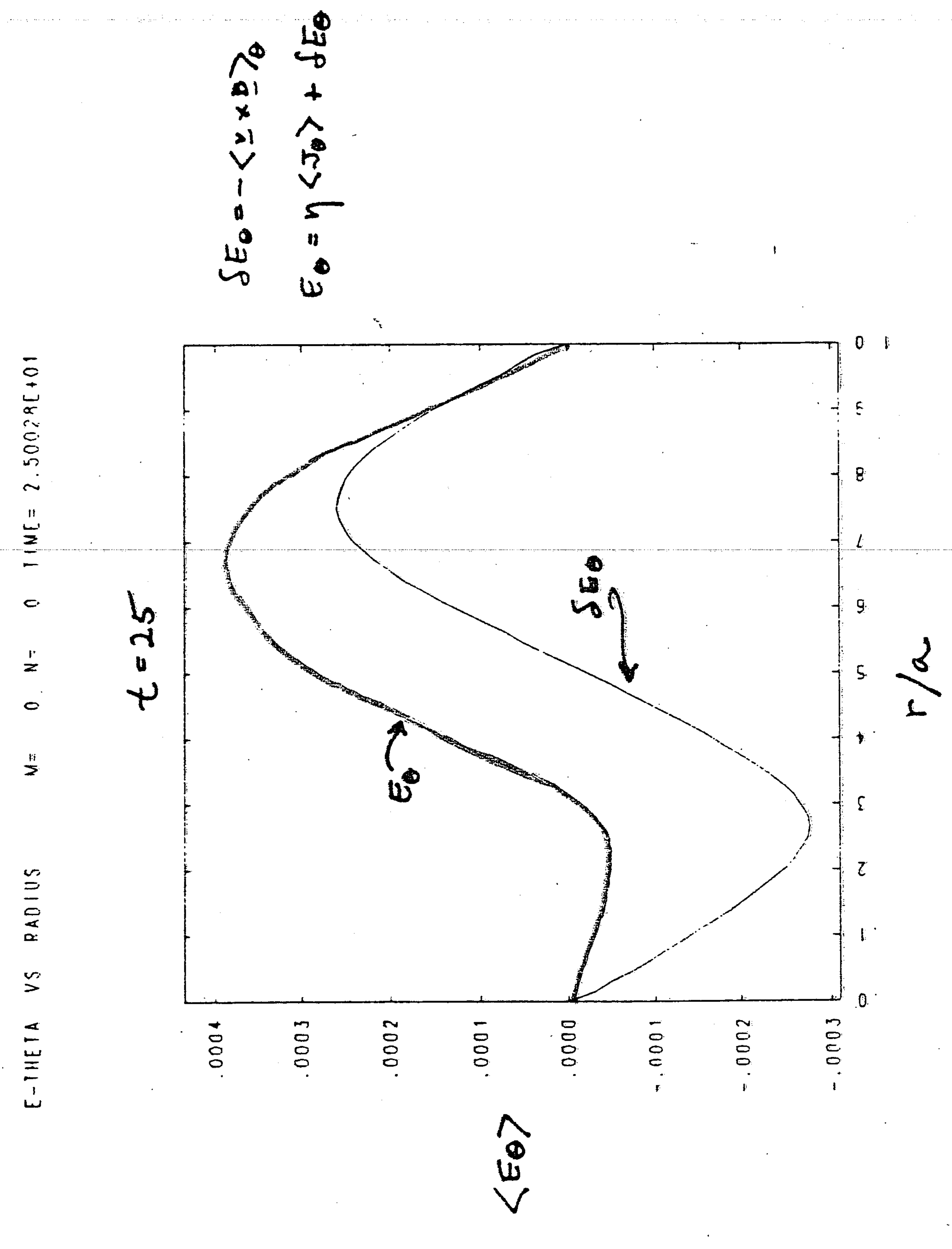

E-THETA VS RADIUS M= 0 N= 0 TIME= 2.50028E+01
t = 25
$\delta E_\theta = -\langle \underline{v} \times \underline{b} \rangle_\theta$
$E_\theta = \eta \langle J_\theta \rangle + \delta E_\theta$
E_θ
δE_θ
$\langle E_\theta \rangle$
r/a
.0004
.0003
.0002
.0001
.0000
-.0001
-.0002
-.0003

E-THETA VS RADIUS M= 0 N= 0 TIME= 3.20019E+01

$t = 32$

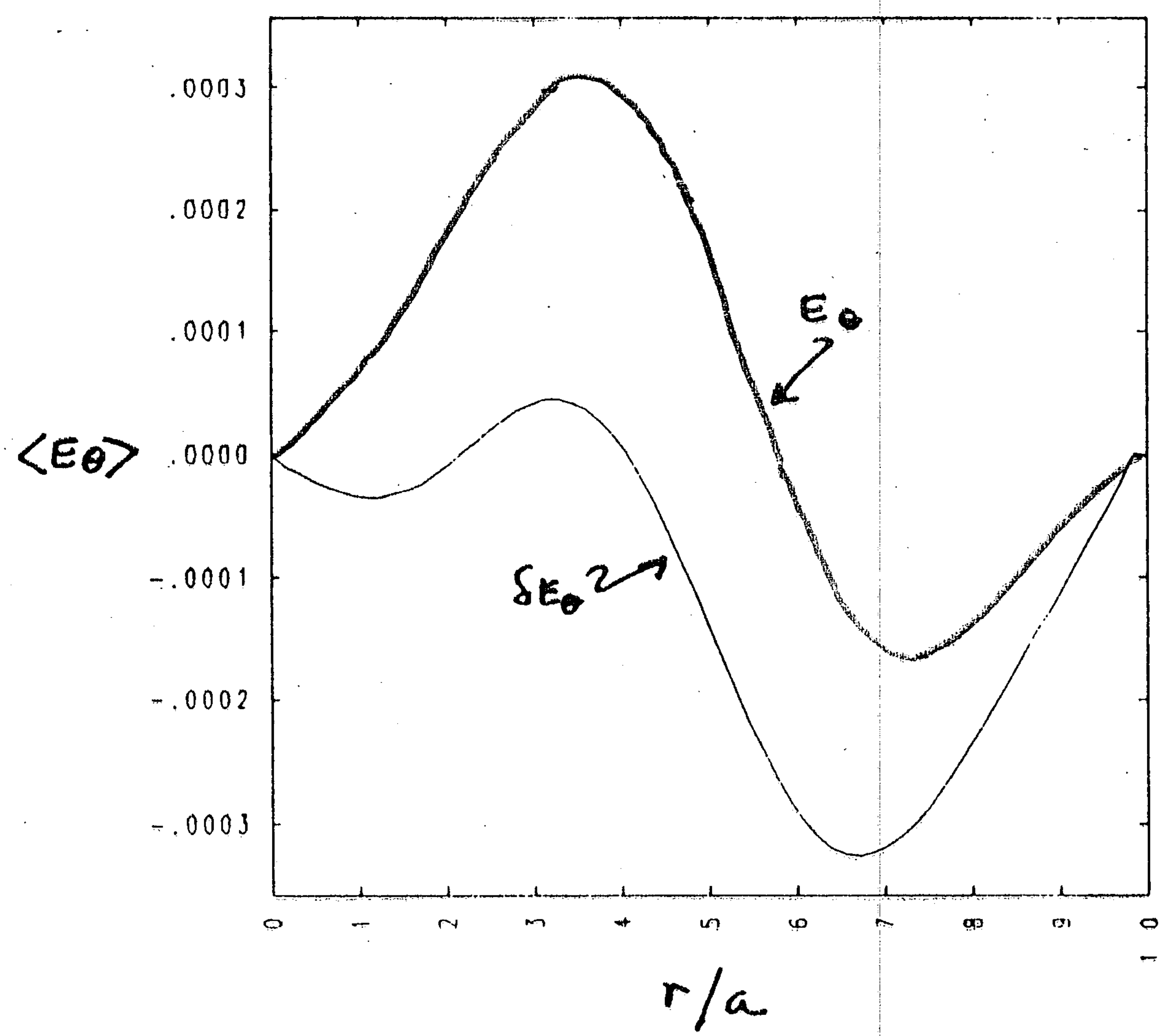

$\delta E_\theta = -\langle \underline{v} \times \underline{B} \rangle_\theta$

$E_\theta = \eta \langle J_\theta \rangle + \delta E_\theta$

E-THETA VS RADIUS M= 0 N= 0 TIME= 3.70007E+01

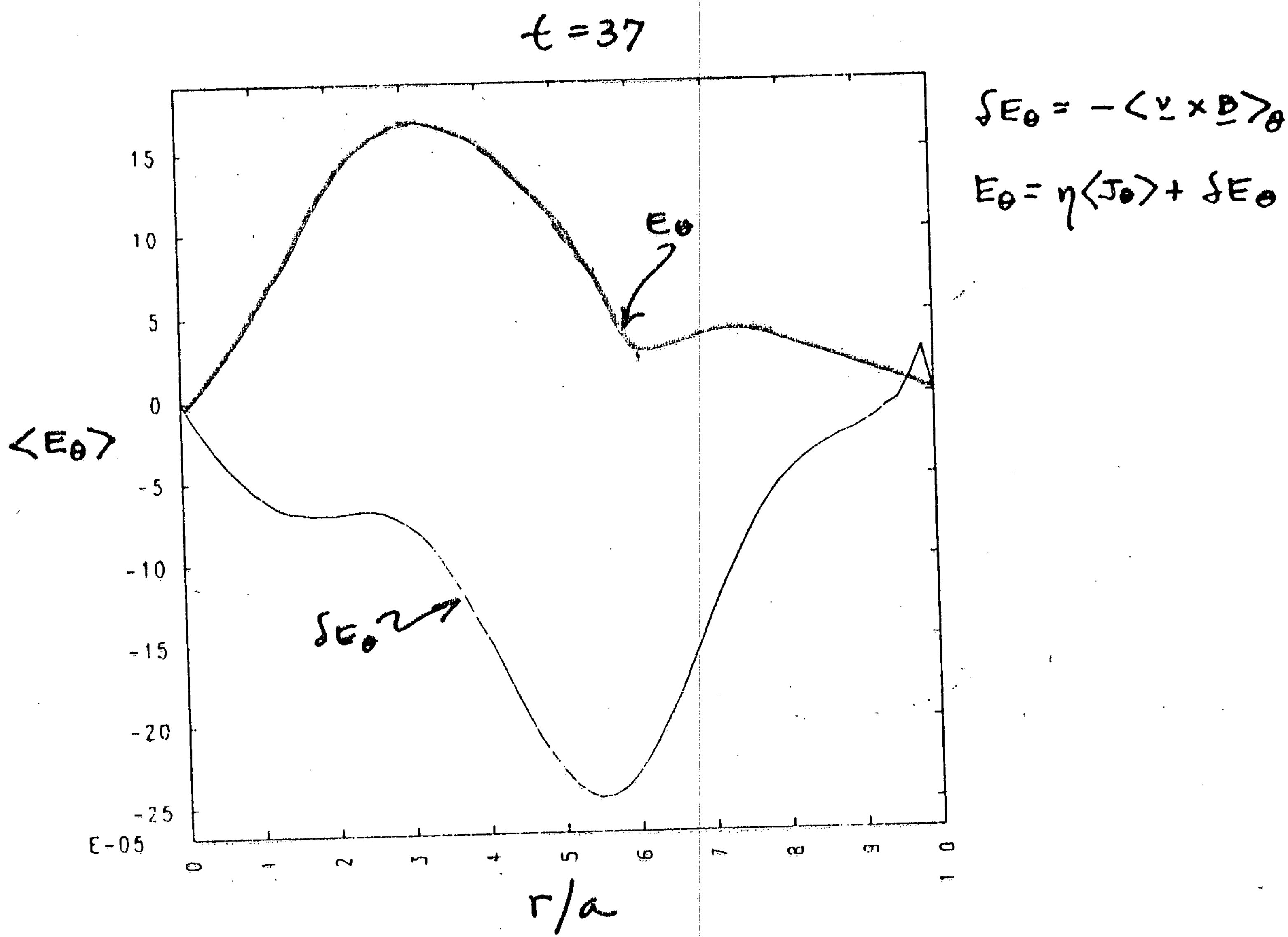

ROLE OF COMPRESSIBILITY IN RFP DYNAMO

3 CASES EXAMINED:

CASE 1: INCOMPRESSIBLE: NO SUSTAINMENT
(INCOMPR) (diffusion)

CASE 2: NOT-SO-INCOMPRESSIBLE, [(0,0) compressible, (m,n) incompressible]:
SUSTAINMENT, NO REVERSAL
(NOTSOINC) (non-reversed Ohmic state)

CASE 3: FULLY COMPRESSIBLE: SUSTAINMENT WITH REVERSAL (reversed Ohmic state)
(SPECTR3)

$\Theta_0 = 1.71$; $\varepsilon = 1$; $N_r = 65, N_\theta = 8, N_z = 16$, NO OHMIC HEATING

All cases dominated by (1,-2) mode. $S = 10^3$

Examine differences in $\langle E_\theta(r) \rangle$ at $t = 100$ (after mode saturation) for each case.

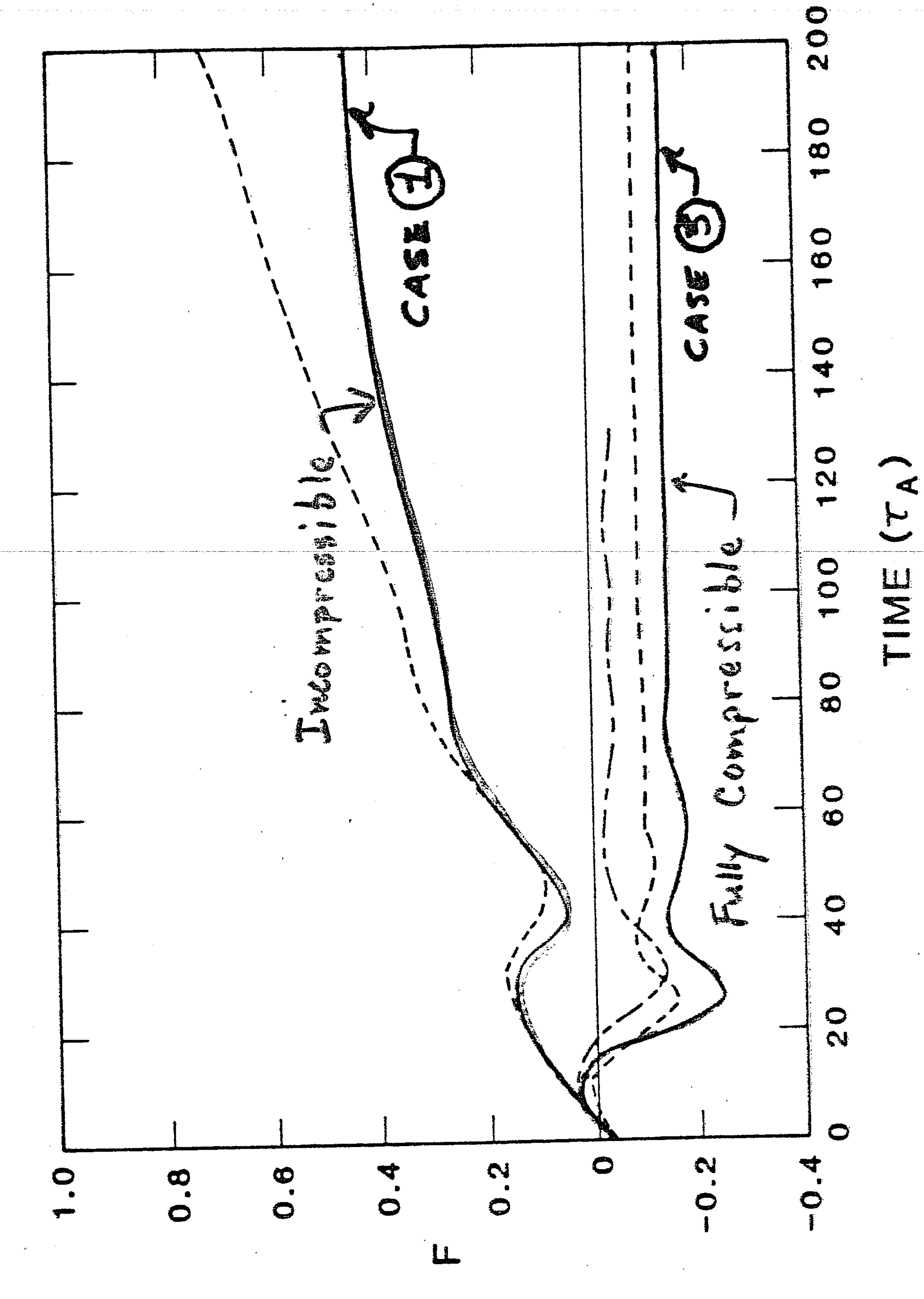
F
1.0
0.8
0.6
0.4
0.2
0
-0.2
-0.4
0
20
40
60
80
100
120
140
160
180
200
TIME (τ_A)
Incompressible
CASE 1
Fully Compressible
CASE 5

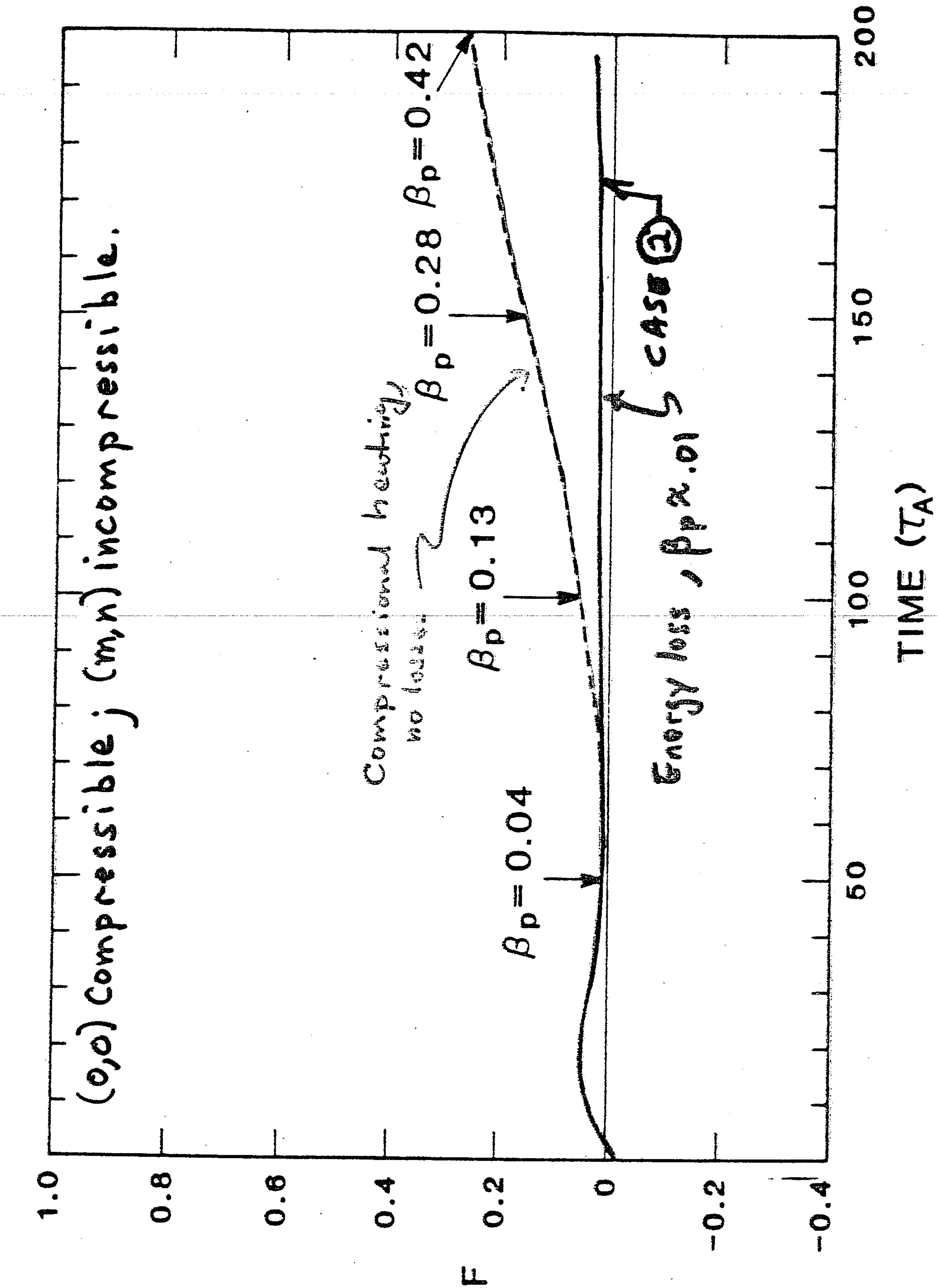
(0,0) Compressible ; (m,n) incompressible.
$\beta_p = 0.04$
$\beta_p = 0.13$
$\beta_p = 0.28$
$\beta_p = 0.42$
Compressional heating no loss
Energy loss , $\beta_p \approx .01$
CASE ②
F
1.0
0.8
0.6
0.4
0.2
0
−0.2
−0.4
50
100
150
200
TIME (τ_A)

10/84

CASE (1) INCOMPRESSIBLE

E-THETA .VS RADIUS M= 0 N= 0 TIME= 1.00046E+02

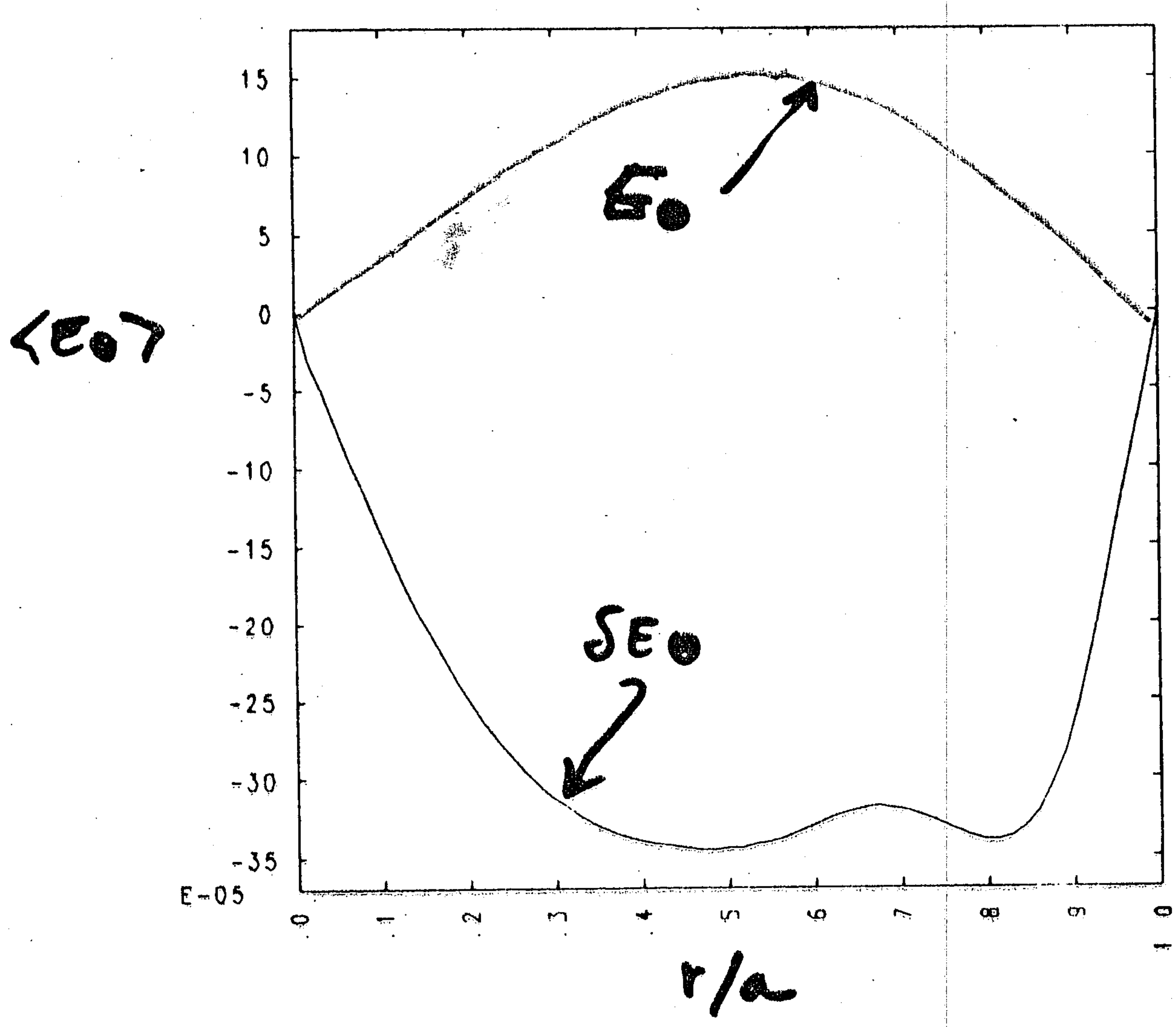

$\delta E_\theta = -\langle \underline{v} \times \underline{B} \rangle_\theta$

$E_\theta = \eta \langle J_\theta \rangle + \delta E_\theta$

CASE ② $\left\{ \begin{array}{l} (0,0)\ \text{COMPRESSIBLE} \\ (m,n)\ \text{INCOMPRESSIBLE} \end{array} \right\}$ NOT-SO-INCOMP.

E-THETA VS. RADIUS M= 0 N= 0 TIME= 1.00038E+02

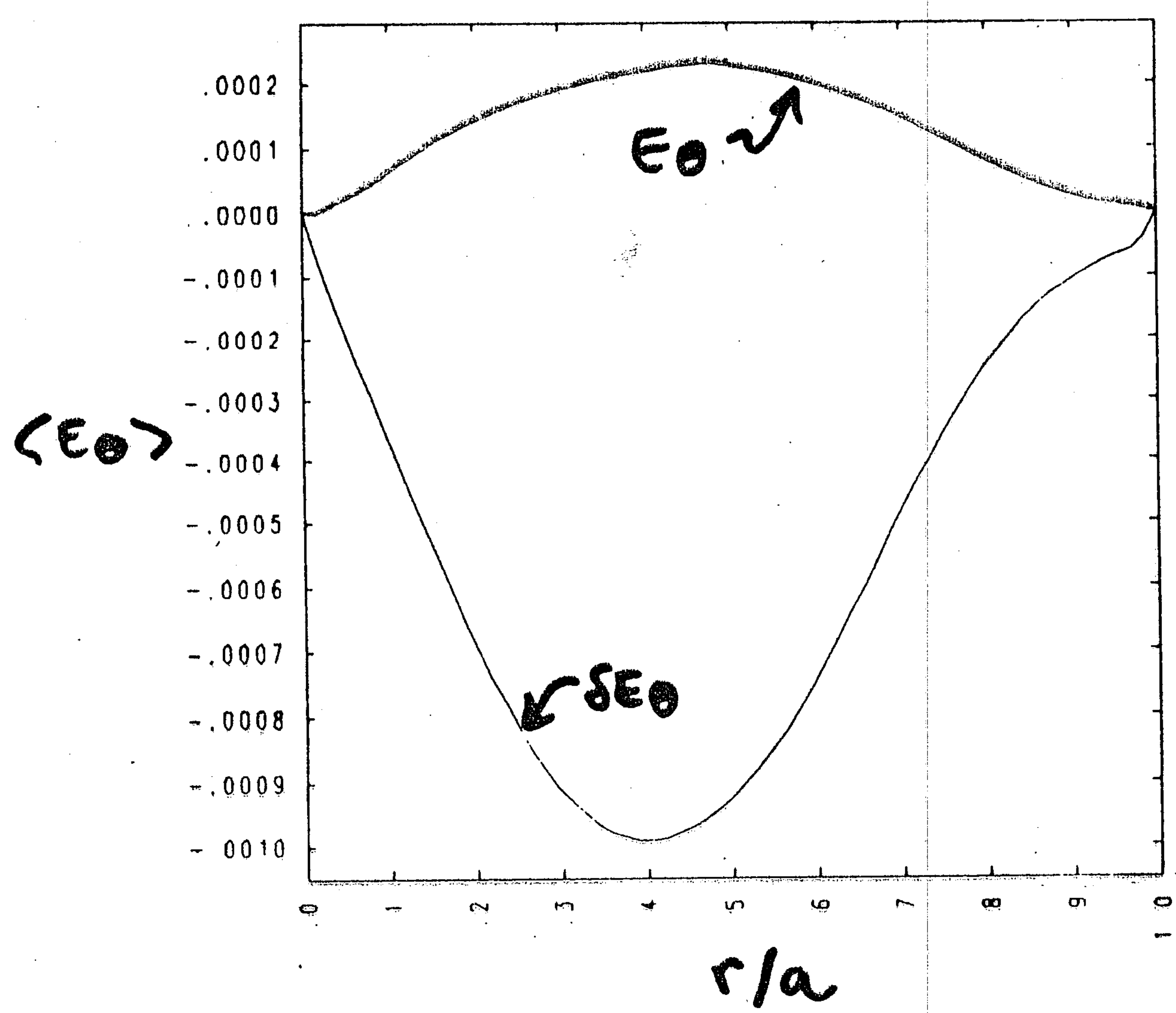

$\delta E_\theta = -\langle \underline{v} \times \underline{B} \rangle_\theta$

$E_\theta = \eta \langle J_\theta \rangle + \delta E_\theta$

CASE (3) FULLY COMPRESSIBLE

E-THETA .VS. RADIUS M= 0 N= 0 TIME= 1.00004E+02

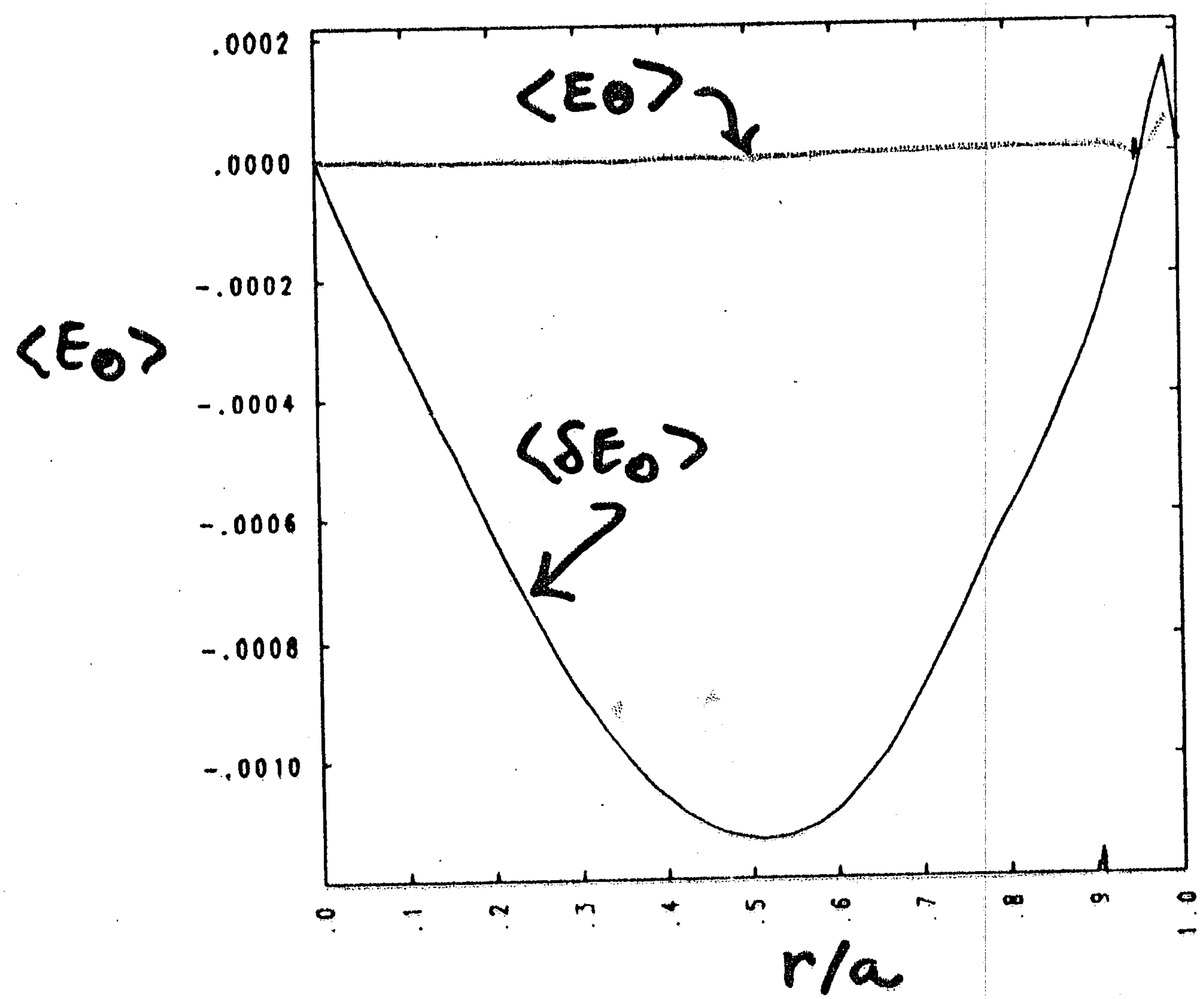

$\langle \delta E_\theta \rangle = -\langle \underline{v} \times \underline{B} \rangle_\theta$

$\langle E_\theta \rangle = \eta \langle J_\theta \rangle + \langle \delta E_\theta \rangle$

COMMENT:

1. Compressible $\langle E_\theta(r)\rangle$ differs only slightly from incompressible $\langle E_\theta(r)\rangle$ (with (0,0) compressible). Perhaps it is just this particular case that gives this difference between compressible and incompressible models. (see, for example, the Ohmic state of Aydemir and Barnes.)

2. Flux is generated (for $\varepsilon = .2$) during short "relaxation" process. If transport, relaxation, and "turbulent" phases well separated, flux generation should appear "Quantized". (Seen experimentally at high Ⓗ, not seen at low Ⓗ). When time-scales not well-separated, perhaps quasi-steady-state between transp., relaxation results (turbulence?)

TURBULENCE

A statistical steady state resulting from the non-linear saturation of MHD instabilities.

- Present computers probably insufficient to study full turbulence.

  Onset of turbulence can be modelled (previous results).

- Spectra (Fourier decomposition)

- Cascades and inverse cascades (motion thru k-space)

- Power laws, inertial range.

- Effect on sustainment, relaxation, dynamo, and transport.

SPECTRAL EVOLUTION

• Peak of $f(k)$:

$$\langle k^2 \rangle = \frac{\int f(k)\, k^2 \, dk}{\int f(k)\, dk}$$

• "Spread" of $f(k)$

$$\langle k - \langle k \rangle \rangle^2 = \frac{\int f(k)\,(k - \langle k \rangle)^2 \, dk}{\int f(k)\, dk}$$

Look at $\langle k^2 \rangle^{1/2}$ and $\langle k - \langle k \rangle \rangle^2$ vs time

for

$$f(k) = \begin{cases} \text{HELICITY SPECTRUM} \\ \text{ENERGY SPECTRUM} \end{cases}$$

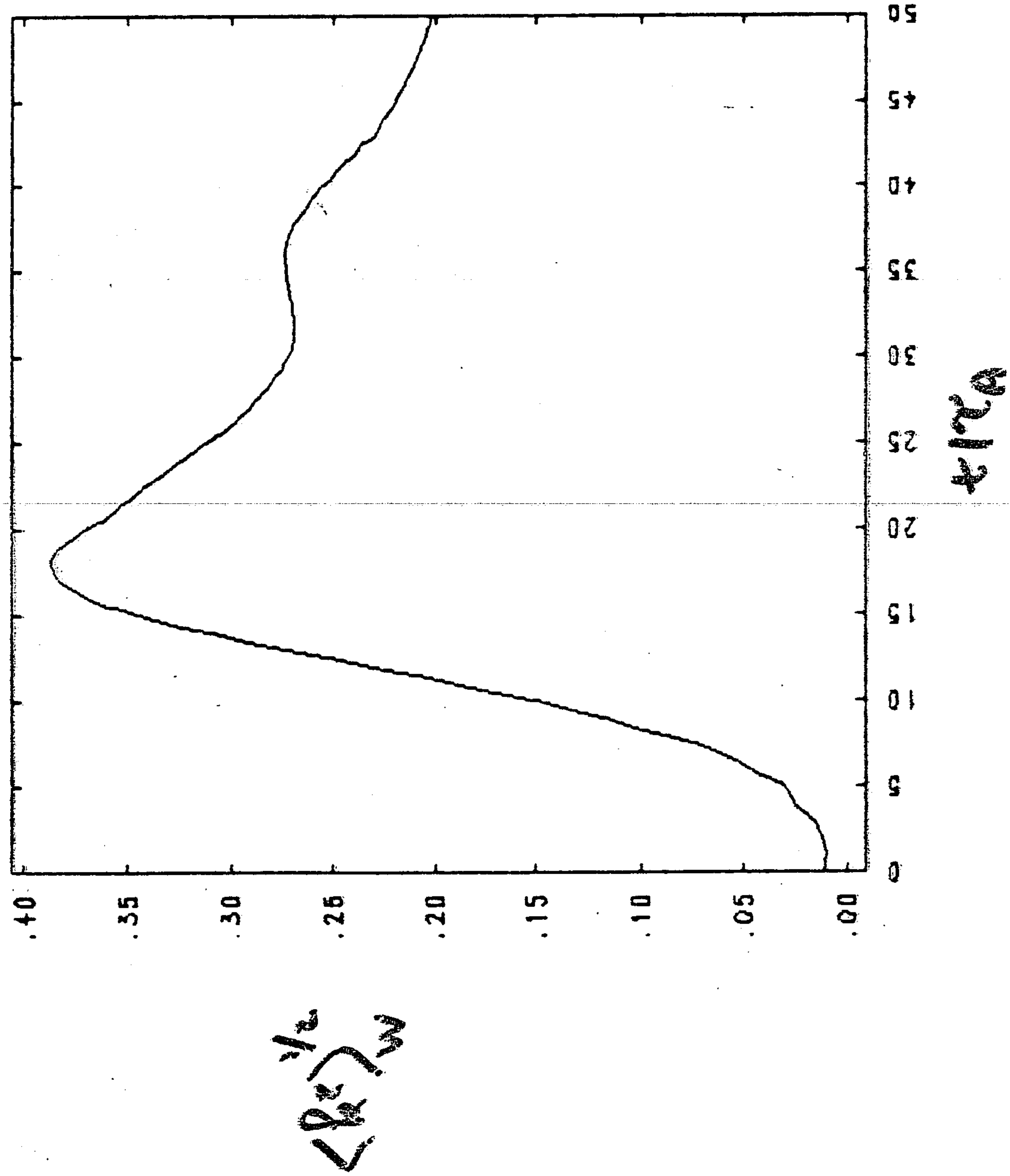

WM PEAK K VS. TIME

WW SPREAD VS. TIME

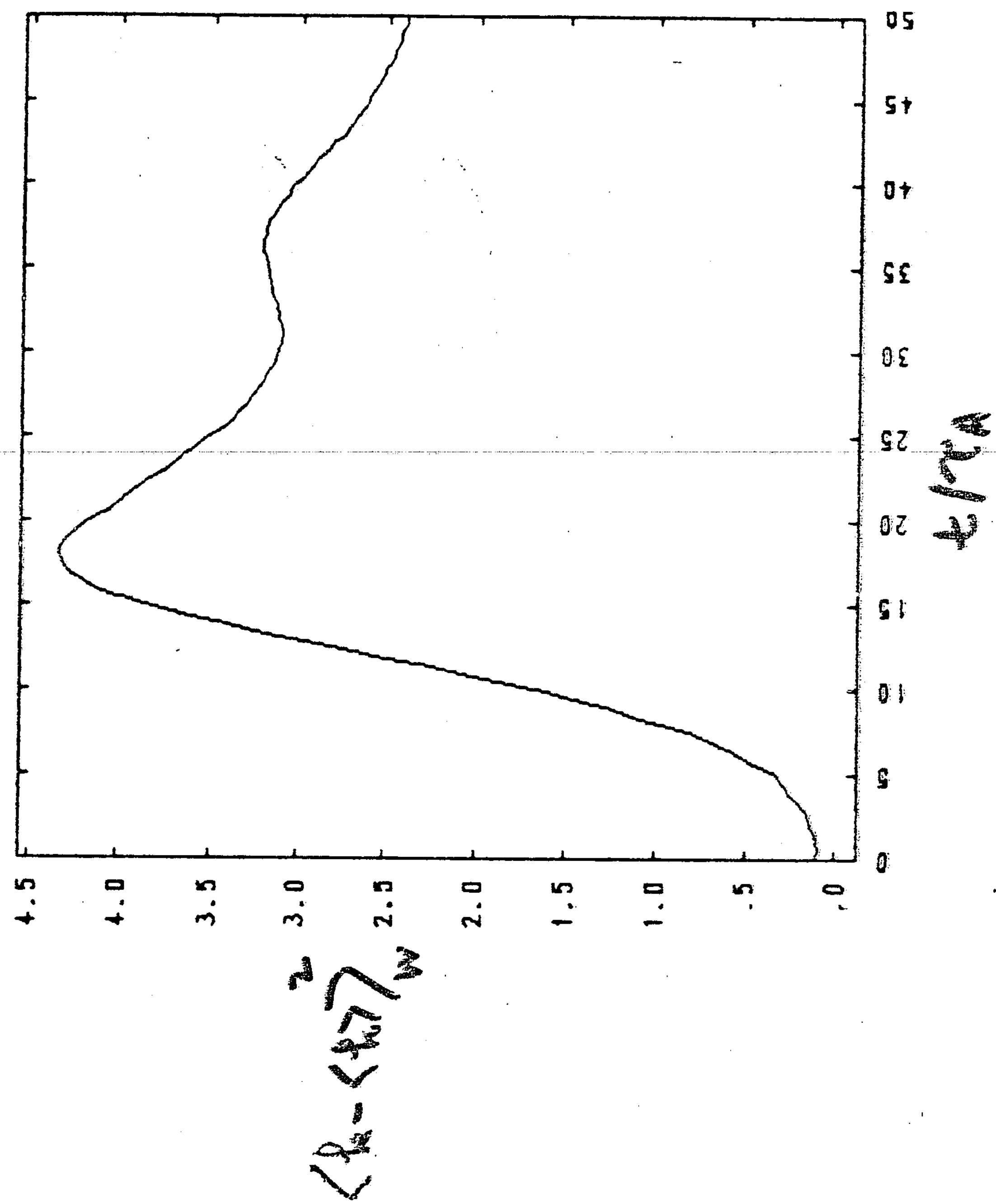

HEL. PEAK K VS. TIME

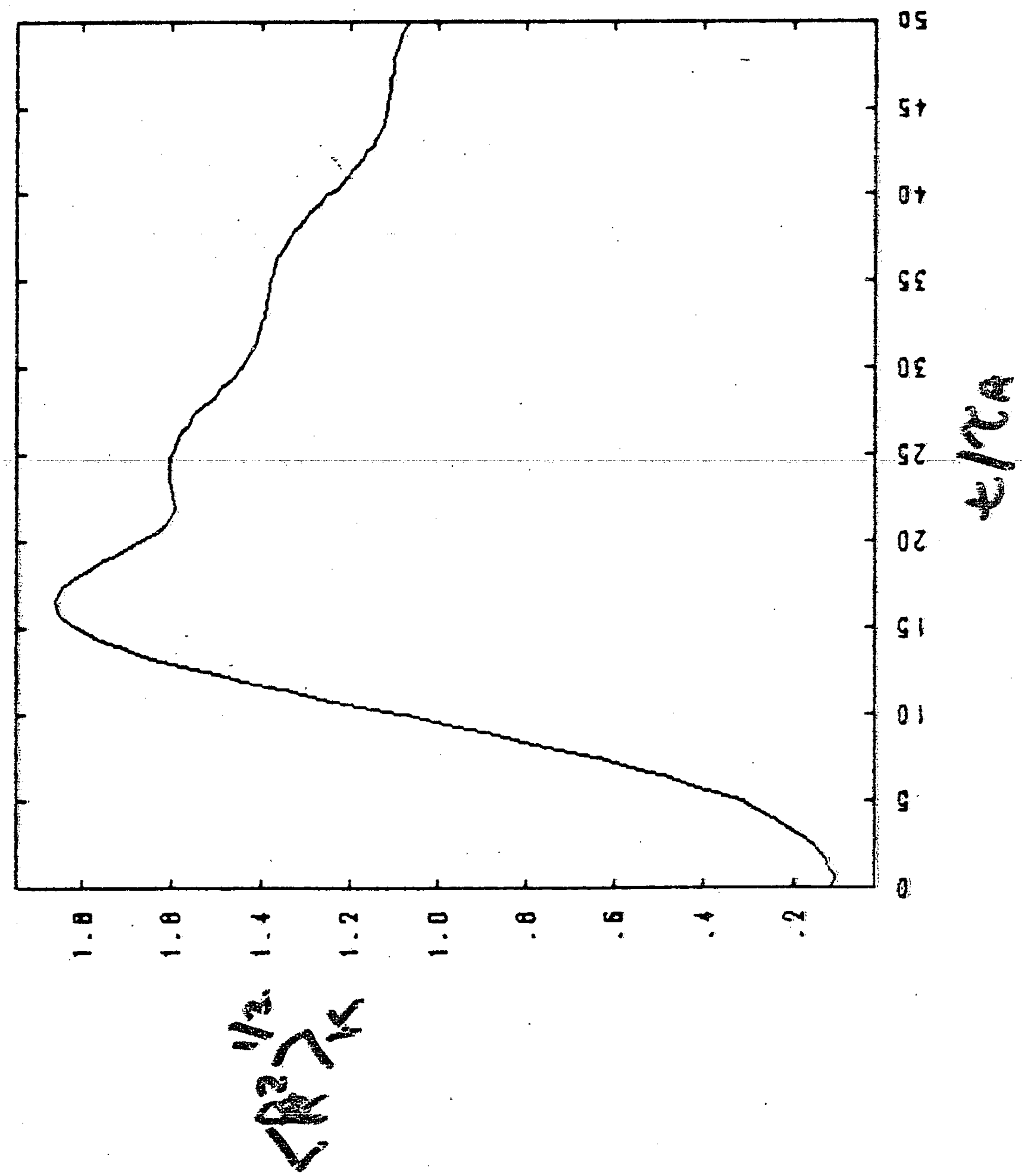

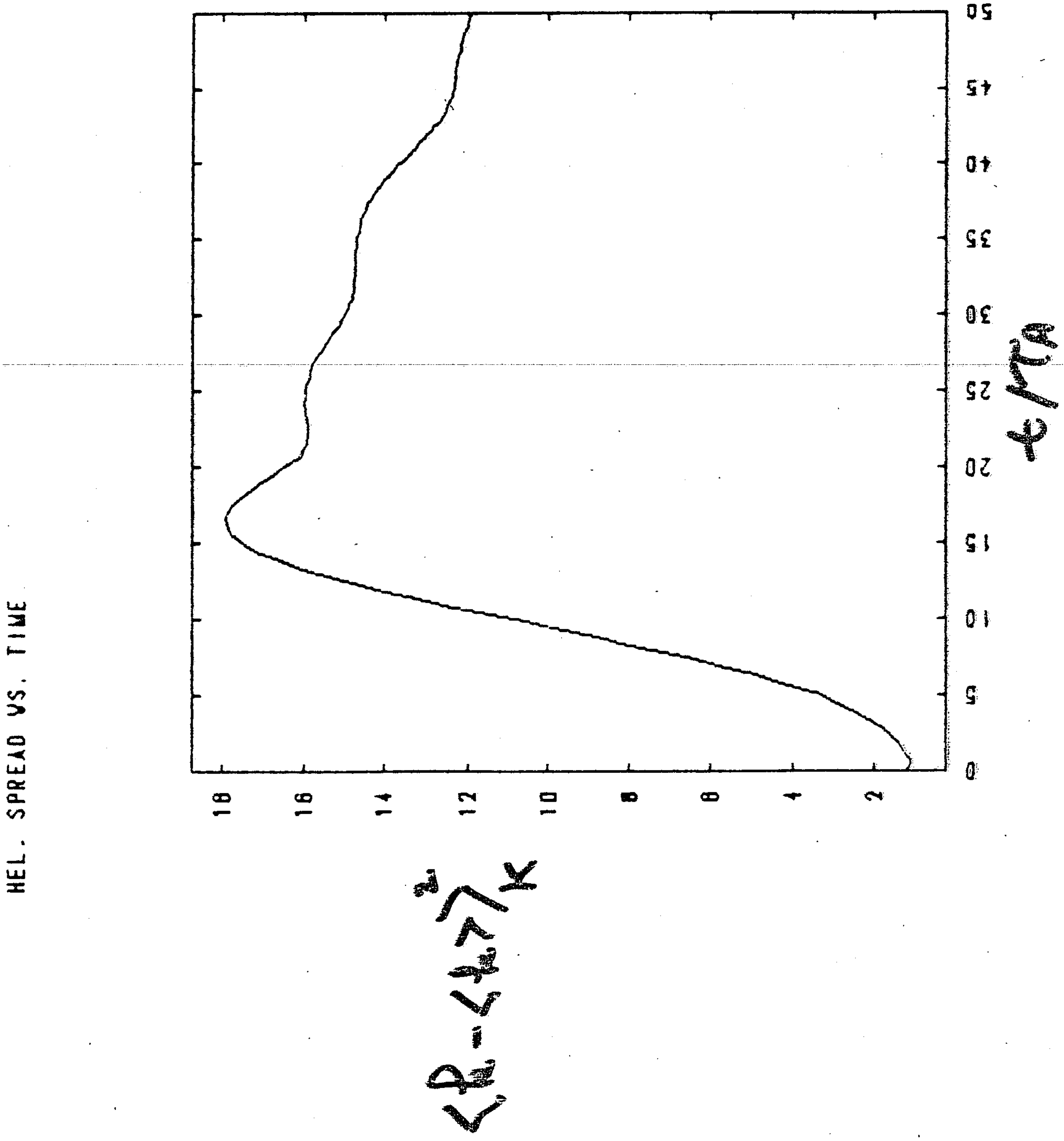
HEL. SPREAD VS. TIME
0
5
10
15
20
25
30
35
40
45
50
2
4
6
8
10
12
14
16
18

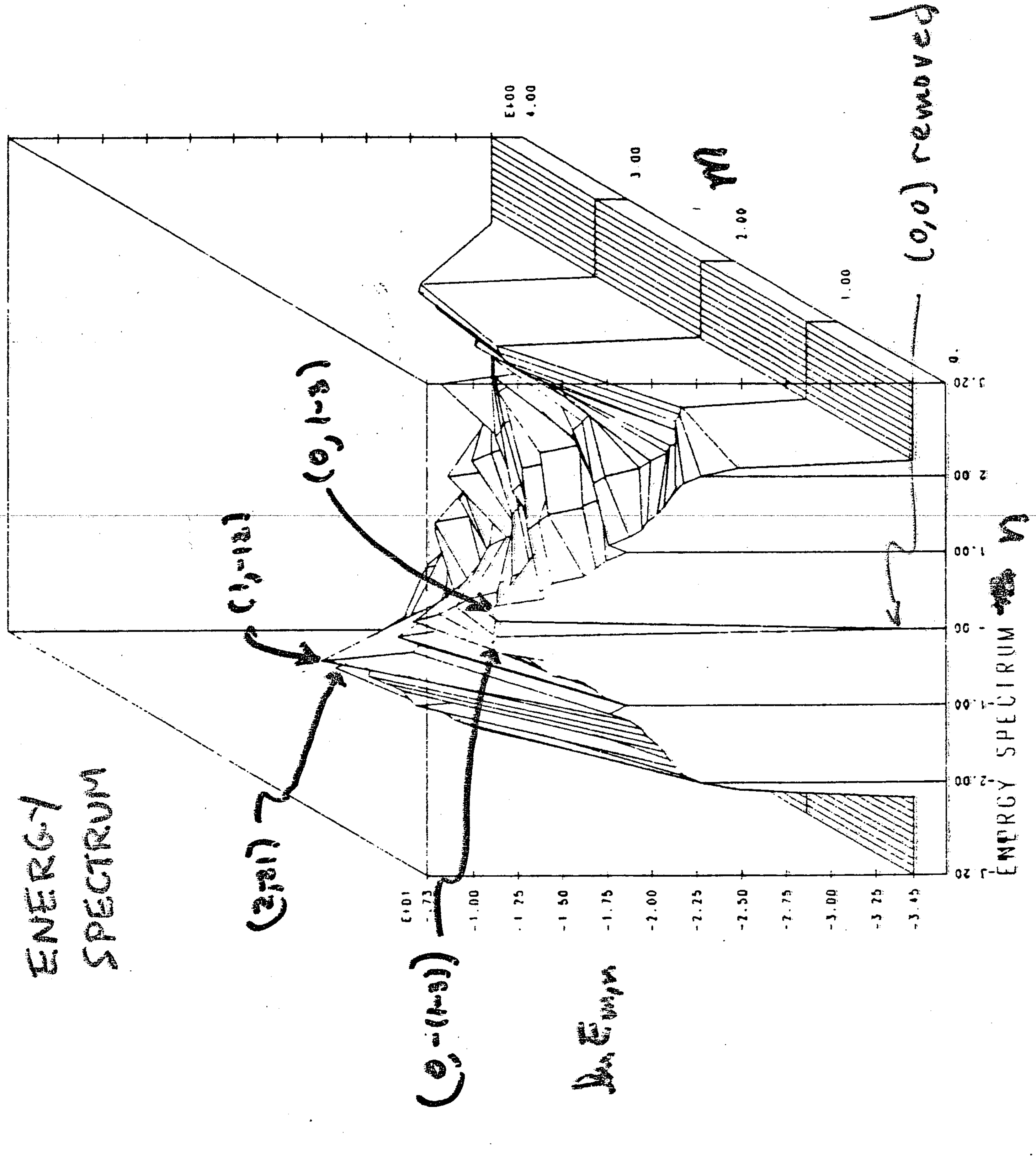
ENERGY SPECTRUM
(0,0) removed
ENERGY SPECTRUM
-1.20
-2.00
-1.00
.00
1.00
2.00
3.20
0.
1.00
2.00
3.00
4.00
-.73
-1.00
-1.25
-1.50
-1.75
-2.00
-2.25
-2.50
-2.75
-3.00
-3.25
-3.45

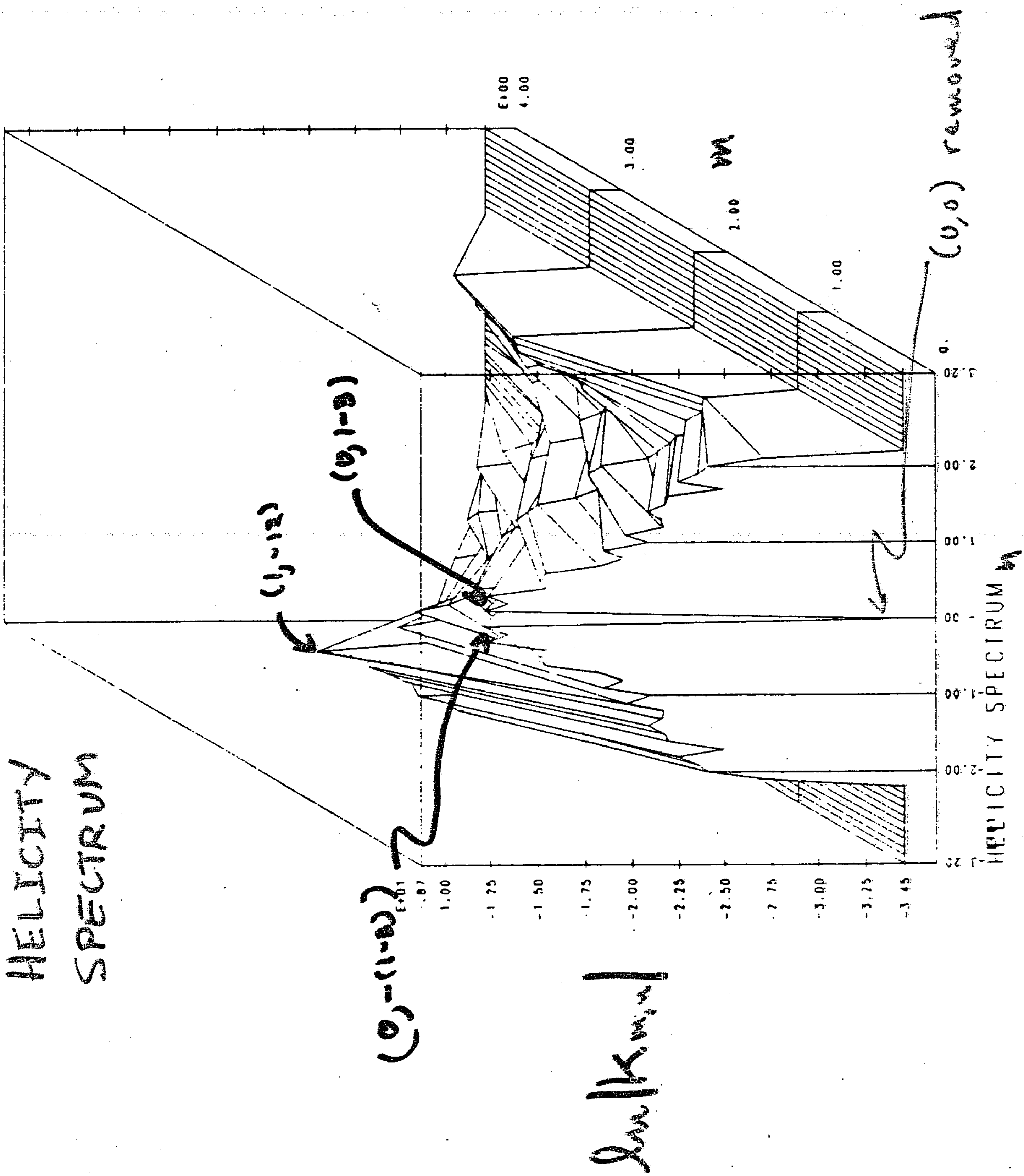
HELICITY SPECTRUM
(0,0) removed
(1,-12)
HELICITY SPECTRUM
m
n
E+00
4.00
3.00
2.00
1.00
0
E+01
.87
1.00
-1.25
-1.50
-1.75
-2.00
-2.25
-2.50
-2.75
-3.00
-3.25
-3.45

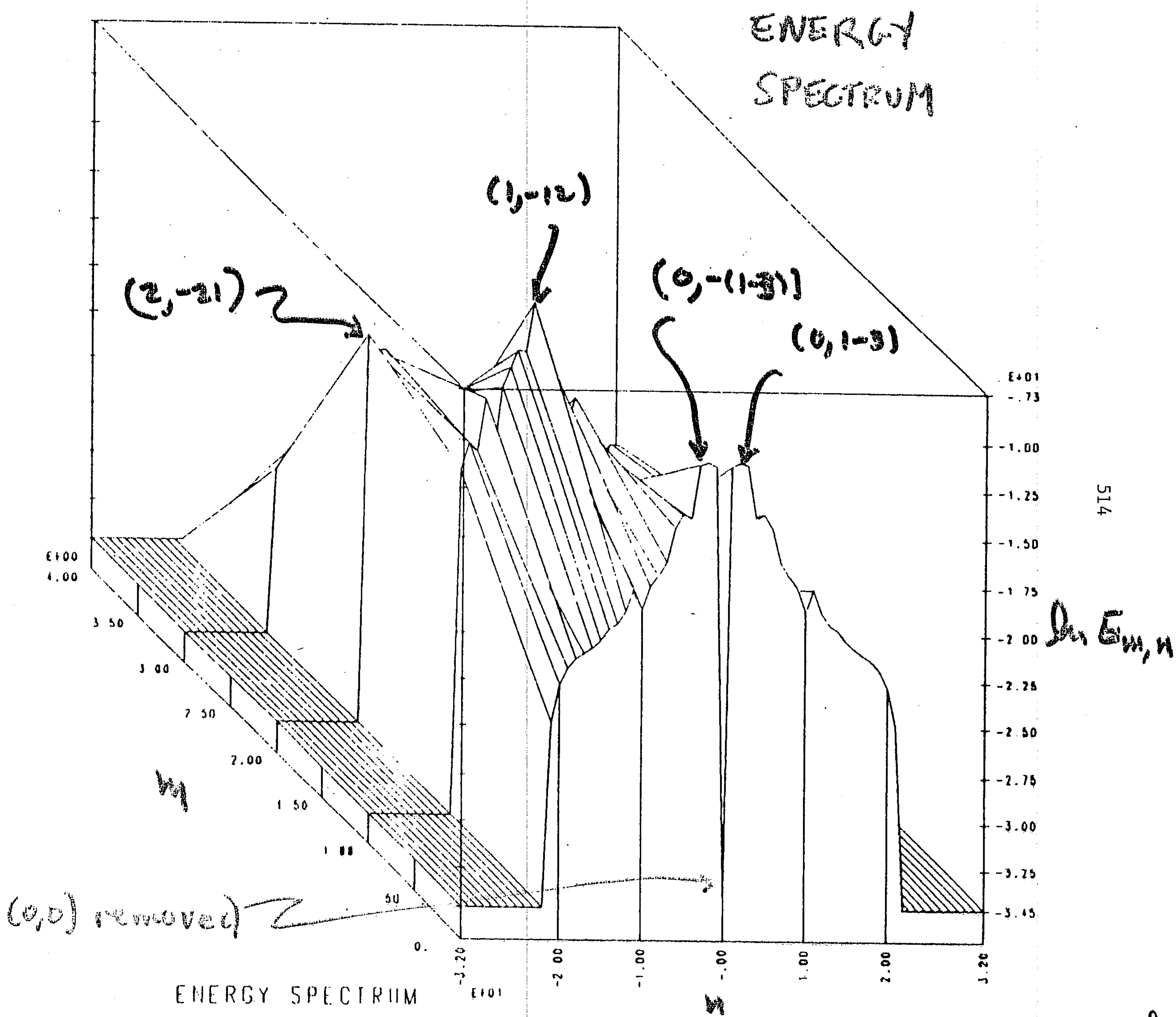
ENERGY SPECTRUM
(2,-21)
(1,-12)
(0,-(1-3))
(0,1-3)
(0,0) removed
E+01
-.73
-1.00
-1.25
-1.50
-1.75
-2.00
-2.25
-2.50
-2.75
-3.00
-3.25
-3.45
ln E m,n
E+00
4.00
3.50
3.00
2.50
2.00
1.50
1.00
.50
0.
-3.20
-2.00
-1.00
-.00
1.00
2.00
3.20
E+01
m
n
ENERGY SPECTRUM

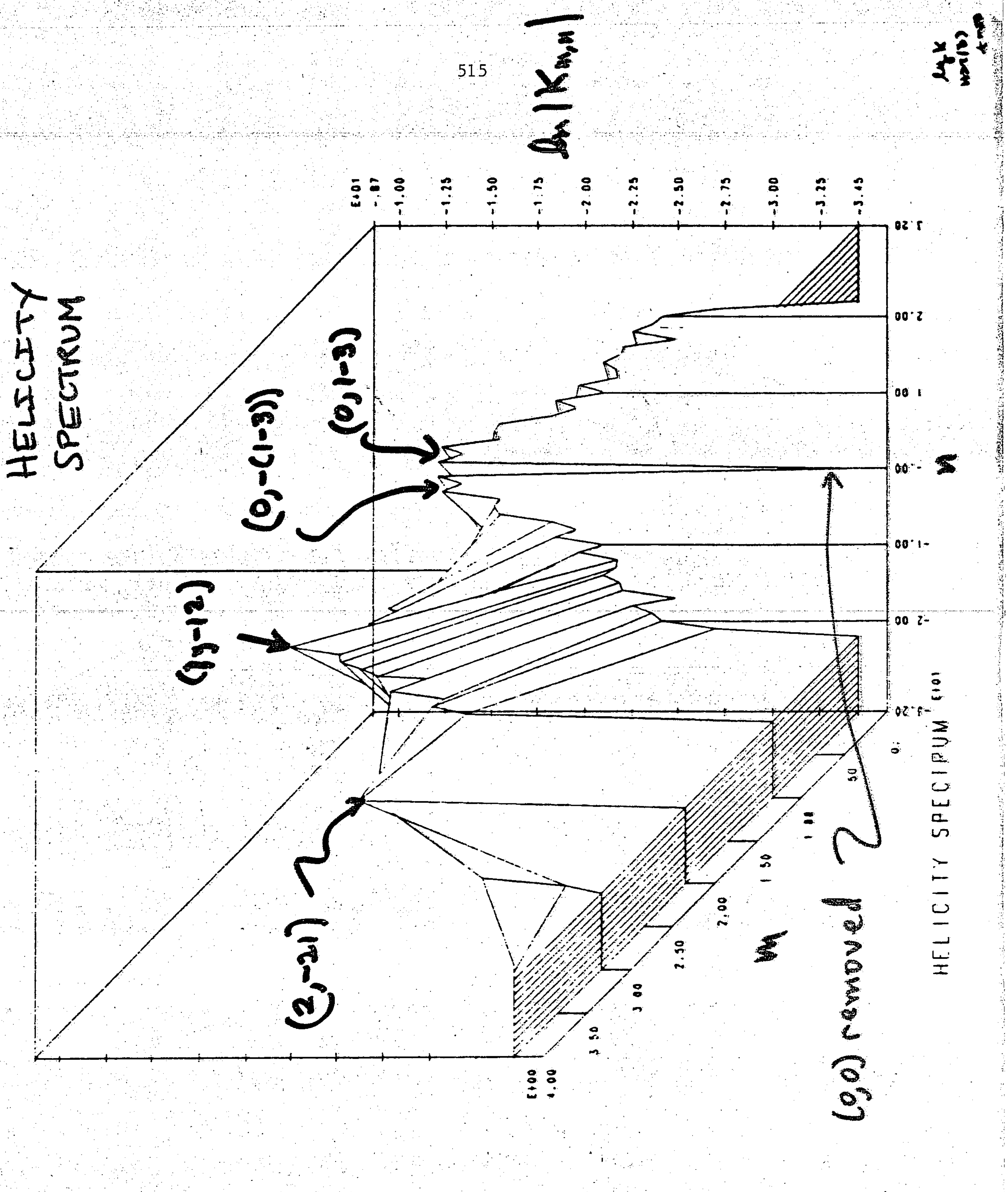

HELICITY SPECTRUM
(0,-(1-3))
(0,1-3)
(0,0) removed
HELICITY SPECTRUM
E+01
-.87
-1.00
-1.25
-1.50
-1.75
-2.00
-2.25
-2.50
-2.75
-3.00
-3.25
-3.45
E+00
4.00
3.50
3.00
2.50
2.00
1.50
1.00
.50
0.

CONCLUSIONS

- Onset of turbulence can be computed.
- W/K is minimized during non-linear growth and saturation of long-wavelength resistive MHD modes (relaxation).
- Relaxation process may cause degradation of confinement.
- Steady-state dynamo computed for $\varepsilon = 1$; transient flux generation for $\varepsilon = .2$. Long wavelength modes sufficient.
- Compressibility of (0,0) essential for RFP studies; compressibility of (m,n) may be important, but needs to be clarified.
- No evidence of inverse cascade for K; however turbulent state not adequately computed.

THE DYNAMICS OF TEARING MODES

S. COWLEY

PRINCETON PLASMA PHYSICS LAB

The Dynamics of Tearing Modes

with. R.M. Kulsrud and T.S. Hahm.

Introduction:

Linear theory.

We have addressed the regime applicable to T.F.T.R. and P.L.T. and shown stability when

$$(1) \qquad \Delta' a < 4\left(\frac{\eta_e}{2}\right)\left(\frac{a}{\rho_i}\right)\beta_p \ln\left(\frac{\rho_i}{\delta}\right)$$

WE CONCLUDE FROM EXPERIMENTAL EVIDENCE THAT:

TEARING MODES ARE PRESENT WHEN THEY ARE LINEARLY STABLE.

we propose the reason for this is:

NONLINEAR INSTABILITY

In a real discharge we expect the low m,n rational surfaces to be broken up into islands or possibly stochastic regions, the break-up can arise in many ways here are two:

- Imperfect coil alignment.
- Toroidal coupling to other modes.

In examining tearing modes one should consider an equilibrium with islands (or a stochastic field?) at the rational surface.

There are 3 types of tearing mode.

(1) Collisional: – Resistive mode of F.K.R.

Width of the current channel is governed by $E_{\parallel} \to 0$ in the outer regions.

(2) Semi-Collisional: – Introduced by Drake & Lee.

Width Δ of the current channel is where parallel diffusion of electrons limits conductivity.

$$\Delta \ll \rho_i$$

$$E_{\parallel} \to 0 \quad \text{for} \quad x \gtrsim \rho_i .$$

$$J_{\parallel}(x) = \sigma(x)\, E_{\parallel}(x)$$

width Δ width ρ_i

$$\Delta \sim \left(\frac{\nu_{ei}}{\omega^*}\right)^{1/2} \rho_e \frac{l_s}{l_n}$$

(3) Collisionless: Current limited by electron inertia, width δ where electrons 'see' D.C. $E_{\parallel}$ i.e. for large $k_{\parallel}$ electrons 'see' A.C. $E_{\parallel}$ and $\sigma_{\parallel}(x)$ is reduced.

$$\omega^* = k_{\parallel} v_{the}$$

$$\delta \sim \rho_e \frac{l_s}{l_n} << \rho_i$$

We consider regimes (2) & (3) since these have been incorrectly treated in the literature. Regime (2) covers most tearing modes in present day large tokamaks.

5/

We make the following general assumptions:

(i) $\omega^* \gg \nu_i$

(ii) $\omega^* \gg k_\parallel v_{thi}$

(iii) $\dfrac{l_n^2}{l_s^2} \ll 1$

(iv) $\rho_e \dfrac{\partial}{\partial x} \ll 1$

(v) $A_\perp \ll A_\parallel$

(vi) $\delta, \Delta \ll \rho_i$

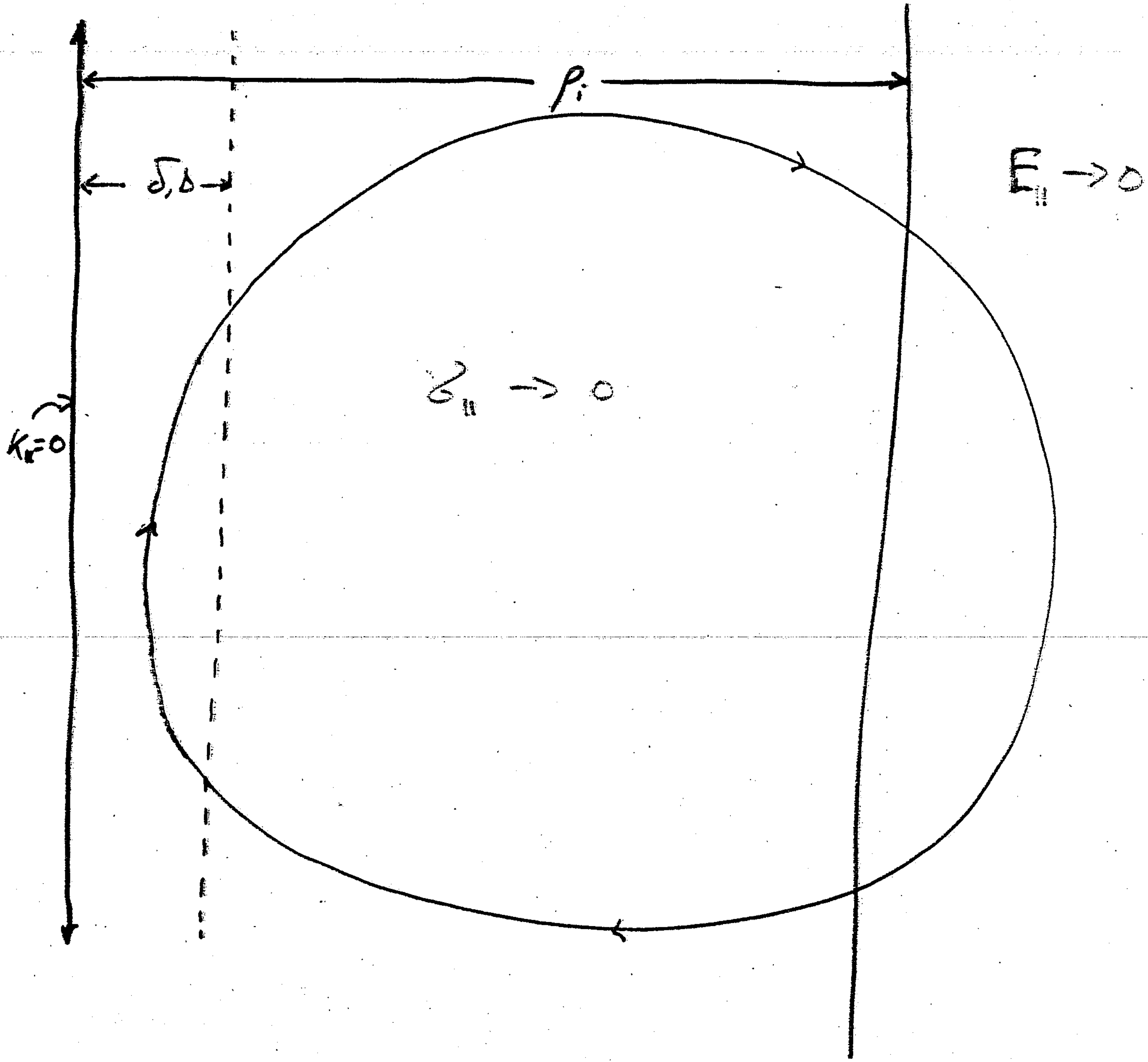

$$\underset{\sim}{B}_0 = B_0 \left(\hat{\underline{z}} + \frac{x}{\ell_s} \hat{y} \right)$$

$$\frac{\partial}{\partial z} \equiv 0$$

GENERAL EQUATIONS

AMPERES LAW

① $$\underbrace{\left(\frac{\omega^*}{\omega}\right)^2 \frac{1}{\beta_p} \frac{d^2 A_\parallel}{dt^2}}_{\nabla^2 A_\parallel} = \frac{1}{t}\int dq\, \Phi(q) F(q) e^{iqt}$$

$$= -\underbrace{\left(A_\parallel - t\phi(t)\right)\delta(t)}_{-J_\parallel}$$

QUASI-NEUTRALITY

② $$\underbrace{-t\left(A_\parallel - t\phi(t)\right)\delta(t)}_{-ik_\parallel J_\parallel} = \underbrace{\int dq\, \Phi(q) F(q) e^{iqt}}_{\nabla_\perp \cdot J_\perp}$$

$\phi(t)$ and $\phi(q)$ are a Fourier transform pair – they are generalised functions.

t, $\delta(t)$ are different for the two modes.

t is a scaled x.

where:

'e' $E \wedge B$ F.L.R. ions.

$$(3) \quad F(q) = \left(\frac{\omega^*}{\omega} + \frac{T_e}{T_i}\right)\left(\Gamma_0 - 1\right) - \frac{\omega^*}{\omega}\frac{\eta_i}{2}\frac{q^2}{\epsilon^2}\left(\Gamma_0 - \Gamma_1\right)$$

ion, Bolzman response

$$\Gamma_n = \exp -\left(\frac{q^2}{2\epsilon^2}\right) I_n\left(\frac{q^2}{2\epsilon^2}\right)$$

$\epsilon = \dfrac{\delta}{\rho_i}$ for collisionless mode.

$\epsilon = \dfrac{\Delta}{\rho_i}$ for semi-collisional mode.

Collisionless:

Electron conductivity comes from the Drift-Kinetic equation; t is defined as.

$$(4) \quad t = \frac{x}{\delta}$$

and $\delta(t)$ is

$$(5) \quad \delta(t) = -\frac{1}{2}\left\{\left(1 - \frac{\omega^*}{\omega}\right)\frac{1}{t^2} Z'\left(\frac{1}{|t|}\right) + \frac{\omega^*}{\omega}\frac{\eta_e}{2}\frac{1}{|t|^3} Z''\left(\frac{1}{|t|}\right)\right\}$$

Semi-Collisional

Solving Braginskii's Eqns for the electrons. In the ordering.

(6) $$k_{\parallel}^2 \frac{V_e^2}{\nu_{ei}} \sim \omega^*$$

Note $\omega^* \ll \nu_{ei}$ and $k_{\parallel} V_e \ll \nu_{ei}$

so that $\omega^* \ll \quad \bar{k}_{\parallel} V_{the} \ll \nu_{ei}$

(7) $$t = \sqrt{i}\,\frac{x}{\Delta} = \sqrt{i}\,\frac{x}{\rho_e}\,\frac{\ell_n}{\ell_s}\left(\frac{\omega^*}{\nu_{ei}}\right)^{1/2}$$

(8) $$\boxed{\sigma(t) = \frac{1 - \frac{\omega^*}{\omega}(1 + 1.71\eta_e) + 2.13\left(1 - \frac{\omega^*}{\omega}\right)t^2}{1 + 5.08t^2 + 2.13t^4}}$$

The boundary condition is as usual.

$$(9) \quad \Delta' = \frac{1}{A_\parallel}\frac{dA_\parallel}{dx}\Big|^{x=+\infty} - \frac{1}{A_\parallel}\frac{dA_\parallel}{dx}\Big|^{x=-\infty}$$

and $E_\parallel \to 0$ as $|x| \to \infty$

Integrate (1) w.r.t. t.

$$(10) \quad \left(\frac{\omega^*}{\omega}\right)^2 \frac{1}{\beta_p} (\Delta' a) \underbrace{\frac{\delta}{a} A_\parallel(\infty)}_{\text{very small}} = \int_{-\infty}^{\infty} dt \, (A_\parallel - t\,\phi(t))\,\delta(t)$$

small since for $\beta_p \ll 1$
$A_\parallel$ is nearly constant

O(1)

Hence dominant current must

cancel upon integration.

This makes $\omega \sim \omega^*$

MAGNETISED: versus :UNMAGNETISED

Two limits to Eqn. (2)

$$-t\,(A_{\parallel} - t\,\phi(t))\,\delta(t) = \int dq\, \phi(q)\, F(q)\, e^{iqt}$$

Magnetised : $\frac{\rho_i}{\delta}\frac{d}{dt} \ll 1$ in our case for $t \gg \frac{\rho_i}{\delta}$

(11) $$t\,(A_{\parallel} - t\,\phi(t))\,\delta(t) = \underbrace{\left[\frac{T_e}{T_i} + \frac{\omega^*}{T_i}\left(1 + \frac{\eta_i}{2}\right)\right]}_{\text{polarisation current}} \frac{\rho_i^2}{\delta^2}\frac{d^2\phi}{dt^2}$$

F.L.R. E×B

Adiabatic or Unmagnetised or Bolzman ions

(12) $$\boxed{-t\,(A_{\parallel} - t\,\phi(t)) = F(\infty)\,\phi(t) = -\left(\frac{\omega^*}{\omega} + \underbrace{\frac{T_e}{T_i}}_{\text{Bolzman ions}}\right)\phi(t)}$$

Valid where $$\phi \gg \int dq\, e^{iqt}\, \Phi(q)\, \Gamma_0\!\left(\frac{q}{\epsilon}\right)$$

or $$\phi \gg \frac{\delta}{2\rho_i}\frac{1}{\sqrt{2\pi}}\int_{-\infty}^{\infty} dt'\, \phi(t')\, \exp\left(\frac{t-t'}{\rho_i/\delta}\right)^2 K_0\left(\frac{t-t'}{\rho_i/\delta}\right)^2$$

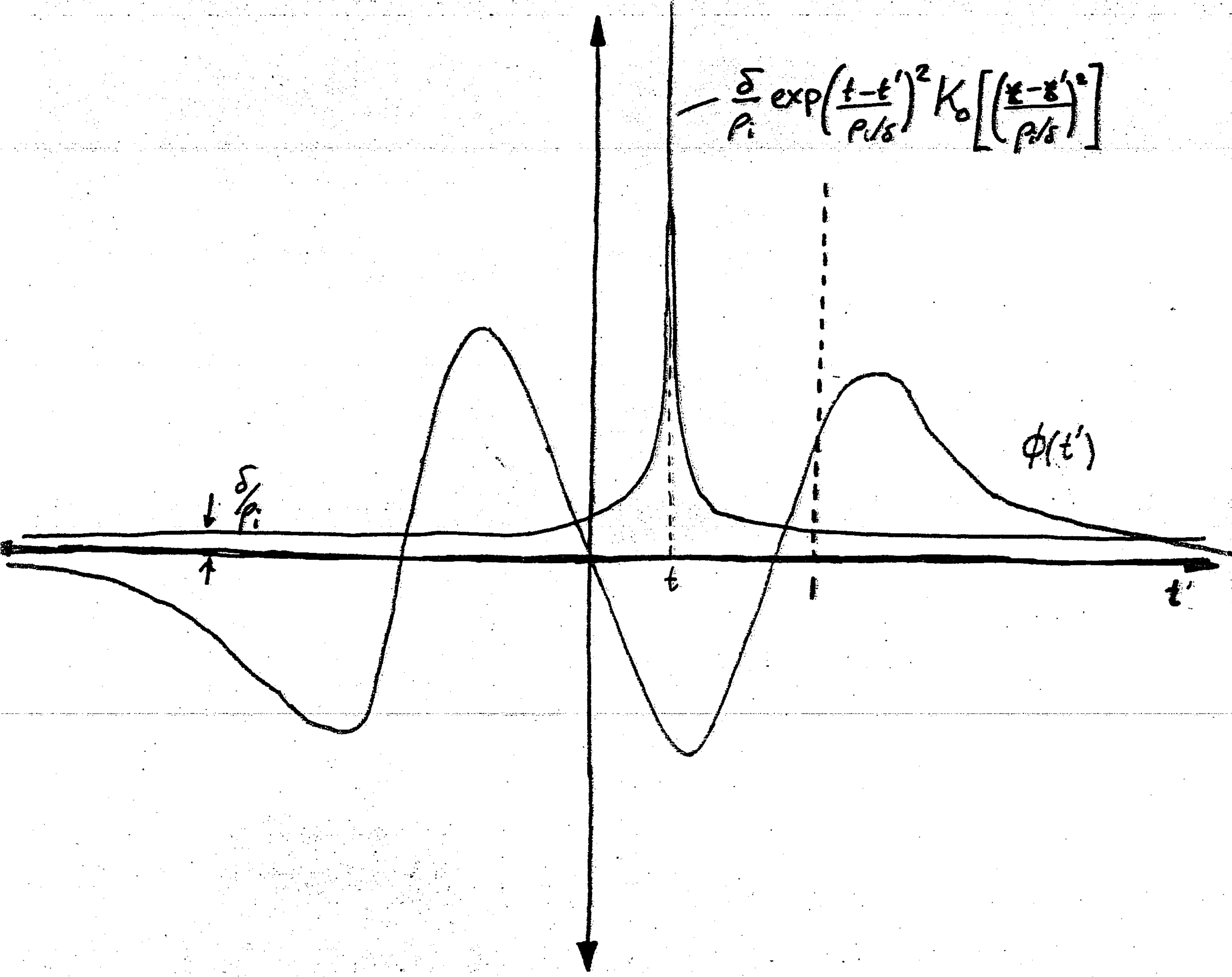

Non-local response

$$\phi \gg ? \quad \frac{\delta}{2\rho_i}\frac{1}{\sqrt{2\pi}}\int_{-\infty}^{\infty} dt'\,\phi(t')\exp\left(\frac{t-t'}{\rho_i/\delta}\right)^2 K_0\left[\left(\frac{t-t'}{\rho_i/\delta}\right)^2\right]$$

Shows (12) is valid for $t \sim 1 \ll \rho_i/\delta$ to order δ/ρ_i

Expansion Technique

Treat $A_{\parallel}$ as known solve

Quasi-Neutrality Equ. (2) for $\phi(q)$ then

substitute into (1) however (2) is an

integral Equ. we solve in powers of δ/ρ:

Call $\phi_u(t)$ the unmagnetised solution

the solution of Equ. (12) i.e.

$$(13) \quad -t\left(A_{\parallel} - t\phi_u(t)\right)\delta(t) = F(\infty)\,\phi_u(t)$$

Valid for $t \ll \rho_i/\delta$

Write (2) as:

$$(14) \quad \boxed{\begin{aligned} &\left(F(\infty) - \delta(\infty)\right)\phi_u(t) + \left(t^2\delta(t) - \delta(\infty)\right)\left(\phi(t) - \phi_u(t)\right) \\ &= \int dq\,\left(F(q) - \delta(\infty)\right)\phi(q)\,e^{iqt} \end{aligned}}$$

$$\lim_{t \to \infty} t^2 \delta(t) = \delta(\infty) = \left(1 - \frac{\omega^*}{\omega}\right)\begin{pmatrix}\text{Bolzmann} \\ \text{response}\end{pmatrix}$$

Define a function $\chi(t)$ which equals $\phi(t)$ for $t \ll \rho_i/\delta$.

Rewrite 2. again.

$$\boxed{\begin{aligned} (15) \quad \left(F(\infty) - t^2\delta(t)\right)\chi(t) &= -t\,\delta(t) A_{11}(t) \\ &\quad + \underbrace{\boxed{\int dq \left[F(\infty) - F(q)\right] \phi(q) e^{iqt}}}_{A} \end{aligned}}$$

14 again

$$\boxed{\begin{aligned} \left(F(\infty) - \delta(\infty)\right)\phi_u(t) &+ \underbrace{\boxed{\left(t^2\delta(t) - \delta(\infty)\right)\left(\phi(t) - \phi_u(t)\right)}}_{B} \\ &= \int dq \left[F(q) - \delta(\infty)\right] \phi(q)\, e^{iqt}. \end{aligned}}$$

(A) produces a small effect for $t \ll (\rho_i/\delta)$

we have shown this is order δ/ρ_i

(B) Is finite for $t \ll \rho_i/\delta$ only

$\phi(t)$ in (B) can be approximated by $\chi(t)$

Dropping (A) as small we obtain the

Orth Order:

(16) $\chi_0(t) = \phi_u(t)$ as before.

(17) $$\phi_0(q) = \frac{(F(\infty) - \delta(\infty))\,\phi_u(q)}{F(q) - \delta(\infty)}$$

We can itterate substituting $\phi_0(q)$ into (A) evaluating $\chi_1(t)$ substituting in (16) etc:

n'th itteration

$$(18) \quad \left(F(\infty) - t^2\delta(t)\right)\chi_n(t) = \int dq \left(F(\infty) - F(q)\right)\phi_{n-1}(q)e^{iqt}$$

$$(19) \quad \phi_n(q) = \frac{1}{F(q) - \delta(\infty)}\int \frac{dt}{2\pi} e^{-iqt}\left\{\left(t^2\delta(t) - \delta(\infty)\right)\left[\chi_n(t) + \phi_{n-1}(t) - \chi_{n-1}(t)\right]\right.$$

Schematically we have

$\boxed{\phi_{n-1}(t)\ \chi_{n-1}(t)\ \text{KNOWN}}$ Non local response propergates

Equ(18) ϕ_{n-1} from outside to inside to change χ by χ_n

$\boxed{\chi_n(t),\ \phi_{n-1},\ \chi_{n-1}\ \text{KNOWN}}$ Taking χ_n

Equ(19) and $\phi_{n-1} - \chi_{n-1}$ as sources in the inside change ϕ by ϕ_n by non-local propergator.

$\boxed{\chi_n,\ \phi_n\ \text{KNOWN}}$

Treating $\beta_p < 1$ we expand $A_{\parallel}$ in β_p first term is $A_{\parallel}$ = constant.

Integrating Eqn (1) Amperes law over + keeping $O(\delta/\rho_i)$ and $O(\beta_p)$ only we obtain.

$$\boxed{\begin{aligned}\left(\frac{\omega^*}{\omega}\right)^2 \frac{1}{\beta_p}(\Delta' a)\left(\frac{\delta}{a}\right) \simeq\ & F(\infty)\int dt\left[\frac{\theta(t)}{t} + \left(\frac{\omega}{\omega^*}\right)^2 \beta_p\left[\int dt' \frac{\theta(t')}{t}\right]^2\right] \\ &+ \int_{-\infty}^{\infty} dq\, \theta(q)\left[\frac{F(\infty) - F(q)}{F(q) - \delta(\infty)}\right]\left[\theta(q)F(\infty) - \delta(\infty) + \frac{T(q)\,F(\infty)}{F(\infty) - \delta(\infty)}\right]\end{aligned}} \tag{20}$$

$$\theta(t) = \frac{-t\,\delta(t)}{F(\infty) - t^2\delta(t)}$$

$$T(t) = -\left(t^2\delta(t) - \delta(\infty)\right)t^{-1}$$

Results

It can be shown that the

$O(1)$ and $O(\beta_p)$ terms give

$\underline{\mathrm{Im}\,\omega = 0}$ for both modes

If $(\Delta' a) < 4\left(\frac{\eta_e}{2}\right)\left(\frac{a}{\rho_i}\right)\beta_p \ln\left(\frac{\rho_i}{\delta}\right)$

mode is stable !

Collisionless

$$\gamma_{damping} \simeq \frac{\omega^* \eta_e}{\sqrt{2}\,8} \frac{\delta}{\rho_i} \ln\left(\frac{\rho_i \sqrt{2}}{\delta}\right)$$

Semi-collisional

$$\gamma_{damping} \simeq \frac{3.71}{4\pi^{1/2}} \omega^*(1 + 0.4\eta_e)\eta_e \frac{\Delta}{\rho_i} \ln\left(\frac{\rho_i}{\Delta}\right)$$

Physics!

Parallel current driven by:-

F_e = Force on electrons = $\nabla_{\parallel} p_e + n e E_{\parallel}$

Drop ∇T_e for this discussion.

$\nabla_{\parallel} p_e$ arises from parallel flows and tilting the field line. From parallel flows.

$$n_e' = n_e \frac{k_{\parallel} v_{\parallel}}{\omega}$$

Tilting field line

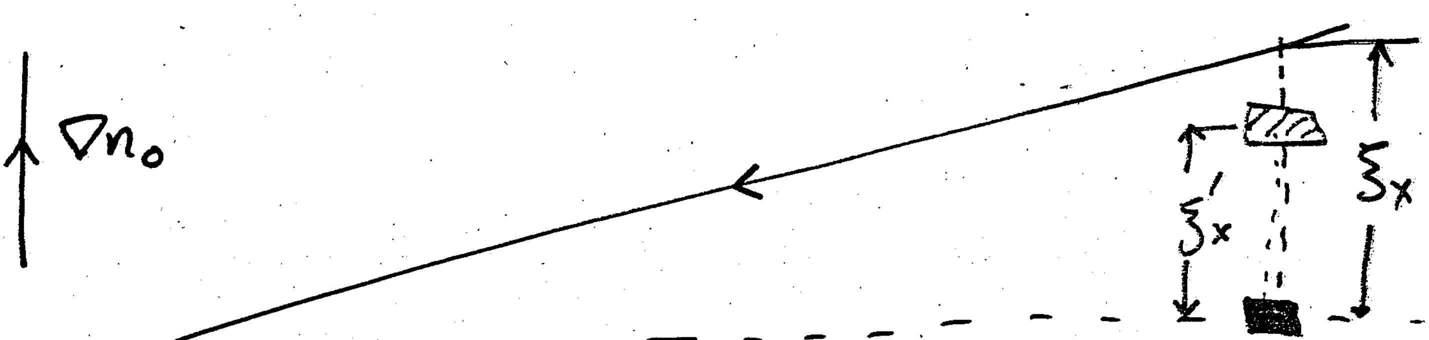

field line displaced ξ_x

Electrons displaced ξ_x'

ξ_x' the electron displacement comes from the $\underset{\sim}{E} \times \underline{B}$ velocity

$$\xi_x' = \frac{k}{\omega} \frac{c\phi}{B_0}$$

ξ_x the displacement of the field line is

$$\xi_x = \frac{\delta B_x}{i k_{\parallel} B_0} = \frac{k A_{\parallel}}{k_{\parallel} B_0}$$

the parallel pressure gradient is then

$$\nabla_{\parallel} P_{\parallel} = + i k_{\parallel} (\xi_x - \xi_x') \cdot \nabla n_0 + n_0 \frac{k_{\parallel}^2 v_{the}^2}{\omega} v_{\parallel}$$

$$= -\frac{\omega^*}{\omega} e E_{\parallel} n_0 + n_0 \frac{k_{\parallel}^2 v_{the}^2}{\omega} v_{\parallel}$$

$$\therefore \quad F_{\parallel} = \underbrace{e n_0 \Big(1 \underbrace{- \frac{\omega^*}{\omega}}_{\text{Tilt term}} \Big) E_{\parallel}}_{\text{driving force}} + n_0 \frac{k_{\parallel}^2 v_{the}^2}{\omega} v_{\parallel}$$

$F_{\parallel}$ balanced by: Friction in semi-collisional case
: inertia in collisionless case.

Simple Physical Picture of Stabilization

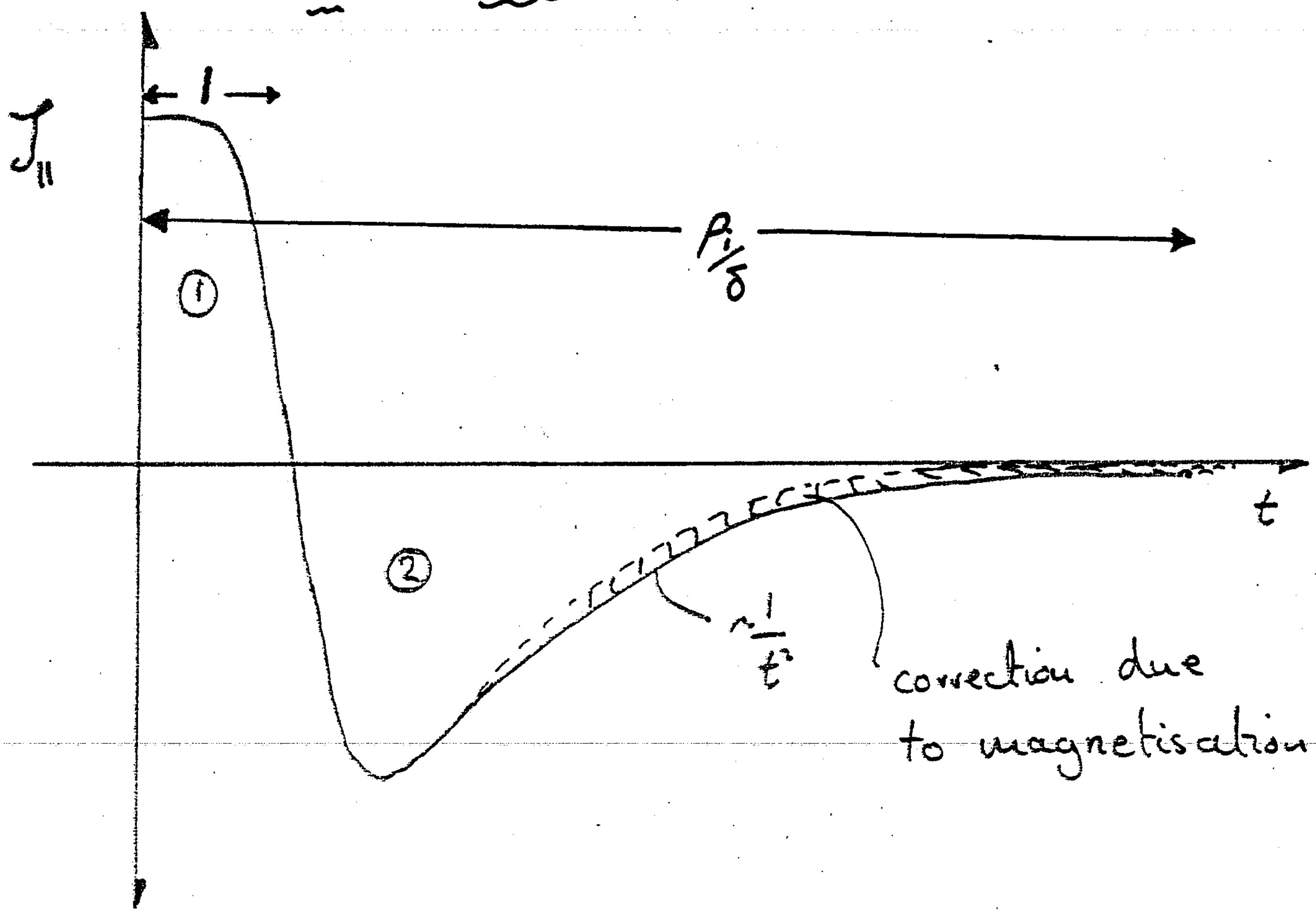

① + ② = 0 dominant current canceling.

Correction to current $\Delta J_{\parallel}$ is approx

$\Delta J_{\parallel} \doteq$ "Magnetised ion current response" − 'Unmagnetised' ion current response. incorrect

for $t > \rho_i/\delta$ only

magnetised current from

$$J_{\parallel} = \frac{\nabla\cdot J_{\perp}}{ik_{\parallel}} \qquad J_{\perp} = \text{polarisation current of ions.}$$

$$\int dt\, \Delta J_{\parallel} = \int_{\alpha\rho_i}^{\infty} dt \left\{ J_{\parallel\,\text{mag}} - J_{\parallel\,\text{unmag.}} \right\}$$

using $J_{\parallel} \simeq A_{\parallel}\, \delta_{\parallel}$ for unmag.

$$\frac{\delta}{a}\left(\Delta' a - \beta_p \frac{a}{\rho_i}\right) \simeq -\frac{4\pi}{c}\int_{-\infty}^{\infty} dt\, J_{\parallel}(t)_{\text{unmag.}}$$

stabalizing from $\Delta J_{\parallel}$

Magnetisation couples ions and field lines

field 'shakes' ions at $\sim\omega^*$ causing currents to

flow that stabilize.

Nonlinear Aspects.

Equilibrium islands. ∇T_e and $\nabla n_e = 0$ around island. All ω^* effects go away in fact when $\nabla T_e = 0$ $\phi = 0$ and ion stabilization goes in linear mode.

The evolution of the island from equilibrium is described well for width of the island $W \gg \rho_i$ by resistive M.H.D.. Equilibrium island is given by ψ_0

$$\frac{\Delta' \psi}{(\psi + \psi_0)^{1/2}} = \frac{16\pi A}{\eta \left(\frac{2B_0}{\ell_s}\right)^{1/2}} \frac{\partial \psi}{\partial t}$$

Exponential growth for $\psi \ll \psi_0$

for $\psi \gg \psi_0$

$$\psi^{1/2} = \eta \left(\frac{2B_0}{\ell_s}\right)^{1/2} \int_0^t \Delta'(t')\, dt'$$

CONCLUSION

We have shown that tearing modes are stable when

$$\Delta' a < 4\left(\frac{\eta_e}{2}\right)\left(\frac{a}{\rho_i}\right)\beta_p \ln\left(\frac{\rho_i}{\delta}\right)$$

The question of stability however must be addressed in the non-linear regime since ripple ~ 1% will make equilibrium islands of size greater than ρ_i. Non-linear growth is expected.

COMPUTER MODELING OF FAST COLLISIONLESS RECONNECTION

J. N. LEBOEUF

INSTITUTE FOR FUSION STUDIES

COMPUTER MODELING OF FAST COLLISIONLESS RECONNECTION

• J.N. LEBOEUF — IFS

F. BRUNEL — IFS
• T. TAJIMA — IFS

J. SAKAI — Toyama U., Japan

• C.C. WU — UCLA
• J.M. DAWSON — UCLA

Acknowledgment:
P.T. Kaw.

TALK OUTLINE

1. BRIEF REVIEW OF OTHER SIMULATION WORK ON COLLISIONLESS TEARING AND/OR RECONNECTION AND/OR COALESCENCE

2. OUR SIMULATION WORK
   - MODEL AND CONFIGURATION
   - RECONNECTION EVENTS
   - ENERGETICS
   - APPLICATION TO SOLAR FLARES

3. SUMMARY AND CONCLUSIONS

OTHER WORK : BRIEF REVIEW

ALL USE MAGNETOSTATIC (DARWIN) PARTICLE OR KINETIC COLLISIONLESS CODES UP TO 2-½ D.

- • – DICKMAN, MORSE, NIELSON, PHYS FLUIDS 12, 1708 (1969)
- – AMANO AND TSUDA, J. Geomag. Geoelect. 29, 9 (1977).
- • – KATANUMA AND KAMIMURA, Phys. Fluids 23, 2500 (1980).
- – HAMILTON AND EASTWOOD, Planet. Sp. Sc. 30, 293 (1982).
- • – TERASAWA, JGR 86, 9007 (1981)

 Dickman et. al. 13
Multimode Tearing

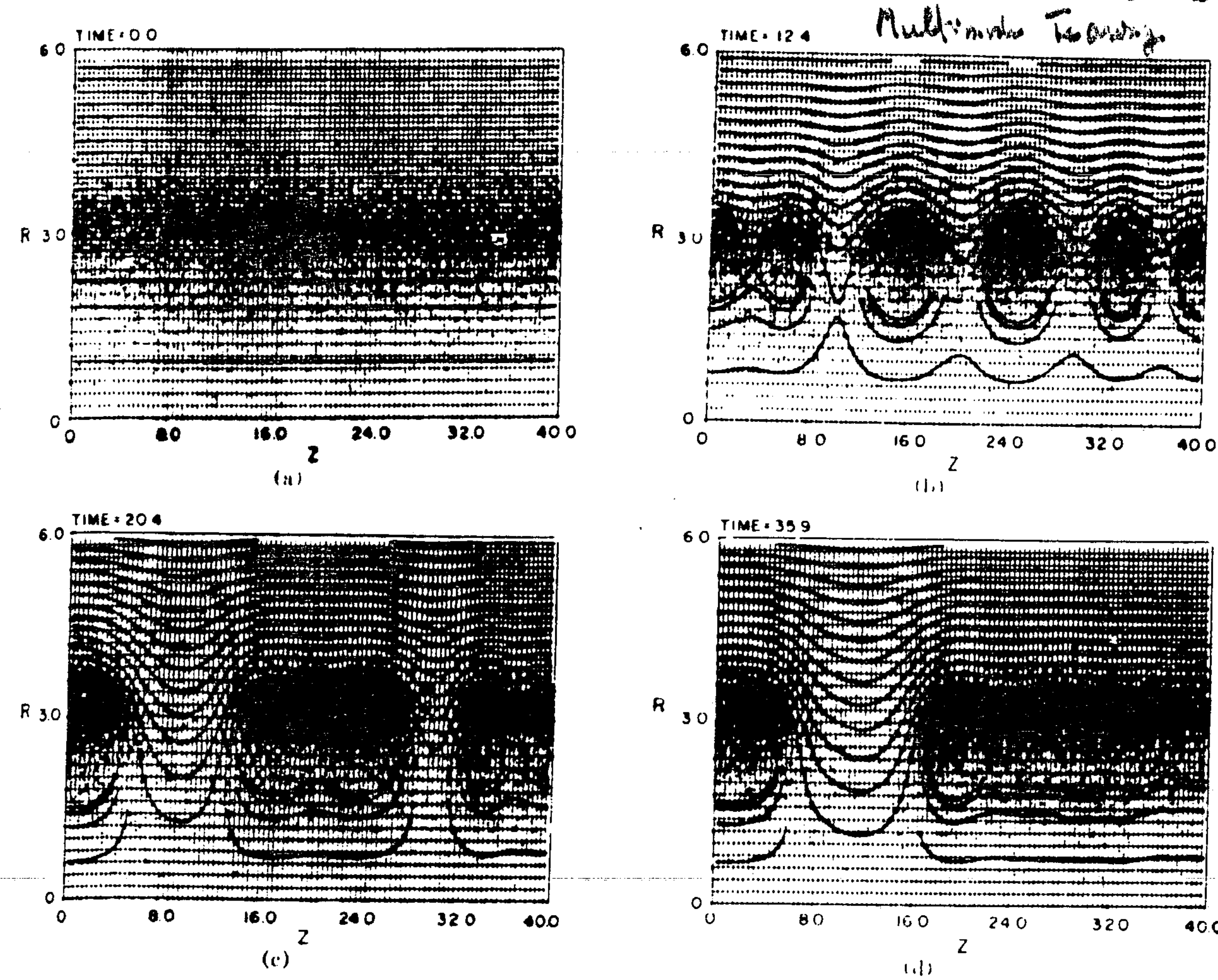

FIG. 6. Time sequence of tearing mode simulation at t = (a) 0, (b) 12.4, (c) 20.4, (d) 35.9 where the gyro-period in the external vacuum field is $2\pi/1.5$. Tearing at about the wavelength of maximum linear growth rate, (b), is subsequently converted into one wavelength in the system, (d), by coalescing.

of that anisotropy which was initially responsible for the instability. This large increase in axial thermal motion should have a large effect on end loss from θ-pinches in times short compared with ion-ion collision times, and in fact is consistent with experimental findings on this point. Some plots like those of Fig. 3 together with a brief discussion of the code appear in a previous paper.[8]

V. ASTRONLIKE CONFIGURATIONS

Figure 5 shows the initial profile for the case $\psi = -0.5$, $r = 3.0$, and $T = 1.0$ in which the diamagnetic current is sufficient to reverse B_z and the plasma is well localized midway between the center axis and the flux conserver at $r_{max} = 6.0$. The same reflective conditions as above apply at

[8] R. L. Morse, presented at the Conference on Pulsed High Density Plasmas of the American Physical Society, Los Alamos, New Mexico (1967).

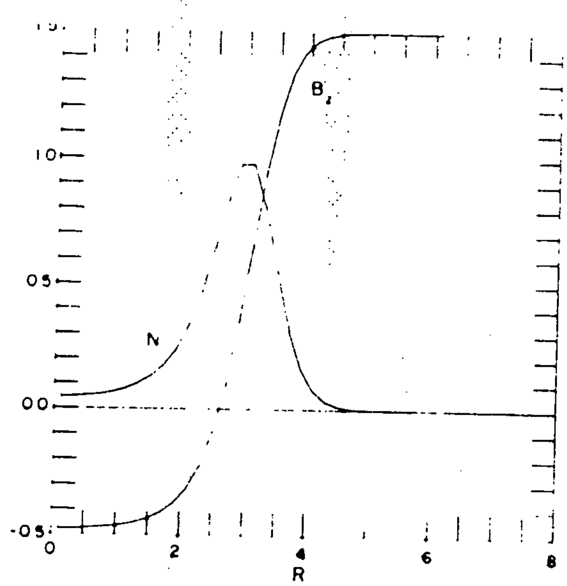

FIG. 5. Initial profiles of $n(r)$ and $B_z(r)$ for the reversed field equilibrium from which the tearing mode simulation of Fig. 6 was begun.

Katanuma + Kamimura
Multi-mode Tearing

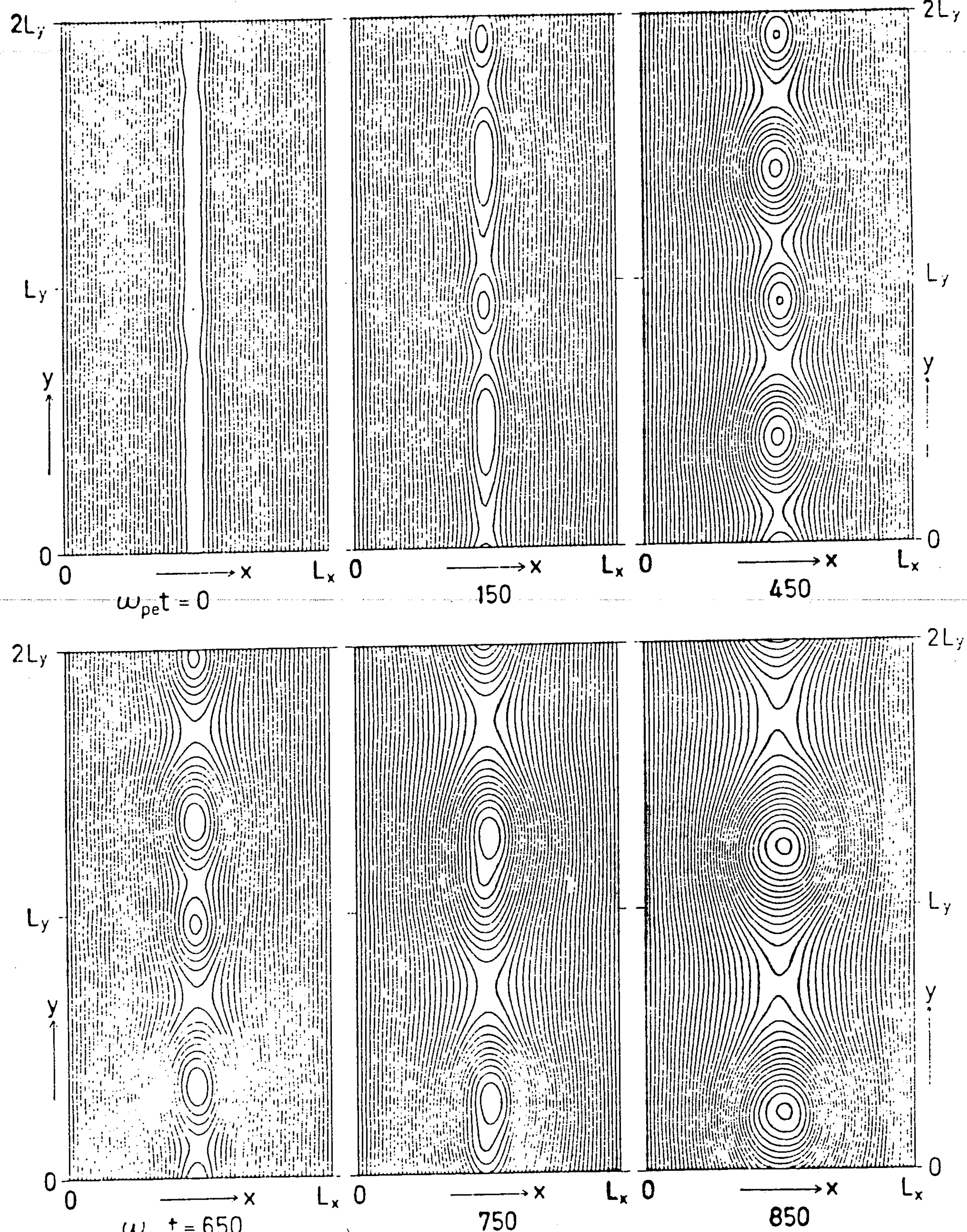

Fig.15

$\tau_A \sim 12 \omega_{pe}^{-1}$

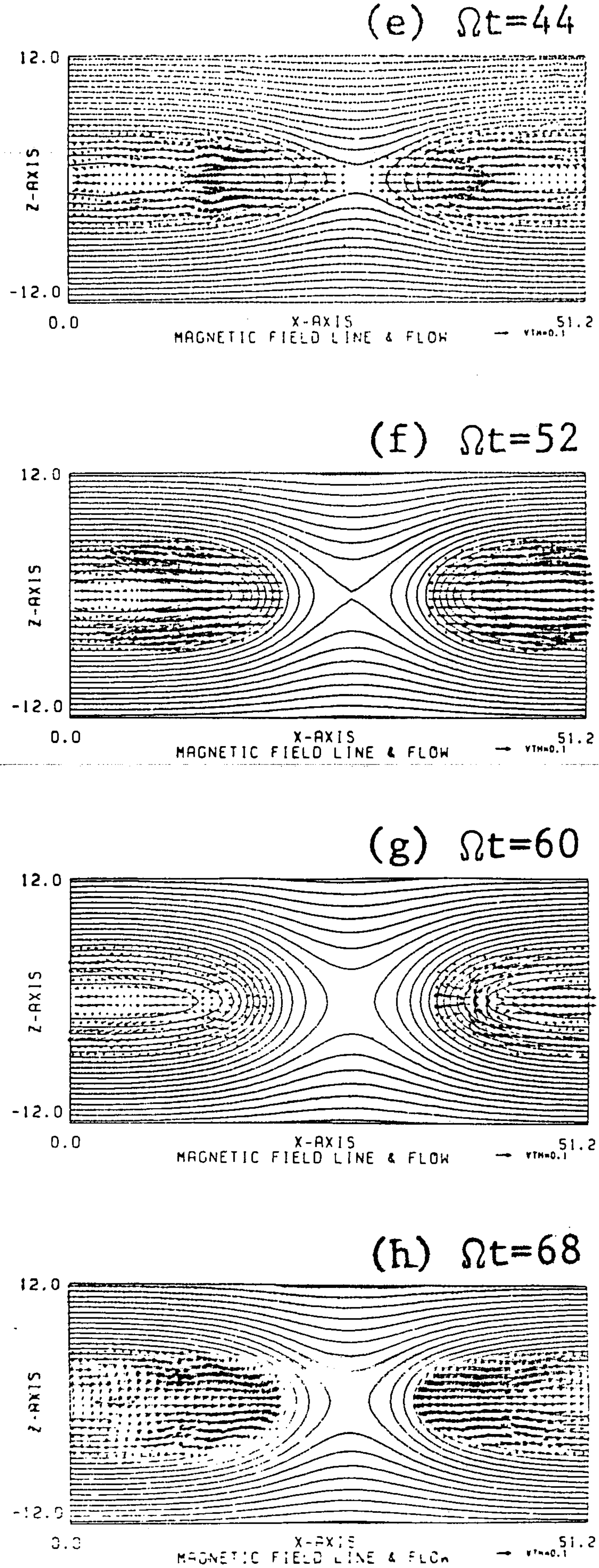
(e) Ωt=44
12.0
Z-AXIS
-12.0
0.0
X-AXIS
51.2
MAGNETIC FIELD LINE & FLOW
VTH=0.1
(f) Ωt=52
12.0
Z-AXIS
-12.0
0.0
X-AXIS
51.2
MAGNETIC FIELD LINE & FLOW
VTH=0.1
(g) Ωt=60
12.0
Z-AXIS
-12.0
0.0
X-AXIS
51.2
MAGNETIC FIELD LINE & FLOW
VTH=0.1
(h) Ωt=68
12.0
Z-AXIS
-12.0
0.0
X-AXIS
51.2
MAGNETIC FIELD LINE & FLOW
VTH=0.1

Fig. 3

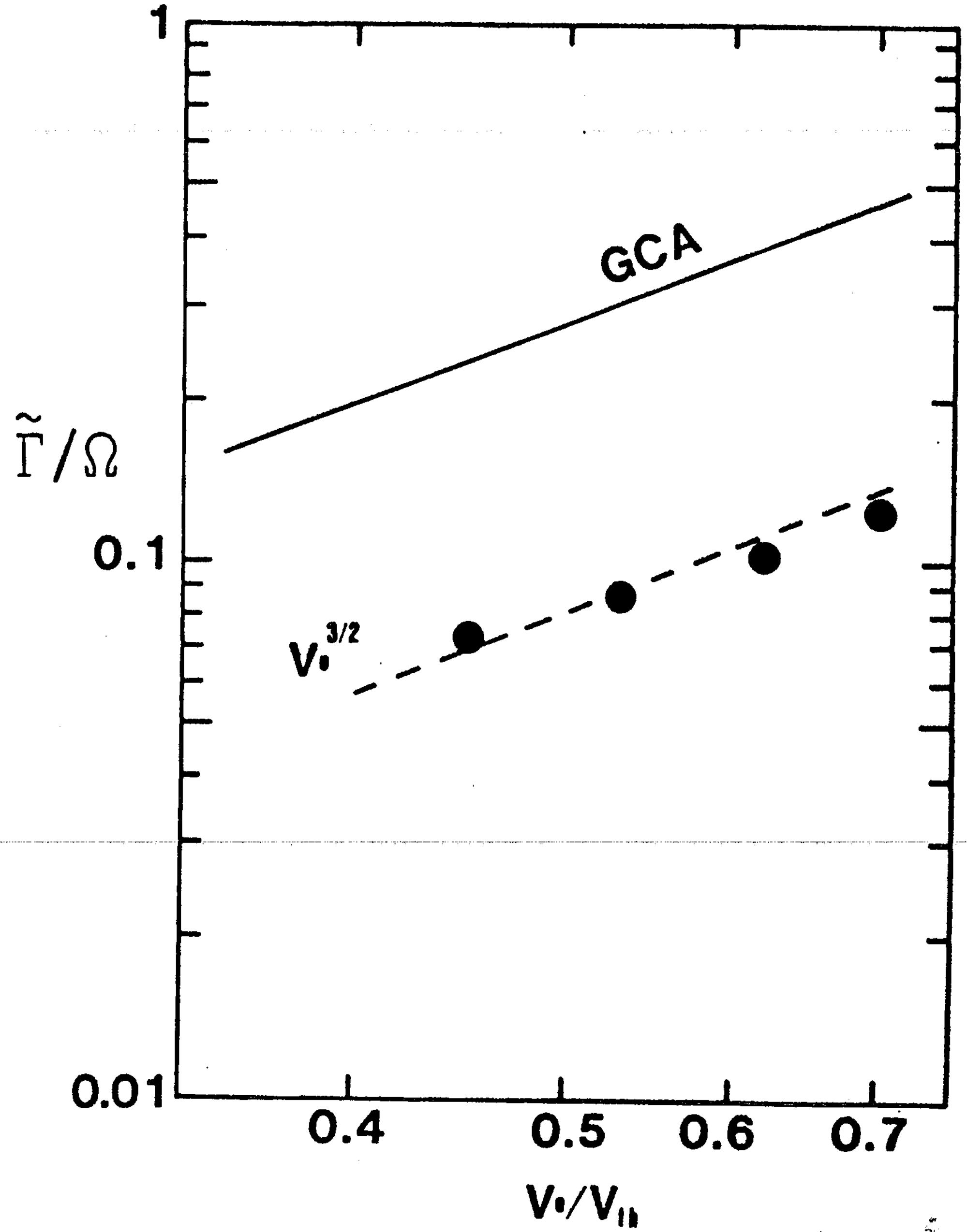

$\gamma \propto b$

$$b(t) = \frac{b(t_0)}{1 - b(t_0)\Gamma(t - t_0)}$$

$$\Gamma_{GCA} \propto \left(V_0/V_{th}\right)^{3/2}$$

Fig. 6

OUR WORK

- PARTICLE SIMULATIONS OF COLLISIONLESS FORCED TEARING, FAST RECONNECTION AND COALESCENCE

  LEBOEUF, TAJIMA, DAWSON, PHYS. FLUIDS 25, 784 (1982); GEOPHYS. MONOGR. 25, 337 (1981).

  TAJIMA, IN FUSION-ENERGY-1981 (INTERNATIONAL CENTER FOR THEORETICAL PHYSICS, TRIESTE, 1982) p. 403.

- VARIOUS MHD (RESISTIVE, COLLISIONAL) SIMULATIONS OF SAME [MENTIONED FOR THE SAKE OF COMPARISON].

  WU, LEBOEUF, TAJIMA, DAWSON, UCLA REPORT PPG # 511, (1980). ([illegible]).

  BRUNEL, TAJIMA, DAWSON, PHYS. REV. LETTS. 49, 323 (1982).

  TAJIMA, BRUNEL, SAKAI, AP. J. 245, L45, (1982). ([illegible]).

  BHATTACHARJEE, BRUNEL, TAJIMA, IFS REPORT # 93 (1983).
  P.F. 26, 3332 (1983)

SIMULATION MODEL

- 2-$\frac{1}{2}$ D ELECTROMAGNETIC FINITE SIZE PARTICLE CODE [TWO SPACE (X AND Y) ; THREE VELOCITIES AND FIELDS (X, Y, AND Z) DIMENSIONS]
- PERIODIC BOUNDARY CONDITIONS
- TYPICAL PARAMETERS

$$L_x \times L_y = 128\Delta \times 32\Delta \quad (\Delta = \lambda_e)$$

$$256\Delta \times 16\Delta \quad (\Delta = 2\lambda_e)$$

$$M_i/m_e = 10$$

$$T_e/T_i = 2$$

SPEED OF LIGHT $c/V_{te} = 5 \quad (\Delta = \lambda_e)$

$c/V_{te} = 6 \quad (\Delta = 2\lambda_e)$

SIMULATION CONFIGURATION

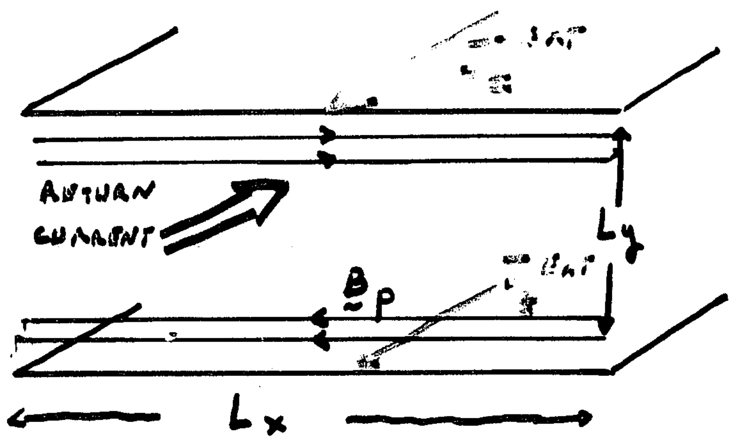

$$J_z^{ext} = J_0 \sin\left(t/t_R\right) \qquad t < t_R \simeq L_y/V_A$$

$$= J_0 \qquad t \gtrsim t_R$$

128 x 32 CASE (POLOIDAL FIELD ONLY)

$\omega_{ce}/\omega_{pe} = 0.77$ $\omega_{ci}/\omega_{pe} = 0.077$

$\rho_e = 1.3\,\lambda_e$ $\rho_i = 2.9\,\lambda_e$

$V_A = 1.22\,V_{te}$ (n_{av}, B_p^{max}) $\beta = 0.2$

$\delta = c/\omega_{pe} = 5\,\lambda_e$

256 x 16 CASE

$\omega_{ce}/\omega_{pe} = 1.17$ $\frac{\omega_{ci}}{\omega_{pe}} = 0.117$

$\rho_e \simeq .85\,\lambda_e$ $\rho_i \simeq 1.9\,\lambda_e$

$V_A = 2.22\,V_{te}$ (n_{av}, B_p^{max}) $\beta = 0.06$

$\delta = c/\omega_{pe} = 6\,\lambda_e$

WE DESCRIBE VERY FEW DEBYE LENGTHS, LARMOR RADII AND COLLISIONLESS SKIN DEPTHS

GENERAL FEATURES OF THE SIMULATIONS

"THICK" PLASMA SHEET IS FORMED

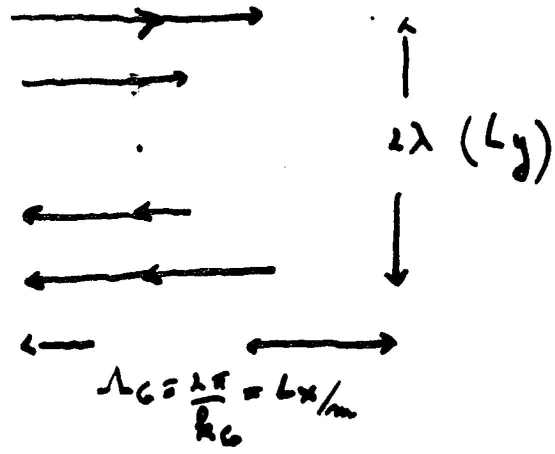

$k\lambda > 1$ STABLE CONFIGURATION

$k\lambda \sim 1$ THRESHOLD

$k\lambda < 1$ UNSTABLE W.R.T. TEARING

MOST UNSTABLE AT SMALL $k_G \lambda$

k_G MAXIMUM GROWTH MODE

ESSENTIALLY
LAVAL PELLAT,
VUILLEMIN, 1966

$\gamma \approx k v_e \left(\rho_e/\lambda\right)^{3/2}$

PERIODIC SHEET STRUCTURE OF DIMENSION

$\Lambda_G, \; 2\lambda$

$\therefore$ NUMBER OF ISLANDS IN OUR CASE $\leq \left(L_x/L_y\right)$

ONCE THE ISLANDS ARE FORMED, THEY ARE UNSTABLE TO COALESCENCE

$\gamma \sim k v_e \left(\rho_e/\lambda\right)^{1/2}$ BISKAMP + SCHINDLER, 1971

PLASMA CURRENT DENSITY
$\beta = 0.2$

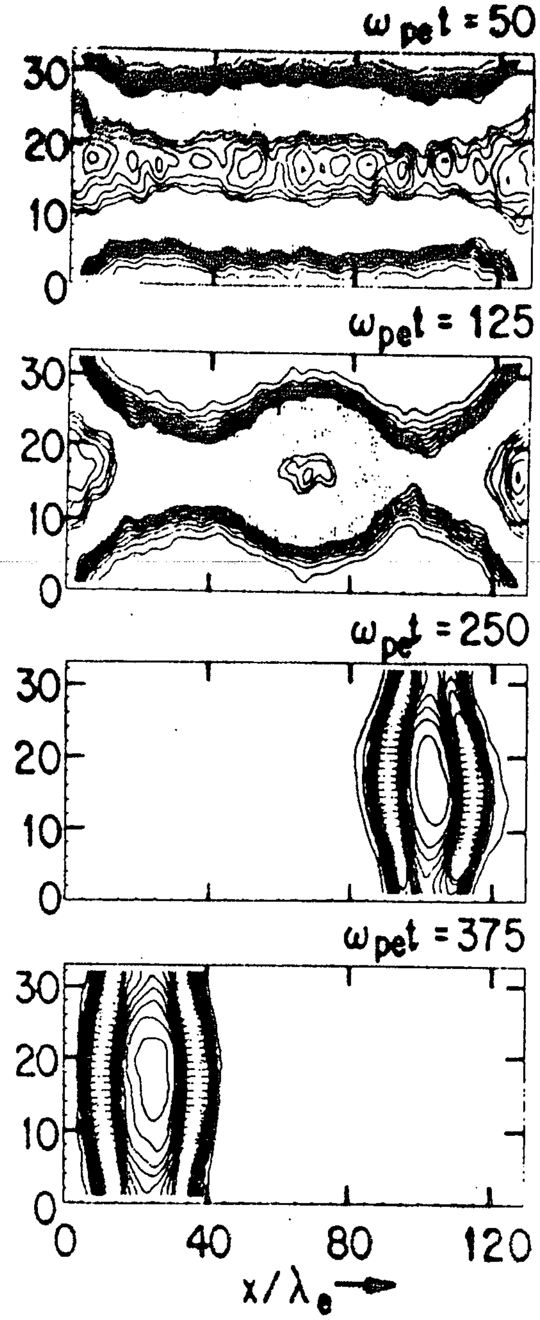

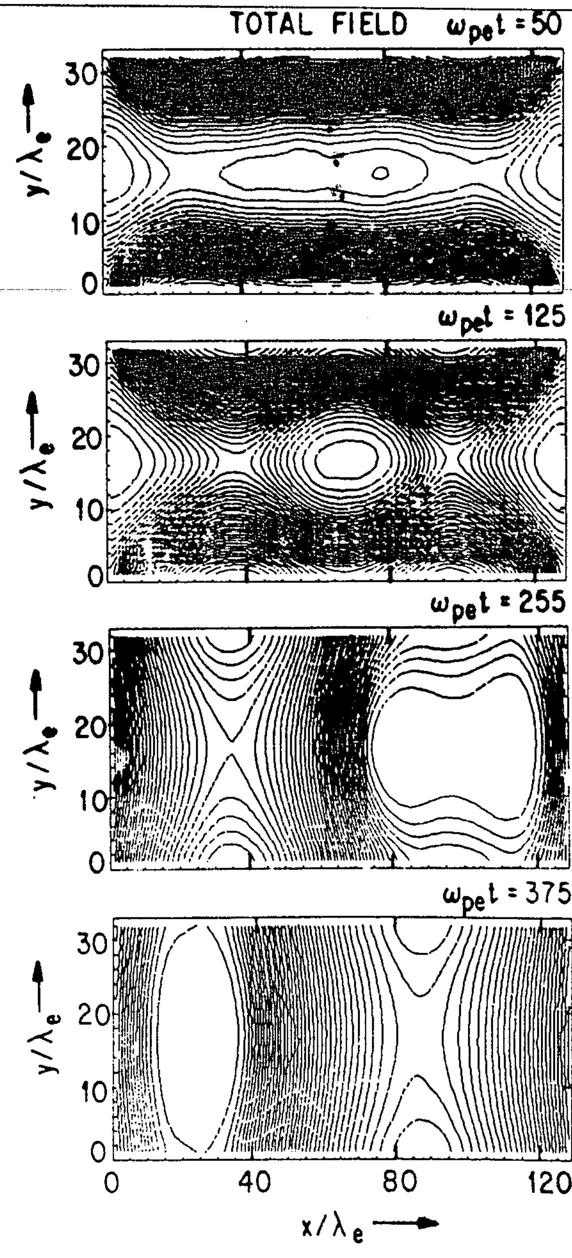
TOTAL FIELD $\omega_{pe}t = 50$
$\omega_{pe}t = 125$
$\omega_{pe}t = 255$
$\omega_{pe}t = 375$
y/λ_e
0
10
20
30
0
40
80
120
x/λ_e

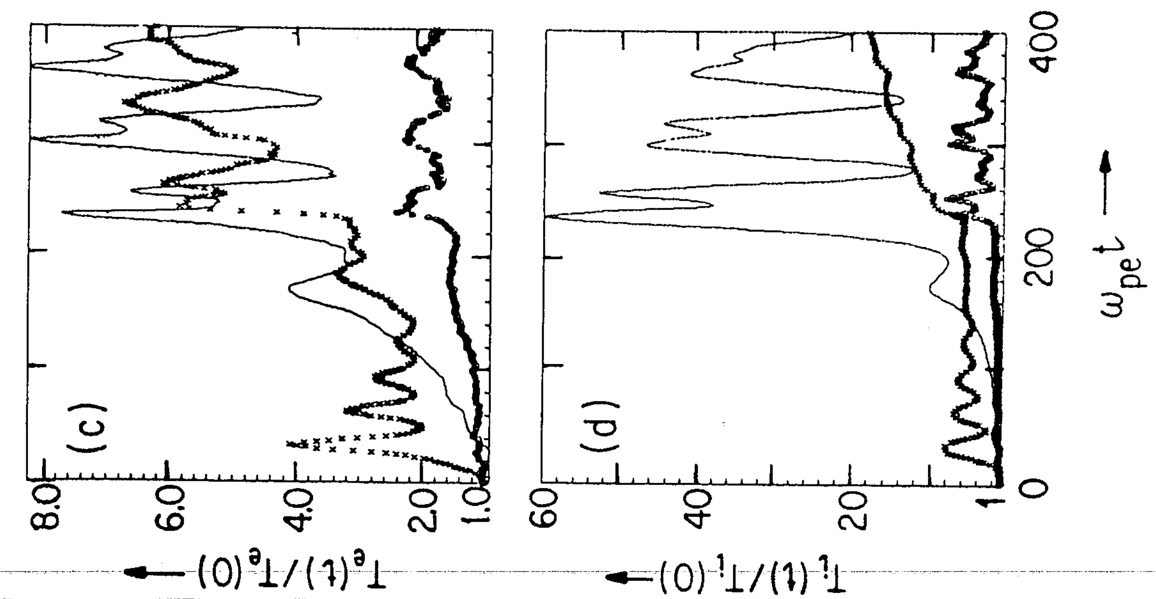
(c)
(d)
$T_e(t)/T_e(0)$
$T_i(t)/T_i(0)$
$\omega_{pe}t$

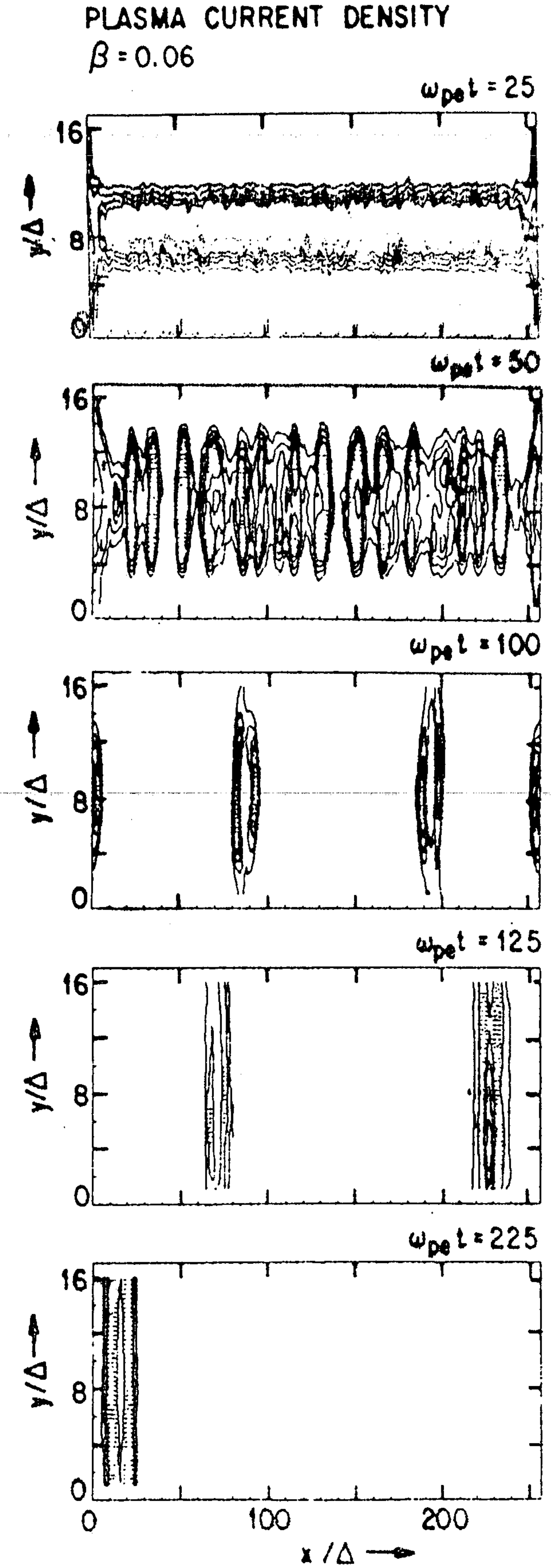
PLASMA CURRENT DENSITY
β = 0.06
ωpe t = 25
ωpe t = 50
ωpe t = 100
ωpe t = 125
ωpe t = 225
y/Δ
16
8
0
100
200
x / Δ

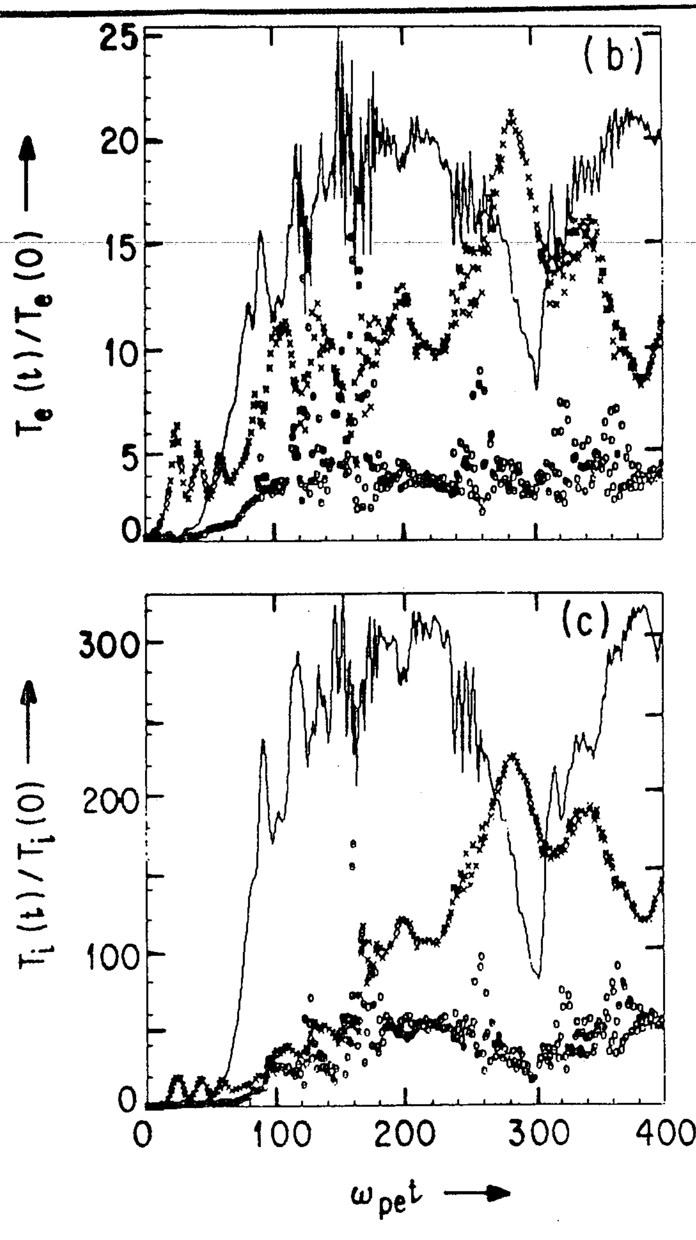
(b)
$T_e(t)/T_e(0)$
25
20
15
10
5
0
(c)
$T_i(t)/T_i(0)$
300
200
100
0
0
100
200
300
400
$\omega_{pe}t$

AN MHD THEORY OF FAST RECONNECTION

(Brunel, Tajima, Dawson, PRL 1982)

Before significant coalescence occurs $(t < t_A)$

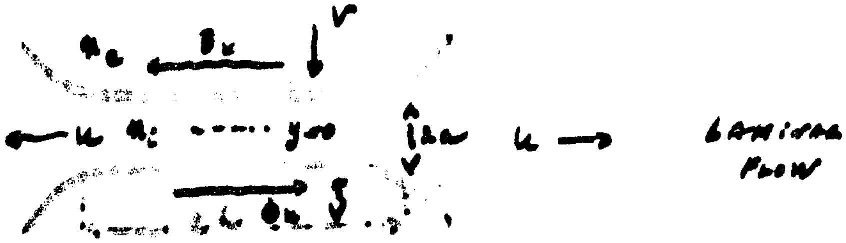

$$\psi_{sp}(t) = \eta^{1/2} B_x(y=a) \left(n_i/n_e\right)^{1/2} \left(v_A/L\right)^{1/2} t$$

After significant coalescence occurs

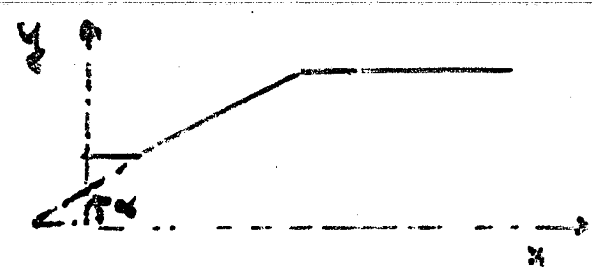

$$\psi(t) = \psi_{sp}(t_A) \left(t/t_A\right)^{n_i/n_e}$$

Compressible plasmas

reconnection induced by pinching $\psi \propto t^{4.5}$

coalescence $\psi \propto t^2$

incompressible plasmas

$\psi \propto t$ or Sweet-Parker all the way

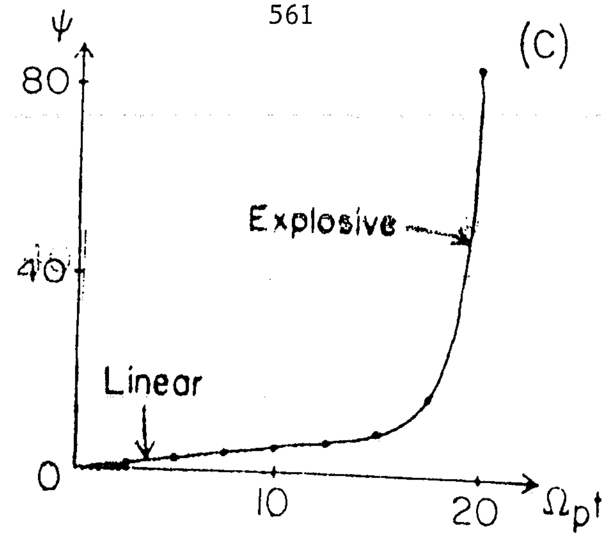

$B_t/B_p = 0.2$

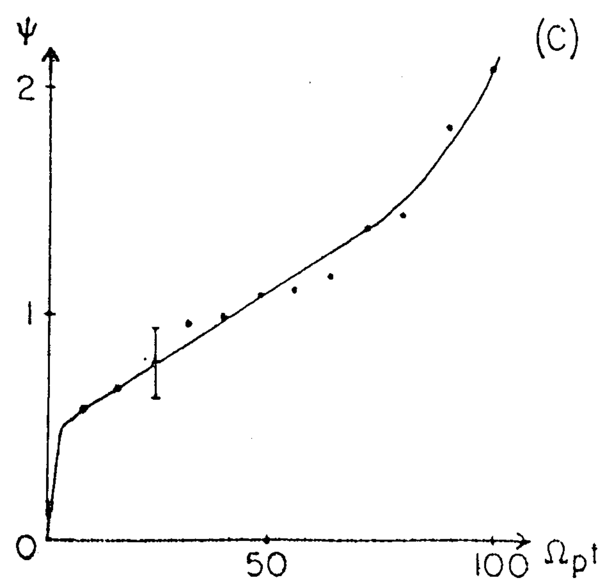

$B_t/B_p = 4$

PRIVATE FLUX VERSUS TIME

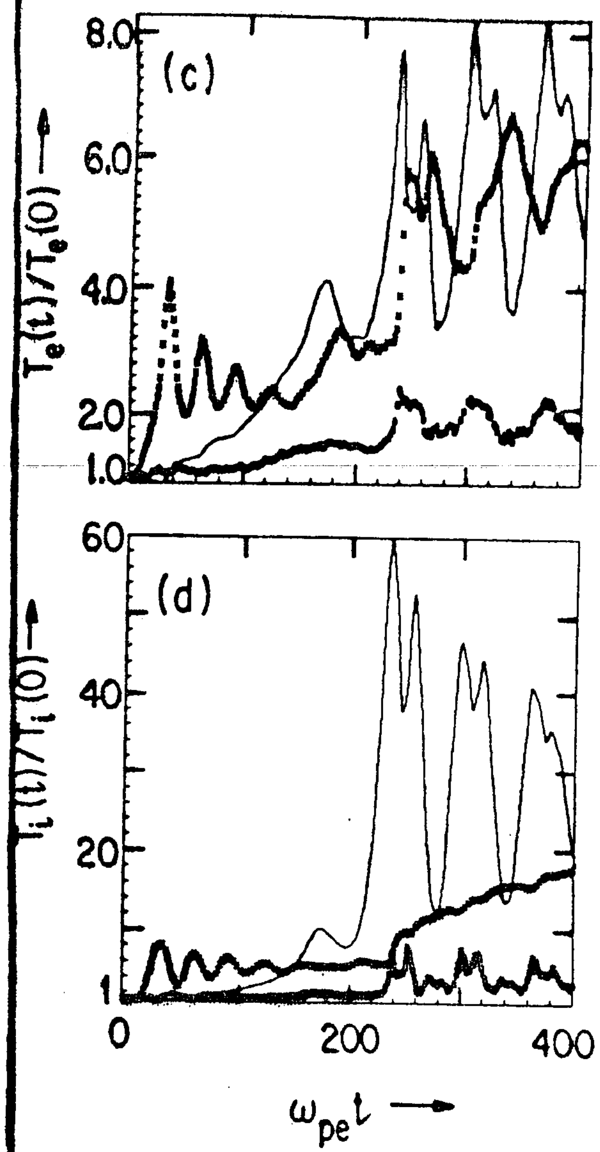

ENERGY THAT CAN BE RELEASED THROUGH ATTRACTION OF THE CURRENT FILAMENTS

$$W_c = -\frac{2I^2}{c^2}\ln\left(\frac{L}{a}\right)$$

$$E_{ion} \approx \frac{1}{6} W_c$$

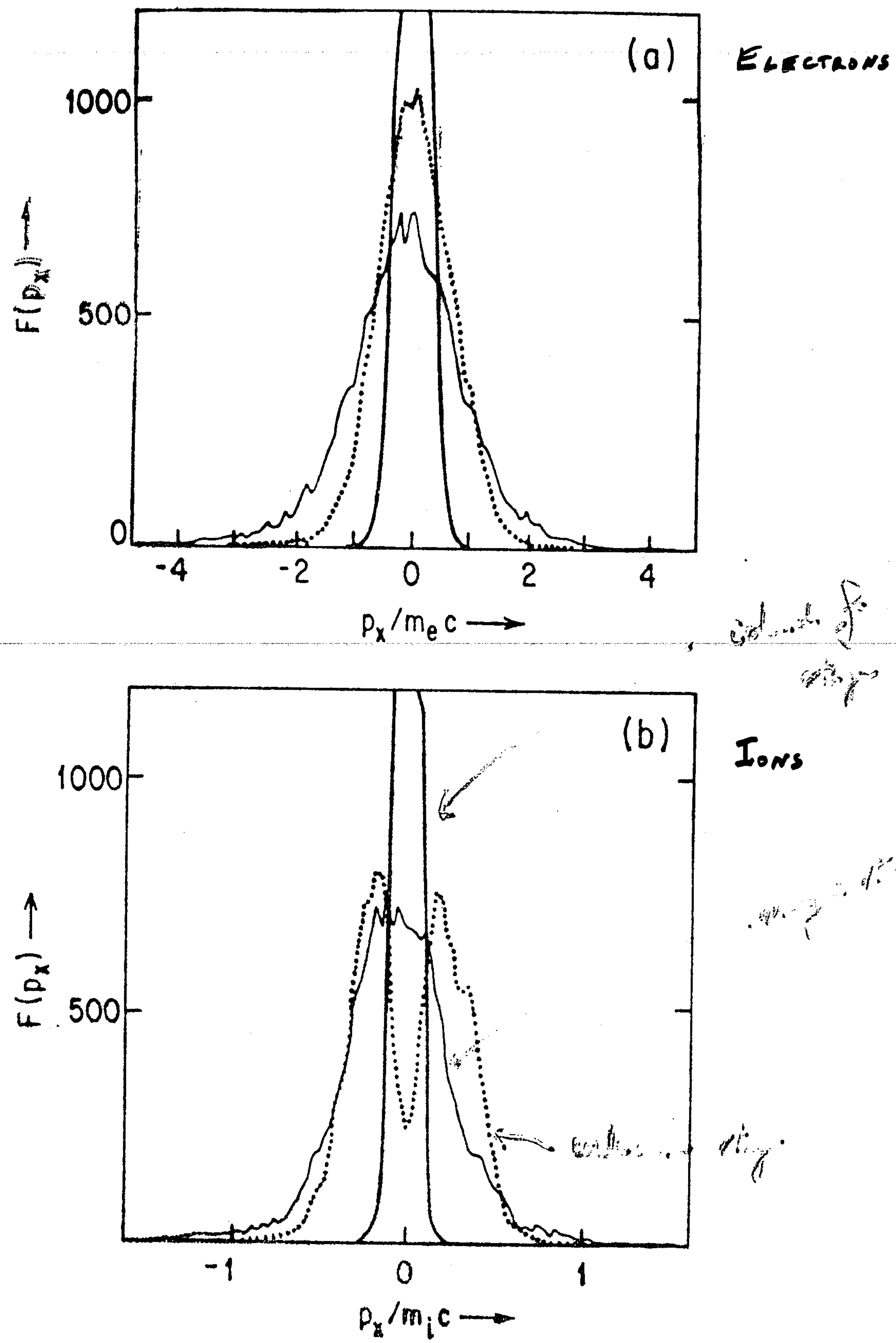
(a)
ELECTRONS
1000
500
0
F(p_x)
-4
-2
0
2
4
p_x/m_e c
(b)
IONS
1000
500
F(p_x)
-1
0
1
p_x/m_i c

564

Tajima, Brunel, Sakai, Ap. J.

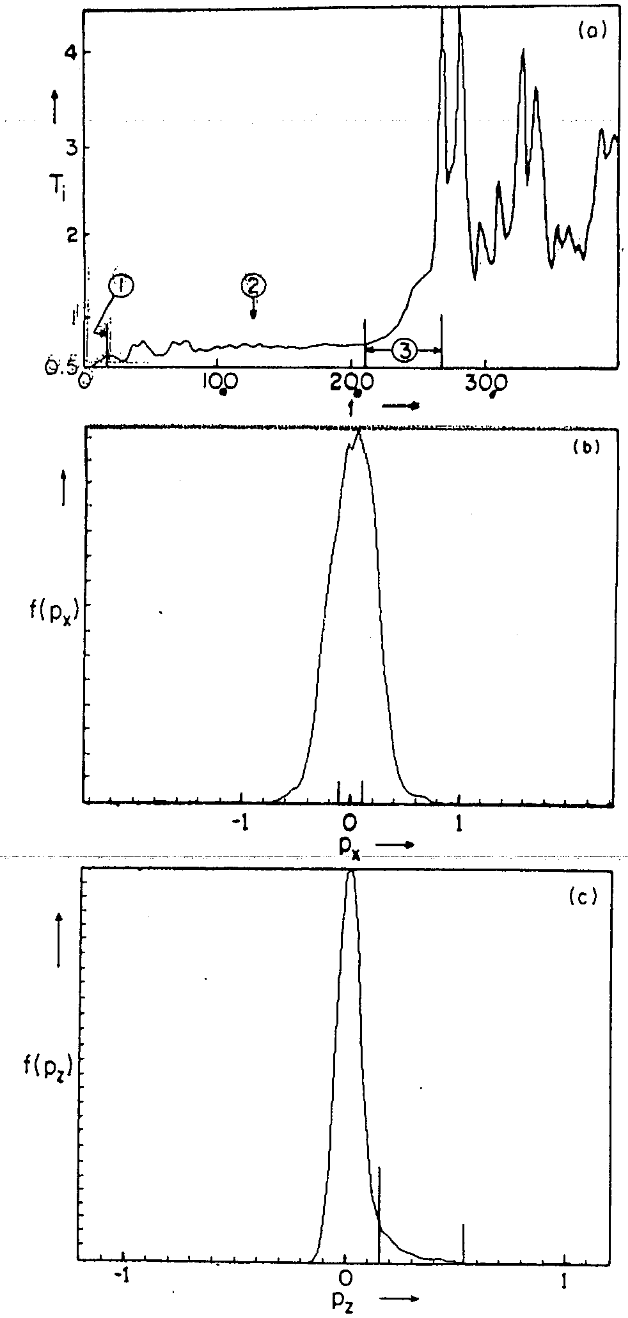

FIG. 2.—Time history of (a) ion temperature during the tearing and coalescence and (b) and (c) of ion distribution functions after coalescence. Data taken from a run on EM code with system size $L_x \times L_y = 128\Delta \times 32\Delta$ (Δ: grid size), $B_t = 0.2\,B_p$, $v_A \approx v_e$ (electron thermal velocity), $T_i/T_e = 0.5$ (at $t = 0$), mass ratio $m/M = 1/10$, particle size $a = \Delta$. (a) Up to $t = 2\Omega_{ci}^{-1}$ (about $0.5\,t_A$), tearing grows and then saturates. From $t = 22\Omega_{ci}^{-1}$ to $t = 26.5\Omega_{ci}^{-1}$ (in about $2t_A$), the coalescence explosively happens and completes. The period of temperature oscillations is $\sim 2t_A$. (b) Ion momentum (p_x) distribution function at $t = 36\Omega_{ci}^{-1}$. (c) Toroidal ion momentum (p_z) distribution function at $t = 36\Omega_{ci}^{-1}$. The thermal momenta are indicated by tick marks near $p = 0$. Momenta are normalized by Mc and $\Omega_{ci} = eB/Mc$.

in one to two Alfvén times. Significantly, there appear to be amplitude oscillations in the temperature, whose frequency matches $\omega \approx k_\perp v_{A\perp}$, where $k_\perp = 2\pi/a$. This temperature oscillation behavior can be attributed to the overshooting of coalescing and colliding two-current blobs. Once two-current blobs coalesce, they are bound by the common magnetic flux, and the coalesced larger island vibrates, "breezing" more oblate and less in turn. Within the coalesced island, the two colliding plasma blobs cause turbulent flows, and the originally directed flow energy quickly dissipates into heat, thereby reducing the amplitude of the temperature oscillations (Fig. 2a).

As a result of this process, the momentum distribution of plasma ions in the poloidal direction shown in Figure 2b exhibits intense bulk heating (including adiabatic heating). The temperature in this direction was increased in our simulation by a factor of 60. The momentum distribution of ions in the toroidal direction (Fig. 2c) shows three regimes, the first being the bulk, the second being the exponential section $f_2(p_x) = \exp(-p_z/p_0)$, and the third being flat distribution up to the relativistic factor $\gamma \sim 2$ in the relativistic region, where $p_0^2/2M \approx 10 \times$ (bulk temperature). The heating in the poloidal direction is due to the intense process of the adiabatic heating and turbulent dissipation as a result of colliding plasma blobs. The heating in the toroidal direction is due to heating and acceleration by the inductive toroidal electric field induced by the annihilated poloidal magnetic flux as a result of coalescence.

III. EXPLANATION OF OBSERVATION

The flare loop slowly expands after it emerges from the photosphere as the toroidal field curvature of the loop makes the centrifugal motion. In time, the toroidal current J_t builds up, increasing the poloidal magnetic field B_p. As the poloidal field B_p reaches the critical value that is of the order of magnitude B_t, the adjacent flare current loop can now coalesce rapidly facilitated by the fast reconnection process governed by equation (1), the faster second phase. Such a fast coalescence of flare current loops proceeds explosively once in its nonlinear regime in a matter of one to two Alfvén times, releasing more than one-tenth of the poloidal magnetic energy into (ion) kinetic energy. Since the flare loop magnetic field (100 gauss) with current rod size ($a = 10^8$ cm) is $W_c \sim 0.5 \times 10^{20} \ln(L/a) \sim 1.5 \times 10^{20}$ ergs cm^{-1} and the energy available in length $d \sim L(\sim 10^9$ cm) is $E = 1.5 \times 10^{29}$ ergs for $a = 10^8$, $d = L = 10^9$ and $E = 1.5 \times 10^{31}$ ergs for $a = 10^9$, $d = L = 10^{10}$. Released ion energy, therefore, is $E_{\rm ion} \sim \frac{1}{6}E$ and is in between 2×10^{28} ergs and 2×10^{30} ergs due to the coalescence. This amount of energy is in the neighborhood of the solar flare energy (Sturrock 1980).

$B_{0x} = 0$

$B_{0y} = \tanh x$

$B_{0z} = (1 - B_{0y}^2)^{1/2}$

$\rho = 1$; $\beta = 1$

$\eta = $ const.

$\tilde{\varphi}_0(L/2) \gg \tilde{\varphi}_0(L)$

$\gamma_L > \gamma_{L/2}$

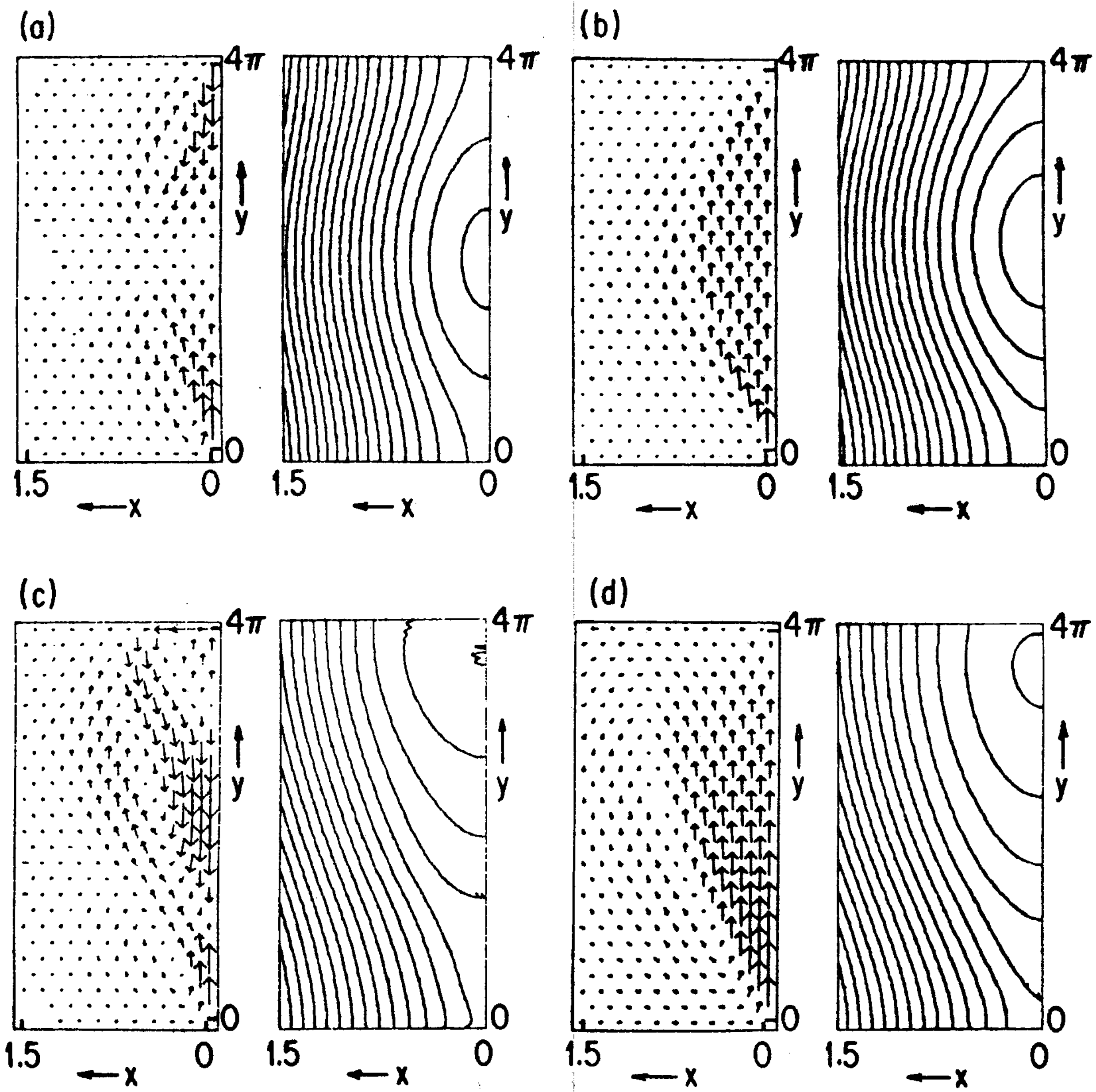

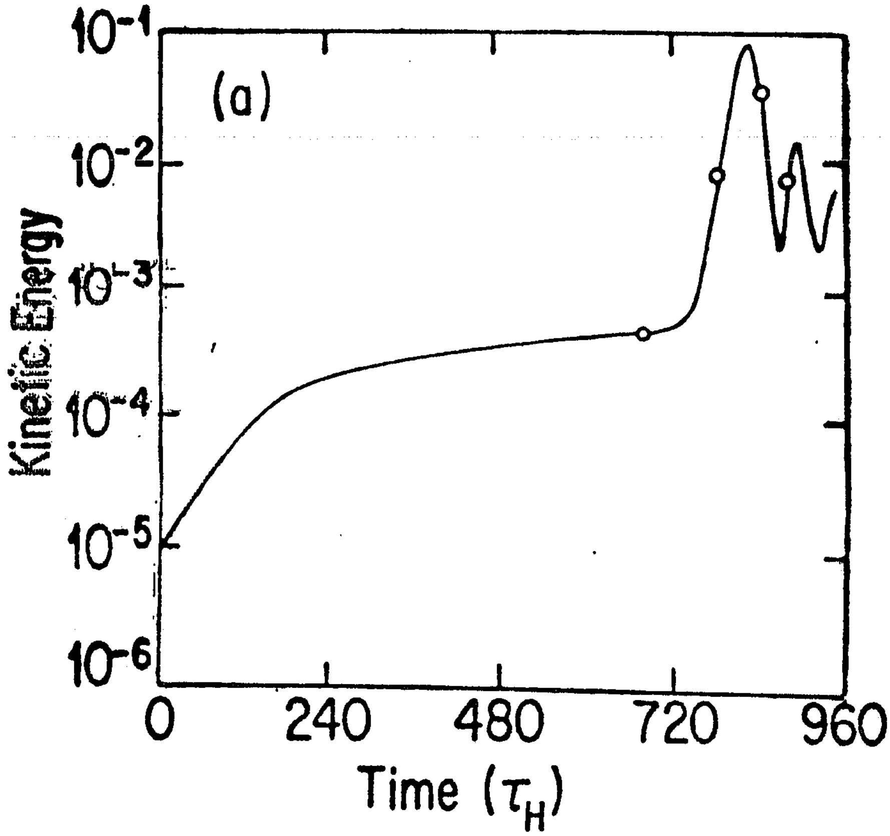

MHD
SIMULATION

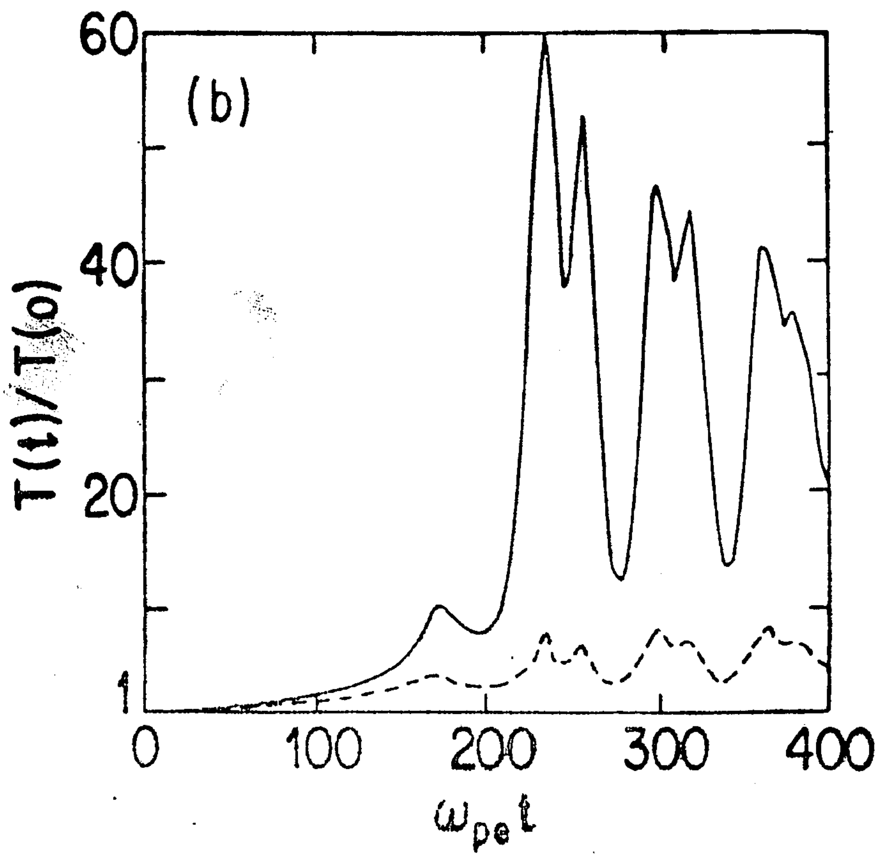

128×32
$B_t = 0.$
PARTICLE
SIMULATION

1980 June 7 Event

The impulsive burst at 0312 UT on 1980 June 7 is one of the most outstanding events which occurred during the SMY period. The burst is composed of seven successive pulses of a quasiperiodicity of ~8 s each of which was observed almost simultaneously in hard X-rays, γ-ray lines, and microwaves[1,2,3,4,5]. From the comparison of the time profiles between hard X-ray and γ-ray emissions recorded with the SMM/GRS, Chupp[3] have reported that the time of peak intensity of the prompt γ-ray line emission (4.1-6.4 MeV; due to de-excitation of excited ions like ^{12}C and ^{16}O) lags the corresponding time of the hard X-ray emission (40-140 keV and 305-355 keV) by ∿2 s.

The burst was observed also with the 17-GHz polarimeter and interferometer at Nobeyama[6]. It also shows seven successive pulses. However, each of the microwave pulses is composed of at least two

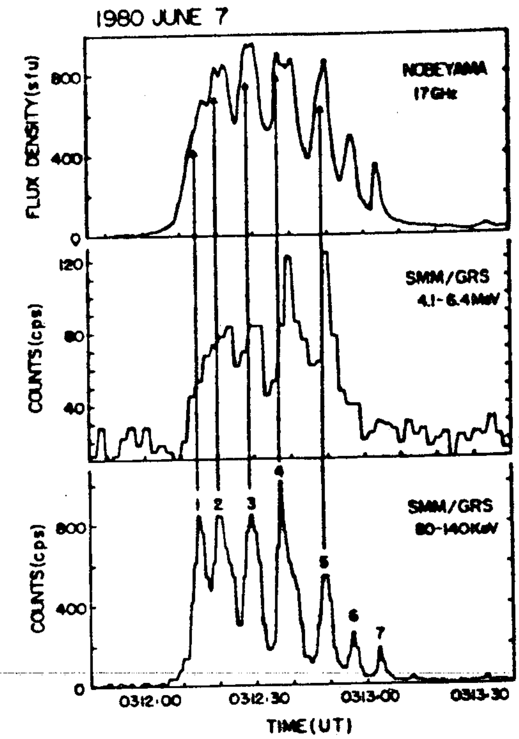

Fig. 1. Time profiles of hard X-ray (80 -140 keV), prompt γ-ray line (4.1-6.4 Mev) and microwave (17 GHz) for the 1980 June 7 event. Both the hard X-ray and prompt γ-ray line emissions were observed with the SMM Gamma-Ray Spectrometer with 1 and 2 sec resolution, respectively. The microwave emission was observed with the 17-GHz polarimeter at Nobeyama at the sampling rate of 0.2 sec (e-floding time constant of 0.3 sec).

REF: Relative Timing of Microwave, X-Ray and γ-ray emissions in the Impulsive Solar Flares on 1980 June 7 and 1980 June 21. Nakajima et. al. Hinotori Symposium on Solar Flares, ISAS, Tokyo, Japan, Jan 27-29, 1982 p. 273.

CHARACTERISTICS OF COALESCENCE PROCESS

CHARACTERISTICS OF SOME FLARES

$B_t > B_p$ NO COALESCENCE

$B_t < B_p$ COALESCENCE

IMPULSIVE NATURE OF FLARES: SWITCH FROM $B_t > B_p$ TO $B_t < B_p$ AS CURRENT BUILDS UP IN THE LOOPS

COALESCENCE HAPPENS WITHIN 1-2 ALFVEN TIMES

FOR FLARE LOOP B-FIELD OF ~ 100 G, TIME SCALE OF IMPULSIVE PHASE $\sim$ 1 SEC OR 1 ALFVEN TIME

ENERGY AVAILABLE

$$W_c = -2I^2/c^2 \ln\left(\frac{L}{a}\right)$$

$a = 10^8$, $L = 10^9$ cm; $W_c \cdot L = 1.5 \times 10^{29}$ erg

$a = 10^9$, $L = 10^{10}$ cm; $W_c \cdot L = 1.5 \times 10^{31}$ erg

$$E_{in} \sim \left(\frac{1}{6} - \frac{1}{10}\right) W_c$$

ENERGY OF FLARE: $2 \times 10^{28} - 2 \times 10^{30}$ erg

SHARP INCREASE IN TEMPERATURE UPON COALESCENCE

TEMPERATURE OSCILLATIONS WITH $\omega \sim k V_A$

TEMPERATURE OSCILLATIONS $\equiv$ SOLAR γ-RAY AMPLITUDE OSCILLATIONS WITH PERIOD $\sim$ 1 ALFVEN TIME

EXPLOSIVE COALESCENCE

T. TAJIMA

INSTITUTE FOR FUSION STUDIES

Explosive Coalescence

T. Tajima
I.F.S.

Magnetic Collapse

Collaborators

J.-I. Sakai

W. Horton
A. Bhattacharjee
F. Brunel

acknowledgments

P. Diamond, J.N. Leboeuf, S.D. Kim,
E. Montalvo, E. Zaidman, A. Aydemir,
J. Todoroki, M. Rosenbluth, J. Dawson,
F. Coroniti

1. Introduction

2. Simulation Results and Indeces of Explosion

3. Dependence of Reconnection Rate on Current Peakedness

4. Self-similarity of Magnetic Collapse and Indeces of Explosion

5. Heuristic Theory of Explosive Coalescence

6. Theory Model and Solution by Stretch Factors

7. Explosive solutions

8. Oscillatory structure (single, double, triple peaked amplitude osc.) and Sagdeev Potential

9. Comments on Sawtooth/Precursor and Relation to Major Disrupti

sunspot

flare loops

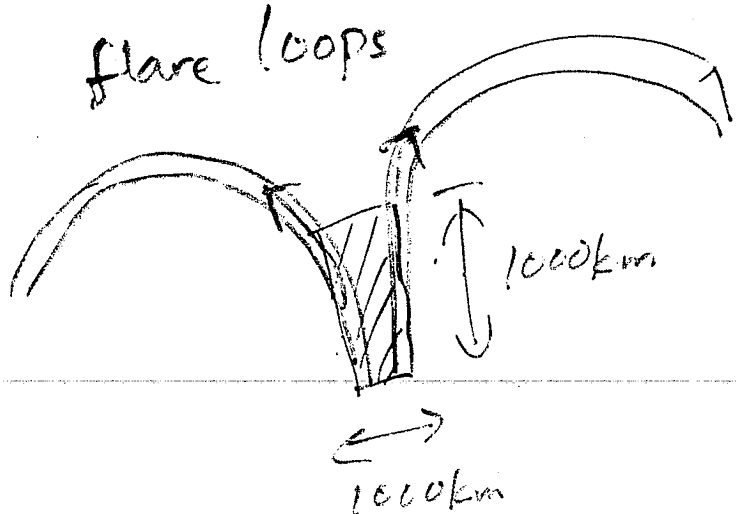

coalescence

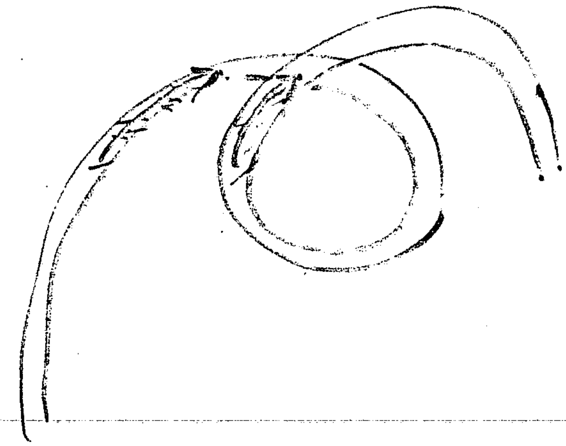

global kink instability

phenomena

- suddenness of impulsive phase of flare
- amount of energy (up to 10^{31} erg) in ~10 sec (~1 Alfven time), number of particles (~10^{34-36}), 40 ~ 300 keV hard X-ray energy
- realignment of quadrupole structure
- post flare phase (quiet soft X rays)
- amplitude oscillations and double hump.

doublet, spheromac
etc.

Coalescence

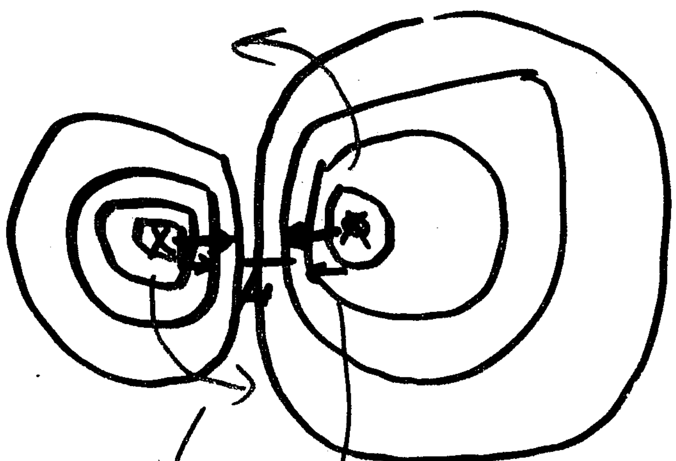

$F \times B_t$ (ideal MHD process)

resistive process
or reconnection process

tokamak internal disruption
etc.

Anti-Coalescence
(or Expulsion
or Half-Coalescence)

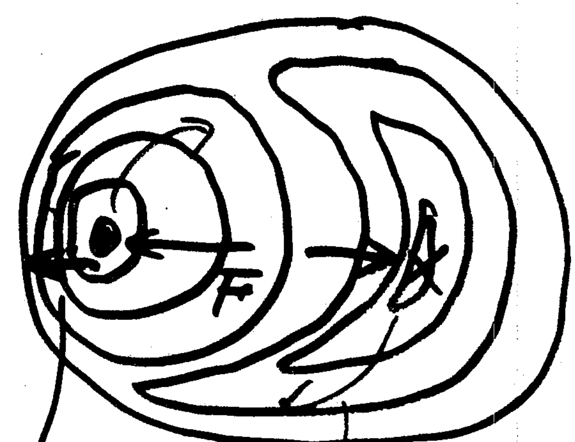

$F \times B_t$ (ideal MHD process)

reconnection process

$\Omega_{et} = 0.2$ (weak rotation)

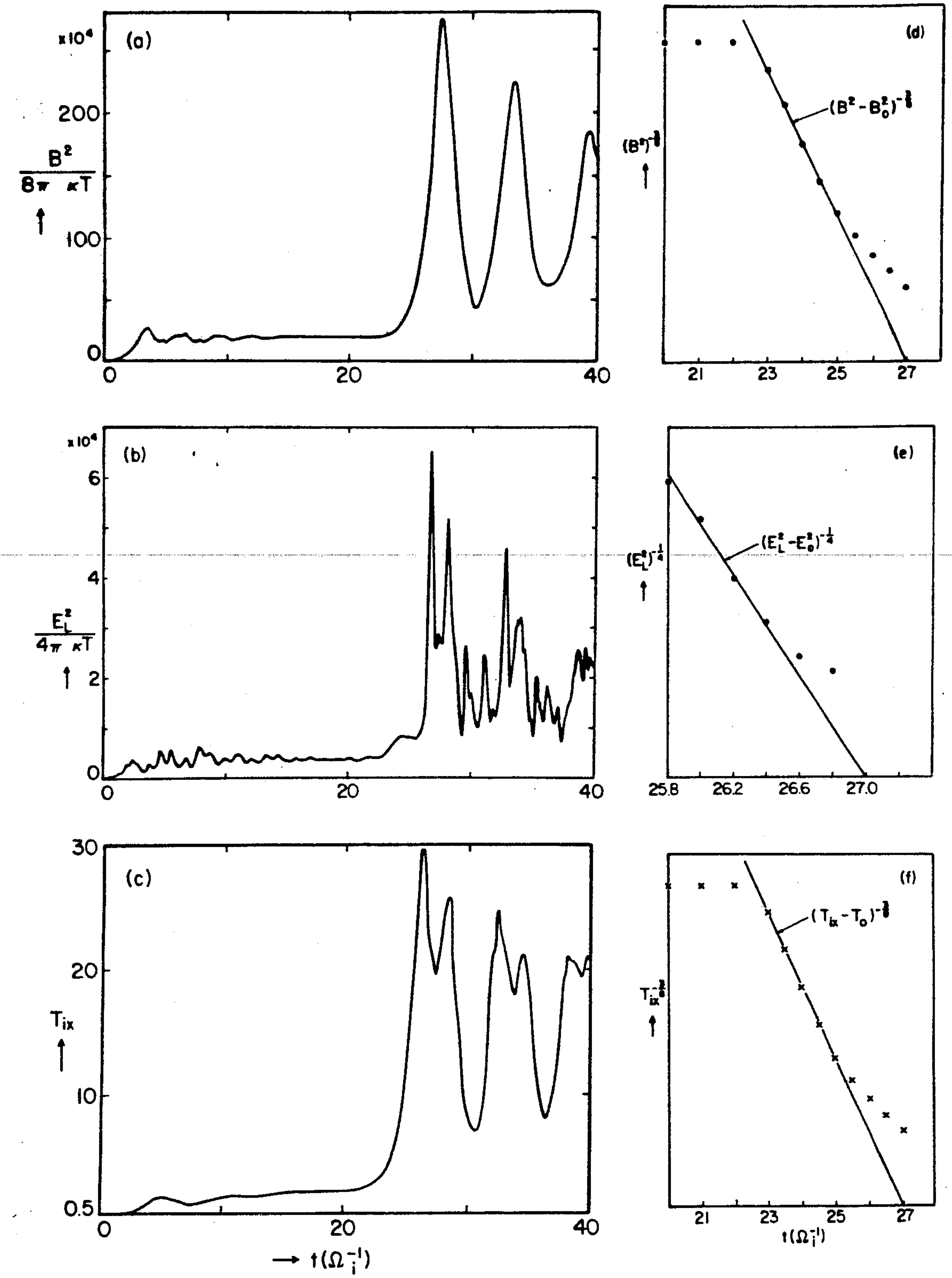

Hot tail distribution during explosive coalescence

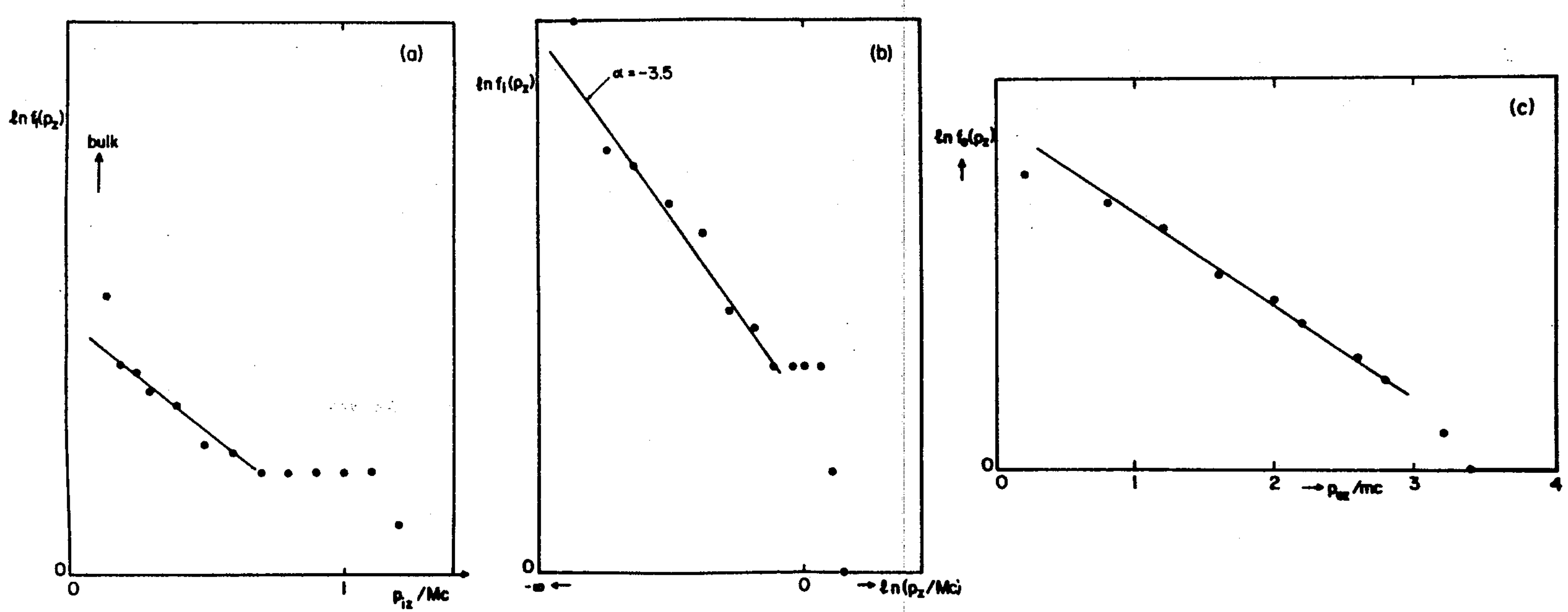

Indeces of Explosion [exponents to the $1/(t_o-t)$] During Coalescence

	$\Omega_{et}=0$ $L_x \times L_y=128\times32$ [NB: $L_x \times L_y=256\times32$ many islands]	$\Omega_{et}=0.2\omega_{pe}$ $L_x \times L_y=128\times32$	$\Omega_{et}=1.0$ $L_x \times L_y=128\times32$	$\Omega_{et}=2.0$ $L_x \times L_y=128\times32$ No formation of islands
simulations →	Leboeuf et al.	Tajima &	Sakai	Tajima
Magnetic Energy S B^2 T	8/3 8/3	8/3 8/3	2 2*	 N/A
Electrostatic Energy S E_L^2 T	4 4	4 4	 4	 N/A
Ion Temperature in x-direction S T_{ix} T	8/3 8/3	8/3 8/3	3 2	 N/A
Explosive Time S t_o	$24.3\Omega_i^{-1}$	$27\Omega_i^{-1}$	$19\Omega_i^{-1}$	N/A
Compressional Alfvén Oscillation S Period τ_{os}	$6.3\Omega_i^{-1}$	$6.0\Omega_i^{-1}$	$8.8\Omega_i^{-1}$	N/A

* incompressibility is assumed. Derivation from observation might be due to plasma rotation in $\Omega_{et}=1$ case.

S: simulations T: theory.

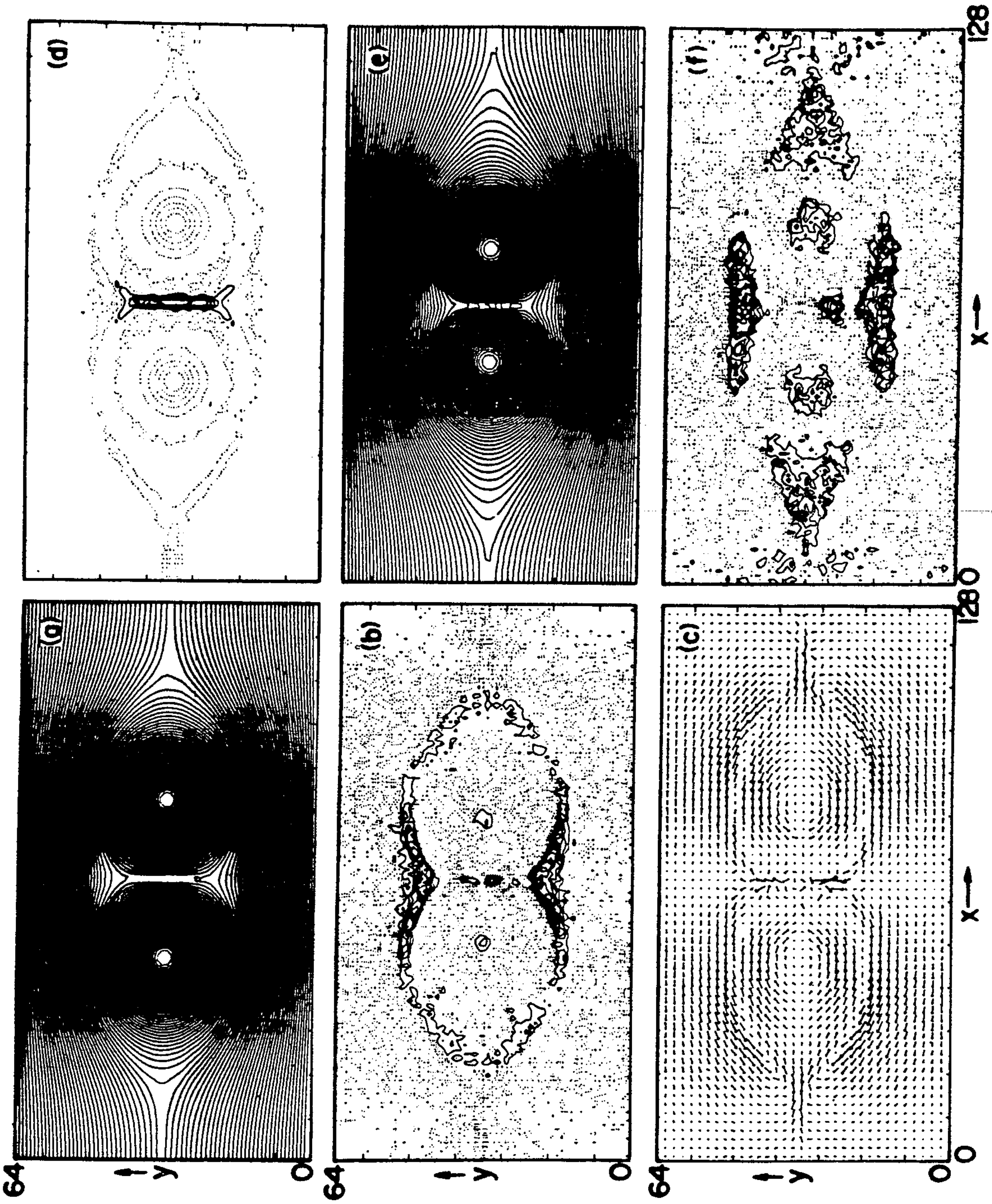

$\epsilon = 0.85$

$\epsilon = 0.85$

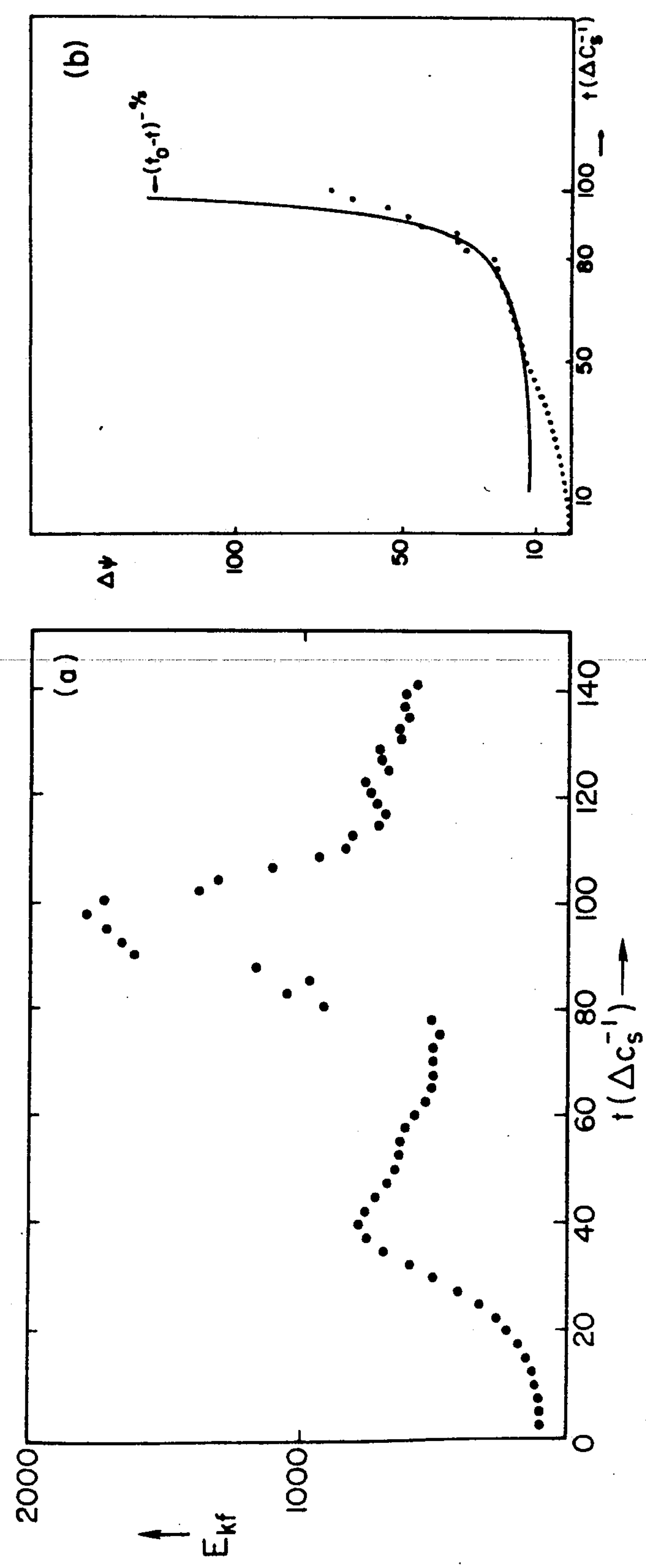
(a)
(b)
E_{kf}
2000
1000
0
20
40
60
80
100
120
140
$t\,(\Delta c_s^{-1})$
$\Delta\psi$
100
50
10
10
50
80
100
$t\,(\Delta c_s^{-1})$
$-(t_0-t)^{-2/3}$

$\epsilon = 0.7$

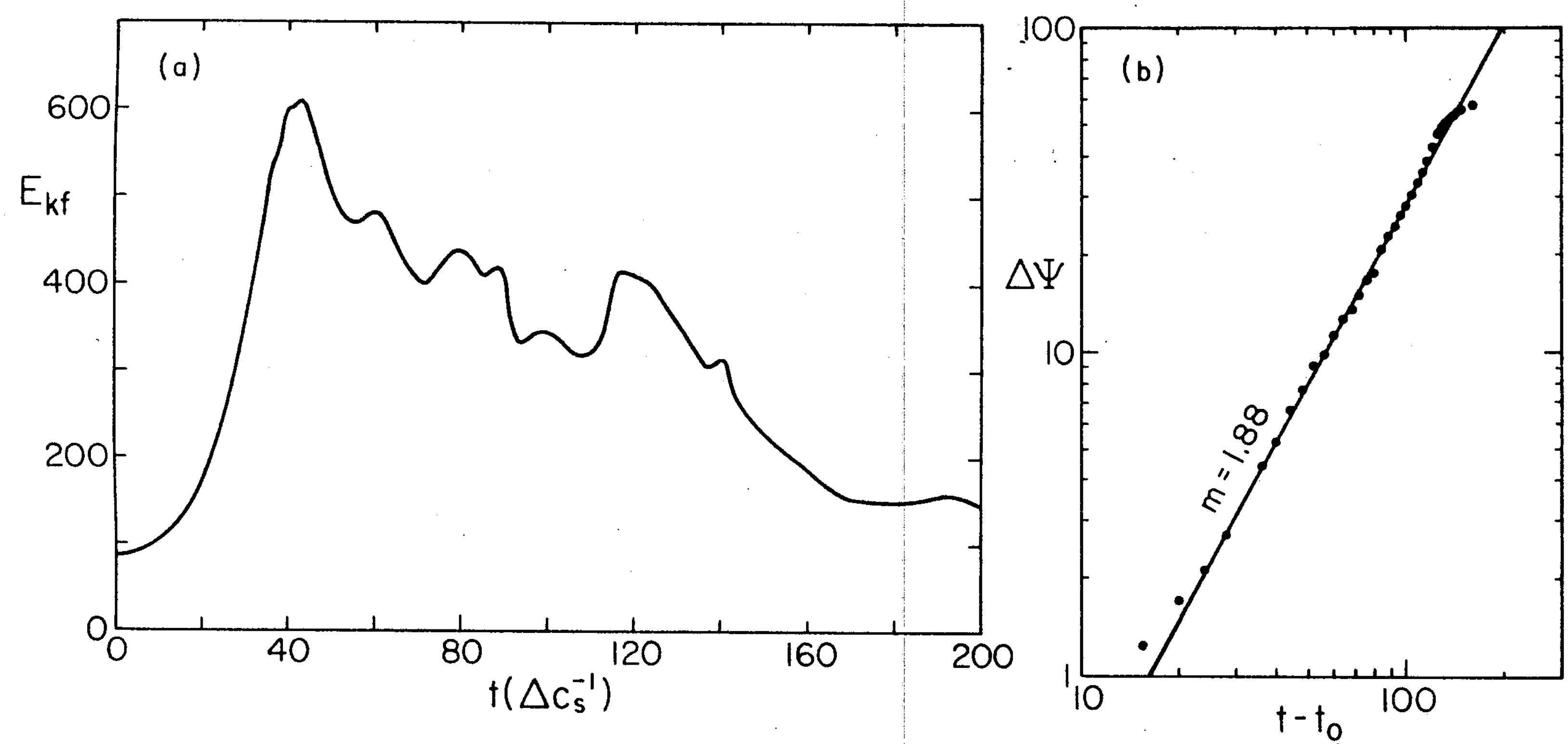
(a)
600
400
200
0
E_{kf}
0
40
80
120
160
200
$t(\Delta c_s^{-1})$
(b)
100
10
1
$\Delta\Psi$
m = 1.88
10
100
$t - t_0$

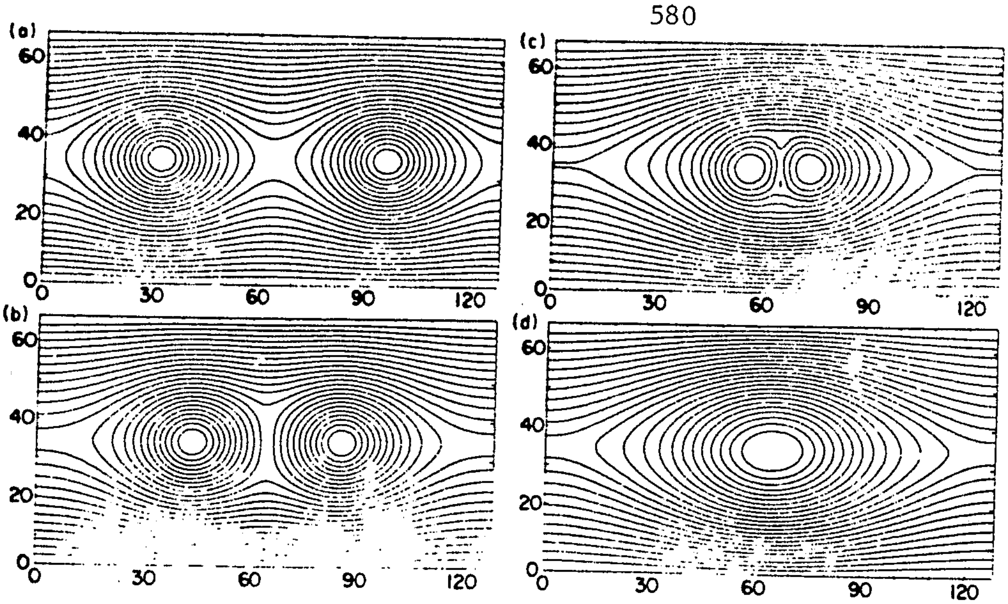

FIG. 1. Typical sequence of frames following the time evolution of the poloidal flux function Ψ. Here (a) displays the initial, and (d) the final configuration.

$\epsilon = 0.3$

study of magnetic reconnection driven by instabilities. The third stage appears when the instability begins to saturate, and the rate of destruction of flux levels off. The demarcation between these three stages is not always sharp, and is sensitively dependent on the Reynolds number.

In Fig. 1, we show a typical sequence of frames following the time evolution of the poloidal flux function Ψ, and in Fig. 2, a typical flow field in the x-y plane.

We now discuss our numerical results on the dynamics of the coalescence instability evolving from equilibria for which $\epsilon = 0.3$ (also studied in Refs. 3 and 8 for incompressible plasmas) and $\epsilon = 0.7$. In what follows, when we refer to the scaling with time of the rate of reconnection, it should be interpreted as the rate of destruction of magnetic flux in the "second stage" of the evolution of the instability.

A. $\epsilon = 0.3$

In Fig. 3 we compare the rates of reconnection as we vary the magnetic Reynolds number for a given number of the subclass of equilibria given by Eq. (9) with $B_{0x} = 3.5$, $B_{0z} = 0$, and $\epsilon = 0.3$. For all values of the Reynolds number ($s = 5\times 10^2$–2×10^3), the destruction of flux proceeds linearly with time. The reconnection process does exhibit self-similar characteristics as the Reynolds number varies, in qualitative agreement with the results of Biskamp and Welter.[8] As mentioned earlier, the separation in time of the three stages of evolution of the coalescence process is less sharp for larger than for smaller values of the resistivity. The explanation for this observation is that for larger values of resistivity, the destruction of flux is effective even in the first stage of the instability and blurs the separation between the first and the second stages.

We have computed the destruction of flux for a member of the second subclass of equilibria, with zero toroidal field, given by Eqs. (9) with $B_{0x} = 3.5$ and $B_z = 0$. Again, as shown in Fig. 4, the destruction of flux proceeds approximately linearly in time. It is seen thus, that for $\epsilon = 0.3$, the rate of reconnection is insensitive to the magnitude of the toroidal field, and the effect of plasma compressibility is negligible. We remark parenthetically that our numerical results for this case with zero toroidal fields are qualitatively different

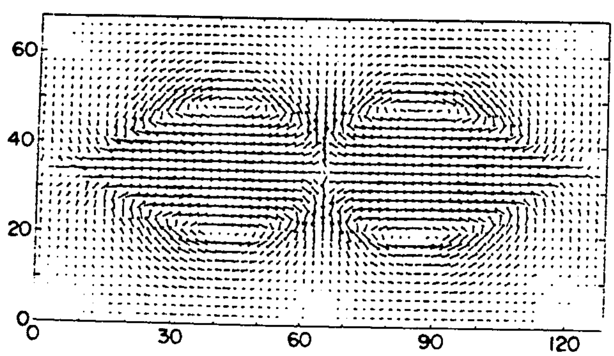

FIG. 2. Plasma flow field in the x-y plane at some instant of time during the evolution of the coalescence instability.

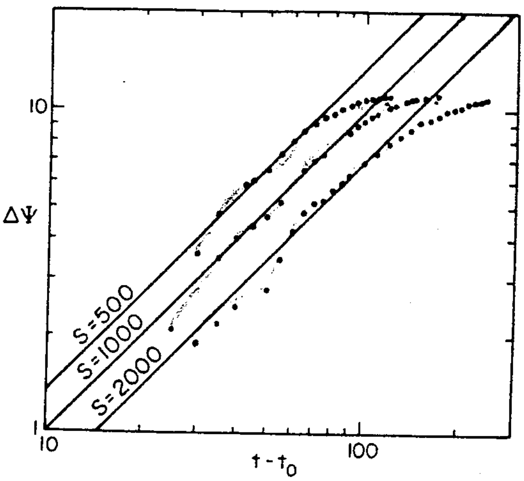

$\epsilon = 0.3$

FIG. 3. Poloidal-flux-destroyed ($\Delta\Psi$) as a function of time (t) for different values of the Reynolds number. The initial configuration is force-free, with $\epsilon = 0.3$, $B_{0x} = 3.5$, and $B_{0z} = 0$.

Reconnection Experiment.

$\Delta\psi \sim t^{\alpha}$

its plasma density goes up to ρ_i, the characteristic density of the internal region. At some distance along the z axis greater than L this flux tube is located outside the diffuse internal region. There, the magnetic field is B and the density is ρ_e. The angle α is $\alpha = B_r/B$, where B_r is the average radial magnetic field in the diffusion layer. This field is given by $B_r = \psi/2\pi RL_t$ where ψ is the total reconnected flux and L_t is the length along z traveled by the ψ flux lines. Setting $L_t = L + vt$ we obtain (Brunel, et al. 1982)

$$L = vt\psi_c/(\psi-\psi_c) \quad , \qquad (4)$$

where ψ_c is $2\pi RaB$. Brunel et al. assume that the fast phase of reconnection sets in when the diffusive length is shortened by the angularity of the lines such that axial convection on perpendicular lines matches radial convention into the diffusive layer. Equating (4) and (3) gives for the reconnected flux:

$$\psi = \psi_o\,(t/t_o)^{\rho_i/\rho_e} + \psi_c \quad , \qquad (5)$$

where $\psi(t_o) = \psi_o$.

Qualitative agreement with this model can be seen in Fig. 6 which shows an abrupt change in slope of reversed trapped flux for each of the two phases. The reconnected flux $\psi_1-\psi_{tr}$ is plotted versus $t-t_o$ for 7 mTorr in Fig. 7. Here $\psi_1 = 22.5 \pm 1.5$ kMx corresponds to the average value of the trapped flux during the plateau phase and ψ_{tr} is the trapped flux (from the axis to the x-circle). Density measurements were not possible in the region between FRC cells because of interference by the mirror coils. Thus the ratio ρ_i/ρ_e in Eq. (5) could not be determined experimentally. However the value of the exponent for the fast phase in Fig. 7 is 4 ± 1, indicating $\rho_i > \rho_e$. This would be expected since ρ_e represents plasma on open field lines and ρ_i that of the originally confined region. The most important feature of the model is that it predicts the onset of a second, fast phase of reconnection in the region of the x-circle, a result which is obtained experimentally.

The merging velocity w of the field lines was obtained experimentally from data similar to those of Figs. 2 and 3 which give the motion of the separatrix radius r_s during the fast phase. The velocity directly obtained from the motion of the separatrix surface at t = 6 μsec is $\dot{r}_s = 2.7\times10^5$ cm/sec. This value can be compared for consistency with that obtained for w using Eq. (1). At t = 6 μsec the value $\dot{\psi} = 4.5$ kMx/μsec is obtained from Fig. 6. From magnetic field profiles in the x-circle region we find B = 1.3 kG and a = 1 cm, giving $w = 2.2\times10^5$ cm/sec in satisfactory agreement with $\dot{r}_s$. (The Alfvén speed calculated using $n = 0.7\times10^{15}$ cm^{-3} is ... cm/sec). We note that the magnetic Reynolds numbers ($8\pi a v_A/c^2\eta$) for the p_o = 7mTorr

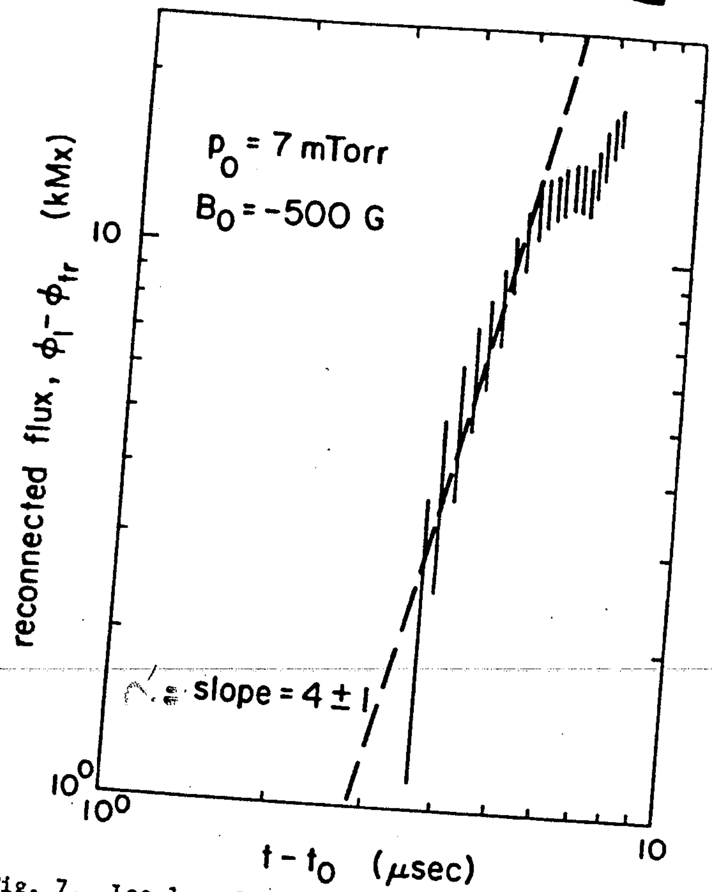

Fig. 7. Log-log plot of the reconnected flux as a function of time at z = -30 cm (the mirror position) for 7 mTorr filling pressure for the fast reconnection phase.

data are 150 for the slow phase and 50 for the fast phase, using a = 1cm and the η values from Section 5.

4.2 Change of Resistivity by Radial Convection of Current Carriers

Both in Fig. 2 and Fig. 3 the breaks in $\dot{\psi}$ (at 5.5 μsec and 3.2 μsec) occur approximately when the separatrix approaches the x-circle where the onset of the sudden increase in $\dot{\psi}$ is measured. As a qualitative second interpretation it is reasonable to assume that a corresponding lower density of current carriers will be convected to the x-circle, leading to increased, anamolous resistivity in the diffusive layer and therefore an increased $\dot{\psi}$.

5. Plasma Resistivity

The values for the resistivity η in the region of the x-circle before and during the second phase of the reconnection were calculated using the equation

$$\dot{\psi} = 2\pi r\eta c J$$

Coalescence and Current Peakedness (ϵ^{-1})

ϵ	0	0.3	0.7	0.85
Process	sheetpinch tearing inst	Coalescence Sweet-Parker Process	Fast Coalescence Brunel-Tajima Process	Explosive Coalescence Tajima-Sakai process
recon. flux $\Delta\psi$	$e^{\gamma_L t}$ $\gamma_L \propto \eta^{3/5}$	$\eta^{1/2} t$	$\eta^{1/2} t^{\alpha}$ $(\alpha \gtrsim 1)$	$\dfrac{\eta^0}{(t_0 - t)^{4/3}}$

ϵ: Faddeev Equilibrium

$$\psi_0 = \frac{B_y}{k} \ln(\cosh kx + \epsilon \cos ky)$$

$$(0 = \epsilon < 1)$$

Temporal Rates of Driven Reconnection in Nonlinear Stages

	reconnected flux vs. time	NB
Sweet-Parker Process	$\Delta\psi = \eta^{1/2} B_y (v_A/L)^{1/2} t$	
*Brunel-Tajima Process	$\Delta\psi = \psi_0 \left(\frac{t}{t_A}\right)^{[illegible]}$	$\psi_0 \approx \eta^{1/2} B_y (v_A/L) t_A$
*Explosive Process	$\Delta\psi \propto \dfrac{\eta^0}{(t_0 - t)^{4/3}}$	$t_\theta \approx \frac{\sqrt{2}}{3} a_0^{3/2} t_A$ η^0. independent of η
Petschek Process	$\Delta\psi \propto \eta^0 t$	

NB: The Rutherford process is essentially a nonlinear stage of non-driven spontaneous tearing instability.

Self-Similarity of Magnetic Collapse

$$\Delta\psi \sim (t_0 - t)^{-\alpha} \quad \text{etc.}$$

temporal universality

---

cf. Kadanoff's spin-block model for phase transition

$$g(r) \sim (r - r_0)^{-\alpha}$$

Kolmogorov's turbulence spectrum

$$E(k) \sim k^{-\alpha}$$

Spatial universality

cf. Lifshitz' explosion of universe

$$a(t) \sim t^{\alpha} \qquad \alpha = 1 \text{ or } 2/3.$$

etc. etc.

Indeces of Explosion and Universality (of Phase Transition etc.)

	Magnetic Collapse of Coalescence Inst.	Phase Transition L-G	Turbulence K
toward critical point	$\epsilon^{-1} - \epsilon_c^{-1}$	$T - T_c$	R_o^{-1} Reynolds #
scale	$t_o - t \to 0$	$r^{-1} \to 0$	$k^{-1} \to 0$
order parameter	?	density fluctuation $\delta n(r)$	vorticity $\Omega(k)$
asymptotic Universal self-similarity	$\Delta\psi \sim (t_o - t)^{-4/3}$	correlation fnc. $g(r) \sim r^{1+\eta} f(\frac{r}{\xi_o})$	energy spectrum $E(k) \sim k^{-5/3} f(\frac{k}{k_d})$
Indeces of explosion (phase transition etc.)	$E_L^2 \sim (t_o - t)^{-4}$ $T_x \sim (t_o - t)^{-8/3}$ $E_z \sim (t_o - t)^{-5/3}$ $a \sim (t_o - t)$ $L \sim (t_o - t)^2$ etc.	$\int_0^\infty r^2 g(r) dr \sim \Delta T^{-\gamma}$ $\nu_{vis} = \xi_o \left(\frac{\Delta T}{T_c}\right)^{-\nu}$ etc.	$\int_0^\infty \Omega(k) dk \propto R_o^{\gamma}$ $k_d = k_o R_o^{\nu}$ etc.

Heuristic Equations

Brunel-Tajima (extended) Eqs.

outside:

$$\frac{\partial \psi}{\partial t} = v B_y$$

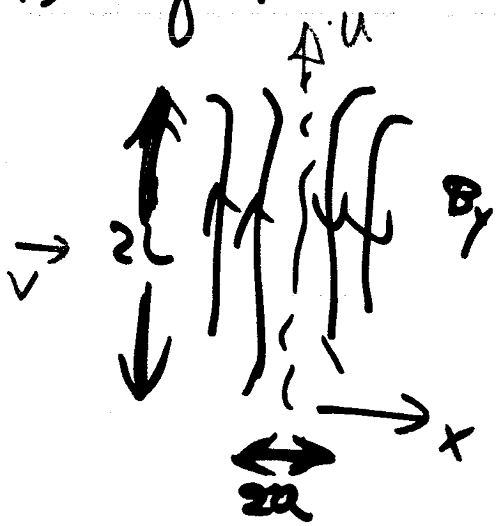

continuity

$$\rho_i u a = \rho_e v L$$

dynamic eq. (non explosive cases)

$$p_i + \frac{B_{iz}^2}{8\pi} = p_e + \frac{B_\perp^2}{8\pi} + \frac{B_{ez}^2}{8\pi}$$

(Inside

$$\frac{\partial \psi}{\partial t} = \eta \nabla^2 \psi$$
)

(explosive case)

$$\frac{\partial V_x}{\partial t} = -\frac{1}{2\rho}\frac{\partial}{\partial x} V_x^2 + \frac{1}{8\pi\rho}\frac{\partial}{\partial x} B_y^2$$

- non-explosive case (Brunel-Tajima reconnection rate)

$$\Delta\psi = \psi_{sp}\left(\frac{t}{t_0}\right)^{\rho_i/\rho_e}$$

reconnection angle

$$\alpha = \frac{a}{L^*} = \frac{\psi}{uB_{ye}\,t} \propto t^{\alpha-1}$$

(Sweet-Parker $\rightarrow$ Petschek)

- explosive case

Let
$$V_x = \frac{V(x)}{t_0-t}$$
$$B_y = \frac{B(x)}{t_0-t}$$
$$\psi = \frac{\Psi(x)}{t_0-t}$$
$$\varphi = \frac{\Phi(x)}{t_0-t}.$$

$\because$) Quadratic nonlinearity.

$$\begin{cases} \Psi = \Psi' V \\ 2V = -\left[(\Psi')^2\right]' - \left[V^2\right]' \end{cases}$$

$$\rightarrow \quad \left[\Psi^2 - \Psi_0^2\right]^{1/4} = \frac{d\Psi}{dx}$$

$$\Psi(x) = \frac{1}{4}(x - x_0)^2$$

$$\rightarrow \quad B^2 \propto (t_0 - t)^{-2}$$

$$E_x^2 \propto (t_0 - t)^{-4}$$

$$E_z \propto (t_0 - t)^{-2}$$

$$J_z \propto (t_0 - t)^{-1}$$

$L \simeq (V_{Ai}/V_x)\, a$ $\qquad V_{Ai} \sim \text{const.}$

$$a \sim t_0 - t$$

$$\therefore L \sim (t_0 - t)^2.$$

reconnection angle

$$\alpha = \frac{a}{L} \; \frac{(\text{small const})}{(t_0 - t)}$$

(Sweet-Parker → Petschek)

Theoretical Model

$$\frac{\partial n_j}{\partial t} + \nabla \cdot (n_j \mathbf{v}_j) = 0$$

$$m_j n_j \frac{d\mathbf{v}_j}{dt} = n_j e_j \left(\mathbf{E} + \frac{\mathbf{v}_j}{c} \times \mathbf{B}\right) - \nabla p$$

$$\nabla \times \mathbf{B} = \frac{4\pi}{c} \sum n_j e_j \mathbf{v}_j$$

$$\nabla \cdot E = 4\pi \sum n_j e_j$$

$$\nabla \times \mathbf{E} = -\frac{1}{c} \frac{\partial \mathbf{B}}{\partial t}$$

$$\frac{\partial p_j}{\partial t} + \mathbf{v}_j \cdot \nabla p_j + \gamma p_j \, \nabla \cdot \mathbf{v}_j = 0$$

---

assumptions $\qquad (\gamma = 1 + \frac{2}{f})$

$\frac{\partial}{\partial x} \gg \frac{\partial}{\partial y}, \frac{\partial}{\partial z}$.

~~self-similarity in t~~

solution expanded near $x = 0$.

[redacted] Solution by Stretch (Scale) factors

Introduce scale factors a and b

$$V_{ex} = \frac{\dot{a}}{a} x$$

$$V_{ix} = \frac{\dot{b}}{b} x$$

consistency:

$$\left.\begin{aligned} n_e &= \frac{n_0}{a} \\ n_i &= \frac{n_0}{b} \end{aligned}\right\} \leftarrow \text{continuity eq.}$$

Substitute these into dynamic eqs of e^- and ions and Maxwell's eqs.

We get:

$$\ddot{a} = -\omega_{pe}^2\left(\frac{a}{b}-1\right) - \frac{B_0^2\, b}{4\pi m n_0 \lambda^2 a^3\left(\frac{b}{a}+\frac{m}{M}\right)} + \frac{2P_{0e}}{m n_0 \lambda^2 a}$$

$$\ddot{b} = \omega_{pi}^2\left(1-\frac{b}{a}\right) - \frac{m}{M}\frac{B_0^2\, b^2}{4\pi M n_0 \lambda^2 a^4\left(\frac{b}{a}+\frac{m}{M}\right)} + \frac{2P_{0i}}{M n_0 \lambda^2 b}.$$

(λ : B-field scale)

$\gamma = 1 + \frac{2}{f}$: gas const.

$$\rightarrow \quad \ddot{a} = -\frac{V_A^2}{\lambda^2 a^2} + \frac{C_s^2}{\lambda^2 a^3}$$

$$= -\frac{\partial V(a)}{\partial a}$$

where the Sagdeev potential

$$V(a) = -\frac{V_A^2}{\lambda^2 a} + \frac{C_s^2}{2\lambda^2 a^2}$$

"grav. potential" "centrifugal force term"

First Integral

$$\dot{a}^2 = \frac{2V_A^2}{\lambda^2 a} - \frac{c_s^2}{\lambda^2 a^2} + \mathcal{E} ,$$

where

$\mathcal{E}$: "energy" in Sagdeev potential.

$\mathcal{E} \sim 0 \Rightarrow$ Explosive sol.

$\mathcal{E} < 0 \rightarrow$ oscillatory sol.

$$T_{os} = 2\int_{a_{t_1}}^{a_{t_2}} \frac{a\, da}{\sqrt{\mathcal{E}\left(a + \frac{V_A^2}{\lambda^2 \mathcal{E}}\right)^2 - \frac{V_A^2}{\mathcal{E}\lambda^2} - \frac{c_s^2}{\lambda^2}}}$$

$$= 2\pi \frac{V_A^2}{\lambda^2} \frac{1}{\mathcal{E}^{3/2}}$$

amplitude oscillations before total reconnection

"Sagdeev" potential $V(a)$

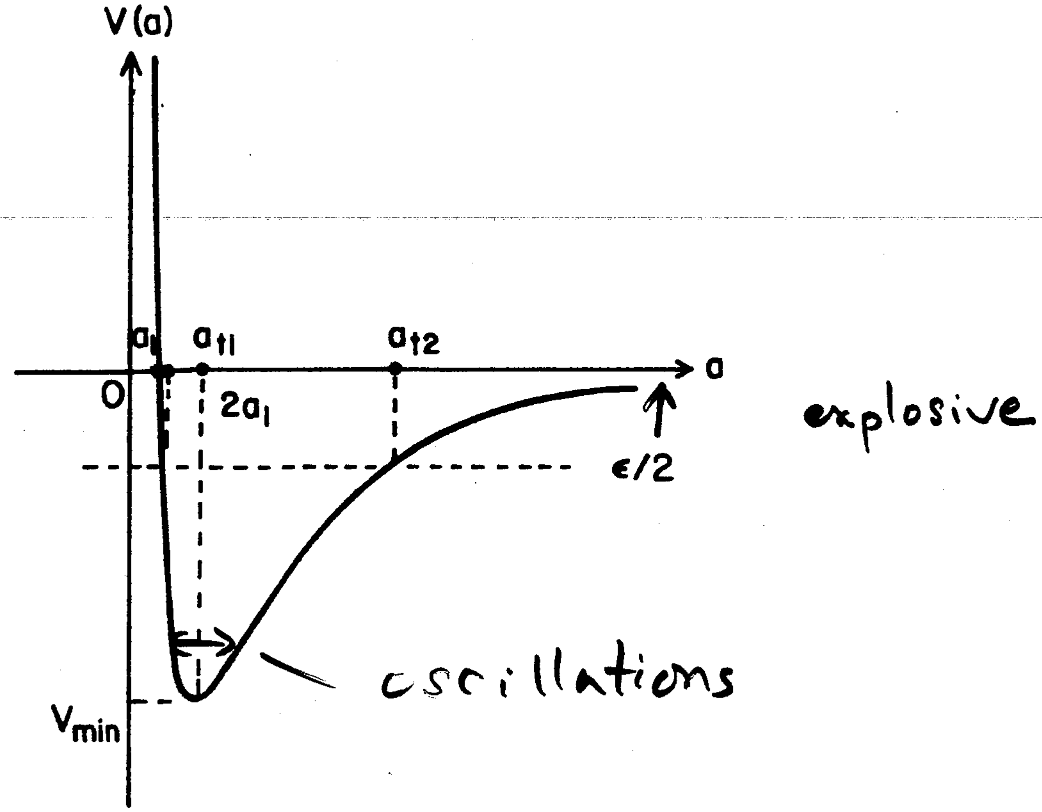

Results for explosive phase:

$$V_x = -\frac{2}{3}\frac{x}{t_0 - t}$$

$$n = \left(\frac{2}{9}\right)^{1/3} \frac{\lambda^{2/3} n_0}{V_A^{2/3}(t_0 - t)^{2/3}}$$

$$E_x = -\frac{2}{9}\frac{M}{e}\frac{x}{(t_0 - t)^2}$$

$$B_y = \left(\frac{2}{9}\right)^{2/3} \frac{B_0 \lambda^{1/3} x}{V_A^{4/3}(t_0 - t)^{4/3}}$$

$$E_z = \mathcal{E}_z^{(1)} \frac{1}{(t_0 - t)^{2/3}} + \mathcal{E}_z^{(2)} \frac{1}{(t_0 - t)^{5/3}}$$

i.e.

(Self-similar phase)

"Sagdeev" potential. V(a)

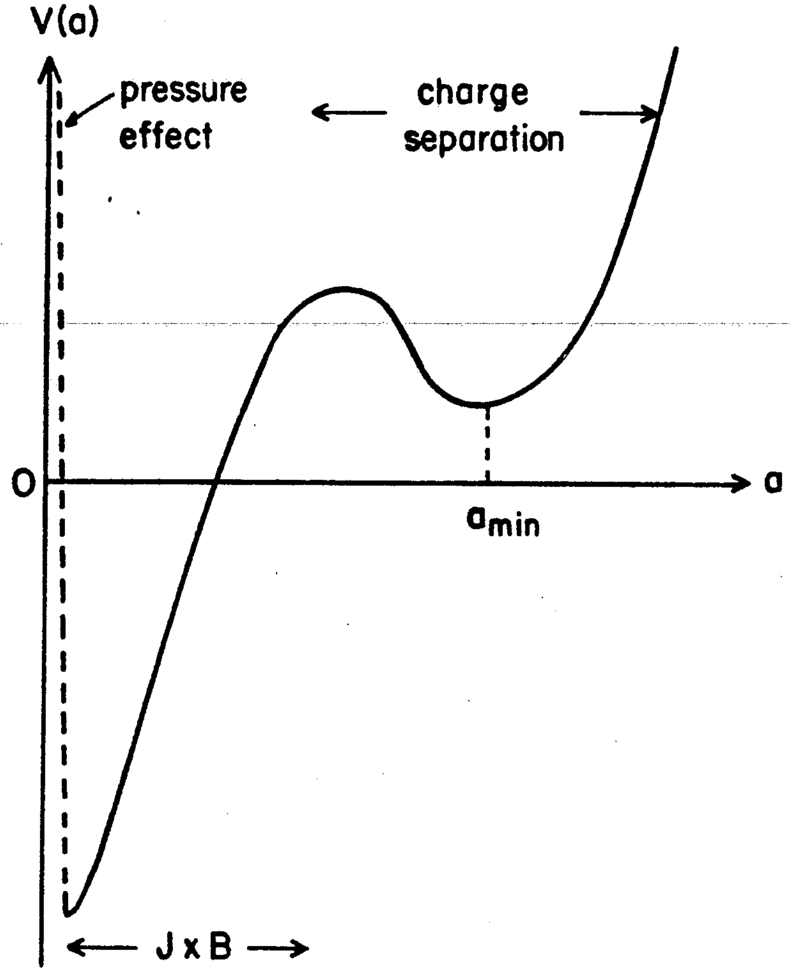

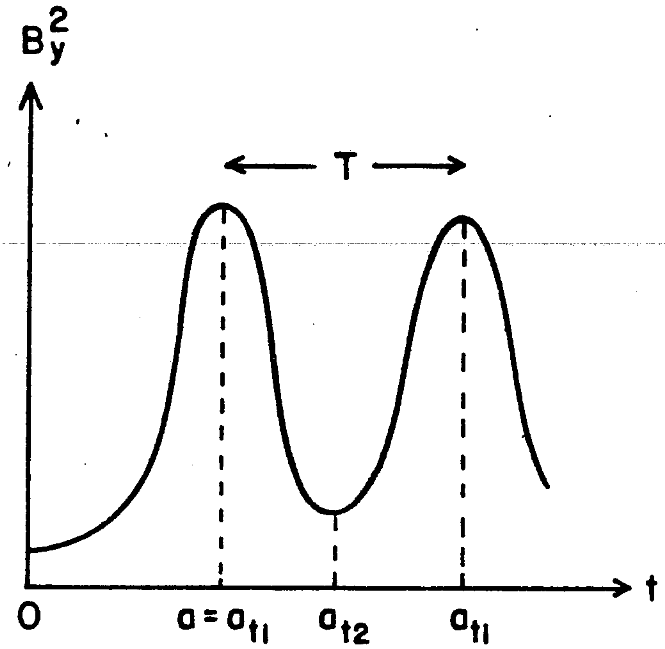
B_y^2
T
O
$a = a_{t1}$
a_{t2}
a_{t1}
t

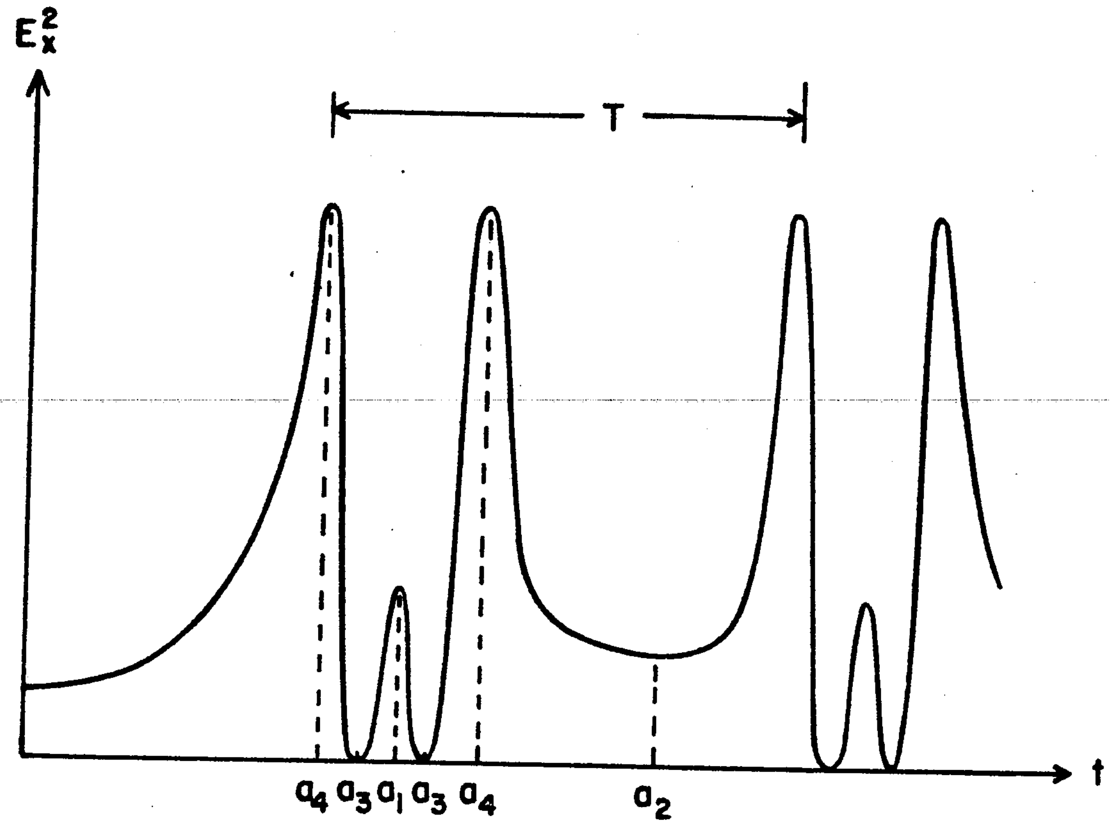

E_x^2
T
t
a_4 a_3 a_1 a_3 a_4
a_2

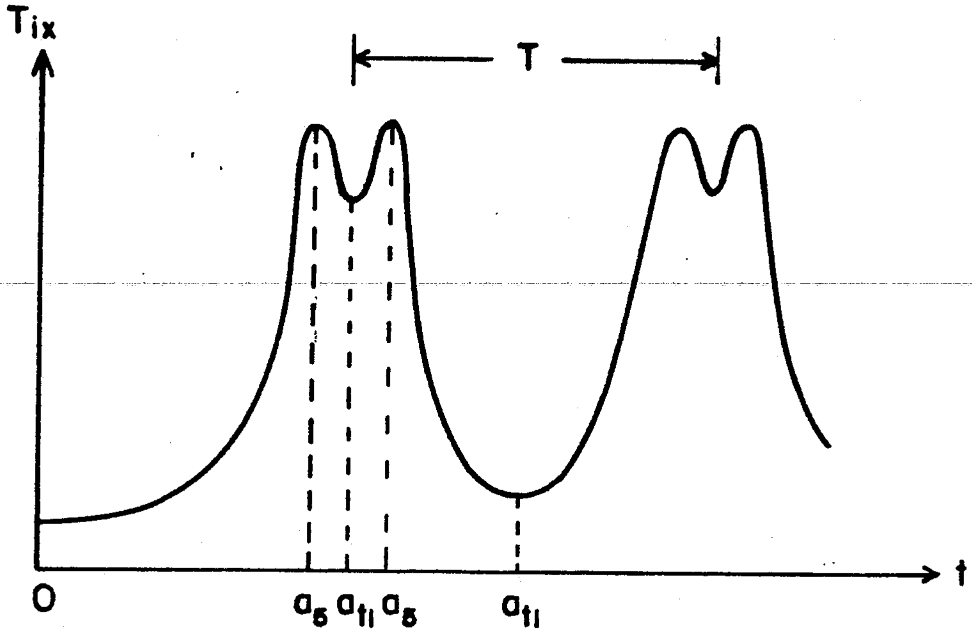

T_{ix}
T
O
a_δ
a_{tl}
a_δ
a_{tl}
t

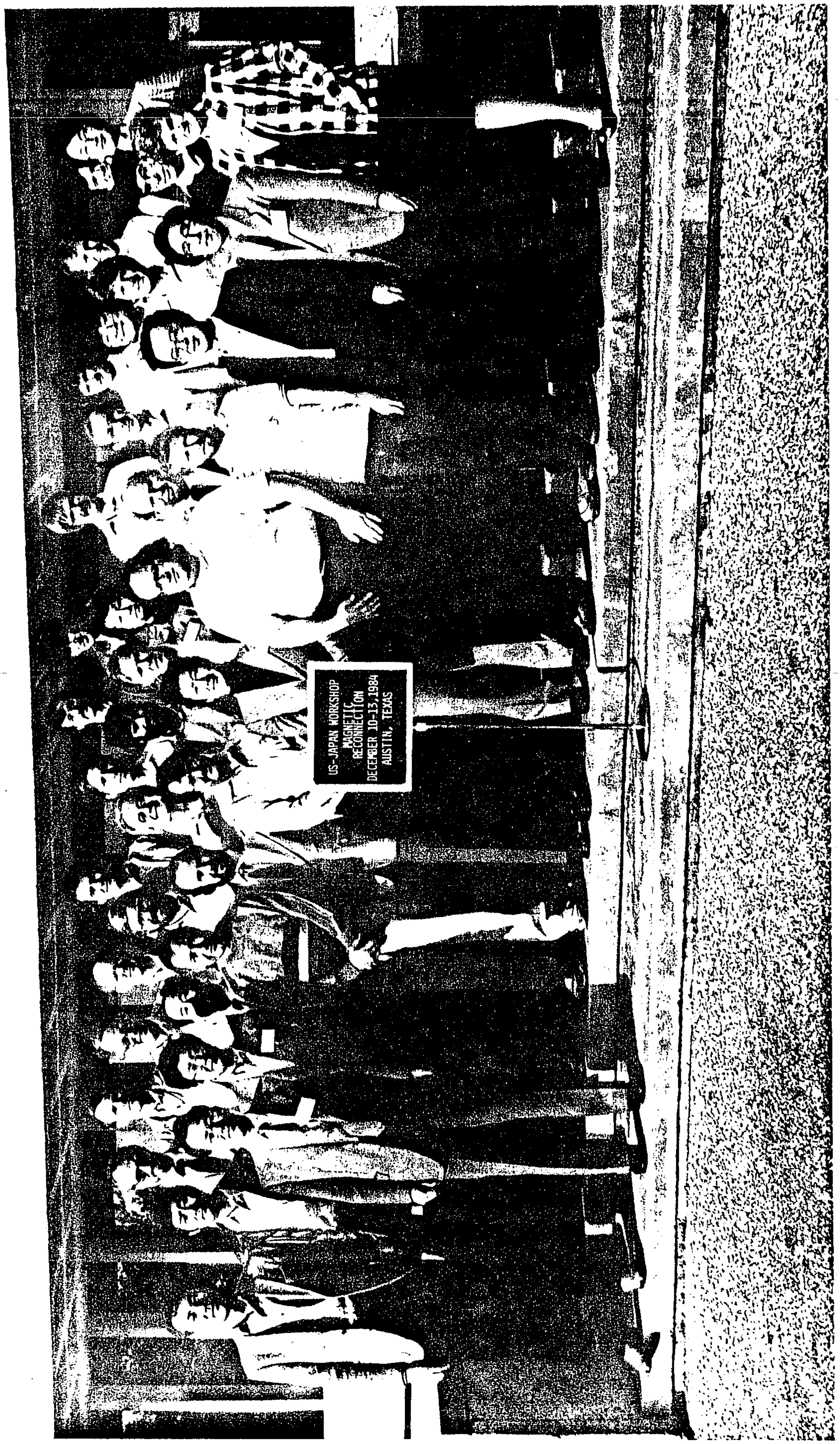
US-JAPAN WORKSHOP
MAGNETIC
RECONNECTION
DECEMBER 10-13,1984
AUSTIN, TEXAS